DELIVERABLE FRONTPAGE

Project number:	243827 FP7-ENV-2009-1
Project acronym:	LC-IMPACT
Project title:	Development and application of environmental Life Cycle Impact assessment Methods for improved sustainability Characterisation of Technologies.
Deliverable number:	D2.3
Deliverable name:	Recommended assessment framework, method and characterisation factors for ecotoxicity and human toxicity
Version:	1
WP number:	2
Lead beneficiary:	DTU
Nature:	R[1]
Dissemination level:	PP[2]
Delivery date Annex I:	M41
Actual delivery date:	30/04/2013
Authors:	R.K. Rosenbaum, A. Anton, B. Ciuffo, P. Fantke, L. Golsteijn, M.Z. Hauschild, S. Hellweg, A.J. Hendriks, H.W.M. Hendriks, M.A.J. Huijbregts, S. Humbert, O. Jolliet, R. Juraske, A. Kounina, M. Margni, D. Marinov, G. Musters, M. Owsianiak, D. Pennington, A.F.H. Pilière, A. Ragas, C.E. Raptis, S. Sala, E. Sevigne Itoiz, M. Trombetti, R. van Zelm
Comments:	**Several parts of this deliverable will be published in scientific journals and need to be treated confidentially until the publishing date (for internal EU review only).**

[1] Please indicate the nature of the deliverable using one of the following codes: **R** = Report, **P** = Prototype, **D** = Demonstrator, **O** = Other

[2] Please indicate the dissemination level using one of the following codes: **PU** = Public, **PP** = Restricted to other programme participants (incl. the Commission Services), **RE** = Restricted to a group specified by the consortium (incl. the Commission Services), **CO** = Confidential, only for members of the consortium (incl. the Commission Services)

Table of Contents

List of abbreviations

AF	bioaccessibility factor
AOX	adsorbable organohalogens
AS	activated sludge
BF	bioavailability factor
BOD	biochemical oxygen demand
CF	characterisation factor
COD	chemical oxygen deman
CTP	comparative toxicity potential
DOC	dissolved organic carbon
EC_x	x % effective concentration
EF	effect factor
FF	fate factor
FIAM	free ion activity model
flow FFF	flow field-flow fractionation
HC_x	x % hazardous concentration
HPSEC	high performance size exclusion chromatography
iF	intake fraction
LCA	life cycle assessment
LCIA	life cycle impact assessment
MW	molecular weight
MWD	molecular weight distribution
NOM	natural organic matter
PAF	potentially affected fraction of organisms
POC	particulate organic carbon
SSD	species sensitivity distribution
TBLM	terrestrial biotic ligand model
TOC	total organic carbon
TU	toxic unit
WEA	whole effluent assessment
WET	whole effluent toxicity
XF	exposure factor

1. Executive summary

The objectives of this work package relevant for this deliverable (as laid out in Annex I of the Grant Agreement) have been met in all tasks. These were respectively:

- improve the characterisation factors of terrestrial ecotoxicity with a specific focus on metals;
- develop an operational method and derive characterisation factors of whole effluent emissions for aquatic ecotoxicity;
- develop an operational method and derive characterization factors to assess the impact of a toxic chemicals on higher predators;
- include direct pesticide exposure via food in the characterisation factor calculations for human toxicity;
- assess the influence of spatial variability on characterization factors for chemicals causing ecotoxicity and human toxicity;

The LCIA methods, characterisation factors and normalisation factors developed within this WP will be applied to the case studies of WP4, to illustrate the use as well as the relevancy. Furthermore, the characterisation factors and normalisation factors will be incorporated into the ILCD system, according to the data format and quality requirements, for easy use by LCA practitioners.

The tasks in work package 2 are essentially related to establishment and improvement of the characterisation modelling of toxic impacts of chemical emissions to humans and ecosystems. In particular, four types of chemical emissions with potential impacts on four different endpoints were considered: 1) metals on terrestrial ecosystems, 2) whole effluents on freshwater ecosystems, and 3) organic chemicals (pesticides) on humans, and organic chemicals on terrestrial ecosystems and higher predators in freshwater ecosystems. These are summarised hereafter.

Terrestrial ecotoxicity of metal emissions: Recent efforts aimed at identifying best practice for characterization modelling in life cycle impact assessment (LCIA) concluded that no method for assessing toxic impacts on terrestrial ecosystems is mature enough to be recommended by the Joint Research Centre of the European Commission (JRC). USEtox is the recommended default model for midpoint evaluation of freshwater ecotoxicity, but lacks scientifically sound characterization factors for terrestrial ecosystems. USEtox, like any other characterization model, ignores the fact that metals can exist in many forms with different behavior and toxicity in terrestrial environments, depending on the ambient conditions. In response, a new framework for characterization modeling of cationic metals in terrestrial environments was developed. The framework distinguishes between two complementary sides of metal availability in soil, that is the solid-phase metal reactivity (captured by the newly introduced accessibility factor) and bioavailability of toxic metal forms in the aqueous phase due to speciation. Geographic differences in fate, accessibility, bioavailability, and terrestrial toxicity were assessed by combining the USEtox characterization model, empirical regression models, and terrestrial biotic ligand models. The median comparative toxicity potentials (CTP) for Cu and Ni with 95% geographic variability intervals are 1.4×10^{3} (1.7×10^{2}

– 2.0×10^4) and 1.7×10^3 (2.1×10^2 – 1.1×10^4) m^3/kg·day, respectively. The geographic variability of 3.5 orders of magnitude in the CTP of Cu is mainly associated with the variability in soil organic carbon and pH. They largely influence the fate and bioavailability of Cu in soils. In contrast, the geographic variability of 3 orders of magnitude in the CTP of Ni can mainly be explained by differences in pore water concentration of magnesium (Mg^{2+}). Mg^{2+} competes with Ni^{2+} for binding to biotic ligands, influencing the toxicity. Empirical regression models were derived that allow calculating CTP of Cu and Ni from soil parameters. Their application was demonstrated with an example of Cu emitted to air from a coal-fired power plant located in Spain. In this particular case, the CTP of Cu is mainly determined by the properties and relative occurrence of soils located within 100 km distance from the power plant. These findings stress the importance of dealing with spatial variability in the calculation of CTPs for terrestrial ecotoxicity of metals. Our framework improves existing life cycle impact assessment schemes for metals by suggesting a modeling approach that is based on the mechanistic understanding of the processes underlying metal behavior in soil. The proposed framework, accompanied by recommendations for Cd, Co, Pb and Zn on how to address their accessibility, give direction for improved characterization of ecotoxic impacts from metals in terrestrial ecosystems.

Aquatic ecotoxicity of whole effluents: Existing freshwater aquatic ecotoxicity fate and effect models employed in LCIA inadequately address the need to characterise complex chemical mixtures, such as industrial effluents. A methodology is proposed to develop a characterisation factor for a commonly measured, all-encompassing organic sum-parameter, namely total organic carbon (TOC). The effect factor ( ) is estimated by appropriately attributing the total measured ecotoxicity to the organic and inorganic fraction of the effluent, which is accomplished by adopting and adapting whole effluent toxicity (WET) studies, the concentration addition concept of mixture toxicity, and state-of-the-art metal toxicity models [biotic ligand models (BLM) and free ion activity models (FIAM)]. The fate factor ( ) is calculated via the USEtox model, after individually estimating all the environmental fate properties of TOC required as an input to the model. These input parameters reflect the average properties of the organic bulk and are estimated either through experimental studies, or through existing empirical relations. Developing freshwater aquatic ecotoxicity characterisation factors (CF) for TOC is expected to make the environmental impact assessment of industrial effluents within LCA much easier than any attempt to measure or assume their individual chemical constituents and carry out LCIA with single chemical CFs. However, achieving such s is in itself particularly data-demanding and dependent on the existence of comprehensive WET studies. The proposed methodology is examined via a test-of-concept study for effluents from the pulp and paper industry. The is found to be equal to 3.31 PAF/(kg m^{-3} TOC), placing it in the lowest 0.5% of all effect factors for organic chemicals in USEtox. At 15.5 d, the is estimated to be within the lowest 38% of fate factors. The then is found equal to 51.3 PAF d/(kg m^{-3} TOC), placing it within the lowest 4.5% of characterisation factors for organic chemicals included in USEtox. Further work with this methodology, when more data are available, could permit the comparison of TOC in effluents from different industries in terms of their ecotoxic potential.

Spatial variability of toxic impacts of organic chemical emissions: This work aims at evaluating key drivers of spatial differentiation for ecotoxicity and human toxicity, selecting an appropriate model and spatial resolution for the freshwater ecotoxicity and human toxicity categories (by all exposure routes) in order to keep a high level of precision while limiting the requirement of a large amount of geographical data. Spatial differentiation has been assessed trough different models at different scales from continental to country, watershed, and grid scale (using MAPPE Global with 1*1° resolution, MAPPE Europe with 1*1 km resolution, IMPACT World with 17 fully interconnected sub-continental regions, and IMPACT 2002 nested and with continent specific parameterization for each continent) along the cause effect chain (removals rates from air, soil, ocean, and freshwater; fate factors; intake fractions). A test set of 36 chemicals, representing different combination of physical chemical properties has been used to explore the environmental behaviour of chemicals. Key parameters for different outputs, different compartments and with different types of chemicals were identified and archetypes for the removal process in different compartments were proposed and partially tested for different chemicals and different geographic regions. Studying *intra-continental variation* at a watershed scale with the spatial IMPACT Europe model, lead to the development of archetypes for freshwater ecotoxicity and human toxicity exposure to drinking water and fish, as a parsimonious proxy to higher resolution spatialization. Results of the analysis of the *spatial variability associated with removal rates* highlighted that the variability is both chemical (highest for volatile and multimedia chemicals) and compartment (highest in air, followed by ocean, and soil) specific. Two archetypes for the coastal zone were identified, based on their capability of behaving as filter or not. For removal from air climate-based archetypes rather than geo-political ones (continent, countries, etc.) were identified as appropriate for removal rate calculations. Regarding *fate factors* for freshwater the watershed scale represents the best trade-off between capability of distinguishing among different landscapes affecting fate factors and complexity of the calculation (e.g. at grid scale). Terrestrial fate factors present a limited overall variability (except for chemicals with high variability in the removal rate from soil) with only the grid scale capturing differences between the factors. Regarding intake fractions (iFs) for inhalation, the results support the distinction between a continental and an urban box (as in USEtox), being mainly affected by the population density. *Inter-continental variation* of fate factors and intake fraction represents more than three orders of magnitude among the 17 zones of IMPACT World and USEtox. However, comparing results from the USEtox nested continental parametrisation (for each continent respectively) with those form IMPACT World shows that surrounding the continental box with either a single global box or a landscape composed of other continents does not have an important influence, as the most important part of the impact occurs in the continent where the pollutant is emitted. Most of result differences between models occur due to model algorithm difference, e.g. modeling of water outflow and volatilization algorithm. Results of IMPACT Europe showed that non-spatial models might overestimate the chemical fate and characterization factors for freshwater ecotoxicity up to a factor five when compared to a spatially differentiated model for unknown emission location (i.e. assumed being uniformly emitted compared over the whole model surface). When the emission location is known, a spatially differentiated model can improve the model accuracy up to 2-3 orders of magnitude, because of its ability to accurately predict the water residence time before advection to the sea (or out of the

system) depending on the emission location. For persistent chemicals, the country/regional differentiation is relevant. The optimization of the variability of spatial model watersheds compared to three archetype watersheds lead to the definition of three archetypes meaningfully distinguishing low water residence time (<2 d to model border, W1), medium water residence time (2 - 60 d to model border, W2), and high water residence time (>60 d to model border, W3). A new version of the model with three watershed archetypes evaluated against a spatial model version, showed the relevance of this archetypical differentiation for aquatic fate and intake fractions. This would constitute a significant improvement in the model accuracy whilst limiting the amount of input data to parameterize detailed geographical watershed data.

Human toxicity of pesticide emissions: A new dynamic plant uptake model is presented to characterize health impacts of pesticides applied to food crops. The model is based on a flexible set of interconnected compartments and assesses various crop types with distinct properties and processes. Crop-specific human toxicity characterization factors are provided for use in life cycle impact assessment along with analyzing their variance between crop types, pesticides and application times. Characterization factors vary up to fourteen orders of magnitude between crops and up to twenty orders of magnitude between pesticides, thereby stressing the importance of considering the specific properties and boundary conditions of different crop-environment systems and related pesticide-specific process characteristics. Crop leaf growth, initial spray drift and food processing are identified to be the main crop-related aspects driving the evolution of pesticide masses in the modeled system along with pesticide properties, mainly octanol-water partition coefficient and degradation half-life in plants. Using the new characterization factors, we demonstrate that toxicity potentials can be reduced up to 99% by defining adequate scenarios for pesticide substitution.

Terrestrial ecotoxicity of organic chemical emissions: Due to insufficient soil toxicity data, terrestrial ecotoxicity is generally hardly addressed. The terrestrial ecotoxic effects depend on the concentration that is dissolved in pore water. Based on sorption equilibrium, the chemical concentration in water and soil can be modelled with the equilibrium partitioning (EP) method. Consequently, aquatic toxicity tests can be used to estimate terrestrial toxicity. An important characteristic in the assessment of toxic chemicals is the hazardous concentration (HC50). *The goal of* the present study was to analyse the validity and uncertainty of estimates of soil toxicity derived from the equilibrium partitioning method. A comparison between freshwater HC50 values derived from standard aquatic tests, and porewater HC50 values derived from terrestrial experimental data by the EP-method, was performed for 48 organic chemicals. Statistical uncertainty was treated with probability distributions propagated by Monte Carlo simulation. For over 65 percent of the chemicals, $HC50_{ex,soil}$ values exceeded $HC50_{ep,soil}$ values, with a systematic uncertainty (i.e. the ratio of $HC50_{ex,soil}/HC50_{ep,soil}$) of typically 1.7. Accompanying confidence intervals were typically four orders of magnitude. For eight percent of the chemicals, a ratio of 1 for $HC50_{ex,soil}/HC50_{ep,soil}$ fell outside the confidence interval.

Higher (warm-blooded) predator ecotoxicity of organic chemical emissions: A method was developed to calculate Characterization Factors (CFs) for the impact assessment of

chemical emissions on warm-blooded predators in freshwater food chains. The CF for these predators was defined as a multiplication of the Fate Factor (FF), Exposure Factor (XF), Bioaccumulation Factor (BF), and Effect Factor (EF). FFs and XFs were calculated with the model USES-LCA 2.0. BFs were calculated with the model OMEGA, for chemical uptake via fresh water, food and air. As a follow-up on the Deliverable 2.1 and a paper published in 2012 by Golsteijn et al., EFs were calculated from hazardous doses based on both experimental and modeled toxicity data. Namely, the effect dataset was enlarged with interspecies correlation estimation (ICE) model predictions. Characterization factors for the ecotoxicological impacts of organic chemicals on warm-blooded predators at the end of freshwater food chains were developed for a list of 1479 non-ionic chemicals for which aquatic ecotoxicity characterization factors have presently been calculated with USEtox.

2. Terrestrial ecotoxicity of metal emissions

M. Owsianiak[1], R.K. Rosenbaum[1], M.A.J. Huijbregts[2], K.S. Christiansen[3], P.E. Holm[3], O.K. Borggaard[3], M.Z. Hauschild[1]

[1]Technical University of Denmark
[2]Radboud University Nijmegen, The Netherlands
[3]University of Copenhagen, Denmark

2.1. Introduction

Current chemical hazard ranking and scoring schemes, including life cycle impact assessment (LCIA), ignore the fact that metals can exist in many forms with different behavior and toxicity in terrestrial environments, depending on the ambient conditions. Efforts have recently been undertaken to improve the situation. Following the "Clearwater Consensus" on assessing metal hazard in freshwater (Diamond et al. 2010), Gandhi et al. (2010) developed a method for calculating comparative toxicity potentials (CTPs) of metals in aquatic systems taking metal speciation into account in environmental fate, bioavailability and effects. The CTPs (in LCIA also known as characterization factors, CF) ranged over three orders of magnitude. The largest contributor to the variability in CTPs was the difference in bioavailability, controlled mainly by pH-dependent dissolution and complexation with dissolved organic matter. These findings highlight the need for taking into account environmental chemistry parameters in ecotoxicity assessment of metals.

For soils, metal distribution between the solid phase and solution phase, and speciation in soil pore water control the availability of toxic forms of metals, while protons and base cations can mitigate their ecotoxicity (Oorts et al. 2006; Thakali et al. 2006a). Several aspects should be considered when including speciation in calculating soil-specific CTPs of metals. First, residence time of metals may be high due to sorption of metal to soil constituents such as clay or organic carbon (Sauvé et al. 2000). Second, a significant fraction of the solid-phase metal is not available for partitioning to the solution phase due to differences in reactivity of solid metal forms (Degryse et al. 2004). Third, geographic variability of environmental chemistry parameters in soil can be high. For example, in soils a variation of six units in pH is not uncommon (Reuter et al. 2008). Due to the effects of pH and other parameters on metal sorption, speciation and ecotoxicity, it can be expected that CTPs of metals in soil will also be controlled by environmental chemistry and will vary depending on soil type, but the magnitude of this variation and controlling factors are unknown.

The aim of our study was to calculate CTPs for copper (Cu) and nickel (Ni) in terrestrial systems taking into account spatial differences in speciation and toxicity as influenced by the soil chemistry. CTPs were calculated for a set of 760 noncalcareous soils from around the world spanning a wide range of properties. USEtox was employed as a fate model to calculate fate factors (FF) of metals in soil after a unit emission to air (Hauschild et al. 2008; Rosenbaum et al. 2008). This emission route was chosen because emissions to air are a major anthropogenic source of metals in soils (Nicholson et al. 2003). Empirical regression models were used to account for differences in metal partitioning in calculation of the distribution coefficient (K_d) and bioavailability factors (BF), while terrestrial biotic ligand

models (TBLM) were chosen as ecotoxicity models to calculate effect factors (EF). Recognizing that the largest metal pool in soil is associated with the solid phase and that only a fraction of this metal pool is reactive (Degryse et al. 2004), a new factor called accessibility factor (ACF) is introduced into the definition of CTP. Geographic variability in CTP is demonstrated for Cu and Ni, which were chosen due to the availability of TBLMs for several terrestrial species for these two metals.

2.2. Methods

2.2.1. Framework

Current Framework for Freshwater Ecotoxicity. The method for calculating CTP of cationic metals in freshwater proposed by Gandhi et al. (2010) was taken as a starting point (eq 2.1). In their method, the CTP is defined as:

$$CTP_{i,s} = FF_{i,s} \cdot BF_s \cdot EF_s \qquad \textbf{2. 1}$$

where $CTP_{i,s}$ ($m^3/kg_{total\ emitted}$·day) is the comparative toxicity potential of total metal s emitted to compartment i; $FF_{i,s}$ (day) is the fate factor calculated for total metal s in freshwater; BF_s ($kg_{bioavailable}/kg_{total}$) is the bioavailability factor defined as the bioavailable fraction of metal s in freshwater; and EF_s ($m^3/kg_{bioavailable}$) indicates the average toxic potency of the bioavailable fraction of metal s expressed as a Potentially Affected Fraction (PAF) of organisms. The bioavailable fraction in the method of Gandhi et al. refers to the "truly" dissolved metal, including free ions and inorganic complexes.

Proposed Framework for Terrestrial Ecotoxicity. The method of Gandhi et al. (2010) is further developed to make it suitable to soils. This is done by introducing the accessibility factor (ACF) into the definition of CTP and modifying the definition of the bioavailability factor (BF) (eq 2.2):

$$CTP_{i,s} = FF_{i,s} \cdot AF_s \cdot BF_s \cdot EF_s \qquad \textbf{2. 2}$$

where $CTP_{i,s}$ ($m^3/kg_{total\ emitted}$·day) is the comparative toxicity potential of total metal s emitted to compartment i; $FF_{i,s}$ (day) is the fate factor calculated for total metal s in soil; ACFs ($kg_{reactive}/kg_{total}$) is the accessibility factor defined as the reactive fraction of total metal s in soil; BF_s ($kg_{free}/kg_{reactive}$) is the bioavailability factor defined as the free ion fraction of the reactive metal s in soil, and EF_s (m^3/kg_{free}) is the terrestrial ecotoxicity effect factor defined as PAF for the free ion form of the metal. We expressed the BF based on the free ion because calculation of the "truly" dissolved metal in soil requires input parameters that are rarely available, such as composition of major anions forming complexes with the free ion.

In the framework proposed by Gandhi et al. (2010) for freshwater, the ACF is in practice part of the BF. The decoupling of the ACF from the BF for the soil assessment is recommended for two reasons. First, the ACF acknowledges the fact that the largest metal pool in soil is the solid-phase metal. Second, the ACF recognizes that not all forms of metal in soil are reactive. Others readily showed that dissolved concentrations of metals can be better predicted from the reactive metal pool instead of the total metal pool (Degryse et al.

2003; Romkens et al. 2009). In freshwater, these aspects are expected to be less important because the particulate-bound metal fraction is often smaller than the total dissolved metal pool (Popp et al. 2008) and because the reactivity of metal sorbed to suspended matter is not expected to be substantially reduced within time until it is removed by outflow and/or sedimentation (Garnier et al. 2006). The term “reactive” refers to the operational definition proposed by Degryse et al. (2009) for the “labile” metal, given as metal in the solid phase that “equilibrates with the solution phase within a few days”.

The terms accessibility and bioavailability are not new and have been used previously in the soil pollution context (Reichenberg and Mayer 2006; Semple et al. 2004). The ACF represents metal that is potentially able to cause ecotoxicity, i.e. metal which can partition to soil solution. This definition is consistent with that proposed by Reichenberg and Mayer (2006) who define accessibility as “the mass quantity of a chemical that is or can become available within a given time span and under given conditions”, and is fundamentally similar to that proposed earlier by Semple et al. (2004) for bioaccessibility, which “encompasses what is actually bioavailable now plus what is potentially bioavailable”. Mechanistically, our ACF is also consistent with the definition of bioaccessibility used in risk assessment of metals (Peijnenburg and Jager 2003; Ruby et al. 1999) except that in the soil context the ACF refers to the partitioning in the natural instead of in the gastrointestinal environment. We find the term accessibility more appropriate as it represents metal pool potentially available for other processes than uptake by biota (as for example leaching from soil). The BF, expressed as a fraction of reactive metal, represents metal that is chemically active on its way to organisms (i.e. free ions), consistently with Semple et al. (2004) who defined the bioavailable compound “as that which is freely available to cross an organism’s cellular membrane from the medium the organism inhabits at a given time”. Note, that both the ACF and the BF are independent of the receptor, because the fate of the free ion within the organism after crossing the membrane does not depend on the soil anymore.

To illustrate these definitions with an example, the comparative toxicity potential of a metal will be the highest if all metal forms in soil are reactive and the only dissolved form are the free ions. However, even if the solid-phase metal is reactive and thus accessible within given time, metal can still become non bioavailable if speciation in soil pore water reduces concentration of the free ions to low levels (soil 1 in Fig. 2.1, left). On the other hand, even if the fraction of free ions in the solution is considerably large, the comparative toxicity potential of the metal can still be reduced if metal is not reactive because the total dissolved metal pool will be lower (soil 2 in Fig. 2.1, right). These two complementary sides of metal accessibility and bioavailability define exposure of terrestrial organisms through soil pore water and (in addition to fate and effects) are expected to control the magnitude of the comparative toxicity potential of metals in terrestrial systems.

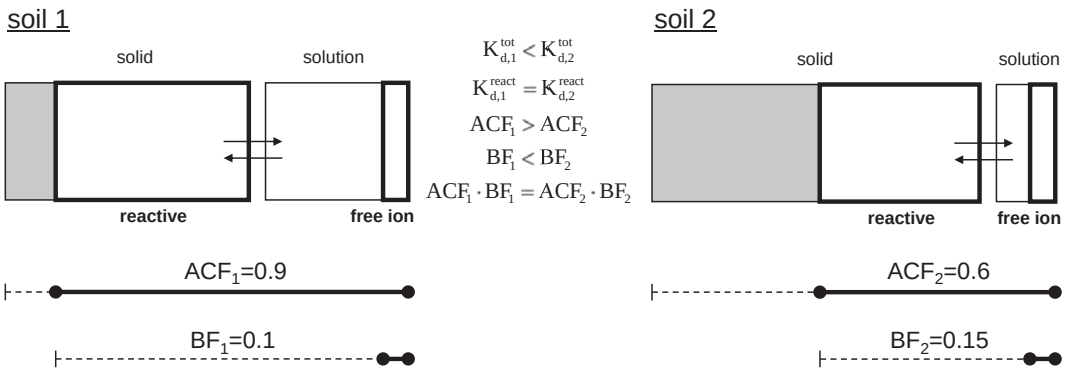

Figure 2.1: The definitions of accessibility (ACF) and bioavailability (BF) factors in the proposed method for calculating CTPs of metals in soil (eq 2.2) illustrated for two hypothetical cases. K_d^{tot} is the distribution coefficient between total solid phase and solution phase; K_d^{react} is the distribution coefficient between reactive solid phase and solution phase. The grey box represents the metal pool that is not reactive, according to the definition given in the main text. The bold boxes represent reactive (solid) and free ion (solution) metal pools. The figure is not up to scale to make it more legible. In reality, the mass of metal in the solid phase is much larger than the mass of metal in the solution (Degryse et al. 2009). The figure is inspired by Fig. 1 in Degryse et al. (2009).

2.2.2. Modeling approach

Fate Factors. The fate factor ($FF_{i,s}$, day) represents the residence time of metal s in soil after emission to compartment i (eq 2.3). Note, that this definition of the FF includes a correction factor to acknowledge the fact that only a fraction of metal emitted to compartment i is transferred to soil, while the residence time of anthropogenically induced metal content in a soil refers to removal processes, such as leaching and runoff. We employed USEtox to calculate the FF of metal in natural soil after unit emission to continental rural air. USEtox is a consensus model developed through comparison and harmonization of seven LCIA-suited models and considers major fate mechanisms. Default USEtox environmental parameters were used combined with metal- and soil-specific K_d values. Calculations were performed for infinite time horizon, assuming instantaneous equilibrium for metal distribution and speciation. Similar approaches to modeling metal fate in soil have been presented previously (Bhavsar et al. 2008).

$$FF_{i,s} = \frac{\Delta C_{total,s} \cdot V \cdot \rho_b}{\Delta M_{s,i}} \qquad \textbf{2. 3}$$

where $\Delta C_{total,s}$ (kg_{total}/kg) is the incremental change in concentration of total metal s in soil; ΔM_s ($kg_{total\ emitted}$/day) is the incremental change in the emission of total metal s to compartment i; V (m^3) is the volume of the soil compartment; and ρ_b (kg/m^3) is the bulk density of the soil.

K_d, defined as the ratio between the concentration of total metal in the solid phase and the total dissolved metal was calculated employing empirical regression models recently proposed by Groenenberg et al. (2012) Empirical regression models (see SI for a review) are equilibrium-based models and find application in deriving soil quality criteria (Lofts et al. 2004) or in human exposure assessment (Pizzol et al. 2011). The following criteria, listed in

order of increasing priority, were applied to select models from available alternatives: (i) models with lower standard errors of estimate in soils outside the parameter range for which they were developed were preferred; (ii) models with lower standard errors of estimate in soils within the parameter range for which they were developed were preferred; (iii) models developed using soils spanning a wide range of environmental properties (pH, the content of organic carbon and total metal) were preferred; (iv) models developed using a large number of soils were preferred.

Due to the lack of measured values of the background content of Cu and Ni in each soil we assumed that they equal 14 and 16 mg/kg respectively. These values are median concentrations measured in European soils (Lado et al. 2008) and were preferred over average (arithmetic mean) concentrations measured in the North America (25 and 19 mg/kg for Cu and Ni, respectively) (Shacklette and Boerngen 1984) because the European set of soils is larger. It was moreover assumed that the content of amorphous, oxalate extractable Al and Fe (hydr)oxides (AlFeox) equals 89 mmol/kg. This value is the sum of median values for Al and Fe measured in Portuguese soils (Rodrigues et al. 2010b) and is close to the sum of median values measured in Dutch soils (44 and 24 mmol/kg for Fe and Al, respectively) (Groenenberg et al. 2010). The concentration of dissolved organic carbon (DOC) was estimated from pH, organic carbon and electrical conductivity using the regression model developed by Römkens et al. (2004).

Accessibility Factors. The accessibility factor (ACF_s, $kg_{reactive}/kg_{total}$) of metal s in soil is proposed as:

$$ACF_s = \frac{\Delta C_{reactive}}{\Delta C_{total}} \qquad \textbf{2. 4}$$

where $\Delta C_{reactive}$ ($kg_{reactive}/kg$) is the incremental change of the concentration of reactive metal in soil; and ΔC_{total} (kg_{total}/kg) is the incremental change in concentration in total metal in soil. The ACF was calculated employing empirical regression models published by Römkens et al. (2004) and Rodrigues et al. (2010b) (see SI). The same selection criteria were applied as for the selection of K_d regression models.

Bioavailability Factors. The bioavailability factor (BF_s, $kg_{free}/kg_{reactive}$) of metal s in soil was calculated as:

$$BF_s = \frac{\Delta C_{free} \cdot \theta_w}{\Delta C_{reactive} \cdot \rho_b} \qquad \textbf{2. 5}$$

where ΔC_{free} (kg_{free}/m^3) is the incremental change of the free ion fraction of metal; $\Delta C_{reactive}$ ($kg_{reactive}/kg$) is the incremental change in concentration in reactive metal content in soil; θ_w (m^3/m^3) is the volumetric soil water content. The BF was calculated using empirical regressions predicting the concentration of free metal ion from reactive metal published in Groenenberg et al. (2010) (see SI). Again, the same selection criteria were applied as for the selection of K_d regression models.

Effect Factors. The effect factor (EF_s, m^3/kg_{free}) of metal s was calculated by assuming a constant value (= 0.5) for a linear dose-response function (Pennington et al. 2004):

$$EF_s = \frac{\Delta PAF}{\Delta C_{free}} = \frac{0.5}{HC50} \qquad \textbf{2. 6}$$

where ΔPAF (dimensionless) is the incremental change in the potentially affected fraction of biological species in the soil ecosystem due to exposure to the free ion concentration of metal; and HC50 (kg_{free}/m^3) is the hazardous free ion concentration affecting 50% of the species, calculated as a geometric mean of free ion EC50 values for individual species.

Terrestrial biotic ligand models (TBLM) were chosen to calculate the EF because the fraction of metal bound to a biotic ligand of terrestrial organisms exposed predominantly via the pore water is expected to be a better descriptor of ecotoxicological response than activity of free ion in soil solution or total metal in soil (Thakali et al. 2006a). Ecotoxicity models that in addition to competitive binding consider electrostatic interactions between metal ions and organism cells have been developed, but their availability is limited to plants (Wang et al. 2012; Wang et al. 2011b). The following criteria were used in selection of TBLMs: (i) models were selected to predict metal toxicity to organisms from at least three trophic levels (plants, microorganisms, and invertebrates); (ii) only models predicting chronic ecotoxicity were used (iii) only models developed in soils were used. The first two criteria were based on the recommended practice to use chronic EC50 values and the representation of the three fundamental trophic levels, both of which are essential to ensure the relevance of the calculated ecotoxicity indicators to terrestrial ecosystems (European Commission 2003). The third criterion relates to the fact that most TBLMs have been developed in experimental model systems such as nutrient solutions or artificial porous media, and their applicability to soils has rarely been evaluated. Christiansen et al. (2011) demonstrated how a biotic ligand model developed in nutrient solution fails to predict ecotoxicity of Cu to lettuce (*L. sativa*) when exposed in soil. In total, six models for Cu and Ni respectively (Thakali et al. 2006a; Thakali et al. 2006b) were selected (Table S2.4).

Soils. A global set of soils containing 760 topsoil profiles was selected from the ISRIC-WISE3 (version 3.1) soil database (Batjes 2008; Batjes 2009). In total, the database holds data on measured soil properties for 10,253 soils collected in 149 countries (Batjes 2009). The majority of soils were excluded from the modeling due to missing information on pH, organic carbon, clay, sand, silt, exchangeable cations and soil electrical conductivity (6608 cases). We also excluded 860 soils with soil electrical conductivity and exchangeable cations assigned “zero” values, because in those cases it was not possible to differentiate whether these parameters equaled “zero”, or whether they were lacking values when accepting soil profile data to the database (Batjes 2008). Another 1,331 profiles were excluded because the method used to measure soil electrical conductivity was either not specified, or it was stated that this parameter was not measured even when a value was assigned to this parameter (in most cases 0.1 dS/m). Because the TBLMs are not applicable to calcareous soils, soils with carbonate content (CaCO3) above 0% (437 cases) and those with pH>6.5 that did not have a value assigned to CaCO3 (252 cases), were also excluded. To the remaining soils that did not report CaCO3, a value of 0% was assigned (57 cases). Finally, saline soils (ionic strength of

soil pore water above 0.5 mol/l) were not included because of uncertainties related to calculations of ion activity coefficients (5 cases). This resulted in 760 noncalcareous soils for which CTPs could be calculated. These soils span a wide range of properties with respect to the most influential parameters affecting metal bioavailability and ecotoxicity, i.e. pH, content of organic carbon, and ionic composition of soil pore water (Table S2.1). Note that the latter is not given in the database and was calculated following the Gaines-Thomas convention for modeling cation exchange, as presented in the SI. The location of those soils for which geographical references are available is shown in Fig. S2.1

Multiple Linear Regression Analysis. Based on the individual soil CTPs, we developed multiple linear regression (MLR) models to analyze the influence of soil properties controlling the CTP (eq 2.7). They can be used to calculate CTPs directly from soil parameters. The MLR models were also derived to analyze the influence of soil properties controlling each model constituent in eq 2.2 (see SI). Only those soil parameters which were included in models used to calculate K_d values, concentrations of reactive, total dissolved, and free metal ions (eq S2.13 - S2.19) were selected as independent variables. Some parameters were excluded due to strong (r>0.8; r=Pearson correlation coefficient) correlation with other parameters (see SI for details).

$$\log_{10}(CTP) = a + b \cdot pH + c \cdot \log_{10}(ORGC) + d \cdot \log_{10}\left[Mg^{2+}\right] + e \cdot \log_{10}(CLAY) \qquad \textbf{2. 7}$$

Normalized Sensitivity Coefficients. Sensitivity of CTPs to uncertain model parameters was analyzed by computing normalized sensitivity coefficients (eq 2.8), as done in Prommer et al. (2006):

$$X_{CTP,k} = \frac{\Delta CTP / CTP}{\Delta a_k / a_k} \qquad \textbf{2. 8}$$

where $X_{CTP,k}$ is the normalized sensitivity coefficient of CTP for perturbance of parameter k, a_k is the k^{th} parameter value, Δa_k is the perturbation of parameter a_k, CTP is the calculated comparative toxicity potential, and ΔCTP is the change of the comparative toxicity potential that resulted from the perturbation of parameter a_k. Note, that in Prommer et al. their analysis was done using constant value of the Δa_k (10%). Here the Δa_k vary between the parameters, and is chosen based on the realistic ranges of uncertain model parameters.

Case Study. Application of comparative toxicity potential in regionalized impact assessment is demonstrated on a case study for emission of Cu from the Compostilla II coal-fired power plant, located in Spain.

2.3. Results and discussion

Below, we present results for CTP and each model constituent in eq 2.2 for a unit emission of Cu and Ni to air. Geographic variability of CTPs accompanied by sensitivity analysis, consideration of method limitations, and a presentation of implications for LCIA, are then discussed.

2.3.1. K_d values

Median (95% geographic variability intervals) values of K_d are 9.1×10^2 (2×10^2 – 2.5×10^3) and 1.8×10^3 (6.2×10^2 – 4.1×10^3) l/kg for Cu and Ni, respectively (Fig. 2.2a). They are within ranges of measured values for different soils (Degryse et al. 2009). If more detailed data on soil characteristics, such as type and properties of organic matter and soil minerals become available, equilibrium multisurface models may be preferred over empirical regressions to obtain more precise values of partitioning coefficients (Dijkstra et al. 2004; Dijkstra et al. 2009).

2.3.2. Fate factors

Median (95% geographic variability intervals) values of FFs are 3.9×10^4 (1.4×10^4 – 1.9×10^4) and 7.1×10^4 (2.7×10^4 – 1.3×10^5) days for Cu and Ni, respectively (Fig. 2.2b). Organic carbon and pH are the major soil properties controlling K_d values and consequently FFs of Cu and Ni, respectively (Table S2.8). Fate factor increases with increase in the partitioning coefficient, which is explained by the latter's strong influence on processes included in the fate model, i.e. leaching to deeper soil layers and runoff from soil (Fig. S2.6). These processes are slow for metals due to their strong binding to soil constituents, resulting in residence times of hundreds of years for a soil layer of 0.1 m. Soil erosion becomes however an important removal process in those soils in which K_d values are very high. As a consequence, FFs level off at high K_d values. USEtox predicts that ca. 1000 years is required for all soil to become eroded to surface water; soil erosion thus determines the maximum residence time of a metal in soil. Residence times in range of hundreds of years indicate that some impacts will be excluded if finite time horizons are chosen in modeling comparative toxicity potentials (Huijbregts et al. 2001).

2.3.3. Accessibility factors

Median (95% geographic variability intervals) values of ACFs equal 0.42 (0.35 – 0.65) and 0.06 (0.022 – 0.13) $kg_{reactive}/kg_{total}$ for Cu and Ni, respectively (Fig. 2.2c). In none of the 760 soils is the reactive fraction equal to 1, as is assumed in current LCIA practice (Pizzol et al. 2011) This is an important aspect to consider because even if metal is initially reactive, the reactive fraction in soil can decrease significantly at time scales of months (Buekers et al. 2008b), reducing the magnitude of CTPs. Here, we assume that the reactive metal is in equilibrium with total metal. This assumption can be justified because the regression models used to calculate reactive metal have been derived from both uncontaminated and contaminated, aged soils. The calculated median value of the reactive fraction of Cu is close to the median value measured in soils from 19 paddy fields of Taiwan (0.56) (Romkens et al. 2009) but is higher than median value measured in 136 soils from Portugal (0.2) (Rodrigues et al. 2010b). By contrast, median reactive fraction for Ni (calculated using the regression developed for the Portuguese soils) is lower than the median value measured in the Taiwanese soils (0.23). The difference can be attributed to the fact that both Dutch and Taiwanese soils have been formed from unconsolidated river sediments of different properties than soils formed from parent material, such as the Portuguese ones. As noted by Römkens et al. (2004) the fraction of reactive metal will be lower in soils derived from parent material, because a larger proportion of metal is included in non-reactive minerals. The

reactive fraction of Cu and Ni predicted by the kinetic model of Crout et al. (2006) using kinetic parameters from Buekers et al. (2008b) for pH 5.7 (median for soils) and infinite time equal to 0.6 and 0.65, respectively. These values are higher than median values calculated here, which may be clarified by the fact that the model of Buekers et al. does not capture those processes which occur after ca. 800 days in soil, such as precipitation of salts and formation of minerals (Amacher 1991). If more information on the type of reactive surfaces and kinetics of reactions becomes available, assemblage models constructed using multisurface models can be employed for modeling both speciation in soil pore water and time-dependent changes in the solid-phase metal reactivity in soils (Buekers et al. 2008b).

Our study corroborates earlier study recommending the use of calibrated bioavailability models to correct for metal leaching and aging (Smolders et al. 2009) by introducing a factor which is based on a mechanistic understanding of processes affecting metal availability in soils. Further work should be devoted to considerations of changes in metal reactivity with time as affected by emitted forms of metal and soil properties. This aspect is particularly relevant if finite time horizons are considered in modeling comparative toxicity potentials for metals.

The ACF is not just relevant for metals in soil. The availability of some organic contaminants can also be reduced in soil by sorption to organic matter and slow diffusion into micropores (Alexander 2000). Indeed, the truly dissolved concentration and bioaccumulation of some hydrophobic organic compounds are better predicted if sorption to carbonaceous materials such as black carbon, coal, and kerogen (collectively called “carbonaceous geosorbents”, GC) constituting approximately 10% of total organic carbon is taken into account (Cornelissen et al. 2005). As for metals fixed in soil, the majority of GC-bound hydrophobic organics is resistant to release. The ACF can be applied to capture the differences in availability in such cases. Then, the BF (for organics known as the exposure factor, XF) can be used to translate between the compound available for partitioning and the truly dissolved fraction, as is practiced today (Henderson et al. 2011). If a compound does not bind strongly to the GC, the ACF=1, and the BF is a sufficient descriptor of the exposure through soil pore water.

2.3.4. Bioavailability factors

Median (95% geographic variability intervals) values of BFs equal 2.3×10^{-6} (1.7×10^{-7} – 4.8×10^{-5}) and 6.8×10^{-4} (1.6×10^{-4} – 3.3×10^{-3}) $kg_{free}/kg_{reactive}$ for Cu and Ni, respectively (Fig. 2.2d). To test the accuracy of these predictions, we calculated the concentrations of free metal ions expressed as a fraction of total dissolved metal using regression models employed to calculate concentration of free ion and total dissolved metal, and compared them with the free ion fraction of total dissolved metal measured by others. The free Cu^{2+} fraction of total dissolved Cu ranges 4.6 orders of magnitude (Fig. S2.3) and decreases with soil pH (data not shown). This is confirmed by measurements in soil solutions from various soils (Degryse et al. 2009; Groenenberg et al. 2010) The lowest fraction of free Cu^{2+} measured by Groenenberg et al. (2010) (3×10^{-7}) is about 2 orders of magnitude lower than the lowest value calculated here (5.4×10^{-5}), while the lowest value calculated here for Ni^{2+} (1.6×10^{-1}) does not reach the lowest value measured by Groenenberg et al. (2010) (2×10^{-2}). This is because only five soils with pH>7 and only two soils with organic carbon content above 20%, in which bioavailability of Cu and Ni is expected to be low, were included in our data set.

Here, in one soil the calculated free ion fraction of total dissolved Cu exceeds the maximum possible value of 1 (by 129%), while the fraction of free Ni^{2+} exceeds the maximum possible value of 1 in five soils (by<12%). We consider these predictions as sufficiently accurate to incorporate the BFs in calculations of CTPs.

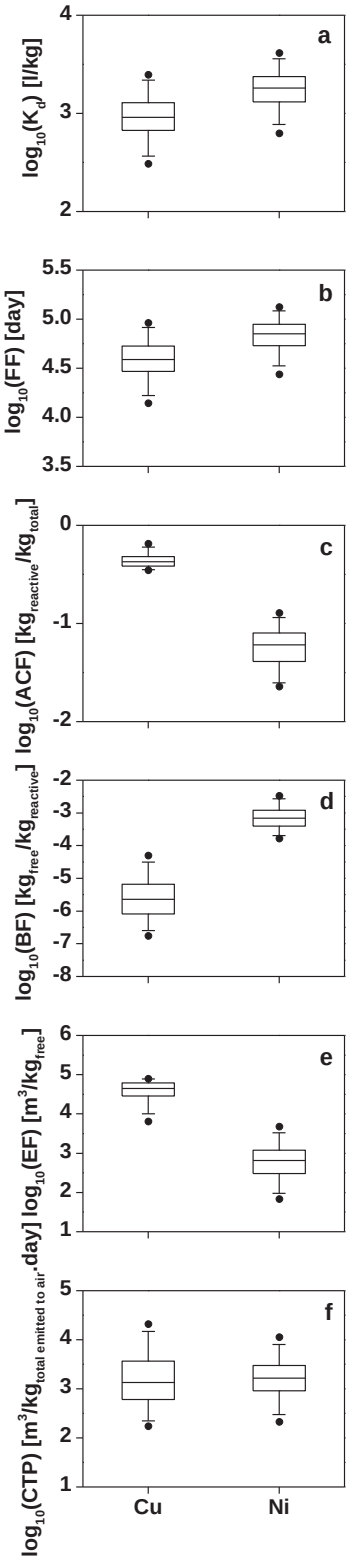

Figure 2.2: Log10-transformed K_d values (a), FFs (b), ACFs (c), BFs (d), EFs (e) and CTPs (f) for Cu and Ni calculated for 760 soils. Boxes with bars indicate the 5th, 25th, 50th, 75th and 95th percentiles; black dots indicate 2.5th and 97.5th percentiles of the calculated values.

2.3.5. Effect factors

Median (95% geographic variability intervals) values of EFs are 4.4×10^4 (6.4×10^3 – 7.8×10^4) and 6.6×10^2 (6.7×10^1 – 4.7×10^3) m^3/kg_{free} for Cu and Ni, respectively (Fig. 2.2e). EFs of Ni span a wider range than those for Cu, because in all cases, except of nitrifying microorganisms, only protons compete with Cu^{2+} for binding to biotic ligands, whereas the toxicity of Ni^{2+} is also alleviated by Mg^{2+}, and sometimes by Ca^{2+}. As a consequence, EFs of Cu strongly correlate with soil pH (Table S2.11). In contrast, the EF of Ni primarily correlates with the concentration of Mg^{2+} dissolved in soil pore water. Comparison between our species sensitivity distributions (SSD) constructed from the TBLM-derived EC50 values, and SSDs derived from species effect data from ecotoxicity experiments shows that even though non-alkaline soils dominate our dataset, and there are differences in species included in the comparison, in many cases our SSDs fall within the 95% confidence interval for the experimental SSD (see SI). We consider these predictions as reasonable and sufficiently accurate to employ our EFs for calculating CTPs.

Haye et al. (2007) showed that EF based on total metal for Cu was 3.2 times higher than that for Ni. Here, the ecotoxicity ranking of Cu and Ni is more similar to what was observed for freshwater organisms by Gandhi et al. (2010) who showed that Cu is about 80 times more toxic than Ni when the EF was based on the "truly" dissolved metal. Toxicity of metals can be related to the strength of their binding to biomass, such as plasma membranes, cell walls, and proteins, and has been shown to correlate with metal softness (Kinraide 2009; Kinraide and Yermiyahu 2007). A property of soft metals is that they have strong binding affinity to soft ligands, such as biomass. If corrected for differences in ionic composition of the environment, only molecular properties of metal ions and the type of biomass will drive the metal uptake and toxicity, which may explain the similarities reported here between toxicity ranking of metal ions for terrestrial and aquatic organisms. Veltman et al. (2008, 2010) have already demonstrated that the absorption rate constant and the conditional affinity constant of various aquatic species were positively correlated with the metal covalent index.

2.3.6. Comparative toxicity potentials

Comparative Toxicity Potentials range 3.5 and 3 orders of magnitude for Cu and Ni, respectively, with median values (95% geographic variability intervals) equal to 1.7×10^2 (1.7×10^1 – 2×10^4) and 1.7×10^3 (2.1×10^2– 1.1×10^4) $m^3/kg_{total\ emitted\ to\ air}\cdot day$ (Fig. 2.2f). They are distributed lognormally (see SI).

Multiple linear regressions show that the CTP of Cu is determined mainly by soil organic carbon (Table 2.1), influencing metal fate. The predictive power of the equation for calculating CTPs of Cu is improved by including the effects of soil pH, influencing bioavailability (Table S2.10). In contrast to Cu, the compensating effects of soil organic carbon on both accessibility and bioavailability result in soil organic carbon being a rather poor descriptor of CTP for Ni. The CTP of Ni is mainly controlled by pore water concentration of Mg^{2+}, through its influence on ecotoxicity. This poses a challenge for global scale modeling of ecotoxic impacts from those metals for which base cations alleviate toxicity to soil organisms, because pore water concentrations of Mg^{2+} and other base cations are neither routinely measured, nor are they specific to soil types (Mertens et al. 2008). As

demonstrated here, however, they can be calculated from electrical conductivity of soil pore water, which can be measured or estimated from soil properties (Sudduth et al. 2005).

Table 2.1: Linear regression coefficients, adjusted R^2 values (R^2_{adj}) and standard error of estimate (se) of regression equations for log_{10}(CTP) of Cu and Ni (eq 2.7). Values in brackets indicate standard error.

Metal	a intercept	B pH	C log_{10}(ORGC)	d $log_{10}([Mg^{2+}])$	e log_{10}(CLAY)	R^2_{adj}	se
Cu	3.327 (0.010)	x	-1.003 (0.019)	x	x	0.784	0.27
	5.653 (0.038)	-0.408 (0.007)	-1.150 (0.008)	x	x	0.965	0.11
	6.006 (0.039)	-0.426 (0.006)	-1.166 (0.007)	0.072 (0.005)	x	0.973	0.093
	6.074 (0.043)	-0.427 (0.006)	-1.156 (0.007)	0.078 (0.005)	-0.035 (0.009)	0.974	0.092
Ni	1.540 (0.037)	x	x	-0.482 (0.010)	x	0.736	0.22
	1.613 (0.033)	x	-0.209 (0.014)	-0.470 (0.009)	x	0.795	0.19
	0.962 (0.079)	0.104 (0.012)	-0.169 (0.014)	-0.486 (0.009)	x	0.815	0.19
	0.701 (0.083)	0.107 (0.011)	-0.209 (0.015)	-0.510 (0.009)	0.134 (0.017)	0.828	0.18

CTP ($m^3/kg_{total\ emitted\ to\ air}$·day) is the comparative toxicity potential of total metal emitted to air; ORGC (%) is the organic carbon content; $[Mg^{2+}]$ (mol/l) is magnesium concentration in soil pore water; and CLAY (%) is the clay content; x indicates that the variable did not pass stepping method criteria ($p<0.05$ for entry, and $p>0.1$ for removal); all coefficients are significant at the probability level $p<0.001$.

2.3.7. Sensitivity analysis

The sensitivity of CTPs to many model parameters is metal- and soil-specific (Fig. 2.3). The parameters affecting ionic composition of soil pore water (such as the Gaines-Thomas selectivity coefficients for cation exchange, K^{GT}) appear important for Ni due to competitive binding of Mg^{2+} to biotic ligands. However, if the full set of three K^{GT} values is in lower and higher range of values typical for clay soils (Table S2.13), median CTPs of Ni change by 4 and 5%, respectively, compared with the base scenario (data not shown). The influence of soil moisture on CTPs of Ni is larger compared to Cu because concentration of dissolved Mg^{2+} is also proportional to the water content (eq S2.1), whereas the precipitation rate can influence CTP of both Cu and Ni due to its control of leaching and runoff. The geographic variability in the CTP of Cu is expected to be higher if data on location-specific content of amorphous Fe and Al (hydr)oxides were available.

The CTPs for both metals are more sensitive to low background metal content, compared with high background levels. However, using a European subset of 24 soils (see SI for details) we show that median CTPs change by 10% for both metals if location-specific background metal is used instead of constant values. For the same subset, an increase in reactive metal to the levels expected in soils from paddy fields of Taiwan (56 and 23% of total, location-specific Cu and Ni, respectively) (Romkens et al. 2009) is to some extent compensated by shorter residence time of a metal. However, a 10% change in K_d or DOC will result in nearly 10% change in CTPs, due to their influence on metal fate. Overall, it can be

concluded that inclusion of location-specific model parameters will improve accuracy of soil-specific CTPs and will probably increase geographic variability in the CTPs, but is not expected to considerably (>10%) influence median values, at least at a global scale. If a regionalized assessment at country levels is to be performed, attention must be paid to the dependency of CTPs on soil moisture and precipitation rates.

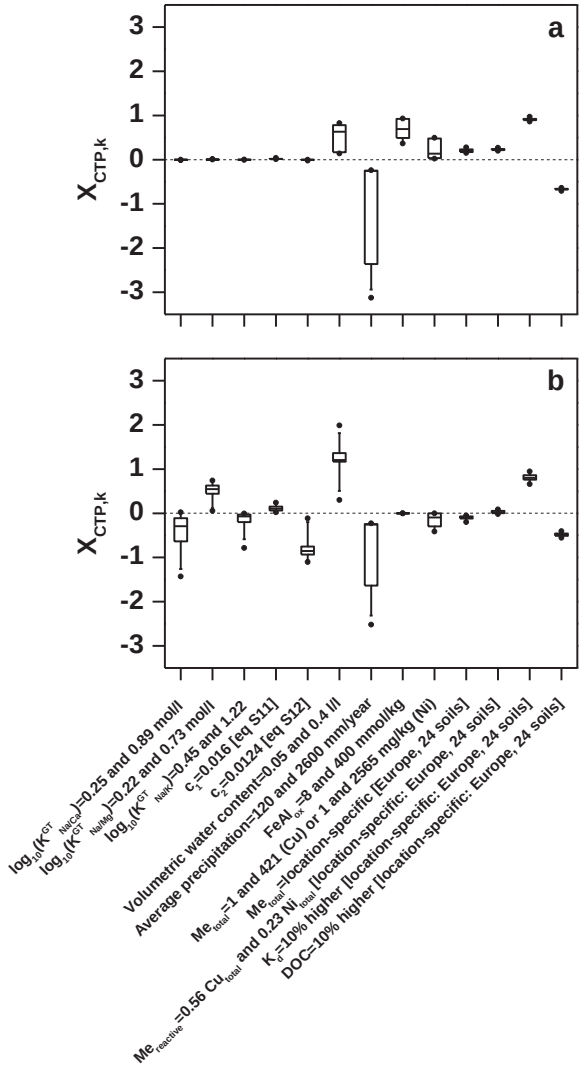

Figure 2.3: **Normalized sensitivity coefficients ($X_{CTP,k}$) computed using eq 2.8 for several uncertain model parameters with respect to the calculated CTPs of Cu (a) and Ni (b) in all 760 soils, or in the European subset of 24 soils. Boxes with bars indicate the 5th, 25th, 50th, 75th and 95th percentiles; black dots indicate 2.5th and 97.5th percentiles of the calculated values. Details on selection of K^{GT} values and location-specific background metal content are given in the SI.**

2.3.8. Method limitations

We propose a new method for calculating CTPs of Cu and Ni in soil, but its extension to other metals or terrestrial systems can be limited. Multisurface speciation models can be applied to metals lacking empirical regressions, and terrestrial free ion activity models (FIAM), or freshwater ecotoxicity EFs can be adapted to cover metals lacking TBLMs. Alternatively, quantitative ion character-activity relationships (QICAR) can be developed, as done for freshwater organisms (Wu et al. 2012). The coverage of saline and calcareous soils will be challenged by the need for validating existing speciation and ecotoxicity models.

Our method does not capture the aspects of metal essentiality, active plant uptake, or microbial adaptation, but it is not obvious how these limitations affect toxicity potentials. Whereas toxic pressure has been demonstrated to relate to biodiversity (Posthuma and De Zwart 2006; Posthuma and de Zwart 2012) positive effects on a species level might not always translate into positive effects on an ecosystem level (Hurd et al. 1971).

It should be also noted that research is needed to evaluate whether the framework can be applied to elements forming anions or organic compounds, whereas the reactivity of massive metal products and metallic nanoparticles is expected to be more dependent on the particle size and/or shape than on the initial chemical form (Ispas et al. 2009; Skeaff et al. 2000; Tourinho et al. 2012).

Finally, we stress that LCIA-suited models are based on an average situation that is appropriate to rank substances according to their toxicity potential for application in LCA. However, environmental risk assessment (ERA) or environmental impact assessment (EIA) usually operate in well-defined settings, and practitioners thus should consider employing site specific fate and exposure models to (ideally) best represent conditions at a site. For example, if our method is used to calculate CTP for a metal emitted directly to an agricultural soil, metal removal via plant harvest can play a role in determining metal fate (Ali et al. 2002).

2.3.9. Application of comparative toxicity potentials in regionalized impact assessment

For applications in regionalized assessments, it is important to evaluate the variability of CTPs as controlled by spatially variable soil properties. The scientifically relevant spatial scales can be different for different metals, due to differences in spatial variability of soil parameters controlling CTPs, as demonstrated here for Cu and Ni. In situations where emission location is unknown, as is often the case in LCIA, it is important to carefully select generic values of CTPs. Weighting of CTPs can be done based on the relative occurrence of soils, with the assumption that metal emissions can be approximated by an average situation. This assumption is considered valid in case of emission with large deposition areas, such a airborne emission from power plants, smelters, or incinerators (Pettersen and Hertwich 2008). Weighting should also be considered also in regionalized assessments, to take into account the fact that deposition load is affected by the distance from the source. Here, we show how to apply calculated CTPs in case of airborne emission of metal from the Compostilla II coal-fired power plant, located in Spain.

We used eq 2.7 combined with regression coefficients from Table 2.1 to calculate CTP of Cu in each 1-km grid cell representing soils affected by emission from the power plant. In case of airborne emissions the deposition (mass per area) increases with increasing distance

from the source until it reaches maximum (typically within a few km range, x' in Fig. 2.4) and then decreases with distance (de Caritat et al. 1997). In practice, airborne metal can travel across thousand of kilometers (Ewing et al. 2010); however, the majority of the emission is deposited within a few hundred km range from the source (de Caritat et al. 1997). Here, the emission is assumed to deposit on the area located within 200 km range from the source and to follow the deposition function published by (de Caritat et al. 1997) for Cu emitted from a smelter. The deposition function is used to calculate a fraction of total emission deposited in each grid cell as affected by the distance from the source. To weight CTPs the total deposition area is split into one circle-shaped and two torus-shaped subareas. In each subarea, CTPs are first weighted based on the occurrence of soils. Then, second weighting is done using weighting factors representing deposition load in each subarea. In this way, case-specific CTP of a metal emitted to air are be derived (Table 2.2). Here, the CTP of Cu mainly depends on the relative occurrence of soils located within 100 km distance from the source.

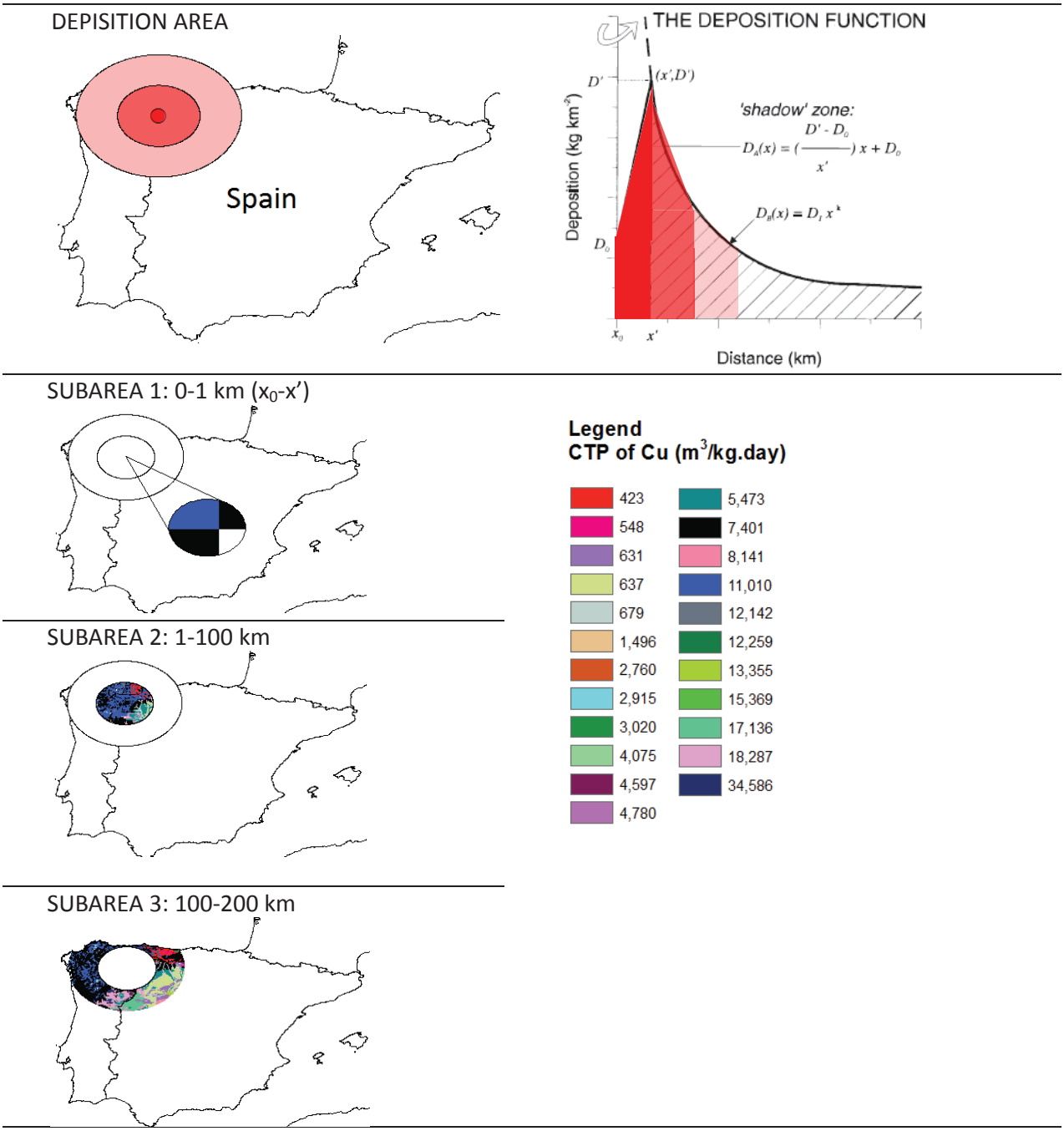

Figure 2.4: Compostilla II coal-fired power plant located in the center of the red circle (upper left) is a source of airborne Cu. CTPs of Cu were calculated using eq 2.7 for each of the 1-km grid cells representing soils from the HWSD database (FAO/IIASA/ISRIC/ISS-CAS/JRC 2012). The deposition area can be divided into subareas of circle (inner part) and torus shape (outer parts). The deposition of metal in each grid cell with subareas is calculated from the deposition function published in de Caritat et al. (1997). Insert in the upper right corner is Fig. 3 from de Caritat et al. (1997).

Table 2.2: Soil- and area-weighted of CTPs for Cu emission from coal-fired power plant.

Subarea	Subarea weight	Soil-weighted CTP in each subarea (m^3/kg·day)	Subarea-weighted CTP (m^3/kg·day)	Soil- and subarea-weighted CTP (m^3/kg·day)
0-1 km (x_0-x')	0.13	7370	958	8115
1-100 km	0.83	8342	6924	
100-200 km	0.04	5833	233	

2.3.10. Implications of metal aging in soils

We propose comparative toxicity potentials (CTP) of a metal in soil being a product of metal fate, accessibility, bioavailability and terrestrial toxicity. The ACF determines the maximum concentration of the bioavailable metal pool (usually, the free ions) in soil pore water through its control of the total dissolved metal pool; a reduction in ACF lowers the total dissolved metal pools and thereby the concentration of free ions, reducing the magnitude of the CTP.

Several aspects should be considered in when deriving ACF for metals in soil. First, high residence time of a metal in soil (in range of hundreds of years) means that reactions of a metal with soil constituent, collectively referred to as aging, can change the magnitude of the time-integrated ACF in soils. For example, metals applied in readily soluble forms (such as soluble salts) are initially reactive, but their reactivity can be reduced within days to months due to interactions of metal ions with soil constituents, such as organic matter or Fe and Me (hydr)oxides (Ma et al. 2006). By contrast, accessibility of metals emitted in solid forms, such as oxides or minerals, is expected to be initially lower as compared with soluble salts because a part of total metal pool is not reactive. However, their reactivity can potentially increase due to dissolution of the solid-phase metal and formation of new, reactive phases (Voegelin et al. 2011). Third, aging models developed for soluble salts may not capture long-term aging mechanism in soil, overestimating the ACF, whereas equilibrium based empirical regression models developed for metal or soils of unknown contamination history may not be directly applicable to metal applied in solid forms. Long-term aging processes, such as formation minerals, can further contribute to the reduction in reactivity or initially reactive metal at time scales of years to decades (Amacher 1991). Forth, little is known how metal accessibility depends on contamination type and kinetics of aging. Empirical regression models have recently been developed for 20 elements using soils contaminated with anthropogenic and/or geogenic metal, but they may not be directly applicable to all contamination types relevant in an impact assessment context, such particle-bound metal emitted to air or metal applied to soil as a biosolid. On the other hand, kinetic aging models developed using soils spiked with soluble salts are expected to overestimate the metal reactivity because they do not capture those aging mechanism in soil that occur at time scales of decades, such as formation of minerals or precipitation of salts.

The aim of this part was to develop predictive models for calculating concentration of reactive Cd, Co, Cu, Ni, Pb and Zn in soils for contamination types constituting major anthropogenic source of metals in soils, such as particle-bound metal in fly ashes, metal occluded within biosolids and other organic matrices, or metal related to mining activities and that associated with industrial waste. The six cationic metals were chosen because of the availability of data on metal reactivity in soils as measured using radioactive or stable isotope dilution techniques. Isotope-based methods are expected to provide more accurate estimates of

concentration of reactive metal in soils, as compared with single or sequential extraction procedures (SEP) (Ahnstrom and Parker 2001; Degryse et al. 2011). In most cases, the information about contamination age had to be assumed and is uncertain, whereas availability of measured data for some potentially important soil properties (such as content of Fe and Mn (hydr)oxides) is low. Insights into aging mechanisms were inferred by comparison with metal reactivity measured in soils spiked with soluble salts and those contaminated with geogenic metal, and by comparison with predictions of empirical regression models and kinetic aging models developed by others.

Data collection. Data were included if they met the following criteria: (i) concentration of reactive metal or reactive fraction of total metal were measured in soils; (ii) contamination type was reported; and (iii) measurement was done using either stable or radioactive isotope exchange dilution methods. The latter criterion was applied to minimize uncertainties associated with method used to measure concentration of reactive metal in soil. Others readily showed the lack of correspondence between metal fractions extracted using sequential extraction procedures (SEP) and the size of reactive metal pool measured using isotope-based methods.(Ahnstrom and Parker 2001)

Data were collected through searching the ISI Web of Knowledge, version 5.7 (Thomson Reuters, New York, NY) using a combination of keywords: (i) isotop*; and either (ii) exchang*, or dilute*; and either (iii) labil*, or soil*; and either (iv) Cd, Co, Cu, Ni, Pb, Zn, cadm*, cobalt*, copp*, nick*, lead, or zinc*. A complementary search was conducted in ISI to retrieve papers which cited papers retrieved in the previous step, and those which were cited in the collected papers but were not found through the search in ISI. The two latter steps were iterated until new data were found. Thereby, we retrieved a total 1885 measured data on concentration of reactive metal or reactive fraction of total metal reported in a total of 65 papers (Fig. S2.9). They span a relatively wide range of properties with respect to contamination type, except of Co for which only airborne contamination types were found. Data availability for the content of Fe, Mn or Al (amorphous, crystalline, or total) is low (<10 %) as compared with data availability for soil pH or organic carbon content.

Classification of contamination type. Data were classified into three major contamination types: (i) “readily soluble” for soils spiked with soluble salts and other readily soluble or dissolved metal forms, such as Cd present as a co-contaminant in phosphate fertilizer, Cu sulfate applied as a fungicide, or aqueous Zn dissolving from galvanized power lines; (ii) “solid” for soils contaminated with primarily solid-phase metal of anthropogenic origin; and (iii) “geogenic” for soils impacted by geogenic metal with no recognized history of anthropogenic metal input. Note, that reactivity of geogenic background contributes to the reactivity of anthropogenic metal because background reactivity of geogenic metal prior anthropogenic input was not measured. These groups represent major contamination types in impacted soils and are expected to show distinct profiles with respect to metal reactivity.

The “solid” type was further classified into four subtypes: (i) “airborne”, including emissions from smelters , metal refineries, factories, combustion of petrol, and unspecified atmospheric deposition; (ii) “organic”, including direct application of biosolids, manure, compost, or wastewater irrigation; (iii) “mining and industrial waste”, including mine spoils, mining-affected sediment, material containing metal ores, alluvial deposition, unspecified industrial waste, and technosols; and (iv) “other”, including Zn oxides in tire debris, isolated ZnO, and mixed, unspecified sources.

Determination of contamination age. For readily soluble metal, the majority of data were retrieved from sources where kinetics of metal aging was studied in detail. No such studies are however available for solid metal forms. In addition, information about contamination age for most solid metal is scarce. To get more insight into the influence of contamination age on metal reactivity, we assumed contamination age equal to half of the interval between start and termination of the emission, and equal to time from the emission peak to the publication year. If emission above or below certain time was reported, contamination age was assumed equal to double or half of that time, respectively. If only a century of emission start was reported, time from the middle of that century to publication year was assumed. If the emission source could be unambiguously identified, information on contamination age was retrieved from sources reporting emission data.

Harmonization of soil properties. Data on soils properties were included if reported. Empirical regression developed by Azevedo et al. (2013) using a set of ca. 10,000 soils was used to convert soil pH between measurements in H_2O and $CaCl_2$ extracts. A ratio of soil organic matter (OM) to soil organic carbon (ORGC) equal to 1.78 was assumed. Total soil organic carbon (TOC) was assumed to contain 75% of ORGC. Values reported as below or above a certain value were assumed equal half or double of that value, respectively. If not measured, the concentration of total metal in soil was assumed equal to nominal value.

Data analysis. For solid metal, the influence of aging on metal reactivity of was analysed by means of multiple linear regression analysis (MLR) with time being an independent variable (eq 2.9). Approaches similar to determining the influence of time on metal reactivity in soils were presented previously (Wendling et al. 2009). To isolate the influence of aging from the influence of soil properties, the analysis was done as follows: (i) only time and concentration of total metal as independent variables; (ii) time, concentration of total metal, and one soil property i as independent variables (this step was repeated for each soil property i; and (iii) time, concentration of total metal, and several soil properties as independent variables (this step was repeated if the number of soil properties varied). The analysis was done for each contamination type per metal, and for combined contamination types per metal. Some soil parameters were excluded due to strong ($r>0.8$; r=Pearson correlation coefficient) correlation with other parameters. For readily soluble metal, the influence of aging was studied in detail by others and is not analysed here. We refer to the SI for a review of published aging models.

Because the number of data for soil properties was higher as compared with data for which contamination age could be estimated, the same procedure was applied as for the analysis of the influence of aging, except that aging time was excluded from the regression. Again, the analysis was done for each contamination type per metal, and for combined contamination types per metal, and some soil parameters were excluded due to strong correlation with other parameters.

$$\log_{10}\left(C_{reactive}\right) = a + b \cdot \log_{10}\left(C_{total}\right) + c \cdot t \qquad \textbf{2. 9}$$

$$\log_{10}\left(C_{reactive}\right) = a + b \cdot \log_{10}\left(C_{total}\right) + c \cdot pH + \sum_i d_i \cdot \log_{10}(soil\ property_i) \qquad \textbf{2. 10}$$

where $C_{reactive}$ and C_{total} (mg/kg) are the concentration of reactive and total metal in soil, respectively; t (day) is the contamination age; pH is measured in H_2O; a, b, c, and d_i are the regression coefficients; and is the index for soil property i.

Influence of type of contamination. Figure 2.5 shows that median reactivity of readily soluble metal is higher as compared with that of either anthropogenic or geogenic metal. Median reactivity of anthropogenic metal is lower for Cd, Ni and Pb, and higher for Co, Cu and Zn, as compared with that of geogenic metal. For Cd, reactivity of both anthropogenic and geogenic is high, and span a range comparable to that of readily soluble Cd. The number of measured data for reactivity of geogenic Pb and Co is low (20), but low variability in reactivity of this metal suggest that geogenic Co is not reactive, and that readily soluble Pb is reactive.

Median and ranges in reactivity are comparable across contamination types. Reactivity of anthropogenic metal across all contamination types is usually between 0.05 and 0.6 and is within 95% variability interval for reactivity of geogenic metal. Median reactivity of Cd related to mining and industrial waste is lower as compared with that of airborne or organic Cd. ZnO (classified as other) can have high reactivity, comparable to that of readily soluble metal.

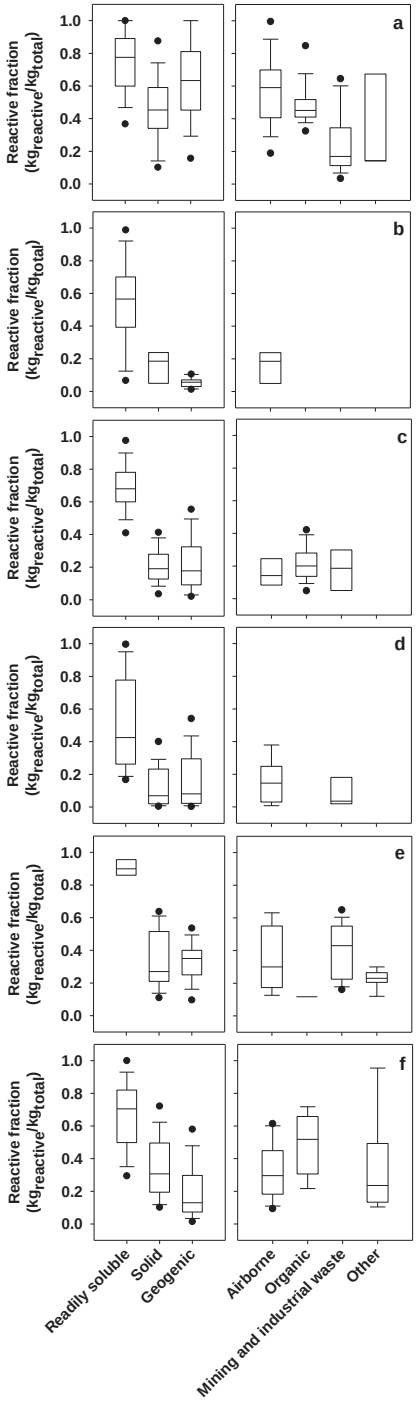

Figure 2.4: Reactive fraction (in $kg_{reactive}/kg_{total}$) of Cd (a), Co (b), Cu (c), Ni (d), Pb (e), and Zn (f) measured in soils contaminated with readily soluble, anthropogenic (solid), or geogenic metal forms (left panel), and in soils contaminated with anthropogenic contamination forms classified as airborne, organic, mining and industrial waste, and other (right panel). Boxes with bars indicate the 10th, 25th, 50th, 75th, and 90th percentiles; black dots indicate 5th and 95th percentiles of the measured values.

Influence of contamination age. Time was found to be a significant variable in regression models for Cd, Cu, Zn and Pb (Table 2.3). For the combined sets of anthropogenic contamination types, regression coefficients ranged from -0.0024 to 0.021 for Cd and Cu, respectively. Yet, the analysis was based on 12 and 14 data points, respectively. In addition, time was not found significant when the analysis was done for each contaminant type separately. For Zn, time appeared to be a significant variable in the regression for airborne metal, but regression coefficients for time change from 0.0026 to -0.01 as more soil properties are included in the regression, and become not significant when all available soil properties are included. Time appears to be significant variable for organic Zn (regression coefficient equal to 0.0034), but the regression is based on 9 data points. Analysis of 16 data points for airborne Pb suggest significant effect of time on reactivity of this contamination type (regression coefficient equal to -0.0074), whereas the significance of time disappears as soil parameters are included in the regression for organic Pb.

Table 2.3: Model, number of measured data (n), linear regression coefficients, adjusted R^2 values (R^2_{adj}), and standard error of estimate (se) of regression equations for $\log_{10}(C_{reactive})$ of geogenic, anthropogenic, and combined anthropogenic and geogenic forms of Cd, Co, Cu, Ni, Pb, and Zn (eq 2.9).

Metal	Solid contamination type	Model	n	a (intercept)	b $\log_{10}(C_{total})$	c (time)	d pH(H_2O)	e $\log_{10}$(ORGC)	f $\log_{10}$(CLAY)	g $\log_{10}$(CEC)	R^2_{adj}	se
Cd	solid (airborne, organic, mining and industrial waste)	*s1*	46	-0.2	0.86	x	NA	NA	NA	NA	0.83	0.29
		s2	46	-0.2	0.86	x	x	NA	NA	NA	0.83	0.29
		s3	42	-0.19	0.84	x	NA	x	NA	NA	0.82	0.3
		s4	36	-0.39	0.66	x	NA	NA	NA	0.42	0.7	0.29
		s5	12	-0.17	0.67	x	NA	NA	x	NA	0.41	0.47
		s6	35	-0.4	0.65	x	x	x	NA	0.44	0.71	0.29
		s7	12	-1.3	x	0.021	x	x	x	0.75	0.8	0.27
	airborne	*s8 (A)*	36	-0.16	0.83	x	NA	NA	NA	NA	0.8	0.3
		s9	36	-0.16	0.83	x	x	NA	NA	NA	0.8	0.3
		s10	35	-0.16	0.83	x	NA	x	NA	NA	0.8	0.31
		s11	29	-0.69	0.69	x	NA	NA	NA	0.73	0.68	0.25
		s12	28	0.81	0.66	x	-0.092	x	x	0.81	0.74	0.23
	organic	*s13*	4	-0.42	1.07	x	NA	NA	NA	NA	0.997	0.042
		s14	4	-0.42	1.07	x	x	NA	NA	NA	0.997	0.042
	mining and industrial waste	*s15*	5	-0.64	1.07	x	NA	NA	NA	NA	0.87	0.29
		s16	5	-0.64	1.07	x	x	NA	NA	NA	0.87	0.29
		s17	5	-0.64	1.07	x	NA	x	NA	NA	0.87	0.29
		s18	5	-0.64	1.07	x	NA	NA	NA	x	0.87	0.29
		s19 (B)	5	-0.64	1.07	x	x	x	NA	NA	0.87	0.29
Cu	solid (airborne and organic)	*s20*	14	0.87	1.34	-0.0041	NA	NA	NA	NA	0.97	0.1
		s21	14	0.87	1.34	-0.0041	x	NA	NA	NA	0.97	0.1
		s22	14	0.87	1.34	-0.0041	NA	x	NA	NA	0.97	0.1
		s23	10	-0.48	1.01	x	NA	NA	x	NA	0.94	0.095
	airborne	*s24*	5	-1.55	1.35	x	NA	NA	NA	NA	0.99	0.096
		s25	5	-4.01	1.67	x	0.33	x	NA	x	0.999	0.033
	organic	*s26*	9	-0.55	1.04	x	NA	NA	NA	NA	0.85	0.1
		s27 (C)	9	-0.55	1.04	x	x	NA	NA	NA	0.85	0.1
Ni	solid (airborne)	*s28*	9	-1.57	1.23	x	NA	NA	NA	NA	0.9	0.44
		s29	9	-1.57	1.23	x	x	x	NA	NA	0.9	0.44
Pb	solid (airborne, mining and waste)	*s30*	37	-0.28	0.91	x	NA	NA	NA	NA	0.84	0.24
		s31	38	0.039	1.02	x	-0.09	x	NA	NA	0.88	0.22
	airborne	*s32*	16	-0.46	1.09	-0.0064	NA	NA	NA	NA	0.84	0.18
		s33	16	0.29	1.15	-0.0072	-0.13	x	NA	NA	0.89	0.15
	mining and waste	*s34*	21	-0.81	0.97	0.003	NA	NA	NA	NA	0.94	0.17
		s35	21	0.076	1.03	x	-0.22	x	NA	NA	0.96	0.13
Zn	solid (airborne, organic)	*s36*	49	-0.43	1	-0.0024	NA	NA	NA	NA	0.91	0.27

		s37	49	0.011	1.04	-0.0028	-0.086	NA	NA	NA	0.91	0.26
		s38	43	-0.54	0.99	x	NA	x	NA	NA	0.91	0.27
		s39	43	-0.065	1.03	x	-0.098	x	NA	NA	0.91	0.26
		s40	36	0.29	0.97	x	-0.12	x	NA	x	0.87	0.26
		s40	32	0.48	0.97	x	-0.15	x	x	x	0.91	0.22
	airborne	*s42*	30	-0.1	1.05	0.0026	NA	NA	NA	NA	0.95	0.23
		s43	30	0.26	1.08	-0.0084	-0.082	x	NA	NA	0.96	0.22
		s44	23	0.99	0.98	-0.01	-0.13	x	NA	x	0.95	0.18
		s45	19	0.74	0.88	x	-0.16	x	x	0.15	0.98	0.12
	Zn organic	*s46*	9	-0.12	0.95	0.0034	NA	NA	NA	NA	0.94	0.11
		s47	9	-0.12	0.95	0.0034	x	NA	NA	NA	0.94	0.11

$C_{reactive}$ (mg/kg) is the concentration of reactive metal in soil; C_{total} (mg/kg) is the concentration of total metal in soil; time (year) is the estimated contamination age (see the Methods section in the main part for details on the estimation of contamination age); pH is measured in H20 (see the Methods section in the main part for details on harmonization of soil pH); ORGC (%) is the organic carbon content; CLAY (%) is the clay content; and CEC ($mmol_c/kg$) is the cation exchange capacity. Other soil parameters were not considered because they were not available, or correlated strongly (r>0.8) with other soil parameters. All coefficients are significant at the probability level $p < 0.001$.

(A) $\log_{10}$(CLAY) was excluded because it correlates strongly with time

(B) $\log_{10}$(CEC) was excluded because it correlates strongly with $\log_{10}$(ORGC)

(C) $\log_{10}$(CLAY) was exclued because correlates strongly with pH; $\log_{10}$(ORGC) was excluded because it correlates with $\log_{10}(C_{total})$

Influence of soil properties. For geogenic metal, results of multiple linear regressions show that concentration of reactive metal can mainly be explained by total metal content (Table 2.4). The predictive power of the equations is improved by inclusion of soil pH or organic carbon content, whereas the inclusion of Fe (hydr)oxides improves predictions for geogenic Ni and Zn. The explained variance (R^2_{adj}) is < 0.8 for geogenic Cd, Ni, and Pb, and is < 0.7 for geogenic Co, Cu and Zn.

Considerable part of the variation in concentration of solid metal in soil can be explained either by total metal alone, or by including the effects of soil pH. The explained variance for regressions for individual contamination types is higher as compared with that for geogenic metal, except airborne Pb. Yet, for airborne Co, organic Zn, and for all individual contaminations types of Cu and Ni, the number of measured data is low (< 11). Except of airborne Cu and airborne Ni, the models predict higher reactivity for anthropogenic metal, as compared with that for geogenic metal. For metals associated with mining and industrial waste (Cd, Ni and Pb), lower reactivity is predicted at higher contamination level. Similar, albeit less strong effect of total metal content, is observed for airborne Cd and airborne Pb. For other metals and contamination types, metal reactivity either increases or does not change with an increase in total metal content.

For the combined set of all anthropogenic contamination types (per metal), the performance of multiple linear regressions for is worse (Cu, Ni) or similar (Cd, Pb, Zn) to those developed for individual contamination types (Table S2.14). The analysis for the combined sets of geogenic and all anthropogenic contamination types show that total metal and soil properties can explain > 0.85 variability in the concentration of reactive Cd, Co, Pb and Zn. For Cu and Ni, however, the fit of such regressions is relatively poor, with the explained variance < 0.6.

Table 2.4: Number of measured data (n), linear regression coefficients, adjusted R^2 values (R^2_{adj}), and standard error of estimate (se) of regression equations for $\log_{10}(C_{reactive})$ of solid forms of Cd, Co, Cu, Ni, Pb, and Zn (eq 2.10)

Metal	Solid contamination type	Model	n	a (intercept)	b $\log_{10}(C_{total})$	c $pH_{(H2O)}$	d $\log_{10}$(ORGC)	e $\log_{10}$(CLAY)	f $\log_{10}$(CEC)	g $\log_{10}(Fe_{ox})$	h $\log_{10}(Fe_d)$	i $\log_{10}(Al_{ox})$	j $\log_{10}(Mn_d)$	R^2_{adj}	se
Cd	geogenic	m1	79	-0.39	0.77	x	x [n=66]	x [n=40]	x [n=35]	x [n=21]	NA	NA	NA	0.74	0.36
		m2	79	0.35	0.88	-0.11	x [n=66]	x [n=40]	x [n=35]	x [n=21]	NA	NA	NA	0.76	0.34
	airborne	m3	40	-0.21	0.89	x	x [n=37]	NA	NA	NA	NA	NA	NA	0.83	0.31
		m4	29	-0.69	0.69	NA (A)	NA (A)	NA	0.73	NA	NA	NA	NA	0.68	0.25
	organic	m5	32	-0.35	1.02	x	x [n=19]	x [n=15]	x [n=17]	x [n=13]	x [n=13]	x [n=13]	x [n=13]	0.98	0.11
	mining and industrial waste	m6	23	-0.14	0.68	x	NA	NA	NA	NA	NA	NA	NA	0.83	0.24
Co	geogenic	m7	20	-1.55	1.24	x	x	x	NA	NA	NA	NA	NA	0.45	0.28
		m8	20	0.73	1.06	-0.34	x	x	NA	NA	NA	NA	NA	0.68	0.21
	airborne	m9	8	-1.98	1.56	x	x	x	0.66	NA	NA	NA	NA	0.94	0.21
Cu	geogenic	m10	103	-1.06	1.15	x	x	NA	NA	NA	NA	NA	NA	0.40	0.51
		m11	97	-0.99	1.07	x	0.20	x [70]	NA	NA	x [25]	NA	NA	0.48	0.46
	airborne	m12	5	-1.55	1.35	NA (B)	NA (B)	NA	x	NA	NA	NA	NA	0.99	0.096
	organic	m13 (C)	9	-0.54	1.04	x	NA (D)	NA (D)	NA	NA	NA	NA	NA	0.85	0.1
Ni	geogenic	m14	68	-0.60	0.72	x	x	NA	NA	see n=45	see n=47	NA	NA	0.46	0.67
		m15	68	-0.77	0.69	x	0.81	NA	NA	see n=45	see n=47	NA	NA	0.60	0.58
		m16	47	-0.82	0.95	x	0.55	NA	NA	see n=45	-0.38	NA	NA	0.72	0.53
		m17	45	-0.26	0.98	x	x	NA	NA	0.84	-0.97	NA	NA	0.78	0.48
	airborne	m18	11	-1.63	1.22	x	x	NA	NA	NA	NA	NA	NA	0.79	0.61
	mining and industrial waste	*m19* (E)	8	1.39	x	x	1.12	x	NA	NA	NA	NA	NA	0.77	0.35
Pb	geogenic	m20	21	-0.82	1.14	x	x	NA	NA	x	x	NA	NA	0.71	0.18
		m21	21	-0.27	1.24	-0.10	x	NA	NA	x	x	NA	NA	0.76	0.17
	airborne	m22	17	-0.48	0.98	x	x	NA	NA	NA	NA	NA	NA	0.64	0.28
	mining and industrial waste	m23	21	-0.15	0.88	x	NA (F)	NA	NA	NA	NA	NA	NA	0.92	0.19
		m24	21	0.076	1.03	-0.097	NA (F)	NA	NA	NA	NA	NA	NA	0.96	0.13
Zn	geogenic	m25	79	-0.62	0.82	x	see n=71	NA	NA	NA	see n=51	NA	NA	0.15	0.64
		m26	71	-0.27	0.62	x	0.52	NA	NA	NA	see n=51	NA	NA	0.45	0.37
		m27	51	0.19	0.67	x	0.56	NA	NA	NA	-0.19	NA	NA	0.60	0.25
	airborne	m28	38	-0.56	1	x	x	NA	NA	NA	NA	NA	NA	0.93	0.25
		m29	38	-0.12	1.04	-0.092	x	NA	NA	NA	NA	NA	NA	0.94	0.24
	organic	m30	10	-0.47	1.05	x	NA	NA	NA	NA	NA	NA	NA	0.85	0.2

NA indicates that the variable parameter was not included in the analysis; x indicates that the variable did not pass stepping method criteria ($p<0.05$ for entry, and $p>0.1$ for removal); $C_{reactive}$ (mg/kg) is the concentration of reactive metal in soil; C_{total} (mg/kg) is the concentration of total metal in soil; pH is measured in H20 (see the Methods section in the main part for details on harmonization of soil pH); ORGC (%) is the organic carbon content; CLAY (%) is the clay content; CEC ($mmol_c$/kg) is the cation exchange capacity; Fe_{ox} (g/kg) is the content of amorphous,

oxalate-extractable Fe (hydr)oxides; Fe_d (g/kg) is the content of the sum of amorphous and crystalline, dithionite-extractable Fe (hydr)oxides; Al_{ox} (g/kg) is the content of amorphous, oxalate-extractable Al (hydr)oxides; and Mn_{ox} (g/kg) is the content of amorphous, oxalate-extractable Mn (hydr)oxides. Other soil parameters were not considered because they were not available, or correlated strongly (r>0.8) with other soil parameters. All coefficients are significant at the probability level $p < 0.001$. (A) the variable was not included because it did not turn out significant in the analysis for larger number of data. (B) pH and $\log_{10}$(ORGC) were excluded because they correlate strongly with $\log_{10}(C_{total})$. (C) the analysis included 8 data points for 2 soils of the same properties, but with different biosolid amendments. (D) $\log_{10}$(ORGC) and $\log_{10}$(CLAY) were excluded because they correlate strongly with $\log_{10}(C_{total})$. (E) $\log_{10}$(ORGC) correlates with $\log_{10}(C_{total})$ (r=0.7) which may explain identification of $\log_{10}(C_{total})$ as an insignificant variable; if $\log_{10}$(ORGC) is excluded the regression coefficients are equal to -0.19 (for a), 0.65 (for b) with R^2_{adj}=0.46 and se=0.53, and n=8. (F) $\log_{10}$(ORGC) excluded because it correlates strongly with pH.

Uncertainty. First, several assumptions had to be made when assigning contamination age in order to increase number of data. Even if approximate time of emission could be specified (for example, when emission peak occurred), little can be said how metal age in the actual soil sample corresponds to the assumed time.

Second, it should be noted that in many cases information about some soil properties was not available. The performance of our regressions is expected to improve when data on the content of Fe, Al or Mn (hydr)oxides, which are expected to play a role in determining metal reactivity (Buekers et al. 2007), become available.

Third, the number of studies for each contamination type differs across metals. For example, studies on mainly airborne metal were found for Co, Ni or Zn, while the range in contamination type is relatively wide for Pb and Cu. The regressions for the combined set of solid forms for the forme metals are thus biased toward airborne metal, and may fail to predict reactive concentrations of metals for other contamination types.

Forth, data we collected if measured using isotope-based methods, as they are expected to be more accurate as compared with single or sequential extraction procedures. We however combined methods using radioisotopes that were used to measure either isotopically exchangeable or isotopically available metal pools. This was necessary in order to increase data availability, but can introduce and error in range of a few percent in determining reactive concentration of a metal (Hamon et al. 2002). Methods with stable isotopes can also be criticized because extraction of a soil solution is a necessary step that may introduce an error in determining a reactive concentration (Hamon et al. 2008).

Accessibility of readily soluble metal. Large part of the variability in reactivity of readily soluble metals in soils can be explained by soil pH which is known to control adsorption of Zn, Cd, Ni, Cu, and Pb ions onto the surface of Fe and Mn (hydr)oxides, thereby facilitating fixation through diffusion into (hydr)oxide structure (Buekers et al. 2008a; Buekers et al. 2008b; Buekers et al. 2007). For Cu and Co, these processes are recognized to occur through hydroxyl intermediates, providing a semi-mechanistic explanation for the role of pH in reactivity of these metals. Indeed, soil pH is a sole soil parameter in published aging models developed for Zn, Cd, Ni, Cu, and Co (Table S2.15).

Little is known about reactivity of readily soluble metals in soils at time scales longer than a few years. So far, only Ma et al. (2006) showed how their kinetic model developed using soils spiked with soluble Cu salts successfully predicts reactivity of Cu in soils contaminated with soluble Cu and aged for up to 40 years. Our comparison of measured and model predicted concentration of reactive metal shows that in most cases, except of readily soluble Cd and Co they overpredict concentration of reactive, solid or geogenic metal in soils (Fig. S2.10 - S2.15). The discrepancies probably originate from the fact that the kinetic aging models do not capture aging mechanisms occurring at time scales of decades, such as precipitation of salts and formation of secondary minerals. For example, reactivity of aqueous Zn corroding from galvanized power lines (classified in our study as readily soluble) varied between 10 and 60% in soils aged for 17-74 years, depended on the content of Zn precipitates in soil (such as Zn-layered double hydroxide, Zn-phyllosilicates, and hydrozincite), and correlated with soil pH only when a soil did not contain Zn-hydroxy interlayered minerals (Degryse et al. 2011). These observations suggest that soil properties controlling aging of Cu, Ni and Pb at time scales of decades can be different as compared to

those occurring at time scales of years. They also indicate that even in soils contaminated with soluble Zn, metal reactivity can be close to that measured for geogenic background.

Accessibility of anthropogenic and geogenic metal. A large part of variability in concentration of reactive metal could be explained by total metal content and/or soil properties. Although some influence of aging cannot be ruled out, our results indicate that aging is not an important parameter in determining reactivity of anthropogenic metals. This does not mean that aging of anthropogenic metal does not take place. It just indicates that possible changes in metal reactivity as a result of aging were not captured in our data set, with no measurements for individual soils sampled at various time intervals and with uncertain information on aging time. In addition, it cannot be ruled out that transformation of metal from one solid-phase form into another as a result of aging does not affect the overall metal reactivity in soils where large variability in metal forms and numerous aging mechanisms can occur simultaneously. For example, dissolution of ZnO that increases reactivity of Zn can be compensated by simultaneous formation of Zn precipitates reducing it reactivity, as both processes occur at time scales of months (Smolders and Degryse 2002; Voegelin et al. 2011)

As is the case for geogenic metal, published aging models developed for soluble salts, overpredict concentration of reactive metal, except of smelter- and biosolid-derived Cd and biosolids-derived Cu and Zn (Fig. S2.10 - S2.15). The bias is smaller for published empirical regression models developed in for both anthropogenic and geogenic metal (where concentration of reactive metal was measured using extraction with 0.43 M HNO_3), and for our regression models developed for either separate or combined sets of anthropogenic and geogenic metal. We argue that this is partly because reactivity of emitted solid metal is similar to that of geogenic metal, and partly because some metal forms in anthropogenically contaminated soils are the same as compared with soils contaminated with geogenic metal.

Cadmium. Regression analysis revealed a small effect of soil pH on concentration of reactive Cd in soils, which is often close to concentration of total Cd. This is in agreement with studies documenting very high (close to 1) initial reactivity of Cd in a fly ash from a medical waste incinerator (Wang et al. 2011a). High reactivity of Cd can mainly be explained by the fact that this metal binds to soil constituents through weak electrostatic forces (Rodrigues et al. 2010b). Ettler et al. (2012) already showed how positively charged or neutral chloro- or sulfate complexes can reduce affinity of smelter-derived Cd to positively charged organic and oxide soil constituents, confirming earlier findings showing that Cd is mostly present in soil solutions in dissolved forms as free ions or labile complexes (Citeau et al. 2003; Denaix et al. 2001). The positive, small effect of soil organic carbon on Cd reactivity for the combined data for geogenic and anthropogenic Cd is consistent with observations for smelter-derived Cd by Chrastny et al. (2012) and Nowack et al. (2010) who reported higher amounts of weakly bound, reactive Cd in organic soils. Our results imply that in a wide range of concentration of total metal and contamination types, the reactivity of Cd can be predicted from total metal load, soil pH and soil organic carbon. Published kinetic aging models and empirical regression models tend to overpredict concentration of reactive Cd in anthropogenic soils, particularly for soils where total Cd concentrations are high, such as in mining-impacted but the bias is smaller for soils contaminated with geogenic Cd (see SI).

Cobalt. Our analysis shows that reactive concentration of anthropogenic Co can mainly be explained by total metal. The role of soil pH and organic carbon, identified by Rodrigues et al. (2010b) as predictors of concentration of reactive Co, is not apparent probably because our low number of data. Indeed, Co adsorbed to organic matter was shown to be readily exchangeable, in contrast to non-reactive Co absorbed on Mn oxides being a major sink for this metal (Gal et al. 2008; Ghabbour et al. 2007; McLaren et al. 1986; McLaren et al. 1987). The kinetic model by Wendling et al. (2009) only slightly overpredicts concentration of reactive airborne Co, whereas the model of Rodrigues et al. (2010b) predicts reactive concentrations close to measured values. Both models however overpredict concentration of geogenic Co, suggesting that at time scales of centuries a further decrease in reactivity of anthropogenic Co is expected to occur.

Copper. We show that organic carbon positively contributes to reactivity of Cu in soils, confirming the observations of Rodrigues et al. (2010b) and Romkens et al. (2004). Although the contribution of Fe and Mn oxides in a biosolid to binding of Cu is debated, organic matter is expected to be a more effective adsorbent for Cu as compared with mineral soil constituents in soils. Indeed, in the long-term, fungicide-contaminated soils Cu was found to be primarily associated with soil organic matters, while no evidence was found for the formation of silicate minerals (Donner et al. 2012; Heemsbergen et al. 2010). Note, that the initial form of Cu in a biosolids, determined by biosolids age, will have a role in determining Cu reactivity in soil; reactive CuS formed in non-aged biosolids will be released in aerobic soil conditions allowing for Cu reaction with soil constituents, whereas oxide- or organic-bound copper in aged biosolids is expected to be less reactive. Our regression models developed for geogenic Cu explains lower part of the variability in reactive Cu, as compared with other metals and the models developed by the others (see SI). This probably reflects the lack of inclusion of Fe (hydr)oxides, recognized to reduce reactivity of Cu in soils (Buekers et al. 2007). Published aging models overpredict reactive concentration of both geogenic and anthropogenic Cu, except the model of Rodrigues et al. (2010b) applied to geogenic Cu.

Nickel. Our results suggest that organic-bound geogenic Ni is reactive, confirming the findings of Rodrigues et al. (2010b) Our results are consistent with known ability of Ni to form minerals with Fe or Mn (hydr)oxides (Echevarria et al. 1998); amorphous iron (hydr)oxides were found to be a significant variable in the regression equation for concentration of reactive, geogenic Ni. Low number of data for anthropogenic Ni limits interpretation of our results. We nevertheless show that 0.7 of the variability in concentration of reactive Ni or airborne and industrial origin can be explained by total Ni concentration. Published kinetic models overestimate concentration of reactive Ni (both geogenic and anthropogenic). The bias is smaller for empirical regression models; yet the explained variability is below 0.55.

Lead. Our analysis shows that concentration of anthropogenically induced Pb in soil depends mainly on soil pH. The role of amorphous Fe (hydr)oxides becomes apparent for the combined set of anthropogenic and geogenic metal. This is in agreement with data presented in Morin et al. (1999) who showed that about half of total Pb originating from mine tailings and smelters was included within Fe- and Mn-(oxyhydr)oxides. These forms of Pb were also identified in geogenic Pb material by Teutsch et al. (1999), suggesting that

transformation of primary Pb in soil occurs at time scale of decades. Ettler et al. (2012) showed how pH-dependent dissolution of a smelter fly ash led to a complete dissolution of primary Pb minerals (caracolite $Na_3Pb_2(SO_4)_3Cl$, and KPb_2Cl_5) with formation of secondary anglesite ($PbSO_4$), minor cerrusite ($PbSO_3$) and trace carbonates in soils. Soil pH appears a controlling factor for Pb, which can be adsorbed on the surface of Fe oxides at pH < 5.5. At historically contaminated sites (from 2 to 19 centuries) impacted by smelting, relatively small proportion of Pb was labile when soil pH was high, but about 40% of Pb was reactive at pH < 5. It was moreover suggested that cerrusite formed in the presence of calcium and carbonate compounds leached from the slag waste. However, we did not find organic carbon to be a significant descriptor of Pb reactivity, although organic-bound Pb can be a predominant form of Pb in organic reach soils (Morin et al. 1999). Regression models of Rodrigues et al. (2010b) underestimate reactive concentration of Pb, particularly for in mining-impacted soils. Better performance is noted for regressions developed by Romkens et al. (2004) applied to airborne Pb.

Zinc. Reactivity of anthropogenic Zn is expected to be reduced by dissolution and reaction with soil minerals. Scheckel et al. (2010) demonstrated how ZnO dissolves and forms Zn^{2+} complexes in kaolinite within few months, while Smolders and McGrath (2003) showed high and low reactivity of Zn in an acidic soil, emitted as isolated ZnO or ZnO in tire debris, respectively. In two smelter impacted soils, Diesing et al. (2008) found considerable amounts of exchangeable species and Zn-phyllosilicates, and speculated that the predominance of the former is most likely due to the dissolution of smelter-inherited primary minerals (franklinite, sphalerite, willemite), while Isaure et al. (2005) showed how smelter-related sphalerite (ZnS) and franklinite ($ZnFe_2O_4$) applied via sediment disposition on land, transformed into poorly-crystalline Zn-sorbed Fe-oxyhydroxides and zinciferous phyllosilicate. In two organic rich soils Jacquat et al. (2009) demonstrated that although Zn primary minerals accounted to 5% of total Zn in the bulk soil, Zn was found to be predominantly speciated as Zn-organic matter complexes, Zn-sorbed phosphate, and Zn-sorbed iron oxyhydroxides. It thus appears that a time scale of about a century is enough for smelter-related Zn to transform into forms that are found within geogenic background. The lack of the influence of soil pH in the regression equations for solid Zn is unexpected, given that most of solid metal forms of Zn were emitted from smelters, but is consistent with observation of Rodrigues et. () who found only small influence of soil pH and larger influence of soil organic carbon on reactivity of Zn. The role of organic carbon in the regression equation for geogenic Zn is also consistent with observation of Rodrigues et al. (2010b). Our results suggest relatively good performance of the regression developed for the combined set of anthropogenic and geogenic Zn may be results of similarities in chemical forms of Zn in contaminated soils. As was the case of other metals, kinetic aging models overpredict concentration of reactive geogenic and anthropogenic Zn.

Influence of accessibility on comparative toxicity potentials of metals. We showed that metal accessibility can be low. This will have an impact on the magnitude of comparative toxicity potentials. The accessibility influences CTP of metals through its control of the distribution coefficient (K_d). First, the ACF determines the concentration of toxic free ions in soil pore water; a reduction in the ACF increases the K_d and thereby reduces the CTP because the dissolved pool of free ions will be lower. Second, the ACF influences metal fate; a

reduction in the ACF increases the K_d and thereby metal residence time in the soil, increasing the CTP. These two effects of the ACF on the CTP only partly compensate each other because metal fate in soil depends also on K_d-independent processes, such as soil erosion (see SI for details).

Figure 2.6 shows that accurate correct estimation of ACF is particularly important for Pb and Cu, for which reduction in the CTP almost linearly correlates to the reduction in the ACF. This is because at high Kd values metal fate is determined mainly by K_d-independent soil erosion (see SI for calculations). The CTP of Co and Ni can also be reduced at low accessibility, whereas For Zn correct estimation of the ACF is only important in lower range of the ACF values (< 0.4). For Cd, reduction in the ACF has small influence on the CTP because fate of Cd in soil is determined mainly by K_d-controlled leaching. Further research efforts on metal accessibility should thus focus on elements with strong affinity to soils constituents, for which metal fate is determined mainly by K_d-independent processes, such as soil erosion (the steady state characterization model Usetox (Rosenbaum et al. 2008) assumes that about 1200 years is required for all soil to become exchanged as a result of erosion to surface water). Our results also suggest that of K_d values typically measured for hydrophobic organics (< 10 L/kg), aging will not influence of CTP substantially; a reduction in accessibility will be compensated by higher residence time of a substance in the soil.

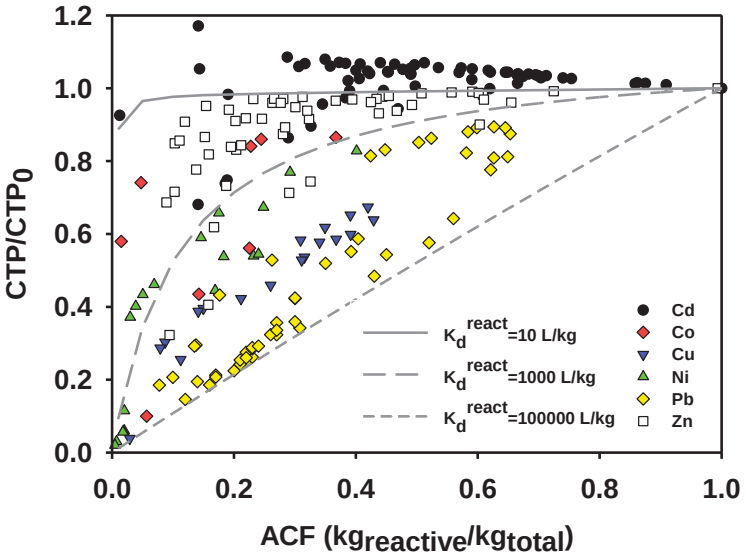

Figure 2.5: Influence of the accessibility factor (ACF) on the comparative toxicity potential (CTP) of anthropogenic Cd, Co, Cu, Ni, Pb, and Zn. CTP_0 is the comparative toxicity potential assuming ACF equal to 1 $kg_{reactive}/kg_{total}$; CTP is the comparative toxicity potential as measured in our soils. Gray solid and dashed lines represent CTP/CTP_0 for three hypothetical cases where the K_d^{react} are equal to (i) 10; (ii) 1000; and (iii) 10000 L/kg. The K_d^{react} (defined as defined as the ratio between the concentration of reactive metal in the solid phase and the total dissolved metal) is related to K_d through the relationship: $K_d^{react}=K_d/ACF$. See SI for details on the analysis.

2.3.11. Recommendations for life cycle inventory

In current chemical hazard ranking and life cycle impact assessment emissions of metals are inventoried according to their symbol and oxidation state (Pettersen and Hertwich 2008). Our results suggest that reporting only the type of metal is sufficient to allow for subsequent characterization ecotoxic impacts. This can be explained by the fact that reactivity of anthropogenic metal in soils is mainly determined by total metal burden and/or soil properties than by the initial form of metal. In regionalized assessments, where detailed information about emitted metal forms is available (as can be in environmental impact assessment, EIA), models developed for specific contamination type or individual metal forms can be considered. If conservative assumptions are deemed necessary (as can be the case of environmental risk assessment, ERA) aging models developed using soils spiked with soluble salts might be sufficient. However, they will overestimate metal accessibility at time horizons larger than a few years.

2.3.12. Recommendations for characterization modeling

An impact assessment practitioner may wish to choose and infinite time horizon for modeling toxicity potential of metals. Our results show than at time scales of decades to centuries, the influence of aging for anthropogenic metal forms is small, and the ACF can be calculated employing empirical regression models assuming equilibrium between concentration of reactive and total metal in the soil using data on total metal burden and/or soil properties. Alternatively, predictive models for calculating reactivity of metals in soils from physicochemical properties of metal ions, can be developed (Laird et al. 2011).

2.4. Conclusions

Our new CTPs of Ni and Cu in soils, taking metal bioaccessibility into account, highlight the need for considering variability in soil properties as drivers of metal CTPs. These aspects of terrestrial ecotoxicity assessment of metals are not included yet in the existing LCIA methodologies (Pizzol et al. 2011). For applications in regionalized assessments, it is important to evaluate the variability of CTPs as controlled by spatially variable soil properties. The scientifically relevant spatial scales can be different for different metals, due to differences in spatial variability of soil parameters controlling CTPs, as demonstrated here for Cu and Ni. In situations where the emission location is unknown, as is often the case in LCA, it is important to carefully select generic values of CTPs. Weighting of CTPs can be done based on the relative occurrence of soils. Alternatively, soil archetypes can be derived for which spatially-determined variability of CTPs can be calculated. In both cases, our empirical CTP-regression can be directly employed to calculate CTPs for Cu and Ni from soil parameters.

2.5. References

Ahnstrom ZAS, Parker DR. 2001. Cadmium reactivity in metal-contaminated soils using a coupled stable isotope dilution-sequential extraction procedure. Environmental Science & Technology 35(1):121-126.

Alexander M. 2000. Aging, bioavailability, and overestimation of risk from environmental pollutants. Environmental Science & Technology 34(20):4259-4265.

Ali NA, Bernal MP, Ater M. 2002. Tolerance and bioaccumulation of copper in Phragmites australis and Zea mays. Plant and Soil 239(1):103-111.

Amacher M. 1991. Methods for obtaining and analyzing kinetic data. In: Sparks DL, Suarez DL, editors. Rates of soil chemical processes Madison, WI: Soil Science Society of America. p 19-59.

Anderson PR, Christensen TH. 1988. Distribution coefficients of Cd, Co, Ni, and Zn in soils. Journal of Soil Science 39(1):15-22.

Azevedo LB, van Zelm R, Hendriks AJ, Bobbink R, Huijbregts MAJ. 2013. Global assessment of the effects of terrestrial acidification on plant species richness. Environmental Pollution 174(0):10-15.

Batjes NH. 2006. ISRIC-WISE derived soil properties on a 5 by 5 arc-minutes global grid (version 1.0). Wageningen: ISRIC –World Soil Information. Report nr 2006／02.

Batjes NH. 2008. ISRIC-WISE harmonized global soil profile dataset (version 3.1). Wageningen: ISRIC –World Soil Information. Report nr 2008／02.

Batjes NH. 2009. Harmonized soil profile data for applications at global and continental scales: updates to the WISE database. Soil Use and Management 25(2):124-127.

Batjes NH. 2012. ISRIC-WISE derived soil properties on a 5 by 5 arc-minutes global grid (version 1.2). Wageningen: ISRIC –World Soil Information. Report nr 2012／01.

Bhavsar SP, Gandhi N, Diamond ML. 2008. Extension of coupled multispecies metal transport and speciation (TRANSPEC) model to soil. Chemosphere 70(5):914-924.

Buekers J, Amery F, Maes A, Smolders E. 2008a. Long-term reactions of Ni, Zn and Cd with iron oxyhydroxides depend on crystallinity and structure and on metal concentrations. European Journal of Soil Science 59(4):706-715.

Buekers J, Degryse F, Maes A, Smolders E. 2008b. Modelling the effects of ageing on Cd, Zn, Ni and Cu solubility in soils using an assemblage model. European Journal of Soil Science 59(6):1160-1170.

Buekers J, Van Laer L, Amery F, Van Buggenhout S, Maes A, Smolders E. 2007. Role of soil constituents in fixation of soluble Zn, Cu, Ni and Cd added to soils. European Journal of Soil Science 58(6):1514-1524.

Chrastny V, Vanek A, Komarek M, Farkas J, Drabek O, Vokurkova P, Nemcova J. 2003. Incubation of air-pollution-control residues from secondary Pb smelter in deciduous and coniferous organic soil horizons: Leachability of lead, cadmium and zinc. Journal of Hazardours Materials 209:40-47.

Christiansen K, Holm P, Borggaard O, Hauschild M. 2011. Addressing speciation in the effect factor for characterisation of freshwater ecotoxicity—the case of copper. The International Journal of Life Cycle Assessment 16(8):761-773.

Citeau L, Lamy I, van Oort F, Elsass F. 2003. Colloidal facilitated transfer of metals in soils under different land use. Colloids and Surfaces A: Physicochemical and Engineering Aspects 217 (1-3):11-19.

Cornelissen G, Gustafsson O, Bucheli TD, Jonker MTO, Koelmans AA, Van Noort PCM. 2005. Extensive sorption of organic compounds to black carbon, coal, and kerogen in sediments and soils: Mechanisms and consequences for distribution, bioaccumulation, and biodegradation. Environmental Science & Technology 39(18):6881-6895.

Corwin DL, Lesch SM. 2003. Application of soil electrical conductivity to precision agriculture: Theory, principles, and guidelines. Agronomy Journal 95(3):455-471.

Crout NMJ, Tye AM, Zhang H, McGrath SP, Young SD. 2006. Kinetics of metal fixation in soils: Measurement and modeling by isotopic dilution. Environmental Toxicology and Chemistry 25(3):659-663.

Davies CW. Ion Association. Butterworth: London, 1962.

de Caritat P, Reimann C, Chekushin V, Bogatyrev I, Niskavaara H, Braun J. 1997. Mass Balance between Emission and Deposition of Airborne Contaminants. Environmental Science & Technology 31(10):2966-2972.

Degryse F, Broos K, Smolders E, Merckx R. 2003. Soil solution concentration of Cd and Zn can be predicted with a CaCl2 soil extract. European Journal of Soil Science 54(1):149-157.

Degryse F, Buekers J, Smolders E. 2004. Radio-labile cadmium and zinc in soils as affected by pH and source of contamination. European Journal of Soil Science 55(1):113-121.

Degryse F, Smolders E, Parker DR. 2009. Partitioning of metals (Cd, Co, Cu, Ni, Pb, Zn) in soils: concepts, methodologies, prediction and applications - a review. European Journal of Soil Science 60(4):590-612.

Degryse F, Voegelin A, Jacquat O, Kretzschmar R, Smolders E. 2011. Characterization of zinc in contaminated soils: complementary insights from isotopic exchange, batch extractions and XAFS spectroscopy. European Journal of Soil Science 62(2):318-330.

Denaix L, Semlali RM, Douay F. 2001. Dissolved and colloidal transport of Cd, Pb, and Zn in a silt loam soil affected by atmospheric industrial deposition. Environmental Pollution 114(1):29-38.

Diamond ML, Gandhi N, Adams WJ, Atherton J, Bhavsar SP, Bulle C, Campbell PGC, Dubreuil A, Fairbrother A, Farley Ket al. 2010. The clearwater consensus: the estimation of metal hazard in fresh water. International Journal of Life Cycle Assessment 15(2):143-147.

Diesing WE, Sinaj S, Sarret G, Manceau A, Flura T, Demaria P, Siegenthaler A, Sappin-Didier V, Frossard E. 2008. Zinc speciation and isotopic exchangeability in soils polluted with heavy metals. European Journal of Soil Science 59(4):716-729.

Dijkstra JJ, Meeussen JCL, Comans RNJ. 2004. Leaching of heavy metals from contaminated soils: An experimental and modeling study. Environmental Science & Technology 38(16):4390-4395.

Dijkstra JJ, Meeussen JCL, Comans RNJ. 2009. Evaluation of a generic multisurface sorption model for inorganic soil contaminants. Environmental Science & Technology 43(16):6196-6201.

Donner E, Ryan CG, Howard DL, Zarcinas B, Scheckel KG, McGrath SP, de Jonge MD, Paterson D, Naidu R, Lombi E. 2012. A multi-technique investigation of copper and zinc distribution, speciation and potential bioavailability in biosolids. Environmental Pollution 166:57-64.

Echevarria G, Morel JL, Fardeau JC, Leclerc-Cessac E. 1998. Assessment of phytoavailability of nickel in soils. Journal of Environmental Quality 27(5):1064-1070.

European Commission. Technical Guidance Document in support of Commission Directive 93/67/EEC on Risk Assessment for new notified substances, Commission Regulation (EC) No 1488/94 on Risk Assessment for existing substances and Directive 98/8/EC of the European Parliament and of the Council concerning the placing of biocidal products on the market. Joint Research Centre, European Chemicals Bureau: Brussels, Belgium, 2003.

Elzinga EJ, van Grinsven JJM, Swartjes FA. 1999. General purpose Freundlich isotherms for cadmium, copper and zinc in soils. European Journal of Soil Science 50(1):139-149.

Ettler V, Mihaljevič M, Šebek O, Matys Grygar T, Klementová M. 2012. Experimental in Situ Transformation of Pb Smelter Fly Ash in Acidic Soils. Environmental Science & Technology.

Ewing SA, Christensen JN, Brown ST, Vancuren RA, Cliff SS, Depaolo DJ. 2010. Pb Isotopes as an Indicator of the Asian Contribution to Particulate Air Pollution in Urban California. Environmental Science & Technology 44(23):8911-8916.

FAO/IIASA/ISRIC/ISS-CAS/JRC. 2012. Harmonized World Soil Database (version 1.2)

Gaines JGL, Thomas HC. 1953. Adsorption Studies on Clay Minerals. II. A Formulation of the Thermodynamics of Exchange Adsorption. The Journal of Chemical Physics 21(4):714-718.

Gal J, Hursthouse A, Tatner P, Stewart F, Welton R. 2008. Cobalt and secondary poisoning in the terrestrial food chain: Data review and research gaps to support risk assessment. Environment International 34(6):821-838.

.

2010. New method for calculating comparative toxicity potential of cationic metals in freshwater: application to copper, nickel, and zinc. Environmental Science & Technology 44(13):5195-5201.

Garnier JM, Ciffroy P, Benyahya L. 2006. Implications of short and long term (30 days) sorption on the desorption kinetic of trace metals (Cd, Zn, Co, Mn, Fe, Ag, Cs) associated with river suspended matter. Science of the Total Environment 366(1):350-360.

Ghabbour EA, Scheinost AC, Davies G. 2007. XAFS studies of cobalt(II) binding by solid peat and soil-derived humic acids and plant-derived humic acid-like substances. Chemosphere 67(2):285-291.

Griffin BA, Jurinak JJ. 1973. Estimation of Activity Coefficients From the Electrical Conductivity of Natural Aquatic Systems and Soil Extracts. Soil Science 116(1):26-30.

Groenenberg JE, Dijkstra JJ, Bonten LTC, de Vries W, Comans RNJ. 2012. Evaluation of the performance and limitations of empirical partition-relations and process based multisurface models to predict trace element solubility in soils. Environmental Pollution 166(0):98-107.

Groenenberg JE, Römkens PFAM, Comans RNJ, Luster J, Pampura T, Shotbolt L, Tipping E, De Vries W. 2010. Transfer functions for solid-solution partitioning of cadmium, copper, nickel, lead and zinc in soils: derivation of relationships for free metal ion activities and validation with independent data. European Journal of Soil Science 61(1):58-73.

Hamon RE, Bertrand I, McLaughlin MJ. 2002. Use and abuse of isotopic exchange data in soil chemistry. Australian Journal of Soil Research 40(8):1371-1381.

Hamon RE, Parker DR, Lombi E. 2008. ADVANCES INISOTOPIC DILUTION TECHNIQUES IN TRACE ELEMENT RESEARCH: A REVIEW OF METHODOLOGIES, BENEFITS, AND LIMITATIONS. In: Sparks DL, editor. Advances in Agronomy, Vol 99. p 289-343.

Hauschild MZ, Huijbregts M, Jolliet O, MacLeod M, Margni M, van de Meent DV, Rosenbaum RK, McKone TE. 2008. Building a model based on scientific consensus for life cycle impact assessment of chemicals: The search for harmony and parsimony. Environmental Science & Technology 42(19):7032-7037.

Haye S, Slaveykova VI, Payet J. 2007. Terrestrial ecotoxicity and effect factors of metals in life cycle assessment (LCA). Chemosphere 68(8):1489-1496.

Heemsbergen DA, McLaughlin MJ, Whatmuff M, Warne MS, Broos K, Bell M, Nash D, Barry G, Pritchard D, Penney N. 2010. Bioavailability of zinc and copper in biosolids compared to their soluble salts. Environmental Pollution 158(5):1907-1915.

Henderson A, Hauschild M, van de Meent D, Huijbregts M, Larsen H, Margni M, McKone T, Payet J, Rosenbaum R, Jolliet O. 2011. USEtox fate and ecotoxicity factors for comparative assessment of toxic emissions in life cycle analysis: sensitivity to key chemical properties. The International Journal of Life Cycle Assessment 16(8):701-709.

Huijbregts MAJ, Guinee JB, Reijnders L. 2001. Priority assessment of toxic substances in life cycle assessment. III: Export of potential impact over time and space. Chemosphere 44(1):59-65.

Hurd LE, Mellinger MV, Wolf LL, McNaughton SJ. 1971. Stability and diversity at three trophic levels in terrestrial successional ecosystems. Science 173(4002):1134-1136.

Isaure MP, Manceau A, Geoffroy N, Laboudigue A, Tamura N, Marcus MA. 2005. Zinc mobility and speciation in soil covered by contaminated dredged sediment using micrometer-scale and bulk-averaging X-ray fluorescence, absorption and diffraction techniques. Geochimica et Cosmochimica Acta 69(5):1173-1198.

Ispas C, Andreescu D, Patel A, Goia DV, Andreescu S, Wallace KN. 2009. Toxicity and developmental defects of different sizes and shape nickel nanoparticles in Zebrafish. Environmental Science & Technology 43(16):6349-6356.

Jacquat O, Voegelin A, Kretzschmar R. 2009. Soil properties controlling Zn speciation and fractionation in contaminated soils. Geochimica et Cosmochimica Acta 73(18):5256-5272.

Janssen RPT, Peijnenburg WJGM, Posthuma L, Van Den Hoop MAGT. 1997. Equilibrium partitioning of heavy metals in dutch field soils. I. Relationship between metal partition coefficients and soil characteristics. Environmental Toxicology and Chemistry 16(12):2470-2478.

Kindler R, Siemens J, Kaiser K, Walmsley DC, Bernhofer C, Buchmann N, Cellier P, Eugster W, Gleixner G, Grunwald Tet al. 2011. Dissolved carbon leaching from soil is a crucial component of the net ecosystem carbon balance. Global Change Biology 17(2):1167-1185.

Kinraide TB. 2009. Improved scales for metal ion softness and toxicity. Environmental Toxicology and Chemistry 28(3):525-533.

Kinraide TB, Yermiyahu U. 2007. A scale of metal ion binding strengths correlating with ionic charge, Pauling electronegativity, toxicity, and other physiological effects. Journal of Inorganic Biochemistry 101(9):1201-1213.

Lado LR, Hengl T, Reuter HI. 2008. Heavy metals in European soils: A geostatistical analysis of the FOREGS Geochemical database. Geoderma 148(2):189-199.

Laird BD, Peak D, Siciliano SD. 2011. Bioaccessibility of Metal Cations in Soil Is Linearly Related to Its Water Exchange Rate Constant. Environmental Science & Technology 45(9):4139-4144.

Lofts S, Spurgeon DJ, Svendsen C, Tipping E. 2004. Deriving soil critical limits for Cu, Zn, Cd, and Ph: A method based on free ion concentrations. Environmental Science & Technology 38(13):3623-3631.

Ma YB, Lombi E, Oliver IW, Nolan AL, McLaughlin MJ. 2006. Long-term aging of copper added to soils. Environmental Science & Technology 40(20):6310-6317.

Massoura ST, Echevarria G, Becquer T, Ghanbaja J, Leclere-Cessac E, Morel JL. 2006. Control of nickel availability by nickel bearing minerals in natural and anthropogenic soils. Geoderma 136(1-2):28-37.

Matschonat G, Ingwersen J, Streck T. 2003. Suitability of the ESS laboratory method to determine the equilibrium soil solution composition of agricultural soils, and suggestions for simplification of the experimental procedure. Journal of Plant Nutrition and Soil Science-Zeitschrift Fur Pflanzenernahrung Und Bodenkunde 166(6):742-749.

McLaren RG, Lawson DM, Swift RS. 1986. THE FORMS OF COBALT IN SOME SCOTTISH SOILS AS DETERMINED BY EXTRACTION AND ISOTOPIC EXCHANGE. Journal of Soil Science 37(2):223-234.

McLaren RG, Lawson DM, Swift RS. 1987. THE AVAILABILITY TO PASTURE PLANTS OF NATIVE AND APPLIED SOIL COBALT IN RELATION TO EXTRACTABLE SOIL COBALT AND OTHER SOIL PROPERTIES. Journal of the Science of Food and Agriculture 39(2):101-112.

Mertens FM, Paetzold S, Welp G. 2008. Spatial heterogeneity of soil properties and its mapping with apparent electrical conductivity. Journal of Plant Nutrition and Soil Science-Zeitschrift Fur Pflanzenernahrung Und Bodenkunde 171(2):146-154.

Morin G, Ostergren JD, Juillot F, Ildefonse P, Calas G, Brown GE. 1999. XAFS determination of the chemical form of lead in smelter-contaminated soils and mine tailings: Importance of adsorption processes. American Mineralogist 84(3):420-434.

Nicholson FA, Smith SR, Alloway BJ, Carlton-Smith C, Chambers BJ. 2003. An inventory of heavy metals inputs to agricultural soils in England and Wales. Science of the Total Environment 311(1-3):205-219.

Nowack B, Schulin R, Luster J. 2010. Metal fractionation in a contaminated soil after reforestation: Temporal changes versus spatial variability. Environmental Pollution 158(10):3272-3278.

Oorts K, Ghesquiere U, Swinnen K, Smolders E. 2006. Soil properties affecting the toxicity of CuCl2 and NiCl2 for soil microbial processes in freshly spiked soils. Environmental Toxicology and Chemistry 25(3):836-844.

Parkhurst DL, Appelo CAJ. User's guide to phreeqc- a computer program for speciation, batch-reaction, one-dimensional transport, and inverse geochemical calculations; U.S. Geological Survey: Denver, CO, 1999.

Paquin PR, Gorsuch JW, Apte S, Batley GE, Bowles KC, Campbell PGC, Delos CG, Di Toro DM, Dwyer RL, Galvez Fet al. 2002. The biotic ligand model: a historical overview. Comparative Biochemistry and Physiology C-Toxicology & Pharmacology 133(1-2):3-35.

Peijnenburg WJGM, Jager T. 2003. Monitoring approaches to assess bioaccessibility and bioavailability of metals: Matrix issues. Ecotoxicology and Environmental Safety 56(1):63-77.

Pennington DW, Payet J, Hauschild M. 2004. Aquatic ecotoxicological indicators in life-cycle assessment. Environmental Toxicology and Chemistry 23(7):1796-1807.

Pettersen J, Hertwich EG. 2008. Critical review: Life-cycle inventory procedures for long-term release of metals. Environmental Science & Technology 42(13):4639-4647.

Pizzol M, Christensen P, Schmidt J, Thomsen M. 2011. Eco-toxicological impact of "metals" on the aquatic and terrestrial ecosystem: A comparison between eight different methodologies for Life Cycle Impact Assessment (LCIA). Journal of Cleaner Production 19(6-7):687-698.

Popp M, Koellensperger G, Stingeder G, Hann S. 2008. Novel approach for determination of trace metals bound to suspended solids in surface water samples by inductively coupled plasma sector field mass spectrometry (ICP-SFMS). Journal of Analytical Atomic Spectrometry 23(1):111-118.

Posthuma L, De Zwart D. 2006. Predicted effects of toxicant mixtures are confirmed by changes in fish species assemblages in Ohio, USA, Rivers. Environmental Toxicology and Chemistry 25(4):1094-1105.

Posthuma L, de Zwart D. 2012. Predicted mixture toxic pressure relates to observed fraction of benthic macrofauna species impacted by contaminant mixtures. Environmental Toxicology and Chemistry 31(9):2175-2188.

Prommer H, Tuxen N, Bjerg PL. 2006. Fringe-controlled natural attenuation of phenoxy acids in a landfill plume: integration of field-scale processes by reactive transport modeling. Environmental Science & Technology 40(15):4732-4738.

Reichenberg F, Mayer P. 2006. Two complementary sides of bioavailability: Accessibility and chemical activity of organic contaminants in sediments and soils. Environmental Toxicology and Chemistry 25(5):1239-1245.

Reuter HI, Lado LR, Hengl T, Montanarella L. 2008. Continental-scale digital soil mapping using European soil profile data: soil pH. Hamburger Beiträge zur Physischen Geographie und Landschaftsökologie 19:91-102.

Robbins CW, Carter DL. 1983. Selectivity coefficients for calcium-magnesium-sodium-potassium exchange in eight soils. Irrigation Science 4(2):95-102.

Rodrigues SM, Henriques B, da Silva EF, Pereira ME, Duarte AC, Groenenberg JE, Römkens PFAM. 2010a. Evaluation of an approach for the characterization of reactive and available pools of 20 potentially toxic elements in soils: Part II – Solid-solution partition relationships and ion activity in soil solutions. Chemosphere 81(11):1560-1570.

Rodrigues SM, Henriques B, da Silva EF, Pereira ME, Duarte AC, Romkens P. 2010b. Evaluation of an approach for the characterization of reactive and available pools of twenty potentially toxic elements in soils: Part I - The role of key soil properties in the variation of contaminants' reactivity. Chemosphere 81(11):1549-1559.

Romkens PF, Guo H-Y, Chu C-L, Liu T-S, Chiang C-F, Koopmans GF. 2009. Characterization of soil heavy metal pools in paddy fields in Taiwan: chemical extraction and solid-solution partitioning. Journal of Soils and Sediments 9(3):216-228.

Römkens PFAM, Groenenberg JE, Bonten LTC, Vries Wd, Bril J. 2004. Derivation of partition relationships to calculate Cd, Cu, Ni, Pb, Zn solubility and activity in soil solutions. Wageningen: Alterra. 75 p.

Rosenbaum RK, Bachmann TM, Gold LS, Huijbregts MAJ, Jolliet O, Juraske R, Koehler A, Larsen HF, MacLeod M, Margni Met al. 2008. USEtox-the UNEP-SETAC toxicity model: recommended characterisation factors for human toxicity and freshwater ecotoxicity in life cycle impact assessment. International Journal of Life Cycle Assessment 13(7):532-546.

Rowell, D. L., Soil science: Methods & applications. Longman Scientific & Technical, Longman Group UK Ltd: Harlow, Essex, UK, 1994.

Ruby MV, Schoof R, Brattin W, Goldade M, Post G, Harnois M, Mosby DE, Casteel SW, Berti W, Carpenter Met al. 1999. Advances in evaluating the oral bioavailability of inorganics in soil for use in human health risk assessment. Environmental Science & Technology 33(21):3697-3705.

Sauvé S, Hendershot W, Allen HE. 2000. Solid-solution partitioning of metals in contaminated soils: dependence on pH, total metal burden, and organic matter. Environmental Science & Technology 34(7):1125-1131.

Scheckel KG, Luxton TP, El Badawy AM, Impellitteri CA, Tolaymat TM. 2010. Synchrotron Speciation of Silver and Zinc Oxide Nanoparticles Aged in a Kaolin Suspension. Environmental Science & Technology 44(4):1307-1312.

Semple KT, Doick KJ, Jones KC, Burauel P, Craven A, Harms H. 2004. Defining bioavailability and bioaccessibility of contaminated soil and sediment is complicated. Environmental Science & Technology 38(12):228A-231A.

Shacklette HT, Boerngen JG. 1984. Element concentration in soils and other surficial materials of the conterminous United States.: USGS (United States Geological Survey) professional paper 1270.

Skeaff J, Delbeke K, Van Assche F, Conard B. 2000. A critical surface area concept for acute hazard classification of relatively insoluble metal-containing powders in aquatic environments. Environmental Toxicology and Chemistry 19(6):1681-1691.

Smolders E, Degryse F. 2002. Fate and effect of zinc from tire debris in soil. Environmental Science & Technology 36(17):3706-3710.

Smolders E, McGrath SP, Lombi E, Karman CC, Bernhard R, Cools D, Van Den Brande K, Van Os B, Walrave N. 2003. Comparison of toxicity of zinc for soil microbial processes between laboratory-contamined and polluted field soils. Environmental Toxicology and Chemistry 22(11):2592-2598.

Smolders E, Oorts K, van Sprang P, Schoeters I, Janssen CR, McGrath SP, McLaughlin MJ. 2009. Toxicity of trace metals in soil as affected by aoil type and aging after contamination: using calibrated bioavailability models to set ecological soil standards. Environmental Toxicology and Chemistry 28(8):1633-1642.

Sonmez S, Buyuktas D, Okturen F, Citak S. 2008. Assessment of different soil to water ratios (1:1, 1:2.5, 1:5) in soil salinity studies. Geoderma 144(1-2):361-369.

Stiven GA, Khan MA. 1966. Saturation percentage as a measure of soil texture in the lower Indus basin. Journal of Soil Science 17(2):255-273.

Sudduth KA, Kitchen NR, Wiebold WJ, Batchelor WD, Bollero GA, Bullock DG, Clay DE, Palm HL, Pierce FJ, Schuler RTet al. 2005. Relating apparent electrical conductivity to soil

properties across the north-central USA. Computers and Electronics in Agriculture 46(1–3):263-283.

Teutsch N, Erel Y, Halicz L, Chadwick OA. 1999. The influence of rainfall on metal concentration and behavior in the soil. Geochimica et Cosmochimica Acta 63(21):3499-3511.

Thakali S, Allen HE, Di Toro DM, Ponizovsky AA, Rooney CP, Zhao F-J, McGrath SP. 2006a. A terrestrial biotic ligand model. 1. Development and application to Cu and Ni toxicities to barley root elongation in soils. Environmental Science & Technology 40(22):7085-7093.

Thakali S, Allen HE, Di Toro DM, Ponizovsky AA, Rooney CP, Zhao F-J, McGrath SP, Criel P, Van Eeckhout H, Janssen CRet al. 2006b. Terrestrial biotic ligand model. 2. Application to Ni and Cu toxicities to plants, invertebrates, and microbes in soil. Environmental Science & Technology 40(22):7094-7100.

Tourinho PS, van Gestel CAM, Lofts S, Svendsen C, Soares AMVM, Loureiro S. 2012. Metal-based nanoparticles in soil: Fate, behavior, and effects on soil invertebrates. Environmental Toxicology and Chemistry 31(8):1679-1692.

Tournassat C, Gailhanou H, Crouzet C, Braibant G, Gautier A, Gaucher EC. 2009. Cation Exchange Selectivity Coefficient Values on Smectite and Mixed-Layer Illite/Smectite Minerals. Soil Science Society of America Journal 73(3):928-942.

Tournassat C, Gailhanou H, Crouzet C, Braibant G, Gautier A, Lassin A, Blanc P, Gaucher EC. 2007. Two cation exchange models for direct and inverse modelling of solution major cation composition in equilibrium with illite surfaces. Geochimica et Cosmochimica Acta 71(5):1098-1114.

Tye AM, Young S, Crout NMJ, Zhang H, Preston S, Zhao FJ, McGrath SP. 2004. Speciation and solubility of Cu, Ni and Pb in contaminated soils. European Journal of Soil Science 55(3):579-590.

U.S. Environmental Protection Agency. 2012. ECOTOX User Guide: ECOTOXicology Database System. Version 4.0. Available: http:/www.epa.gov/ecotox/

Veltman K, Huijbregts MAJ, Hendriks AJ. 2010. Integration of biotic ligand models (BLM) and bioaccumulation kinetics into a mechanistic framework for metal uptake in aquatic organisms. Environmental Science & Technology 44(13):5022-5028.

Veltman K, Huijbregts MAJ, Van Kolck M, Wang WX, Hendriks AJ. 2008. Metal bioaccumulation in aquatic species: Quantification of uptake and elimination rate constants using physicochemical properties of metals and physiological characteristics of species. Environmental Science and Technology 42(3):852-858.

Voegelin A, Jacquat O, Pfister S, Barmettler K, Scheinost AC, Kretzschmar R. 2011. Time-Dependent Changes of Zinc Speciation in Four Soils Contaminated with Zincite or Sphalerite. Environmental Science & Technology 45(1):255-261.

Vulava VM, Kretzschmar R, Rusch U, Grolimund D, Westall JC, Borkovec M. 2000. Cation competition in a natural subsurface material: Modelling of sorption equilibria. Environmental Science & Technology 34(11):2149-2155.

Wang C, Zhu N, Wang Y, Zhang F. 2011a. Co-Detoxification of Transformer Oil-Contained PCBs and Heavy Metals in Medical Waste Incinerator Fly Ash under Sub- and Supercritical Water. Environmental Science & Technology 46(2):1003-1009.

Wang P, De Schamphelaere KAC, Kopittke PM, Zhou DM, Peijnenburg W, Lock K. 2012. Development of an electrostatic model predicting copper toxicity to plants. Journal of Experimental Botany 63(2):659-668.

Wang P, Kinraide TB, Zhou D, Kopittke PM, Peijnenburg WJGM. 2011b. Plasma membrane surface potential: dual effects upon ion uptake and toxicity. Plant Physiology 155(2):808-820.

Wendling LA, Ma YB, Kirby JK, McLaughlin MJ. 2009. A Predictive Model of the Effects of Aging on Cobalt Fate and Behavior in Soil. Environmental Science & Technology 43(1):135-141.

Wu F, Mu Y, Chang H, Zhao X, Giesy JP, Wu KB. 2012. Predicting Water Quality Criteria for Protecting Aquatic Life from Physicochemical Properties of Metals or Metalloids. Environmental Science & Technology 47(1):446-453.

4. Toxicity of organic chemical emissions

4.1. Spatial differentiation of ecotoxicity and human toxicity: the assessment of drivers of variability in fate and exposure

S. Sala[1], A. Kounina[2], D. Marinov[1], B. Ciuffo[1], M. Trombetti[1], S. Humbert[2], O. Jolliet[2], M. Margni[2], D. Pennington[1]

[1]Joint Research Centre, Italy
[2]Quantis, Lausanne, Switzerland

4.1.1. Introduction

4.1.1.1. Project scope

Multimedia and multi-pathways exposure models have been recognized as being suitable characterization models to generate characterization factors for ecotoxicity and human toxicity impact categories in Life Cycle Assessment (LCA) (Udo de Haes et al. 2002; Finnveden et al. 2009).

Inter-continental variation has been analysed, e.g., by a nested parameterization of the IMPACT 2002 model (Rochat et al. 2004), a nested continent in a global box, similar to USEtox ,but with continent specific parameterization for each continent. At this scale, the results of these models have been estimated to vary because of spatial inhomogeneity by a factor of 5 to 10 between continents. However, it is still to be demonstrated whether regionally differentiated nested models correctly mimic the results of spatially resolved model that model advection exchanges between multiple continents. To test this, nested model can be compared with the IMPACT World model (Shaked 2011) that model media specific concentrations and intake fractions in 17 fully interconnected sub-continental regions.

For higher resolutions, *intra-continental variation* can be represented at several resolutions, e.g., 1*1 degree grid cells for the MAPPE Global and 1*1 km for the MAPPE Europe model (Pistocchi et al. 2010), ecological zones with a continental coverage for the BETR North America model (MacLeod et al. 2004) or subwatershed resolution for emissions in water in a parametrization of the IMPACT 2002 model (Manneh et al. 2010). Intake fractions vary up to six (MacLeod et al. 2004) or 10 orders of magnitude (Manneh et al. 2010).

However, the choice of resolution should consider both the required differentiation from a scientific relevance standpoints and the constraints from a practical standpoint (Sedlbauer et al. 2007). Indeed, limiting the requirement for a large amount of geographical data e.g., meteorological, population, agricultural zones whilst keeping a high level of precision is possible by simplifying the spatial regionalization approach. Humbert et al. (2011) showed that intake fraction from inhalation of primary matter can be modeled based on emission release height and “archetypal” environment (indoor versus outdoor; urban, rural, or remote locations). Several other authors have already used the archetype approach for the

estimation of human toxicity impact from emissions to air (indoor – Wenger et al. (2012), urban continental (Rosenbaum et al., 2011). For water , Pennington et al. (2005) showed that for a spatialized model in Europe at 2x2.5 degree scale, differences of several orders of magnitude can occur between watersheds, but no archetype has been developed so far for water related fate and exposure.

This work is divided in two parts. The first is performed by JRC (only part on marine ecotoxicity is developed by Quantis) and addresses several aspects of regionalization, analyzing drivers of spatial differentiation (affecting removal rates and fate) at several scales. The objectives of this part are as follows:

- Clustering organic pollutants according to their chemical properties
- Analysing spatial differentiation of removal rate from air, soil, ocean and freshwater with the MAPPE global model
- Performing a sensitivity analysis of the MAPPE Global model (air/soil/water) supporting the development of emission archetypes based on climatic region
- Analysing spatial variability of fate factors for freshwater and soil compartment for aquatic ecotoxicity
- Evaluating the variability of FFs for terrestrial and marine ecotoxicity
- Analysing spatial variability of intake fractions for human toxicity due to inhalation calculated with MAPPE Europe
- Provide a proposal for compartment specific archetypes based on key parameter influencing chemical fate

The second part of the work is developed by Quantis and aims at selecting an appropriate model and spatial resolution for the freshwater ecotoxicity and human toxicity categories (by all exposure routes) in order to keep a high level of precision while limiting the requirement of a large amount of geographical data. More specifically, it primarily focuses on fate in water and ecosystem and human exposure through water pathways, aiming to:

1. Develop continent specific parameters for USEtox
2. Evaluate *inter-continental variation* by comparing a nested USEtox model with continent specific parameterization versus a fully connected IMPACT World model.
3. Study *intra-continental* variation and develop archetypes for freshwater ecotoxicity and human toxicity exposure to drinking water and fish, as a parsimonious surrogate to higher resolution spatialization.

4.1.1.2. Overview of current multimedia models

In the context of chemical impact assessment, an assessment of some key existing models was undertaken in order to assess whether spatial differentiation is needed, and in which cases taking account of geographical variability is crucial. The overview of methods and models typology able to calculate spatially differentiated characterisation factors was carried out in light of balancing the uncertainties related to site-independent models and the complexity/workload of those that are site-dependent.

The main criteria for assessing strengths and weaknesses of the selected models were focused on:

- Environmental compartment/media modelled and considered
- Accounting for transboundary transport
- Exposure pathways considered

- Capability of identifying hot spots (high exposure intensity)
- Geographical coverage
- Model's resolution

Table 4.1.1:Synoptic scheme of the main model type for assessing spatial differentiation in the context of Life Cycle Impact Assessment (modified from Shaked, 2011).

Model type	Model name	Multiple Environmental Media	Transboundary transport	Multi-pathway exposure	High exposure intensity	Global coverage
Generic/ nested Multimedia	CALTox (Maddalena et al, 1995)	one-box	One-box	Ingestion/ inhalation/ dermal	-	no
	USETox (Rosenbaum et al, 2008)	Urban/cont/global	Water and air advection	Ingestion/ Inhalation	Urban compartment	Global
	USES-LCA (Van Zelm et al, 2009)	Local/region/cont/hemispheric	Water and air advection	Ingestion/ Inhalation	Local environment.	Hemispheric
Spatial Multimedia	IMPACTEurope (Pennington et al 2005) and NorthAmerica (Humbert et al, 2009)	136 watersh./ 157aircells 523 watersh./	Water and air advection	Ingestion/ Inhalation	Urban compartment/ + watershed agr.Product	Europe/North America
	GLOBOX (Wegener Sleeswijk and Heijungs, 2010)	239 countries	Water and air advection	Ingestion/ Inhalation	country	Global
	IMPACTWorld (Shaked, 2011)	17 sub-cont. regions 9 oceans + 33 coastal regions	Water & air advection and food trade	Ingestion/ Inhalation	Urban compartment/ costal area	Global
	Mappe Europe (Pistocchi et al, 2010)	1x1 km	Source-receptor matrix		Local condition	Europe
	Mappe Global (Pistocchi et al, 2011)	1x1 degree	Advection from cell accounted		Local condition	Global
Global Climate + Atmospheric transport.	GEOS-Chem (Bey et al, 2001)	Air 2x2.5 degree air cells	-		-	Global

Table 4.1.1 presents a synoptic overview of the typology of models (with few key examples) for assessing spatial differentiation in the context of LCIA and evaluates the extent to which different types of models (generic/nested multimedia, spatial multimedia and global multimedia) meet the key criteria described above.

Generic multimedia models like USEtox (Rosenbaum et al.2008) simulate pollutant transport through air, water and soil, with the one-box version (or a nested box) using averaged environmental and exposure parameters to estimate concentrations, intake fractions, and endpoint impacts in the emission region. These models do not account for spatial differentiation.

Impact Europe spatial (Pennington et al. 2005) and Impact North America (Humbert et al. 2009) and MAPPE Europe (Pistocchi et al. 2010) are able to predict monitored concentration but the geographical coverage cannot cover the entire world. Nevertheless, MAPPE Europe

is highly spatially resolved and provides a user-friendly way to simulate fluxes and concentrations of chemical pollutants at a resolution of 1x1 Km in Europe.

MAPPE Global (Pistocchi et al. 2011) is a spatially-resolved steady state multimedia model capable of calculating removal rate at a resolution of 1x1 degree for the entire globe but lack of a fully integrated atmospheric transport model. It computes the removal rate due to advection from each cell but does not model the transport.

The recent development of the GLOBOX model (Wegener Sleeswijk and Heijungs 2010) represents the first global multimedia model to include exposure. The model could calculate spatially differentiated LCA toxicity characterisation factors on a global scale for human toxicity, aquatic (distinguishing freshwater, lake and marine) and terrestrial ecotoxicity. It builds upon EUSES 2.0 multimedia model, supplemented by specific equation to account for advection of air and water. However, it does not account for urban exposure and it has not yet been compared with or evaluated against measurements. Moreover, some limitations related to pollutant transport between regions were identified (Shaked 2011).

IMPACT World (Shaked 2011) enables determination of Intake Fractions (iF) and characterization factors (CF) for 17 regions of the world, differentiating between location of emission and location of impact.

Therefore, none of the above models fully meet the criteria required for evaluating the globally-distributed human toxicity and ecotoxicity impacts associated with pollutant emissions. This means that different models have to be used to explore different aspects of variability.

Actually, there are two major trends in model development. One is a trend toward more detailed models with higher fidelity to the real system, driven by the availability of highly resolved environmental data, increases in computer power, and progress in atmospheric and earth sciences. The other trend is toward models that are tailor-made to specific scientific questions or decision-making problems, driven by the philosophy of parsimony and the increase in the need for scientific results as a basis for decision-making (MacLeod et al 2010).

Even the most sophisticated mathematical models can only provide a simplified representation of reality. Hence, the choice of the model to be used in assessing spatial variability was done considering that the set of models and their results, despite their uncertainties, are robust enough to draw some preliminary conclusion. Actually, Mappe Europe and Impact Europe model were also separately assessed against monitoring data (Pennington et al2005; Vizcaino and Pistocchi 2010) and they represent a good combination toward robust conclusions, at least at European scale.

The present study capitalises on the strength of four models (MAPPE global, MAPPE Europe, IMPACT world and IMPACT Europe) in order to provide insight on different aspects of spatial differentiation. The analysis of the varaibility is performed along several steps of the cause effect chain: from the analysis of the variability of removal rates (MAPPE GLOBAL) and variability of fate factors in water and soil at high resolution (MAPPE Europe) to the assessment intra- and inter-continental variation with IMPACT World and Europe. The methodological section and the related results section is organised as in the following scheme.

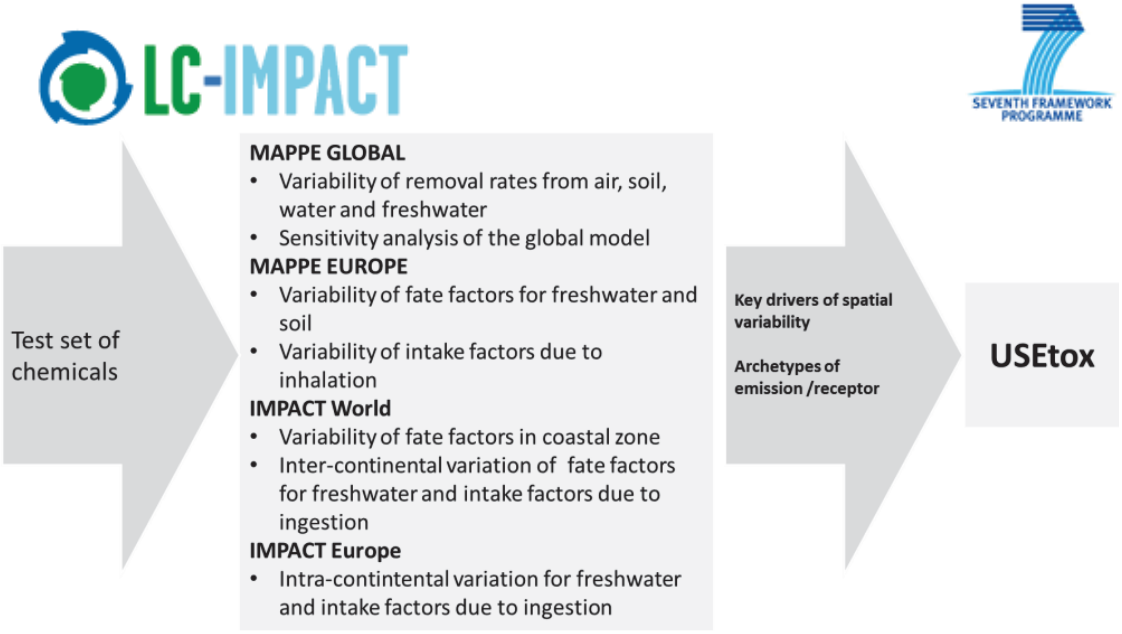

Figure 4.1.1 Overview of the adopted models and the key issues addressed in term of spatial differentiation

4.1.2. Methodology

In the following sections, the methodology adopted to analyse each of the issues illustrated in Figure 4.1.1 is described.

4.1.2.1. Clustering of organics according to their chemical properties

All analyses performed in this work are based on a test set of 36 chemicals. These substances form a set of non-dissociating and non-amphiphilic organic chemicals that represent well the variability of physico chemical properties of organic substances (Margni et al. 2002; Margni et al. 2003). This set covers all relevant combinations in terms of environmental partitioning and exposure routes, overall persistence, long-range transport and feedback fraction (fraction of an emission that returns to the medium of release after transfer to other media). The physical and chemical properties of these organic chemicals are presented in supporting information (Table S4.1). Following the guidelines presented by Gouin et al. (2000) and Margni (2004), the substances were clustered in group and classified as substances that will likely be found mainly in water, soil or the air compartment. The position of the different chemicals within the chemical space is presented in supporting information (SI) (Figure S4.1). In running the models, we use all the chemicals or only some representative ones depending on specific issues to be addressed and in order to highlight relevant aspects of spatial differentiation.

4.1.2.2. Method for the assessment of spatial differentiation with MAPPE Global

According to Sala et al. 2011, a complete assessment of spatial differentiation requires at least two levels of analysis:

- Assessment of spatial distribution (the range of potential environmental geographical distribution of chemicals) in order to understand at which scale a chemical is typically distributed (local, regional, global etc.) and

- Assessment of spatial variability (the variability of the distribution and fate of a chemical among various scenarios, continents, countries).

We use the multimedia models MAPPE Global and MAPPE Europe, whose main characteristics and details are described in SI, for exploring the spatial distribution and spatial variability of fate of chemicals in the environment.

The spatial differentiation evaluation was organized as follows:

- Spatial distribution. We propose a framework to assess the hypothetical spatial distribution and optimal geographical resolution for the fate assessment of chemicals on the basis of their physical chemical properties. Organic chemicals were clustered dividing chemical space according to likely similar environmental behaviour. A range of likely geographical distribution was assigned to each chemical group.
- Spatial variability. The representative test set of 36 chemicals were used to run MAPPE Global and MAPPE Europemodels in order to identify the relevance of performing a spatially differentiated assessment, considering different steps in the environmental cause-effect chain (from removal rates to FFs and iFs).

4.1.2.2.1. Method for assessing spatial distribution based on physical chemical properties

Reviewing the literature, we develop a screening guidance on spatial distribution based solely on physical chemical properties and persistence of chemicals. Sala et al 2011 assigned to each cluster of chemicals a potential spatial distribution, defined as the scale of likely distribution of a chemical (local, regional, continental and global). The spatial distribution is assigned to each combination of chemical properties and overall persistence as presented in

Table 4.1.2. This was built upon the result of the OECD tool (Wegmann et al. 2009) and a literature review on spatial distribution/range of different class of chemicals (Wania and Mackay 1993; Fenner et al. 2005, Scheringer et al. 2002; Wania 2006; Wania and Su 2004, Scheringer et al. 2000; Leip and Lammel2004; Hollander et al. 2009; Von Waldow et al. 2010, Liu et al. 2010, Weber et al. 2010). The OECD tool is a multimedia fate models designed for estimating overall persistence (POV) and long-range transport potential (LRTP) of organic chemicals at a screening level. The literature review as been focused on better defining environmental behaviour of chemical in specifical area of the chemical space.

As a first step, screening level guidance on spatial distribution can be based just on physical- chemical properties and may support the identification of the range/distribution of the chemical (from local to global scale). However, it is necessary to run multimedia models in order to perform a comprehensive analysis of spatial variability and assess the spatial resolution necessary to reduce uncertainties in assessing chemical fate. e.g., a chemical with a limited spatial range/distribution doesn't require a high resolution model if the variability in fate at global scale is low. This is usually related to strong partitioning properties that are more relevant compared to environmental properties. On the contrary, a chemical that distributes at global scale may require a continental or sub-continental model if the area of emission affects the pattern related to the fate (when there is a clear influence of the continent where the emission occurs as, e.g., in Leip and Lammel, 2004). This represents a fundamental step for further identification of appropriate archetypes as a simplified approach to spatial modeling.

Table 4.1.2: Guidance on spatial distribution of the chemicals based on Long Range Transport metrics (physical chemical properties and persistence)

Subsections	Log Kow	Log Kaw	Log Koa	<1 day	1 day <x<1 week	1 week <x< 1 month	>1 month	Main fate compartment
1a		>-0.5	<4	L	R/C	Co/G	Co/G	Air
1a[a]		>0	<6.5	R/C	G	Co/G	Co/G	Air (fliers)
2a	<1	<-6		L	R/C	Co/G	Co/G	Water
2b	<1	-6<x<-4.5		L	R/C	Co/G	Co/G	Water
3a	>6		>8	L	L	R/C	Co/G	Solid
3a[b]	>6	<-6		L	L	R/C	R/C	Solid
3a[c]	>6		>10	L	L	R/C	R/C	Solid
3b	5<x<6		>8	L	L	Co/G	Co/G	Solid
4a	1<x<5	-4<x<-0.5	4<x<6	L	R/C	Co/G	Co/G	Multimedia
4b	1<x<5	-4.5<x<-0.5	6<x<8	L	R/C	Co/G	Co/G	Multimedia
5a		-4.5<x<-0.5	<4	L	R/C	Co/G	Co/G	Air-water
6a	1<x<4	-6<x<-4.5	<8	L	L	Co/G	Co/G	Water-solid
6b	1<x<2	<-6		L	L	R/C	Co/G	Water-solid
6c	2<x<5		>8	L	L	R/C	Co/G	Water-solid
7a		>-0.5	4<x<6	L	R/C	Co/G	Co/G	Air-solid
7b	>5		6<x<8	L	R/C	Co/G	Co/G	Air-solid

Subsection's number (1a, 2 a, 2b etc) refers combination of Log Kow and Log Kaw, identifying specific areas in the chemical space. More details in Sala et al 2011. The coloumns with <1 day, 1 day<x< 1 week etc. refer to persistence of the chemical. For each combination of Log Kow, Log Kaw and persistence, a spatial scale could be assigned: L= local scale (up to 10^1 Km); R= regional scale; C= country scale (up to10^3 Km); Co/G= continental/global scale (10^4 -10^5 Km) ;[a] So volatile that they don't deposit to the Earth's surface, even under the condition of the Artic Environment (Wania 2006);[b] Transport reduced by deep sea export (Scheringer et al 2002) ;[c] Single hoppers, tending to be associated with particles in the atmosphere, usually deposited irreversibly to the Earth's surface (Wania 2006)

4.1.2.2.2. Method for assessing spatial variability of removal rates (air/soil/water) with MAPPE GLOBAL

Spatial variability of removal rates was analysed using MAPPE Global in order to identify drivers and patterns of variability related to key environmental parameters. For each chemical of the test set, the spatially explicit multimedia model MAPPE GLOBAL was run to assess the variability of removal rates from different compartments. We analysed the variability of removal rates from air (k_{air}), from soil (k_{soil}) and from sea/ocean (k_{sea}) governing environmental fate of chemicals emitted in air, soil and sea/ocean.

k_{air} total is the sum of 5 removal rate processes: Particle dry deposition (k_{part}), Wet deposition (k_{wet}), Gas absorption (k_{gas}), Degradation ($k_{deg,a}$) and Advection (k_{adv}).

$$k_{air} = k_{part} + k_{wet} + k_{gas} + k_{deg,a} + k_{adv} \quad 4.1.1$$

k_{soil} is the sum of Volatilization (k_{vol}), Runoff (k_Q), Degradation in soil ($k_{deg,s}$), Erosion (k_{er})

$$k_{soil} = k_{vol} + k_q + k_{deg,s} + k_{er} \quad 4.1.2$$

k_{sea} is the sum of sinking with organic carbon (k_{settl}), volatilisation (k_{vol}), degradation in water ($k_{deg,w}$), and advection due to sea flow (k_{adv})

$$k_{sea} = k_{settl} + k_{vol} + k_{deg,w} + k_{adv} \quad 4.1.3$$

Detail for calculation of k_{air}, k_{soil} and k_{sea} are reported in Pistocchi et al 2011.

An additional removal rate, the load to the sea, was assessed specifically for analyzing the capability of a chemical emitted in a watershed to reach the sea/ocean. At watershed level, the load to the sea is influenced by the K_{soil} and by the specific river's characteristics.

Additionally, we performed a variance-based sensitivity analysis of the MAPPE model in order to identify key parameters influencing the overall variability of the results and driving the spatial patterns.

Results of the model run for 36 chemicals are presented in the following sections, where representative patterns of removal rate from air, soil, sea and freshwater are reported.

4.1.2.3. Sensitivity analysis of MAPPE Global for supporting the development of emission archetypes

The sensitivity analysis (SA) or *importance ranking* aims at understanding "how uncertainties in the model outputs can be apportioned to different sources of uncertainties in the model inputs" (Saltelli et al. 2004). In other words *the objective of the sensitivity analysis is to inform the modeller of the relative importance of the uncertain inputs in determining the variables of interest*. For this reason it plays an important role in model understanding, simplification and, in particular, in supporting the identification of the crucial parameters to be optimised to reduce the uncertainty in themodel outputs.

Model sensitivity analysis generally involves some statistical treatment of the input/output relations drawn within the uncertainty propagation step.

Attempts at applying sensitivity analysis techniques to spatial multimedia models are reported in literature and have focussed on evaluating:

- the behaviour of a spatially resolved multimedia model and its comparison with the results of a non spatially resolved one (Pennington et al., 2005);
- the influence of a specific environmental input on the final result,e.g. analysis of role of forest (Wania and McLachlan 2001), or the influence of precipitation (Jolliet and Hauschild 2005) on the outputs of the model;
- the relative influence of environmental or chemical based inputs in affecting the final results (e.g. Hollander et al. 2009, using stepwise multiple regression analysis; Schenker et al. 2009 adopting rank correlation based approach to provide new insight into important processes that govern the global fate and persistence of DDT in the environment, Macleod et al. 2002 adopting an analytical approach to map the propagation of the uncertainty in the inputs to the uncertainty in the outputs of chemical fate and accumulation models).

Hence, in the context of multimedia models, sensitivity analysis may play a relevant role in evaluating the robustness of models but also in supporting the assessment of spatial differentiation.

Approaches applied so far, however, have not included an exhaustive exploration of the inputs' domains and therefore do not ensure the correct evaluation of the relative influence of model inputs. As an example, the Spearman Rank Correlation Coefficients used in Shenker et al. (2009) is an easy to compute and powerful tool for assessing the relative importance of model inputs. In contrast to other methods it is able to consider non-linear models, but not non-monotonic ones, which could be the case of fate models. Most importantly, none of the approaches used so far has considered influence on the model outputs of inputs' interactions. If this might be reasonable when the objective of the study is to get preliminary

insights into the model behaviour, inputs' interactions cannot be neglected when the objective of the analysis is the model simplification as in the present case. In fact, if the interactions of two or more inputs account for a considerable share of the output variance - and one of the inputs involved is kept fixed because it is considered not influential, then-- there is the risk of significantly distorting the capability of the model to reproduce the reality.

For the abovementioned reasons, in this work, we adopt a Monte Carlo framework to perform global sensitivity analysis. The approach is based on the calculation of the Sobol sensitivity indices, that is, the conditional variances of the model outputs with respect to the different model inputs (Saltelli et al. 2008). The Monte Carlo framework is based on Sobol quasi-random sequences, used to evaluate the model in different combinations of model inputs, following the methodology described in Saltelli et al. (2008, 2010). Both first order and total effects indices are considered in order to capture the importance of each single input and their interactions.

It is worth noting that Monte Carlo approach applied to the spatial parameters of box models has been criticized in Hollander et al. (2009), where the authors argued that in this case, Monte Carlo approach may lead to a significant overestimation of the spatial variation effects. Further arguments to support this thesis are not provided by the authors. In our opinion, this criticism can be motivated by the risk that the analyst is not able to reasonably identify possible correlations among the inputs and to define reasonable ranges and distributions for the same inputs. In the present study, we claim to have been careful enough in order for this criticism not to hold. We also deem that the Monte Carlo framework with a sufficient coverage of the inputs' domain is the most appropriate tool for this kind of analysis.

Sensitivity analysis techniques have been applied to MAPPE Global (Pistocchi et al 2011) to identify key parameters and support the development of emissions' archetypes (Ciuffo et al. 2012). Using a Monte Carlo framework, we applied variance-based sensitivity analysis techniques to find out those environmental parameters explaining the highest share of the variability (namely the variance) in the model outputs.

4.1.2.4. Method for assessing the spatial variability of FFs in freshwater and soil compartment

In order to understand the spatial variability of chemicals distribution and fate, it is necessary to test models at high resolution. For this purpose, we run the multimedia models MAPPE Europe (for the freshwater and soil compartments assessing freshwater ecotoxicity) and MAPPE Global (for the soil compartment linked also to terrestrial ecotoxicity).

MAPPE Europe is a GIS based model which provides a user-friendly way to simulate fluxes and concentrations of chemical pollutants emitted by industrial activities, other diffusive or point source chemical emission, or widespread-used substances within households or the urban environment. The target contaminants are organic compounds such as Persistent Organic Pollutants (e.g. polychlorinated biphenyls, dioxins), pesticides, pharmaceuticals, volatile organic compounds, or other industrial chemicals. Spatial extent is the European continent with resolution of 1x1 km. The spatial variability of fate factors has been evaluated at higher resolution with MAPPE Europe. The results for freshwater were already presented in deliverable 1 (further details reported in supporting information S9),

showing that, for Europe, the average value at continental scale is close to the value of a box model, such as USEtox. Nevertheless, at higher resolution, the variability increases up to 6/7 orders of magnitude with significant differences between major rivers/watershed and minor ones.

Therefore, we ran the spatially resolved model MAPPE Europe, under an agricultural emission scenario, to further exploring the spatial variability at different scales. Two emission scenarios were adopted:

(1) uniform emission of 1 kg/Km^2 of the pesticide endosulfan in agricultural areas across Europe;

2) uniform emission of 1 kg/Km^2 of the pesticide endosulfan everywhere in Germany.

The agricultural emission related to a soil/water scenario assumes an emission into soil with a 1% of drift.

We then, ran MAPPE Global, under the scenario of uniform emission everywhere on land at global scale.

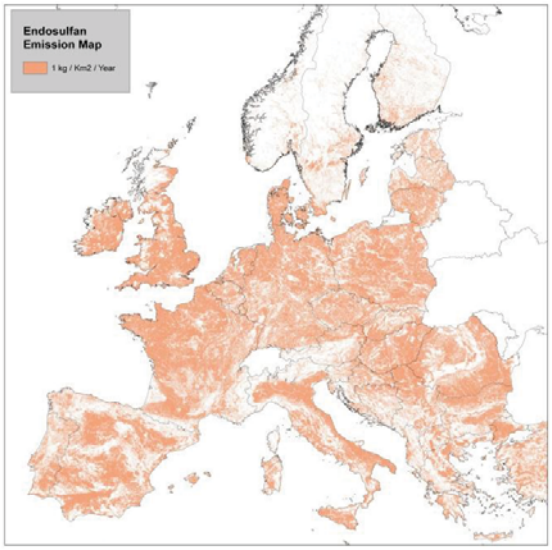

Figure 4.1.2: Emission scenario for Europe: 1kg/km2 per year of endosulfan in agricultural areas

4.1.2.5. Method for the calculation of intake fraction due to inhalation

Several other authors have already used the archetype approach for estimation of human toxicity impact from emissions to air: namelyindoor – Wenger et al. 2012); urban - Humbert et al. 2011); continental and global (Rosenbaum et al. 2011.

Intake fraction (iF) is defined as the fraction of mass of a chemical released into the environment that is ultimately taken in by the human population as a result of food contamination, inhalation, and dermal exposure (Bennett et al, 2002a). The intake fraction iFx, [$kg_{intake}/kg_{emitted}$] can be interpreted as the fraction of an emission into a source compartment m that is taken in by the overall population through a given intake pathway x. A high value, such as iF=0.001 for dioxin (Margni et al. 2004a; Bennett et al. 2002b), indicates that humans will take in 1 part of 1000 of the mass of a chemical released. iF is calculated by multiplying the fate with the exposure factor. This work focuses on the iF as a result only of inhalation. The impact related to intake due to food is presented in latersection, applying the Impact model.

4.1.2.5.1. Calculation of intake fractions (iFs) due to inhalation with MAPPE EUROPE

We calculate the intake fraction due to an emission (E) with MAPPE Europe (resolution 1*1km^2) in three steps:

1. Calculation of Intake Rate coefficient (iR)

4.1.4

First of all we calculated the Intake Rate coefficient at the resolution of 1*1 km for Europe. For each cell, the iR correspond to the quantity that could be inhaled.
The population is specified as the number of inhabitants per km^2 (inhab/km^2). The inhalation through air (direct) depends on the individual's breathing rate, which is averaged over the entire population and assumed to be 13 m^3/day on an individual level (USEPA 1997, the same value is used in USEtox). Other outhors reported breathing rate of 20 m^3/day (e.g. Tainio et al. 2009), leading to higher IR. For allowing comparison with USEtox, we adopted the same values.
The input maps (population density and atmospheric boundary layer height) employed to calculate the *iR* are presented below. The overall volume of air in Europe relative to the 32 countries considered in MAPPE is equal to 1.84 E+15 m^3 (volume of air in USEtox: urban box 5.76 E+10 m^3, continental box 1.00 E+10 m^3).

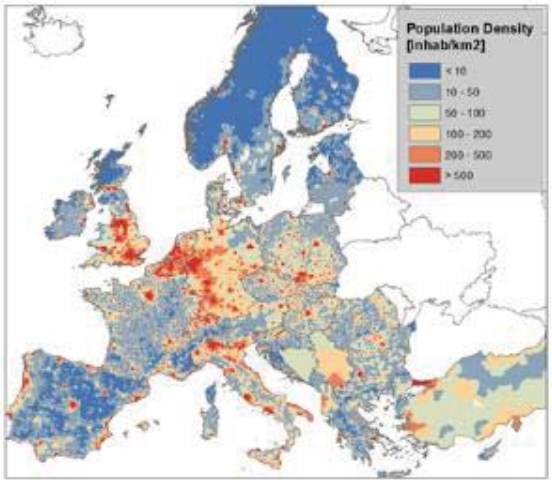

Figure 4.1.3: Map of the population densities across Europe (inhab/km^2). Values: min=0, max= 21022, mean=102.5, SD=299.5. In the legend, last class identify urban zone with population density with more then 500 inhabitants per km^2

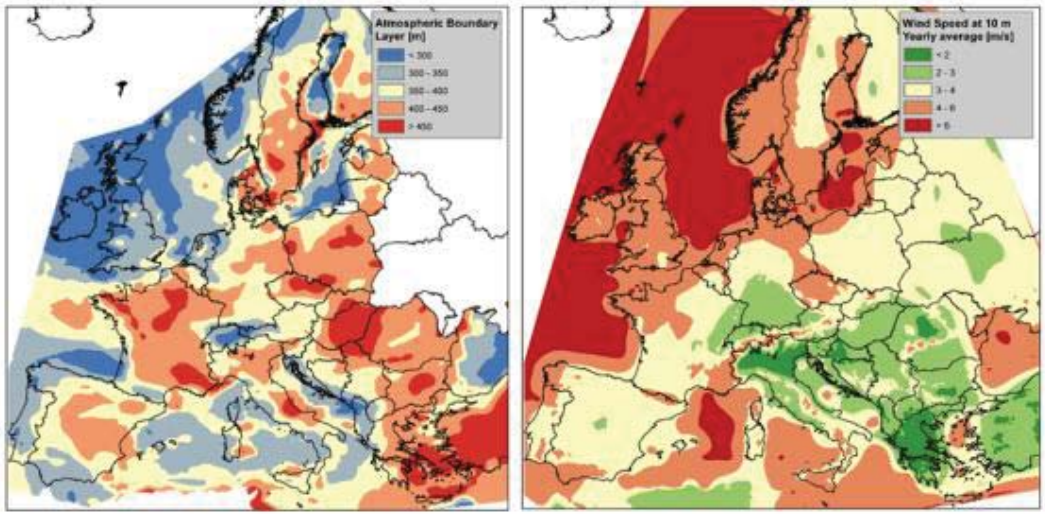

Figure 4.1.4: Map of the distribution of the atmospheric boundary layer height (m) across Europe (Values: min=180, max= 573, mean=374, SD=60) and average wind speed at 10 meters

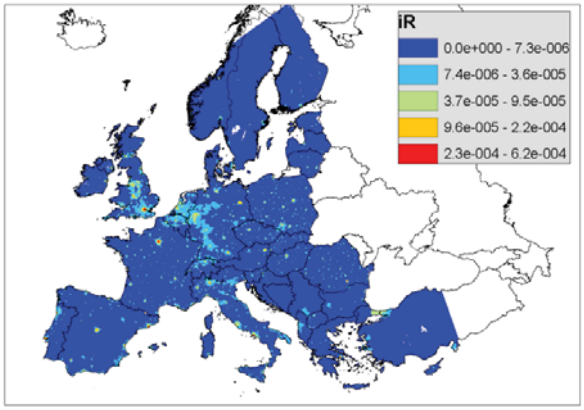

Figure 4.1.5: Map of the distribution of the intake rate coefficient (d-1) across Europe. Values: min=0, max= 6.18 10-4, mean=3.64 10^{-6}, SD=1.06 10^{-5}

As shown in figure 4.1.5, iR across Europe represents a variability of two orders of more than two orders of magnitude. Areas with high population density present higher values. Differences across countries are, then correlated to the distribution of the population (e.g. high values in cities and relatively low in the rural areas as, e.g. France or more uniform distribution across the country as, e.g. in Netherlands).
Obviously, the iR map for Europe is chemical independent but it gives a general idea where higher impact as a result of human inhalation caused by the atmospheric pollution could be expected.

2. Calculation of chemical mass (M) in the air

Pistocchi (2008) and Pistocchi et al. 2010, report the MAPPE model algorithms used for calculating the chemical concentration C [µg/m^3] due to an emission into air.
The current variant of MAPPE model allows computing air concentrations at any point under a specific scenario, namely under the assumption that emissions occur with the same spatial distribution as population density, according to the ADEPT model (Roemer et al., 2005). At

grid cell level the concentrations are computed as the sum of the contributions from *n* emitting countries:

$$C(x,y) = \sum_{i=1}^{n} SR_i(x,y) EMISS_i \exp(-K_{air} * SR\_TT_i(x,y)) \quad \textbf{4.1.5}$$

Where:

- SRi(x,y) is the source-receptor relation for country i-th (i.e. the concentration at point (x,y) provoked by an emission of 1 Mt/year of a non-decaying chemical in the country i-th)
- EMISSi is the annual total emission in i-th country
- SR_TTi (x,y) is the time required on average for a pollutant to travel from sources in country i-th to point (x,y)
- K_{air} is the European average decay rate for the chemical (including all forms of deposition, and atmospheric degradation).

The structure and main features of the SR matrix are reported in supporting information (Figure S4.2-S4.6).

Accordingly, the chemical mass M in the air is calculated, for each grid cell in Europe, as a product of concentration C and volume of air cells V (m^3):

4.1.6

To respect the units the resulting mass M is converted to kg multiplying by 10^{-9}.

3. Calculation of Intake fraction

The intake fraction iF for each grid cell is then calculated as follows:

_____ **4.1.7**

where iR is the intake rate calculated as mentioned above, M [kg] is the mass of the chemical in air and E [kg/day] is the emission.

4.1.2.6. Methods for the selection of an appropriate model and spatial resolution for toxicity categories

Parametrization of USEtox landscape data

We developed parametrized sub-continental and continental specific landscapes in USEtox based on the sub-continental IMPACT World model resolution of 17 zones (Shaked 2011) as in Figure 4.1.6. In a second step, we grouped these 17 zones into 8 continental zones, to match the need for continent specific characterization factors for Life Cycle Assessment studies. The landscape parameters for the continental 8 zones and sub-continental 17 zones are given in supporting information (Table S4.2) where this parametrization is applied to generate impact results for a pollutant as an example (Table S4.3).

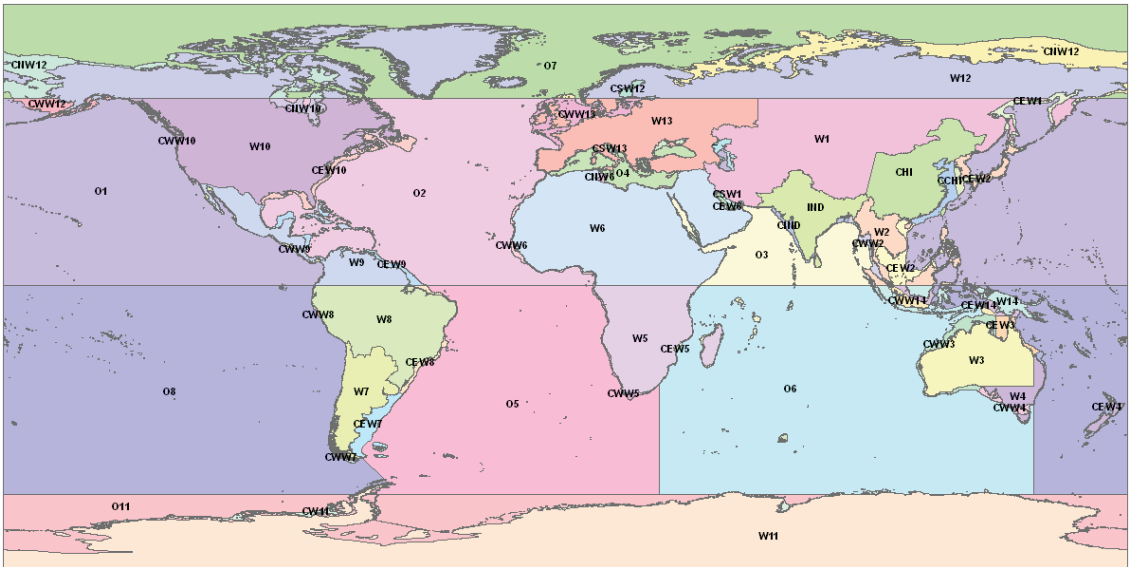

Figure 4.1.6: Sub-continental zones in the IMPACT World model (Shaked 2011)

Inter-continental variation

Nested USEtox 17 zone model and interconnected IMPACT World models have the same resolution and landscape parameters. Beyond this initial similarity, however, fate and intake fraction estimation by these two models vary depending on (1) model fate and exposure algorithms and (2) the landscape definition of the zone surrounding the considered continent, i.e. a single global box for the USEtox parametrized model and multiple other sub-continental zones for the interconnected IMPACT World model. Between these two models, we compared the fate and intake fractions by inhalation, as well as by ingestion through drinking direct water, fish, exposed produce, unexposed produce, dairy and meat products. We also calculated transfer fractions from air to water ($TF_{a,w,}$ *unitless*) and from water to air ($TF_{w,a}$, unitless) based on the following fate factors:

——— **4.1.8**

——— **4.1.9**

Equations of the Transfer fraction from air to water and from water to air calculated based on fate factors

With $FF_{a,w}$ the fate factor in water for an emission to air (days, equal to the mass at steady state in water in kg for an emission flow of 1 kg/day in air), $FF_{w,a}$ (days) the fate factor in air for an emission to water, $FF_{w,w}$ (days) the fate for an emission to water in water and $FF_{a,a}$ (days), the fate factor in air for an emission to air.

We used a set of 36 pollutants selected from the OMNIITOX project (Margni et al. 2002) for this comparison.

Intra-continental variation and development of archetypes

Intra-continental variation was analyzed on a finer resolution with IMPACT Europe model (Pennington et al. 2005).

The model allows two consistent scenarios; one adopting the typical multimedia approach without spatial distinction (i.e. IMPACT Europe single zone model with one homogeneous compartment per environmental medium), the other accounting for spatial differentiation based on watershed resolution. The IMPACT Europe spatial model comprises 135 land zones (watersheds), 124 oceanic zones, 2 x 2.5 degree air grid, nested in a non-spatial global model.

We first compared the water fate factors of the IMPACT Europe single zone model with the IMPACT Europe spatial model, looking both at uniform emissions (i.e. emission distributed in each watershed proportionally to their surface) and emissions into selected watersheds with short, medium and long residence time of water to the sea. We then analyzed the interaction between chemical properties and landscape properties specific to each spatially differentiated watershed to identify the key parameters influencing the fate. Watershed archetypes were defined based on the identified key parameters and compared to the spatial model to evaluate their relevance.

4.1.3. Results and discussion

4.1.3.1. Spatial variability of removal rates in air, soil, ocean and freshwater

4.1.3.1.1. Variability and spatial patter for removal rates – air

The results of the variability of removal rate from air are reported in the figure below.

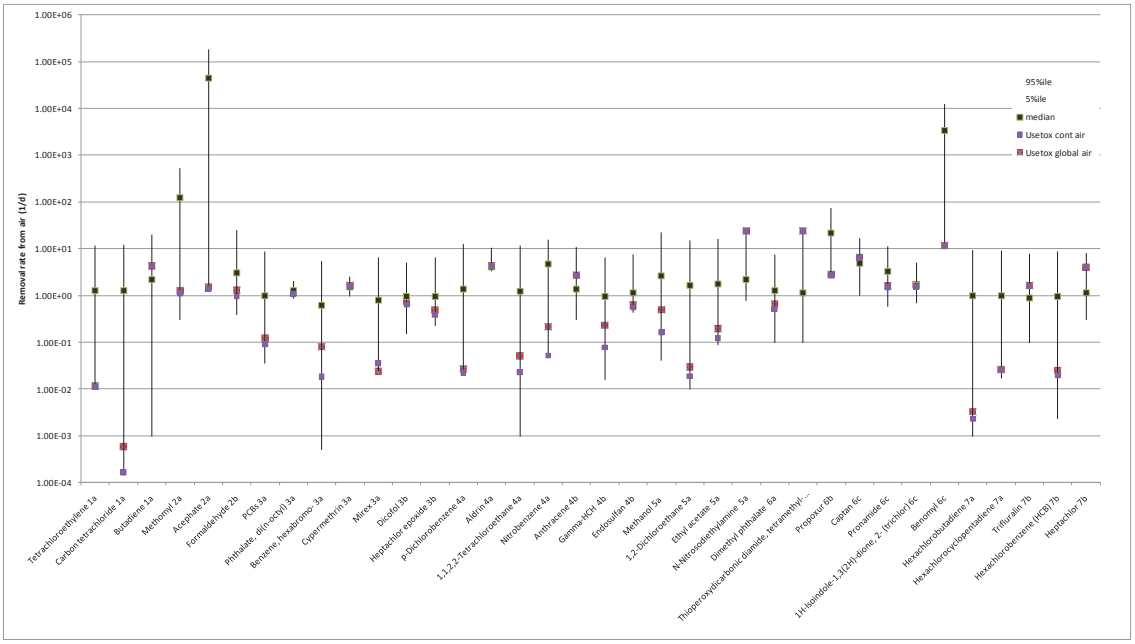

Figure 4.1.7: Removal rates from air for the chemicals in the test set (no advection case)

For air, amongst different clusters of chemicals (1a, 2a etc), the variability is associated with different spatial patterns reflecting key environmental drivers affecting the total removal rate. Example of patterns for Methomyl/Acephate and Butadiene/PCB's dominated by specific removal rates are reported in Figure 4.1.8.

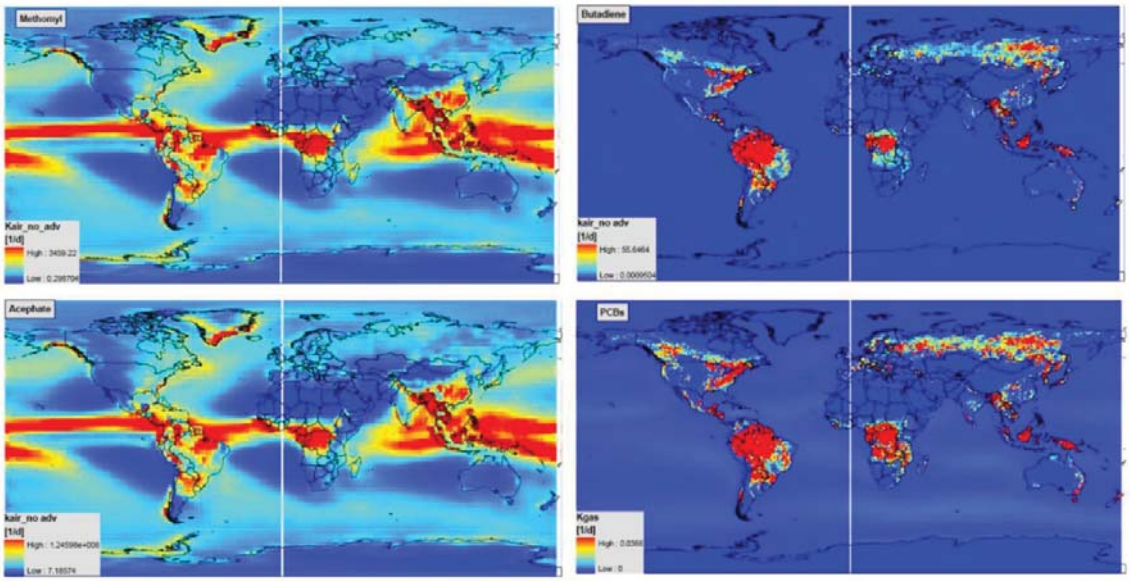

Figure 4.1.8: Patterns of variability for methomyl/acephate (due to wet deposition) and Butadiene/PCB's (due to gas exchange)

For multimedia chemicals, like e.g. lindane, the pattern of spatial variability reflects the relative influence of several removal rates. Figure of each pattern are reported in the SI of the first deliverable. A detailed explanation of this variability is reported in Sala et al. 2011 (and a summary of key finding for the different clusters is in supporting information of the paper, reporting key results of Deliverable 2.1- LC-impact). Comparing the results with USEtox, the results showed that USEtox is close to the 5th percentile of the removal rates from air, water and soil calculated with MAPPE for the majority of chemicals, both considering continental and global air in USEtox. The results for air can be explained considering the roles of gas exchange and wet and dry deposition in the two models. This is due to the fact that we ran the MAPPE model with the same chemical properties of USEtox, and as the removal from stratosphere is a constant value in USEtox. For the wet and dry deposition, MAPPE may overestimate the removal rate as it doesn't account for intermitting rain events but it takes an average annual rain. For the gas exchange, MAPPE distinguishes among various land use, accounting for high gas exchange especially in forested areas. This finding has been further assessed through a sensitivity analysis of key input parameters in MAPPE (see next section).

For multimedia chemicals, like those in 4b, the pattern of variability is related to the interplay of different removal rates (see Figures in Sala et al. 2011) even if substantial contribution is still related to gas exchange since the Kgas is the prevailing removal rate compared to the others. In addition, K_{gas}, Kwet and Kdeg shape the total air removal rates due to their variability at country scale. In Sala et al 2011, the variability of removal rates by countries is presented. Amongst countries, Kgas and Kwet represent variability over 3 orders of magnitude, while Kdeg and K part around one order of magnitude.

Basically, it is not possible to assign spatial variability to a certain group of chemicals based only on their partitioning properties without accounting for the role of degradation. Figure 4.1.9 shows the correlation between variability and persistence in air. There is a good

correlation between persistence and order of magnitude of variability in air. The two "outliners" are methomyl and acephate (both 2a) that have high affinity for water.

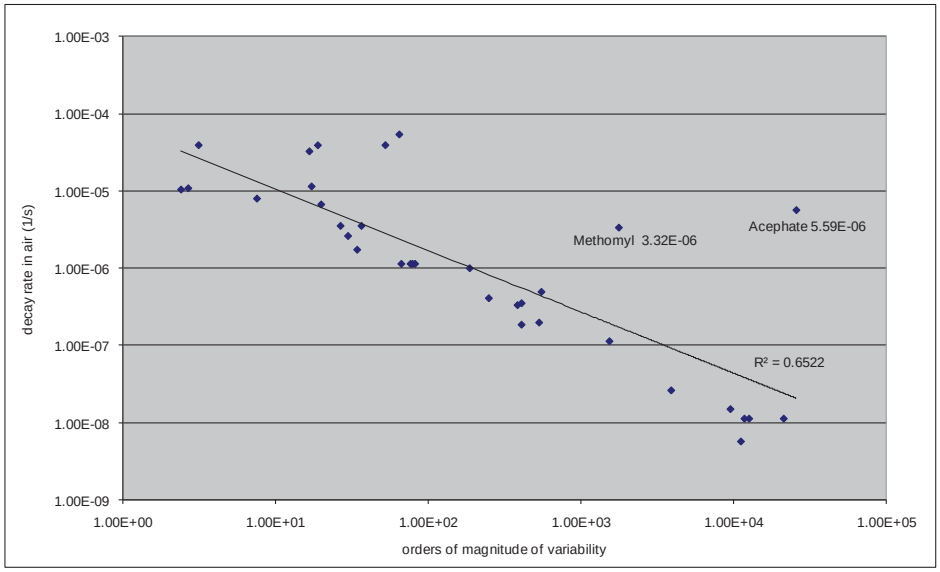

Figure 4.1.9: Correlation between variability (orders of magnitude) and persistence of the chemicals

Potentially, one additional source for the changeability of the intermedia transfer rates is related to the influence of temperature on the spatial variability of the substance physical chemical properties.

To assess this influence, MAPPE Global (Pistocchi et al., 2011) was run considering the impact of variation with temperature of Kaw and Kdeg on the total removal rates (excluding advection) of Lindane. The input parameters vary as follows: kaw for lindane spans over 3 orders; of magnitude of variability Kdeg for lindane span over order of magnitude. The output removal rates were comparend against the case of application of a default global mean value for Kaw and kdeg, as it is the usual practice in fate modelling (USEtox or Impact World among the others). However, the comparison for lindane demonstrated that for multimedia chemicals the impact of ambient temperature seems to be low as shown in the figure below, because the medians and the range of variability of results with and without accounting environmental temperature are quite similar.

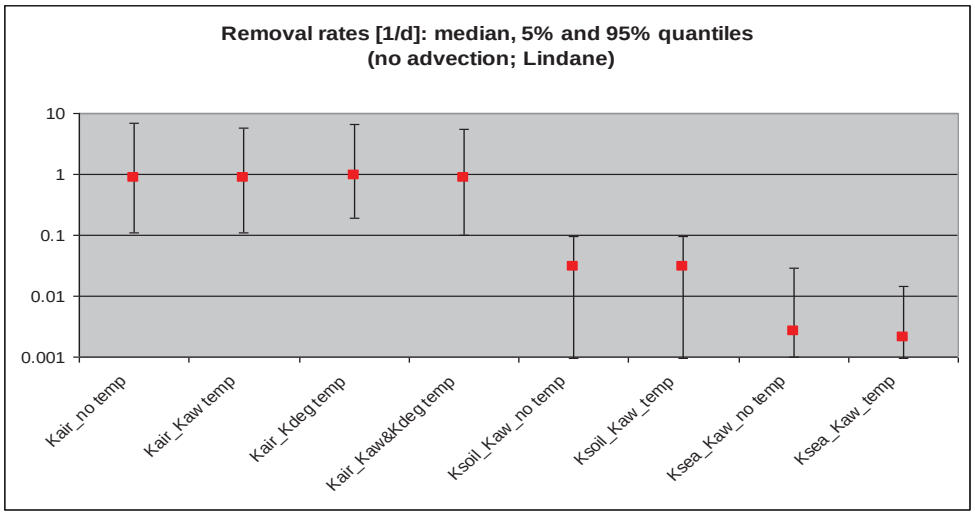

Figure 4.1.10: Effect of ambient temperature on total removal rates (no advection case) for lindane according to MAPPE Global model: medians and range of variability (given by 5 and 95 quantiles) of the air removal rate (1/d) accounting for different scenarios: kair no temperature variation, variation only of Kaw, only of Kdeg, variation of both Kaw and K deg; K soil with and without Kaw variation and Ksea eith and without kaw variation with temperature.

4.1.3.1.2. Variability and spatial patter for removal rates – soil and sea

Unlike removal rate from air, the variability related to removal rates from soil and sea is low for almost all the chemicals in the test set. The results of K soil and K sea are reported in the figures below with the associated patterns of spatial variability.

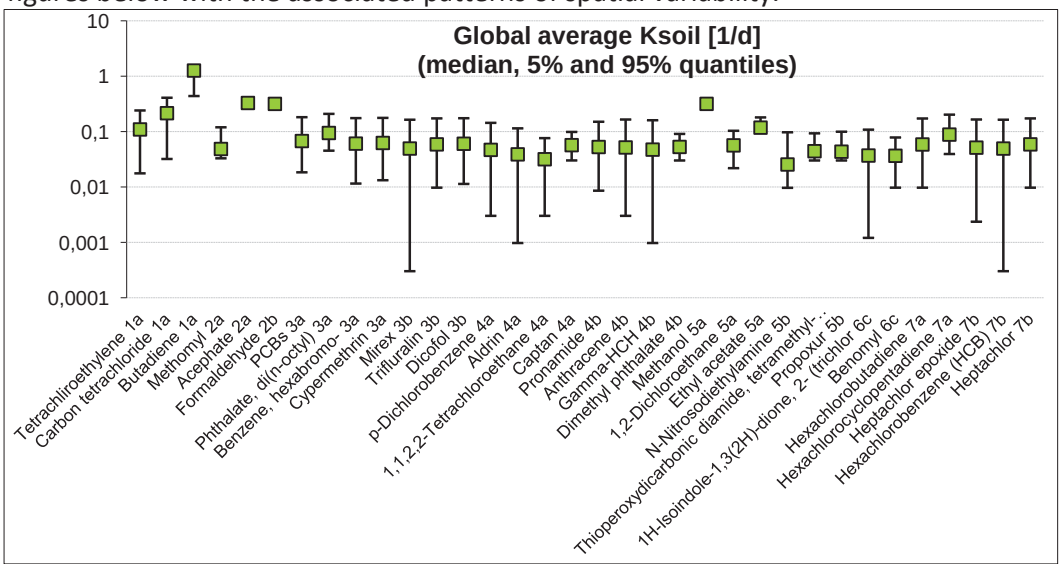

Figure 4.1.11: Removal rates from soil for the chemicals in the test set

In general, the global variability of total removal rates for different chemicals and media spans from less than one up to more than four orders of magnitude depending whether or not the advection is accounted for. As expected, a wider range of variability was observed for the atmosphere and least one for the soil.

For the soil compartment the variability in the total removal rates remains below 2.5 orders of magnitude but for 68% of the chemical groups (23 out of 34) the variability does not exceed more than one order of magnitude.

Furthermore, in order to identify the cause of variation and trying to answer whether or not the variation follows similar spatial patterns, distribution maps at global scale were calculated for all chemicals.

For hydrophobic chemicals, such as those from the 3a group, considering the model results for PCBs, it was confirmed that the environmental fate in soil is basically regulated by degradation followed by erosion (see also the table 4.1.3).

COMPARTMENT		RELATIVE REMOVAL RATE (%)				
AIR		**kgas**	**kwet**	**kpart**	**kdeg**	**kadv**
	No Advection	77.3230	4.7205	0.0002	17.9562	n.a.
	With Advection	46.4402	0.8009	0.0001	2.1495	50.6093
SOIL		**kerosion**	**kvol**	**krun-off**	**kdeg**	
		16.9001	0.6734	3.3080	79.1185	
OCEAN		**ksettling**	**kvol**	**kdeg**	**kadv**	
	No Advection	4.98e-01	23.72169	75.780235	n.a.	
	With Advection	3.99e-02	0.88736	1.01e+00	98.06723	

Table 4.1.3: global average relative removal rates (as % from the total) for lindane in different environmental compartments.

Therefore, a possible reason for the 'homogenisation" of soil removal rates could be the elimination through erosion which is an "chemical independent" process from a hydrological point of view but of course will act on different substances according to their physico-chemical properties (affinity for binding to particles, solubility and volatility).

Therefore, for soil, for the majority of chemicals in the test set the variability is less than one order of magnitude as hydrophobic chemicals tend to remain in soil locally and highly hydrophilic chemicals are subject to runoff/leaching. Amongst the other chemicals, mirex (soil decay rate 3.5 E-9, spatial pattern in figure below), heptachlor epoxide and hexachlorobenzene (soil decay rate 3.5E-9) showed the highest variability because they also have high persistence.

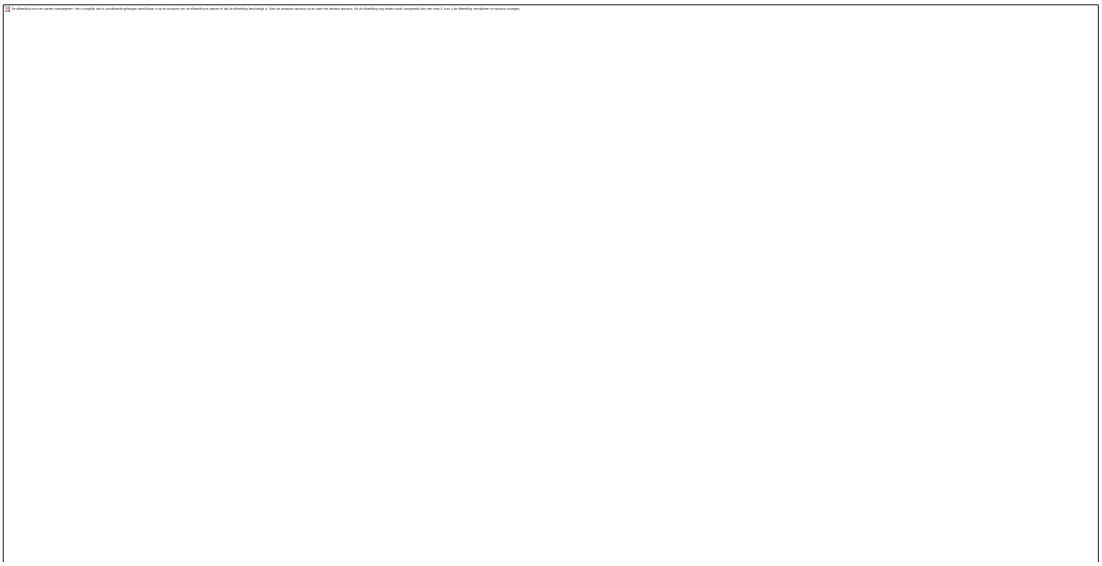

Figure 4.1.12: Spatial distribution of the values of removal rate from soil - Mirex

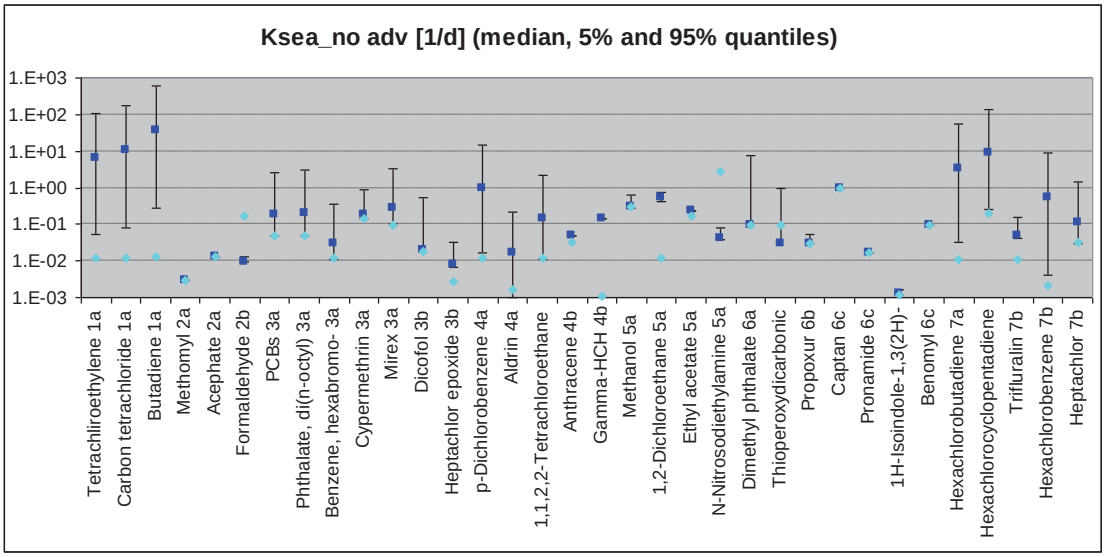

Figure 4.1.13: Removal rates from ocean for the chemicals in the test set (no marine advection case)

For the ocean, the variation in removal rates within the different clusters is:

- 1a; 4a;7a;7b; very high (from 2.5 to 4 orders of magnitude). These are the clusters related to substances potentially subject to high volatilization
- 3a; 3b; 6a; medium (from 1 to 2 orders of magnitude). These are clusters in which the main fate compartment is solid
- 2a; 2b; 4b; 5a; 6b;6c; (less than 1 order of magnitude). These are the clusters where the main fate compartment is water, or the water-solid

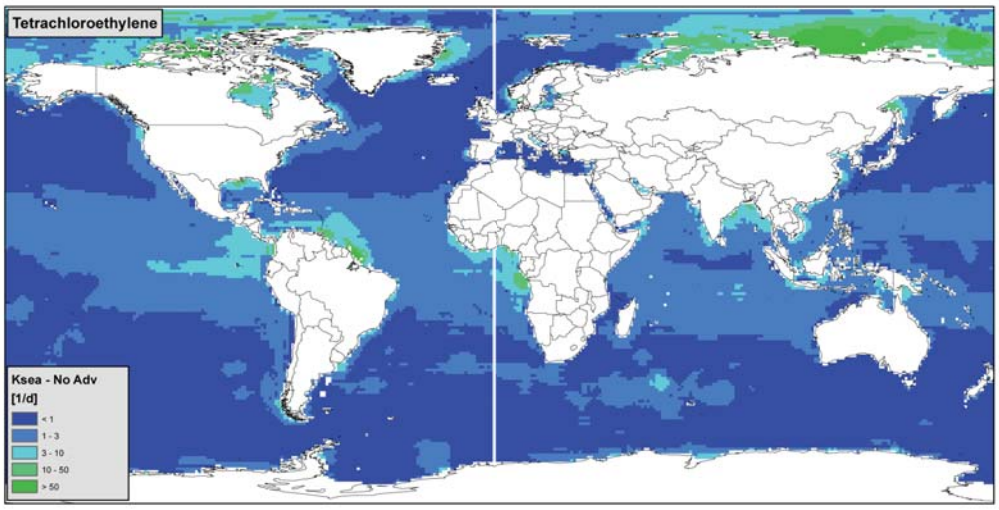

Figure 4.1.14: Pattern of variability of removal rate from ocean for tetrachloroethylene (no marine advection case)

For soil and sea, the use of global default factor for removal rates implies uncertainties that span from less than 1 to 2 orders of magnitude for soil and from less than 1 to 3 orders of magnitude for sea.

Table 4.1.4 reports chemical properties of each cluster of chemicals, the test set of chemicals and their persistence (USEtox database), and a synopsis of variability of removal rates. 1a is the group with higher variability in all the three removal rates; 6a and 6 b show low variability for both air, water and soil; 3a has a low variability except for hexabromobenzene, which is highly persistent in air.

Table 4.1.4 Synopsis of chemicals clusters, associated physico chemical properties, variability of removal rates

Subsections	Log Kow	Log Kaw	Log Koa	Main fate compartment	1day>x>1 week	1 week>x< 1 month	>1 month	Chemicals	Clus	Air decay rate [1/s]	Soil decay rate alpha_s [1/s]	Water decay rate [1/s]	Orders of magnitude of variability in removal rates		
													air	soil	sea
1a		> -0.5	<4	air	R/C	Co/G	Co/G	Tetrachloroethylene	1a	3.50E-07	1.13E-07	1.10E-07	2.50E+00	1.50E+00	3.00E+00
1a*		>0	<6.5	Air (fliers)	G	Co/G	Co/G	Carbon tetrachloride	1a	1.13E-08	3.19E-08	1.13E-07	4.00E+00	1.50E+00	3.00E+00
								Butadiene	1a	1.13E-08	3.50E-07	1.13E-07	4.00E+00	1.50E+00	3.00E+00
2a	<1	<-6		water	R/C	Co/G	Co/G	Methomyl	2a	3.32E-06	3.83E-07	3.49E-08	3.00E+00	<1	<1
								Acephate	2a	5.59E-06	3.64E-06	1.50E-07	4.00E+00	<1	<1
2b	<1	-4.5<x<-6		water	R/C	Co/G	Co/G	Formaldehyde	2b	5.31E-05	3.50E-06	2.01E-06	2.00E+00	<1	<1
3a	>6		>8	solid	L	R/C	Co/G	PCBs	3a	4.07E-07	2.14E-07	5.70E-07	2.00E+00	<1	1.50E+00
3a**	>6	<-6		Solid	L	R/C	R/C	Phthalate. di(n-octyl)	3a	1.03E-05	5.72E-07	5.73E-07	<1	<1	1.50E+00
3a***			>10	Solid	L	R/C	R/C	Benzene. hexabromo-	3a	5.73E-09	1.34E-07	1.34E-07	4.00E+00	1.00E+00	1.50E+00
								Cypermethrin	3a	1.07E-05	1.54E-07	1.60E-06	<1	1.00E+00	1.00E+00
								Mirex	3a	1.13E-06	3.50E-09	1.13E-06	2.00E+00	2.50E+00	1.50E+00
3b	5<x<6		>8	solid	L	Co/G	Co/G	Dicofol	3b	1.72E-06	1.32E-07	2.14E-07	1.50E+00	1.00E+00	1.50E+00
								Heptachlor epoxide	3b	2.59E-06	2.74E-08	2.74E-08	1.50E+00	1.50E+00	<1
4a	1<x<5	-4.5<x<-0.5	4<x<6	Multimedia	R/C	Co/G	Co/G	p-Dichlorobenzene	4a	3.50E-07	3.50E-08	1.13E-07	2.00E+00	1.50E+00	3.00E+00
								Aldrin	4a	3.86E-05	1.13E-08	1.10E-08	<1	1.00E+00	2.00E+00
								1.1.2.2-Tetrachloroethane	4a	1.13E-08	3.50E-08	1.13E-07	4.00E+00	1.50E+00	2.00E+00
								Nitrobenzene	4a	3.90E-05	1.56E-07	1.10E-07	2.00E+00		
4b	1<x<5	-4.5<x<-0.5	6<x<8	Multimedia	R/C	Co/G	Co/G	Anthracene	4b	3.50E-06	3.50E-08	3.50E-07	1.00E+00	<1	<1
								gamma-HCH	4b	1.85E-07	1.13E-08	1.13E-08	2.00E+00	1.00E+00	<1
								Endosulfan	4b	5.00E-06	9.14E-07	1.70E-06	1.00E+00		
5a		-4.5<x<-0.5	<4	air-water	R/C	Co/G	Co/G	Methanol	5a	4.91E-07	3.50E-06	3.50E-06	3.00E+00	<1	<1
								1.2-Dichloroethane	5a	1.13E-07	3.50E-08	1.13E-07	3.00E+00	<1	<1
								Ethyl acetate	5a	9.92E-07	1.13E-06	2.01E-06	2.00E+00	<1	<1
								N-Nitrosodiethylamine	5a	3.21E-05	1.13E-07	3.21E-05	1.00E+00	1.00E+00	<1
6a	1<X<	-4.5<X<-6	6<X<8	water-solid	L	Co/G	Co/G	Dimethyl phthalate	6a	1.13E-06	3.50E-07	1.13E-06	1.50E+00	1.00E+00	2.00E+00
								Thioperoxydicarbonic diamide. tetramethyl-	6a	1.13E-06	3.50E-07	1.13E-06	1.00E+00	<1	1.50E+00
6b	1<x<2	<-6		water-solid	L	R/C	Co/G	Propoxur	6b	3.85E-05	3.50E-07	3.50E-07	1.00E+00	<1	<1
								Captan	6c	1.13E-05	3.50E-07	1.13E-05	<1	<1	<1
6c	2<x<5	<-4.5	>8	water-solid	L	R/C	Co/G	Pronamide	6c	6.62E-06	9.97E-08	1.97E-07	4.00E+00	<1	<1
								1H-Isoindole-1.3(2H)-dione. 2-(trichloromethyl)thio -	6c	7.87E-06	1.40E-08	1.40E-08	1.00E+00	2.00E+00	<1
								Benomyl	6c	3.86E-05	1.13E-07	1.13E-06	<1	1.00E+00	<1
7a		>-0.5	4<x<6	air-solid	R/C	Co/G	Co/G	Hexachlorobutadiene	7a	1.50E-08	1.13E-07	1.10E-07	4.00E+00	1.00E+00	3.50E+00
								Hexachlorocyclopentadiene	7a	1.97E-07	4.58E-07	2.23E-06	3.00E+00	<1	2.50E+00
7b	>5		6<x<8	air-solid	R/C	Co/G	Co/G	Trifluralin	7b	1.13E-06	1.13E-07	1.13E-07	2.00E+00	<1	<1
								Hexachlorobenzene	7b	2.62E-08	3.50E-09	3.50E-09	3.50E+00	2.00E+00	3.50E+00
								Heptachlor	7b	3.50E-06	1.13E-07	3.50E-07	1.50E+00	1.00E+00	1.50E+00

4.1.3.1.3. Variability in the removal rate from watershed: load to the sea and coastal zones

We ran MAPPE Global also to explore the potential contribution of the watersheds across the Globe to marine pollution. The assessment is based on the analysis of the variability of the rate of chemical load to seas and an evaluation of the capability of a chemical to reach the sea after being emitted to soil within a watershed. The unit of the load rate is the same as for the other removal rates (1/d). The load rate to the sea is an indication of the "speed" of the removal processes occuring in the surface water system and the contaminant discharge from catchments to the seas.

The rate of load to oceans (d^{-1}) through surface water, as a fraction of emissions (direct or indirect) occurring to soil, is given as a sum of dissolved and sediment fractions by:

$$\_ \quad \_\_\_\_ \quad \_ \quad \_\_\_\_ \qquad \textbf{4.1.10}$$

where A is the catchment area, dt50,w (d) is the half-life of the chemical in dissolved phase, while the half-life of the sediment phase (dt50,s) is represented by the rate in the dissolved phase (dt50,w) and the ratio of the residence times of the chemical in sediments and in water for the catchment (see Pistocchi et al., 2011)

At the present stage of development of the MAPPE Global model, due to the practical difficulty to assign a value of α for each catchment, and considering the uncertainty in half lives in sediments and in *SSY*, we simply assume that all load with sediments is eventually delivered to the oceans, i.e. α=0 meaning that the exponent in the second term in the above integral is just zero. Moreover, assuming that τ is a single value for each catchment and the half-life is a non-spatial variable but chemical-specific constant, the above expression simplifies to:

$$\_ \quad \_\_\_\_ \quad \_ \qquad \textbf{4.1.11}$$

As an illustrative example a map of the load rate to the sea, following the approach of Pistocchi et al 2011 (the chemical load from soil is transferred to oceans passing only through an exponential decay process accounting for the inland retention time in surface water), has been calculated for mirex. The choice of mirex is based on the fact that this is the chemical with highest variability in ksoil among the chemicals considered. The results show that the pollutant load rate is lower for big watersheds, whereas very high for small basins discharging directly to the sea. The variability is at least 2 orders of magnitudes: from less than 0.05 d^{-1} to over 5 d^{-1}. The hot spots are represented by the right 5% tail of the results (over with values over 5). These are very small catchements in which the chemical emitted is easily and quickly transferred to the sea.

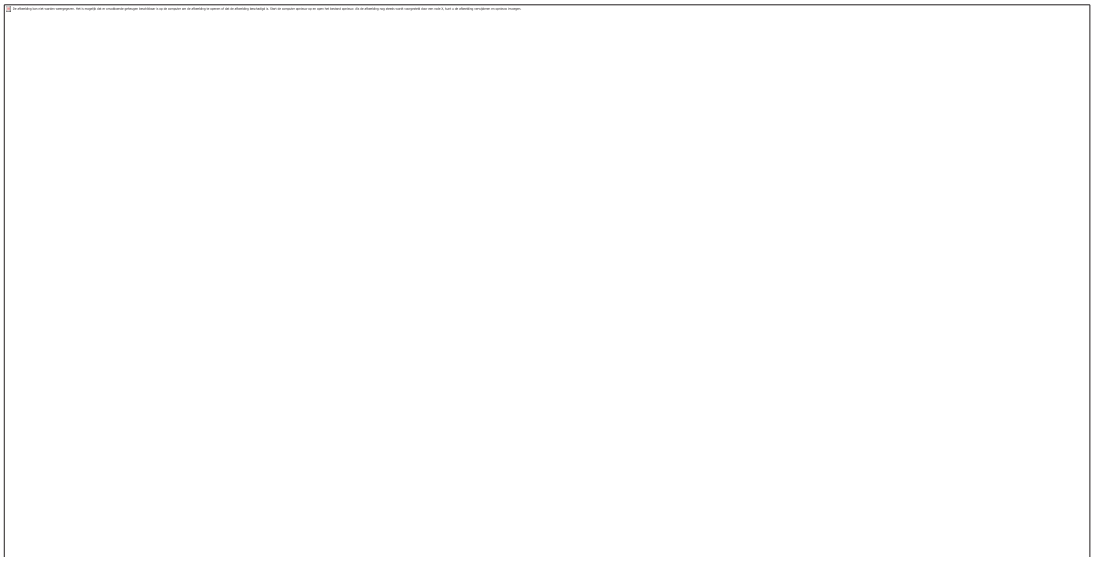

Figure 4.1.15: Average load to the sea for the major watershed across the world. (Statistics: min=0, max=24.3, mean=1.06, SD=2.20; 5% = 0, 95% = 5.9)

A part from the landscape conditions of each basin, the potential of a chemical to reach the sea is also affected by the specific features of the coastal zone. For istance, a spatially explicit global overview of nearshore coastal types, based on hydrological, lithological and morphological criteria has been developed by Durr et al 2011, see figure 4.1.16. Amongst the different types of coastal area, four are considered able to act as filters of both dissolved and suspended material entering the ocean from land: small deltas (type I), tidal systems (II), lagoons (III) and fjords (IV). Large rivers (V) largely bypass the nearshore filter, while karstic (VI) and arheic coasts (VII) act as inactive filters. This typology provides new insight into the spatial distribution and inherent heterogeneity of estuarine filters worldwide. Types I, II, III and IV account for 32%, 22%, 8% and 26% of the global coastline, respectively, while 12% have a very limited nearshore coastal filter.

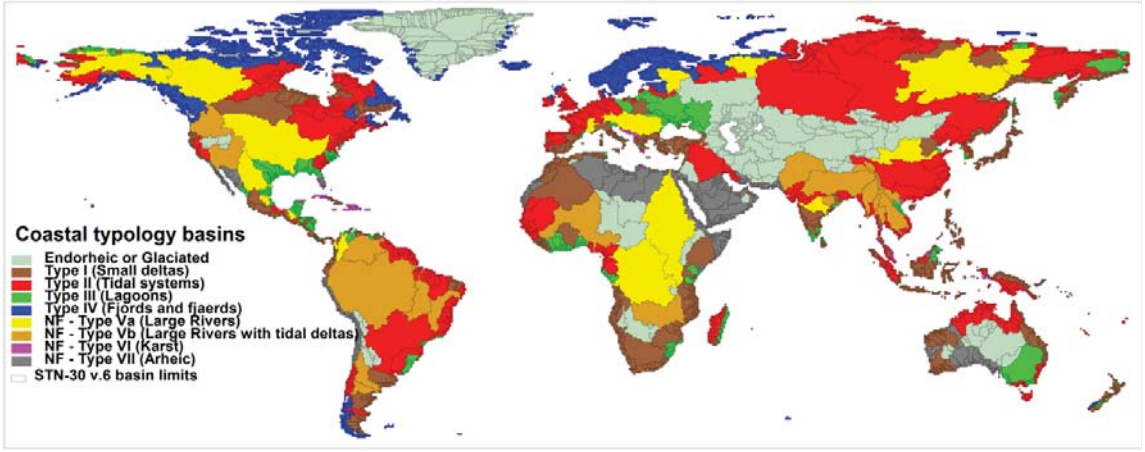

Figure 4.1.16: Coastal typology in the world, from Durr et al 2011. Coastal type with NF in the legend are consider as inactive filter

Accordingly, we prepared a map distinguishing between watershed acting as an active or inactive filter globally and with a further detail for European watersheds.

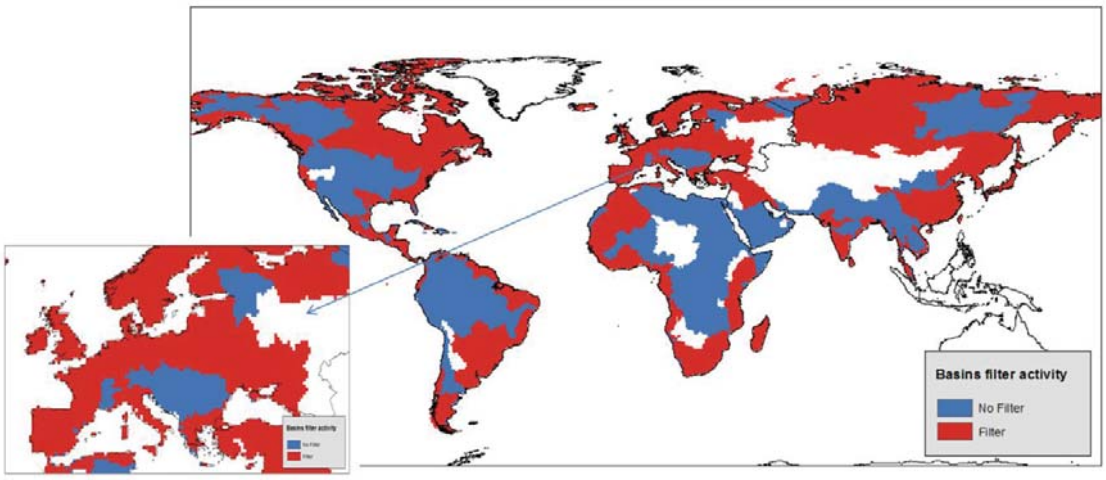

Figure 4.1.17: Distinction between watershed as active and inactive filter. Catchments in white are endoreic, thus not directly involved in the load to the sea. Detailed map on the left presents the distinction between watersheds as active and inactive filter in Europe

By attributing an arbitrary role of filtering to active filtering catchements (in this case of 25%), it is possible to higlight the basins where a reduced chemical load to the sea could be expected. This implies the necessity of taking into account two potential archetypes for marine ecotoxicity based on the filter activity of coastal zone. The first, associated with watershed with filtering activities, should be considered as contributing less to marine ecotoxicity (even if an higher impact may occour in the delta itself); the second (non filtering activitity), in which all of the load to the sea coming from the catchement contributes to marine ecotoxicity.

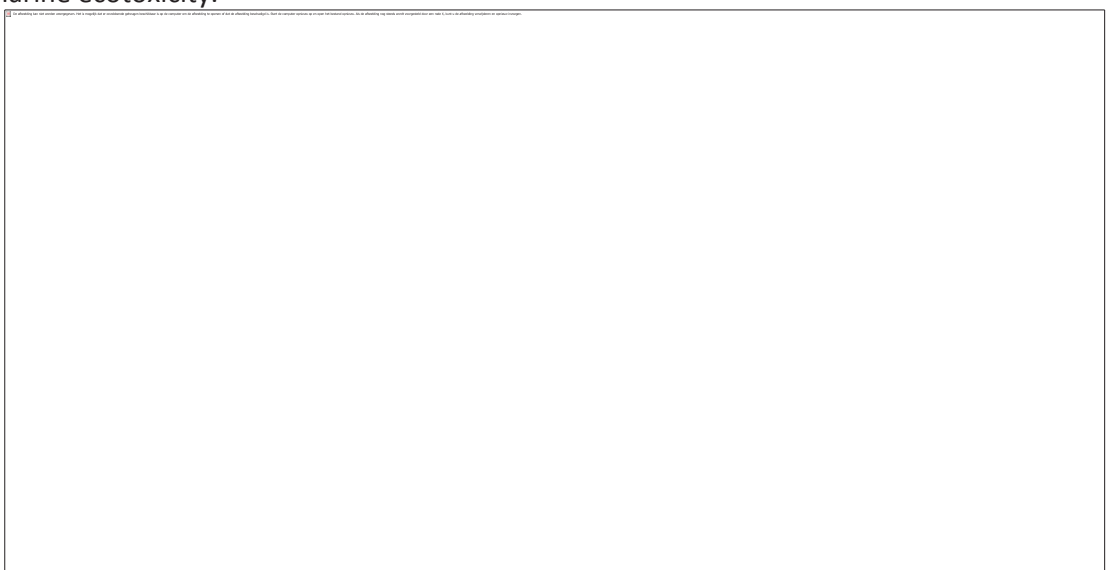

Figure 4.1.18: Basins presenting a reduction of load to the sea due to coastal zone and related value of the load to the sea

4.1.3.2. Sensitivity analysis of MAPPE GLOBAL

4.1.3.2.1. Air compartment

In the logic adopted in MAPPE Global, the main output for the air compartment is the removal rate for air (k_{air}), that is, the amount of a certain chemical emitted in the air compartment that is removed from the place where it is emitted in a reference time period. Different phenomena are considered to mimic the removal process. Among these, the most important for the air compartment is the wind advection. In the approach adopted by MAPPE it is considered that the real removal rate is bounded by the removal rates calculated with and without the advection component (Pistocchi et al. 2011). For this reason, in the present work, the sensitivity analysis has been carried out considering two model outputs: k_{air} and k_{air} (no advection).

Once the relevant outputs have been identified, the second key step for the sensitivity analysis is the identification of the relevant model inputs and their distributions (to be used in the Monte Carlo sampling of their values). In MAPPE we identify three types of model inputs: i) environmental inputs, ii) chemical specific inputs and iii) model parameters. The latter category concerns those inputs calibrated in the process of developing the model and considered as fixed. Though their inclusion in the sensitivity analysis would be interesting (especially with the aim of improving the model behaviour) and meaningful, in the present case, since the interest is more related to understanding how the current modelbehaves, only the first two categories of inputs are considered. In particular, environmental parameters used in MAPPE Global are:

- Atmospheric Boundary Layer (*ABL*)
- Wind Speed (u_{10})
- Organic carbon concentration in atmosphere (*OC*)
- Deposition flux of atmospheric organic carbon (f_{OC})
- Temperature (*T*)
- Precipitation (*P*)
- Coverage/land use, such as forest, impervious surface etc. (*cov*)

while chemical specific parameters are:

- Chemical molecular weight (MW)
- Chemical octanol-water partition coefficient (K_{ow})
- Chemical air-water partition coefficient (K_{aw})
- Chemical degradation rate at a given temperature ($k_{deg,T}$)
- Coefficient of the relation between the degradation rate and the temperature (β)

It is worth mentioning here that i) β is not available in MAPPE for all the chemicals. For this reason in the results of the sensitivity analysis the temperature will always have zero influence; ii) the five chemical parameters are strongly inter-correlated. Hence it is not possible to independently sample them (in the Monte Carlo framework). In this study we have therefore used a single variable (named “chemical”) to identify a specific chemical. Then the value of the five parameters is assigned on the basis of the chemical specified. Though correct and efficient, this approach will not allow identification of the influence of the single chemical parameters on the model outputs.

A final aspect considered in this study concerns the selection of the type of coverage. As already pointed out, as for the case of the chemical parameters, also for the different

coverage we used one single variable identifying the possible combinations of ocean, lakes, forests etc. In addition, in the analysis, we considered only the combinations of coverage adopted by MAPPE with their real frequency. In this way, however, in more than 50% of samples, the coverage selected resulted in ocean coverage. For this reason we performed two analyses, one considering both land and sea coverage and another only considering land coverage.

Results are presented in the following figures in two main blocks.

- *sensitivity analysis of environment specific inputs*. In this case, chemical-specific inputs were considered as fixed, the values corresponding to four different chemicals: acephate, γ-HCH (lindane), di(n-octyl) phthalate and Butadiene. The selection of four chemicals, with very different physical-chemical properties[14], allows in any case understanding the role played by the chemical properties.
- *sensitivity analysis of environment and chemical specific inputs*. All the parameters are included explicitly or implicitly. In particular chemical specific input factors were only implicitly considered to compare the impact of the chemical chosen with respect to the environment specific inputs.

The detailed results are reported in SI.

Results confirm the conclusions of Hollander et al. (2009) concerning the predominance of the chemical properties in the quantification of the removal rate. However, for a specific chemical (or at least the specific cluster the chemical pertains to), the definition of the more influential environmental parameters leads now to new insight in the drivers of variation. A summary of the results is provided in the following Table.

Table 4.1.5: Results' summary: key environmental parameters for different chemical archetypes as resulting from the sensitivity analysis of the MAPPE model (air compartment)

Chemical Archetype	Key parameters for archetypes Air compartment
Hydrophilic	Precipitation, ABL
Lipophilic	Wind, Precipitation, ABL, OC, Coverage
High volatility	Wind, Coverage, ABL
Multimedia	Wind, Coverage, ABL

Results highlight the following issues:

- the Atmospheric Boundary Layer (ABL) parameter always has an effect on the model outputs (though it is never the most influential parameter) independent of the chemical;
- the wind speed (the main driver of the advection process) has an effect on most of the chemicals and therefore the advection is really the uppermost process of removal from air for all but hydrophobic chemicals;

[14] In the chemical space defined by Kow and Kaw (Sala et al. 2011), Acephate represents a hydrophilic chemical, whilst di(n.octyl) phatalate a hydrophobic one and Butadiene an extremely volatile one. Lindane, instead, is a multimedia chemical, meaning that it represents those chemical that are close to equal affinity for air, soil and water

- land coverage and the forest have a significant effect on the model outputs, especially for multi-media chemicals and especially when assessing removal from land surface;
- the role of precipitation, especially for hydrophilic chemicals, is significant.

4.1.3.2.2. Soil and freshwater compartments

In the present section, results of the sensitivity analysis for the soil/freshwater compartment are reported and discussed. The framework is the same as for the air compartment. Soil and freshwater are considered together as in MAPPE Global they are treated in very close relationship, having part of the calculation of the freshwater compartment coming from a calculation of the soil one. Most of the considerations for the air compartment can be repeated in this case. In particular, the main output of MAPPE Global is the soil removal rate (k_{soil}), that is, the amount of a certain chemical emitted in the soil compartment that is removed from the place where it is emitted in a reference time period. As for air compartment, k_{soil} is connected to different phenomena (chemical degradation, erosion, runoff, partitioning. volatilization) that are evaluated separately and then aggregated (Pistocchi et al. 2011). Runoff and erosion are the phenomena driving the removal of the chemical from the soil to the surface water bodies. For this reason, the sensitivity analysis is also performed on the chemical load in liquid form to surface water bodies (*LoadQ*) and on the chemical load in solid form to surface water bodies (*LoadS*). *LoadQ* and *LoadS* are then the two inputs to be used to evaluate the total chemical load to the sea (*Load2Sea*), namely, the main output of MAPPE for the inland water compartment.

Also in the case of the soil/fresh-water compartment, the parameters kept as fixed in MAPPE are not considered in the sensitivity analysis. In the same way, again, the following environmental inputs are considered:

- Organic carbon concentration in soil (*OC*)
- Temperature (*T*)
- Coverage/land use, such as lakes, impervious surface etc. (*cov*)
- Annual discharge per unit area (*Q*)
- Specific sediment yield (*sSy*)
- Average catchment retention time (*tau*)

As for the chemical specific parameters in the air compartment, the same considerations also hold here (that is, the necessity to group them in 1 single input responsible for the choice of the chemical to use within a given iteration of the sensitivity analysis), as well as for the unavailability of the coefficient β and therefore the impossibility for temperature to account for any share in the outputs' variance.

In summary, as in the previous case, two different analyses have been carried out:

- *sensitivity analysis of environment specific inputs*. In this case, chemical-specific inputs were considered as fixed the values corresponding to five different chemicals: acephate, γ-HCH (lindane), di(n-octyl) phthalate, butadiene and mirex. The selection of five chemicals, with very different physical-chemical properties[15], allows assessment of the role played by the chemical properties.

[15] In the chemical space defined by Kow and Kaw (Sala et al. 2010), Acephate represents a hydrophilic chemical, whilst di(n.octyl) phatalate and mirex are hydrophobic and butadiene is an extremely volatile one.

- *sensitivity analysis of environment and chemical specific inputs*. All the parameters are included explicitly or implicitly. In particular chemical specific input factors were only implicitly considered to compare the impact of the chemical chosen with respect to the environment specific inputs.

The detailed results are reported in SI.

As in the case of the air compartment, the effect of the chemical selection seems to be predominant in determining the value of the soil compartment removal rate. On the contrary, this seems not to be the case for the freshwater compartment, where the chemical selection, in its first order effect, accounts for just the 10% of the variability in total load to the sea, while the environmental parameters together have a first order effect accounting for around 25% of the variability. The remaining output variability is explained by parameter' interactions. A summary of the results is provided in Table 4.1.6.

Table 4.1.6: Results' summary: key environmental parameters for different chemical archetypes as resulting from the sensitivity analysis of the MAPPE model (soil-freshwater compartment)

Chemical Archetype	Key parameters for archetypes Soil compartment	Key parameters for archetypes Freshwater compartment
Hydrophilic	Q	Q, tau
Lipophilic	sSy	sSy
High volatility	Cov, OC	Q, tau, sSy, OC
Multimedia	sSy, Q, OC	sSy, Q, OC, tau

Results highlight the following issues:

- there are no parameters that account for outputs' variability for all chemicals. Specific sediment yield and annual discharge rate exert an effect in most chemical types. Interestingly, sSy does not show up as an important parameter in the sensitivity analysis involving both environment and chemical specific inputs. As already pointed out this might be connected to the fact that the sensitivity analysis looks at the absolute variability and not in terms of orders of magnitude. An analysis using the logarithmic transformation of the outputs may provide additional insights;
- the catchment retention time is never the most important parameter of the freshwater compartment. In particular, it is totally non-influential for lipophilic chemicals and almost non-influential for multimedia ones. This is explained by the fact that in MAPPE Global the retention time only influences the runoff component of the load2Sea and not the erosion component;
- as expected temperature has no effect on the outputs;
- coverage and organic carbon come into play when volatilisation influence the soil removal rate.

Lindane, instead, is a multimedia chemical, meaning that it represents those chemical that are close to equal affinity for air, soil and water

4.1.3.2.3. Ocean compartment

In this section, results of the sensitivity analysis for the ocean compartment are reported and discussed. The framework is the same as for the other cases. Most of the considerations for the other compartments can be repeated in this case. In particular, the main output of MAPPE Global is the sea removal rate (k_{sea}), that is, the amount of a certain chemical emitted in the ocean compartment that is removed from the place where it is emitted in a reference time period. As for the air compartment, k_{sea} is influenced by different phenomena (chemical degradation, partitioning, volatilization, sinking with organic carbon and advection) that are evaluated separately and then aggregated.

As for the case of the air compartment, in this case we have also evaluated the model with and without considering advection.

As with the other compartments, the fixed parameters in MAPPE are not considered in the sensitivity analysisThe following environmental inputs are considered:

- Concentration of chlorophyll (*chi*)
- Wind speed at 10m (u_{10})
- Temperature (*T*)
- Ocean mixing layer depth (*MLD*)
- Average ocean current velocity (*u*)

For what concerns chemical specific parameters, as previously mentioned, there is the need for groping them in 1 single input responsible for the choice of the chemical to use within a given iteration of the sensitivity analysis. Besides, there is the unavailability of the coefficient β and therefore the impossibility for the temperature to account for any share in the outputs' variance.

In summary, as in the previous cases, two different analyses have been carried out:

- *sensitivity analysis of environment specific inputs*. In this case, chemical-specific inputs were considered as fixed the values corresponding to four different chemicals: acephate, γ-HCH (lindane), di(n-octyl) phthalate and butadiene.
- *sensitivity analysis of environment and chemical specific inputs*. All the parameters are included explicitly or implicitly. In particular chemical specific input factors were only implicitly considered to compare the impact of the chemical with respect to the environment specific inputs.

The detailed results are reported in SI.

Again the effect of the chemical selection seems to be the predominant factor determining the value of the compartment removal rate. Advection still represents an important process but, overall, its contribution seems outweighed by the role played by volatilization. A summary of the results is provided in Table 4.1.7.

Table 4.1.7: Results' summary: key environmental parameters for different chemical archetypes as resulting from the sensitivity analysis of the MAPPE model (ocean compartment)

Chemical Archetype	Key parameters for archetypes Ocean compartment
Hydrophilic	u

Lipophilic	MLD, u, chi
High volatility	MLD, u_{10}, u
Multimedia	u, MLD, u_{10}

Results highlight the following issues:

- the average speed of marine currents that drive advection always account for a share of the outputs' variability. Its influence , however, varies withdifferent chemicals.
- the ocean mixing layer depth is the second most important factor. It affects both volatilization and sinking with organic carbon (both chlorophyll concentration and wind speed only exert an effect in combination with it).
- classes of marine currents and mixing layer depth should be sufficient to determine robust archetypes for emission calculations.

4.1.3.3. Discussion on the implication of sensitivity analysis results in order to build archetypes of emissions

Considering the results obtained from the sensitivity analysis of MAPPE Global for the different compartments, it would be interesting to try to evolve the concept of spatial differentiation from the traditional approaches to scale/resolution (cell, country, and basin) to a "scenario-oriented" approach. In this context, scale is linked to specific environmental parameters leading to the development of archetypes. The emission archetype is meant as the geographical unit, showing similar behaviour in the removal rates of a chemical. It is suitable for building representative scenarios of the distributions of chemicals in the environment and is consequently able to reduce the computational burden related to complex and high-resolution multimedia models.

More specificallyarchetypes should be developed to be:

- Compartment specific: each compartment having different characteristics, the archetypes should account for compartment's related influential parameters.
- Chemical specific: as different clusters of chemicals present different behaviours due to inherent physical chemical properties and may require different scale of assessment
- Target specific: the impacts on ecotoxicity (aquatic freshwater and marine and terrestrial hypogean and epigean) and human toxicity (route of exposure: inhalation, ingestion) occur at different scales and through different pathways. Hence the archetypes should reflect this difference in impact targets.

In the next section, we will test the hypothesis of basing environmental archetypes of emission for the air compartment on climatic zones (based on wind, precipitation and coverage) and we will compare the resulting uncertainty in the evaluation of the removal rates for four chemicals with that resulting from the calculation of the same removal rates on geo-political boundaries (in particular on continents).

4.1.3.3.1. Comparison of the uncertainty in the air removal rate calculated using climatic versus continental archetypes

As the adoption of a specific scale for running a multimedia model is still an open issue in the impact assessment of chemicals, we tested two different spatial approaches for building archetypes of emissions.

We analysed how the uncertainty in the calculation of the air removal rate from the MAPPE Global model varies considering two different archetypes:

- *Climatic zone-based archetypes*. Climatic zones are identified on the basis of the updated Koppen-Geiger Climate Classification (Kottek et al. 2006), considering 30 different zones on the basis of main climates, precipitation and temperature.
- Geo-political archetypes based on continent.

The basic idea is based on the results of the sensitivity analysis carried out for removals rates from air, in which landscape parameters affecting the variability in removal rates could be associated with the typical parameters defining climates, as in the abovementioned Koppen-Geiger Climate Classification. The resulting map of climates is reported in figure 4.1.19.

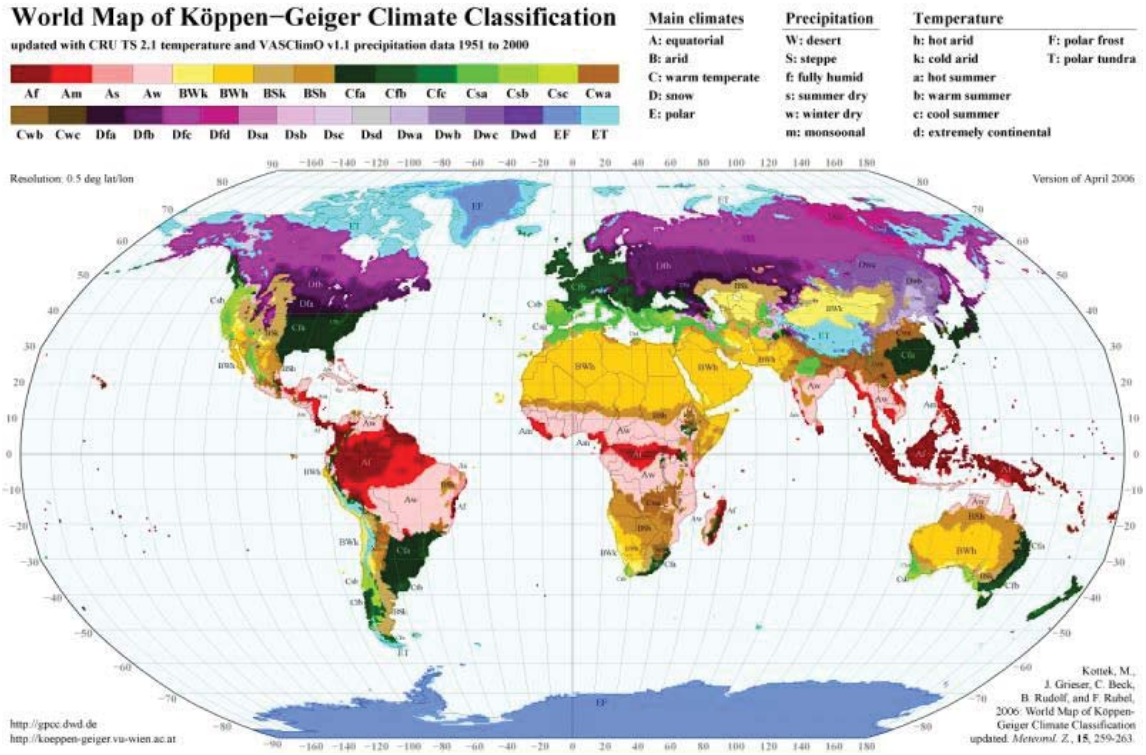

Figure 4.1.19: Map of climate according to Koppen-Geiger classification (from Kottek et al. 2006)

The uncertainty analysis has been carried out considering the air removal rate (with and without advection) for the four different chemicals used in the sensitivity analysis (acephate, γ-HCH (lindane), di(n-octyl) phthalate, butadiene). The removal rates are calculated in the cells of four different climatic zones: *Zone 11+12*: equatorial fully humid and equatorial moonsonal; *Zone 22*: arid, winter dry, hot arid; *Zone 32*: Warm temperate, fully humid,

warm summer; *Zone 42+43*: Snow fully humid warm summer and snow fully humid cool summer. And in the cells of four continents: *South America, Africa, Europe, North America*

The uncertainty comparison has been carried out by visually analysing the distributions of the removal rates in the cells composing the climatic zones and the continents. In order to be as fair as possible we have compared continents with their predominant climatic zones, therefore South America with Zone 11+12, Africa with Zone 22, Europe with Zone 32 and North America with Zone 42+43. Further to the visual analysis, an indicator of small or large uncertainty has been considered to be the kurtosis of the distributions. The larger the kurtosis is, the narrower the distribution is expected to be and the smaller the uncertainty is also expected to be. In Figure 4.1.20 the distributions of the kurtosis for zone-base archetype and continent-based archetype is shown. From the picture it is clear that, overall, the zone-based approach is able to provide removal rate estimations with lower uncertainty (almost 75% of the distribution have kurtosis higher than 3, which corresponds to the kurtosis of a Normal distribution) if compared with the continent-based distributions (in which only the 55% of the distributions have kurtosis higher than 3).

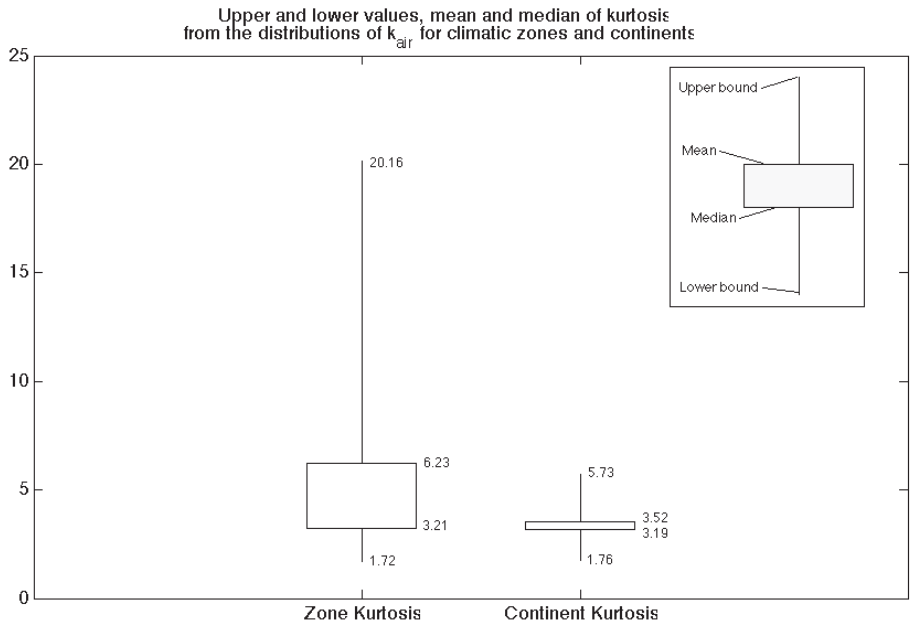

Figure 4.1.20: Kurtosis upper and lower values, mean and median for the distributions of k_{air} from different combinations of chemicals and geographic zones. Data are summarized in the form of candlestick charts

Although the results are overall satisfactory and confirm the higher suitability of climatic zones to act as archetypes for removal rates calculation with respect to the continent approach, if the distributions are compared case by case (as in the figures S4.28-4.35 in the supporting information), it is easy to recognize that the climate-based archetype not always outperform the continent-based one. This is also due to the limitations of the MAPPE Global in accounting for the several aspects of the removal process, in particular for what concerns the role of the temperature. Further research is therefore required to investigate this aspect in a more careful way. Details of the results are elaborated in SI.

4.1.3.4. Spatial variability of fate factor in freshwater and soil for Europe

Masses in soil and in water were computed with MAPPE Europe as a basis for calculating fate factors at various scales, from cells (1x1 km^2) to country, basin and continental level. Maps and statistics for fate factors at each scale are provided in the figures and tables below The results of the calculation described above are reported in SI

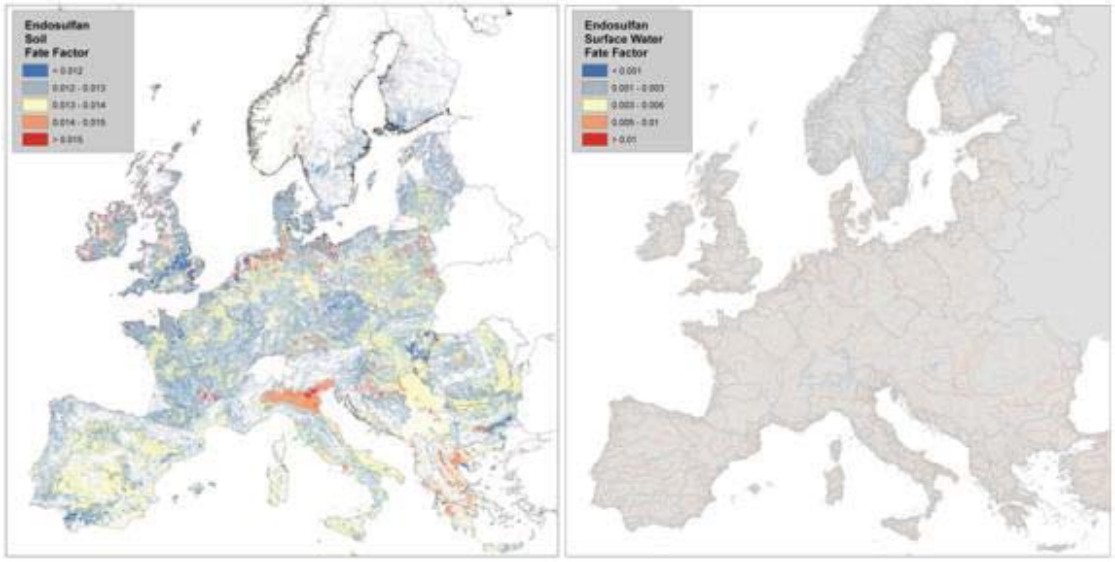

Figure 4.1.21: Fate factors in soil [calculated as Kg in soil/Kg emitted] and for freshwater [calculated as ∑mass upstream / ∑emission upstream] (per cell)

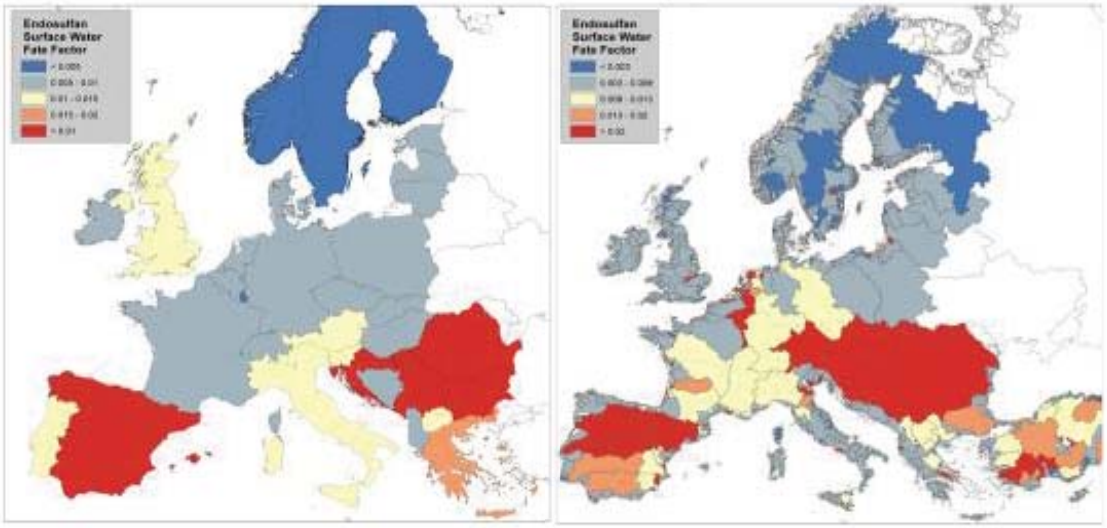

Figure 4.1.22: Fate factors in freswater calculated at country (left) and basins (right) scale calculated as – country: ∑Mass in rivers /∑emission in the country; - basin: ∑Mass in rivers /∑emission in basin

Figure 4.1.23: Fate factors in freswater calculated at country scale- after an emission in Germany only-calculated as ∑Mass in rivers /∑emission in Germany only

The summary of the statistics of the different analysis are reported in table 4.1.8. The mapping of fate factors (FFs) at various scales, highlights the magnitude and the relevance of spatial differentiation.

The results for soil FFs, under the European emission scenario , illustrates that the range of variability at cell and country level differs (1 order for countries, 2 orders for cells).

The freshwater FFs express higher variability. At country scale, the range of FFs is over one order of magnitude whereas at basin and cell scale, the variability is up to 4 orders. The basin scale , therefore, appears as the most appropriate scale to identify the wider variations in fate due to landscape and climatic parameters.

For sea/ocean FFs, again the basin level is the most relevant to capture spatial differences.

The example of emissions only in Germany, reinforce the general conclusions that river basins represent the optimal trade-off in terms of spatial unit for freshwater fate factors assessment.

Table 4.1.8: Statistics showing the variability of FF in soil, water and sea across Eu

		EUROPE - 1kg/km² Emissions on agricultural land					GERMANY - 1kg/km² Emissions everywhere			
Compartment	Unit	Avg	Stdv	Max	Min		Avg	Stdv	Max	Min
SOIL	Europe	1.2E-02					1.0E-02			
	Country	1.2E-02	9.6E-04	1.4E-02	9.9E-03		1.0E-02			
	Cell (1 Km²)	1.2E-02	2.0E-03	2.8E-02	2.0E-04		1.0E-02	4.0E-03	2.7E-02	1.0E-04
WATER	Europe	2.3E-02					8.5E-03			
	Country	1.1E-02	1.1E-02	5.7E-02	3.0E-03		8.5E-03			
	River Basin	7.0E-03	9.0E-03	1.0E-01	1.0E-05		8.0E-03	1.4E-02	1.3E-01	1.0E-03
	Cell (1 Km²)	5.3E-03	4.0E-03	1.3E-01	5.3E-05		8.0E-03	1.3E-02	1.9E-01	5.1E-19
OCEAN	Europe	6.0E-03					7.0E-03			
	Sea Basin	5.5E-03	2.2E-03	8.0E-03	3.4E-03		9.0E-03	6.0E-03	1.6E-02	4.0E-03
	River Basin	5.8E-03	2.7E-03	1.4E-02	1.0E-06		6.0E-03	3.9E-03	2.4E-02	2.4E-03

4.1.3.5. Spatial variability of fate factors for terrestrial ecotoxicity (at global scale)

The soil compartment has been further analysed for supporting the calculation of spatially resolved characterization factors for terrestrial ecotoxicity. We ran both MAPPE Europe (reported in the previous section and coupled with freshwater FF evaluation) and MAPPE Global to explore spatial variability in the fate factors associated with an emission of chemicals into soil.

In order to calculate fate factors at the global level for the soil compartment, we ran MAPPE global. In the section on removal rates we presented the calculation for the 36 chemicals of the test set related to Ksoil and the result of the sensitivity analysis of the model. The results showed that the variability in the removal rates from soil is relatively low at global level, apart from a few clusters of substances (3a, 3b, 4a, 4b, 6b and 7b) in which the variability is up to 3 orders of magnitude. This implies that the variability in terrestrial ecotoxicity resulting from the chemicals emitted to soil and that remain in soil is relatively low. From the sensitivity analysis we have already shown that the value of Ksoil is strictly connected with the type of chemical under analysis. The variability due to environmental parameters is mainly related to precipitation, the type of coverage, the concentration of organic carbon and the specific sediment yield (sSy). In particular, this latter parameter results the most important one for lipophilic and multi-media chemicals (namely most of the clusters mentioned above). For this reason, in Figure 4.1.24 and Figure 4.1.25, the geographical distribution of Ksoil of the four chemicals showing the highest variability is shown and compared with the distribution of sSy. From the two figures, the similarity in the variability patterns of sSy and Ksoil results are evident (the reader can focus the attention, e.g. on the Southern part of Chile, on the Japan, on the Himalayan Region etc.).

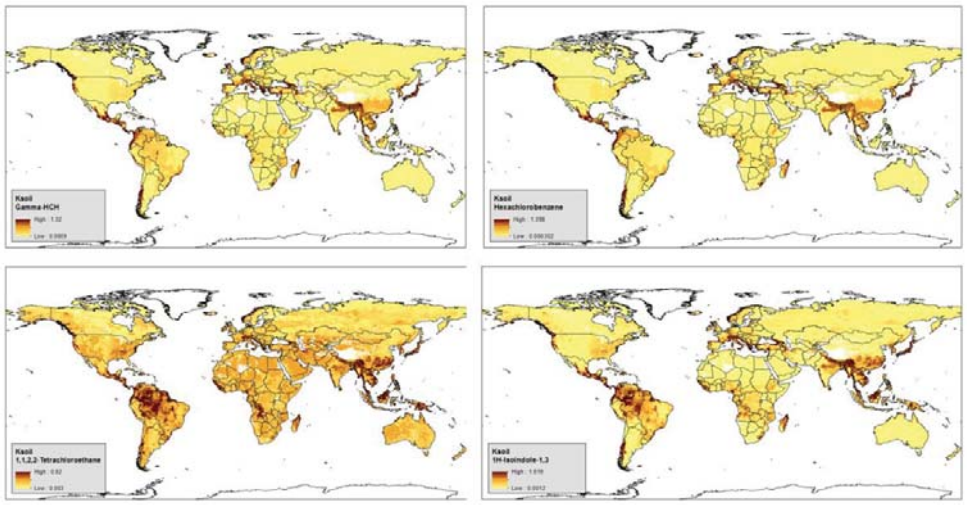

Figure 4.1.24: Variability of K soil for lindane, hexachlorobenzene, 1,1,2,2 tetracloroethane and phthalimide at cell scale

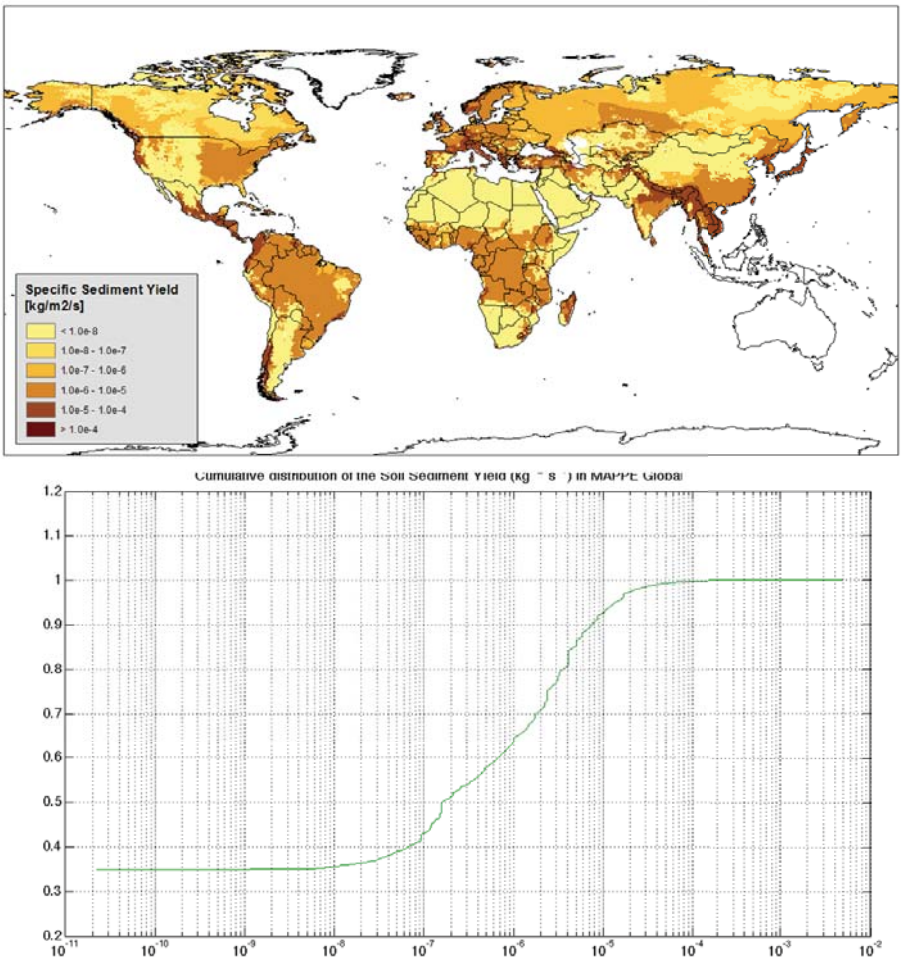

Figure 4.1.25: Geographical and cumulative distribution of sSy among the geographic cells of MAPPE Global

In addition, since in almost 60% of the cells sSy is in the range [10^{-7},10^{-4}] and since this is the range in which the specific sediment yield mainly affects the value of Ksoil, it is straightforward to hypothesizethe archetypes connected with the value of sSy. This will be the objective of future research activities.

As heptachlor is one of the chemicasl for which an effect factor has been calculated in section 5.3 we have calculated the fate factor and the associated characterisation factors at different resolutions. The variability of Ksoil is 3 orders of magnitude if we consider the results at cell scale.

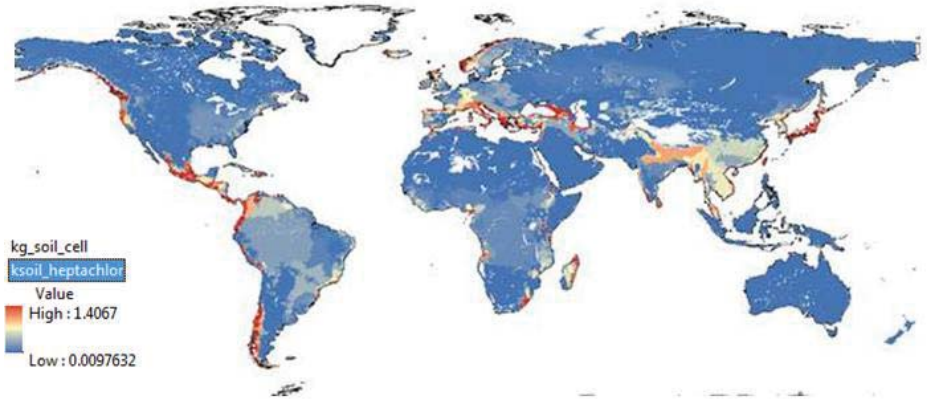

Figure 4.1.26: Variability of K soil for Heptachlor at cell scale

The variability of FF is also up to 3 orders (mean= 96.04, stdv = 11.85, max = 102.42, min = 0.71, 5% = 70.11, 95% = 102.02). Considering soil compartement features, highly lipofilic chemicals are expected to remain locally and to exert effect mainly at the local scale. Hence, even if the 5% and 95% valuesindicate a low variability, the presence of hot spots should be taken into account (in this case, the presence of a 5% of cells with a value over 102.2). The FF in USEtox is 4.11E+2 (if a chemical has been emitted in agricultural soil or natural soil and if the receiving compartement is the same as the emission). Therefore, USEtox may overestimate the FF in soil for Heptachlor up to a factor of 6.

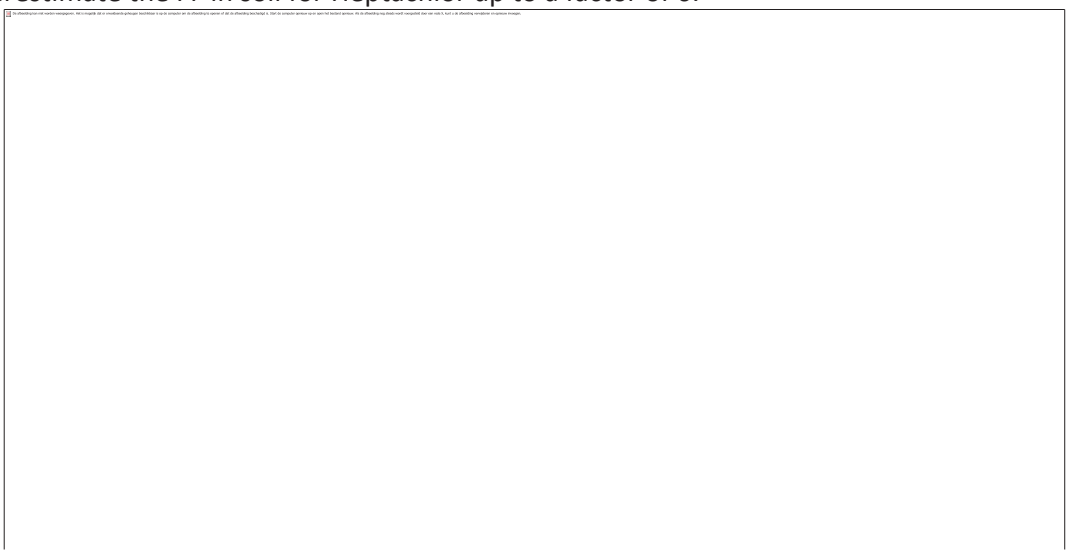

Figure 4.1.27: Characterisation factors at global scale for heptachlor (5% = 28.80 and 95% = 42.03)

The characterisation factors may then be calculated from the FF, multiplying the FF for the effect factor. The effect factor has been calculated in section 5.3 and is equal to 4.12E-01 (kgsoildryw/mg chemical). The map (Figure 4.1.27) reports the characterisation factors at cell scale, which vary up to a factor of 3 (with a minimum value lower than 1 in eight cells in the South of Chile), and also at country level, where the minimum value is in Lebanon (15.63) and the maximum in Greenland (42.19).

4.1.3.6. Spatial variability of fate factors for marine ecotoxicity

We used the IMPACT World model to estimate the fate in 33 model coastal zones presented in Figure 4.1.28. Figure 4.1.29 presents fate in coastal zones. Water residence time in these zones as recalculated in Table 4.1.9 varies from 0.59 y in CWW8 (Western South America) to 359 y for CNW10 (Northern North America). However, only the later value exceeds 1.0 and is due to the transformation of water into ice. Pollutants with persistence less than 1 year will thus disappear by degradation, sedimentation or volatilization, while pollutants with longer persistence, e.g., Folpet ($t_{1/2}$=1.57 y in water) can be transferred to an oceanic zone.

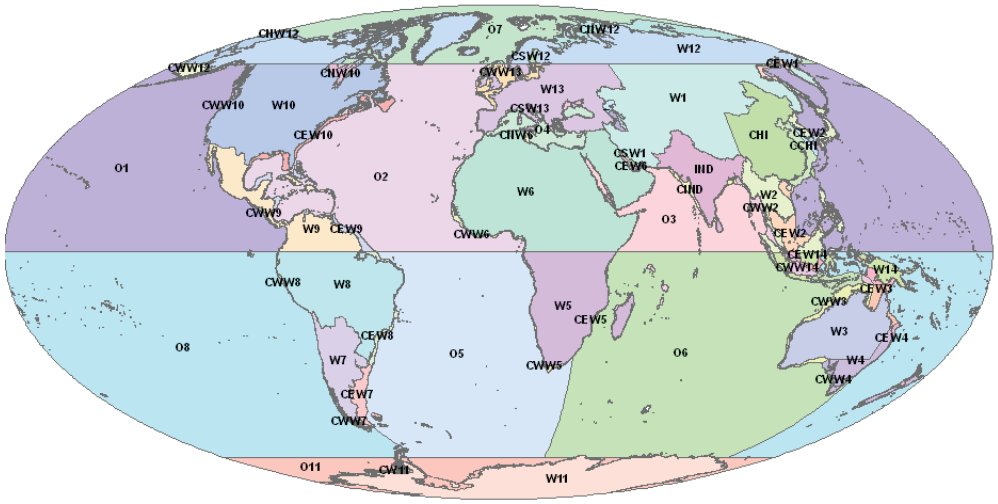

Figure 4.1.28: Map of IMPACT World model (Shaked 2011)

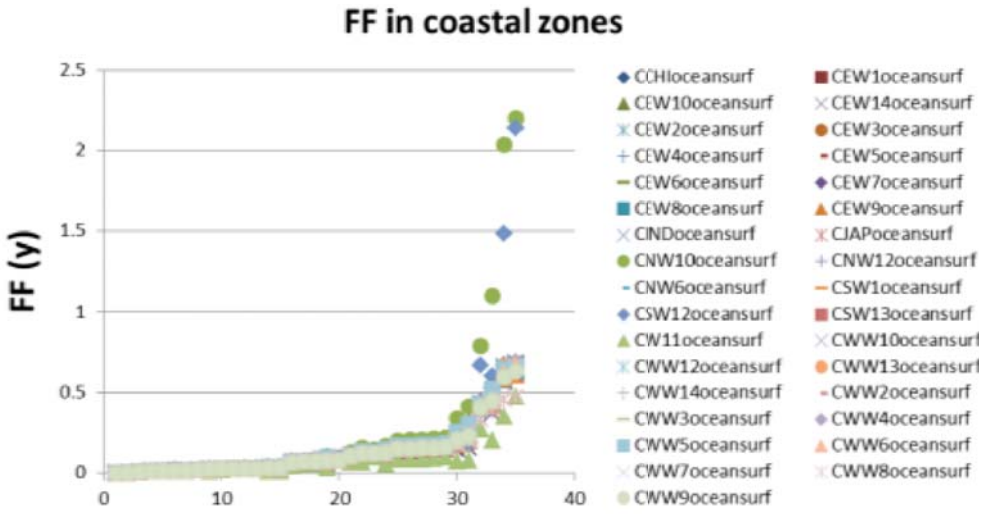

Figure 4.1.29: Fate factors in coastal zones modeled with Impact World, classified by coastal zones (Shaked 2011)

Table 4.1.9: Residence time of coastal zones in Impact World model

	Volume (m^3)	Advection (m^3/hour)	residence time	residence time (y)
CCHI	4.55E+13	5.44E+09	8.36E+03	0.95
CEW1	4.25E+13	5.06E+09	8.41E+03	0.96
CEW10	7.34E+13	8.52E+09	8.62E+03	0.98
CEW14	2.49E+13	3.05E+09	8.17E+03	0.93
CEW2	9.19E+13	1.06E+10	8.64E+03	0.99
CEW3	2.11E+13	2.41E+09	8.75E+03	1.00
CEW4	2.09E+13	2.41E+09	8.68E+03	0.99
CEW5	1.58E+13	1.92E+09	8.20E+03	0.94
CEW6	1.47E+13	1.77E+09	8.31E+03	0.95
CEW7	7.32E+13	8.4E+09	8.71E+03	0.99
CEW8	2.38E+13	3.16E+09	7.52E+03	0.86
CEW9	4.40E+13	5.25E+09	8.39E+03	0.96
CIND	2.39E+13	2.96E+09	8.08E+03	0.92
CJAP	2.30E+13	2.65E+09	8.66E+03	0.99
CNW10	3.15E+13	10000000	3.15E+06	359
CNW12	2.68E+14	3.12E+10	8.59E+03	0.98
CNW6	8.32E+12	1.04E+09	8.00E+03	0.91
CSW1	5.51E+12	8.15E+08	6.76E+03	0.77
CSW12	3.76E+12	0	-	-
CSW13	2.14E+13	2.57E+09	8.33E+03	0.95
CW11	5.94E+12	1.1E+09	5.42E+03	0.62
CWW10	7.27E+12	9.69E+08	7.50E+03	0.86
CWW12	3.96E+13	4.53E+09	8.74E+03	1.00

CWW13	8.05E+13	9.31E+09	8.64E+03	1.00
CWW14	2.53E+13	3.09E+09	8.18E+03	0.93
CWW2	2.27E+13	2.71E+09	8.40E+03	0.96
CWW3	5.83E+13	6.66E+09	8.76E+03	1.00
CWW4	1.76E+13	2.02E+09	8.74E+03	1.00
CWW5	2.03E+13	2.44E+09	8.31E+03	0.95
CWW6	1.79E+13	2.13E+09	8.39E+03	0.96
CWW7	5.78E+12	7.09E+08	8.16E+03	0.93
CWW8	5.69E+12	1.1E+09	5.19E+03	0.59
CWW9	1.52E+13	1.95E+09	7.77E+03	0.89

4.1.3.7. Spatial variability of inhalation intake fractions from MAPPE Europe

4.1.3.7.1. Scenarios of emission and chemicals used

Intake fraction for Europe has been calculated with MAPPE Europe under an industrial emission scenario considering different substances and location of the sources of emissions.

As first step, we ran MAPPE Europe with a uniform emission coming from highly populated and industrialised areas. The amount of emission in each European country has been scaled up by the population density. In these runs, two substances were evaluated:

- 1,1,2,2 tetrachloroethane- representative of highly volatile chemicals;
- nitrobenzene- representative of multimedia chemicals;

Secondly, we ran the model assuming an emission coming only from a single country (Spain or Luxemburg or Slovenia).

Thirdly, we ran the model with real industrial emission data for 1,2 dichloroethene (representative of volatile chemicals) from the country where this emission are reported and then for Belgium only.

4.1.3.7.2. Results-1-Emission of 1,1,2,2 tetrachloroethane in all Europe

An emission of 1,1,1,2 tetrachloroethane was chosen to run the model considering a scenario of atmospheric emissions from industrialized (urban) areas in Europe.

1,1,2,2 tetrachloroethane has the highest solvent power of any chlorinated hydrocarbon and it was widely used as a solvent and as an intermediate in the industrial production of trichloroethylene, tetrachloroethylene, and 1,2-dichloroethylene.

The scenario assumes an overall amount of 100 tons emitted to air per year, scaled by country on the basis of population density. Thus, the emissions from the smaller European countries (like Estonia or Slovenia) are in a range 0.1-1 t/y, while the industrial states (as Germany, UK France and Italy) emitted more than 10t/y (besides, Spain and Poland are also close to this amount emitting 7-8 t/y); for the other cases the emissions vary between 1-4 t/y. Figure 4.1.30 shows the distribution of the emission by country, whereas the specific values of the emissions from each country are reported in the accompanying table.

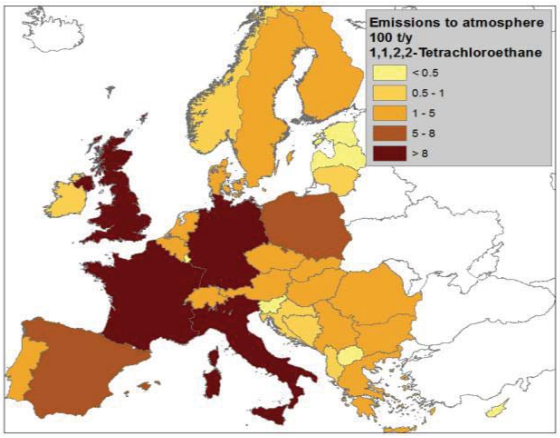

Country	t/year	Country	t/year	Country	t/year
Albania	0.69	Greece	2.12	Poland	7.32
Austria	1.55	Cyprus	0.14	Portugal	2.01
Belgium	2.00	Hungary	1.94	Spain	7.87
Bulgaria	1.49	Ireland	0.78	Romania	4.16
Czech Republic	1.96	Italy	11.03	Slovakia	1.03
Denmark	1.04	Latvia	0.44	Sweden	1.72
Estonia	0.26	Lithuania	0.66	Switzerland	1.42
Finland	1.00	Luxembourg	0.09	Bosnia and Herzegovina	0.88
France	11.50	Macedonia	0.39	Croatia	0.85
Germany	15.82	Netherland	3.12	Slovenia	0.38
Great Britain	11.42	Norway	0.88	Serbia	2.07

Figure 4.1.30: Map of the emission scenario by country into air across Europe in ton per year (t/y) per country and quantities per country. Total emission for Europe is 100 tonnes

Following the abovemnetioned assumption that the air pollution is coming mainly from the highly populated areas, the distribution of the emissions specific locations in Europe is shown in figure 4.1.31.

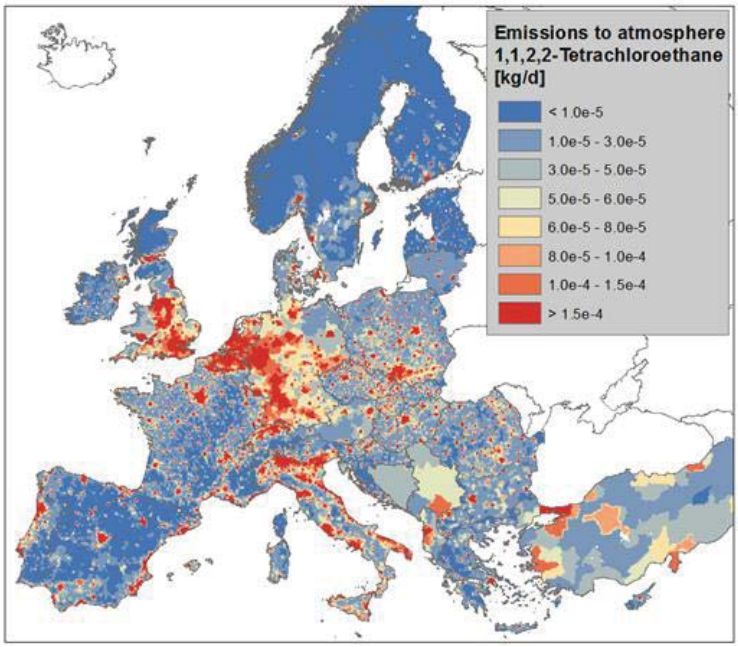

Figure 4.1.31: Map of the emission scenario by source of emissions into air across Europe according to the source receptor matrix. Emission in (kg/day) are spatially distributed according to the population density (resolution 1km^2. Values: min=0, max= 0.011, mean=5.38 10-5, SD=1.57 10^{-4})

Under the adopted industrial emission scenario, the atmospheric concentration in air and the resulting mass (Figure 4.1.32) in air could be calculated. The areas representing higher concentrations and masses in the atmosphere are related to the source of emissions (populated areas under the considered scenario) but also to climatic and removal conditions (for instance, even if there are higher emissions in Spain or Italy, the elevated air removal rate leads to relatively lower concentrations in the southern areas compared to those in the central part of Europe).

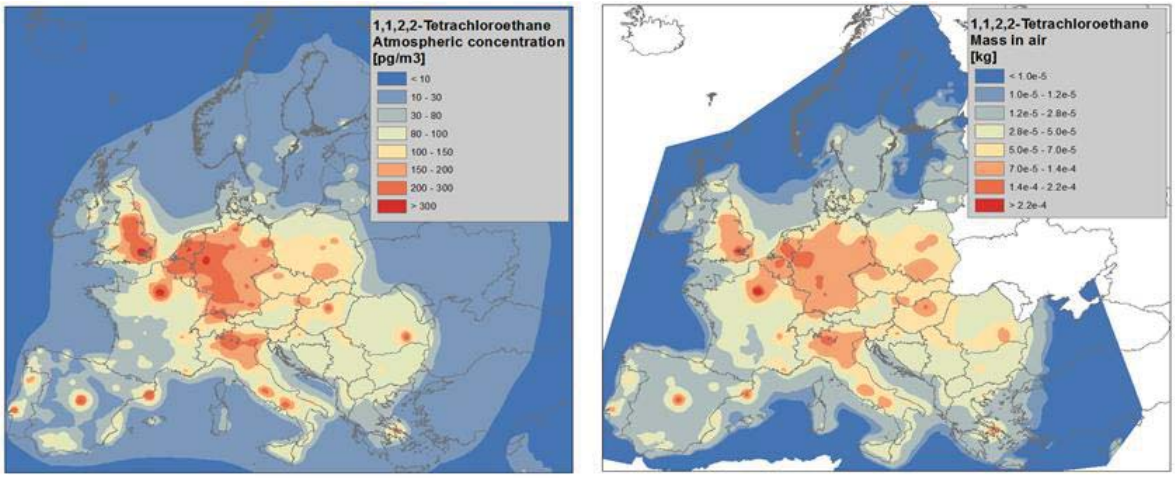

Figure 4.1.32: Concentration (pg/m^3) and mass kg of 1,1,2,2 tetrachloroethane in air after an emission in air from highly industrialized areas (Statistics are evaluated on land only, values for concentration: min=0, max=942.24, mean=99.58, SD=81.65; 5% = 7.39 and 95% = 284.52)

In order to calculate the intake fraction, firstly we calculate the numerator of its governing equation, namely the (mass in air)*IR, at 1*1 Km^2 of resolution (Figure below).

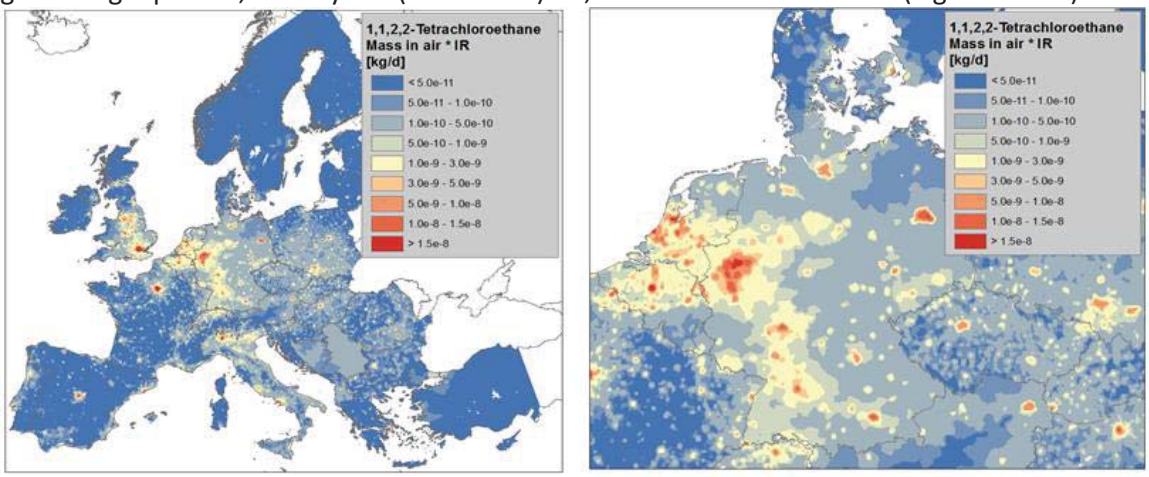

Figure 4.1.33: iR multiplied by mass after an emission of 1,1,2,2 tetrachloroethane in air. (Statistics calculated over land only, values: min=0, max=1.36 10-7, mean=2.3 10-10, SD=1.21 10-9). A detail, related to Germany and neighbouring countries is presented on the right

Emissions and masses in the air are highly correlated (R^2=0.8931). Nevertheless, the values show a difference amongst countries with high emission but relatively low masses in air (due to the transport of the masses elsewhere, e.g. Romania, Poland, Spain, Italy and France) and countries with high emission and relatively high mass in the air (due also to contribution of masses coming from other countries, e.g. UK, Germany, Netherland and Belgium).

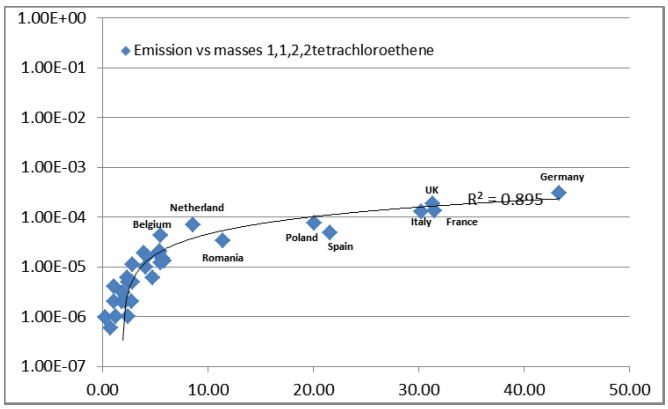

Figure 4.1.34: Correlation between emissions (in kg) and masses (in kg) in the air in EU countries after an emission of 1,1,2,2 tetrachloroethane in air

The intake fractions (iFs) were calculated adopting two approaches:

i. dividing the numerator (mass in air *iR) by the actual emission in each country;
ii. dividing the numerator by the overall emissions in Europe (100 t).

The two resulting maps in the figure 4.1.36 show similar patterns but highlight different aspects of spatial variability.

In case i), the relative importance of the intake associated to urban areas is more evident, and the iF in the urban areas (max value in a single cell 2.3E-5 to be multiplied by the average size of urban areas) is much higher compared to the value reported for the urban box in USEtox (6.8 E-5). For example, Paris has IF equal to 1.4E-3, Berlin to 5.1E-3, Madrid to 3.4E-3. The average iF per km^2 in the four cities is different: Paris 1.33E-5, Berlin 5.72E-6, Madrid 5.61E-6 iF/km^2. The differences amongst cities are due to different population densities (in Paris the highest, 21000 inhabitants/km^2) atmospheric conditions driving the advection and the atmospheric boundary layer. The difference from USEtox could be explained mainly by the differences in the air volume (USEtox 5.76E+10, e.g Paris 4.5E+10 m^3) and population (USEtox 1.86E+6, e.g. Madrid 3.2E+6).

The distribution of iFs values in the cells in Europe is reported in the following histrogram, fig 4.1.35. Few cells, representing major cities contribute the most to the overall intake value.

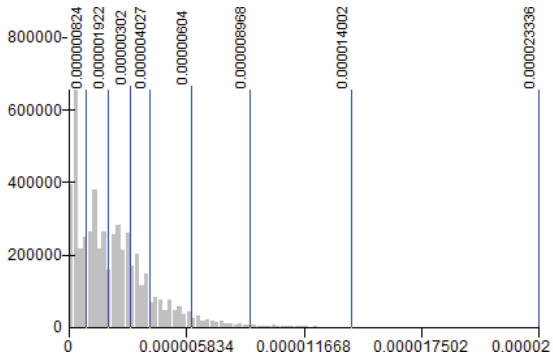

Figure 4.1.35: Histogram of the distribution of the intake fraction in the grid cells of 1*1 Km^2 in Europe, under case i)

In case ii), the iF calculation is similar to a continental approach in box model, in which the overall emissions are taken as single amount not spatially resolved over the continent. In this case the iF for Europe is equal to 4.40E-6 (USEtox value 4.38E-5) and the relative contribution of each country is given in fig 4.1.37. In the map, high value of iFs are associated with the relative contribution of each country to the overall continental iF.

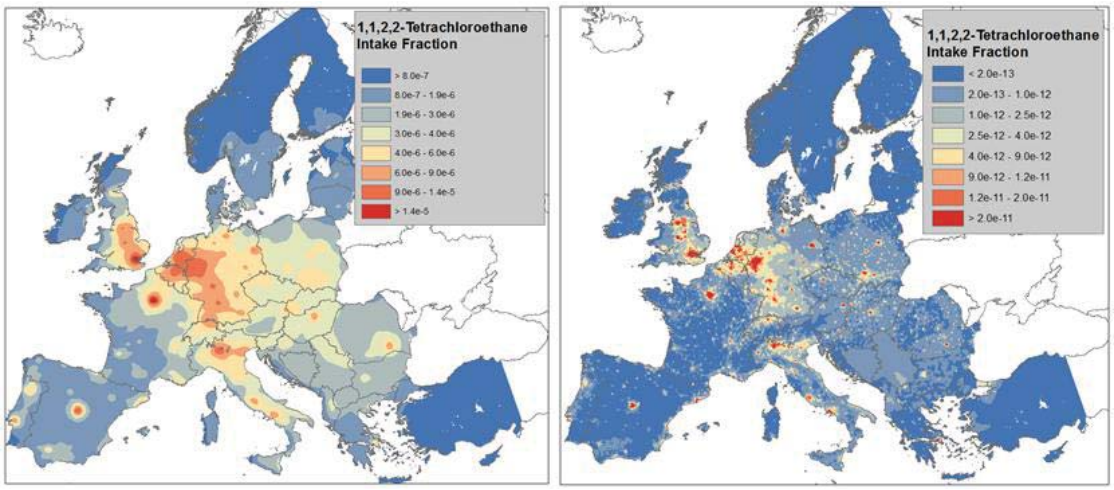

Figure 4.1.36: Intake fraction in Europe after an emission of 1,1,2,2 tetrachloroethane in air calculated at 1*1 km. On the left, the map of iF calculated dividing the numerator in each country by the actual emission in the country (Values: min=0, max=2.33 10-5, mean=2.34 10-6, SD=2.01 10-6). On the right, the map of iF calculated dividing by the overall emission (Values: min=0, max=4.9 10-10, mean=8.5 10-13, SD=4.4 10-12)

Figure 4.1.37 shows the IFs plotted with the emission quantity in each country, highlighting where the iF is relatively high compare to the emission amount and vice versa.

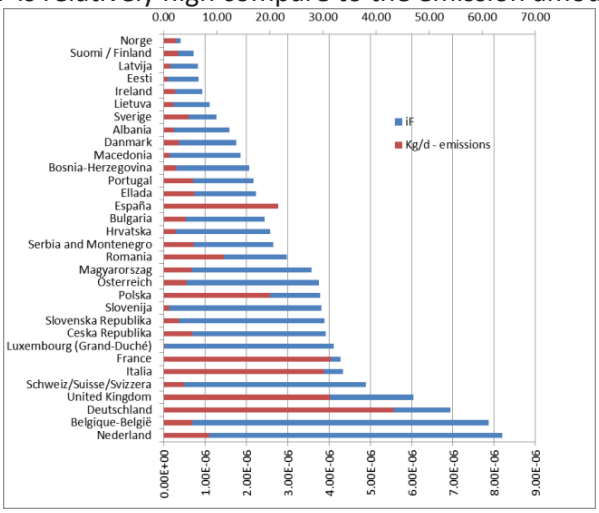

Figure 4.1.37: Intake fraction (under case i) in Europe after an emission of 1,1,2,2 tetrachloroethane in air and emission in each country (Kg)

Following the calculation done for case i), the iFs for each country could be calculated aggregating the iF in each cell of the country. Results are reported in Table 4.1.10. The iFs span over one order of magnitude (min 4.15E-07 in Norway; max 8.19E-06 in Netherlands),

and the difference is due to the combination of emission, resulting mass in air and population density; the latter having a crucial role, as the correlation between emission and iF is very low (R^2=0.25).

Table 4.1.10: iF in European countries due to an emission into air of 1,1,2,2 tetrachloroethane under case i). The reported values are the sum of the IFs in the cells of each country.

Country	IF	Country	IF	Country	IF
Albania	1.59E-06	Suomi / Finland	7.29E-07	Nederland	8.19E-06
Österreich	3.76E-06	France	4.29E-06	Norge	4.15E-07
Bosnia-Herzegovina	2.07E-06	Ellada	2.24E-06	Polska	3.79E-06
Belgique-België	7.87E-06	Hrvatska	2.58E-06	Portugal	2.18E-06
Bulgaria	2.45E-06	Magyarorszag	3.58E-06	Romania	2.99E-06
Suisse	4.89E-06	Ireland	9.41E-07	Sverige	1.27E-06
Ceska Republika	3.92E-06	Italia	4.34E-06	Slovenija	3.81E-06
Deutschland	6.95E-06	Lietuva	1.11E-06	Slovenska Republika	3.89E-06
Danmark	1.76E-06	Luxembourg	4.12E-06	United Kingdom	6.04E-06
Eesti	8.47E-07	Latvija	8.23E-07	Serbia and Montenegro	2.65E-06
España	2.27E-06	Macedonia	1.86E-06		

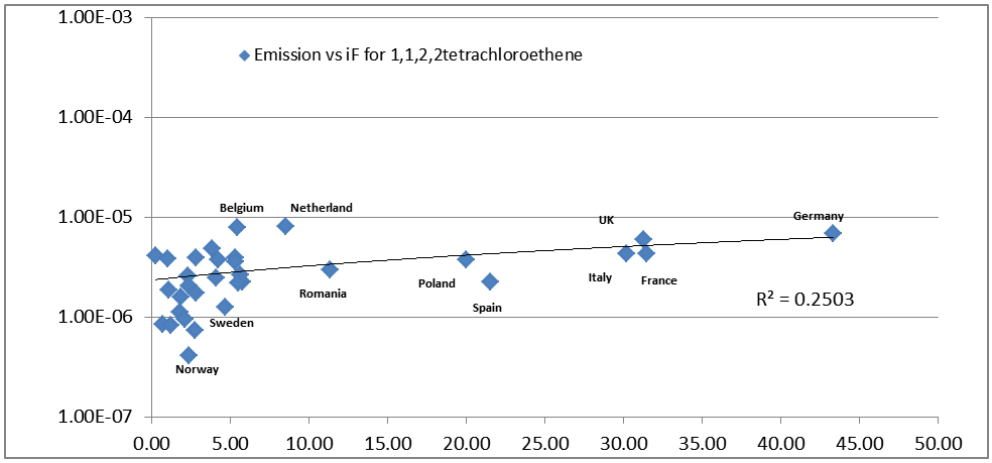

Figure 4.1.38: Correlation between emissions and iF in the air in EU countries after an emission of 1,1,2,2 tetrachloroethane in air

The relative contribution of the countries to the overall iF at continental scale has been assessed under case ii), and it is reported in figure 4.1.39. Under the scenario of an intensity of emissions related to population density, the countries presenting the higher iF - as results of local and "imported" masses of chemical - are Germany, United Kingdom, France, Italy, Poland and Netherlands.

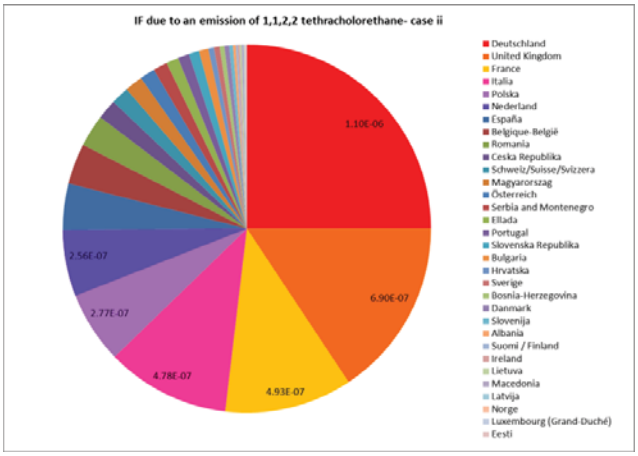

Figure 4.1.39: Relative contribution of EU countries to the overall continental iF after an emission of 1,1,2,2 tetrachloroethane in air. iF calculated under case ii)

Differences up to one order of magnitude, have been observed under the 1,1,2,2-tetrachloroethane scenario described above, when comparing estimates produced by the MAPPE with non-spatial USEtox model. USEtox tends to underestimate the values forecasted by MAPPE model for urban areas and overestimate the continental iF, if Europe is the selected continent.

4.1.3.7.3. Results-2-Emission of nitrobenzene in all Europe

To test the spatial variability for another chemical, we ran MAPPE Europe for nitrobenzene - a multimedia chemical produced on a large scale from benzene as a precursor to aniline. The concentration in air after an emission of 100 tons of nitrobenzene in air from highly populated areas in Europe is displayed in the map below, fig 4.1.40. The concentrations follow a similar pattern of spatial distribution even if the absolute values are lower compared to 1,1,2,2 tetrachloroethane. Due to the multimedia behaviour of nitrobenzene and its degradation rate, the mean concentrations of nitrobenzene (0.023 ng/m^3) are one fourth lower compared to 1,1,2,2 tetrachloroethane (0.099 ng/m^3).

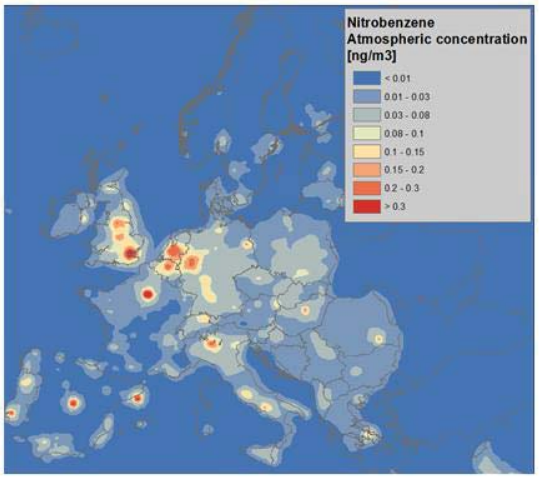

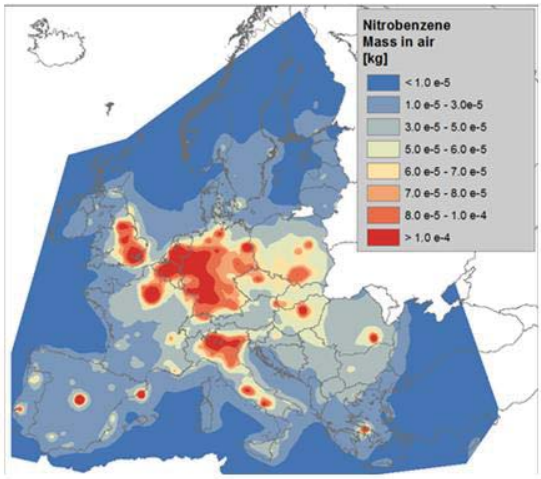

Figure 4.1.40: Concentration in ng/m^3 and mass in Kg of nitrobenzene in air after an emission in air from highly industrialized areas (statistics computed over land only, concentration: min=0, max=0.64, mean=0.023, SD=0.032; 5% = 0, 95% = 0.11)

The iFs have been calculated adopting the two abovementioned approaches i) and ii). The variability of the iR*mass in air has the same pattern and very similar values compared to 1,1,2,2 tetrachloroethane.

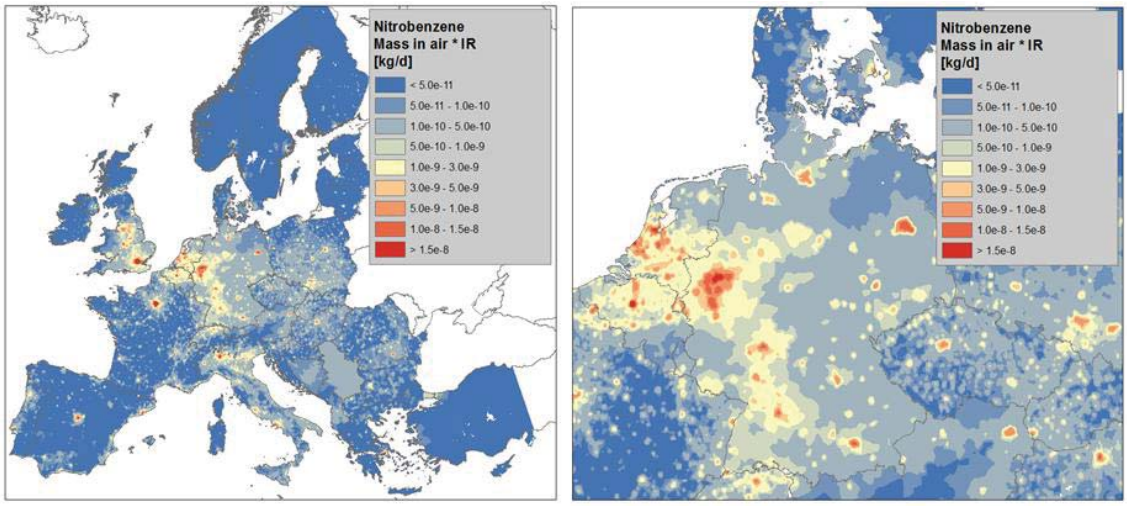

Figure 4.1.41: IR multiplied by mass after an emission of Nitrobenzene in air. Values: min=0, max=1.33 10^{-7}, mean=2.22 10^{-10}, SD=1.17 10^{-9}. A detail on Germany and neighbouring countries is also provided

Therefore, the calculation of the iFs according to i) and ii) lead to similar results, as reported in the maps below, fig 4.1.41. Intake fraction of nitrobenzene due to an emission in the urban box of USEtox is equal to 3.3 E-5 whereas in the continental box is equal to 9.05E-6. Under assumption ii), the iF at EU scale is 4.16E-6 with the relative contribution of each EU country (Table 4.1.11) as shown for 1,1,2,2 tetrachloroethane.

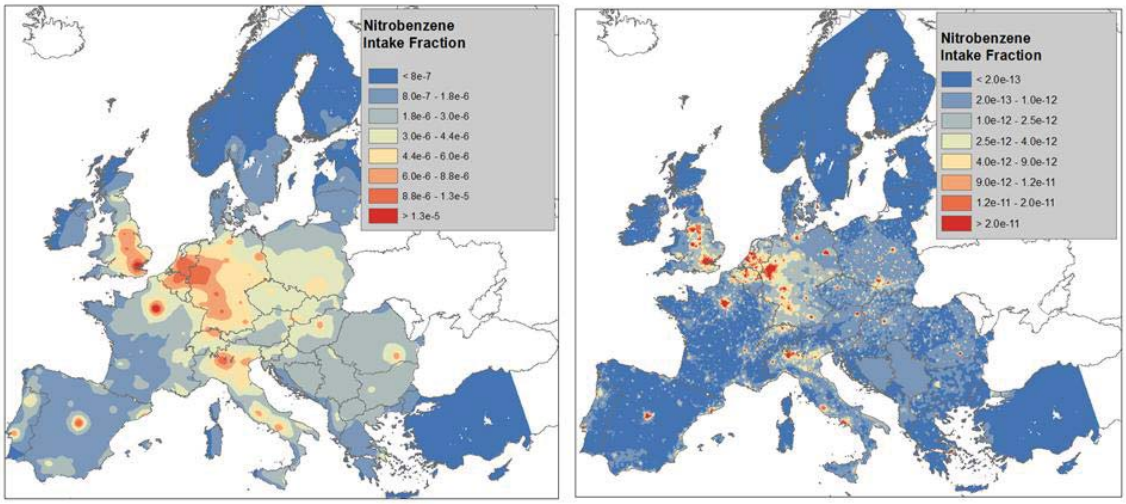

Figure 4.1.42: Intake fractions in Europe after an emission of nitrobenzene in air after an emission in air calculated at 1*1 km^2 On the left, the map of iF calculated dividing the numerator in each country by the actual emission in the country (Values: min=0, max=2.3 10^{-5}, mean=2.2 10^{-6}, SD=1.9 10^{-6}; 5% = 9 10^{-8} 95% = 6 10^{-6}). On the right, the map of iF calculated dividing by the overall emission (Values: min=0, max=4.8 10^{-10}, mean=8.1 10^{-13}, SD =4.2 10^{-12}; 5% = 0 95% = 8.2 10^{-11})

Table 4.1.11: iF in European countries due to an emission into air of nitrobenzene case i)

Country	IF	Country	IF	Country	IF
Albania	1.59E-06	Suomi / Finland	7.29E-07	Nederland	7.84E-06
Österreich	3.53E-06	France	4.06E-06	Norge	4.15E-07
Bosnia-Herzegovina	1.66E-06	Ellada	2.07E-06	Polska	3.54E-06
Belgique-België	7.50E-06	Hrvatska	2.15E-06	Portugal	1.99E-06
Bulgaria	2.20E-06	Magyarorszag	3.21E-06	Romania	2.63E-06
Suisse	4.63E-06	Ireland	9.41E-07	Sverige	1.27E-06
Ceska Republika	3.73E-06	Italia	4.10E-06	Slovenija	2.86E-06
Deutschland	6.60E-06	Lietuva	1.11E-06	Slovenska Republika	3.54E-06
Danmark	1.41E-06	Luxembourg	3.81E-06	United Kingdom	5.85E-06
Eesti	7.36E-07	Latvija	8.23E-07	Serbia and Montenegro	2.30E-06
España	2.18E-06	Macedonia	1.86E-06		

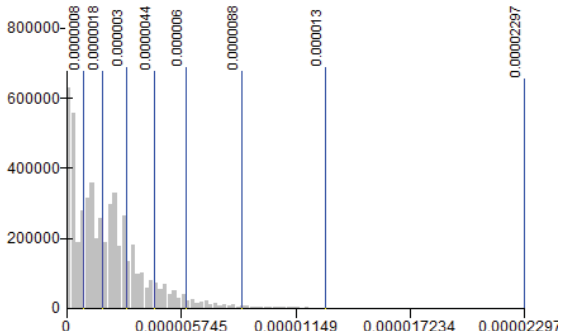

Figure 4.1.43: Histogram of the distribution of the intake fraction in the grid cells of 1*1 Km2 in Europe under the case i)

4.1.3.7.4. Results-3-Variability in air deposition after an emission in all Europe

The maps of the concentration in soil due to deposition from air have been calculated for both substances. The spatial variability of 1,1,1,2-tetrachloroethane and nitrobenzene mass in soil, as a result of the atmospheric deposition after an emission in air, are similar. In this case, the concentrations span over two orders of magnitude and follow the pattern of the atmospheric deposition which explains why higher concentrations are predicted in the mountain areas, in which typically comparatively lower temperatures are expected. The related FFs also vary up to two orders of magnitude.

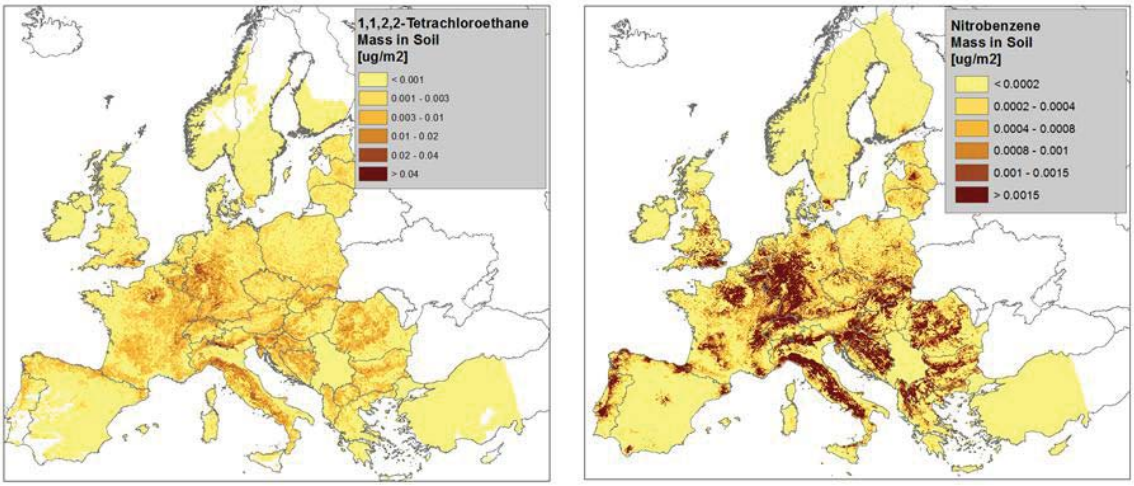

Figure 4.1.44: Concentration (µg/m^2) of 1,1,1,2 tetrachloroethane (left) and nitrobenzene (right) in soil after an emission in air. Statistics [Tetrachloroethane: min=0, max=0.21, mean=2.1 10^{-3}, SD=5.5 10^{-3}; 5% =0, 95% = 0.032. Nitrobenzene: min=0, max=0.16, mean=5.3 10^{-4}, SD=1.8 10^{-3}; 5% =0, 95% = 0.021]

4.1.3.7.5. Results -4- Intake fraction due to an emission from a single country

In order to calculate the intake fractions (iFs) related to an emission from a single country, highlighting the effect of the emission on neighbouring countries, we ran MAPPE for an emission of 1,1,2,2 tetrachloroethane under four scenarios:

- atmospheric emissions of 10t only in Spain (population 47M)
- atmospheric emission of 0.7t only in Luxemburg (population 0.517M), representing the same amount of emission as in Madrid, downscaled by the population of Luxemburg city
- atmospheric emissions of 0.7t only in Luxemburg city, representing approximately the same emission per unit area as in Madrid, which equates to total of 3.5t for the state of Luxembourg .
- atmospheric emission of 3.5t only in Slovenia (population 2.052 M), representing the same amount of emissions as in the country of Luxembourg

4.1.3.7.5.1. Emission in Spain

The distribution of the concentration due to an emission from Spainish major cities clearly shows that the highest range of concentrations (>110 pg/m^3) are mainly located within the same country. France and Portugal are also affected in the range 10-50 pg/m^3, whereas concentrations below 10 pg/m^3 have a distribution towards eastern countries, encompassing France, Belgium, Switzerland, Germany and Italy. The resulting iF for these countries is equal to 2.41E-6. The iF map indicates, as expected, the highest values in Spain contributing 85% to the overall value (iF 2.04E-6), followed by France (6%), Portugal, Germany and Italy (1.5% each). The details of contribution of each country are reported in fig 4.1.47.

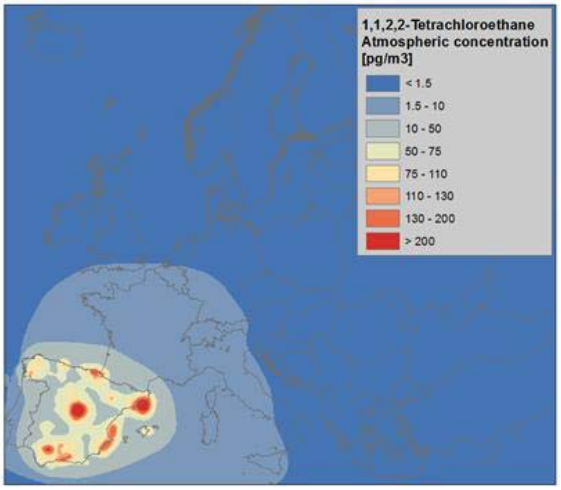

Figure 4.1.45: Concentration of 1,1,1,2 tetrachloroethane in air after an emission in air (10 ton) in Spain (statistics computed over land only Values: min=0, max=648.2, mean=8.71, SD=26.3; 5% = 0; 95% = 134.7)

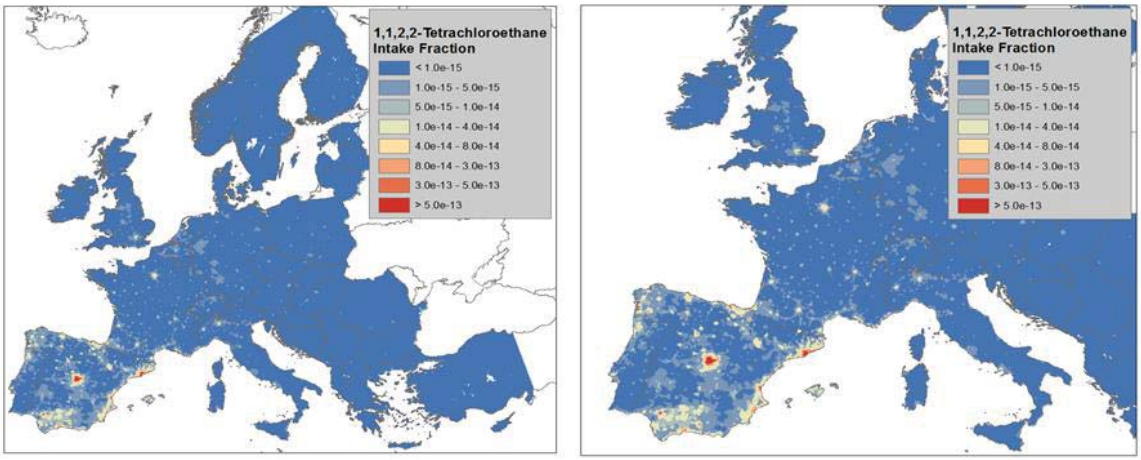

Figure 4.1.46: Intake fraction of 1,1,1,2 tetrachloroethane in air after an emission (10 ton) in air in Spain. (Values: min=0, max=4.2 10^{-12}, mean=1.3 10^{-15}, SD=2.6 10^{-14}; 5% = 0; 95% = 1.4 10^{-12}). The iF values are calculated over a year. To compare the results with previous map, values have to be multiplied by 365

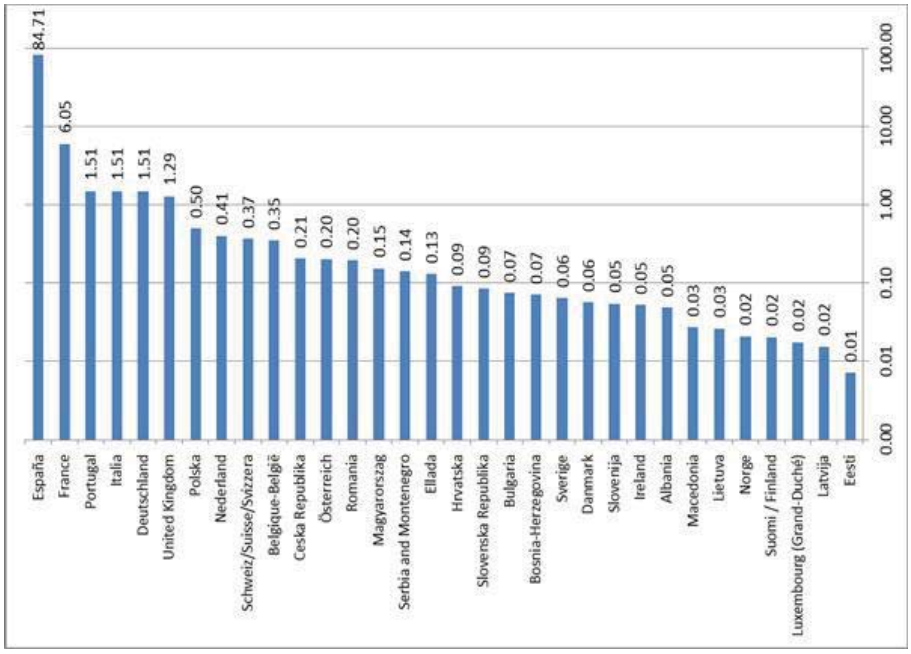

Figure 4.1.47: Relative contribution of each European country to the overall iF associated to an emission from Spain. Values are in percentage

4.1.3.7.5.2. Emission in Luxemburg, scenario A and B

We ran MAPPE for an emission from Luxemburg under two scenarios: A) atmospheric emission of 0.7t t only in the country of Luxemburg representing the same amount of emission as in Madrid, downscaled by the population of Luxemburg city; B) atmospheric emissions of 0.7 t only in Luxemburg city, representing approximately the same emission per unit area as in Madrid, which equates to a total 3.5t for Luxembourg.As a result of increasing the emission in scenario B, the area of dispersion of masses in air is wider, involving more countries compared to scenario A, but the overall iF is only slightly affected (in scenario A, iF is equal to 5.75E-6 whereas in scenario B, it is equal to 6.20E-6 with a variation of 8%). The most influential factor is the dispersion over Germany, where an 8% increase in iF is observed (scenario A 3.66E-6, scenario B 3.97E-6) followed by a 59% of variation in France which results in an increase of the relative contribution of the country from 5.24E-7 in scenario A to 8.35E-7 in scenario B. iF in other countries remain basically the same.

The results confirm the importance of the spatial distribution of the dispersion of an emission. If higher masses reach the air in densely populated areas, the intake fractions is affected.

In scenario B, the relative contribution of the countries to the overall iF is presented in the figure below. Even if Luxemburg is the emitting country, the contribution is only at third highest, after Germany (64%) and France (13.8%). The Luxemburg contribution is 5.5% (as Belgium) followed by Italy, Netherland, UK (1.38% each).

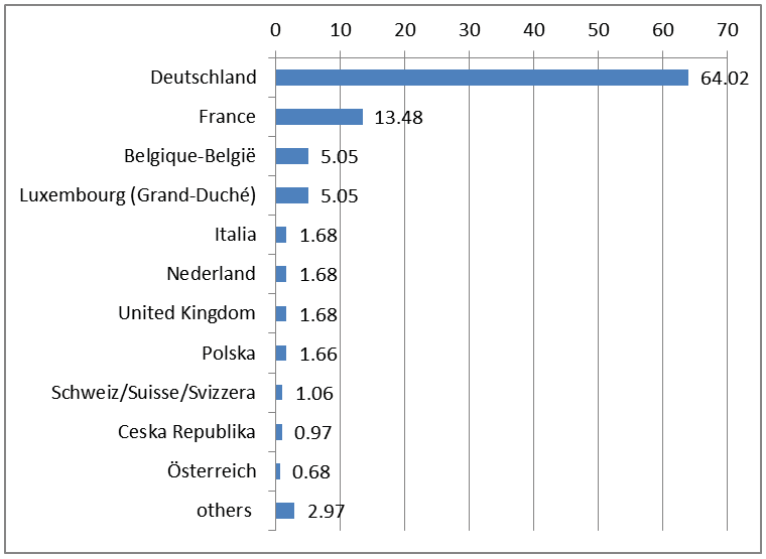

Figure 4.1.48: Relative contribution of Eu countries to the intake fraction of 1,1,2,2 tetrachloroethane in air after an emission (3.5 ton) in air in Luxemburg. Values are in percentage. Countries contributing less than 0.5% are reported as "others"

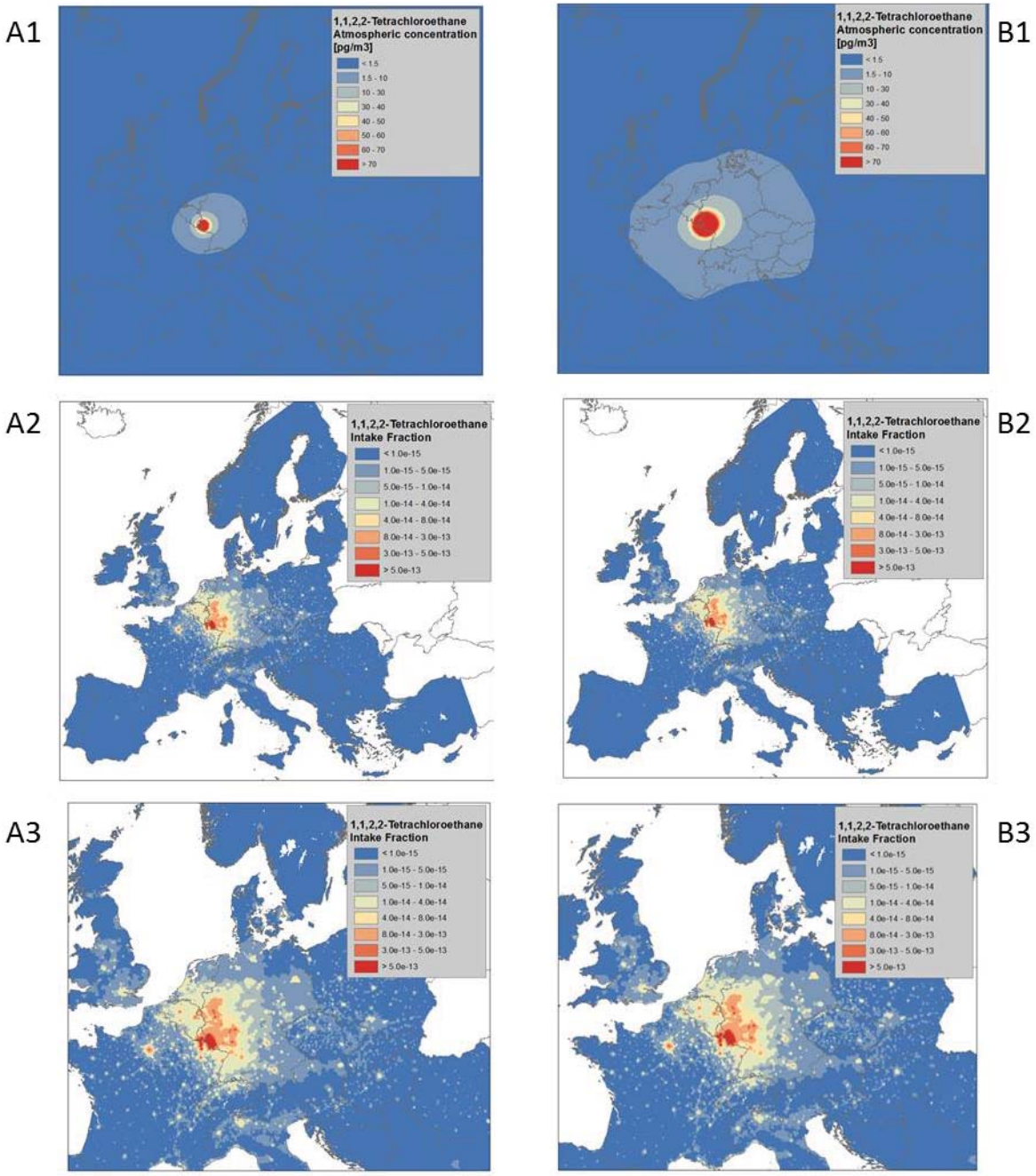

Figure 4.1.49: Map of concentration and intake fraction in Europe due to an emission from Luxemburg under two scenarios, A and B. A [Emission scaled to compare the emission per person from Madrid (7 ton); Concentration in air (min=0, max=369.6, mean=0.98, SD=7.95 (5% = 0, 95% = 152.2) ; Intake fraction (Values: min=0, max=4.0 10^{-12}, mean=3.3 10^{-15}, SD=3.6 10^{-14} (5% = 0; 95% = 1.4 10^{-12})] and B [Emission scaled to compare the unit emission per Km^2 from Madrid (3.5 ton); Concentration in air (min=0, max=1847.9, mean=4.89, SD=39.8 (5% = 0, 95% = 760.93); Intake fraction (Values: min=0, max=4.0 10^{-12}, mean=3.3 10^{-15}, SD=3.6 10^{-14} (5% = 0; 95% = 1.4 10^{-12})]. Statistics calculated over land. The iFs values are calculated over a year. To compare the results with maps of uniform emission in EU, values have to be multiplied by 365

4.1.3.7.5.3. Emission in Slovenia

We ran MAPPE also considering the emission from Slovenia (3.5t), representing the same emissions as for Luxembourg (scenario B, above). The mean value of the concentration across EU is similar (4.89 pg/m^3 for Luxemburg compared to 4.39 for Slovenia) whereas the peak concentrations, expressed by the 95%, are lower in Slovenia (403.34 pg/m^3) than in Luxemburg (760.93 pg/m^3) as the intensity of emission is different (in Kg/km^2). The resulting iF due to the emission from Slovenia is 3.57E-6, 57% lower than in the case of Luxemburg (6.20E-6). Even if several countries are affected by the dispersion of the chemical, the lower population density affects the final iF.

The relative contribution of the countries is presented in fig 4.1.52: Slovenia and Croatia account respectively for 32% and 29 %of the iF, followed by Italy 8.7%, Austria and Hungary 5,8% each.

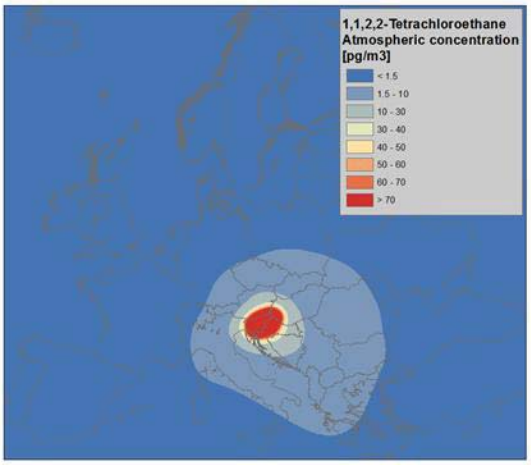

Figure 4.1.50: Concentration of 1,1,2,2 tetrachloroethane in air after an emission (3.5 ton) in air in Slovenjia (min=0, max=745.3, mean=4.39, SD=29.01 ; 5% = 0, 95% = 403.34)

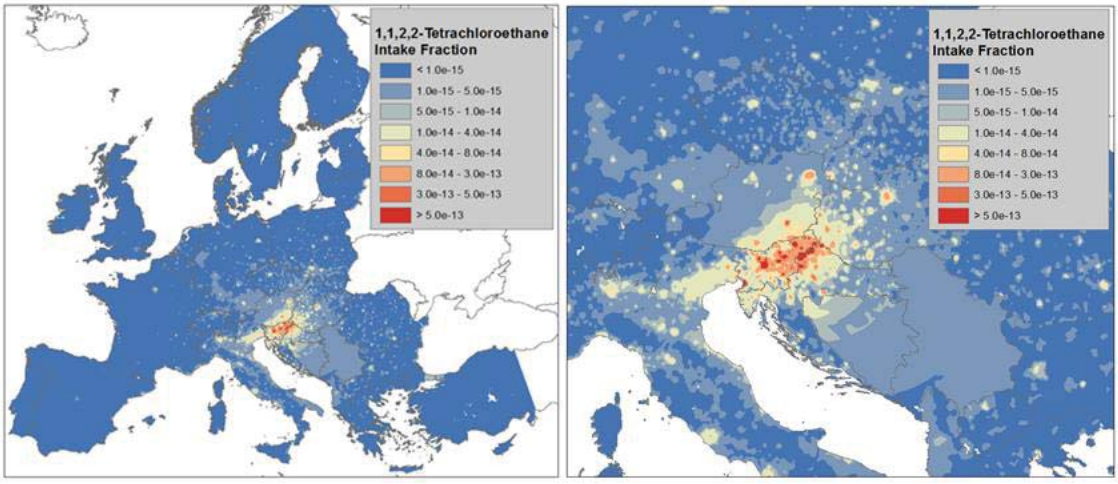

Figure 4.1.51: Intake fraction of 1,1,2,2 tetrachloroethane in air after an emission (3.5 ton) in air in Slovenjia (Values: min=0, max=1.6 10-11, mean=2.02 10-15, SD=6.08 10-14 (5% = 0; 95% = 1.4 10-12). On the right a detail on Slovenia and neighbouring countries. The iF values are calculated over a year. To compare the results with maps of uniform emission in EU, values have to be multiplied by 365

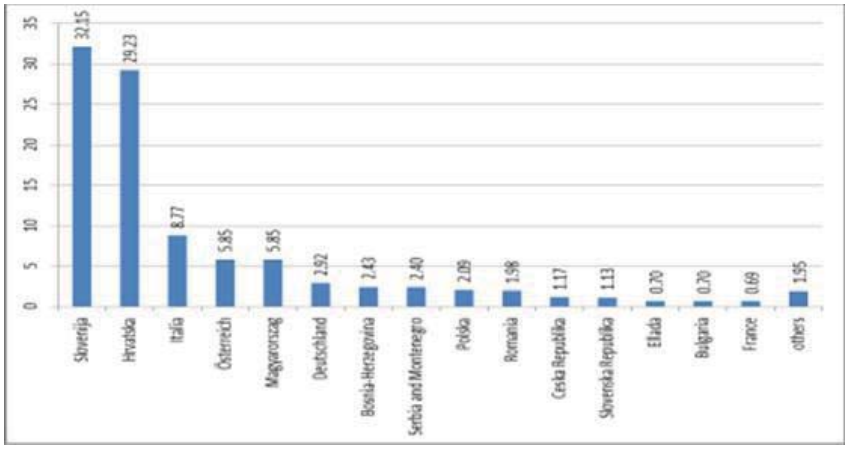

Figure 4.1.52: Relative contribution of Eu countries to the intake fraction of 1,1,2,2 tetrachloroethane in air after an emission (3.5 ton) in air in Slovenia. Values are in percentage. Countries contributing less than 0.5% are reported as "others"

4.1.3.7.5.4. Synopsis of the results per country and discussion

The summary of the results is reported in figure 4.1.53. In the four scenarios, the iFs are always of the same order of magnitude (E-6) and the difference amongst emitting countries are explained by the differences in the pattern of chemical dispersion, leading to higher or lower iF depending on higher or lower population densities.

The iFs are one order of magnitude higher than in USEtox, where the iF due to an emission to continental air is 4.38E-5. The specific reasons behind this difference have to be further explored with regard of the continental box. Known differences include: i) volume of the air compartment (1E+16 m^3 in USEtox vs 1.84E+15 m^3 in MAPPE); ii) population (9.98E+08 in USEtox vs 5.2 E+8 in MAPPE); iii) area of land (9.01E+6 km^2 in USEtox vs 4.9E+6 km^2 in MAPPE).

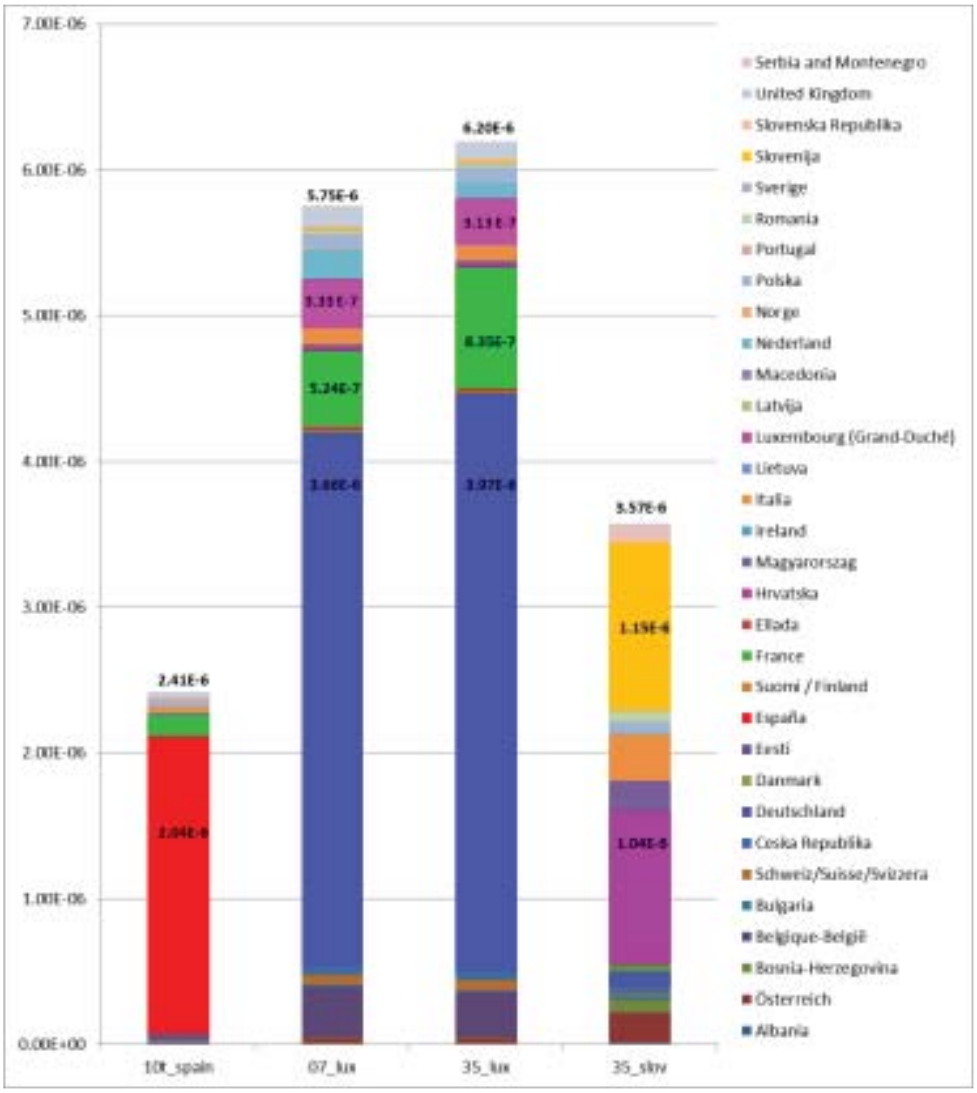

Figure 4.1.53: Summary of the iF results of the emission by single country. Overall iF are reported on top of each bar

4.1.3.7.6. Results-5-Intake fraction due to an emission in Europe- scenario based on real emission

4.1.3.7.6.1. Emission of 1,2-Dichloroethane in Europe

From the European Pollutant Release and Transfer Register (E-PRTR) it is possible to extrapolate the emission reported by industrial facilities across Europe for 91 pollutants. Considering emission into air, the organic chemical with highest emission in air is 1,2-Dichloroethane(DCE). Most releases to the environment are from its use in chemical manufacture. Data on emission into air over years have been collected and are plotted in figure 4.1.54.

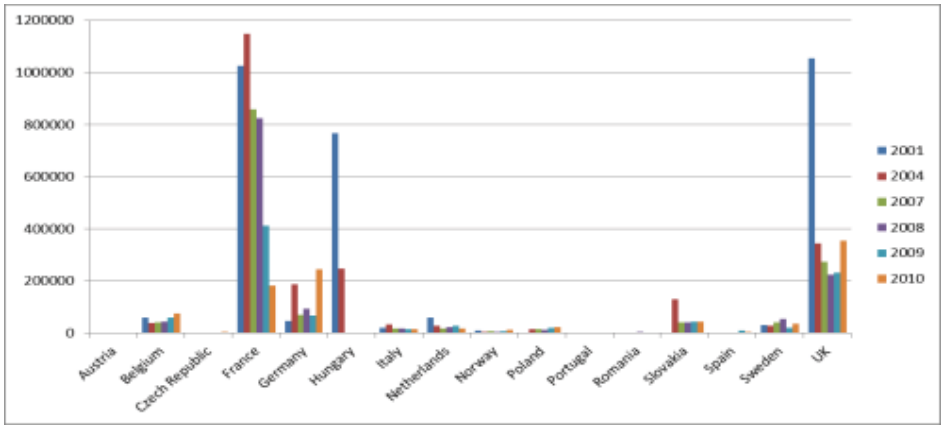

Figure 4.1.54: Emission in air of 1,2 dichloroethene by country by year from industrial facilities (source E-PRTR)

To run MAPPE under a realistic scenario of emissions, we assigned to each European country the emission as reported in the E-PRTR register. We ran the model considering the emissions in 2010, reported in table 4.1.12.

Table 4.1.12: Emission in air of 1,2 dichloroethane by country in 2010

Country	kg/2010	Country	kg/2010	Country	kg/2010
Albania	0	Greece	0	Poland	22310
Austria	3220	Cyprus	0	Portugal	0
Belgium	75770	Hungary	0	Spain	5820
Bulgaria	0	Ireland	0	Romania	0
Czech Republic	4450	Italy	14820	Slovakia	43400
Denmark	0	Latvia	0	Sweden	35500
Estonia	0	Lithuania	0	Switzerland	0
Finland	0	Luxembourg	0	Bosnia and Herzegovina	0
France	182700	Macedonia	0	Croatia	0
Germany	244450	Netherland	18900	Slovenia	0
Great Britain	356000	Norway	13700	Serbia	0

The following maps show the distribution of the concentration and the mass*iR over Europe and the distribution of the resulting iFs. The overall iF at continental level is equal to 5.88E-6, with a contribution mainly related to emitting countries. In fact 96.62% of the overall iF is associated to emitting countries, as highlighted in table 4.1.13.

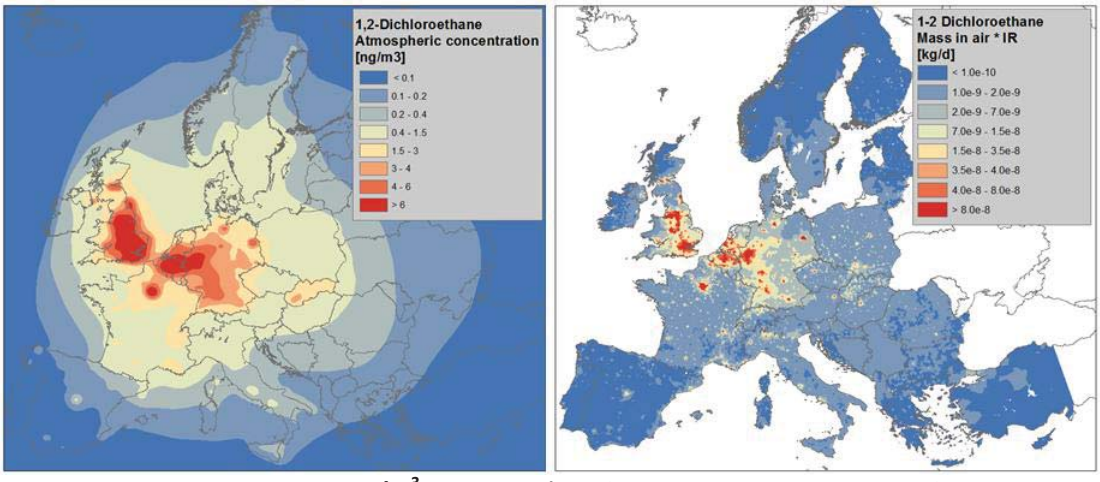

Figure 4.1.55: Concentration in ng/m^3 and mass *iR of 1,2-dichloroethene in air after an emission into air according to the table above. Statistic calculated over land only (concentration: min=0, max=23.6, mean=1.01, SD=1.63 ; 5% = 0, 95% = 6.02) (mass*iR: min=0, max=2.12 10^{-6}, mean=3.15 10^{-9}, SD=2.4 10^{-8})

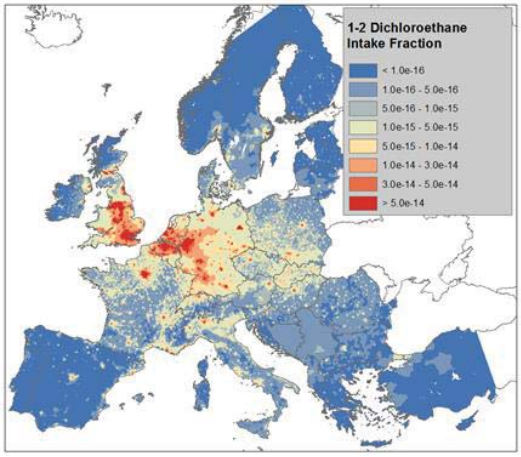

Figure 4.1.56: Intake fraction of 1,2 dichloroethene in Europe after an emission into air. (Values: min=0, max=2.14 10^{-12}, mean=3.08 10^{-15}, SD=2.3 10^{-15} ; 5% = 0, 95% = 4.45 10^{-13})

Table 4.1.13: Synoptic table of percentage contribution to overall emission and to overall iF (5.88E-6) at country scale co for Europe. In bold emitting countries

Country	% of emission	% of iF	Country	% of emission	% of iF	Country	% of emission	% of iF
Albania		0.03	Greece		0.08	Poland	2.19	2.90
Austria	0.32	0.69	Cyprus		0.00	Portugal		0.01
Belgium	7.42	7.06	Hungary		0.69	Spain	0.57	0.46
Bulgaria		0.11	Ireland		0.12	Romania		0.96
Czech Republic	0.44	1.14	Italy	1.45	2.12	Slovakia	4.25	0.96
Denmark		0.26	Latvia		0.04	Sweden	3.48	0.65
Estonia		0.01	Lithuania		0.07	Switzerland		0.81
Finland		0.05	Luxembourg		0.10	Bosnia and Herzegovina		0.08
France	17.89	13.09	Macedonia		0.02	Croatia		0.13
Germany	23.94	27.46	Netherland	1.85	5.52	Slovenia		0.09
Great Britain	34.87	34.38	Norway	1.34	0.18	Serbia		0.21

4.1.3.7.6.2. Emission of 1,2-Dichloroethane in Belgium

In order to highlight the relative contribution of Belgium on the overall intake fraction, MAPPE was run considering an emission from Belgium only. The iF due to the emission in Belgium is equal to 9.26E-06, for which Belgium is representing the highest contribution (45.15%) followed by Germany (23.86%) and Netherlands (18.86%). France and UK contribute with 6.31% and 2.21% respectively whereas the other countries are less affected.

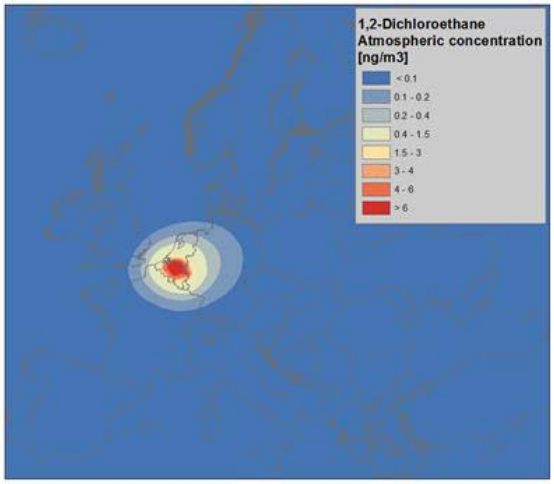

Figure 4.1.57: Concentration of dichloroethene1,2 in Belgium after an emission into air accordingly to the table above (Statistic calculated over land only, min=0, max=13.7, mean=0.086, SD=0.53 (5% = 0, 95% = 7.11)

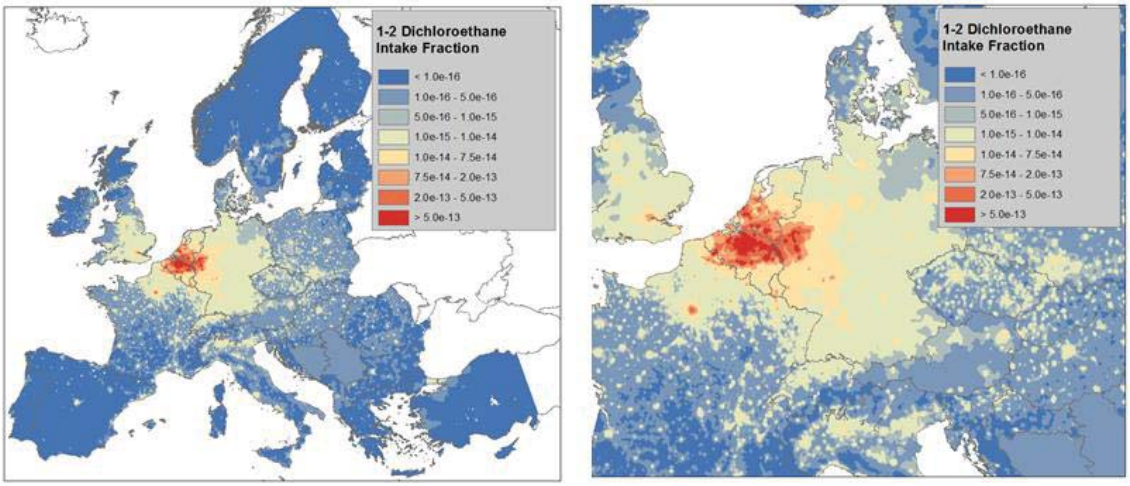

Figure 4.1.58: Intake fraction of 1,2 dichloroethene in Belgium after an emission into air. Values: min=0, max=1.41 10^{-11}, mean=4.86 10^{-15}, SD=6.7 10^{-14} (5% = 0, 95% = 4.45 10^{-13}). A detail map on central Europe on the right

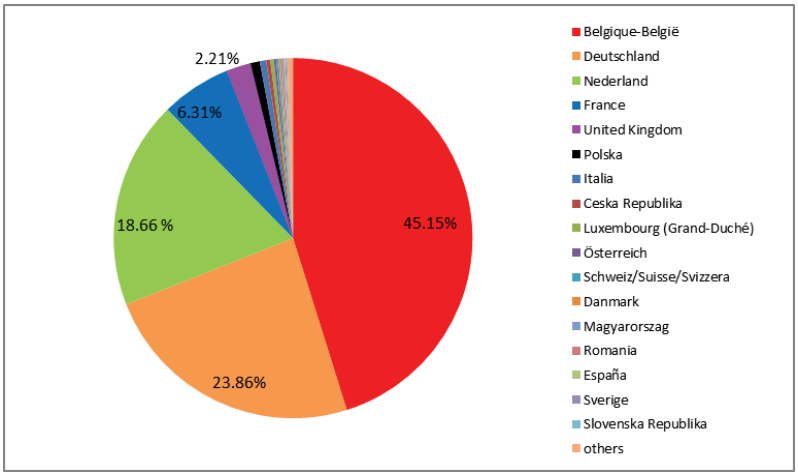

Figure 4.1.59: Relative contribution of EU countries to the intake fraction of 1,2- dichloroethene in Belgium in air after an emission in air in Belgium. Values are in percentage. Countries contributing less than 0.5% are reported as "others"

4.1.3.8. Selection of an appropriate model and spatial resolution for toxicity categories

4.1.3.8.1. Inter-continental variation: comparison of IMPACT World regionalized and USEtox nested model

Table 4.1.14 shows some key landscape parameters of the USEtox parametrization. The full set of parameters is provided in supporting information Table S4.2. Land area varies from 6.0E+05 km^2 for Japan (JAP) to 2.4E+07 km^2 for North Africa (W6). Other physical landscape parameters such as area of sea, freshwater, rain rate, freshwater depth also represent more than one order of magnitude between the lowest and the highest value. Exposure is based on regional values of population and food production (Pennington et al. 2005; Margni et al. 2004).

Table 4.1.14: Key landscape parameters for the USEtox 17 zone parametrization

ID #	Name	Area	Area	Areafrac	Rain rate	Depth	Human pop	Human pop	Exposed produce	Unexposed produce	Meat	Dairy products	Fish freshwater	Fish coastal marine water
		land	sea	freshwater		Freshwater	continent	urban	continent	continent	continent	continent	continent	continent
		km^2	km^2	[-]	$mm.y^{-1}$	m	[-]	[-]	kg/(day*capita)	kg/(day*capita)	kg/(day*capita)	kg/(day*capita)	kg/(day*capita)	kg/(day*capita)
W1	West Asia	1.7E+07	7.4E+05	1.7E-02	2.2E+02	1.3E+01	2.35E+08	1.47E+06	1.39	0.65	0.08	0.26	0.011	0.05
W2	Indochina	3.3E+06	2.2E+06	3.6E-02	2.4E+03	1.3E+01	4.65E+08	1.30E+06	1.55	1.21	0.05	0.01	0.008	0.06
W3	N. Australia	6.6E+06	1.6E+06	9.9E-03	1.5E+03	3.0E+00	3.20E+06	8.24E+05	6.10	4.54	0.51	1.39	0.006	6.65
W4	S. Australia+	1.5E+06	6.4E+05	1.2E-02	5.1E+02	3.0E+00	2.12E+07	1.03E+06	5.34	3.89	0.60	2.84	0.004	0.61
W5	S. Africa	1.0E+07	6.2E+05	2.2E-02	1.0E+03	4.6E+01	3.24E+08	1.25E+06	0.38	1.08	0.03	0.06	0.006	0.03
W6	N. Africa	2.4E+07	9.7E+05	1.9E-02	5.1E+02	4.6E+01	7.89E+08	2.30E+06	0.65	0.78	0.04	0.10	0.006	0.01
W7	Argentina+	4.2E+06	1.1E+06	1.5E-02	7.0E+02	8.0E+00	6.67E+07	2.89E+06	3.74	1.64	0.23	0.57	0.002	0.31
W8	Brazil+	1.1E+07	5.8E+05	8.3E-03	1.8E+03	8.0E+00	2.42E+08	2.62E+06	1.41	5.03	0.20	0.28	0.004	0.05
W9	Central America	5.9E+06	1.3E+06	3.6E-02	2.0E+03	2.0E+01	3.05E+08	2.76E+06	0.62	2.10	0.09	0.20	0.003	0.04
W10	US+	1.4E+07	1.8E+06	3.4E-02	7.1E+02	2.0E+01	3.28E+08	1.32E+06	4.28	0.96	0.35	0.69	0.003	0.04

W12	N. Eur. + N. Canada	1.8E+07	5.6E+06	4.9E-02	4.9E+02	1.7E+01	1.67E+07	6.56E+05	1.61	0.60	0.15	0.75	0.008	1.43
W13	Europe+	8.6E+06	1.7E+06	1.6E-02	5.5E+02	1.5E+01	7.59E+08	1.41E+06	2.34	1.35	0.19	0.80	0.003	0.02
W14	East Indies	2.0E+06	1.4E+06	3.0E-02	1.5E+03	3.0E+00	2.07E+08	1.30E+06	0.77	0.58	0.02	0.01	0.013	0.13
IND	India	4.6E+06	4.6E+05	4.2E-02	1.2E+03	1.3E+01	1.57E+09	1.76E+06	0.77	0.81	0.01	0.20	0.008	0.00
CHI	China	6.4E+06	8.4E+05	4.6E-02	1.2E+03	1.3E+01	1.33E+09	1.47E+06	1.49	0.79	0.12	0.03	0.029	0.01
JAP	Japan	6.0E+05	4.2E+05	4.4E-02	2.4E+03	1.3E+01	1.51E+08	4.56E+06	0.94	0.44	0.09	0.19	0.027	0.06

Figure 4.1.60 presents the residence time of freshwater (a), the residence time of substances emitted into freshwater (i.e. $F_{w,w}$) (b), the transfer fraction from air to freshwater (c) and transfer fraction from freshwater to air (d).

Figure 4.1.60a shows that water residence time is similar in both models for all sub-continental zones, except for North Australia (W3) overestimated in IMPACT World, East Indies (W14) and North Canada + North Europe (W12) both underestimated in IMPACT World. For the latter zone, the difference in water residence time comes from a model artifact in IMPACT World due to the way the flow modeling is calculated between W12 and W10 (define the region). Indeed, 1E10 m^3/h flows from W10 to W12 and 1E9 m^3/h flows back from W10 to W12. While the flows pertain to rivers exchanging between W12 and W10 without discharging directly to the sea, it creates a model artifact: a loop of water stuck between W10 and W12. This loop results in an underestimation of water residence time due to an artificial increased outflow in IMPACT World compared to USETOX, where flows are modeled based on a mass balance between precipitation, evapotranspiration and infiltration. IMPACT World instead calculates absolute hydrological advective flows from river discharges out from the sub-continental zone. On the same line the overestimation of the water residence time compared to USEtox in W3 is explained by an underestimation of outflows in IMPACT World to adjacent costal zones CEW3 and CWW3.

Figure 4.1.60b compares fate factors in water for chemical emissions into water ($FF_{w,w}$) for each sub-continental zone between the IMPACT World and USEtox. Discrepancies between the results from the two models are correlated with the sub-continental zones already showing different water residence time for W14 East Indies, W12 North Canada + North Europe, W3 N. Australia as per a. For W3 N. Australia, the USEtox fate factors reach a maximum of 28 days (corresponding to the freshwater residence time) for pollutants which disappearance is not driven by processes such as degradation, evaporation or sedimentation (e.g., Folpet, Methomly). Similarly the observed trend of fate results for W14 East Indies can be explained by the difference in water residence time, limiting the fate factors to a maximum of 19 days in the IMPACT World model (equals the freshwater residence time in W14). Chemicals which disappearance is not limited by processes such as degradation, evaporation or sedimentation (e.g., Folpet) are thus to be found at the high end of the asymptote set at 19 days. However, an outlier (Hexachlorobenzene) is observed exceeding this maximum the fate factor of 19 days. This is explained by inherent structure of a spatially differentiated vs non-spatial model. In the former a pollutant can be transferred from a watershed into another and remain in the system as long as the water residence time of the receiving system. As the fate factor is the product between the transfer fraction from the emission to the receiving compartment and the residence time of this latter (see Equation 4.1.8 and 4.1.9), in a spatially differentiated model it can therefore exceed the fate factor of the emission compartment. In our case, the fate of Hexachlorobenzene is driven by the residence time of the pollutant that reaches Antartica (W11), and the capability of the pollutant to be transferred in that sub-continental zone. Hexachlorobenzene is highly volatile

(K_H=170 Pa m^3 mol^{-1}) and persistent ($t_{1/2air}$=0.84 yr and $t_{1/2water}$=6.3 yr). The IMPACT World model water residence time in Antartica (W11) is 8220 yr. The fate of Hexachlorobenzene in W11 is thus not limited by water residence time of the emitting compartment. Results for South Australia (W4) show that differences in chemical fate that are not correlated with the residence time of water. This difference is important for chemicals with a large K_H (e.g., Hexachlorobenzene with K_H = 170 $Pa.m^3.mol^{-1}$, tetrachloroethylene with K_H = 1770 $Pa.m^3.mol^{-1}$; 1,3-butadiene K_H = 7360 $Pa.m^3.mol^{-1}$;) which main disappearance pathway is volatilization to continental air for both IMPACT World and USEtox models. The observed discrepancies originate from the volatilization algorithm: the volatilization rate constant equals 2.7 m/day in USEtox and 0.24 m/day in IMPACT World. This order of magnitude difference is then reflected in the fate factor results.

Figure 4.1.59c shows that IMPACT World tends to overestimate the transfer factor from air to water in relation to pollutant properties by about 1 order of magnitude compared to USEtox. The dominant disappearance pathway of pollutants with high K_H (e.g., Hexachlorobenzene K_H=170 $Pa.m^3.mol^{-1}$, carbon tetrachloride K_H=2760 $Pa.m^3.mol^{-1}$, N-Nitrosodiethylamine K_H=0.362 $Pa.m^3.mol^{-1}$) emitted to continental air is transfer to global air. The transfer factor from air to water is higher than 1 for Hexachlorobenzene in IMPACT World for emission to several regions, e.g., W8 Brazil and W14 East Indies. This is due to the fact that when Hexachlorobenzene is emitted to air, there is deposition in freshwater of other continents (Hexachlorobenzene is persistent in air and water), which can exceed the fate when directly emitted to freshwater. For example, when emitted to East Indies (W14), there is an important fate in Antartica (W11) deposited from air. As residence time in W11 is higher than in W14 (>8000 y compared to 19 days), the pollutant disappears in W11 by degradation rather than transfer to seawater.

Figure 4.1.59d shows that when emitted to water, Thiram and N-Nitrosodiethylamine transfer fraction to air are under-estimated by USEtox by respectively 2 and 1 orders of magnitude. This discrepancy can be again explained by the volatilization rate difference in both models.

From these observations, we can conclude that deviations in fate results are rather due to model algorithm difference, i.e., modeling of water outflow and volatilization algorithm, than influence of global or continental zone surrounding.

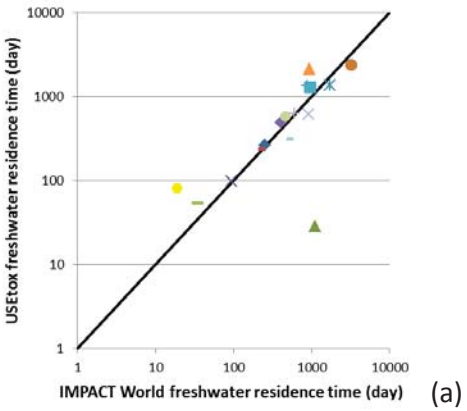

(a)

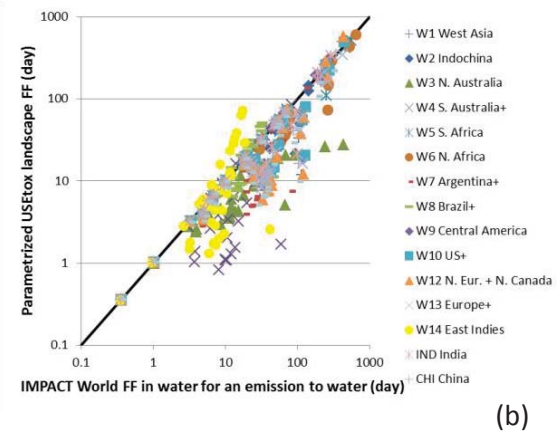

(b)

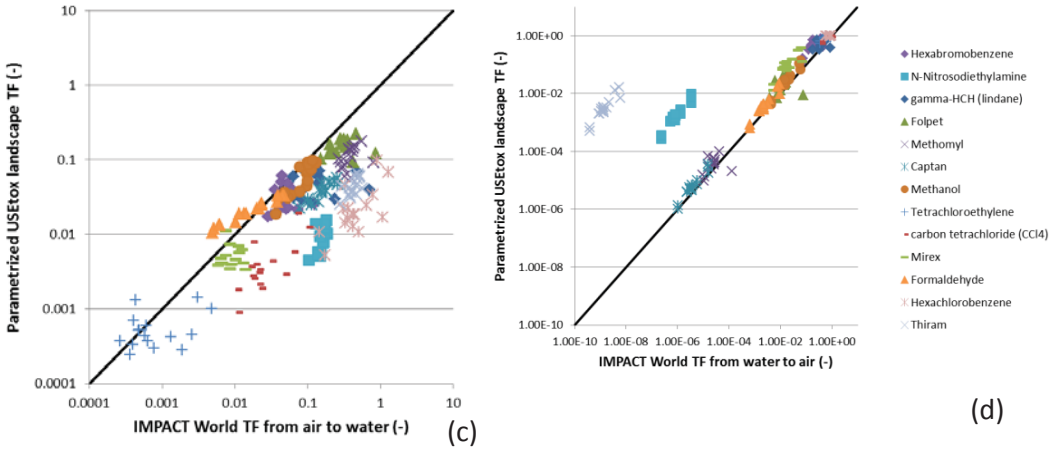

Figure 4.1.60: Comparison between non-spatial USEtox model and the spatially differentiated IMPACT World model regarding: a) Freshwater residence time in each sub-continent, b) Residence time in water of 36 representative chemicals emitted in each sub-continent, c) Transfer fraction from air to water and d) Transfer fraction from water to air

Figure 4.1.61 displays the comparison of human intake fractions for emission into water by inhalation (a), total ingestion (b), water ingestion (c) and fish ingestion (d). Figure 4.1.60a shows that results for both models are aligned except for Thiram and N-Nitrosodiethylamine. This difference is correlated with the discrepancies observed for transfer fraction from water to air (see d), and thus due to a difference in fate factor $F_{w,a}$. Intake fractions for an emission into water for total ingestion (b), water ingestion (c) and fish ingestion (d) are within one order of magnitude between the two models. Neither differences in spatialization nor in model algorithms result in a significant deviation of intake fraction results. Intake fraction results for other pathways for an emission to water as well as intake fraction for all pathways for an emission to air are presented in Figures S4.53 and S4.54 of supporting information 5.3.12.

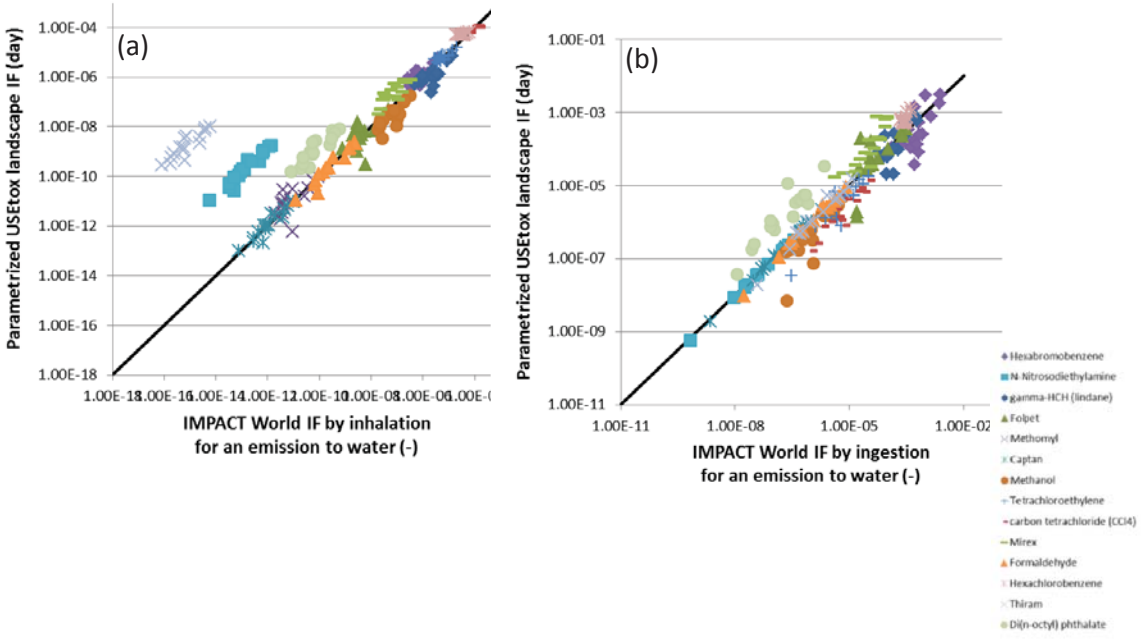

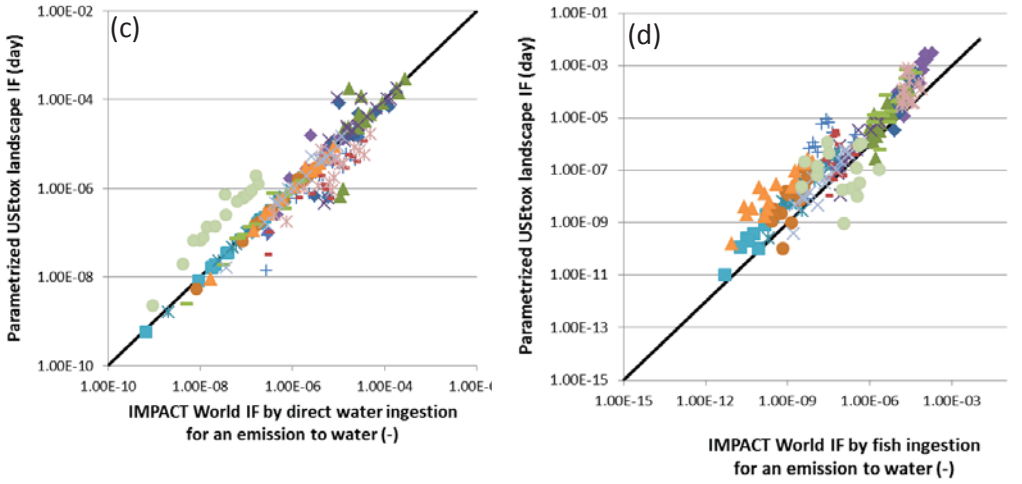

Figure 4.1.61: Comparison between non-spatial USEtox model and the spatially differentiated IMPACT World model regarding: a) Inhalation intake fraction for an emission to water, b) Total ingestion intake fraction for an emission to water, c) Ingestion intake fraction through water ingestion for an emission to water, d) Ingestion intake fraction through fish ingestion for an emission to water

4.1.3.8.2. Intra-continental variation and importance of spatialization: Europe a-spatial and Europe spatial IMPACT model

This part focuses on the analysis of intra-continental variation of fate and intake fraction in Europe on a watershed scale.

Figure 4.1.62 displays results for the comparison of fate factors (a,b) and intake fractions (c-f) between the a-spatial and spatial IMPACT model for both uniform and point emission (in red).

Figure 4.1.62a shows that for highly degradable pollutants ($t_{1/2}$, <. 0.01 y), fate for a uniform emission modelled with the spatial model is similar to fate in the a-spatial single box model (bottom left hand side of the graph). For persistent pollutants ($t_{1/2}$ > 0.01 y), fate is over-estimated in the a-spatial single box model due to a higher residence time of freshwater. A-spatial models might thus overestimate the chemical fate up to a factor 5 when compared to a spatially differentiated model for unknown emission location (i.e. assumed being uniformly emitted compared over the whole model surface).

Figure 4.1.62b shows that for point emissions, the a-spatial model accuracy depends on the watershed where the pollutant is emitted, additionally to the pollutant persistence. While for highly degradable pollutants ($t_{1/2}$, <0.01 y), a-spatial results are aligned with the spatial ones for all watersheds, it is not the case for highly persistent pollutants ($t_{1/2}$ > 0.01 y) where the water residence time to the sea of the emitting comparatment is a key parameter. As per the example of an emission into the lake of Geneva, results are slightly under-estimated in the a-spatial single box model due to a water residence time in the spatial model about 3 times higher than the a-spatial one (a-spatial model water residence time: 4.1 y; spatial model water residence time in lake of Geneva watershed: 13.6 y). Results for an emission into the Danube are slightly over-estimated in the a-spatial model (spatial model water residence time in Danube watershed: 1.4 y) and results for Brittany are over-

estimated in the a-spatial model given the 3 order of magnitude difference in water residence time (spatial model water residence time in Brittany watershed: 0.81 d = 0.002 y). When an emission location is known, a spatially differentiated model can thus improve the model accuracy up to 2-3 orders of magnitude.

Human intake fractions for water and fish ingestion are represented in Figure 4.1.62c to f. For a uniform emission (c and e), both intake fractions by water and freshwater fish ingestion are under-estimated by the a-spatial model, up to 2 orders of magnitude. This trend does not follow the one for the fate estimation and arises from differences in exposure estimation. Population in watersheds with high water residence time is indeed lower than in coastal watersheds, where water residence time is low (population is generally concentrated nearby coastal zones). The a-spatial model thus overestimate the intake compared to the spatial model given they do not account the fact that an important part of the exposed population lives in watersheds with low residence time where pollutants are rapidly advected to the sea. For a point source emission into water (d and f), variation of population density also influence the over-estimation of intake fraction by the a-spatial model compared to an emission in Brittany. Results for emission into the watersheds of lake of Geneva and Danube are further explained in the section *Development of water archetype, Evaluation of the performance of the archetype model*.

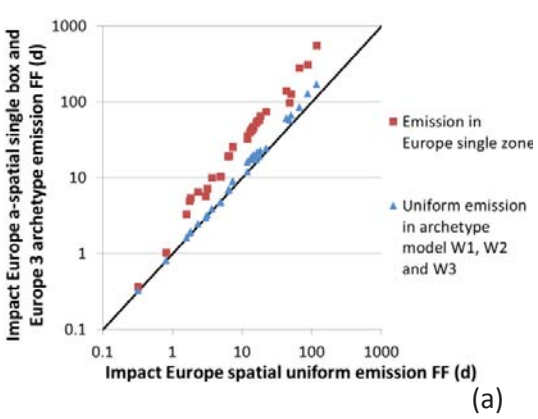

(a)

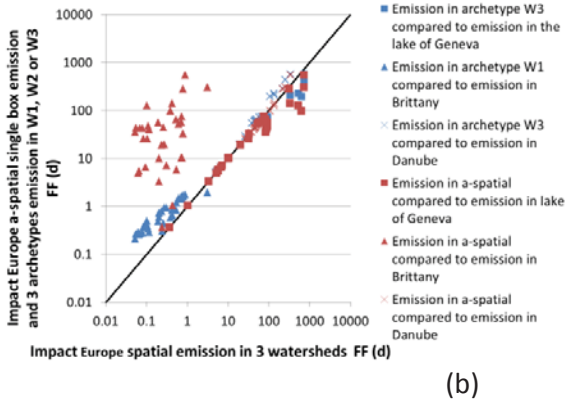

(b)

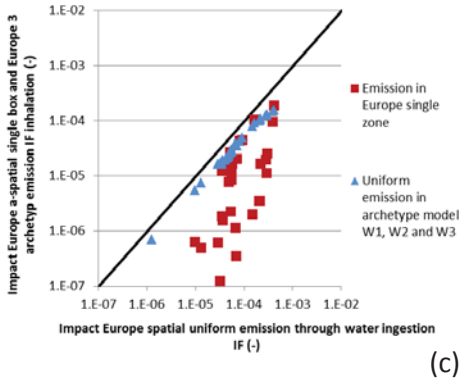

(c)

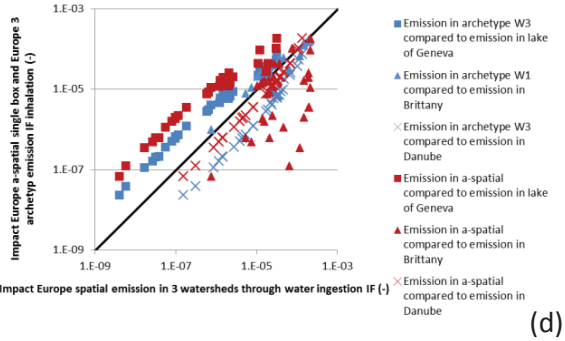

(d)

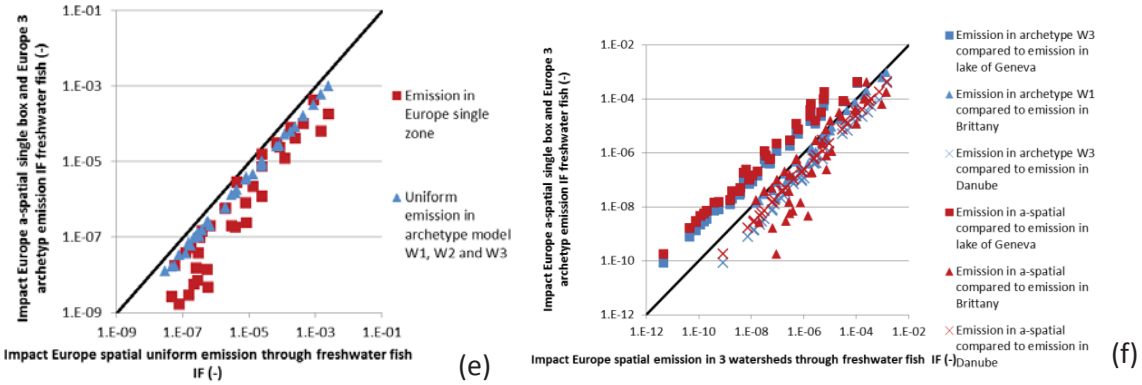

Figure 4.1.62: a) Impact Europe spatial fate factor uniform emission compared to emissions in Europe a-spatial model and uniform emission in W1, W2 and W3 archetype landscapes, b) Impact Europe spatial fate factor emission in lake of Geneva (water residence time 13.6 y), Danube (water residence time 1.4 y) and Brittany (water residence time 0.002 y = 0.81 d), c) Impact Europe intake fraction through water ingestion spatial uniform emission compared to emissions in Europe a-spatial model and uniform emission in W1, W2 and W3 archetype landscapes, d) Impact Europe intake fraction through water ingestion spatial emission in lake of Geneva, Danube and Brittany, e) Impact Europe intake fraction through freshwater fish ingestion spatial uniform emission compared to emissions in Europe a-spatial model and uniform emission in W1, W2 and W3 archetype landscapes, f) Impact Europe intake fraction through freshwater fish ingestion spatial emission in lake of Geneva, Danube and Brittany

The analysis of influential parameters for the spatial differentiation of fate is further explored in Figure 4.1.62a, which shows an evaluation of the variability of chemical fate according to an emission in each of the watersheds of the spatially differentiated European model. The analysis of the relationship between the chemicals half-life in water and their fate in water leads to the observation that for pollutants with very low persistence, i.e., $t_{1/2}$<1 d, fate value for each European watershed varies less than one order of magnitude, e.g., 57% variation for N-Nitrosodiethylamine ($t_{1/2}$=6.00 h in water). On contrary, fate can vary up to four orders of magnitude for persistent pollutants, i.e., $t_{1/2}$>100 d., e.g., 775% variation for Folpet ($t_{1/2}$=1.38E+04 h in water).

Figure 4.1.63b displays the fate factor in function of water residence time for four pollutants with different persistences, i.e., Folpet ($t_{1/2}$=573 d in water), Hexabromobenzene ($t_{1/2}$=73 d in water), Captan ($t_{1/2}$=0.71 d in water) and N-Nitrosodiethylamine ($t_{1/2}$=0.25 d in water). While the fate factor of Nitrosodiethylamine is not influenced by water residence time t, fate factors for Folpet show a linear dependence on water residence time. Outliers are likely to be influenced by other loss processes, such as volatilization or deposition rates, these latter being inversely proportional to the depth of dilution. The higher the freshwater depth, the lower the volatilization and deposition rates.

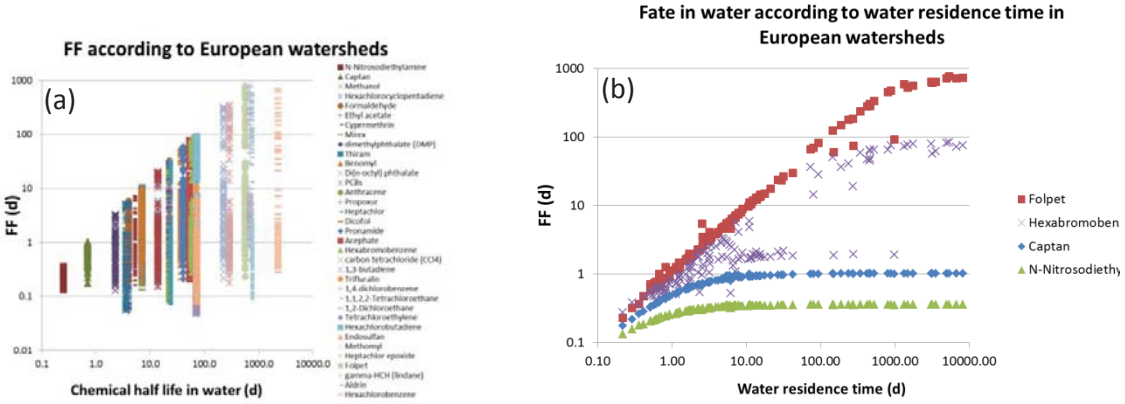

Figure 4.1.63: a) Chemical fate factors of 36 chemicals (plotted on the X-axes) emitted in each single watershed of the European spatial model versus their chemical half-life in water, b) Chemical fate factors as a function of water residence time for each of the 136 European watersheds for N-Nitrosodiethylamine (t1/2=0.25 d in water), Captan (t1/2=0.71 d in water), Hexabromobenzene (t1/2=73 d in water) and Folpet (t1/2=573 d in water)

4.1.3.8.3. Development of archetypes for aquatic ecotoxicity

Previous observations show that within an open system (1) the regionalization for aquatic ecotoxicity is only relevant for persistent pollutants, i.e., pollutants with a degradation rate higher than the advection rate; and (2) for these persistent pollutants, the variation of fate results is driven by the water residence time until the model boundaries (i.e. until the sea or any other advection into the global system). Given that the water residence time (= inverse of the advection rate) depends on the water advective flow and the volume of water in a given watershed, the influence of parameters such as average depth of water on other loss processes, such as volatilization or sedimentation might also play a role but are not further investigated in this work.

The first observation is linked to the pollutant properties and not to a spatial archetype, only the latter observation is thus analyzed in this part. We developed a model with three watersheds with archetypical residence time to improve the performance of the a-spatial model while reducing the amount of input data for its implementation.

Definition of archetypical water residence time: Based on the IMPACT Europe spatial model, we developed an archetypical model where we aggregated the spatial model 127 watersheds in 3 archetypical watersheds defined by lower and upper water residence time thresholds as well as a mean residence time. In order to have meaningful and representative archetypes which overcome as far as possible the limitations of the a-spatial model, we defined archetypes by minimizing the variation of the spatial model water residence times compared to the mean value of the archetype watershed they are related to. According to Equation 4.1.12 using the variables defined in Table 4.1.15, we minimized the standard deviation $SD_{tot,}$ sum of the standard deviations between the watershed residence time τ_{Wi} related to $\tau_{1,}$ τ_2 and τ_3. We used the logarithmic values in order to prevent from giving importance to high values.

Calculation of the total standard deviation of spatial model water residence time compared to mean water residence time of the archetype model. By minimizing this value, we obtained optimal values for τ_1, τ_2, τ_3, τ_{T1} and τ_{T2}

Table 4.1.15: Definition of variables and results of

Variable name	Variable definition	Unit	Mathematical	Final values
τ_{Wi} with 2≤i<136	residence time in watershed i	d	—	-
$\tau_{downstream}$	water residence time in watersheds downstream of watershed i	d	-	-
V_i	volume in watershed i	m^3	-	-
Q_i	advection out of watershed i	m^3/d	-	-
τ_1, τ_2 and τ_3	water residence time for the 3 archetype watersheds calculated from the archetype model	d	— — —	τ_1: 1.7 d τ_2: 8.6 d τ_3: 1600 d
τ_{T1} and τ_{T2}	threshold water residence between the 3 archetype watersheds	d	-	τ_{T1}: 2 d τ_{T2}: 60 d

Figure 4.1.64 shows the new archetype model limits: low water residence time archetype (less than 2 d until the model border, W1), medium water residence time (between 2 and 60 d until the model border, W2), and high water residence time (more than 60 d until the model border, W3), respectively. The classification of IMPACT Europe spatial model watersheds into archetype category is presented in Table S4.5 of supporting information 5.3.13.

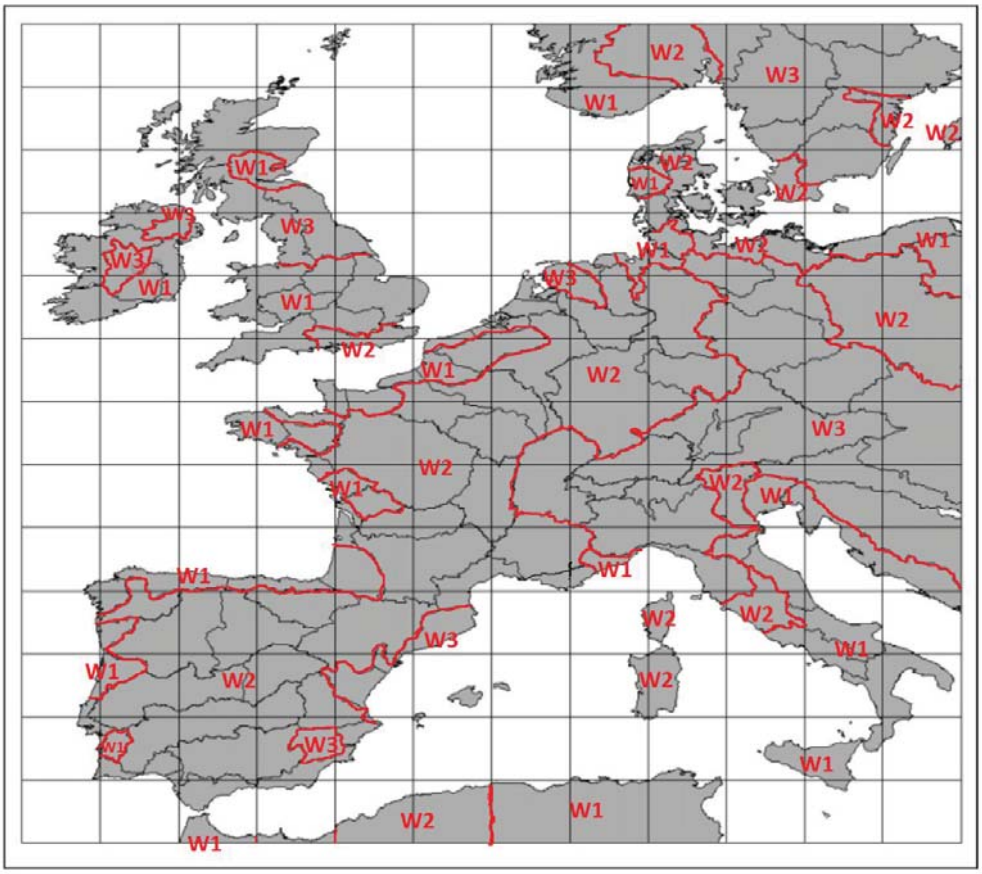

Figure 4.1.64: Limits of the archetypical model based on the IMPACT Europe spatial model (Pennington et al. 2005)

Evaluation of the performance of the archetype model: We evaluated the performance of the archetype model compared to the IMPACT Europe spatial model for the evaluation of chemicals fate and intake fraction for a uniform and punctual emission in Figure 4.1.61a to f (in blue).

Figure 4.1.61a shows that chemical fate factors of the archetype model are aligned with the Europe spatial model for a uniform emission. For an emission in Brittany (b), chemical fate is under-estimated by less than a factor 5 when using the archetype model (water residence time being 0.81 d in Brittany and 2 d in the archetype model), which represents a significant improvement compared to the a-spatial model. For intake fractions by water and freshwater fish ingestion, the archetype model improves the a-spatial model estimation by reducing the difference in results to a factor two compared to the spatial model for a uniform emission (c and e). This reflects the improvement in exposure modelling related to population density compared to the a-spatial model, given that the archetype W1 is composed of coastal areas and thus mimics more adequately the intake fraction of coastal zones.

For a punctual emission (Figure 4.1.62d and f), the fate modelling for an emission in Britanny is improved in the spatial model compared to the a-spatial one, due to improvement in coastal zones exposure modelling. For an emission to Geneva lake, the

difference between emission to the spatial model and to the a-spatial and archetype model is also explained by the difference in exposure.

We recalculated for a persistent pollutant (Folpet) the exposure factor for water and freshwater fish ingestion based on intake fraction and fate factor as follows:

—— **4.1.13**

Where XP_i is the exposure factor an emission in watershed, archetype or a-spatial zone *i*, IF_i is the intake fraction and FF_i is the fate factor for an emission to *i*. Figure 4.1.65 presents XP_i for a water ingestion as a function of FF_i for all watersheds of the spatial model, archetypes and a-spatial model. While W1 archetype and the Brittany watershed as well as the W3 archetype and the Danube watershed have a proportional difference in fate and exposure, W3 archetype and the Geneva lake do not follow this rule. Population difference between the W3 archetype and Geneva lake explain why the archetype and a-spatial model overestimate the intake compared to the spatial model, where population is lower than in the generic and archetype boxes. Difference for pollutants with short persistence is more important because it is directly influenced by population.

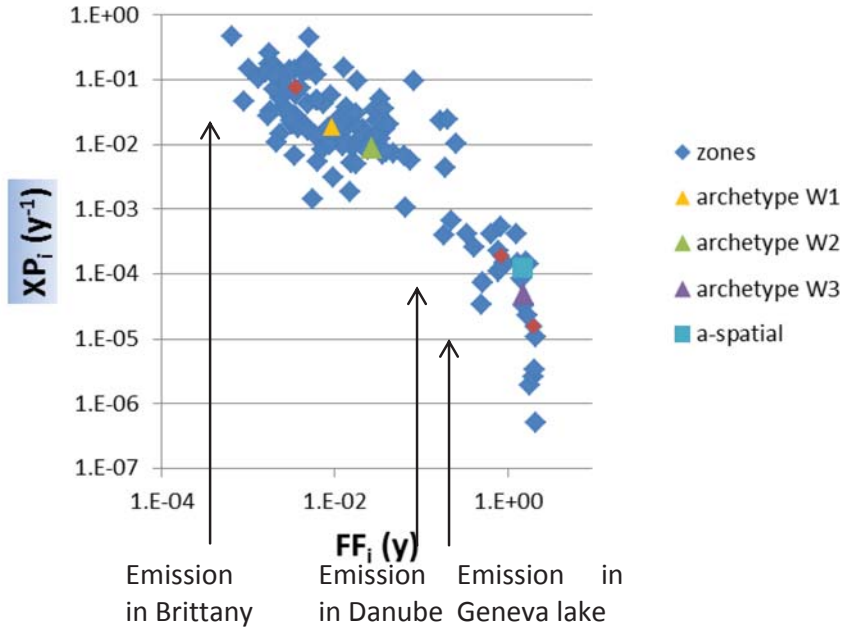

Figure 4.1.65: Variation of exposure for water ingestion according to fate factor for the spatial, archetype and a-spatial models for Folpet

4.1.3.9. Summary on archetype development

According to the results presented in the previous sections, several archetypes could be proposed in order to integrate in box models key elements affecting spatial variability.

Ideally, as already done for freshwater archetypes, key parameters may be used to re-parametrize USEtox. In the table below, we present an overview of possible archetypes for each compartment.

For each compartment, key parameters related to the results of the sensitivity analysis of MAPPE and the proposed archetypes are reported. In some cases, as for air emission, the

archetypes are based on an existing classification, reflecting a combination of key parameters.

As the chemicals in the different clusters show a different spatial variability, some archetypes are considered relevant only for those clusters presenting high variability. For chemicals presenting a very low spatial variability (below one order of magnitude), the box model doesn't need to be reparametrized.

Table 4.1.16: Summary of suggested archetypes and related compartment, key parameters and chemical cluster for which the archetype should be applied

Compartment	Key parameter/s	Proposed archetypes	Chemical cluster for which the archetype should be applied
Freshwater (already applied for Impact world/Europe)	Residence time	3 archetypes	The archetypes have been applied on all the substances, reparametrising USEtox. According to the variability of the load to the sea, the clusters of hydrophyilic and high volatility are the most affected
Coastal zone/marine	Filtrating capacity of coastal zone	2 archetypes based on capability or not of coastal zone to reduce the load to the sea	All chemicals
Air	Wind, coverage and precipitation	5 archetypes of emission based on climate zone of Koppen-Geiger	All chemicals
Air, regarding the intake due to inhalation	Area and population density	Archetypes for continental box/urban box as in USEtox very important. Combinations of area and population density in urban box to be further explored	Especially for volatilizing and multimedia chemicals in case of urban box
Soil	Specific sediment yield (Ssy)	4 archetypes, based on orders of magnitude of SSy	Only for cluster 3a,3b,4a,4b,6b,7b where the variability is higher
Ocean	ocean current velocity (u), Ocean mixing layer depth (MLD),	Combination of u and MLD to be further explored	Only for clusters 1a, 3a, 3b,4a,6a, 7a, 7b

4.1.4. Conclusions

The analysis of the spatial variability associated with removals rates highlighted that the variability is chemical specific and compartment specific. The compartment showing highest variability is the air, followed by ocean and soil. The chemical clusters showing highest variability for all the removals is the cluster related to chemicals having high degree of volatilisation and multimedia (up to 4 orders of magnitude in air, 1.5 orders in soil and 3 orders in sea). Single cases of high variability for chemicals portioning in water and solid are mainly due to the persistence of the chemical in the environment. Regarding the load to the sea, namely the removal rate from freshwater, the overall variability is 3 orders of magnitude for the chemicals with the highest variability in soil. Furthermore, the results support the identification of two archetypes for the coastal zone, accounting for their filtering capability.

Results of the model sensitivity analysis suggest the necessity to identify chemical-specific archetypes in all compartments. As for different types of chemicals the removal process is influenced by different sub-processes. Apart from the role played by the choice of the specific chemical, environmental inputs accounting for the highest share of the output variance are reported in order of importance. For the air compartments, the inputs are wind speed, type of land coverage, precipitation and atmospheric boundary layer. In particular, the influence of coverage and precipitation would suggest the possibility of adopting climate-based archetypes rather than geo-policy-based ones (continent, countries, etc.) for removal rate calculations. This hypothesis has been confirmed from analysis of the distributions of the air removal rates calculated for different chemicals and on different climate and continental regions: when not equivalent, climate-based distributions revealed significantly narrower than the continent-based ones.

Yet, for the soil compartment MAPPE is particularly sensitive to the variation in the quantity of organic carbon, precipitation and specific sediment yield in certain region. Similarly, this input also affects the freshwater compartment in which, however, an important role is also played by the average catchment retention time. Finally, for the ocean compartment, main inputs affecting the results of MAPPE are the marine current speed, the ocean mixing layer depth and the wind speed. The identification of the most sensitive inputs in these two compartments should also help the identification of more robust archetypes of emission.

Regarding the fate factors, the results of MAPPE Europe for freshwater confirm the relevance of accounting for spatial variability at a watershed scale, as this scale represents the best trade-off between capability of distinguishing among different landscape affecting fate factors and complexity of the calculation (e.g. at grid scale). The variability of FFs for freshwater is up to 4 orders of magnitude. Marine ecotoxicity fate factors generated for coastal zones of the IMPACT World model vary between 0.59 and 1 y (in coastals zones where water is not transformed and stored as ice). Terrestrial ecotoxicity fate factors represents a limited overall variability except for 3 orders of magnitude associated with chemicals with high variability in the removal rate from soil. For terrestrial fate factors, only the grid scale is able to capture the differences between the factors as the country or the continental scale present a variability of the average values of a factor of 3.

Regarding the intake fractions (iFs) due to inhalation, the results of MAPPE Europe support the need to distinguish between a continental and an urban box as in USEtox. The

iFs for the chemical representing one of the highest variabilities in removal rate from air (1,1,2,2 tetrachloroethane) vary of 1 order of magnitude amongst countries and it is mainly affected by population density. For example, emitting the same quantity from Luxemburg and Slovenia implies a factor of 2 (iF for Luxemburg 6.20E-6 and for Slovenia 3.57E-6). On average, the iFs at continental scale are one order of magnitude higher than in USEtox whereas at urban scale iFs are two orders of magnitude higher than in USEtox.

Inter-continental variation of fate and intake fraction represents more than 3 orders of magnitude among the 17 zones of IMPACT World and USEtox model. Differentiation of continents and their landscape and population parameters is a key step towards model relevance and consistency. However, the comparison between the USEtox nested parametrisation and the IMPACT World model shows that the surrounding of the continental box, i.e., a single global box or a landscape composed of other continents, does not have an important influence on results. As proved by Shaked (2011), the most important part of the impact occurs in the continent where the pollutant is emitted. Most differences in results between models occur due differencein model algorithms, e.g., modeling of water outflow and volatilization algorithm. We also developed a nine zone model that provides results on a continental scale and has a higher applicability from a life cycle inventory perspective.

The results for Europe showed that a-spatial models might overestimate the chemical fate and characterization factors for fresh water ecotoxicity by up to a factor 5 when compared to a spatially differentiated model for unknown emission location (i.e. assuming the emission is uniformly emitted per unit of surface area). When the emission location is known, a spatially differentiated model can improve the model accuracy by up to 2-3 orders of magnitude, because of its ability to accurately predict the water residence time to the sea (or out of the system) depending on the emission location. Is therefore spatial differentiation always required? The answer depends on the physico-chemical properties of the chemical: for persistent chemicals only the water residence time plays a key role in determining the chemical fate for freshwater ecosystem. Highly degradable or volatile chemicals for example would disappear before being advected out of the system. This indicates that, for persistent chemicals with those properties, the country/ regional differentiation is relevant.

The optimization of the variability of spatial model watersheds compared to three archetype watersheds lead to the definition of a meaningful situation: the distinction of low water residence time archetype (less than 2 d until the model border, W1), medium water residence time (between 2 and 60 d until the model border, W2), and high water residence time (more than 60 d until the model border, W3). The new version of the model with three watersheds was evaluated against the spatial model and showed the relevance of this archetypical differentiation for aquatic fate and intake fractions.

The assessment of spatial variability in removal rates demonstrates the need of archetypes of emission chemical specific. In addition, the sensitivity analysis of MAPPE global may support the further development of box models, accounting for the variability of key input parameters, and their potential re-parametrisation based on climate zone instead of continent. The variability of fate factors for freshwaters supports the use of watershed as best resolution for addressing spatial variability, whereas for soil the cell scale only is able to fully address the variability.

To improve accuracy for aquatic fate and intake fraction modelling at the global scale we recommend using a nested continental model that distinguishes three freshwater compartments with low, medium and high water residence times. This would constitute a

significant improvement in the model result accuracy whilst limiting the amount of input data needed to parameterize detailed geographical watersheds.

4.1.5. References

Bennett DH, McKone TE, Evans JS, Nazaroff WW, Margni MD, Jolliet O, et al. 2002a. Defining intake fraction. Environmental Science and Technolology 36(9):207A-11A.

Bennett DH, Margni M, McKone TE, Jolliet O. 2002b. Intake fraction for multimedia pollutants: a tool for life cycle analysis and comparative risk assessment. Risk Analysis 22(5):903-16.Ciuffo B, Miola A, Punzo V, Sala S. 2012. Dealing with uncertainty in sustainability assessment - Report on the application of different sensitivity analysis techniques to field specific simulation models. JRC68035. EUR 25166. ISBN 978-92-79-22725-7. Available at http://publications.jrc.ec.europa.eu/repository/handle/111111111/26231

Dürr HH, Laruelle GG, van Kempen CM, Slomp CP, Meybeck M, Middelkoop H. 2011. Worldwide typology of nearshore coastal systems: defining the estuarine filter of river inputs to the oceans. Estuaries and Coasts 34(3) 441-458.

Fenner K, Scheringer M, MacLeod M, Matthies M, McKone T, Stroebe M et al (2005) Comparing Estimates of Persistence and Long-Range Transport Potential among Multimedia Models. Environ Sci Technol 39(7):1932-1942

Finnveden G, Hauschild MZ, Ekvall T, Guinée J, Heijungs R, Hellweg S, Koehler A, Pennington D, Suh S. 2009. Recent developments in life cycle assessment. Journal of Environmental Management 91 (1):1-21.

Hollander A, Pistocchi A, Huijbregts MAJ, Ragas AMJ, Meent DV. 2009. Substance or space ? The relative importance of substance properties and environmental characteristics in modeling the fate of chemicals in Europe. Environmental Toxicology Chemistry 28(1):44-51.

Humbert S, Marshall JD, Shaked S, Spadaro JV, Nishioka Y, Preiss P, McKone TE, Horvath A, Jolliet O. 2011. Intake fraction for particulate matter: recommendations for life cycle impact assessment. Environmental Science and Technology 45 (11):4808-4816.

Jolliet O, Hauschild M. 2005. Modeling the influence of intermittent rain events on long-term fate and transport of organic air pollutants . Environmental Science and Technology. 39(12): 4513-4522.

Liu W., Chen D., Liu X., Zheng X., Yang W., Westgate J. N., Wania F. 2010. Transport of Semivolatile Organic Compounds to the Tibetan Plateau: Spatial and Temporal Variation in Air Concentrations in Mountainous Western Sichuan, China. Environmental Science & Technology 44 (5):1559-1565

Leip, A.; Lammel, G. 2004 . Indicators for persistence and long-range transport potential as derived from multicompartment chemistry-transport modeling. Environ. Pollut. 128 (1-2): 205– 221.

MacLeod M, Bennett D, Perem M, Maddalena R, McKone T, Mackay D. 2004. Dependence of intake fraction on release location in a multimedia framework: a case study of four contaminants in North America. Journal of Industrial Ecology 8 (3):89-102.

MacLeod M, Fraser AJ, Mackay D. 2002. Evaluating and expressing the propagation of uncertainty in chemical fate and bioaccumulation models. Environmental Toxicology and Chemistry 21(4):700-709

Manneh R, Margni M, Deschênes L. 2010. Spatial variability of intake fractions for canadian emission scenarios: a comparison between three resolution scales. Environmental Science and Technology 44 (11):4217-4224.

Margni M, Pennington D, Amman C, Jolliet O. 2004. Evaluating multimedia/multipathway model intake fraction estimates using POP emission and monitoring data. Environmental Pollution 128 (1-2):263-277.

Margni M, Pennington D, Birkved M, Larsen HF, Hauschild MZ. 2002. Test set of organic chemicals for life cycle impact assessment characterisation method comparison. OMNITOX project report.

Margni M, Pennington DW, Amman C, Jolliet O. 2004. Evaluating multimedia/ multipathway model intake fraction estimates using POP emission and monitoring data. Environmental Pollution 128(1-2):263-277

Pennington DW, Margni M, Ammann C, Jolliet O. 2005. Multimedia fate and human intake modeling: spatial versus nonspatial insights for chemical emissions in Western Europe. Environmental Science and Technology 39 (4):1119-1128.

Pistocchi A, Marinov D, Pontes S, Zulian G, Trombetti M. 2011. Multimedia assessment of pollutant pathways in the environment - Global scale model. Office for Official Publications of the European Communities, Luxembourg EUR 24911 EN.

Pistocchi A, Zulian G, Vizcaino P, Marinov D. 2010. Multimedia assessment of pollutant pathways in the environment, European scale model (MAPPE-EUROPE). Office for Official Publications of the European Communities, Luxembourg, EUR 24256 EN.

Pistocchi A. 2008. A GIS-based approach for modeling the fate and transport of pollutants in Europe. Environmental Science and Technology 42(10):3640-3647.

Potting J, Hauschild M. 2006. Spatial differentiation in life cycle impact assessment: a decade of method development to increase the environmental realism of life cycle impact assessment. The International Journal of Life Cycle Assessment 11 (1):11-13.

Rochat D, Margni M, Jolliet O. 2006. Continent-specific intake fractions and characterization factors for toxic emissions: does it make a difference? International Journal of Life Cycle Assessment 11 (1):55-63.

Roemer M, Baart A, Libre JM. 2005. ADEPT: Development of an atmospheric deposition and transport model for risk assessment, TNO report BandO- A R 2005-208, Apeldoorn, The Netherlands.

Rosenbaum R, Huijbregts M, Henderson A, Margni M, McKone T, van de Meent D, Hauschild M, Shaked S, Li D, Gold L, Jolliet O. 2011. USEtox human exposure and toxicity factors for comparative assessment of toxic emissions in life cycle analysis: sensitivity to key chemical properties. The International Journal of Life Cycle Assessment 16 (8):710-727.

Sala S, Marinov D, Pennington D. 2011. Spatial differentiation of chemical removal rates from air in Life Cycle Impact Assessment. International Journal of Life Cycle Assessment 16(8):748-760.

Saltelli A, Annoni P, Azzini I, Campolongo F, Ratto M, Tarantola S. 2010. Variance based sensitivity analysis of model output. Design and estimator for the total sensitivity index. Computer Physics Communications 181(2):259-270.

Saltelli A, Ratto M, Anres T, Campolongo F, Cariboni J, Gatelli D, Saisana M, Tarantola S. 2008. Global Sensitivity Analysis – The Primer. John Wiley and Sons Ltd, Cheichester, England.

Saltelli A, Tarantola S, Campolongo F, Ratto M. 2004. Sensitivity Analysis in Practice: A Guide to Assessing Scientific Models. John Wiley and Sons Ltd, Cheichester England.

Scheringer, M.; Wegmann, F.; Fenner, K.; Hungerbuthler, K. 2000. Investigation of the cold condensation of persistent organic pollutants with a global multimedia fate model. Environ. Sci.Technol. 34 (9), 1842–1850

Scheringer M, Stroebe M, Held H. 2002. Chemrange 2.1 - A Multimedia Transport Model for Calculating Persistence and Spatial Range of Organic Chemicals. ETH Zurich, www.sust-chem.ethz.ch/research/groups/prod_assessment/Projects/chemrange/index

Schenker U, Scheringer M, Sohn MD, Maddalena RL, McKone TE, Hungerbühler K. 2009. Using information on uncertainty to improve environmental fate modeling: a case study on DDT. Environmental Science and Technology 43(1):128-134.

Sedlbauer K, Braune A, Humbert S, Margni M, Schuller O, Fischer M. 2007. Spatial differentiation in life cycle assessment: moving forward to more operational sustainability. Technikfolgenabschätzung - Theorie und Praxis (Technology assessment) 16 (3):24-31.

Shaked S. 2011. Multi-continental multimedia model of pollutant intake and application to impacts of global emissions and globally traded goods. PhD thesis. The University of Michigan, Ann Arbour.

Tainio M, Sofiev M, Hujo M, Tuomisto JT, Loh M, Jantunen M, et al. 2009. Evaluation of the European population intake fractions for European and Finnish anthropogenic primary fine particulate matter emissions. Atmospheric Environment, 43(19): 3052-3059

Udo de Haes HA, Finnveden G, Goedkoop M, Hauschild MZ, Hertwich E, Hofstetter P, Jolliet O, Klöpffer W, Krewitt W, Lindeijer E, Mueller-Wenk R, Olsen I, Pennington D, Potting J, Steen B. 2002. Life cycle impact assessment: striving towards best practice. Society of Environmental Toxicology and Chemistry (SETAC). Pensacola, United States of America.

USEPA. 1997. Exposure factors handbook – volume I. Office of Research and Development, Washington DC.

Von Waldow H., MacLeod M., Scheringer M., Hungerbuhler K. 2010.Quantifying Remoteness from Emission Sources of Persistent Organic Pollutants on a Global Scale. Environmental Science and Technology, 44 (8), pp. 2791-2796

Wania, F.; Mackay, D. 1993. Global fractionation and cold condensation of low volatility organochlorine compounds in polar regions. Ambio 22, 10–18.

Wania F, McLachlan MS. 2001. Estimating the influence of forests on the overall fate of semivolatile organic compounds using a multimedia fate model. Environmental Science and Technology 35(3):582-590.

Wania, F.; Su, Y. 2004.Quantifying the global fractionation of polychlorinated biphenyls. Ambio, 33 (3), 161–168.

Wania F. 2006. Potential of degradable organic chemicals for absolute and relative enrichment in the arctic. Environ Sci Technol 40:569–77

Weber J., Halsall C.J., Muir D., Teixeira C., Small J.,Solomon K. et al. 2010. Endosulfan, a global pesticide: a review of its fate in the environment and occurrence in the Arctic, Science of the Total Enviroment **408**: 2966–2984

Wegmann F, Cavin L, Macleod M, Scheringer M, Hungerbuhler K. 2009. The OECD software tool for screening chemicals for persistence and long-range transport potential. Environ Modell Softw 24(2):228–237.

Wenger Y, Li D, Jolliet O. 2012. Indoor intake fraction considering surface sorption of air organic compounds for life cycle assessment. The International Journal of Life Cycle Assessment 17 (7):919-931.

4.2. Human toxicity of pesticides

P. Fantke[1], R. Juraske[2], A. Anton[3], E. Sevigne Itoiz[3], A. Kounina[4], S. Humbert[4], O. Jolliet[4]

[1]University of Stuttgart, Germany
[2]Swiss Federal Institute of Technology Zurich, Switzerland
[3]IRTA, Spain
[4]Quantis, Switzerland

4.2.1. Introduction

The work presented in this deliverable is further detailed in several scientific publications (Fantke et al. 2013; Fantke et al. 2012a; Fantke et al. 2012b; Itoiz et al. 2012; Juraske et al. 2012; Fantke et al. 2011a; Fantke et al. 2011b).

Human health impacts of pesticides are poorly represented in existing LCIA approaches, since only effects from diffuse emissions are considered, thereby disregarding ingestion exposure from residues in field crops after direct pesticide application. While in the case of diffuse emissions environmental media, such as air and soil, are the emission target compartments, in case of direct application it is the cultivated crop that is finally consumed. As a first attempt to account for effects of direct application, recent studies contrasted residues from direct and diffuse sources for human intake fractions (iF) in fruits and vegetables (*Pennington et al., 2005; Rosenbaum et al., 2008*) and concluded that ingestion of directly treated food crops is the most important human exposure route. As a result, detailed exchange processes between environmental media and vegetation have been introduced in multimedia models, traditionally considering steady-state conditions. However, for pesticide residues and related impacts, steady-state is usually not obtained during the short time period from substance application to ultimate crop harvest, which is why the evolution of residues needs to be assessed dynamically. In addition, it is stated in (*Trapp et al., 2006*) that pesticide uptake and translocation mechanisms vary considerably between crop species and may indicate significant differences in related health impacts. Consequently, differing crop-specific characteristics need to be considered as provided for single crop species by recently developed uptake models (*Fantke et al., submitted; Juraske et al., 2007; Juraske et al., 2011; Trapp et al., 2007*). However, no existing tool assessing environmental fate of pesticides after direct application is able to contrast various crops consumed by humans. Since this implies a major drawback in characterizing human toxicity for LCIA, the present study aims at introducing a consistent approach for answering the following related questions:

How can human intake of pesticides via ingestion of different food crops and related health impacts be characterized and evaluated in a transparent, consistent and concise way?

What is the influence of crop characteristics, substance properties and application times on the dynamic behavior of pesticides in field crops and on subsequent human intake?

What are the differences between crop-specific characterization factors from direct pesticide application onto different food crops and generic characterization factors from continuous, diffuse emissions to the environment?

How can substitution of pesticides applied to the same crop be evaluated and their health impacts compared on a similar functional basis?

To answer these questions, we developed a new dynamic assessment model for human health impacts due to uptake of pesticides into multiple crop types (dynamiCROP) based on a transparent matrix algebra framework. We selected six food crops covering a large fraction of the worldwide consumption of vegetal origin, thereby representing the most important crop archetypes. For each archetype, substance-specific human ingestion intake fractions are calculated and evaluated. In addition, the influence of crop and substance characteristics as well as the time between application and harvest on pesticide characterization is discussed. Finally, crop-specific characterization factors are provided – differentiated according to human cancer and non-cancer effect information – along with generic characterization factors to also account for diffuse pesticide emissions.

4.2.2. Methodology

Selection of Crops. We introduce six characteristic plant species representing the most relevant crop archetypes with respect to human vegetal food based on a systematic criteria approach. Selection criteria are human consumption quantity, expected pesticide residues in harvest, crop characteristics (cropping practice, plant phenotype, and harvested components), availability of knowledge from other crop-specific models, and finally availability of experimental data for comparison with modeled residues. Human consumption is analyzed based on global FAO statistics of 159 food crops (*FAO, 2011*). Ranges of expected residues in food products are estimated based on maximum residue levels (MRL) stated by (*UNDA, 2011*), considering MRL data from 70 countries, the European Commission (*EU, 2008*) and the Codex Alimentarius Commission (*2010*). Table 4.2.1 summarizes the criteria analysis and lists selected crop species accounting for 45% of the global vegetal consumption in 2007 (*FAO, 2011*). These crops cover the most important archetypes, i.e. cereals, paddy cereals, herbaceous fruits and vegetables, fruit trees, leafy vegetables as well as roots and tubers. Based on these archetypes, the model framework can be easily adapted to assess additional species.

Table 4.2.10: Selected crops and represented archetypes according to a set of systematic criteria including share of crop on human consumption of archetype (ϕ_{crop}) and share of archetype on total human vegetal consumption ($\phi_{archetype}$)

Crop	archetype	human consumption share		residues	characteristics	knowledge base	
		ϕ_{crop}	$\phi_{archetype}$			adaptable models	experimental residue data
Wheat	cereals	68%	24%	medium	grass like; grain harvested	(Fantke et al., submitted; Charles, 2004)	(Cao, 2011)
paddy rice	paddy cereals	97%	13%	medium	grass like; paddy water; grain harvested	(Fantke et al., submitted; Inao et al. 2008)	(Ishii, 2004; Wang et al., 2007)
Tomato	herbaceous	15%	26%	high	herbaceous; fruit	(Juraske et	(Juraske et al.,

	fruits and vegetables				harvested	al., 2008; Juraske et al., 2009)	2008; Juraske et al., 2008)
Apple	fruit trees	13%	17%	high	treelike; perennial; fruit harvested	(Trapp, 2007; Paraíba., 2007)	(Kumar et al., 2005; Xu et al., 2008)
Lettuce	leafy vegetables	14%	2%	high	herbaceous; high adsorption; leaves harvested	(Kulhanek et al., 2005)	(Fenoll et al., 2008, Fenoll et al., 2009)
potato	roots and tubers	51%	18%	medium	herbaceous; root or stem tuber harvested	(Juraske et al., 2011; Paraíba et al., 2008)	(Juraske et al., 2011; Abdel-Gawad et al., 2008)

Description of the dynamic plant uptake model. The multimedia plant-environment modeling system was originally developed for wheat with environmental compartments (atmospheric ground layer, root-zone soil layer) and vegetation compartments (leaf and fruit surface deposit, leaf and fruit interior, stem and root system), and adjusted to also cover other food crops. In contrast to most existing uptake models (e.g. *Trapp and Mc Farlane, 1995; Charles, 2004; Contreras et al., 2008*), the protected grains are explicitly taken into account as separate compartment for substance accumulation.

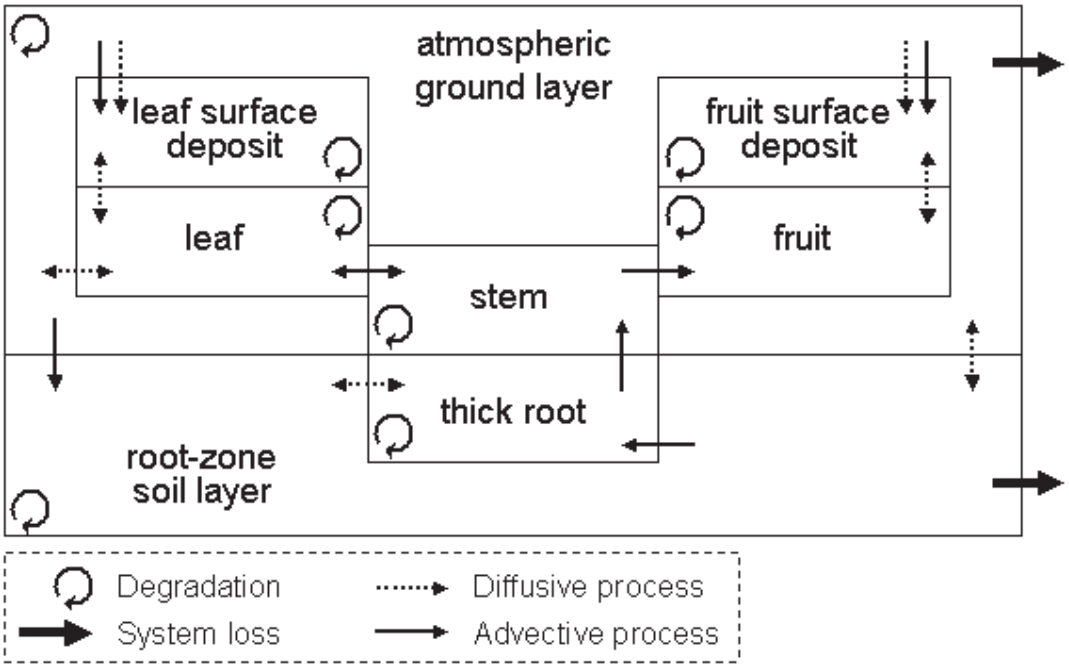

Figure 4.2.24: Graphical representation of model setup, consisting of environmental compartments (atmospheric boundary layer, root-zone soil layer), wheat plant components (leaf and fruit surface deposit, leaf and fruit interior, stem, root) and process rates within/between compartments

Depending on application technique (foliar spray, soil application, etc.), atmospheric ground, root-zone soil and vegetation leaf/fruit surface deposit are primary compartments receiving the applied pesticide. Furthermore, pesticides can bioaccumulate in each compartment as a function of their source compartments and of the plant-internal translocation processes via xylem and phloem as shown in Fout! Verwijzingsbron niet gevonden.**. When sprayed onto wheat, three components are directly exposed: leaves, grains and stem, while the fraction reaching the soil can be taken up through roots. Environmental compartments and their characteristic parameters are considered to remain constant, whereas plant components evolve over time. The dynamic plant development is accounted for by its growth influencing diverse fate processes. Substance transformation within and translocation between compartments is described using first-order rate coefficients aggregating underlying physical processes including degradation, diffusive and advective transfers. These rate coefficients form the basis for an analytical matrix algebra framework for solving the system's mass balance. All rate coefficients summarizing intermedia transport and loss from the model domain are formulated in**

Table 4.2.11. Mathematically, this homogeneous dynamical system consists of *n* compartments, where each compartment can receive from and emit to all other compartments. Such a system is described by an $n \times n$ matrix **K**, whose line and column indices indicate the receiving and source compartments, respectively. The mass balance of a substance in such a system over time, hence, can be described by a set of ordinary linear differential equations (vector-matrix notation):

$$\frac{\mathrm{d}\vec{\mathbf{m}}(t)}{\mathrm{d}t} = \mathbf{K}\,\vec{\mathbf{m}}(t) \qquad \textbf{4.2.1}$$

with $\vec{\mathbf{m}} \in \mathbf{P}^{n}$ as *n*-dimensional column vector of substance masses in the compartments [kg], *t* as time [day], and $\mathbf{K} \in \mathbf{P}^{n \times n}$ representing the square matrix of first-order rate coefficients [day^{-1}], where each main diagonal element of **K**, i.e. $k_{i \leftarrow j}$ with $i = j$, contains the bulk removal rate in compartment *i*, $k_{i,\mathrm{loss}}$, plus the sum of transfer rates from compartment *i* to all other compartments *j*, and where each off-diagonal element of **K**, i.e. $k_{i \leftarrow j}$ with $i \neq j$, contains a single transfer rate from compartment *j* to compartment *i*. For any compartment $i \in \{1, \ldots, n\}$, the differential equation, hence, becomes:

$$\frac{\mathrm{d}m_i(t)}{\mathrm{d}t} = -\left(k_{i,\mathrm{loss}} + \sum_{l=1; l \neq i}^{n} k_{l \leftarrow i}\right) m_i(t) + \sum_{j=1; j \neq i}^{n} k_{i \leftarrow j} m_j(t) \qquad \textbf{4.2.2}$$

The common solution of the system in Equation 4.2.1 for a direct pesticide application, i.e. pulse release with $\vec{\mathbf{m}}_0 = \vec{\mathbf{m}}(0)$ for $t = 0$, is given based on the matrix exponential of **K**:

$$\vec{\mathbf{m}}(t) = \mathrm{e}^{\mathbf{K}t}\vec{\mathbf{m}}(0) \qquad \textbf{4.2.3}$$

The physical processes behind the rate coefficients, $k_{i \leftarrow j}$, in Equation 4.2.2 are summarized in Table 4.2.11.

Table 4.2.11: Rate coefficients for intermedia mass transport processes considered in the modeled system (including system losses, i.e. processes towards compartments not included in the model domain)

Intermedia transfer process	Equation of transfer rate coefficient
Atmospheric ground layer to root-zone soil layer	$k_{a\to s} = (k_{a,dep,dry} + \Delta k_{a,dep,wet,int}) \times e^{-(LAI+FAI)\times CCS}$
Atmospheric ground layer to vegetation leaf surface deposit	$k_{a\to vld} = (k_{a,dep,dry} + \Delta k_{a,dep,wet,int}) \times (1 - e^{-LAI\times CCS})$
Atmospheric ground layer to vegetation fruit surface deposit	$k_{a\to vfd} = (k_{a,dep,dry} + \Delta k_{a,dep,wet,int}) \times (1 - e^{-FAI\times CCS})$
Atmospheric ground layer to vegetation leaf interior	$k_{a\to vl} = \frac{A_{vl} \times \varphi_{a/vl}}{K_{aw} \times V_a}$
Root-zone soil layer to atmospheric ground layer	$k_{s\to a} = \frac{A_s \times fc_{L\,to\,m3} \times \varphi_{a/s}}{K_{sa} \times M_s}$
Root-zone soil layer to surface water	$k_{s\to w} = \frac{(fc_{s,paq} + fc_{s,ps} \times fr\_M_{s,run,ps}) \times p_{rain} \times fr\_p_{rain,run}}{h_s}$
Root-zone soil layer to saturated sub-soil (groundwater) layer	$k_{s\to u} = \frac{fc_{s,paq} \times (p_{rain} \times fr\_p_{rain,leach} \times fr\_V_{s,paq} - \varphi_s)}{h_s}$
Root-zone soil layer to vegetation root	$k_{s\to vr} = \frac{(A_{vr} \times fc_{L\,to\,m3} \times \varphi_{vr} + Q_{xylem}) \times K_{ws}}{M_s}$
Leaf surface deposit to vegetation leaf interior	$k_{vld\to vl} = \frac{A_{vl} \times \varphi_{cut}}{V_{vld}} = k_{cut} \times K_{cuw}$
Fruit surface deposit to fruit interior	$k_{vfd\to vf} = \left(\frac{2}{k_{cut} \times K_{cuw}} + \frac{K_{vlc} \times M_{lemma}}{A_{lemma} \times fc_{L\,to\,m^3} \times \varphi_{cut}} \right)^{-1}$
Vegetation leaf interior to atmospheric ground layer	$k_{vl\to a} = \frac{A_{vl} \times fc_{L\,to\,m3} \times \varphi_{a/vl}}{K_{vlw} \times M_{vl}}$
Vegetation leaf interior to vegetation leaf surface deposit	$k_{vl\to vld} = \frac{A_{vl} \times fc_{L\,to\,m3} \times \varphi_{cut}}{K_{vlcut} \times M_{vl}}$
Vegetation leaf interior to vegetation stem	$k_{vl\to vs} = \frac{Q_{vf,phloem}}{K_{vlw} \times M_{vl}}$
Vegetation fruit interior to vegetation fruit surface deposit	$k_{vf\to vfd} = \left(\frac{K_{vlc} \times (M_{vf} + M_{lemma})}{A_{vf} \times fc_{L\,to\,m^3} \times \varphi_{cut}} + \frac{1}{k_{cut} \times K_{cuw}} \right)^{-1}$

Intermedia transfer process	Equation of transfer rate coefficient
Vegetation stem to vegetation leaf interior	$k_{vs\rightarrow vl} = \frac{Q_{vl,xylem}}{K_{vsw} \times M_{vs}}$
Vegetation stem to vegetation fruit interior	$k_{vs\rightarrow vf} = \frac{Q_{vf,phloem}}{K_{vsw} \times M_{vs}}$
Vegetation root to root-zone soil layer	$k_{vr\rightarrow s} = \frac{A_{vr} \times fc_{L\ to\ m3} \times \varphi_{vr}}{K_{vrw} \times M_{vr}}$
Vegetation root to vegetation stem	$k_{vr\rightarrow vs} = \frac{Q_{xylem}}{K_{vrw} \times M_{vr}}$

Key: Where *A* area [m^2]; *LAI* and *FAI* leaf and fruit area indices [m^2/m^2]; *CCS* substance capture coefficient [$(kg/m^2)/(kg/m^2)$]; $fc_{L\ to\ m3}$ conversion factor of 1,000L per $1m^3$; fc_{paq} correction factor between aqueous phase and bulk soil [L/L]; fc_{ps} correction factor between solid phase and bulk soil [L/L]; fr_M_{ps} fraction of soil mass in solid phase [kg/kg]; fr_p_{rain} rain rate related fraction [m/day per m/day]; fr_V_{paq} fraction of volumetric water in soil [m^3/m^3]; *h* vertical dimension (height or depths) [m]; *k* rate coefficient [1/day]; *Δk* equivalent rate coefficient [1/day]; *K* partition coefficient [kg/m^3 per kg/m^3 for air/water and cuticular wax/water, L/kg for soil/air, leaf/cuticle, leaf/water, stem/water and root/water, kg/L for water/soil]; *M* mass of compartment or phase [kg]; p_{rain} rain rate [m/day]; *φ* conductance (diffusion velocity) [m/day]; *Q* volume related flow rate [L/day]; *V* volume [m^3]. Indices: a, s, vf, vl, vld, vfd, vr, vs, u, w denote the compartments atmospheric ground layer, root-zone soil layer, vegetation fruit, leaf, leaf surface deposit, fruit surface deposit, root, stem, saturated sub-soil layer and water; cut, cuw, lemma, paq, ps denote the compartment phases/components leaf/fruit cuticle, leaf/fruit cuticular wax, fruit lemma, aqueous phase and solid phase; dep, dry, int, leach, phloem, rain, run, wet, xylem denote processes related to deposition, dry deposition, intermittent or interval periods, leaching, phloem flow, rain, runoff, wet deposition and xylem flow, respectively.

Assessment Framework. For human impacts, we followed the general LCIA cause-effect chain by linking applied pesticide masses to health impacts via environmental fate, exposure and effects (*Udo de Haes et a.l, 2002*). When taking DALY (Disability Adjusted Life Years) as measure for overall population impacts, the human-toxicological population impact score, $\mathrm{IS}_i(t)$ [DALY·ha^{-1}], caused by intake of active ingredient *i* (hereafter referred to as 'pesticide') applied to crop *x* that is harvested at time *t* is expressed as product of the characterization factor for human toxicity, $\mathrm{CF}_{i,x}(t)$ [DALY·$kg_{applied}^{-1}$], and the life cycle inventory output, i.e. total mass of pesticide applied, $\mathrm{m}_{app,i,x}$ [$kg_{applied}$·ha^{-1}]:

$$\mathrm{IS}_{total,x} = \sum_{i=1}^{n} \mathrm{IS}_{i,x}(t) = \sum_{i=1}^{n} \mathrm{CF}_{i,x}(t) \times \mathrm{m}_{app,i,x} \qquad \textbf{4.2.4}$$

with $\mathrm{IS}_{total,x}$ as total impact score per crop. We describe the characterization factor by multiplying the human effect factor for pesticide *i*, EF_i [DALY·kg_{intake}^{-1}], with the total population intake fraction of the pesticide via ingestion of crop *x*, $\mathrm{iF}_{i,x}(t)$ [kg_{intake}·$kg_{applied}^{-1}$]:

$$\mathrm{CF}_{i,x}(t) = \mathrm{EF}_i \times \mathrm{iF}_{i,x}(t) = \beta_i \times \mathrm{DF} \times \mathrm{iF}_{i,x}(t) \qquad \textbf{4.2.5}$$

EF_i consists of a dose-response slope factor, β_i [incidence risk·kg_{intake}^{-1}], and – for distinguishing between cancer and non-cancer effects – of a severity factor, DF [DALY·$incidence^{-1}$]. Severity factors of 11.5 and 2.7 DALY·$incidence^{-1}$ for cancer and non-cancer effects, respectively, are based on global human health statistics as described in (*Huijbregts et al., 2005*). Slope factors relating potential risks of pesticides in humans to their quantities ingested via intake of food crops are derived from the chronic lifetime dose of pesticide *i* affecting 50% of a population, $ED50_i$ [risk·kg_{intake}^{-1}·$person^{-1}$]. For non-carcinogenic effects, chronic ED50 values are only rarely available. Hence, assuming linear dose-response relationships, $ED50_{i,s}$ is estimated from no-observed effect levels of exposed animal species *s*, $NOEL_{i,s}$ [mg·kg_{BW}^{-1}·day^{-1}]:

$$\beta_i = \frac{cf_{\mathrm{ED50}}}{\mathrm{ED50}_i} = cf_{\mathrm{ED50}} \times \left(\frac{\mathrm{NOEL}_{i,s} \times cf_{\mathrm{NOEL}} \times \mathrm{BW} \times \mathrm{LT} \times \mathrm{d\_to\_y}}{cf_{\mathrm{s}} \times cf_{\mathrm{time}} \times \mathrm{mg\_to\_kg}} \right)^{-1} \qquad \textbf{4.2.6}$$

BW=70 kg·$person^{-1}$ denotes average body weight, LT=70 years is the average human life time, d_to_y=365 days·$year^{-1}$ corrects for number of days per year, mg_to_kg=1E+06 mg·kg^{-1} corrects for mg per kg, and *cf* [-] denotes an extrapolation factor. cf_{ED50}=0.5 accounts for the human response level corresponding to ED50, cf_{NOEL}=9 is the NOEL-to-ED50 extrapolation factor, cf_s corrects for interspecies differences, i.e. between the studied animal and humans, and cf_{time} accounts for differences in exposure time. Extrapolation factors are derived from (*Huijbregts et al., 2005*; *Huijbregts et al., 2010*). Details are provided in supporting information.

Intake fractions are commonly used in LCIA to express source-to-intake relationships (*Bennett et al. 2002*) and are introduced to describe the mass fractions of applied pesticides that are ultimately taken in by the human population via food ingestion:

$$\mathrm{iF}_{i,x}(t) = \frac{\mathrm{m}_{\mathrm{intake},i,x}(t)}{\mathrm{m}_{\mathrm{app},i,x}} = \mathrm{hF}_{i,x}(t) \times \mathrm{PF}_x \qquad \textbf{4.2.7}$$

with the mass of pesticide *i* taken in via ingestion of crop *x*, $\mathrm{m}_{\mathrm{intake},i,x}(t)$ [kg_{intake}·ha^{-1}], mass fraction of applied pesticide that is found as residue in harvest, $\mathrm{hF}_{i,x}(t)$ [$kg_{in\ harvest}$·$kg_{applied}^{-1}$] at harvest time *t* [day], and finally crop-specific food processing factor, PF_x [-], accounting for reduction of pesticide residues between harvest and final consumption. Mass in harvest is a result of the mass balance underlying the fate assessment, which builds upon the dynamical framework developed in (*Fantke et al., submitted*). In contrast to other plant uptake models focusing on a single-species environment, the present model accounts for system characteristics of various crops based on a flexible set of interconnected compartments. This allows to directly compare modeled crop-specific residues with experimentally derived concentrations in harvested plants and to contrast model results against existing MRLs. Parameters determining the fate processes are physicochemical properties of applied pesticides, system initial and boundary conditions as well as crop-specific characteristics as discussed in (*Fantke et al., submitted*).

Crop Characteristics. Initial deposition of pesticides on plant surfaces directly after application depends on the crop-specific leaf area index (LAI) representing leaf growth

stage, and furthermore the pesticide capture coefficient being a measure of a crop's capture efficacy (*Gyldenkaerne et al., 1999*). While the latter can be seen as a fixed value, LAI is time-dependent. Crop-specific LAI curves are fitted based on experimental data (see supporting information). After a pesticide is applied to a crop, a certain fraction of the initial dose has the potential for drifting from the agricultural site. In most cases, drift mainly depends on application method, pesticide formulation, environmental conditions and crop type (*Wolters et al., 2008*). Typical crop type- and application method-specific drift values are applied as loss fractions. Finally, in order to evaluate the effect of food processing on the magnitude of pesticide residues in the studied crops, food processing factors for washing, peeling, cooking, juicing and baking are introduced from (*Kaushik et al., 2009*).

Model Evaluation. Internal model consistency was continuously examined by checking the underlying mass balance, i.e. ensuring that the sum of elimination and biodistribution pathways at any time equals the total pesticide mass applied. Secondly, modeled residues are evaluated by analyzing whether model simulations adequately represent collected experimental data from the literature. A measure to estimate model prediction quality compared with experiments is the residual error, also known as standard deviation of the log of residuals between observed and modeled concentrations as discussed in (*Hamburg et al., 1994*). A residual error of e.g. 0.5 implies a deviation between modeled and experimental data of approximately a factor $10^{\text{Student's } t \times 0.5}$. For a Student's *t*-value of ~2, we would then arrive at a factor 10 deviation. Thirdly, we performed sensitivity analyses to determine the influence of the most important parameters on model output variability, i.e. changing parameter values from best estimate to upper and lower limits. Finally, generic characterization factors additionally accounting for diffuse emission pathways as calculated with the USEtox model (*Rosenbaum et al., 2008*) are presented for the set of selected substances.

4.2.3. Results

Pesticide Residues in Crops. Modeled residues are compared with measured concentrations of eleven different pesticides applied to the six selected crops (**Fout! Verwijzingsbron niet gevonden.**). Experimentally derived maximum concentrations are reported to range from 28.91 mg·kg^{-1} in apples at the day of application to 0.01 mg·kg^{-1} in potato tubers measured 15 days after the tested pesticide was applied, demonstrating a variability of three orders of magnitude between crops. Measurements and model estimates correspond well with total crop-specific residual errors ranging between 0.08 (factor 1.5 deviation) for fenitrothion applied to lettuce and 0.64 (factor 37) for propisochlor sprayed on rice with an overall residual error of 0.33 (factor 32) over all 12 substance-crop combinations. A higher accuracy of prediction is observed in crops where the final commodity stands in direct contact with the applied pesticide (apple, lettuce, tomato, and wheat). In comparison, crops in which the pesticide has to pass an additional medium like paddy water (rice) or soil (potato) in order to reach the harvested good, on average showed higher uncertainties.

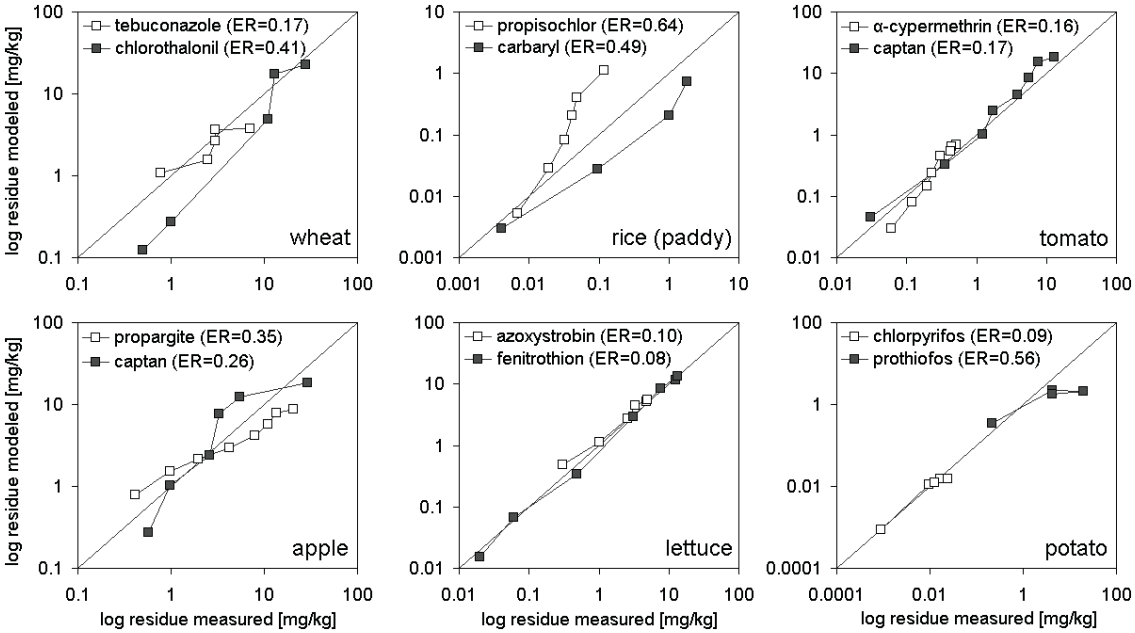

Figure 4.2.25: Measured and modeled evolution of pesticide residues in plant components harvested for human consumption for each of the six studied crops with residual error (ER) for each substance-crop combination

Human Intake Fractions. We calculated intake fractions and characterization factors as measures normalized to one unit mass of applied pesticide for 726 potential substance-crop combinations, i.e. 121 substances applied to six crops. Overall impact per ha is calculated for a subset of 181 substance-crop combinations authorized for use in at least one of the countries listed in the *Codex Alimentarius* (*2010*) with given recommended amounts applied. Intake fractions of a pesticide can vary between four and fourteen orders of magnitude for fungicide ferbam and herbicide thiobencarb, respectively, when applied to different crops at recommended doses and harvested at typical times after applications. In contrast, iF between all pesticides applied to the same crop can vary between five (potato) and nineteen (apple) orders of magnitude, thereby indicating that substance properties are almost as influential on iF as crop properties. The lowest intake fraction is found for metribuzin applied to apple with iF=4.8E-21 $kg_{intake} \cdot kg_{applied}^{-1}$, whereas the highest intake fraction is found for benomyl applied to lettuce with iF=5.6E-02 $kg_{intake} \cdot kg_{applied}^{-1}$. Intake fractions for all potential substance-crop combinations are provided in Table S4.7 (Supporting Information).

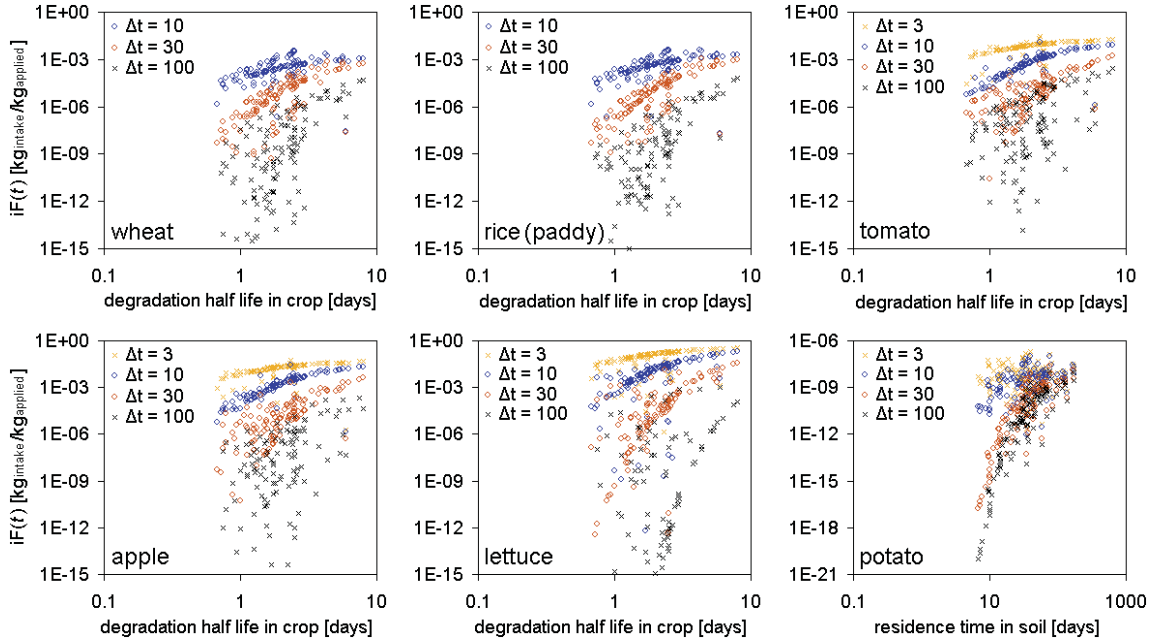

Figure 4.2.26: Intake fractions as a function of degradation half-lives of pesticides (n=121) in plants for different time periods between substance application and crop harvest (Δt) for each of the six studied crops

Substance degradation in plants and the time between pesticide application and crop harvest are known to predominantly determine model sensitivity (*Charles, 2004; Juraske et al., 2008*). In **Fout! Verwijzingsbron niet gevonden.**, we present intake fractions as a function of the substance degradation half-life in plants – typically varying between one and ten days – for different times to harvest. For all crops but potato, intake fractions are usually in the range of 1E-02 and 1E-08 $kg_{intake} \cdot kg_{applied}^{-1}$ for typical times between application and harvest. Decreasing the half-life in plants results in continuously decreasing iF, with the magnitude of decrease being amplified with higher time lag before harvest. However, for given half-lives below ten days, intake fractions are significantly reduced along with larger variation. At the upper range of time lags, iF variation of up to ten orders of magnitude for a given half-life in plant is mainly attributable to the difference in degradation of pesticides within crops by having more time to establish a significant influence. When looking at potato, there is little influence of the degradation half-life in plant. Instead, the residence time in soil is a main factor of influence affecting iF variation in **Fout! Verwijzingsbron niet gevonden.**. Residence times are, hence, more adequate to examine iF variation for potato, since the pesticide always has to pass the heterogeneous soil layer, before entering the tuber. In this case, soil characteristics become predominant, which is in line with (*Juraske et al., 2011; Paraíba et al., 2008*).

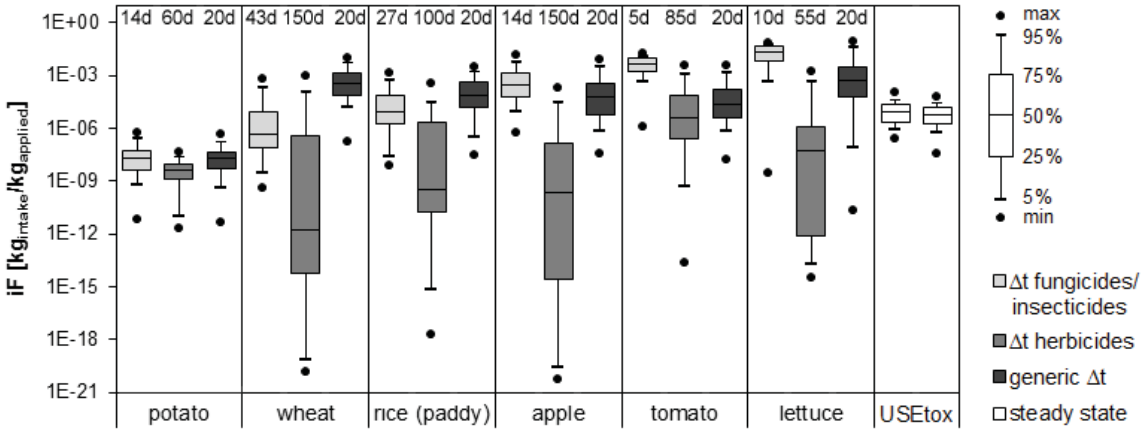

Figure 4.2.27: Box and whisker plot of human intake fractions for pesticides directly applied to the six selected crops (n=121, dynamic assessment for different times between application and harvest Δt) and from diffuse emissions (n=97, assessed with USEtox, steady state, left box: emissions to air, right box: emissions to soil)

How crop and substance characteristics as well as time to harvest are influencing the variation of intake fractions is contrasted in Figure 4.2.27. For the same generic time between application and harvest of 20 days (dark boxes) potato shows the lowest range of intake fractions with a median of 1.3E-08 $kg_{intake} \cdot kg_{applied}^{-1}$ and less than three orders of magnitude variation between 5th and 95th percentiles. Potato is followed by cereals and fruit crops, for which we basically obtain a similar behavior with median iF ranging from 2.0E-05 to 2.5E-04 $kg_{intake} \cdot kg_{applied}^{-1}$ and typical variation ranges from two to four orders of magnitude between pesticides. In contrast, lettuce as leafy crop shows highest iF with a median of 4.3E-04 $kg_{intake} \cdot kg_{applied}^{-1}$ and six orders of magnitude variation. For fixed times to harvest, consequently, all the variation is attributable to intrinsic crop characteristics, mainly due to losses during application via wind drift, LAI growth over time and food processing after harvest. Drift fractions, however, are not only crop-specific, but also depend on application method, e.g. foliar spray or soil injection, whereas loss fractions due to food processing also differ between substances. Generally, substance-specific processing factors are rarely available and, hence, aggregated for each processing step. In practice, times between application and harvest depend on crop species, pest occurrence, weather conditions and a pesticide's mode of action. However, since for LCIA we are interested in providing best estimates, we also need to distinguish between pesticide target classes for arriving at typical times to harvest. For fungicides and insecticides, officially reported minimum pre-harvest intervals are selected. Herbicides, in contrast, are usually applied pre-emergent or during early crop growth resulting in relatively long times to harvest between 55 and 150 days as discussed in the supporting information. Overall, average times to harvest range between 5 days for fungicides/insecticides applied to tomato and 150 days for herbicides applied to wheat and apple (Table S4.6). Varying application times lead to additional iF variation between pesticides with herbicides showing lower intake fractions and higher variation due to their longer time lags between application and harvest (Figure 4.2.27, grey middle box-plots). For fungicides and insecticides, the later application leads to higher intake fraction, especially for tomato and lettuce, for which application can take place only 5 to 10 days before harvest (Figure 4.2.27, left box plots). Figure 4.2.27 also

enables us to compare direct pesticide application modeled dynamically with diffuse emissions calculated by USEtox assuming steady-state conditions and continuous input (see two white box-plots at the right end of Figure 4.2.27). With the generic time to harvest of 20 days, all crops except potato show higher iF due to direct application residues compared to iF due to continuous, diffuse emissions. For recommended times to harvest, median iF of herbicides applied to all crops and of fungicides/insecticides applied to cereals decrease below USEtox values. In contrast, for fungicide/insecticide applied shortly before harvest (tomato, lettuce), median intake fractions from diffuse emissions strongly underestimate overall intake by up to four orders of magnitude. Finally, in the case of potatoes, residues from direct application of all pesticides remain of minor importance, i.e. with lower median iF values, than diffuse emissions.

Characterization Factors and Impact Scores. The whole source to impact pathway from pesticide application to human impacts is summarized in Table 4.2.12. Characterization factors for the set of 121 pesticides applied to the six selected food crops are calculated according to Equation 4.2.5 to characterize the direct impact per kg of pesticide applied. However, characterization factors for substance-crop combinations not known to be officially authorized shall only be used as reference for further crops. Following the chain from intake fractions to characterization factors, additional variation is introduced by human effect factors, more specifically by substance-specific dose-response slope factors. Information related to cancer effects is given in (*Rosenbaum et al., 2008*) for less than 20% of the 121 pesticides, which is in line with (*Huijbregts et al., 2005*). In addition, 77% of substances with available information related to cancer do not show any cancer potential (effect factors set to zero). This indicates that most of today's pesticides are rather leading to non-cancer effects. All in all, effect factors vary by 3.5 orders of magnitude between pesticides leading to a variation in characterization factors of 21 orders of magnitude due to the combination of large variations in intake fractions with lower variations in effect factors (Table 4.2.12). Detailed information is provided in the supporting information on cancer and non-cancer potentials, crop-specific and generic characterization factors, and finally impact scores.

Table 4.2.12: Median values with 5th and 95th percentiles (in brackets) of crop-specific application amount m_{app} [$kg_{applied}$·ha^{-1}], intake fraction iF [kg_{intake}·$kg_{applied}^{-1}$], characterization factor CF [DALY·$kg_{applied}^{-1}$] and impact score IS [DALY·ha^{-1}], as well as crop-independent effect factor EF [DALY·kg_{intake}^{-1}] for 121 pesticides

Crop	m_{app}	iF	EF	CF	IS
Wheat	0.16 (0.01 – 2.87)	2.1E-07 (3.7E-17 – 1.9E-04)	cancer*: 0.17 (0.007 – 1.6) non-cancer: 0.11 (0.009 – 2.5)	5.2E-08 (4.1E-18 – 3.3E-05)	7.6E-09 (4.3E-16 – 9.8E-06)
rice (paddy)	0.75 (0.04 – 3.75)	4.3E-06 (4.1E-13 – 4.3E-04)		6.8E-07 (8.7E-14 – 9.8E-05)	3.7E-07 (2.6E-14 – 7.3E-05)
Tomato	0.27 (0.02 – 4.82)	2.1E-03 (3.4E-08 – 9.8E-03)		2.0E-04 (4.2E-08 – 8.2E-03)	1.3E-05 (3.3E-08 – 1.7E-03)
Apple	0.86 (0.04 – 3.16)	1.0E-04 (1.2E-17 – 5.2E-03)		1.3E-05 (4.1E-19 – 1.8E-03)	1.6E-05 (3.2E-10 – 3.0E-04)
Lettuce	0.2 (0.03 – 1.59)	8.4E-03 (5.6E-13 – 4.8E-02)		8.1E-04 (2.8E-14 – 4.2E-02)	2.4E-04 (3.2E-07 – 4.8E-03)

Crop	m_{app}	iF	EF	CF	IS
Potato	0.89 (0.03 – 100.6)	9.9E-09 (2.7E-10 – 2.0E-07)		9.6E-10 (1.4E-11 – 1.1E-07)	9.2E-10 (6.8E-12 – 3.9E-07)

* See text for explanation.

Functional Assessment and Pesticide Substitution. When assessing the change in impacts linked to substitution of pesticides, a functional assessment is required, ensuring that the combination and quantities of pesticides applied are able to control a set of distinct pests in an equivalent way.

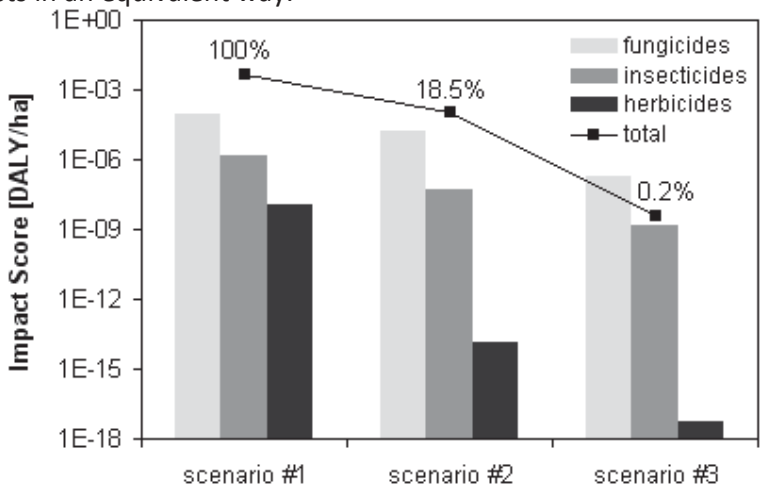

Figure 4.2.28: Human toxicity impact scores of different scenarios expressed in DALY per ha of applied fungicides, insecticides, herbicides and total pesticides applied on wheat and relative impact scores normalized to scenario#1

Figure 4.2.28 presents an example of how to conduct crop-specific substitution of different pesticides. Pesticide target classes focus on distinct pest categories, e.g. fungi, insects, weeds. Substitution, hence, must be discussed separately for pesticides within each target class., i.e. insecticides can only be substituted by other insecticides etc. In scenario#1, we exemplarily combined applications of β-cyfluthrin and carbaryl on wheat against a set of common wheat-damaging insects (wheat bulb fly, cereal leaf beetle, aphids and thrips). This insecticide mix is substituted by a combination of the less impacting insecticides α-cypermethrin and deltamethrin in scenario#3. Individual insecticides and application rates are chosen to ensure a similar ability to control the same unwanted insects in both scenarios. Figure 4.2.28 demonstrates that substituting scenario#1 by scenario#3 reduces the total impact score of applied insecticides by almost three orders of magnitude to only 0.2% of the impact score of scenario#1. This approach is similarly applied to fungicides and herbicides, where substituting scenario#1 by scenario#3 results in impact scores reduced by more than one and nine orders of magnitude, respectively. Scenario#2 represents an intermediary situation showing some, but not as much reduction in impact scores for all target classes as scenario#3. Background information for this example of pesticide substitution is provided in supporting information.

4.2.4. Discussion

Potential and Limitations. The presented approach demonstrates the importance of dynamic pesticide assessment and enables us to distinguish between various food crops. By identifying the combined influence of crop characteristics, application times and substance properties we demonstrate that it is crucial to choose appropriate times to apply pesticides and that diffuse emission pathways may be significant for early application, but strongly underestimate human intake for late application before harvest. For practical implementation, we therefore recommend to use our crop-specific characterization factors to account for direct application residues. We thereby stress that results must always be interpreted as a function of times to harvest, i.e. re-calculations are required to account for changing the date of pesticide application. To account for impacts from diffuse emissions in addition to direct residues, initial loss fractions to air and soil during application should be multiplied by the USEtox characterization factors for emissions to urban air and agricultural soil, respectively. For typical foliar application, crop-specific loss fractions to air range from 5-25% and to soil from 5-70%, respectively, where the latter also depends on crop development stage. All presented crop-specific characterization factors are global averages and based on generic values for most underlying parameters, such as human life time and body weight. However, for a spatial assessment, these parameters need to be adjusted accordingly. The present approach is so far limited to organic substances, since inorganics require a different consideration of e.g. their partitioning behavior.

Differences between Crops. Variation in crop-specific intake is mainly driven by distinct characteristics between crop archetypes, e.g. with respect to harvested plant components, from which we can basically classify food crops into roots and tubers, fruits and cereals as well as leafy vegetables. Overall, leafy vegetables only contribute to 2% of the total human vegetal consumption, but may nevertheless lead to human impacts comparable or even higher than via ingestion of cereals. Cereals, on the other hand, contribute to 37% of the human vegetal consumption (including paddy cereals), but substances are usually applied earlier for these crops, leading to lower intake fractions. Highest impacts are expected via consumption of herbaceous crops and fruit trees with usually high intake fractions and consumption, while roots and tubers only contribute little due to very low intake fractions.

Pesticide Substitution. Whenever developing substitution scenarios, we strongly recommend considering aspects related to pesticide authorization, since a substance may be authorized for use on particular crops in some countries, but not in others, because of decreased susceptibility of target pests (resistance) to certain pesticides. Furthermore, for considering multiple applications at different application times, Equation 5.2.4 can be summed up over various applications in addition to summing up over pesticides. However, in line with findings from (*Juraske et al., 2011*), usually only the latest application plays a predominant role due to increasing reduction of intake fractions with time.

4.2.5. References

Abdel-Gawad H, Afifi LM, Abdel-Hameed RM, Hegazi B. 2008. Distribution and Degradation of ^{14}C-Ethyl Prothiofos in a Potato Plant and the Effect of Processing. Phosphorus, Sulfur, and Silicon and the Related Elements 183:2734-2751.

Bennett DH, McKone TE, Evans JS, Nazaroff WW, Margni MD, Jolliet O, Smith KR. 2002. Defining Intake Fraction. Environmental Science and Technology 36:207A-211A.

Cao, T. T. 2001. Fate and a Prediction Model of Pesticides Residues Evolution in Plants. École Polytechnique Fédérale de Lausanne, Lausanne.

Charles R. 2004. Modelling Pesticides Residues. Ph.D. Dissertation, Ecóle Polytechnique Fédérale de Lausanne, Lausanne,.

Codex Alimentarius Commission; Codex pesticides residues in food online database. Joint FAO/WHO Food Standards Programme: 2010.

Contreras WA, Ginestar D, Paraíba LC, Bru R. 2008. Modelling the pesticide concentration in a rice field by a level IV fugacity model coupled with a dispersion-advection equation. Computers & Mathematics with Applications 56(3): 657-669.

European Commission; Commission Regulation (EC) No 149/2008 setting maximum residue levels for products covered by Annex I thereto. (January 29, 2008).

Fantke P, Wieland P, Wannaz C, Friedrich R, Jolliet O. 2013. Dynamics of pesticide uptake into plants: From system functioning to parsimonious modeling. Environmental Modelling & Software 40: 316-324.

Fantke P, Wieland P, Juraske R, Shaddick G, Sevigné E, Friedrich R, Jolliet O. 2012a. Parameterization models for pesticide exposure via crop consumption. Environmental Science & Technology 46(23): 12864-12872.

Fantke P, Friedrich R, Jolliet O, 2012b. Health impact and damage cost assessment of pesticides in Europe. Environment International 49: 9-17.

Fantke P, Juraske R, Antón A, Friedrich R, Jolliet O. 2011a. Dynamic multicrop model to characterize impacts of pesticides in food. Environmental Science & Technology 45(20): 8842-8849.

Fantke P, Charles R, de Alencastro LF, Friedrich R, Jolliet O. 2011b. Plant uptake of pesticides and human health: Dynamic modeling of residues in wheat and ingestion intake. Chemosphere 85(10): 1639-1647.

Fenoll J, Hellín P, López J, González A, Lacasa A, Flores P. 2009. Dissipation rates of fenitrothion in greenhouse grown lettuce and under cold storage conditions. International Journal of Food Science and Technology 2009 44:1034-1040.

Fenoll J, Helln P, Camacho MdM, Lpez J, Gonzlez A, Lacasa A, Flores P. 2008. Dissipation rates of procymidone and azoxystrobin in greenhouse grown lettuce and under cold storage conditions. International Journal of Environmental Analytical Chemistry 88:737-746.

Food and Agriculture Organization of the United Nations; FAOSTAT. faostat.fao.org (updated March 03, 2011).

Gyldenkaerne S, Secher B JM, Nordbo E. 1999. Ground deposit of pesticides in relation to the cereal canopy density. Pesticide Science 55:1210-1216.

Hamburg M, Young P. 1994. Statistical analysis for decision making. 6th Edition. Dryden Press: Fort Worth, London.

Huijbregts M, Hauschild M, Jolliet O, Margni M, McKone T, Rosenbaum RK, van de Meent D. 2010 USEtox™ User Manual Version 1.01.

Huijbregts MAJ, Rombouts LJA, Ragas AMJ, van de Meent D. 2005. Human-Toxicological Effect and Damage Factors of Carcinogenic and Noncarcinogenic Chemicals for Life Cycle Impact Assessment. Integrated Environmental Assessment and Management 1:181-244.

Humbert S, Margni MD, Charles R, Salazar OMT, Quirós AL, Jolliet O. 2007. Toxicity assessment of the main pesticides used in Costa Rica. Agriculture, Ecosystems and Environment 118:183-190.

Inao K, Watanabe H, Karpouzas DG, CapriE. 2008. Simulation Models of Pesticide Fate and Transport in Paddy Environment for Ecological Risk Assessment and Management. Japan Agricultural Research Quarterly 42:13-21.

Ishii Y. 2004. A comparative study of the persistence of organophosphorous and carbamate insecticides in rice plants at harvesting. Bulletin of the National Institute of Agro-Environmental Sciences 23:1-14.

Itoiz E, Fantke P, Juraske R, Kounina A, Antón Vallejo A. 2012. Deposition and residues of azoxystrobin and imidacloprid on greenhouse lettuce with implications for human consumption. Chemosphere 89(9): 1034-1041.

Juraske R, Fantke P, Romero Ramírez AC, González A. 2012. Pesticide residue dynamics in passion fruits: Comparing field trial and modeling results. Chemosphere 89(7): 850-855.

Juraske R, Antón A, Castells F, Huijbregts MAJ. 2007. Human intake fractions of pesticides via greenhouse tomato consumption: Comparing model estimates with measurements for Captan. Chemosphere 67: 1102-1107.

Juraske R, Antón A, Castells F. 2008. Estimating half-lives of pesticides in/on vegetation for use in multimedia fate and exposure models. Chemosphere 70:1748-1755.

Juraske R, Castells F, Vijay A, Muñoz P, Antón A. 2009. Uptake and persistence of pesticides in plants: Measurements and model estimates for imidacloprid after foliar and soil application. Journal of Hazardous Materials, 165:683-689.

Juraske R, Mutel CL, Stoessel F, Hellweg S. 2009. Life cycle human toxicity assessment of pesticides: Comparing fruit and vegetable diets in Switzerland and the United States. Chemosphere 77:939-945.

Juraske R, Vivas CSM, Velsquez AE, Santos GG, Moreno MBB, Gomez JD, Binder CR, Hellweg S, Dallos JAG. 2011. Pesticide Uptake in Potatoes: Model and Field Experiments. Environmental Science and Technology 45:651-657.

Kaushik G, Satya S, Naik SN. 2009. Food processing a tool to pesticide residue dissipation - A review. Food Research International 2009 42:26-40.

Kulhánek A, Trapp S, Sismilich M, Janku J, Zimová M. 2005. Crop-specific human exposure assessment for polycyclic aromatic hydrocarbons in Czech soils. Science of the Total Environment 339:71-80.

Kumar V, Sood C, Jaggi S, Ravindranath SD, Bhardwaj SP, Shanker A. 2005. Dissipation behavior of propargite - an acaricide residues in soil, apple (Malus pumila) and tea (Camellia sinensis). Chemosphere 58:837-843.

Margni MD, Rossier D, Crettaz P, Jolliet O. 2002. Life cycle impact assessment of pesticides on human health and ecosystems. Agriculture, Ecosystems and Environment 93:379-392.

Paraíba LC, Kataguiri K, Model approach for estimating potato pesticide bioconcentration factor. Chemosphere 73:1247-1252.

Paraíba LC. 2007. Pesticide bioconcentration modelling for fruit trees. Chemosphere 66:1468-1475.

Pennington DW, Margni MD, Ammann C, Jolliet O. 2005. Multimedia Fate and Human Intake Modeling: Spatial versus Nonspatial Insights for Chemical Emissions in Western Europe. Environmental Science and Technology 39:1119-1128.

Rosenbaum RK, Bachmann TM, Gold L S, Huijbregts MAJ, Jolliet O, Juraske R, Koehler A, Larsen H. F, MacLeod M, Margni MD, McKone TE, Payet J, Schuhmacher M, van de Meent D, Hauschild MZ 2008. USEtox - the UNEP-SETAC toxicity model: recommended characterisation factors for human toxicity and freshwater ecotoxicity in life cycle impact assessment. The International Journal of Life Cycle Assessment 13:532-546.

Trapp S, Mc Farlane JC. 1995. Plant Contamination: Modeling and Simulation of Organic Chemical Processes. Lewis Publishers, Boca Raton , Florida, U.S.

Trapp S. 2007. Fruit Tree model for uptake of organic compounds from soil and air. SAR and QSAR in Environmental Research 18: 367-387.

Trapp, S.; Kulhánek, A. Human Exposure Assessment for Food - One Equation for all Crops is not enough. 2006. In Phytoremediation and Rhizoremediation., Mackov, M, Dowling D, Macek T, Eds. Springer Press: Dordrecht, The Netherlands 285-300.

Udo de Haes HA, Finnveden G, Goedkoop M, Hauschild MZ, Hertwich E, Hofstetter P, Jolliet O, Klöpffer W, Krewitt W, Lindeijer E, Müller-Wenk R, Olsen S, Pennington DW, Potting J, Steen B. 2002 Life-Cycle Impact Assessment: Striving Towards Best Practice. SETAC Press: Pensacola, FL.

United States Department of Agriculture; International Maximum Residue Limit Database. www.mrldatabase.com (last accessed April 15, 2011).

Wang S-L, Liu F-M, Jin S-H, Jiang SR. 2007. Dissipation of propisochlor and residue analysis in rice, soil and water under field conditions. Food Control 18:731-735.

Wolters A, Linnemann V, Zande JCvd, Vereecken H. 2008. Field experiment on spray drift: Deposition and airborne drift during application to a winter wheat crop. Science of the Total Environment 405:269-277.

Xu X-M, Murray RA, Salazar JD, Hyder K. 2008. The temporal pattern of captan residues on apple leaves and fruit under field conditions in relation to weather and canopy structure. Pest Management Science 64:565-578.

4.3. Terrestrial ecotoxicity

L. Golsteijn, A.F.H. Pilière, R. van Zelm, A.J. Hendriks, and M.A.J. Huijbregts

Radboud University Nijmegen, The Netherlands

4.3.1. Introduction

Soil has only recently become an important topic for ecotoxicologists, despite the fact that the terrestrial environment is of crucial importance (Traas and van Leeuwen 2007). The risk assessment of contaminated soil is complex and has been neglected and avoided frequently (Jensen and Mesman 2006). Also in life cycle assessments, terrestrial ecotoxicity is in most cases not addressed, or to a very limited extent, as a consequence of insufficient soil toxicity data (Rosenbaum et al. 2008a). Nevertheless, several countries have already established soil quality standards (Nortcliff 2002), and the awareness of the importance of soil is increasing. An important metric to describe the toxicity of chemical exposure and uptake is the environmental concentration of a chemical toxic to 50 percent of all species. This hazardous concentration (HC50) can be applied directly in life cycle assessments to determine a median estimate for the effect of chemicals (Hauschild, 2005). Another application can be found in the Sediment Quality Triad concept: the integrated use of site-specific chemical, toxicological and ecological information (Long and Chapman, 1985). Therefore, in order to assess terrestrial ecotoxicity it is important to know the HC50 values and the accompanying uncertainty of the chemicals of interest.

The ecotoxic effects of organic chemicals in soil are found to depend on the concentration that is bioavailable via dissolution in pore water. Pavlou and Weston (1983) and Adams et al. (1985) were the first to suggest that pore water is the primary route of exposure for soil dwelling organisms, a theory that was later confirmed (Belfroid et al. 1994a; 1994b; 1996; Jager 1998; Jager et al. 2003). Hence, exposure is controlled by both substance specific and soil specific parameters (Loibner et al. 2006). In the so-called equilibrium partitioning (EP) method of Shea (1988), a chemical's concentration in water and sediment can be modeled on the basis of its sorption equilibrium. Van der Kooij et al. (1991) described an approach to use the EP-method to derive coherent environmental quality objectives for aquatic systems, that is for the dissolved water phase, the suspended particles, the total concentrations, and the sediment. Quality criteria for water are based on standard aquatic toxicity tests, and much more abundant than soil toxicity data. Therefore, the EP-method makes it possible to estimate terrestrial ecotoxicity from measured aquatic toxicity data.

The applicability of the EP-method is dependent on the validity of the sorption equilibrium model, and the availability of soil water partitioning coefficients (Van der Kooij et al. 1991). An important assumption when applying the equilibrium partitioning method to aquatic toxicity data in order to estimate terrestrial ecotoxicity is that the sensitivity for the aquatic and terrestrial species is similar. Van Beelen et al. (2003) tested aquatic to terrestrial extrapolation for ten organic substances and eight metals and found that using the EP-method gave an equal chance of underestimation or overestimation of terrestrial toxic concentrations. Thus, they stated that the method could be used in case there is a very limited number of terrestrial toxicity data available. Loibner et al. (2006) state that since

other uncertainties associated with the risk assessment of contaminated land are much larger, the EP-method is a sensible tool. Occasionally, the relative toxicity of chemicals to different terrestrial and aquatic species has been determined within the same study (for instance, Siegfried 1993). However, rigorous comparisons of terrestrial and aquatic toxicity are lacking for large sets of chemicals and species. Furthermore, to the best of our knowledge, an analysis of uncertainty in the EP-method has not been performed yet.

The goal of the present study was to analyse the validity and uncertainty of estimates of soil toxicity derived by the equilibrium partitioning method. We made a comparison between freshwater HC50 values derived from standard aquatic tests, and porewater HC50 values derived from terrestrial experimental data by the EP-method. Statistical uncertainty in input parameters was treated with probability distributions propagated by Monte Carlo Simulations. In the end, the practical use of the EP-method was discussed.

4.3.2. Methodology

4.3.2.1. Equilibrium Partitioning Method

The relationship between concentrations in water and solids is described by a partition coefficient (K_p in L water/kg solids). In case of equilibrium, which is required for application of the EP-method, K_p values can be derived from chemical properties and soil characteristics as is commonly done for organic chemicals (Van der Kooij et al. 1991). Specifically the equilibrium partitioning between organic carbon and pore water is an important descriptor of terrestrial ecotoxicity for organic chemicals (DiToro et al. 1991). Then, the partition coefficient is often normalized to the organic matter content in solids and called K_{oc} (L water/kg organic carbon), according to:

$$K_p = f_{oc} \cdot K_{oc} \qquad \textbf{4.3.1}$$

where f_{oc} is the mass fraction of organic carbon in the soil (kg organic carbon/ kg soil).

The Kp values were used in the equilibrium partitioning method as described by Van Beelen et al. (2003) to estimate toxic porewater concentrations:

$$\log L(E)C50_{ep,pw} = \log L(E)C50_{ex,soil} - \log K_p \qquad \textbf{4.3.2}$$

The L(E)C50 value of a chemical is the environmental concentrations expected to cause an effect, e.g. mortality, in at least 50 percent of the individuals in a given population. In this equation $L(E)C50_{ep,pw}$ is the toxic concentration in pore water derived by the EP-method (mg/L), and $L(E)C50_{ex,soil}$ is the toxic concentration in soil derived from experimental data (mg/ kg of soil dry weight; $mg \cdot kg_{dw}^{-1}$). Subsequently, all available L(E)C50 values were used to calculate so-called hazardous concentrations.

The hazardous porewater concentration ($HC50_{ep,pw}$ in $mg \cdot L^{-1}$) was estimated by the geometric mean of all available species-specific log-normally distributed L(E)C50 values. Therefore, log HC50 equals the arithmetic mean of the log-transformed L(E)C50 values.

$$\log HC50_{ep,pw} = \frac{1}{n} \cdot \sum_{i=1}^{n} \log L(E)C50_{ep,pw,i} \qquad \textbf{4.3.3}$$

where *n* is the number of species for which aquatic toxicity tests have been performed for chemical x, and $L(E)C50_{ep,pw,i}$ is the concentration of chemical x that causes an effect to 50 percent of the individuals of species i ($mg \cdot L^{-1}$). The HC50 implies that at least 50 percent of the individuals in 50 percent of all species is expected to be protected against the chemical's

toxic effects. Similar to Equation 4.3.3, a hazardous freshwater concentration ($HC50_{ex,fw}$ in mg/L) was derived from all available experimental freshwater L(E)C50 values.

4.3.2.2. Uncertainty

Several sources of statistical uncertainty influenced the estimates of the hazardous concentrations for pore water and fresh water. Here, the focus was on chemical-specific uncertainties, whereas environment related uncertainties were excluded. The uncertainty distributions of the hazardous freshwater concentrations depended on the number of species for which L(E)C50 values were available. Therefore, we assigned a student t-distribution to log $HC50_{ep,pw}$ values and to log $HC50_{ex,fw}$ values, with n-1 degrees of freedom and a standard deviation calculated directly from the individual L(E)C50 data. Estimated log K_{oc} values (see par. Data Collection) were assigned a normal distribution with a residual error of 0.34 log-unit (EPI Suite KOCWIN, Meylan et al. 1992). Subsequently, the uncertainties in the predictive modeling output were propagated with Monte Carlo simulations using the spreadsheet-based application Crystal Ball (Oracle©, Release 11.1.2.0.00) in MS Excel with 10,000 iterations per run.

By comparing $HC50_{ex,fw}$ values and $HC50_{ep,pw}$ values, we tested the assumption underlying the EP-method that chemicals' sensitivity for aquatic and terrestrial species is similar. The ratio of $HC50_{ep,pw}$ and $HC50_{ex,fw}$ functioned an indicator of the similarity:

$$Ratio_{ter/aq} = HC50_{ep,pw} / HC50_{ex,fw} \qquad \textbf{4.3.4}$$

In order to use standard aquatic tests for the derivation of hazardous concentrations in soil or soil quality criteria, a value of 1 should be within the confidence interval of the $Ratio_{ter/aq}$.

4.3.2.3. Data Collection

Terrestrial toxicological data for organic chemicals were collected from the U.S. Environmental Protection Agency TERRETOX Database (2007), and from the Dutch National Institute for Public Health and the Environment (Huijbregts 1999; RIVM 2011; Verbruggen et al. 2001). We collected experimental L(E)C50 values per unit of soil dry weight from studies that reported the chemical and species tested, toxic endpoint (i.e. LC50 or EC50), and fraction of organic matter or carbon in the soil sample. For chemicals with more than one measurement for the same species, the geometric mean was used. For chemicals whose toxic concentration was expressed as a range, the median was used. Frequently, experimental studies reported the total fraction of organic matter, rather than the fraction of organic carbon. In that case we assumed that the fraction of organic carbon was a factor of 1.7 lower than the total fraction of organic matter (Verbruggen et al. 2001).

Hazardous concentrations for fresh water were obtained from the Dutch National Institute for Public Health and the Environment (RIVM 2008). For porewater as well as freshwater, we used HC50 values based on toxicity data for at least three test species, as Van Zelm et al. (2009a) demonstrated that uncertainty decreases drastically when three instead of two test species are available.

Organic carbon-water partitioning coefficients (Koc in L/kg) were estimated with the EPI Suite™ chemical estimation program version 4.0 on the basis of the chemicals' molecular connectivity index (MCI).

4.3.3. Results

Hazardous porewater concentrations were estimated with the equilibrium partitioning method, and derived from standard aquatic toxicity tests for 48 organic chemicals. Typical porewater HC50 values ranged between $1.2 \cdot 10^{-3}$ and $3.3 \cdot 10^{4}$ mg·L^{-1} based on the EP-method, and typical freshwater HC50 values between $7.8 \cdot 10^{-3}$ and $6.5 \cdot 10^{3}$ based on standard aquatic toxicity tests. Confidence intervals of median $HC50_{ep,pw}$ values as well as median $HC50_{ex,fw}$ values ranged typically 2 orders of magnitude. For almost 65 percent of the chemicals, $HC50_{ep,pw}$ values exceeded $HC50_{ex,fw}$ values (see Figure 4.3.29). Overall, median $Ratio_{ter/aq}$ values ranged from $5.8 \cdot 10^{-3}$ to $1.5 \cdot 10^{2}$, with a typical value of $1.7 \cdot 10^{0}$. Accompanying confidence intervals of the $Ratio_{ter/aq}$ values ranged from < 2 up to 10 orders of magnitude, typically 4 orders of magnitude (see Figure 4.3.30). For 8 percent of the chemicals (4 out of 48), a value of 1 for the $Ratio_{ter/aq}$ fell outside the confidence interval. Table 4.3.1 gives the chemical-specific HC50 values for porewater and fresh water, the $Ratio_{ter/aq}$ values, and the accompanying uncertainty ranges.

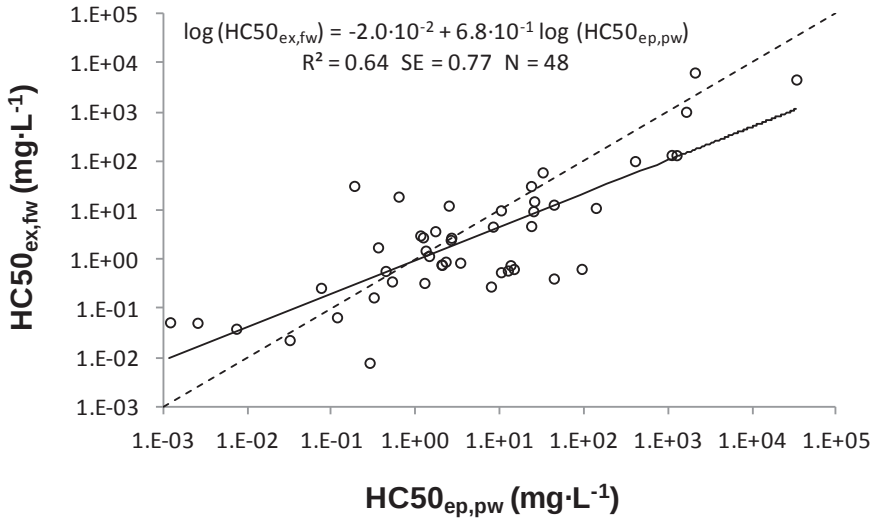

Figure 4.3.29. Porewater hazardous concentrations (HC50ep,pw) versus freshwater hazardous concentrations (HC50ex,fw). N indicates the number of chemicals.

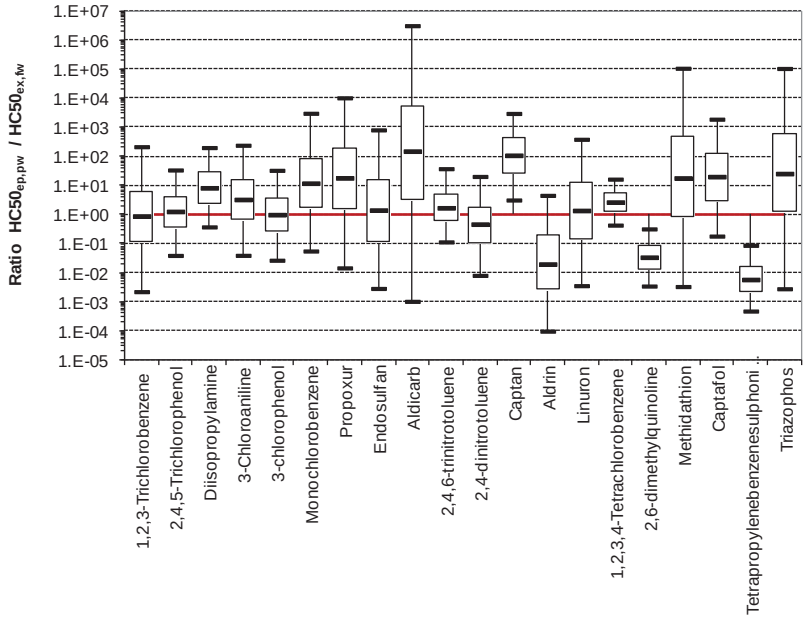
Ratio HC50ep,pw / HC50ex,fw
1.E+07
1.E+06
1.E+05
1.E+04
1.E+03
1.E+02
1.E+01
1.E+00
1.E-01
1.E-02
1.E-03
1.E-04
1.E-05
1,2,3-Trichlorobenzene
2,4,5-Trichlorophenol
Diisopropylamine
3-Chloroaniline
3-chlorophenol
Monochlorobenzene
Propoxur
Endosulfan
Aldicarb
2,4,6-trinitrotoluene
2,4-dinitrotoluene
Captan
Aldrin
Linuron
1,2,3,4-Tetrachlorobenzene
2,6-dimethylquinoline
Methidathion
Captafol
Tetrapropylenebenzenesulphoni
Triazophos

(a)

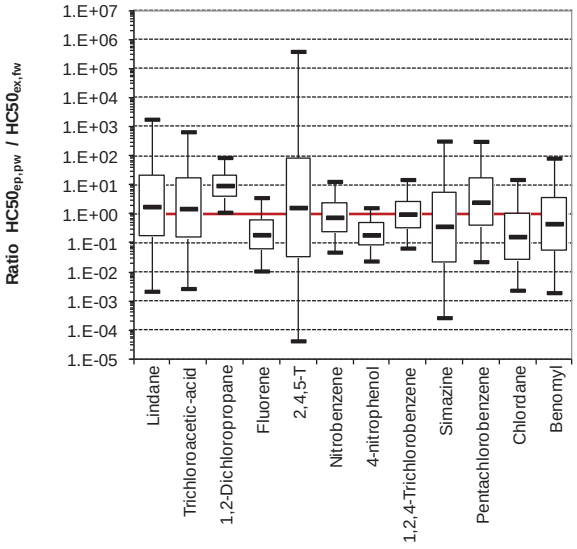
Ratio HC50ep,pw / HC50ex,fw
1.E+07
1.E+06
1.E+05
1.E+04
1.E+03
1.E+02
1.E+01
1.E+00
1.E-01
1.E-02
1.E-03
1.E-04
1.E-05
Lindane
Trichloroacetic-acid
1,2-Dichloropropane
Fluorene
2,4,5-T
Nitrobenzene
4-nitrophenol
1,2,4-Trichlorobenzene
Simazine
Pentachlorobenzene
Chlordane
Benomyl

(b)

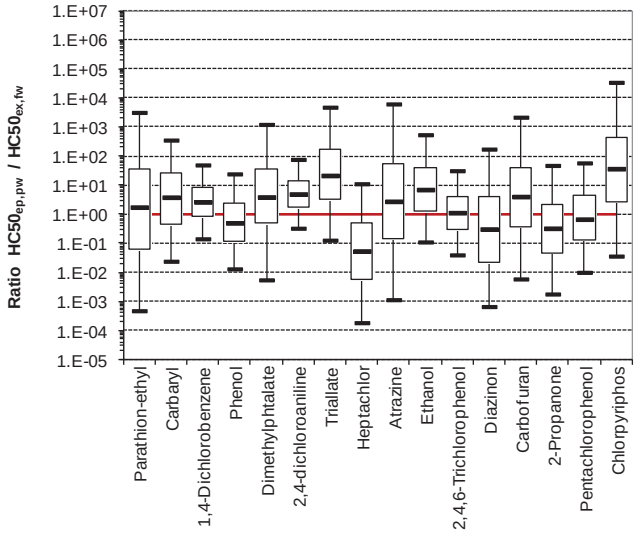

(c)

Figure 4.3.30. Ratio of the typical porewater HC50 values based on the EP-method ($HC50_{ep,pw}$), and typical freshwater HC50 values based on standard aquatic toxicity tests ($HC50_{ex,fw}$), for chemicals with 3 (a), 4 (b), or ≥5 (c) species tested in soil toxicity experiments. The columns represent the 25th and 75th percentile, and the whiskers the 5th and 95th percentiles. In the columns, the median ratio is marked.

Table 4.3.1. Chemical-specific HC50 values for porewater and fresh water, the $Ratio_{ter/aq}$ values, and the accompanying uncertainty ranges.

Chemical Name	Log Koc (log L/kg)	P_{50} $HC50_{ep,pw}$	P_5 $HC50_{ep,pw}$	P_{95} $HC50_{ep,pw}$	n ep,pw	# trophic levels	P_{50} $HC50_{ex,fw}$	P_5 $HC50_{ex,fw}$	P_{95} $HC50_{ex,fw}$	n ex,fw	# trophic levels	P_{50} Ratio $HC50_{ep,pw}$ /$HC50_{ex,fw}$	P_5 Ratio $HC50_{ep,pw}$ /$HC50_{ex,fw}$	P_{95} Ratio $HC50_{ep,pw}$ /$HC50_{ex,fw}$	Ratio of 1 not in 90%-CI
1,2,3-Trichlorobenzene	3.14	1.31E+00	[5.81E-03 -	1.81E+02]	3	2	1.52E+00	[1.68E-01 -	2.01E+01]	7	3	8.80E-01	[2.21E-03 -	2.13E+02]	
2,4,5-Trichlorophenol	3.25	1.43E+00	[5.62E-02 -	3.60E+01]	3	2	1.18E+00	[4.32E-01 -	3.45E+00]	18	4	1.26E+00	[3.88E-02 -	3.37E+01]	
Ddiisopropylamine	1.80	1.09E+03	[2.30E+02 -	4.41E+03]	3	1	1.35E+02	[9.03E+00 -	1.86E+03]	15	4	8.21E+00	[3.72E-01 -	1.99E+02]	
3-Chloroaniline	2.05	4.35E+01	[2.66E+00 -	1.03E+03]	3	2	1.31E+01	[6.77E-01 -	4.41E+02]	7	4	3.26E+00	[3.91E-02 -	2.39E+02]	
3-Chlorophenol	2.48	1.02E+01	[5.50E-01 -	1.62E+02]	3	2	1.01E+01	[1.73E+00 -	5.81E+01]	8	3	9.80E-01	[2.66E-02 -	3.28E+01]	
Monochlorobenzene	2.37	1.37E+02	[2.89E+00 -	8.17E+03]	3	2	1.13E+01	[3.74E-01 -	3.66E+02]	16	3	1.18E+01	[5.51E-02 -	3.01E+03]	
Propoxur	1.78	1.33E+01	[4.47E-02 -	1.64E+03]	3	1	7.66E-01	[1.15E-02 -	5.83E+01]	59	3	1.80E+01	[1.45E-02 -	1.02E+04]	
Endosulfan	3.83	3.16E-02	[9.31E-04 -	1.14E+00]	3	1	2.28E-02	[1.43E-04 -	3.19E+00]	152	4	1.41E+00	[2.84E-03 -	8.08E+02]	
Aldicarb	1.39	9.32E+01	[1.63E-03 -	6.38E+05]	3	1	6.44E-01	[7.37E-03 -	5.16E+01]	43	4	1.50E+02	[1.02E-03 -	3.10E+06]	
2,4,6-Trinitrotoluene	3.45	8.23E+00	[1.09E+00 -	6.64E+01]	3	1	4.68E+00	[8.48E-01 -	2.56E+01]	12	2	1.68E+00	[1.13E-01 -	3.74E+01]	
2,4-Dinitrotoluene	2.76	1.70E+00	[6.38E-02 -	4.29E+01]	3	1	3.78E+00	[3.98E-01 -	3.78E+01]	17	4	4.62E-01	[8.01E-03 -	2.02E+01]	
Captan	2.40	4.36E+01	[1.11E+01 -	1.76E+02]	3	1	4.10E-01	[1.76E-02 -	1.01E+01]	40	3	1.08E+02	[3.13E+00 -	2.97E+03]	*
Aldrin	4.91	1.20E-03	[4.85E-05 -	3.14E-02]	3	1	5.25E-02	[9.89E-04 -	2.82E+00]	77	2	1.96E-02	[9.66E-05 -	4.52E+00]	
Linuron	2.53	5.20E-01	[4.58E-02 -	4.67E+00]	3	1	3.57E-01	[2.26E-03 -	8.50E+01]	25	3	1.36E+00	[3.55E-03 -	3.83E+02]	
1,2,3,4-Tetrachlorobenzene	3.36	2.04E+00	[5.33E-01 -	7.79E+00]	3	2	7.77E-01	[2.30E-01 -	2.97E+00]	4	3	2.65E+00	[4.28E-01 -	1.63E+01]	
2,6-Dimethylquinoline	3.60	6.23E-01	[1.25E-01 -	2.65E+00]	3	1	1.92E+01	[3.19E+00 -	1.08E+02]	17	4	3.37E-02	[3.44E-03 -	3.17E-01]	*
Methidathion	1.33	1.24E+01	[9.18E-03 -	8.99E+03]	3	1	5.96E-01	[1.36E-03 -	1.58E+02]	24	3	1.79E+01	[3.31E-03 -	1.06E+05]	
Captafol	2.89	1.03E+01	[3.01E+00 -	3.69E+01]	3	1	5.51E-01	[6.44E-03 -	4.41E+01]	22	3	1.99E+01	[1.80E-01 -	1.88E+03]	

Tetrapropylenebenzenesulphonic-acid	4.86	1.85E-01	[	2.41E-02	-	1.39E+00	]	3	1	3.17E+01	[	6.17E+00	-	1.49E+02	]	18	4	5.77E-03	[	4.75E-04	-	8.65E-02	]	*
Triazophos	3.27	7.80E+00	[	2.79E-02	-	2.99E+03	]	3	2	2.81E-01	[	7.14E-04	-	2.37E+02	]	7	3	2.54E+01	[	2.78E-03	-	1.05E+05	]	
lindane	3.45	3.15E-01	[	1.99E-03	-	3.18E+01	]	4	1	1.69E-01	[	1.58E-03	-	1.36E+01	]	181	4	1.78E+00	[	2.17E-03	-	1.81E+03	]	
Trichloroacetic-acid	0.51	1.62E+03	[	2.87E+01	-	1.24E+05	]	4	2	1.03E+03	[	9.75E+00	-	1.17E+05	]	13	2	1.52E+00	[	2.70E-03	-	6.71E+02	]	
1,2-Dichloropropane	1.78	1.25E+03	[	3.19E+02	-	5.18E+03	]	4	1	1.34E+02	[	2.59E+01	-	6.62E+02	]	9	3	9.45E+00	[	1.14E+00	-	8.69E+01	]	*
Fluorene	3.96	3.55E-01	[	9.61E-02	-	1.35E+00	]	4	1	1.77E+00	[	1.32E-01	-	2.54E+01	]	12	3	1.91E-01	[	1.08E-02	-	3.63E+00	]	
2,4,5-T	2.03	2.55E+01	[	4.54E-04	-	2.25E+06	]	4	2	1.53E+01	[	7.06E-01	-	4.03E+02	]	28	3	1.65E+00	[	4.27E-05	-	3.90E+05	]	
Nitrobenzene	2.35	2.33E+01	[	5.60E+00	-	8.89E+01	]	4	1	3.15E+01	[	2.54E+00	-	2.98E+02	]	17	4	7.62E-01	[	4.83E-02	-	1.31E+01	]	
4-Nitrophenol	2.46	2.46E+00	[	7.03E-01	-	1.10E+01	]	4	1	1.25E+01	[	2.85E+00	-	6.19E+01	]	33	4	1.89E-01	[	2.39E-02	-	1.63E+00	]	
1,2,4-Trichlorobenzene	3.13	2.63E+00	[	4.33E-01	-	1.28E+01	]	4	2	2.78E+00	[	2.61E-01	-	2.24E+01	]	37	4	9.87E-01	[	6.65E-02	-	1.52E+01	]	
Simazine	2.17	1.13E+00	[	5.37E-03	-	1.21E+02	]	4	1	3.09E+00	[	3.43E-02	-	3.16E+02	]	57	4	3.73E-01	[	2.68E-04	-	3.20E+02	]	
Pentachlorobenzene	3.57	2.01E+00	[	1.83E-01	-	2.11E+01	]	4	2	7.90E-01	[	1.49E-02	-	4.06E+01	]	13	3	2.53E+00	[	2.27E-02	-	3.13E+02	]	
Chlordane	4.53	7.33E-03	[	5.22E-04	-	1.03E-01	]	4	1	3.88E-02	[	1.12E-03	-	1.45E+00	]	41	3	1.65E-01	[	2.36E-03	-	1.53E+01	]	
Benomyl	2.53	1.21E+00	[	7.66E-02	-	2.64E+01	]	4	1	2.83E+00	[	3.44E-02	-	2.26E+02	]	21	3	4.60E-01	[	1.95E-03	-	8.29E+01	]	
Parathion-ethyl	3.38	1.16E-01	[	3.31E-04	-	3.12E+01	]	5	1	6.65E-02	[	2.77E-04	-	1.77E+01	]	142	4	1.75E+00	[	4.78E-04	-	3.19E+03	]	
Carbaryl	2.55	3.36E+00	[	2.87E-01	-	3.59E+01	]	5	1	8.61E-01	[	1.69E-02	-	5.74E+01	]	200	4	3.84E+00	[	2.41E-02	-	3.56E+02	]	
1,4-Dichlorobenzene	2.57	2.49E+01	[	3.67E+00	-	1.82E+02	]	5	2	9.67E+00	[	1.07E+00	-	7.54E+01	]	17	3	2.65E+00	[	1.43E-01	-	4.97E+01	]	
Phenol	2.27	3.21E+01	[	5.55E+00	-	1.67E+02	]	5	2	5.98E+01	[	2.20E+00	-	2.08E+03	]	224	4	5.03E-01	[	1.32E-02	-	2.44E+01	]	
Dimethylphtalate	1.50	4.02E+02	[	1.02E+00	-	8.84E+04	]	5	2	1.01E+02	[	2.27E+01	-	4.19E+02	]	15	3	3.91E+00	[	5.51E-03	-	1.23E+03	]	
2,4-Dichloroaniline	2.27	2.35E+01	[	4.46E+00	-	1.15E+02	]	5	2	4.82E+00	[	5.29E-01	-	4.76E+01	]	18	4	4.95E+00	[	3.30E-01	-	7.70E+01	]	
Triallate	3.00	1.46E+01	[	2.46E-01	-	8.82E+02	]	5	1	6.40E-01	[	2.55E-02	-	1.33E+01	]	17	3	2.16E+01	[	1.28E-01	-	4.82E+03	]	
Heptachlor	4.62	2.54E-03	[	2.48E-05	-	2.45E-01	]	6	1	5.13E-02	[	1.88E-03	-	1.16E+00	]	83	3	5.41E-02	[	1.85E-04	-	1.12E+01	]	
Atrazine	2.35	2.26E+00	[	2.58E-03	-	1.98E+03	]	6	2	9.03E-01	[	1.81E-02	-	3.89E+01	]	136	4	2.78E+00	[	1.15E-03	-	6.25E+03	]	
Ethanol	0.02	3.32E+04	[	1.47E+03	-	6.59E+05	]	7	2	4.68E+03	[	1.93E+02	-	1.30E+05	]	17	4	7.05E+00	[	1.11E-01	-	5.45E+02	]	
2,4,6-Trichlorophenol	3.25	2.60E+00	[	1.48E-01	-	6.33E+01	]	7	2	2.51E+00	[	6.51E-01	-	9.64E+00	]	28	4	1.13E+00	[	3.98E-02	-	3.15E+01	]	
Diazinon	3.48	7.46E-02	[	1.74E-03	-	4.04E+00	]	7	1	2.64E-01	[	1.75E-03	-	2.55E+01	]	118	4	3.09E-01	[	6.65E-04	-	1.75E+02	]	

Carbofuran	1.98	1.26E+00	[	2.28E-02	-	8.81E+01	]	7	1	3.33E-01	[	2.74E-03	-	3.41E+01	]	69	3	4.05E+00	[	5.92E-03	-	2.18E+03	]	
2-Propanone	0.37	2.06E+03	[	2.39E+01	-	1.44E+05	]	8	2	6.49E+03	[	4.65E+02	-	8.85E+04	]	46	3	3.28E-01	[	1.80E-03	-	4.78E+01	]	
Pentachlorophenol	3.70	4.36E-01	[	2.56E-02	-	8.36E+00	]	9	2	5.85E-01	[	2.37E-02	-	1.33E+01	]	166	4	6.75E-01	[	9.99E-03	-	5.84E+01	]	
Chlorpyriphos	3.86	2.82E-01	[	1.66E-03	-	6.28E+01	]	9	2	7.84E-03	[	7.02E-05	-	6.93E-01	]	164	3	3.69E+01	[	3.62E-02	-	3.46E+04	]	

4.3.4. Discussion

In this study we assessed the validity and uncertainty of estimates of soil toxicity derived by the equilibrium partitioning method. We made a comparison between freshwater HC50 values derived from standard aquatic tests, and porewater HC50 values derived from terrestrial experimental data by the EP-method. There was a positive correlation between them, demonstrating that chemicals that were among the most toxic in fresh water were also among the most toxic in soil. However, uncertainty was high, due to uncertainty in input values.

Interspecies variations in species sensitivity is an important source of uncertainty for toxicity assessments on the basis of a few single test data (Kooijman 1987). In soil toxicity experiments, the number of species tested ranged from 3 to 9, typically 4. After distinguishing primary producers (i.e. plants); consumers (e.g. insects, earthworms, nematodes); decomposers (e.g. micro-organisms); and others, data were from one trophic level only for 56 percent of the chemicals, and from two trophic levels for the remaining chemicals. In the standard aquatic toxicity tests, the number of species ranged from 4 to 224, typically 23. The distinction between 4 trophic levels: i.e. bacteria/archaea/protista; plantae/fungi; invertebrates; and vertebrates-ectotherm, showed that data came from 2 trophic levels for 6 percent of the chemicals, from 3 trophic levels for 48 percent of the chemicals, and from 4 trophic levels for 46 percent of the chemicals. For the four chemicals for which a $Ratio_{ter/aq}$ value of 1 fell outside the 90% CI, soil toxicity data from only one trophic level were available.

Ideally the $Ratio_{ter/aq}$ values would be 1. However, a ratio of 1 fell outside the 50% CI for 55 percent of the chemicals with 3 species tested in soil toxicity experiments, for 25 percent of the chemicals with 4 species tested in soil toxicity experiments, and for 31 percent of the chemicals with ≥5 species tested in soil toxicity experiments. Furthermore, a ratio of 1 fell outside the 90% CI for 15 percent of the chemicals with 3 species tested in soil toxicity experiments (i.e. Captan, 2,6-Dimethylquinoline, Tetrapropylenebenzenesulphonic acid), for 8 percent of the chemicals with 4 species tested in soil toxicity experiments (i.e. 1,2-Dichloropropane), and for none of the chemicals with ≥5 species tested in soil toxicity experiments. For Captan, a fungicide which inhibits sporulation, we found a $Ratio_{ter/aq}$ of $1.1 \cdot 10^{2}$ (90% CI: $3.1 \cdot 10^{0}$-$3.0 \cdot 10^{3}$). Plants and fungi were present in the aquatic test set, but not in the soil test set. The specific mode of action of Captan could explain the lower HC50 for the aquatic dataset. For 2,6-Dimethylquinoline, which is a precursor of several herbicides, we found a $Ratio_{ter/aq}$ of $3.4 \cdot 10^{-2}$ (90% CI: $3.4 \cdot 10^{-3}$-$3.2 \cdot 10^{-1}$). Seven out of the 17 species tested in the aquatic test set were plants or fungi, whereas the soil test set was completely composed of plants. Also for 2,6-Dimethylquinoline, the specific mode of action could be a reason for the lower HC50 in the soil dataset.

Porewater concentrations have been proven to determine the toxicity of polycyclic aromatic hydrocarbons (Swartz et al. 1990), heavy metals (Kemp and Swartz 1988; Swartz et al. 1985), polychlorinated biphenyls (Pavlou and Weston 1983), and pesticides (Houx and Aben 1993; Schuytema et al. 1989; Ziegenfuss et al. 1986). In addition, it has be shown for different species that toxicity can be expressed in terms of porewater concentrations, e.g. for sediment-dwelling organisms like midges (Knezovich and Harrison 1988; Ziegenfuss et al. 1986) and oligochaetes (Connell et al. 1988), and for earthworms (Van Gestel and Ma 1988). In their aquatic to terrestrial extrapolation for ten organic substances and eight metals, Van Beelen et al. (2003) found that using the EP-method gave an equal chance of underestimation or overestimation of terrestrial toxic concentrations. They recommend the use of the EP-method for the estimation of HC5 values

(i.e. the toxic concentration for sensitive species) if less than 5 terrestrial toxicity data were available.

Both confidence intervals of median $HC50_{ep,pw}$ values as well as median $HC50_{ex,fw}$ values ranged typically 2 orders of magnitude. Although the comparison of $HC50_{ep,pw}$ values and $HC50_{ex,fw}$ values showed a typical $Ratio_{ter/aq}$ of 1.7, a ration of 1 fell inside the 90% CI for 92 percent of the chemicals, indicating that the EP-method could give a valid estimate of soil toxicity.

4.3.5. References

Adams WJ, Kimerle RA, Mosher RG. 1985. Aquatic safety assessment of chemicals sorbed to sediments. In: Cardwell RD, Purdy R, Bahner RC, editors. Aquatic toxicology and hazard assessment:seventh symposium. Philadelphia, PA: American Society for Testing and Materials. p. 429-453.

Belfroid A, Meiling J, Sijm D, Hermens J, Seinen W, Vangestel K. 1994a. Uptake of hydrophobic halogenated aromatic-hydrocarbons from food by earthworms (eisenia-andrei). Archives of Environmental Contamination and Toxicology 27(2):260-265.

Belfroid A, Sikkenk M, Seinen W, Vangestel K, Hermens J. 1994b. The toxicokinetic behavior of chlorobenzenes in earthworm (eisenia-andrei) experiments in soil. Environmental Toxicology and Chemistry 13(1):93-99.

Belfroid AC, Sijm DTHM, van Gestel CAM. 1996. Bioavailability and toxicokinetics of hydrophobic aromatic compounds in benthic and terrestrial invertebrates. Environmental Review 4:276-299.

Connell DW, Bowman M, Hawker DW. 1988. Bioconcentration of chlorinated hydrocarbons from sediment by oligochaetes. Ecotoxicology and Environmental Safety 16(3):293-302.

DiToro DM, Zarba CS, Hansen DJ, Berry WJ, Swartz RC, Cowan CE, Pavlou SP, Allen HE, Thomas NA, Paquin PR. 1991. Technical basis for establishing sediment quality criteria for nonionic organic-chemicals using equilibrium partitioning. Environmental Toxicology and Chemistry 10(12):1541-1583.

Houx NWH, Aben WJM. 1993. Bioavailability of pollutants to soil organisms via the soil solution. Science of The Total Environment 134, Supplement 1(0):387-395.

Huijbregts MAJ. 1999. Ecotoxicological effect factors for the terrestrial environment in the frame of LCA. Interfaculty Department of Environmental Science, University of Amsterdam.

Jager T. 1998. Mechanistic approach for estimating bioconcentration of organic chemicals in earthworms (Oligochaeta). Environmental Toxicology and Chemistry 17(10):2080-2090.

Jager T, Fleuren R, Hogendoorn EA, De Korte G. 2003. Elucidating the routes of exposure for organic chemicals in the earthworm, Eisenia andrei (Oligochaeta). Environmental Science & Technology 37(15):3399-3404.

Jensen J, Mesman M. 2006. Foreword. In: Jensen J, Mesman M, editors. Ecological risk assessment of contaminated land. Bilthoven, the Netherlands: National Institute for Public Health and the Environment. p. 5.

Kemp PF, Swartz RC. 1988. Acute toxicity of interstitial and particle-bound cadmium to a marine infaunal amphipod. Marine Environmental Research 26(2):135-153.

Knezovich JP, Harrison FL. 1988. The bioavailability of sediment-sorbed chlorobenzenes to larvae of the midge, chironomus-decorus. Ecotoxicology and Environmental Safety 15(2):226-241.

Kooijman S. 1987. A safety factor for LC50 values allowing for differences in sensitivity among species. Water Research 21(3):269-276.

Loibner A, Jensen J, Ter Laak T, Celis R, Hartnik T. 2006. Sorption and aging of soil contamination. In: Jensen J, Mesman M, editors. Ecological risk assessment of contaminated land. Bilthoven, the Netherlands: National Institute for Public Health and the Environment. p. 19-29.

Meylan W, Howard PH, Boethling RS. 1992. Molecular topology fragment contribution method for predicting soil sorption coefficients. Environmental Science & Technology 26(8):1560-1567.

Nortcliff S. 2002. Standardisation of soil quality attributes. Agriculture, Ecosystems & Environment 88(2):161-168.

Pavlou SP, Weston DP. 1983. Initial evaluation of alternatives for development of sediment related criteria for toxic contaminants in marine waters (Puget Sound). Phase I: Development of conceptual framework. Bellevue, Washington.

RIVM; National Institute for Public Health and the Environment. 2008. e-toxBase [Internet]. [cited]. Available from: http://www.e-toxbase.com/.

RIVM; National Institute for Public Health and the Environment. 2011. e-toxBase [Internet]. [cited]. Available from: http://www.e-toxbase.com/.

Rosenbaum RK, Bachmann TM, Gold LS, Huijbregts MAJ, Jolliet O, Juraske R, Koehler A, Larsen HF, MacLeod M, Margni M et al. . 2008. USEtox-the UNEP-SETAC toxicity model: recommended characterisation factors for human toxicity and freshwater ecotoxicity in life cycle impact assessment. The International Journal of Life Cycle Assessment 13(7):532-546.

Schuytema GS, Nebeker AV, Griffis WL, Miller CE. 1989. Effects of freezing on toxicity of sediments contaminated with ddt and endrin. Environmental Toxicology and Chemistry 8(10):883-891.

Shea D. 1988. Developing national sediment quality criteria. Environmental Science & Technology 22(11):1256-1261.

Siegfried BD. 1993. Comparative toxicity of pyrethroid insectidicdes to terrestrial and aquatic insects. Environmental Toxicology and Chemistry 12(9):1683-1689.

Swartz RC, Ditsworth GR, Schults DW, Lamberson JO. 1985. Sediment toxicity to a marine infaunal amphipod: Cadmium and its interaction with sewage sludge. Marine Environmental Research 18(2):133-153.

Swartz RC, Schults DW, Dewitt TH, Ditsworth GR, Lamberson JO. 1990. Toxicity of fluoranthene in sediment to marine amphipods - a test of the equilibrium partitioning approach to sediment quality criteria. Environmental Toxicology and Chemistry 9(8):1071-1080.

Traas TP, van Leeuwen CJ. 2007. Ecotoxicological effects. In: van Leeuwen CJ, Vermeire TG, editors. Risk assessment of chemicals: an introduction. Springer. p. 281-356.

US EPA. 2007. ECOTOX User Guide: ECOTOXicology Database System. Version 4.0 [Internet]. [cited]. Available from: http:/www.epa.gov/ecotox/.

Van Beelen P, Verbruggen EMJ, Peijnenburg W. 2003. The evaluation of the equilibrium partitioning method using sensitivity distributions of species in water and soil. Chemosphere 52(7):1153-1162.

Van der Kooij LA, Van de Meent D, Van Leeuwen CJ, Bruggeman WA. 1991. Deriving quality criteria for water and sediment from the results of aquatic toxicity tests and product standards: Application of the equilibrium partitioning method. Water Research 25(6):697-705.

Van Gestel CAM, Ma WC. 1988. Toxicity and bioaccumulation of chlorophenols in earthworms, in relation to bioavailability in soil. Ecotoxicology and Environmental Safety 15(3):289-297.

Van Zelm R, Huijbregts M, Posthuma L, Wintersen A, Van de Meent D. 2009. Pesticide ecotoxicological effect factors and their uncertainties for freshwater ecosystems. The International Journal of Life Cycle Assessment 14(1):43-51.

Verbruggen EMJ, Posthumus R, van Wezel AP. 2001. Ecotoxicological Serious Risk Concentrations for soil, sediment and (ground)water: updated proposals for first series of compounds. Bilthoven, the Netherlands: National Institute for Public Health and the Environment. No. RIVM report 711701 020.

Ziegenfuss PS, Renaudette WJ, Adams WJ. 1986. Methodology for assessing the acute toxicity of chemicals sorbed to sediments: testing the equilibrium partitioning theory. In: Poston TJ, Purdy R, editors. Aquatic toxicology and environmental fate. Philadelphia, PA: American Society for Testing and Materials. p. 479-493.

4.4. Higher (warm-blooded) predator ecotoxicity

L. Golsteijn[1], R. van Zelm[1], H.W.M. Hendriks[1], A.J. Hendriks[1], G. Musters[1], A. Ragas[1], K. Veltman[2], M.A.J Huijbregts[1]

[1]Radboud University Nijmegen, The Netherlands
[2]Norwegian University of Science and Technology, Norway

4.4.1. Introduction

As a follow-up on the Deliverable 2.1 and the paper by Golsteijn et al. (2012b), we developed characterization factors for the ecotoxicological impacts of organic chemicals on warm-blooded predators at the end of freshwater food chains, for the chemicals in USEtox. To this end, we calculated fate and exposure factors for water and air. Subsequently, we calculated bioaccumulation factors for warm-blooded predators, based on exposure via water, food, and air. Internal effect factors were calculated based on LD50-values for mammals and birds.

We enhanced the effect database with interspecies correlation estimation (ICE) models of toxicity. This deliverable gives characterization factors for the impact of organic chemicals on warm-blooded predators at the end of freshwater food chains for a list of 1479 non-ionic chemicals for which aquatic ecotoxicity characterization factors have presently been calculated with USEtox.

4.4.2. Methodology

4.4.2.1. Ecotoxicity Characterization Factors

The paper by Golsteijn et al. (2012ba) describes a method to calculate Characterization Factors (CFs) for the impact assessment of chemical emissions on warm-blooded predators in freshwater food chains. The CF for warm-blooded predators in freshwater food chains was defined as the change in ecotoxic effects of a chemical x on warm-blooded predators, resulting from a change in emission of chemical x. It consists of a multiplication of the Fate Factor ($FF_{x,i,j}$), Exposure Factor ($XF_{x,j}$), Bioaccumulation Factor ($BF_{x,j}$), and Effect Factor (EF_x) of a chemical:

$$CF_{x,i} = \underbrace{\sum_j (FF_{x,i,j} \cdot XF_{x,j} \cdot BF_{x,j})}_{CB_{x,i}} \cdot EF_x \qquad 4.4.5$$

where $CF_{x,i}$ is the ecotoxicological characterization factor of a chemical x emitted into an environmental compartment of emission (i) ($yr \cdot kg^{-1}$). The fate factor describes the fraction of the chemical x transferred from the emission compartment i to a compartment of reception (j), and its subsequent residence time in compartment j ($yr \cdot m^{-3}$). The dimensionless exposure factor is the fraction of the chemical x in the receiving compartment j that is bioavailable for uptake by organisms. The bioaccumulation factor for substance x represents the predators' uptake potential of the bioavailable concentration in fresh water, food and air ($m^3 \cdot kg_{wwt}^{-1}$). EF_x is the effect factor of chemical x describing the effects of chemical x on warm-blooded predators per unit of internal concentration ($kg_{wwt} \cdot kg^{-1}$). For the remainder of this paper, we will refer to the product of $FF_{x,i,j}$,

$XF_{x,j}$, and $BF_{x,j}$, summed for uptake from fresh water, food, and air as the chemical's Concentration Buildup ($CB_{x,i}$ in $yr \cdot kg_{wwt}^{-1}$). $CB_{x,i}$ is the change in the internal concentration of chemical x in warm-blooded predators, resulting from a change in emission of chemical x of 1 kilogram per year.

The freshwater food chain modeled in this study consists of four trophic levels, i.e. algae, invertebrates, fish, and warm-blooded predators such as mammals or birds (see Figure 4.4.31). In order to quantify the predators' internal concentration for each chemical, the exposure and bioaccumulation in trophic level 1 up to and including trophic level 3 were taken into account.

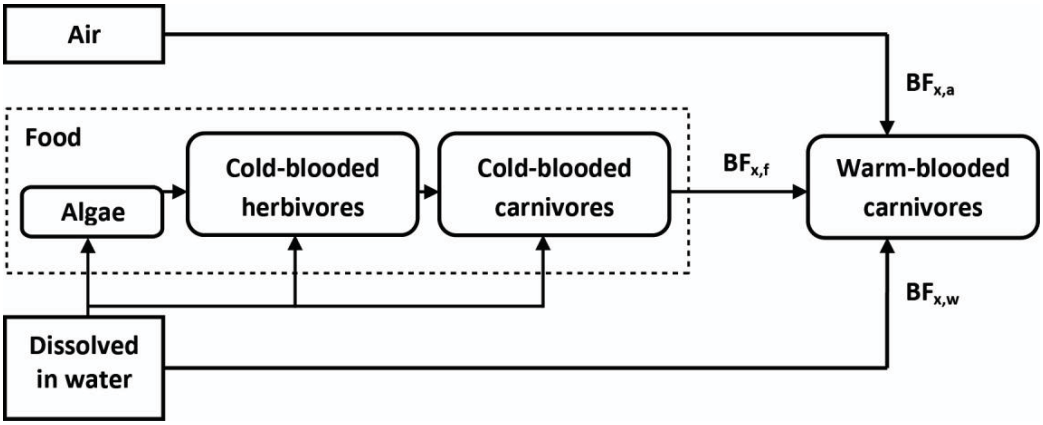

Figure 4.4.31: Scheme of the freshwater food chain applied in the bioaccumulation calculations of this study.

4.4.2.2. Fate and Exposure

FFs and XFs were calculated with the model USES-LCA 2.0 (Van Zelm et al. 2009b).

4.4.2.3. Bioaccumulation

BFs were calculated with the model OMEGA, for chemical uptake via fresh water, food and air (Hendriks et al. 2005; Hendriks et al. 2001; Veltman et al. 2009). For bioaccumulation modeling, the biotransformation rate constants in fish of the third trophic level were taken from EPI Suite™ 4.0 (Arnot et al. 2008). Biotransformation rates in warm-blooded predators were assumed to be five times faster than biotransformation rates in fish of the third trophic level on a per body weight basis, based on the work of Arnot and others (2010). Ionic chemicals were excluded from our assessment.

4.4.2.4. Effects

Initially, in the Deliverable 2.1 and the paper by Golsteijn et al. (2012b), the method was applied to 329 organic chemicals, selected on the basis of the availability of effect data. Ultimately, we enlarged the effect dataset used for calculation of the hazardous dose (which is underlying the effect factor for warm-blooded species) with interspecies correlation estimation (ICE) models. Now, characterization factors could be calculated for 1479 chemicals. With ICE models, acute toxicity values of a chemical to multiple species can be predicted from a single experimental acute toxicity value of the chemical to a so-called surrogate species (Asfaw et al. 2003) For more

information, see also next paragraph. We used the ICE models of Raimondo et al. (2010) to enhance the number of toxicity data. Input values were obtained from experimental studies reported in the Registry of Toxic Effects of Chemical Substances (RTECS, CCOHS 2011). If both experimental and estimated average toxicity values were available, we chose the value based on the largest sample size of species.

4.4.2.5. Uncertainty in Effects

We enlarged our experimental dataset with interspecies correlation estimates, and quantified uncertainty in the hazardous dose before and after enlargement of the sample size (Golsteijn et al. 2012a). The goal of this study was to quantify the possible gain in reliability of the hazardous doses for warm-blooded wildlife species after enlargement of the sample size with ICE predictions. For warm-blooded species, the hazardous dose of a chemical (HD50) is an upcoming and important characteristic in the assessment of toxic chemicals. Generally, experimental information is available for a limited number of warm-blooded species only, which causes statistical uncertainty. Furthermore, when small datasets contain an unrepresentative sample of species, they can cause systematic uncertainty in chemicals' hazardous doses. The number of species can be enlarged with interspecies correlation estimation (ICE) models, but these are uncertain themselves. Therefore, we compared systematic uncertainty and statistical uncertainty between HD50 values based on experimental data ($HD50_{Ex}$) and on datasets combining experimental data and ICE predictions ($HD50_{Co}$).

We used the ICE models available from Raimondo et al. (2010), in order to enhance the dataset of experimental LD50 values. The ICE statistical models are log-linear least square regression models (Asfaw et al. 2003). The slope (b) and intercept (a) for each ICE-regression were derived from the equation:

$$log(LD50_{j,x}) = a + b \cdot log(LD50_{i,x}) \qquad 4.4.6$$

where $LD50_{j,x}$ refers to the predicted toxicity value of chemical x for species j, and $LD50_{i,x}$ refers to the toxicity value of chemical x for surrogate species i. The ICE models were applied only within the toxicity range they were derived from by Raimondo et al. (2010). For species' toxicity values that could be predicted from more than one surrogate species, we chose the prediction with the lowest standard deviation.

We estimated HD50 values based on experimental data only, and on a combined dataset of experimental values and ICE predictions, and calculated systematic uncertainty as follows:

$$UF_{sys,x} = HD50_{Ex,x} / HD50_{Co,x} \qquad 4.4.7$$

in which $UF_{sys,x}$ is the systematic uncertainty factor for the hazardous dose of chemical x, $HD50_{Ex,x}$ and $HD50_{Co,x}$ are the hazardous doses for chemical x based on the experimental dataset and the combined dataset, respectively. We calculated the systematic uncertainty for datasets including all wildlife species for which data were available (i.e. mammals and birds), and for datasets with only mammalian data.

We quantified the statistical uncertainty separately for the HD50 values based on experimental toxicity values and on a combination of experimental and predicted toxicity data. In both cases, statistical uncertainty in the HD50 values was quantified by an Uncertainty Factor, based on the 90% confidence interval (CI) of the log HD50 values. To be exact, we described the uncertainty in the log HD50 predicted from a sample with normally distributed log LD50 values and unknown

variance (Roelofs et al. 2003). Subsequently, we calculated a statistical uncertainty factor ($UF_{stat,x}$) according to:

$$UF_{stat,x} = P_{0.95}/P_{0.05} = 10^{2 \cdot t_{0.90} \cdot SEM_x} \quad \textbf{4.4.8}$$

were $P_{0.95}$ and $P_{0.05}$ are the 95th- and 5th-percentile of the log $HD50_x$ distribution, $t_{0.90}$ is the value of the t-distribution for the log $HD50_x$ that corresponds to the 90% CI depending on the degrees of freedom, and SEM_x is the standard error of the log $HD50_x$.

Experimental Dataset – The standard error of the log $HD50_x$ based on experimental data only ($SEM_{Ex,x}$) was calculated according to:

$$SEM_{Ex,x} = \sqrt{s^2_{Ex,x}/n} \quad \textbf{4.4.9}$$

in which

$$s^2_{Ex,x} = \frac{1}{n-1}\sum_{i=1}^{n}(logLD50_{i,x} - logHD50_{Ex,x})^2 \quad \textbf{4.4.10}$$

In these equations, $s^2_{Ex,x}$ is the variance of the experimental log LD50 values for chemical x; n is the number of experimental $LD50_x$ values in the $HD50_x$ calculation; $LD50_{i,x}$ are the LD50 values for chemical x per experimentally tested species i; and $HD50_{Ex,x}$ is the hazardous dose for chemical x in the experimental dataset.

Combined Dataset – For the combination of experimental and predicted toxicity data, the standard error of the log HD50 ($SEM_{Co,x}$) was calculated according to:

$$SEM_{Co,x} = \sqrt{\frac{s^2_{Co,x}}{n+m} + \frac{m^2}{(n+m)^2}s^2_{ICE,x}} \quad \textbf{4.4.11}$$

in which

$$s^2_{Co,x} = \frac{1}{n+m-1}\sum_{i+j=1}^{n+m}(logLD50_{Co,x} - logHD50_{Co,x})^2 \quad \textbf{4.4.12}$$

$$s^2_{ICE,x} = \left(\frac{1}{m}\sum_{j=1}^{m}s_{j,x}\right)^2 \quad \textbf{4.4.13}$$

In these equations, $s^2_{Co,x}$ is the variance of all log LD50 values available for chemical x, both tested and predicted; n is the number of experimental $LD50_x$ values in the $HD50_x$ calculation; m is the number of predicted $LD50_x$ values in the $HD50_x$ calculation; $s^2_{ICE,x}$ is the squared average regression error of the ICE models used for predicting the log LD50 of chemical x; $LD50_{Co,x}$ is the experimentally tested (i) or predicted (j) toxicity value of chemical x; $HD50_{Co,x}$ is the hazardous dose of chemical x for the combined dataset; and $s_{j,x}$ is the standard deviation of the predicted log LD50 for chemical x in species j, calculated according to Mendenhall and Beaver (1994). For the calculation steps of $s_{j,x}$, we refer to the supporting information of this task (par. Conservative calculation of uncertainty). Equation 9 holds for situations in which the residual errors in the ICE-predictions are fully correlated (r=1), and is further explained in the supporting information (par. Correlations in residual standard errors).

4.4.3. Results and discussion

4.4.3.1. Characterization Factors for Higher Predator Toxicity

Characterization factors for the impact of organic chemicals on warm-blooded predators at the end of freshwater food chains are available in Table S4.14 (Supporting information) for 1479 non-ionic chemicals for which aquatic ecotoxicity characterization factors have presently been calculated with USEtox.

4.4.3.2. Uncertainty in Effects

The uncertainty analysis of the effect data showed that $HD50_{Ex}$ values ranged between $1.0 \cdot 10^{-1}$ and $9.5 \cdot 10^{3}$ $mg \cdot kg_{wwt}^{-1}$, and $HD50_{Co}$ values between $1.1 \cdot 10^{0}$ and $6.1 \cdot 10^{3}$ $mg \cdot kg_{wwt}^{-1}$. For over 97 percent of the chemicals, $HD50_{Ex}$ values exceeded $HD50_{Co}$ values, with a systematic uncertainty (i.e. the ratio of $HD50_{Ex}/HD50_{Co}$) of typically 3.5. The limited availability of experimental toxicity data, predominantly for mammals, resulted in a systematic underestimation of the wildlife toxicity of a chemical. Statistical uncertainty factors (i.e. the ratio of the $95^{th}/5^{th}$ percentile) quantified the statistical uncertainty in the HD50 values. The statistical uncertainty factors ranged between $1.0 \cdot 10^{0}$ and $2.5 \cdot 10^{22}$ for the experimental dataset, and between $4.8 \cdot 10^{0}$ and $1.1 \cdot 10^{2}$ for the combined dataset. For all sample sizes, median statistical uncertainty factors were the largest for combined datasets. However, combining experimental toxicity data with ICE predictions makes it possible to reduce the upper limit of the range for statistical uncertainty factors. We conclude that, by combining experimental data with ICE model predictions, the validity of the HD50 value can be improved and high statistical uncertainty can be reduced, particularly in cases of limited toxicity data, i.e. data for mammals only or a sample size of $n \leq 4$.

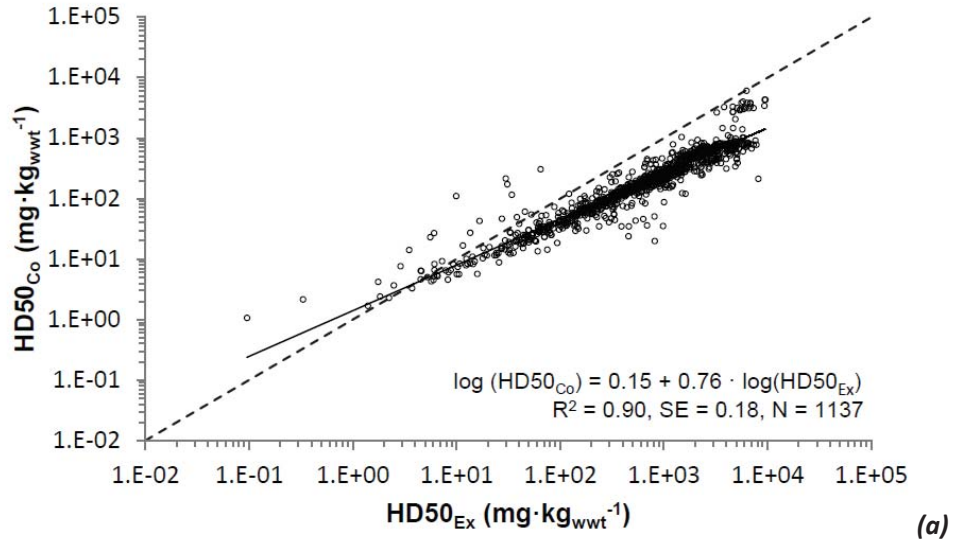

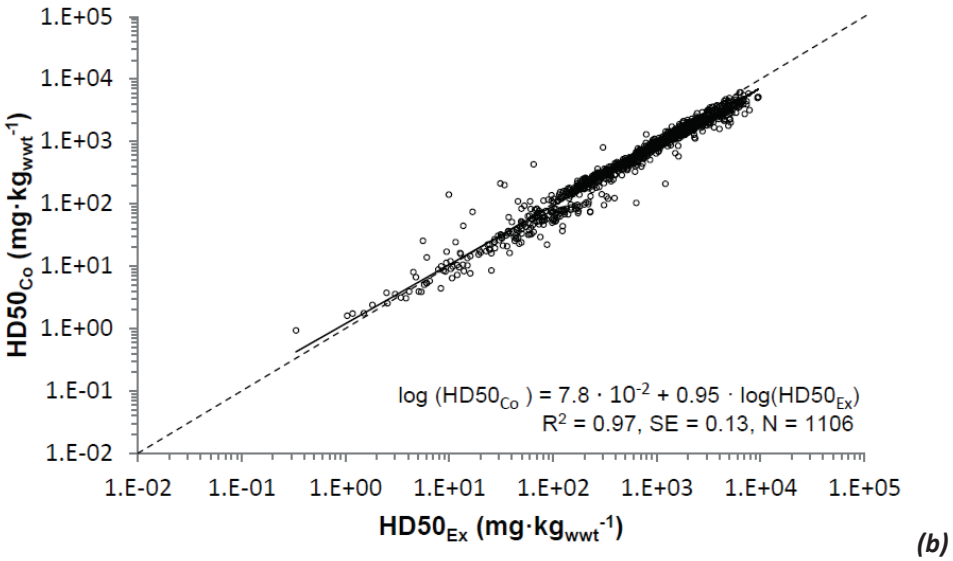

Figure 4.4.32: Hazardous doses based on a dataset of experimental toxicity data ($HD50_{Ex}$) plotted against hazardous doses based on a combined dataset of experimental and predicted toxicity data ($HD50_{Co}$), for all species (a) and for mammals only (b). N is the number of chemicals. The dashed line indicates the 1:1 relation.

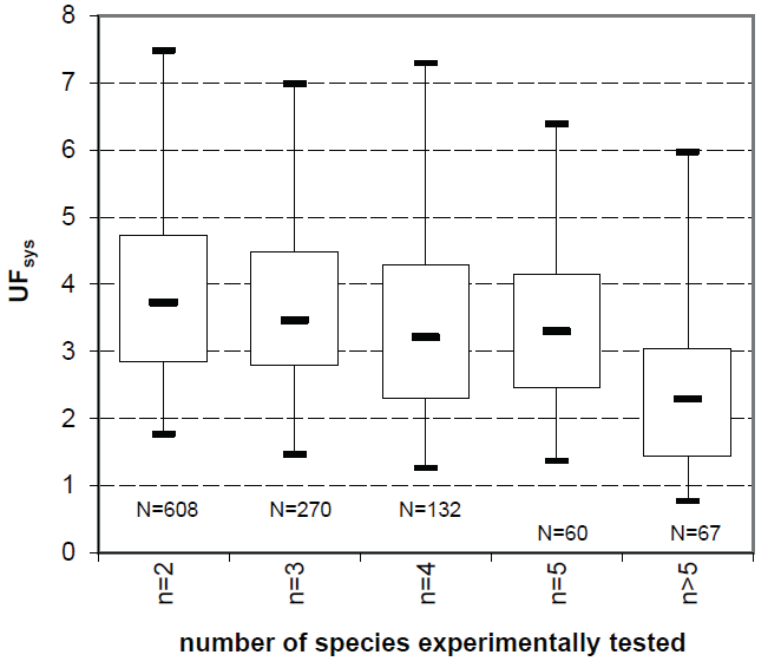

(a)

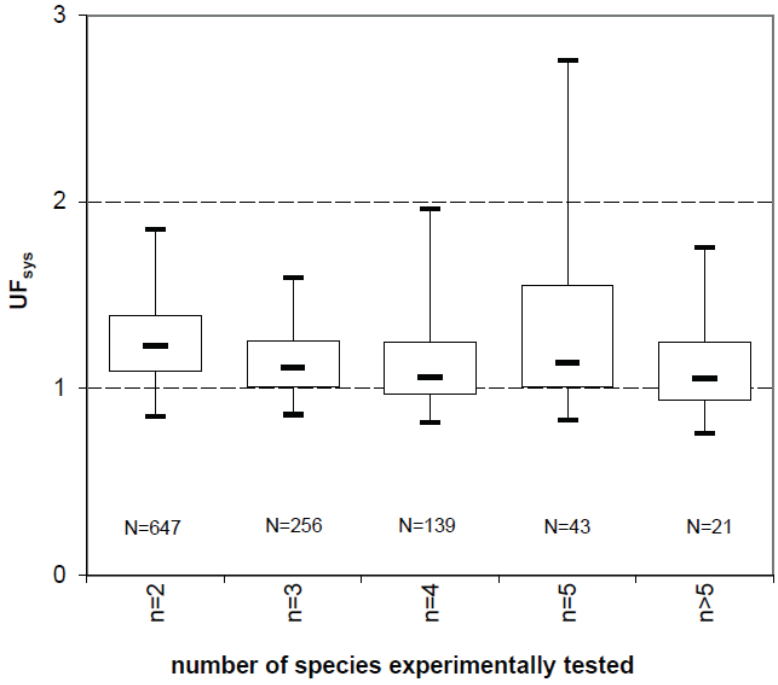

(b)

Figure 4.4.33: Relationship between the number of species for which toxicity was experimentally tested (n) and the systematic uncertainty factor of the HD50 value (UF_{sys} calculated as the ratio of the HD50 value based on experimental data and the HD50 value based on both experimental data and model predictions), for all species (a) and for mammals only (b). The columns represent the 25th and 75th percentile, and the whiskers the 5th and 95th percentiles. In the columns, the median UF_{sys} value is marked. N is the number of chemicals.

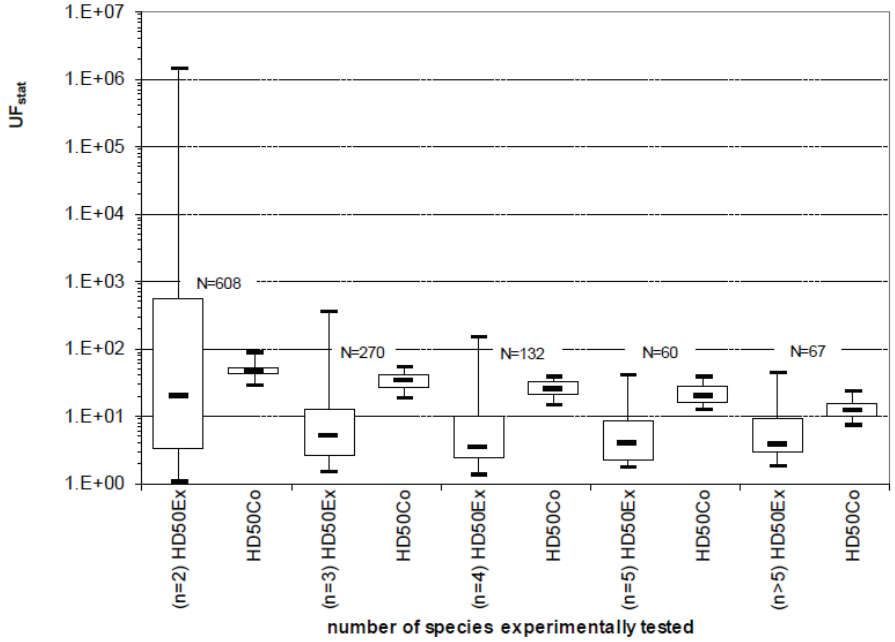

Figure 4.4.34: Box plots of the statistical uncertainty factors of the HD50 values (UF_{stat}) per number of species for which toxicity was experimentally tested (n), for HD50 values based on experimental data ($HD50_{Ex}$) and on both experimental data and model predictions ($HD50_{Co}$). The columns represent the 25th and 75th percentile, and the whiskers the 5th and 95th percentiles. In the columns, the median UF_{stat} value is marked. N is the number of chemicals.

4.4.4. References

Arnot JA, Mackay D, Bonnell M. 2008. Estimating metabolic biotransformation rates in fish from laboratory data. Environmental Toxicology and Chemistry 27(2):341-351.

Arnot JA, Mackay D, Parkerton TF, Zaleski RT, Warren CS. 2010. Multimedia modeling of human exposure to chemical substances: The roles of food web biomagnification and biotransformation. Environmental Toxicology and Chemistry 29(1):45-55.

Asfaw A, Ellersieck MR, Mayer FL. 2003. Interspecies correlation estimations (ICE) for acute toxicity to aquatic organisms and wildlife. II. User manual and software. EPA/600/R-03/106. United States Environmental Protection Agency. Washington, DC.

Canadian Centre for Occupational Health and Safety (CCOHS). 2011. Registry of Toxic Effects of Chemical Substances (RTECS) [Internet]. [cited 2011, July]. Available from: http://ccinfoweb.ccohs.ca/rtecs/search.html.

Golsteijn L, Hendriks HWM, van Zelm R, Ragas AMJ, Huijbregts MAJ. 2012a. Do interspecies correlation estimations increase the reliability of toxicity estimates for wildlife? Ecotoxicology and Environmental Safety Volume 80:238–243.

Golsteijn L, Van Zelm R, Veltman K, Musters G, Hendriks AJ, Huijbregts MAJ. 2012b. Including ecotoxic impacts on warm-blooded predators in life cycle impact assessment. Integrated Environmental Assessment and Management 8(2):372–378.

Hendriks AJ, Traas TP, Huijbregts MAJ. 2005. Critical body residues linked to octanol-water partitioning, organism composition, and LC50 QSARs: Meta-analysis and model. Environmental Science & Technology 39(9):3226-3236.

Hendriks AJ, Van der Linde A, Cornelissen G, Sijm D. 2001. The power of size. 1. Rate constants and equilibrium ratios for accumulation of organic substances related to octanol-water partition ratio and species weight. Environmental Toxicology and Chemistry 20(7):1399-1420.

Mendenhall W, Beaver RJ. 1994. Introduction to probability and statistics.: Duxbury Press, Belmont, California, USA.

Raimondo S, Vivian DN, Barron MG. 2010. Web-based Interspecies Correlation Estimates (Web-ICE) for acute toxicity: user manual. Version 3.1. EPA/600/R-10/004. Office of Research and Development, U.S. Environmental Protection Agency. Gulf Breeze, FL.

Roelofs W, Huijbregts MAJ, Jager T, Ragas AMJ. 2003. Prediction of ecological no-effect concentrations for initial risk assessment: Combining substance-specific data and database information. Environmental Toxicology and Chemistry 22(6):1387-1393.

Van Zelm R, Huijbregts MAJ, Van de Meent D. 2009. USES-LCA 2.0-a global nested multi-media fate, exposure, and effects model. The International Journal of Life Cycle Assessment 14(3):282-284.

Veltman K, McKone TE, Huijbregts MAJ, Hendriks AJ. 2009. Bioaccumulation potential of air contaminants: Combining biological allometry, chemical equilibrium and mass-balances to predict accumulation of air pollutants in various mammals. Toxicology and Applied Pharmacology 238(1):47-55.

5. Appendices (supporting information)

5.1. Appendix for section 2 Terrestrial ecotoxicity of metal emissions

5.1.1. Location and properties of soils

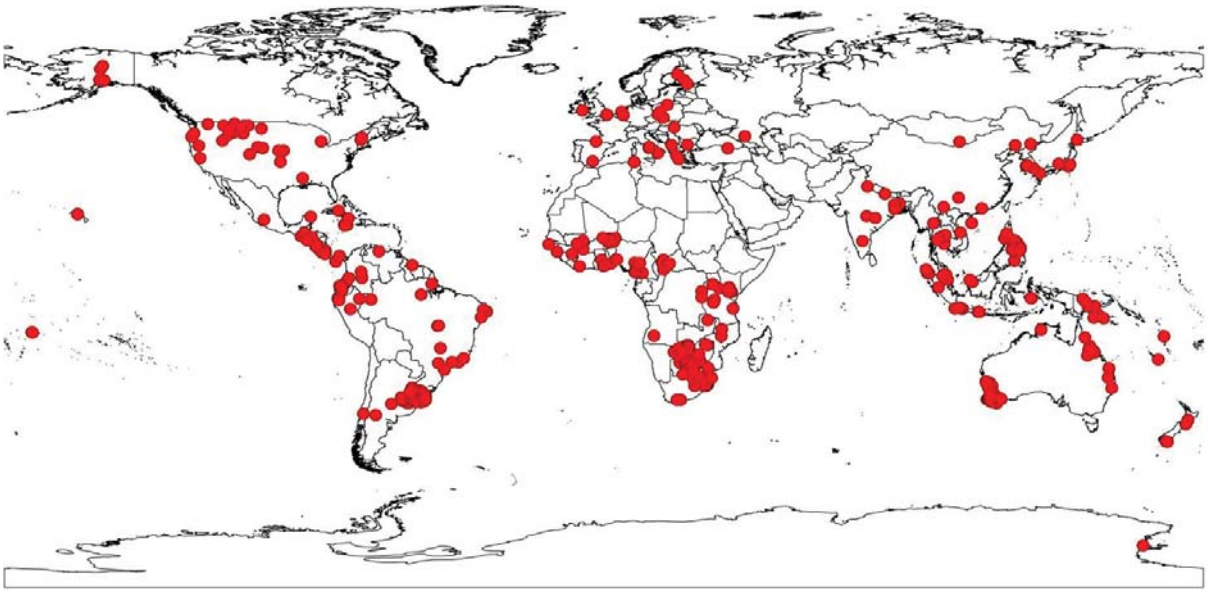

Figure S2.1: Red dots indicate location of 747 soils within the whole set of 760 soils employed for calculating CTPs.

Table S2.1: Parameter ranges over 760 soils employed for calculating CTPs. The soils were selected from the ISRIC-WISE database (version 3.1) (Batjes 2006; Batjes 2009) based on the availability of parameters required in modeling, as described in the main text. Calculation of ionic composition of soil pore water

Parameter	Definition	Unit	Range (min – max)	Median	Source
pH	pH, measured in water	-	3.5 – 9.0	5.7	(Batjes 2006)
ORGC	Organic carbon content	%	0.02 – 38	1.6	(Batjes 2006)
CLAY	Clay content	% (w/w)	1 – 82	21	(Batjes 2006)
SAND	Sand content	% (w/w)	1 – 98	49	(Batjes 2006)
SILT	Silt content	% (w/w)	1 – 81	22	(Batjes 2006)
CEC	Cation exchange capacity	$cmol_c/kg$	1 – 159	14.5	(Batjes 2006)
BSAT	Base saturation	%	1 – 100	74	(Batjes 2006)
EXCA	Exchangeable calcium	$cmol_c/kg$	0.1 – 78	5.9	(Batjes 2006)
EXMG	Exchangeable magnesium	$cmol_c/kg$	0.1 – 35	1.8	(Batjes 2006)
EXNA	Exchangeable sodium	$cmol_c/kg$	0.01 – 19	0.2	(Batjes 2006)
EXK	Exchangeable potassium	$cmol_c/kg$	0.01 – 6.8	0.4	(Batjes 2006)
β_{CaX2}	Fraction of the exchanger sites occupied by Ca^{2+}	-	0.027 – 0.98	0.67	(Batjes 2006)
β_{MgX2}	Fraction of the exchanger sites occupied by Mg^{2+}	-	0.0062 – 0.71	0.22	(Batjes 2006)
β_{NaX}	Fraction of the exchanger sites occupied by Na^{+}	-	0.0012 – 0.64	0.026	(Batjes 2006)
β_{KX}	Fraction of the exchanger sites occupied by K^{+}	-	0.0024 – 0.45	0.05	(Batjes 2006)
ECP	Electrical conductivity of saturation paste extract [1)]	dS/m	0.04 – 11	0.1	(Batjes 2006)
$CaCO_3$	Calcium carbonate content	%	0 – 0	0	(Batjes 2006)
ρ_b	Bulk soil density [2)]	kg/l	0.76 – 1.61	1.36	(Batjes 2008)
θ_w	Volumetric water content	l/l	0.2 – 0.2	0.2	assumed

$FeAl_{ox}$	Sum of amorphous Fe and Al (hydr)oxides	mmol/kg	89 – 89	89	assumed
IS	Effective ionic strength of soil pore water	mol/l	1.1e-3 – 4e-1	6.5e-3	calculated
f_{mono}	Activity coefficient for monovalent cations in soil pore water	-	0.73 – 0.96	0.92	calculated
f_{di}	Activity coefficient for divalent cations in soil pore water	-	0.28 – 0.86	0.71	calculated
ECW	Electrical conductivity of soil pore water	dS/m	0.088 – 31	0.5	calculated
$[Ca^{2+}]$	Calcium concentration in soil pore water in soil pore water	mol/l	4.2e-7 – 5.7e-2	7.4e-4	calculated
$[Mg^{2+}]$	Magnesium concentration in soil pore water	mol/l	6e-8 – 7.5e-2	3.8e-4	calculated
$[Na^{+}]$	Sodium concentration in soil pore water	mol/l	1.5e-4 – 9e-2	1.8e-3	calculated
$[K^{+}]$	Potassium concentration in soil pore water	mol/l	1.5e-5 – 3.4e-2	6.6e-4	calculated
DOC	Dissolved organic carbon	mg/l	0.2 – 1008	36	calculated

1) several methods are used to measure soil electrical conductivity; the values provided here are normalized to the electrical conductivity in the saturation paste extract (ECP), as described later

2) derived by location-specific sampling (nearest neighbor) from the ISRIC-WISE derived soil properties on a 5 by 5 arc-minutes global grid (version 1.2) (Batjes 2012). For the 13 soils missing coordinates, the ρ_b was assumed equal to 1.38 kg/l.

5.1.2. Calculation of Ionic Composition of Soil Pore Water

In order for TBLMs to predict activities of metals ions in pore water resulting in toxic response, activities of base cations in the soil pore water must to be known. These are derived using data on soil electrical conductivity and exchangeable cations by means of cation exchange modeling.

Electrical conductivity of soil pore water. Several methods are used to measure soil electrical conductivity, which include measurements in saturated soil paste, or in soil solutions at various soil to water ratios. To estimate electrical conductivity of the soil pore water, values in the WISE3 database were normalized to electrical conductivity in saturated paste extracts (ECE), following the approach of (Sonmez et al. 2008). Later, electrical conductivity in the soil pore water (ECW) was calculated with the formula given by (Corwin and Lesch 2003):

$$ECW = \left(\frac{ECE \cdot \rho_b \cdot SP}{100 \cdot \theta_w} \right) \qquad \textbf{S2.1}$$

Where SP (%) is the saturation percentage; θ_w is the soil water content (l/l) and ρ_b is the bulk soil density (kg/l). The SP is related to the mechanical constituents of a soil (Stiven and Khan 1966):

$$SP = 578.72 - 4.54 \cdot CLAY - 5.40 \cdot SILT - 5.56 \cdot SAND \qquad \textbf{S2.2}$$

Due to the lack of measured data on soil moisture, and the variability of this parameter over time (which is difficult to take into account in a hazard ranking or life cycle impact assessment) the θ_w was assumed to be constant and equal to 0.2 l/l. When better data on soil moisture become available, this parameter can be implemented to derive more correct estimates of pore water electrical conductivity.

Cation exchange equilibria. Cation exchange was modeled following the Gaines-Thomas convention for exchange equilibria (Gaines and Thomas 1953; Vulava et al. 2000). In this convention, the activity of the exchanger-bound cation is assumed to equal the charge fraction of

the cation in the exchanger. The approach similar to that presented in Matschonat et al. (2003) was applied, with three exchange reactions for the four major cations:

$$NaX + K^+ \longleftrightarrow KX + Na^+ \quad \textbf{S2.3}$$

$$2NaX + Mg^{2+} \longleftrightarrow MgX_2 + 2Na^+ \quad \textbf{S2.4}$$

$$2NaX + Ca^{2+} \longleftrightarrow CaX_2 + 2Na^+ \quad \textbf{S2.5}$$

where X is a surface site of charge equal -1. The equilibrium constant for the exchange of Na^+ with Ca^{2+} is:

$$K^{GT}_{Na/Ca} = \frac{\beta_{CaX_2} [Na^+]^2}{\beta^2_{NaX} [Ca^{2+}]} \quad \textbf{S2.6}$$

The sorbed fraction of a cation, here shown for Ca^{2+}, is:

$$\beta_{CaX_2} = \frac{EXCA}{CEC} \quad \textbf{S2.7}$$

where the total concentration of exchanger sites X, equal to the cation exchange capacity, is:

$$CEC = EXCA + EXMG + EXNA + EXK \quad \textbf{S2.8}$$

In addition to eq S2.6, two other equilibrium reactions can be formed for the remaining cations. In practice, soil can contain exchangeable protons or aluminum (so called, soil acidity), which contribute to total CEC. Out of the selected 1,419 soils, most of them are saturated mainly with base cations (median 92%), although in some cases the contribution of total acidity to CEC is high. These soils were not excluded from the modeling, but the fraction of adsorbed base cations is normalized to base saturation. The activity of cations in pore water, here presented for Ca^{2+}, is:

$$[Ca^{2+}] = f_{di} [Ca^{2+}] \quad \textbf{S2.9}$$

where f_{di} is the activity coefficient for a divalent cation, and square bracket indicate molar concentrations (mol/l). The activity coefficient for each cation was calculated with the modified Debye-Hückel equation proposed by Davies (1962):

$$\log_{10} f_i = -0.512 z_i^2 \left[\frac{IS^{0.5}}{1 + IS^{0.5}} - 0.3IS \right] \quad \textbf{S2.10}$$

where f_i is the activity coefficient for the ion i; z_i is the electric charge of the ion i; and IS is the effective ionic strength of soil pore water (mol/l). The IS was estimated from the relationship between electrical conductivity and ionic strength given by Griffin and Jurinak (1973). The relationship has been developed for river waters and soil extracts and we assume that it is valid for soil pore water:

$$IS = c_1 \cdot ECW \quad \textbf{S2.11}$$

where c_1=0.0113. Equation S2.6 was coupled with equilibrium reactions for K^+ and Mg^{2+}, resulting in three independent equations with four variables. The missing information on solution cations was obtained from the empirical relationship between concentration of base cations and the electrical conductivity (Rowell 1994):

$$2[Ca^{2+}] + 2[Mg^{2+}] + [Na^+] + [K^+] = c_2 \cdot ECW \quad \textbf{S2.12}$$

where c_2=0.01.

Selectivity coefficients. Selectivity coefficients for cation exchange (K^{GT}) depend on exchanger composition and are usually derived from experimental data. It has been shown that they are within the same order of magnitude for different soils (Robbins and Carter 1983). Very recently, empirical methods to model K^{GT} values as a function of exchanger composition and ionic strength have been proposed, but these are available only for a few clay systems (Tournassat et al. 2009; Tournassat et al. 2007). Due to the lack of measured values for the 1,419 soil profiles, default values of selectivity coefficient from the llnl.dat (Lawrence Livermore National Laboratory) database of the PHREEQC are used (Table S2.2) (Parkhurst and Appelo 1999). The sensitivity and uncertainty of the calculated CTPs to the K^{GT} values are discussed later.

Table S2.2: Gaines-Thomas selectivity coefficients for cation exchange reactions used in this study, from the llnl.dat database of the PHREEQC (Parkhurst and Appelo 1999).

Selectivity coefficient, $\log_{10}(K^{GT}_{Na/Me})$		
Ca^{2+}	Mg^{2+}	K^+
0.8	0.6	0.7

5.1.3. Review and Selection of Empirical Regression Models

Recall, that the following criteria (listed in order of increasing priority) were applied to select empirical regression models:

(i) models with lower standard errors of estimate in soils outside the parameter range for which they were developed were preferred
(ii) models with lower standard errors of estimate in soils within the parameter range for which they were developed were preferred
(iii) models developed using soils spanning a wide range of environmental properties (pH, the content of organic carbon and total metal) were preferred
(iv) models developed using a large number of soils were preferred

Empirical Regression Models for Calculating K_d values. Several studies provide empirical regression models for calculating K_d values or total dissolved metal (Table S3). Table S3 shows that the majority of models have been developed for European soils spanning considerably wide range of properties, albeit very alkaline soils were rarely included. The regressions developed by

Groenenberg et al. (2012) (eq S2.13 and S2.14) were chosen because they have been validated for large and independent set of soils, some of which were outside parameter range (pH 2-12) in which they were developed. The models of Groenenberg et al. utilize information on both soil organic carbon and dissolved organic carbon, which is important in case of metals like Cu with high affinity to organic ligands. They predict total dissolved metal from reactive metal (calculated as described in the following paragraph). K_d values were derived from the calculated total dissolved metal and total metal in the solid phase. Parameter units for the models of Groenenberg et al. are given in Table S2.3.

$$\log_{10}(Cu_{total\ dissolved}) = -3.74 + 0.60 \cdot \log_{10}(Cu_{reactive}) - 0.28 \cdot \log_{10}(OM) - 0.79 \cdot \log_{10}(AlFe_{ox}) + 0.79 \cdot \log_{10}(DOC) \quad \text{S2.13}$$

$$\log_{10}(Ni_{total\ dissolved}) = -1.95 + 0.80 \cdot \log_{10}(Ni_{reactive}) - 0.77 \cdot \log_{10}(OM) - 0.17 \cdot \log_{10}(CLAY) + 0.63 \cdot \log_{10}(DOC) - 0.25 \cdot pH \quad \text{S2.14}$$

The DOC was calculated using empirical regression developed by Römkens et al. (2004) (eq S2.15). The regression (standard error of estimate, se = 0.3) was developed using a set of 49 Dutch soils spanning relatively wide ranges of pH (1.9 – 7.9) and organic carbon content (0.2 – 73.4%).

$$\log_{10}(DOC) = 2.25 + 0.75 \cdot \log_{10}(OM) - 0.20 \cdot pH - 0.30 \cdot \log_{10}(ECW) \quad \text{S2.15}$$

where DOC (mg/l) is the dissolved organic carbon, and OM (%) is the soil organic matter content. It was assumed that the OM contains 50% of organic carbon (ORGC). The median (range) DOC calculated for our set of 760 soils equal to 36 (0.2 – 1008) mg/l is within range of DOC measured in various soils(Groenenberg et al. 2012) (0.64 – 1966 mg/l), and is relatively close to median values leached from topsoils of grasslands (7 mg/l), croplands (13 mg/l) and forests (24 mg/l) (Kindler et al. 2011). We consider these predictions as sufficiently accurate to include them for calculating concentration of total dissolved metal, and thereafter the K_d values.

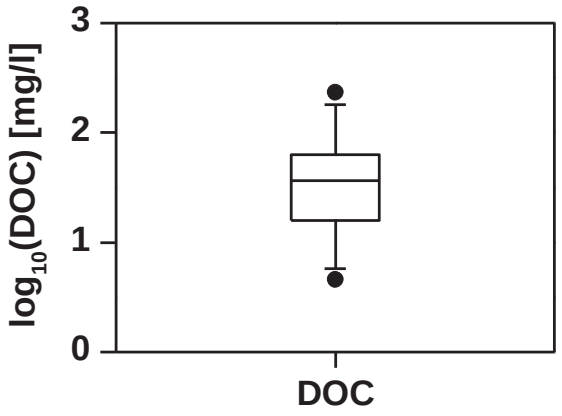

Figure S2.2:. Concentration of dissolved organic carbon (DOC) in 760 soils calculated using eq S2.15. Boxes with bars indicate the 5th, 25th, 50th, 75th and 95th percentiles; black dots indicate the 2.5th and 97.5th percentiles of the calculated values.

Empirical Regressions Models for Calculating Accessibility Factors. The model of Rodrigues et al. (2010b) developed for a set of 136 Portuguese soils, and that of Römkens et al. (2004) developed for the Dutch set of 49 soils were employed for calculating the reactive metal content, and thereafter the AFs for Ni and Cu, respectively (eq S2.16 and S2.17). In contrast to the Dutch set, the Portuguese one does not include soils with high content of organic carbon. Total metal concentration of Cu is representative for Europe and North America, but concentrations of total Ni are in the lower range of measured values (Lado et al. 2008; Shacklette and Boerngen 1984). Little is known about the performance of these models in other soils than those in which they were developed. Their applicability to our soils is discussed in the main text. Parameter units for these models are given in Table S2.4.

$$\log_{10}(Cu_{reactive}) = -0.331 + 0.023 \cdot \log_{10}(OM) + 0.171 \cdot \log_{10}(CLAY) + 1.152 \cdot \log_{10}(Cu_{total}) \quad \textbf{S2.16}$$

$$\log_{10}(Ni_{reactive}) = -1.9 + 0.84 \cdot \log_{10}(Ni_{total}) + 0.14 \cdot pH + 0.42 \cdot \log_{10}(RGC) \quad \textbf{S2.17}$$

Empirical Regression Models for Calculating Bioavailability Factors. Two studies developed empirical regression models for calculating free ion activity from reactive metal. The models of Groenenberg et al. (2010) (eq S2.18 and S2.19) were chosen because they have been validated for an independent, large set of soils. Parameter units for these models are given in Table S2.5.

$$\log_{10}(Cu_{free}) = 0.48 + 0.81 \cdot \log_{10}(Cu_{reactive}) + 0.89 \cdot \log_{10}(OM) - 1.00 \cdot pH \quad \textbf{S2.18}$$

$$\log_{10}(Ni_{free}) = -0.98 + 0.74 \cdot \log_{10}(Ni_{reactive}) + 0.51 \cdot \log_{10}(OM) - 0.42 \cdot pH \quad \textbf{S2.19}$$

The predictions of the free ion fraction of total dissolved metal (FI), estimated using empirical regression models (eq S2.13 - S2.19) for each of the 760 soils, are shown in Fig. S2.3. Their accuracy is discussed in the main text.

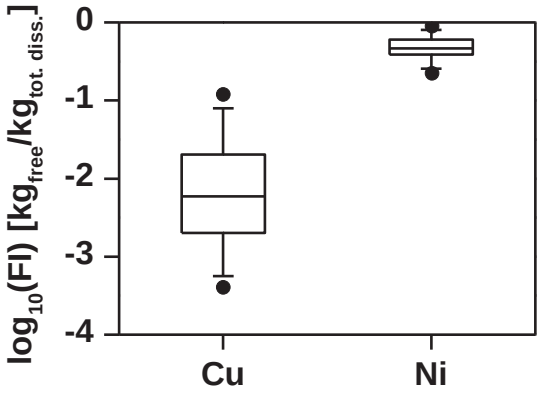

Figure S2.3: Free Cu^{2+} and Ni^{2+} fractions (FI) of total dissolved metal in 760 soils calculated using eq S2.18 - S2.19 (for free ion) and eq S2.13 - S2.14 (for total dissolved metal). Equations S2.15 and S2.16-S2.17 were employed to calculate DOC and reactive metal, respectively. Boxes with bars indicate the 5th, 25th, 50th, 75th and 95th percentiles; black dots indicate the 2.5th and 97.5th percentiles of the calculated values.

Table S2.3: Empirical regression models for calculating K_d values (based on total dissolved metal) or concentration of total dissolved Cu and Ni. Different extractants are used to extract total the total dissolved metal (sometimes referred to as the available metal (Rodrigues et al. 2010a; Romkens et al. 2009)). The type of extractant is shown for comparison, but is not a criterion for model selection. We assume that all models predict total dissolved metal including the free ions, inorganic and organic complexes, and metal bound to colloids in soil pore water. If several models in the same study were provided, only those based on variables which are available for our set of 760 soils were included.

Reference and regression model	Property ranges of soils used to develop regressions			Number, country of origin, and standard error of estimate (se) for soils used to develop regressions (A)	Number, country of origin and standard error of estimate (se) for independent set of soils used to validate regressions		Extractants for total dissolved metal
	pH	ORGC [%]	M_{total} [mg/kg]		within property range	outside property range	
Groenenberg et al. 2012: $\log_{10}(Cu_{total\ dissolved}) = -3.74 + 0.60 \cdot \log_{10}(Cu_{reactive}) + 0.28 \cdot \log_{10}(OM) - 0.79 \cdot \log_{10}(AlFe_{ox}) + 0.79 \cdot \log_{10}(DOC)$ $\log_{10}(Ni_{total\ dissolved}) = -1.95 + 0.80 \cdot \log_{10}(Ni_{reactive}) + 0.77 \cdot \log_{10}(OM) - 0.17 \cdot \log_{10}(CLAY) + 0.63 \cdot \log_{10}(DOC) + 0.25 \cdot pH$ The units are: [mol/L] and [mol/kg] for total dissolved and reactive metal, respectively; [%] for organic matter (OM); [mmol/kg] for $AlFe_{ox}$; [%] for CLAY; and [mg/L] for DOC.	3.7-7.3	0.5-36	Cu: 0.1-326 Ni: 0.4-64.5	118 (NL) Cu: se=0.42 Ni: se=0.40	115 (NL, PT) Cu: se=~0.35 (B) Ni: se=~0.45 (B)	8 (NL, PT) Cu: se=~1.6 (B) Ni: se =~1.1 (B)	0.002 and 0.01 M $CaCl_2$; 0.002, 0.003 and 0.01 M $Ca(NO_3)_2$; extraction of soil pore water
Rodrigues et al. 2010a: $\log_{10}(Ni_{total\ dissolved}) = 0.87 \cdot \log_{10}(Ni_{reactive}) + 0.15 \cdot pH - 0.98 \cdot \log_{10}(ORGC)$ $\log_{10}(Ni_{total\ dissolved}) = 0.56 + 0.56 \cdot \log_{10}(Ni_{reactive}) + 0.18 \cdot pH - 0.84 \cdot \log_{10}(ORGC)$ The units are: [µg/L] and [mg/kg] for total dissolved and reactive metal, respectively; and [%] for ORGC.	3.1-7.0	1.1-5.3	Cu: 7.4-7635 Ni: 4.5-45	136 (PT) Cu: se=0.39 Ni: se=0.27	not done	not done	0.01 M $CaCl_2$
Degryse et al. 2009: $\log_{10}(K_d^{Cu}) = 0.6 + 0.37 \cdot pH$ $\log_{10}(K_d^{Ni}) = 0.99 + 0.30 \cdot pH$ The K_d [L/kg] values are based on total metal.	Cu: 3.09-8.77 (C) Ni: 3.09-7.7 (C)	Cu: 0.2-32.3 (C) Ni: 0.1-33.1 (C)	0.6-326 (C)	Cu: 129 (NL, BE, DE) se=no data Ni: 63 (NL, BE, DE, F, GB, DK, SE, IT, GR, ES) se= not reported	not done	not done	Cu: 0.01 M $CaCl_2$; extraction of soil pore water (C) Ni: 0.01 M $CaCl_2$ (C)
Römkens et al. 2004: $\log_{10}(Cu_{total\ dissolved}) = 0.86 \cdot \log_{10}(Cu_{reactive}) + 0.57 \cdot \log_{10}(ORGC) - 0.09 \cdot pH - 0.33 \cdot \log_{10}(CLAY) + 0.53 \cdot \log_{10}(DOC)$ $\log_{10}(Ni_{total\ dissolved}) = 2.78 + 0.91 \cdot \log_{10}(Ni_{reactive}) + 0.68 \cdot \log_{10}(ORGC) - 0.4 \cdot pH - 0.22 \cdot \log_{10}(CLAY) + 0.28 \cdot \log_{10}(DOC)$ The units are: [µg/L] and [mg/kg] for total dissolved and reactive metal, respectively; [%] for ORGC; [%] for CLAY; and [mg/L] for DOC.	1.8-7.9	0.2-73.4	Cu: 0.2-305 Ni: 0.02-20.5	49 (NL) (D) Cu: se=0.43 Ni: se=0.39	not done	not done	0.002 and 0.01 M $CaCl_2$; 0.002, 0.003 and 0.01 M $Ca(NO_3)_2$; water

Sauvé et al. 2000: $\log_{10}(Cu_{total}) = 0.21 \cdot pH + 0.51 \cdot \log_{10}(ORGC) + 1.75$ The K_d [L/kg] values are based on total metal. The unit is [%] for ORGC.	Cu: ~2.7-8.8 (B) Ni: ~3.4-8.7(B)	not reported	Cu: ~10-10000 (B) Ni: ~1-100(B)	Cu: 353 (origin not reported) se=0.55 Ni: 69 (origin not reported) se=0.61	not done	not done	water or neutral salts; extraction of soil pore water
Elzinga et al. 1999 (model 1): $\log_{10}(Cu_{total\ solid}) = -0.775 + 0.567 \cdot \log_{10}(Cu_{total\ dissolved}) + 0.445 \cdot \log_{10}(CEC) + 0.225 \cdot pH - 0.625 \cdot \log_{10}(SR)$ The $Cu_{total\ solid}$ [mg/kg] is the total sorbed metal; and SSR [g/mL] is the solid:solution ratio. The units are: [mg/L] for $Cu_{total\ dissolved}$; and [$mmol_c$/kg] for CEC.	2.8-8.4	0.1-15.8	0.2-10000 mg/kg	408 (origin not reported) se= not reported	20 (NL) se=no data	not done	not reported
Janssen et al. 1997: $\log_{10}(K_d^{Cu}) = 0.15 \cdot pH + 0.45 \cdot \log_{10}(Fe_{ox}) - 0.71 \cdot \log_{10}(DOC) + 1.33$ $\log_{10}(K_d^{Ni}) = 0.17 \cdot pH + 0.84 \cdot \log_{10}(OM) - 0.84 \cdot \log_{10}(DOC) + 1.95$ The K_d [L/kg] values are based on total metal. The units are: [mmol/kg] for amorphous Fe (hydr)oxides (Fe_{ox}); [mmol/L] for DOC; and [%] for organic matter (OM).	3.8-7.9	2-21.8	Cu: 1.3-110 Ni: 0.6-48	20 (NL) Cu: se=0.31 Ni: se=0.22	16 (NL, UK) Cu: se=0.47 Ni: se=0.33	not done	0.1 M $CaCl_2$
Anderson and Christensen 1989: $\log_{10}(K_d^{Ni}) = 0.529 \cdot pH + 0.291 \cdot \log_{10}(Mn_{ox}) + 0.339 \cdot \log_{10}(ORGC) + 0.597 \cdot \log_{10}(Fe_d)$ The K_d [L/kg] values are based on total metal. Mn_{ox} [mg Mn/g] is the amorphous Mn; Fe_d [mg Fe/g] is the sum of amorphous and crystalline (dithionite-extractable) Fe. The unit is: [mg/g] for ORGC.	4.6-7.3	0.17-2.3	not reported	38 (DK) se= not reported	not done	not done	extraction of soil pore water

(A) ISO country codes (NL=The Netherlands, PT=Portugal, BE=Belgium, DE=Germany, FR=France, GB=United Kingdom DK=Denmark, SE=Sweden, IT=Italy, GR=Greece, ES=Spain)
(B) values estimated from the figures in the original reference
(C) data from Smolders et al. (2000) were not included due to no access to the original report
(D) some soils were sampled at various horizon depths, resulting in 69 sam)les

Table S2.4: Empirical regression models for calculating concentration of reactive Cu and Ni.

Reference and regression model	Property ranges of soils used to develop regressions			Number, country of origin, and standard error of estimate (se) for soils used to develop regressions (A)	Number, country of origin and standard error of estimate (se) for independent set of soils used to validate regressions		Extractants for reactive metal
	pH	ORGC [%]	M_{total} [mg/kg]		within property ranges	outside property ranges	
Rodrigues et al. 2010b: $\log_{10}(Cu_{reactive}) = -0.74 + 0.94 \cdot \log_{10}(Cu_{total}) + 0.45 \cdot \log_{10}(ORGC)$ $\log_{10}(Ni_{reactive}) = -1.9 + 0.84 \cdot \log_{10}(Ni_{total}) + 0.14 \cdot pH + 0.42 \cdot \log_{10}(ORGC)$ The units are: [mg/kg] for total and reactive metal, respectively; and [%] for ORGC.	3.1-7.0	1.1-5.3	Cu: 7.4-7635 Ni: 4.5-45	136 (PT) se= not reported	not done	not done	0.43 M HNO_3
Römkens et al. 2004: $\log_{10}(Cu_{reactive}) = -0.331 + 0.023 \cdot \log_{10}(OM) - 0.171 \cdot \log_{10}(CLAY) + 1.152 \cdot \log_{10}(Cu_{total})$ The units are: [mg/kg] for reactive and total metal; [%] for organic matter (OM); and [%] for	1.8-7.9	0.2-73.4	Cu: 0.2-305	49 (NL) (B) se=0.13	not done	not done	A.43 HNO_3

CLAY.							

A) ISO country code (PT=Portugal, NL=The Netherlands)
B) some soils were sampled at various horizon depths, resulting in 69 samples

Table S2.5: Empirical regression models for calculating free ion activity of Cu and Ni. The type of extractant, and method used to derive activity of free ion are shown for comparison, but are not a criterion for model selection.

Reference and regression model	Property ranges of soils used to develop regressions			Number, country of origin, and standard error of estimate (se) for soils used to develop regressions (A)	Number, country of origin and standard error of estimate (se) for independent set of soils used to validate regressions		Extractants for total dissolved metal and free ion
	pH	ORGC [%]	M_{total} [mg/kg]		within property ranges	outside property ranges	
Groenenberg et al. 2010: $\log_{10}(Cu_{free}) = 0.48 + 0.81 \cdot \log_{10}(Cu_{reactive}) - 0.89 \cdot \log_{10}(OM) - 1.00 \cdot pH$ $\log_{10}(Ni_{free}) = -0.98 + 0.74 \cdot \log_{10}(Ni_{reactive}) - 0.51 \cdot \log_{10}(OM) - 0.42 \cdot pH$ The units are: [mol/L] and [mol/kg] for free ion and reactive metal, respectively; and [%] for organic matter (OM).	3.7-8.3	1-48.9	Cu: 0.1-326 Ni: 0.4-64.5	216 (NL, UK) Cu: se=0.65 Ni: se=0.33	Cu: 626 (UK, CL,CN, AU, US, CA, DK, NL, HU, RU, FR, CH) se=1.1 (B) se=0.75 (C) Ni: 131 (UK, NL, RU, DK, CN) se=1.0 (B) se=0.71 (C)	no data (D)	0.002 and 0.01 M $CaCl_2$; 0.002 M $Ca(NO_3)_2$; 0.002 M $Ca(NO_3)_2$+nitric acid; free ion activities measured or calculated
Tye et al. 2004: $\log_{10}\left(\frac{Cu_{total}}{Cu_{free}^{1.307}}\right) = -2.908 + 1.707 \cdot pH - 1.492 \cdot \log_{10}(S)$ $\log_{10}\left(\frac{Ni_{total}}{Ni_{free}^{1.378}}\right) = -3.532 + 1.124 \cdot pH - 2.296 \cdot \log_{10}(S)$ The units are: [mol/L] and [mol/kg of organic carbon] for free ion and total metal, respectively; and [mol/L] for IS.	3.3-7.6	0.8-15.4	Cu: 5.2-4710 Ni: 6.4-502	23 (UK) Cu: se=0.36 Ni: se=0.39	Cu: 113 (CA, US, DK, UK,CL, CN) (E) se=0.47-1.26 (F) Ni: not done	no data (D)	extraction of soil pore water; free ion activities calculated
Elzinga et al. 1999 (model 3): $\log_{10}(Cu_{total\,solid}) = -2.15 + 0.598 \cdot \log_{10}(Cu_{free}) + 0.403 \cdot \log_{10}(CEC) + 0.564 \cdot pH - 0.608 \cdot \log_{10}(SR)$ The $Cu_{total\,solid}$ [mg/kg] is the total sorbed metal; and SSR [g/ml] is the solid:solution ratio. The units are: [mg/l] for Cu_{free}; and [$mmol_c$/kg] for CEC.	2.8-8.4	0.1-15.8	0.2-10000	408 (origin not reported) se= not reported	20 (NL) se= not reported	not done	not reported

(A) ISO country codes (UK=United Kingdom, CL=Chile, CN=China, AU=Australia, US=United States, CA=Canada, DK=Denmark, NL=The Netherlands, HU=Hungary, RU=Russian Federation, FR=France, CH=Switzerland)
(B) based on measured free ion activities
(C) based on calculated free ion activities
(D) some soils in the validation set fall outside property ranges of soils in which the regressions were developed, but no details are available
(E) origin of 23 soils from the whole dataset is unknown
(F) range for three soil sets

5.1.4. Structure, Parameters, and Predictions of Terrestrial Biotic Ligand Models

Structure and Parameters. The biotic ligand model concept is based on a semi-empirical assumption that metal ecotoxicity depends on the amount of metal ion bound to active site in the organism (biotic ligand, BL), while protons and other cations can alleviate metal toxicity by competitive binding to the BL (Paquin et al. 2002). The biotic ligand model assumes:

$$R = \frac{100}{1+\left(\frac{f}{f_{50}}\right)^{\beta}} \qquad \textbf{S2.20}$$

where R is biological response as % of the control; f is the fraction of the total BL sites occupied by the divalent free metal ion M^{2+}; f_{50} is the fraction of the total BL sites occupied by M^{2+} at which a 50% response is observed; and β is the shape parameter. The f depends on the binding affinity of M^{2+} to the BL and the presence and binding affinity of competing cations:

$$f = \frac{K_{MBL}\{M^{2+}\}}{1+K_{MBL}\{M^{2+}\}+\sum K_{XBL}\{X^{z+}\}} \qquad \textbf{S2.21}$$

where K_{MBL} is the conditional binding constant of metal M^{2+} to the BL, K_{XBL} is the conditional binding constant of cation X^{z+} binding to the BL; $\{M^{2+}\}$ is the free metal ion activity in the pore water solution; and $\{X^{z+}\}$ is the activity of the respective cation in the solution. The binding constants, f_{50} and β are determined from experimental data, and are listed in Table S2.6 for the TBLMs employed in this study.

$$\{M^{2+}\}_{EC50} = \frac{f_{50}}{(1-f_{50})K_{MBL}}\left(1+\sum K_{XBL}\{X^{z+}\}\right) \qquad \textbf{S2.22}$$

Table S2.6: Parameters of TBLMs used in modeling ecotoxicity of Cu and Ni. All models are from Thakali et al. (2006b) Values in brackets are standard errors (± values).

Metal	Organism	Toxic endpoint	TBLM parameters, $\log_{10}(K_{XBL})$ (X-cation; BL-biotic ligand)						
			f_{50}	β	{Me}	$\{H^+\}$	$\{Ca^{2+}\}$	$\{Mg^{2+}\}$	$\{Na^+\}$
Cu	barley (*Hordeum vulgare* cv. Regina)	BRE: root elongation, 4-d EC50	0.05	0.96 (0.11)	7.41 (0.23)	6.48 (0.26)	-	-	-
Cu	tomato (*Lycopersicon esculentum* cv. Moneymaker)	TSY: shoot yield, 21-d EC50	0.05	1.11 (0.16)	5.65 (0.10)	4.38 (0.21)	-	-	-
Cu	redworm (*Eisenia fetida*)	FJP: juvenile production, 4-w EC50 chronic	0.05	0.70 (0.08)	4.62 (0.12)	2.97 (0.62)	-	-	-
Cu	springtail (*Folsomia candida*)	ECP: cocoon production, 4-w EC50 chronic	0.05	1.14 (0.15)	6.50 (0.25)	5.9 (0.29)	-	-	-
Cu	soil microbes	GIR: glucose induced respiration, 7-d EC50	0.05	0.58 (0.07)	6.69 (0.10)	7.5 1)	-	-	-
Cu	soil microbes	PNR: potential nitrification rate, 7-d EC50	0.05	0.78 (0.13)	4.93 (0.48)	4.45 (0.58)	-	1.64 (5.80)	-
Ni	barley (*Hordeum vulgare* cv. Regina)	BRE: root elongation, 4-d EC50	0.05	2.37 (0.33)	3.6 (0.53)	4.53 (0.62)	1.5 1)	3.81 (0.60)	-
Ni	tomato (*Lycopersicon esculentum* cv. Moneymaker)	TSY: shoot yield, 21-d EC50	0.05	2.65 (0.54)	6.05 (0.15)	6.52 (0.18)	5.0 1)	5.23 (0.47)	-
Ni	redworm (*Eisenia fetida*)	FJP: juvenile production, 4-w EC50 chronic	0.05	1.52 (0.26)	5.12 (0.06)	6.02 (0.22)	-	5.0	-

Ni	springtail (*Folsomia candida*)	ECP: cocoon production, 4-w EC50 chronic	0.05	2.18 (0.35)	5.33 (0.05)	6.70 (0.12)	-	5.0	-
Ni	soil microbes	GIR: glucose induced respiration, 7-d EC50	0.05	0.99 (0.15)	4.53 (0.10)	6.09 (0.21)	-	5.0	-
Ni	soil microbes	PNR: potential nitrification rate, 7-d EC50	0.05	1.63 (0.22)	5.72 (0.06)	5.10 (4.05)	-	5.0	-

1) fixed values, see Thakali et al. (2006b)

EC50 values. By employing eq S2.22 for the TBLMs listed in Table S2.6 the activities of free metal ion activity causing 50% response in each of the 760 soils, were calculated (Fig S4).

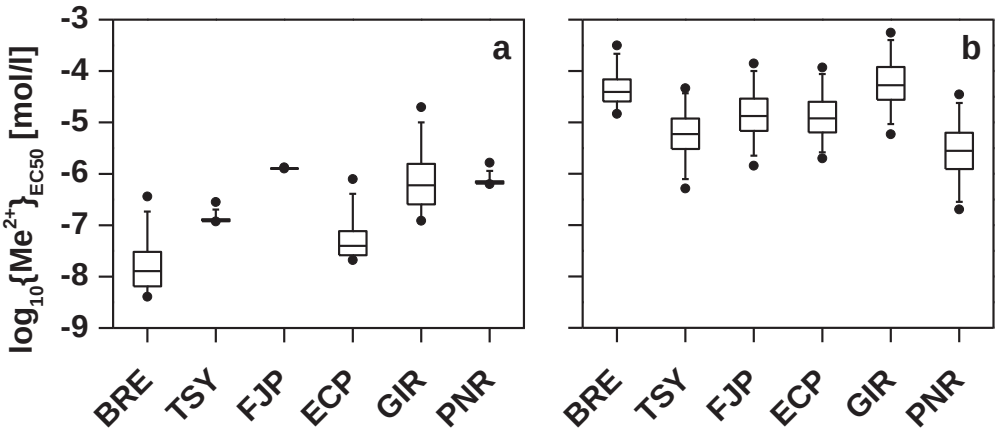

Figure S2.4: Activities of Cu^{2+} and Ni^{2+} corresponding to EC50 values of Cu (a, left) and Ni (b, right) in 760 soils predicted by TBLMs listed in Table S2.6 for six biological endpoints: barley root elongation (BRE); tomato shoot yield (TSY); F. candida juvenile production (FJP); E. fetida cocoon production (ECP); glucose induced respiration (GIR); and potential nitrification rate (PNR). Boxes with bars indicate the 5th, 25th, 50th, 75th and 95th percentiles; black dots indicate the 2.5th and 97.5th percentiles of the calculated values.

Comparison with Published Terrestrial Effect Data. Species sensitivity distributions (SSD) constructed from the TBLM-derived EC50 values for each of our 760 soils were compared with SSDs derived from species effect data from ecotoxicity experiments retrieved from the ECOTOX database (version 4.0) (U.S. Environmental Protection Agency 2012). The following criteria were applied for inclusion of experimental data: (i) they must be derived from experiments with soils freshly spiked with soluble metal salts; (ii) they must be derived from experiments lasting for at least 14 days; (iii) they must be derived from experiments performed in soils. This resulted in a total of 166 and 18 effect data for Cu and Ni, respectively. Note that in the experiments all metal forms are assumed to be 100% reactive. In reality, reactivity of Cu and Ni applied as soluble salts can decrease within one month by up to ~10 and ~20%, respectively (Buekers et al. 2008b). To allow for a direct comparison, our free ion based EC50 values were recalculated to be based on reactive metal, employing the empirical regression model of Groenenberg et al. (2010) for the K_f relation (where K_f is defined as the ratio between the concentration of reactive metal in the solid phase and the free metal ions; eq 6 and Table 7 in Groenenberg et al.). The comparison shows that even though non-alkaline soils dominate our dataset, and there are differences in species included in SSDs (no effect data for microbial endpoints for Cu, while worms are the

dominating species for Ni), in many cases SSDs fall within the 95% confidence interval for the experimental SSD (Fig. S2.5). We consider these predictions as reasonable and sufficiently accurate to employ our EFs for calculating CTPs.

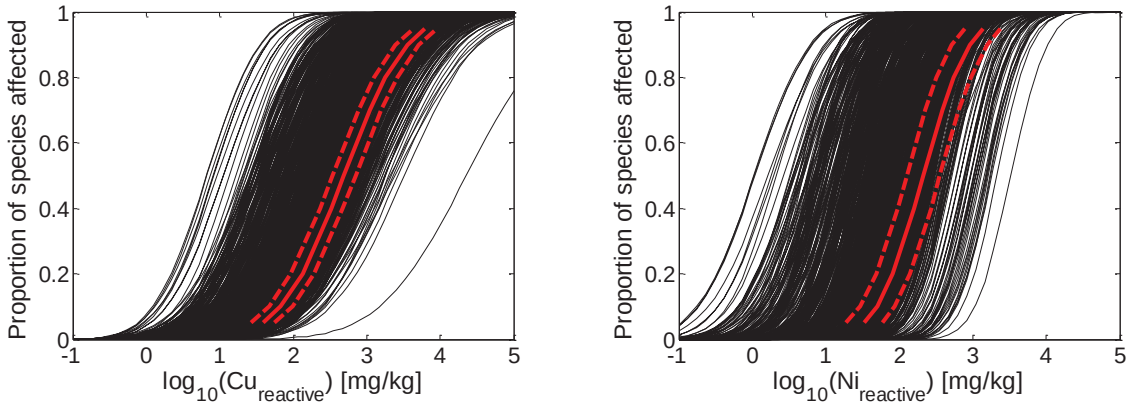

Figure S2.5: Chronic species sensitivity distributions (SSD) for Cu (left) and Ni (right) constructed from the TBLM-derived EC50 values for each of our 760 soils (black lines), and SSDs derived from species effect data from ecotoxicity experiments retrieved from the ECOTOX database (version 4.0) for 166 (Cu) and 18 (Ni) effect data (red lines). The red dashed lines indicate 95% confidence intervals for the SSD generated for organisms used in ecotoxicity experiments. It is assumed that all metal in ecotoxicity experiments with soils freshly spiked with soluble salts was reactive.

5.1.5. Correlation between K_d values and Fate Factors

Fate factors are related to K_d values due to the control of this parameter on metal removal processes in the USEtox model, i.e. leaching from soil and runoff (Fig. S2.6). At higher K_d values, runoff is dominated by soil erosion, and FFs level off.

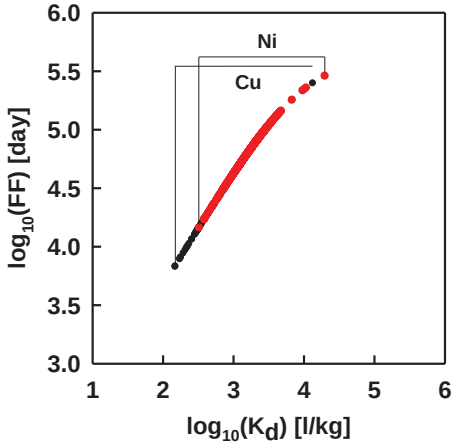

Figure S2.6: Correlation between Kd values and FF for Cu (black) and Ni (red) for 760 soils.

5.1.6. Multiple Linear Regression Analysis

Multiple linear regression (MLR) analysis was done to determine soil properties controlling each model constituent in eq 2.2, and to develop predictive models for calculating CTPs from soil properties (see below and main text). Only those soil parameters which were included in models used to calculate K_d values or concentrations of reactive, total dissolved, and free metal ions (eq S2.13 - S2.19) were selected as independent variables for the stepwise-based method. Some parameters were excluded because they correlate strongly ($r>0.8$) with other soil parameters. The analysis shows that DOC correlates strongly with ORGC, whereas electrical conductivity of soil pore water EWC correlates strongly with both [Mg^{2+}] and [Ca^{2+}]. Thus, concentration of DOC and ECW were excluded from the analyses for the CTP. ECW was however included in the analyses for FFs. Concentration of Mg^{2+} was included because this parameter is an input to TBLMs, whereas concentration of Ca^{2+} was excluded because it correlates strongly with [Mg^{2+}].

Table S2.7: Pearson correlation coefficients (r) between log_{10}-transformed soil parameters. Values in red italics indicate strong correlation (r>0.8).

	pH	log_{10}(ORGC)	log_{10}(DOC)	log_{10}(CLAY)	log_{10}(ECW)	$log_{10}([Mg^{2+}])$	$log_{10}([Ca^{2+}])$
pH	1						
log_{10}(ORGC)	-0.291	1					
log_{10}(DOC)	-0.541	*0.921*	1				
log_{10}(CLAY)	-0.077	0.380	0.273	1			
log_{10}(ECW)	0.104	-0.053	-0.338	0.237	1		
$log_{10}([Mg^{2+}])$	0.161	0.092	-0.183	0.348	*0.809*	1	
$log_{10}(Ca^{2+})$	0.217	0.092	-0.188	0.304	0.773	*0.904*	1

ORGC (%) is the organic carbon content; DOC (mg/l) is the concentration of dissolved organic carbon; CLAY (%) is the clay content; ECW (dS/m) is the electrical conductivity of soil pore water; $[Ca^{2+}]$ (mol/l) is the concentration of magnesium in soil pore water; $[Mg^{2+}]$ (mol/l) is the concentration of calcium in soil pore water.

Soil Properties Controlling Fate Factors. The FFs of Cu are mainly determined by the content of organic carbon (Table S2.8). This parameter controls concentrations of total dissolved metal and DOC, influencing the K_d values (eq S2.13, S2.15 and S2.16). The organic carbon is not a controlling factor of FF for Ni because the effects of this parameter on both the total dissolved and reactive metal compensate each other (eq S2.14 and S2.17). The FF of Ni is mainly determined by soil pH. The inclusion of electrical conductivity of soil pore water and clay content improve predictions of FFs because these parameters affect reactive (eq S2.16) or total dissolved metal (eq S2.13 - S2.15).

$$\log_{10}(FF) = a + b \cdot \log_{10}(ORGC) + c \cdot pH + d \cdot \log_{10}(ECW) + e \cdot \log_{10}(CLAY) \qquad \textbf{S2.23}$$

Table S2.8: Linear regression coefficients, adjusted R^2 values (R^2_{adj}) and standard error of estimate (se) of regression equations for log_{10}(FF) of Cu and Ni. Values in brackets indicate standard error for each parameter. The analysis was done using parameters for the whole set of 760 soils.

Metal	a intercept	b log_{10}(ORGC)	c pH	d log_{10}(ECW)	e log_{10}(CLAY)	R^2_{adj}	se
Cu	4.633 (0.005)	-0.322 (0.01)	x	x	x	0.577	0.14
	4.681 (0.004)	-0.311 (0.007)	x	0.256 (0.008)	x	0.811	0.093
	3.872 (0.014)	-0.261 (0.003)	0.142 (0.002)	0.236 (0.004)	x	0.966	0.039
	3.754 (0.004)	-0.294 (0.001)	0.141 (0.001)	0.209 (0.001)	0.097 (0.001)	0.997	0.011
Ni	3.540 (0.032)	x	0.229 (0.006)	x	x	0.684	0.096
	3.651 (0.020)	x	0.216 (0.003)	0.191 (0.005)	x	0.884	0.058
	3.430 (0.008)	x	0.225 (0.001)	0.156 (0.002)	0.130 (0.002)	0.985	0.021
	3.453 (0.005)	-0.034 (0.001)	0.218 (0.001)	0.151 (0.001)	0.145 (0.001)	0.993	0.014

ORGC (%) is the organic carbon content; CLAY (%) is the clay content; x indicates that the variable did not pass stepping method criteria (p<0.05 for entry, and p>0.1 for removal); all coefficients are significant at p<0.001.

Soil Properties Controlling Accessibility Factors. The AFs for both metals are controlled mainly by clay and soil organic carbon (Table S2.9), consistently with models used for calculating reactive metal (eq S2.16 and S2.17).

$$\log_{10}(AF) = a + b \cdot \log_{10}(ORGC) + c \cdot pH + d \cdot \log_{10}(CLAY) \qquad \text{S2.24}$$

Table S2.9: Linear regression coefficients, adjusted R^2 values (R^2_{adj}) and standard error of estimate (se) of regression equations for $\log_{10}$(AF) of Cu and Ni. Values in brackets indicate standard error. The analysis was done using parameters for the whole set of 760 soils.

Metal	a intercept	b $\log_{10}$(ORGC)	c pH	d $\log_{10}$(CLAY)	R^2_{adj}	se
Cu	-0.159 (0.001)	x	NA	-0.161 (0.001)	0.977	0.011
	-0.150 (<0.001)	0.023 (<0.001)	NA	-0.171 (<0.001)	1.0	1.7e-9
Ni	-1.295 (0.003)	0.370 (0.006)	x	NA	0.833	0.083
	-2.093 (<0.001)	0.420 (<0.001)	0.140 (<0.001)	NA	1.0	0e-15

ORGC (%) is the organic carbon content; x indicates that the variable did not pass stepping method criteria (p<0.05 for entry, and p>0.1 for removal); NA indicates that the variable was not included in the analysis; all coefficients are significant at p<0.001.

Soil Properties Controlling Bioavailability Factors. The pH and soil organic carbon control the BFs for both Cu and Ni (Table S2.10). These parameters are input to models for calculating reactive metal content and free metal ion concentration (eq S2.18 and S2.19).

$$\log_{10}(BF) = a + b \cdot pH + c \cdot \log_{10}(ORGC) + d \cdot \log_{10}(CLAY) \qquad \text{S2.25}$$

Table S2.10: Linear regression coefficients, adjusted R^2 values (R^2_{adj}) and standard error of estimate (se) of regression equations for $\log_{10}$(BF) of Cu and Ni. Values in brackets indicate standard error. The analysis was done using parameters for the whole set of 760 soils.

Metal	a intercept	b pH	c $\log_{10}$(ORGC)	d $\log_{10}$(CLAY)	R^2_{adj}	se
Cu	-1.064 (0.137)	-0.807 (0.024)	x	x	0.597	0.41
	0.183 (0.019)	-1.007 (0.003)	-0.848 (0.004)	x	0.993	0.053
	0.155 (0.019)	-1.008 (0.003)	-0.857 (0.004)	0.027 (0.005)	0.994	0.052
Ni	-3.096 (0.011)	x	-0.417 (0.020)	NA	0.357	0.28
	-0.449 (0.018)	-0.465 (0.003)	-0.583 (0.004)	NA	0.978	0.052

ORGC (%) is the organic carbon content; x indicates that the variable did not pass stepping method criteria (p<0.05 for entry, and p>0.1 for removal); NA indicates that the variable was not included in the analysis; all coefficients are significant at p<0.001;

Soil Properties Controlling Effect Factors. The EF of Cu is controlled by pH because protons are the main cations competing with Cu^{2+} for binding to biotic ligands. In addition to protons, the toxicity of Ni^{2+} is alleviated mainly by Mg^{2+}.

Table S2.11: Linear regression coefficients, adjusted R^2 values (R^2_{adj}) and standard error of estimate (se) of regression equations for $\log_{10}$(EF) of Cu and Ni. Values in brackets indicate standard error. The analysis was done using parameters for the full set of 760 soils.

Metal	a intercept	b pH	c $\log_{10}([Mg^{2+}])$	R^2_{adj}	se
Cu	2.055 (0.021)	0.448 (0.004)	x	0.951	0.063
Ni	0.924 (0.037)	x	-0.535 (0.010)	0.780	0.22
	-0.401 (0.069)	0.217 (0.010)	-0.563 (0.008)	0.862	0.17

$[Mg^{2+}]$ (mol/l) is the concentration of magnesium in soil pore water; x indicates that the variable did not pass stepping method criteria ($p<0.05$ for entry, and $p>0.1$ for removal); all coefficients are significant at $p<0.001$.

5.1.7. Statistical Distribution of Comparative Toxicity Potentials

Goodness-of-fit tests (Anderson-Darling, Chi-square and Kolmogorov-Smirnov) for CTPs of Cu and Ni were performed for all continuous distribution types available in Crystal Ball, v. 7.2 (Oracle Corporation, Redwood Shores, CA), that is, normal, triangular, uniform, lognormal, beta, gamma, Weibull, max extreme, min extreme, logistic, Student's t, exponential, and Pareto. Results show that CTPs of Cu and Ni are distributed lognormally (Table S2.12).

Table S2.12: Descriptive statistics and results of goodness of fit tests (Anderson-Darling, Chi-square and Kolmogorov-Smirnov) for non-transformed CTPs calculated for 760 soils. Geometric standard deviation was normalized by N, where N=760.

Metal	Geometric mean	Geometric standard deviation	Results of goodness-of-fit tests		
			Anderson-Darling	Chi-square	Kolmogorov-Smirnov
Cu	1541	3.71	lognormal; A^2=1.72	lognormal; X^2=58.18	lognormal; D=0.04
Ni	1639	2.69	lognormal; A^2=0.78	lognormal; X^2=30.4	lognormal; D=0.03

5.1.8. Uncertain Model Parameters

Several model parameters were assumed constant during modeling CTPs. Below, details are given on the sensitivity analysis for two of these assumptions.

Selectivity Coefficients for Cation Exchange. First, we perturbed Gaines-Thomas selectivity coefficients (K^{GT}) for cation exchange for individual cation exchange reactions to be in lower and higher range of typical values for clay soils (that is, $\log_{10}(K^{GT})$ equal to 0.25 and 0.89; 0.22 and 0.73; 0.45 and 1.22 for Na/Ca, Na/Mg and Na/K, respectively, Fig. S2.7) (Tournassat et al. 2009). The sensitivity of the CTPs to the K^{GT} values was then analyzed. We also assessed model performance using two sets of K^{GT} values perturbed simultaneously for all three cation exchange reactions. Again, two sets typical for clay soils were used (Fig. S2.7 and Table S2.13) (Tournassat et al. 2009). In these two cases computation of the normalized sensitivity coefficients was not possible because the perturbation of each of the K^{GT} values varied between reactions. The model sensitivity was

analyzed however on a CTP level by comparing calculated median CTP with median CTP in the base scenario. Results are discussed in the main text.

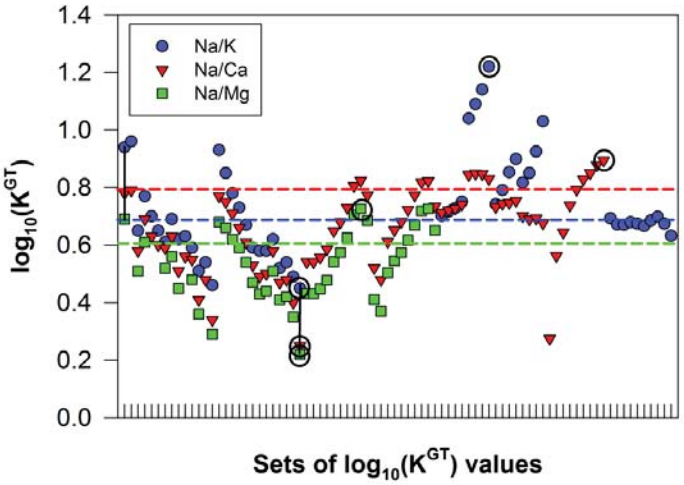

Figure S2.7: Ranges of log_{10}-transformed Gaines-Thomas selectivity coefficients for cation exchange (K^{GT}) in clay soils. All 82 sets given in Tournassat et al. (2009) are shown, but in some cases the full set of three K^{GT} values was not available. Dashed horizontal lines indicate default K^{GT} values for cation exchange used in the base scenario. Black circles indicate values used in the sensitivity analysis with perturbation of single K^{GT} values. These values are reported in Fig. 2.3. Black vertical lines indicate the two sets used in the analysis with simultaneous perturbation of all three K^{GT} values. The values for these two sets are reported in Table S2.13.

Table S2.13: Two sets of Gaines-Thomas selectivity coefficients (K^{GT}) for cation exchange reactions (Na/Ca, Na/Mg and Na/K) in lower and higher range for clay soils.

Selectivity coefficient, $\log_{10}(K^{GT}_{Na/Me})$			
	Ca^{2+}	Mg^{2+}	K^{+}
Set 1	0.77	0.68	0.93
Set 2	0.25	0.22	0.45

Background Metal Content. The sensitivity of CTPs to background metal content was analyzed using a subset of 24 European soils. Location-specific background metal content was retrieved by coordinate specific sampling (nearest neighbor) from Lado et al. (2008) who estimated background metal on a 5 × 5 km grid (Fig. S2.8). Results are discussed in the main text.

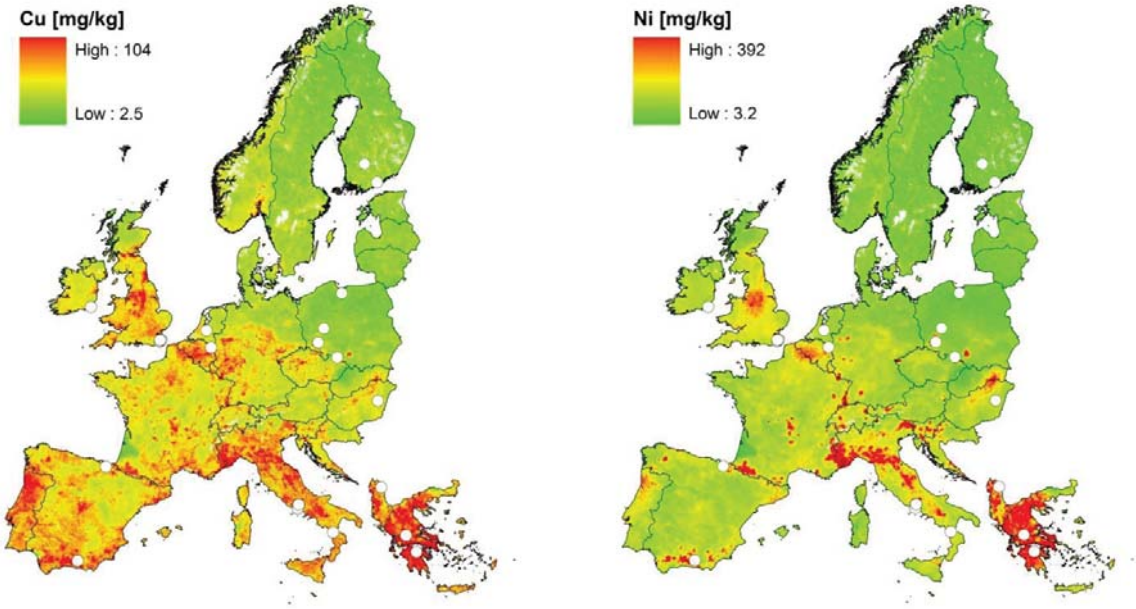

Figure S2.8: White dots indicate locations of 24 European soils selected from the set of 747 soils for which geographical references were available. Note that scales are different for the two metals. One soil located at the coast of Finland was excluded because it falls outside the area covered by the grid.

5.1.9. Accessible fraction in relation to contamination age

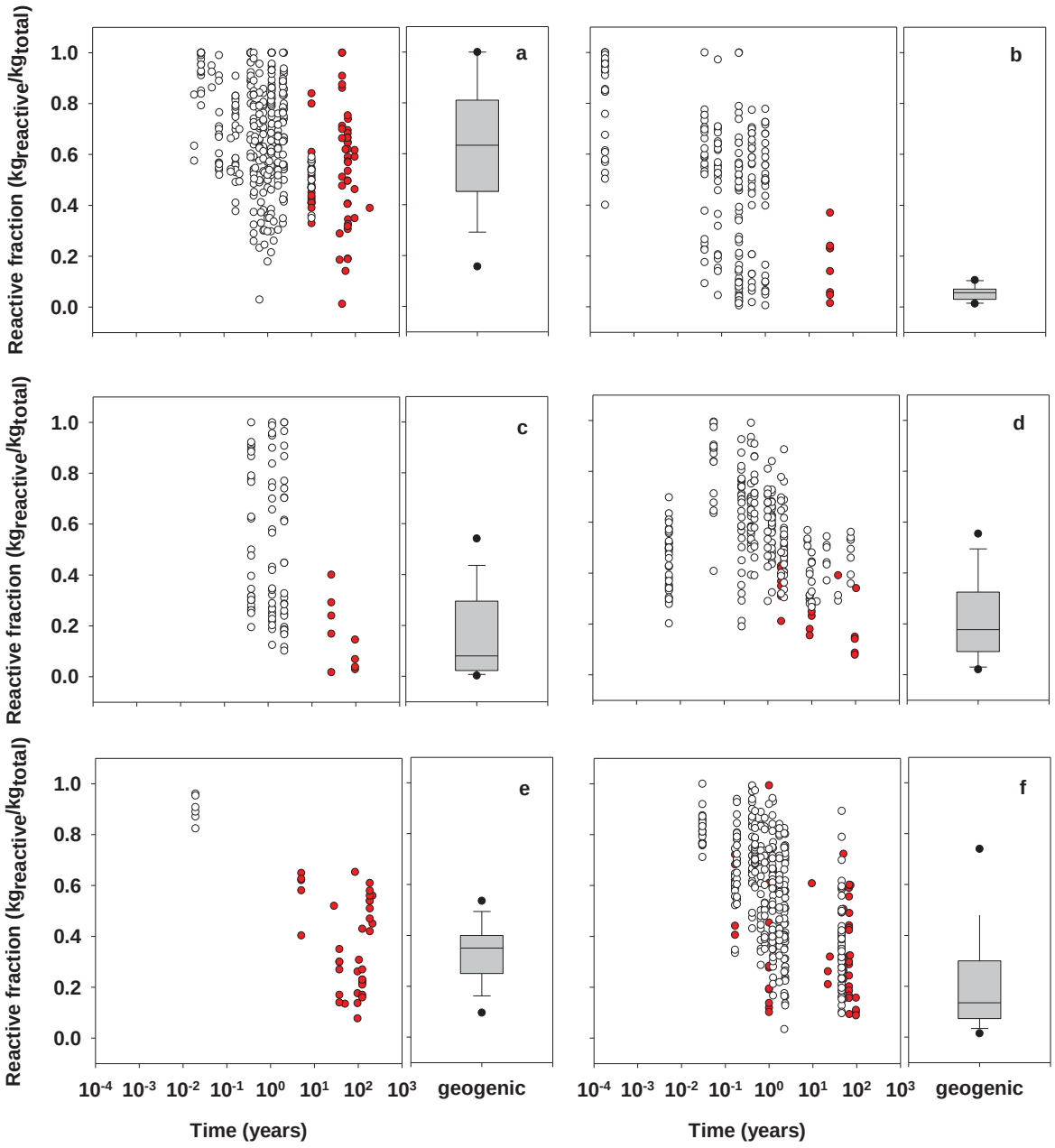

Figure S2.9: Reactive fraction of Cd (a), Co (b), Cu (c), Ni (d), Pb (e), and Zn (f) measured in soils contaminated with readily soluble (hollow circles), solid (red circles) and geogenic (box plots) metals. Boxes with bars indicate the 10th, 25th, 50th, 75th, and 90th percentiles; black dots indicate 5th and 95th percentiles of the measured values.

5.1.10. Additional Results on the Influence of Metal Accessibility Soil Properties

Table S2.14: Model, number of measured data (n), linear regression coefficients, adjusted R^2 values ($R2_{adj}$), and standard error of estimate (se) of regression equations for $log^{10}(C_{reactive})$ of geogenic, anthropogenic, and combined anthropogenic and geogenic forms of Cd, Co, Cu, Ni, Pb, and Zn (eq 2.10).

Metal	Contamination type	Model	n	a (intercept)	b $log_{10}(C_{total})$	c $pH(H_2O)$	d $log_{10}(ORGC)$	e $log_{10}(CLAY)$	d $log_{10}(CEC)$	e $log_{10}(Fe_{ox})$	f $log_{10}(Fe_d)$	R^2_{adj}	se
Cd	solid (airborne, organic, mining, industrial, and various)	*m3*	98	0.24	0.82	x	x [n=65]	x [n=29]	x [n=29]	NA	NA	0.87	0.29
		m4	19	-0.20	0.94	NA	NA	NA	NA	-0.24	NA	0.94	0.08
	geogenic and solid (airborne, organic, mining, industrial, and various)	*m5*	177	-0.31	0.85	x	x	x [n=63]	x [n=88]	x [n=40]	NA	0.90	0.32
		m6	177	0.31	0.88	-0.09	x	x [n=63]	x [n=88]	x [n=40]	NA	0.91	0.31
		m7	131	0.17	0.89	-0.09	0.18	x [n=63]	x [n=88]	x [n=40]	NA	0.88	0.32
Co	solid (airborne)	*m10*	8	-1.98	1.78	x	x	x	NA	NA	NA	0.84	0.34
		m11	8	-1.54	1.43	x	0.44	x	NA	NA	NA	0.92	0.24
		m12	8	-1.98	1.56	x	x	x	0.66	NA	NA	0.94	0.21
	geogenic and solid (airborne)	*m13*	28	-1.93	1.69	x	x	x	NA	NA	NA	0.79	0.30
		m14	28	-0.94	1.63	-0.15	x	x	NA	NA	NA	0.82	0.28
		m15	28	-0.63	1.61	-0.22	0.39	x	NA	NA	NA	0.87	0.24
Cu	solid (airborne, organic, mining and industrial waste)	*m18*	18	-0.38	0.87	x	x	x [n=14]	NA	NA	NA	0.81	0.19
	geogenic and solid (airborne, organic, mining, and industrial)	*m19*	121	-0.97	1.10	x	see [n=115]	x [n=84]	NA	NA	NA	0.61	0.49
		m20	121	-0.32	1.07	-0.09	see [n=115]	x [n=84]	NA	NA	NA	0.63	0.48
		m21	115	-0.98	1.10	x	x	x [n=84]	NA	NA	NA	0.66	0.45
		m22	115	-0.92	1.03	x	0.21	x [n=84]	NA	NA	NA	0.67	0.44
Ni	solid (airborne, and industrial)	*m27*	19	-1.11	0.97	NA	x	x [15]	NA	NA	NA	0.70	0.61
	geogenic and solid (airborne, and industrial)	*m28*	87	-0.74	0.81	x	x	see [n=52]	NA	NA	NA	0.57	0.66
		m29	87	-0.86	0.76	x	0.67	see [n=52]	NA	NA	NA	0.64	0.60
		m30	52	0.76	0.55	x	0.82	-0.73	NA	NA	NA	0.46	0.65
Pb	solid (airborne, organic, mining, industrial, and various)	*m33*	49	-0.40	0.95	x	x	NA	NA	see [n=26]	NA	0.83	0.24
		m34	49	0.00	1.06	-1.04	x	NA	NA	see [n=26]	NA	0.88	0.21
		m35	26	0.23	1.24	-0.26	x	NA	NA	-0.59	NA	0.94	0.08
	geogenic and solid (airborne, organic, mining, industrial, and various)	*m36*	70	-0.43	0.96	x	x	NA	NA	see [n=46]	NA	0.83	0.23
		m37	70	0.00	1.05	-0.09	x	NA	NA	see [n=46]	NA	0.87	0.20
		m38	46	-0.46	1.11	-0.23	x	NA	NA	-0.45	NA	0.90	0.11
Zn	solid (airborne, organic, oxide, and tire debris)	*m42*	58	-0.48	0.99	x	x	NA	x	x [n=40]	NA	0.90	0.26
	geogenic and solid (airborne, organic, oxide, and	*m43*	137	-1.06	1.15	x	x	see [n=81]	NA	NA	NA	0.71	0.54

	tire debris)	*m44*	137	-0.39	1.19	-0.13	x	see [n=81]	NA	NA	NA	0.73	0.53
		m45	123	-0.43	1.06	-0.08	0.30	see [n=81]	NA	NA	NA	0.85	0.36
		m46	81	-0.69	1.13	x	0.52	-0.39	NA	NA	NA	0.86	0.36

NA indicates that the variable parameter was not included in the analysis; x indicates that the variable did not pass stepping method criteria ($p<0.05$ for entry, and $p>0.1$ for removal); C_{total} (mg/kg) is the concentration of total metal in soil; $pH(H_2O)$ is soil pH measured in water; ORGC (%) is the organic carbon content; CLAY (%) is the clay content; CEC ($mmol_c/kg$) is cation exchange capacity; Fe_{ox} (g/kg) is the content of amorphous, oxalate-extractable Fe (hydr)oxides; Fe_d (g/kg) is the content of the sum of amorphous and crystalline, dithionite-extractable Fe (hydr)oxides. Fe_{ox} (g/kg) is the content of amorphous, oxalate-extractable Fe (hydr)oxides; Fe_d (g/kg) is the content of the sum of amorphous and crystalline, dithionite-extractable Fe (hydr)oxides; Al_{ox} (g/kg) is the content of amorphous, oxalate-extractable Al (hydr)oxides; and Mn_{ox} (g/kg) is the content of amorphous, oxalate-extractable Mn (hydr)oxides. All coefficients are significant at the probability level $p<0.001$.

5.1.11. Review of Published Aging Models

Table S2.15: Published aging models developed using soils spiked with soluble salts.

Model ID	Reference and model	Reactive fraction at equilibrium and reaction kinetics	Major model properties	Major soil properties and aging period	Method used to measure reactive metal
a	Crout et al. (2006): $Cd_{reactive}(t) = \left[f_{AC,eq}\left(1 - f_{AC,eq}\right)\exp\left(K \cdot t\right)\right] Cd_{total}$ where Cdreactive (mg(kg) is the concentration of reactive metal in soil; Cdtotal (mg(kg) is the concentration of total metal in soil; fAC,eq (kgreactive/kgtotal) is the reactive fraction at equilibrium; K (day-1) is the equilibrium rate constant; and t (day) is time	$f_{AC,eq} = 1.28 - 0.122 \cdot pH_{H_2O}$ $K = 0.025 day^{-1}$	First-order kinetics for exchange between accessible and non-accessible metal pools assumed	Soils: 23; mainly from the UK (A) pH: 3.3 – 7.6 ORGC: 0.6 – 4 % Metal source: soluble salts Aging: ~800 days	isotope dilution with the radioisotopes 109Cd and 65Zn
b	$Zn_{reactive}(t) = \left[f_{AC,eq}\left(1 - f_{AC,eq}\right)\exp\left(K \cdot t\right)\right] Zn_{total}$	$f_{AC,eq} = 1.37 - 0.146 \cdot pH_{H_2O}$ $K = 0.0078 day^{-1}$			
c	$Zn_{reactive}(t) = \left[f_{AC,eq}\left(1 - f_{AC,eq} - f_{NAC,0}\right)\exp\left(K \cdot t\right)\right] Zn_{total}$ where fNAC,0 (kgreactive/kgtotal) is the fraction of metal that is immediately rendered non-reactive.	$f_{AC,eq} = 1.433 - 0.159 \cdot pH_{H_2O}$ $K = 0.0049 day^{-1}$ $f_{NAC,0} = 0.16$			
d	Buekers al. (2008b): $Cd_{reactive}(t) = \left[f_{AC,eq}\left(1 - f_{AC,eq}\right)\exp\left(-t \cdot \frac{1}{T_c}\right)\right] \cdot Cd_{total}$ where Tc (days) is the response time of the reaction (equal to 1/K)	$f_{AC,eq} = 1.24 - 0.11 \cdot pH_{CaCl_2}$ $T_c = 800 days$	Model based on that of Crout et al. (Crout et al. 2006)	Soils: 28; from ES, VN, BE, FR, NL, GR, SE, IT pH: 3.4 – 7.8 ORGC: 0.2 – 23 % Metal source: soluble salts Aging: 850 days	isotope dilution with the radioisotopes 109Cd, 63Ni and 65Zn; and the stable isotope 65Cu
e	$Cu_{reactive}(t) = \left[f_{AC,eq}\left(1 - f_{AC,eq}\right)\exp\left(-t \cdot \frac{1}{T_c}\right)\right] \cdot Cu_{total}$	$f_{AC,eq} = 0.83 - 0.04 \cdot pH_{CaCl_2}$ $T_c = 181 days$			
f	$Ni_{reactive}(t) = \left[f_{AC,eq}\left(1 - f_{AC,eq}\right)\exp\left(-t \cdot \frac{1}{T_c}\right)\right] \cdot Ni_{total}$	$f_{AC,eq} = 1.62 - 0.17 \cdot pH_{CaCl_2}$ $T_c = 124 days$			
g	$Zn_{reactive}(t) = \left[f_{AC,eq}\left(1 - f_{AC,eq}\right)\exp\left(-t \cdot \frac{1}{T_c}\right)\right] \cdot Zn_{total}$	$f_{AC,eq} = 1.6 - 0.2 \cdot pH_{CaCl_2}$ $T_c = 478 days$			
h	Buekers al. (2008b): $Cd_{reactive}(t) = \left[f_{AC,eq}\left(1 - f_{AC,eq}\right)\exp\left(-t \cdot \frac{1}{T_c}\right)\right] \cdot Cd_{total}$	$f_{AC,eq} = f_{AC,eq,ox}\frac{1+K}{1+K \cdot f_{AC,eq,ox}}$ $\log_{10}\left(\frac{1 - f_{AC,eq,ox}}{f_{AC,eq,ox}}\right) = 0.17 - 0.92 \cdot pH_{CaC}$ $T_C = T_{c,ox}\frac{1+K}{1+K \cdot f_{AC,eq,ox}}$	Two-component model predicting metal partitioning between reversible components (humic acid and clay) and the irreversible component (oxyhydroxides); speciation calculations are required to obtain the values of K		

		If no fixation to organic matter: $T_{c,ox} = 595 days$ If immediately 10% fixation to organic matter: $T_{c,ox} = 695 days$ where fAC,eq,ox (kgreactive/kgtotal) is the metal fraction at equilibrium bound to oxyhydroxide; Tc,ox (days) is the response time for reaction of a metal with the oxyhydroxide; K (-) is the relative partitioning of metal between the reversible component and the labile part of the oxyhydroxide			
i	$Ni_{reactive}(t) = \left[f_{AC,eq} \cdot \left(1 - \exp\left(-t \cdot \frac{1}{T_c} \right) \right) \right] \cdot Ni_{total}$	$f_{AC,eq} = f_{AC,eq,ox} \frac{1+K}{1+K \cdot f_{AC,eq,ox}}$ $\log_{10}\left(\frac{1 - f_{AC,eq,ox}}{f_{AC,eq,ox}} \right) = 0.32 - 1.81 \cdot pH_{CaCl_2}$ $T_C = T_{c,ox} \frac{1+K}{1+K \cdot f_{AC,eq,ox}}$ If no fixation to organic matter: $T_{c,ox} = 141 days$ If immediately 10% fixation to organic matter: $T_{c,ox} = 150 days$			
j	$Zn_{reactive}(t) = \left[f_{AC,eq} \cdot \left(1 - \exp\left(-t \cdot \frac{1}{T_c} \right) \right) \right] \cdot Zn_{total}$	$f_{AC,eq} = f_{AC,eq,ox} \frac{1+K}{1+K \cdot f_{AC,eq,ox}}$ $\log_{10}\left(\frac{1 - f_{AC,eq,ox}}{f_{AC,eq,ox}} \right) = 0.39 - 2.1 \cdot pH_{CaCl_2}$ $T_C = T_{c,ox} \frac{1+K}{1+K \cdot f_{AC,eq,ox}}$ If no fixation to organic matter: $T_{c,ox} = 294 days$ If immediately 10% fixation to organic matter: $T_{c,ox} = 313 days$			
k	Ma et al. (2006): $Cu_{reactive}(t) = \left(100 - \frac{89.8}{10^{(7 - pH_{H_2O})} + 1} \cdot t^{\frac{1}{t}} - 4.92 \cdot \ln(t) \right) \cdot 0.01 \cdot Cu_{total}$	Model predicts decrease in concentration of reactive metal until depletion of the reactive metal	Model based on a simplified Elovich equation, with two-stage micropore diffusion. Precipitation/nucleation process is considered to be related to the formation of	Soils: 19; from DE, UK, BE, NL, SE, GR, FR, IT, ES pH: 3.0 – 7.5 ORGC: 0.4 – 23 % Metal source:	isotope dilution with the radioisotope 64Cu

			Cu(OH)+ in clay minerals and Fe oxides in soils.	soluble Cu salt Aging: 180 days	
l	Wendling et al. (2009): $Co_{reactive}(t) = \left(84.1 - \frac{59.1}{10^{6.06 - pH_{H_2O}} + 1} \cdot t^{0.0097} - 3.64 \cdot \ln(\quad)\right) \cdot 0.01 \cdot Co_{total}$	Models predicts a decrease in concentration of reactive metal until depletion of the reactive metal	Model similar to that of Ma et al.	Soils: 14; from AU, BE, CA, DK, GR, FR, IT, UK pH: 4.4 – 8.2 ORGC: not measured Metal source: soluble Co salt Aging: 365 days	isotope dilution with the radioisotope 57Co(II)
m	$Co_{reactive}(t) = \left(83.4 - \frac{64.7}{10^{6.5 - pH_{H_2O}} + 1} \cdot t^{0.013} - 4.65 \cdot \ln(\quad)\right) \cdot 0.01 \cdot Co_{total}$				

(A) ISO country codes (NL=The Netherlands, BE=Belgium, DE=Germany, FR=France, GB=United Kingdom DK=Denmark, SE=Sweden, IT=Italy, GR=Greece, ES=Spain, VN=Vietnam, AU=Australia, CA=Canada, DK=Denmark)

Table S2.16: Published aging models developed using soils contaminated with geogenic and/or anthropogenic, solid-phase metal.

Model ID	Reference and model	Reactive fraction at equilibrium and reaction kinetics	Major model properties	Major soil properties	Method used to measure reactive metal
n	Rodrigues et al. (2010b): The units are: [mg/kg] for total and reactive metal; [%] for ORGC; and [%] for CLAY. $\log_{10}(Cd_{reactive}) = -1.1 + 0.91 \cdot \log_{10}(Cd_{total}) + 0.041 \cdot pH_{CaCl_2} + 0.59 \cdot \log_{10}(ORGC) + 0.17 \cdot \log_{10}(CLAY)$	Models assume equilibrium between reactive and total metal	Several models with more significant variables were developed (A)	Soils: 136; from PT (B) pH: 3.1 – 7.0 ORGC: 1.1 – 5.3 Metal source: both geogenic and anthropogenic contamination, sampled away from any known point-source of contamination, as well as from areas of mining and industrial activities Aging: unknown contamination age	single extraction using 0.43 M HNO_3
o	$\log_{10}(Co_{reactive}) = -1.7 + 1.1 \cdot \log_{10}(Co_{total}) + 0.11 \cdot pH_{CaCl_2} + 0.51 \cdot \log_{10}(ORGC)$				
p	$\log_{10}(Cu_{reactive}) = -0.74 + 0.94 \cdot \log_{10}(Cu_{total}) + 0.45 \cdot \log_{10}(ORGC)$				
q	$\log_{10}(Ni_{reactive}) = -1.9 + 0.84 \cdot \log_{10}(Ni_{total}) + 0.14 \cdot pH + 0.42 \cdot \log_{10}(ORGC)$				
r	$\log_{10}(Pb_{reactive}) = 0.78 \cdot \log_{10}(Pb_{total}) + 0.35 \cdot \log_{10}(ORGC) + 0.23 \cdot \log_{10}(CLAY)$				
s	$\log_{10}(Zn_{reactive}) = -1.9 + 1.1 \cdot \log_{10}(Zn_{total}) + 0.11 \cdot pH_{CaCl_2} + 0.55 \cdot \log_{10}(ORGC)$				
t	Römkens et al. (2004): The units are: [mg/kg] for reactive and total metal; [%] for organic matter (OM); and [%] for CLAY. $\log_{10}(Cd_{reactive}) = -0.089 + 0.022 \cdot \log_{10}(OM) - 0.062 \cdot \log_{10}(CLAY) + 1.075 \cdot \log_{10}(Cd_{total})$	Models assume equilibrium between reactive and total metal		Soils: 49 topsoils an 11 (C) soils sampled at various horizon depth; from NL pH: 1.8 – 7.9 ORGC: 0.2 – 73.4 Metal source: both geogenic and anthropogenic contamination, sampled from areas impacted by smelters, waste material, and contaminated river sediment Aging: unknown contamination age	single extraction using 0.43 M HNO_3
u	$\log_{10}(Cu_{reactive}) = -0.331 + 0.023 \cdot \log_{10}(OM) - 0.171 \cdot \log_{10}(CLAY) + 1.152 \cdot \log_{10}(Cu_{total})$				
v	$\log_{10}(Pb_{reactive}) = -0.263 + 0.031 \cdot \log_{10}(OM) - 0.112 \cdot \log_{10}(CLAY) + 1.089 \cdot \log_{10}(Pb_{total})$				
x	$\log_{10}(Zn_{reactive}) = -0.703 + 0.183 \cdot \log_{10}(OM) - 0.298 \cdot \log_{10}(CLAY) + 1.235 \cdot \log_{10}(Pb_{total})$				

(A) other models of Rodrigues et al. were not included because not all significant variables were available for our dataset
(B) ISO country codes (NL=The Netherlands, PT=Portugal)
(C) some soils were sampled at various horizon depths, resulting in 69 samples for 11 soils

5.1.12. Evaluation of Published Aging Models

Published aging models shown in Tables S2.15 and S2.16 were evaluated against measured data collected in this study, except models *h*, *i*, and *j* for which no information was available about relative partitioning (K values) of a metal between the reversible (humic acid and clay) and the irreversible component (oxyhydroxides) in the soils.

Cadmium. The kinetic models *a* and *d* developed using soils spiked with soluble salts both explain 0.77 of variability in the concentration or reactive Cd in soils contaminated with geogenic metal (Fig. S2.10). The error is however large for two deeper soil horizons formed from calcareous parent materials enriched in geogenic Cd. Both empirical regression models n and t perform worse than the kinetic models *a* and *d*.

For anthropogenically contaminated soils, the kinetic models *a* and *d* perform reasonably well (R2 > 0.85) but they overpredict the concentration of reactive Cd in several soils impacted by mine spoils with high total Cd content (> 100 mg/kg), and in one soil impacted by smelter in which Cd concentration was relatively high (50 mg/kg). Note, that for the models *a* and *d* we assumed that reactive Cd was in equilibrium with total Cd even when contaminant age could not be estimated. (the models *a* and *d* predict that equilibrium will be reached at times scales of months to years). The regression model *t* consistently overpredicts the concentration of reactive Cd across all anthropogenic contaminant types. The performance of the regression model *n* is better as compared with that of the model *t*, but worse as compared with that of the kinetic models *a* and *d*. Given that for both regression models concentration of reactive Cd was measured using single extraction with 0.43 M HNO_3, the difference can be attributed to the fact that the model *t* does not consider the effects of soil pH. Soil pH is an important parameter determining Cd reactivity in soils (ref). Overall, our comparison suggests that across all contamination types, reactive Cd is in equilibrium with total Cd. They also suggest that large part of the variability in concentration of reactive Cd can be explained from total metal content, considering the effects of soil pH, except of soils impacted with relatively high (> 50 mg/kg) total concentrations of Cd.

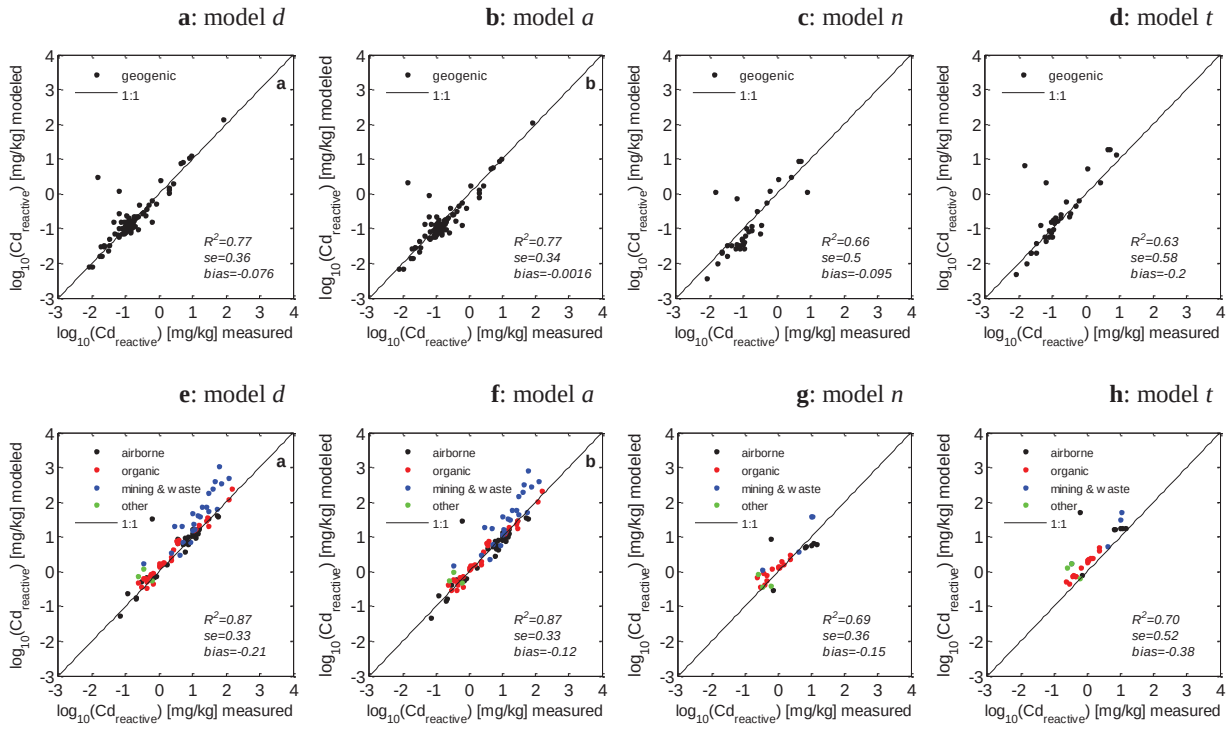

Figure S2.10: Comparison of measured and model predicted concentration of reactive Cd as influenced by contaminant type. Models are shown in Tables S2.15 and S2.16. A perfect agreement between model and measured values would result in alignment of the data points on the first diagonal (1:1 line).

Cobalt. The kinetic models *l* and *m* developed for soluble Co in many cases overpredict concentration of reactive Co in soils contaminated with geogenic metals (Fig S2.11). Here, we assumed contamination age equal to 10 or 500 years. In alkaline soils, the kinetic model *l* underpredicts the size of reactive Co pool, but also allows for negative values to be calculated. Concentration of reactive geogenic Co is also overpredicted by the empirical regression model *o*. By contrast, the models *l*, *m* and *o* successfully predict concentration of reactive, airborne Co, except

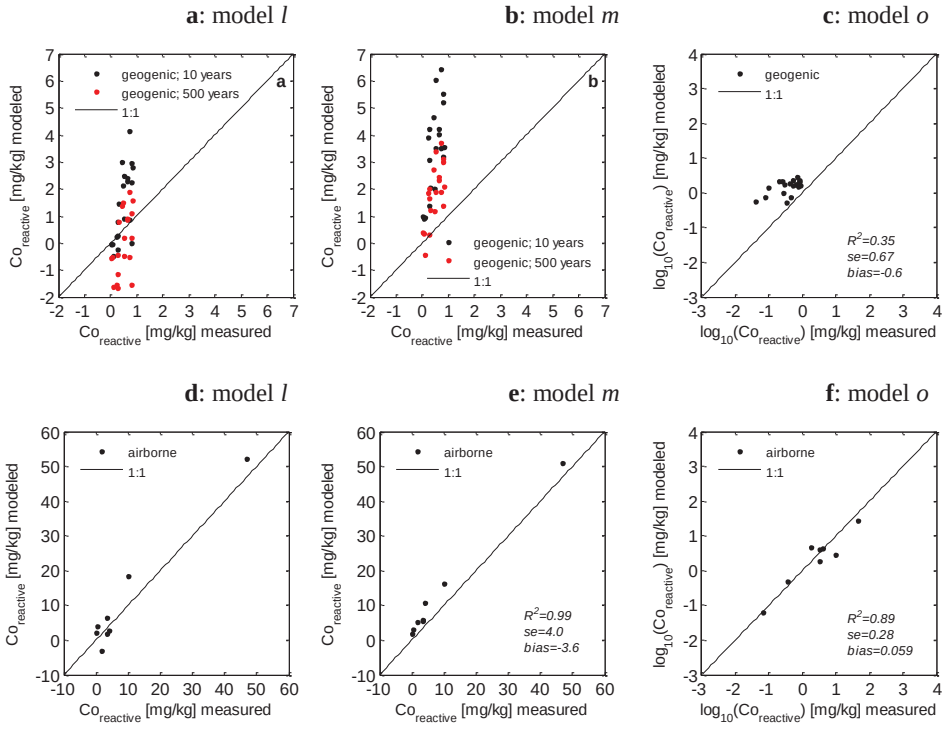

Figure S2.11: Comparison of measured and model predicted concentration of reactive Co as influenced by contaminant type. Models are shown in Tables S2.15 and S2.16. A perfect agreement between model and measured values would result in alignment of the data points on the first diagonal (1:1 line). Note that scales are different in the figures.

Copper. Kinetic aging models *e* and *k* developed for soluble salts overpredict (*e*) or fail to predict (*k*) concentration of reactive geogenic Cu, respectively (Figure S2.12). The error for the model *e* is particularly large larger at low concentrations of reactive Cu. This indicates that the model *e* does not capture those aging mechanisms that bring down reactive concentrations of Cu to low levels. The models *e* and *k* overpredict reactive concentrations of Cu emitted from smelters and in mine spoils, but perform better for Cu present in biosolids. The performance of empirical regression models *p* and *u* is better for geogenic Cu and comparable to that for anthropogenic Cu, as compared with the kinetic models *e* and *k*.

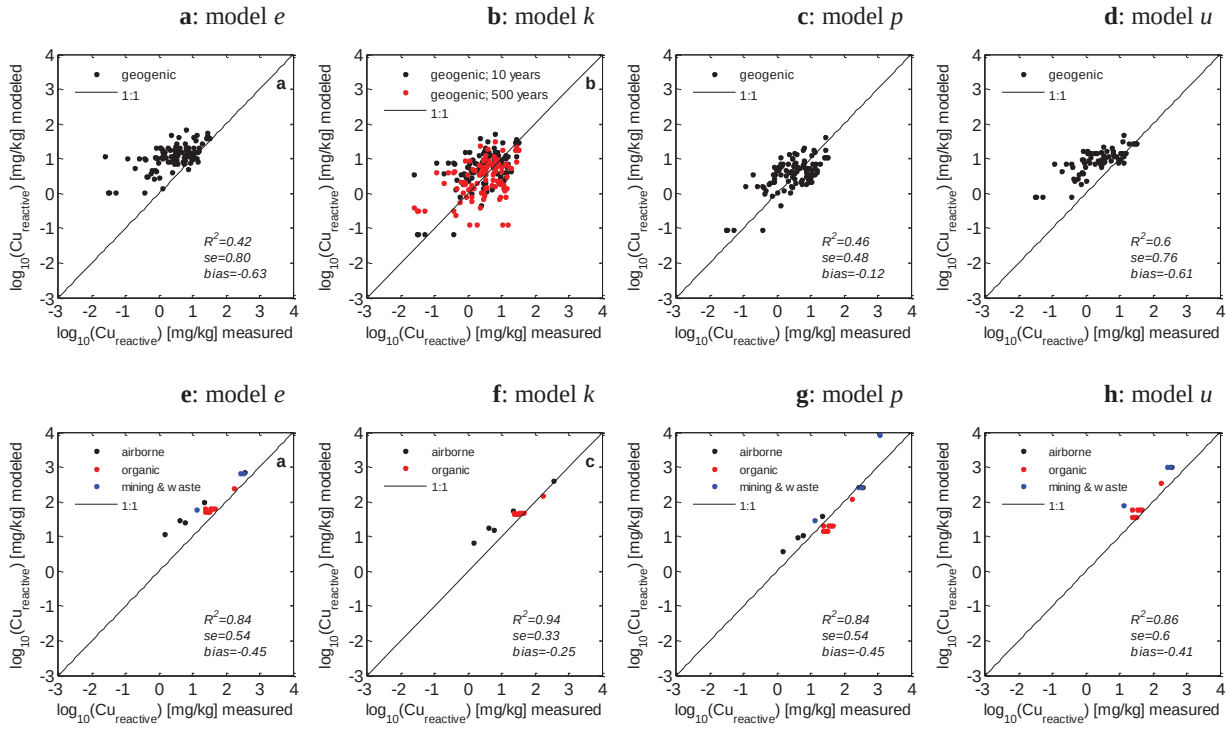

Figure S2.12: Comparison of measured and model predicted concentration of reactive Cu as influenced by contaminant type. Models are shown in Tables S2.15 and S2.16. A perfect agreement between model and measured values would result in alignment of the data points on the first diagonal (1:1 line).

Nickel. The kinetic model *f* developed using soils spiked with soluble salt overestimates concentration of reactive Ni in soils, irrespectively of the type of contamination (Fig. S2.13). The bias is close to zero for the empirical regression model *q*, with explained variability being < 0.55. Large errors are noted for soils developed on Ni-rich rocks, where Ni from weathered rock was mainly present in association with the Fe or Mn oxides (Massoura et al. 2006).

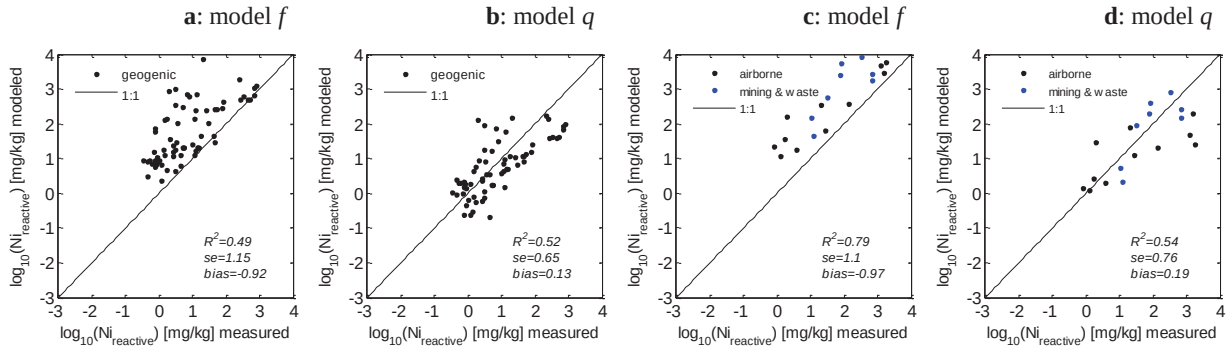

Figure S2.13: Comparison of measured and model predicted concentration of reactive Ni as influenced by contaminant type. Models are shown in Tables S2.15 and S2.16. A perfect agreement between model and measured values would result in alignment of the data points on the first diagonal (1:1 line).

Lead. Empirical regression model *r* underpredicts the concentration of reactive Pb in soils contaminated with geogenic and anthropogenic Pb (Fig. S2.14). The bias probably originates from the fact that due to the lack of measured data we used the version of the where the effects of soils organic carbon on Pb reactivity are not included. The model *v*, where the effects of soil organic carbon are included, performs better as compared with the model *v*. Yet, the comparison was done using only 5 soils.

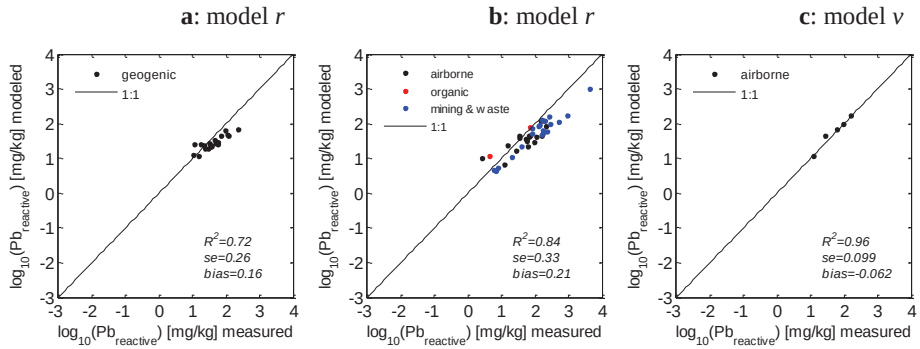

Figure S2.14: Comparison of measured and model predicted concentration of reactive Pb as influenced by contaminant type. Models are shown in Tables S2.15 and S2.16. A perfect agreement between model and measured values would result in alignment of the data points on the first diagonal (1:1 line).

Zinc. The kinetic models *g* and *b* overpredict concentration of reactive Zn for both geogenic and anthropogenic Zn (Fig. S2.15). The bias is larger for soils contaminated with geogenic metal, but is close to zero in soils where Zn was applied in biosolids. Very low reactive Zn was measured in two soils with geogenic Ni but too little information was given

about these soils to allow for drawing any conclusions. For geogenic Zn, the empirical regression models *s* and *x* are less biased as compared with the kinetic models and explain larger part of the variability in concentration of reactive Ni. The regression model *s* underpredicts reactive concentration of anthropogenic Zn.

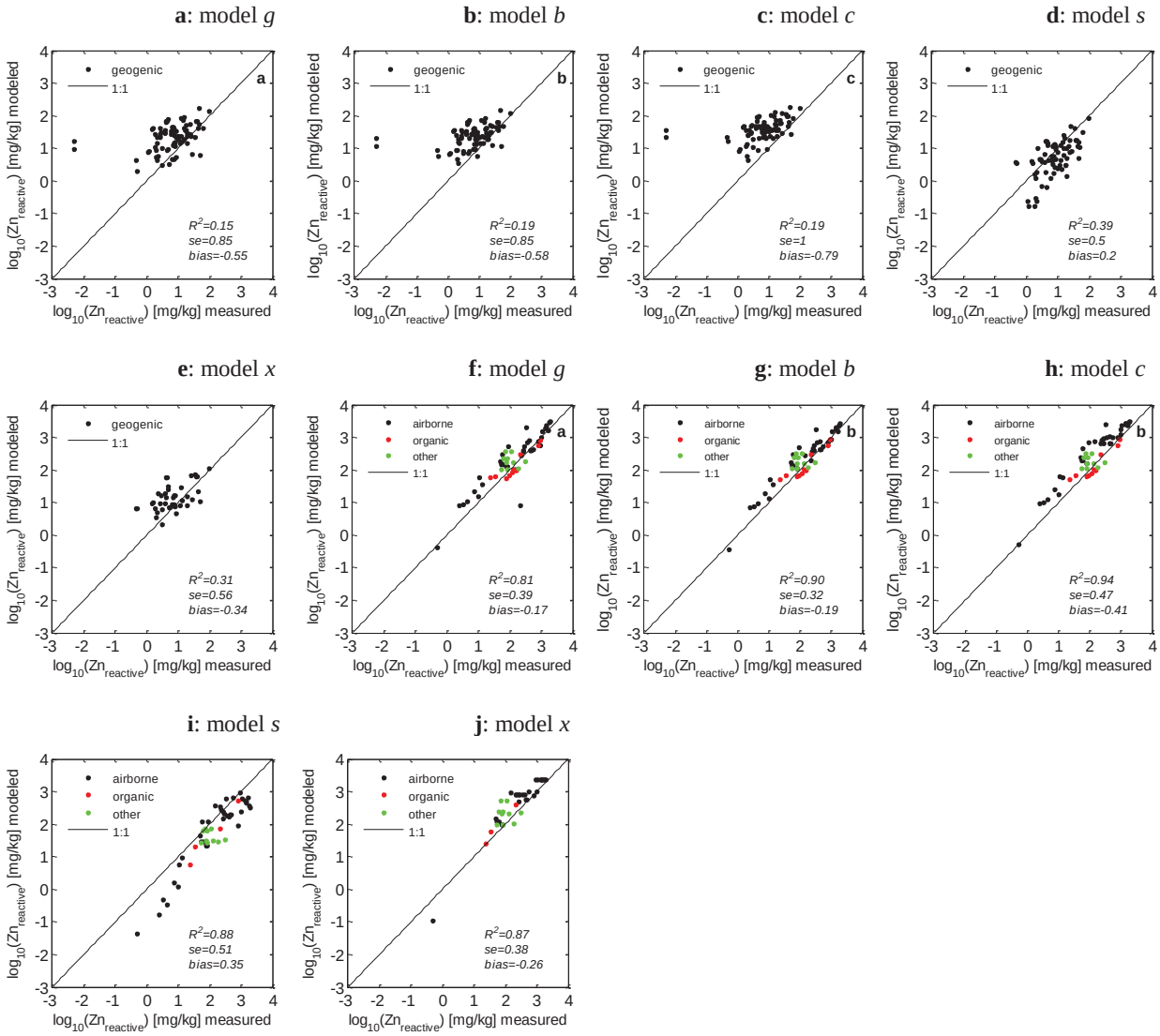

Figure S2.15: Comparison of measured and model predicted concentration of reactive Zn as influenced by contaminant type. Models are shown in Tables S2.15 and S2.16. A perfect agreement between model and measured values would result in alignment of the data points on the first diagonal (1:1 line).

5.1.13. Details on the Influence of Metal Accessibility on Comparative Toxicity Potentials

Comparative Toxicity Potentials. Recall, that comparative toxicity potential for a metal s in soil after a unit emission to compartment i is (eq S2.27, or eq 2.2 in the main part):

$$CTP_{i,s} = FF_{i,s} \cdot ACF_s \cdot BF_s \cdot EF_s \qquad \textbf{S2.27}$$

where $CTP_{i,s}$ ($m^3/kg_{total\ emitted}$·day) is the comparative toxicity potential of total metal s emitted to compartment i; $FF_{i,s}$ (day) is the fate factor calculated for total metal s in soil; ACF_s ($kg_{reactive}/kg_{total}$) is the accessibility factor defined as the reactive fraction of total metal s in soil; BF_s ($kg_{free}/kg_{reactive}$) is the bioavailability factor defined as the free ion fraction of the reactive metal s in soil, and EF_s (m^3/kg_{free}) is the terrestrial ecotoxicity effect factor defined as PAF for the free ion form of the metal.

Accessibility Factor. Accessibility factor (ACF, in $kg_{reactive}/kg_{total}$) was defined as:

$$ACF = \frac{\Delta C_{reactive}}{\Delta C_{total}} \qquad \textbf{S2.28}$$

where $\Delta C_{reactive}$ ($kg_{reactive}/kg$) is the incremental change of the concentration of reactive metal in soil; and ΔC_{total} (kg_{total}/kg) is the incremental change in concentration in total metal in soil.

The ACF influences the CTP directly in eq S2.27, and indirectly through its control of the K_d-dependent fate factor (FF), according to eq S2.29:

$$K_d^{tot} = \frac{K_d^{react}}{ACF} \qquad \textbf{S2.29}$$

Earlier, we showed how FF increases with an increase in the K_d^{tot} (defined as the ratio between the concentration of total metal in the solid phase and the total dissolved metal), which can be explained by the latter's control of leaching and runoff (Fig. S2.6). At high K_d^{tot} values, the fate is however controlled by K_d^{tot}-independent soil erosion. In those cases, the direct effects of the ACF on the CTP are higher as compared with the indirect effects of the ACF on the K_d^{tot}-controlled FF. We will demonstrate this by calculating fate factors for soils in our data sets and computing the ratio of toxicity potential with (CTP) and without (CTP_0) influence for metal accessibility.

Calculations. The ratio of CTP/CTP_0 was computed for anthropogenic contamination types retrieved in this study, as follows:

$$\frac{CTP}{CTP_0} = \frac{FF \cdot ACF \cdot BF \cdot EF}{FF_0 \cdot ACF_0 \cdot BF_0 \cdot EF_0} = ACF \cdot \frac{FF}{FF_0} \qquad \textbf{S2.30}$$

because $BF=BF_0$; $EF=EF_0$; and ACF_0=1 $kg_{reactive}/kg_{total}$.

Because time was not found to influence accessible fraction in our study, the ACF was assumed equal to measured values of the reactive fraction.

K_d^{react} values were calculated from measured concentration of reactive metal and calculated concentration of total dissolved metal. The latter was derived using empirical regression models published in Groenenberg et al. (2012) using measured concentration of reactive metal and soil properties. If data on soil properties were not available, the sum of amorphous Fe and Al (hydr)oxides was assumed equal to 89 mmol/kg, clay content was assumed equal to 21 (median across 760 soils). Dissolved organic carbon (DOC) was calculated from soil organic carbon and electrical conductivity of soil pore water using the empirical regression model developed by Romkens et al. (2004). Soil organic matter was assumed equal to 1.78 of soil organic carbon, whereas electrical conductivity of soil pore water was assumed equal to 0.5 dS/m (median across 760 soils).

Fate factors were calculated employing the steady state characterization model USEtox, (Rosenbaum et al. 2008) as done earlier. Default environmental properties were used combined with soil and metal specific K_d^{tot} values. Computations were done with (for the FF) and without (for the FF_0) the influence of metal accessibility. The ratio CTP/CTP_0 was then calculated (eq S2.30). The same computations with and without correction for metal accessibility were done to calculate FFs for three hypothetical cases with K_d^{react} equal to (i) 10; (ii) 1000; and (iii) 10000 L/kg. Results are discussed in the main text (Fig. 2.6).

5.2. Appendix for section Aquatic ecotoxicity of whole effluents

5.2.1. Estimation of lower horizontal asymptotes for the *P. subcapitata* growth bioassays

To justify the use of the 3-parameter log-logistic function for the WET bioassay for *P. subcapitata* with growth as the endpoint, it will be shown that the lower horizontal asymptote is sufficiently close to zero. The lower horizontal asymptote for the WET bioassay for *P. subcapitata* would be the cell density (measured as absorbance) at the beginning of the test. However the initial cell density is unknown, since the short term WET bioassay for *P.subcapitata* as described by the USEPA (USEPA 2002) requires that absorbance measurements (indicative of cell density) are taken at the end of the 96 h test duration. Nonetheless, the initial cell density, or absorbance, can be estimated by back calculating from the absorbance measurement for the control at 96 h with information obtained from the growth curve of *P. subcapitata*. This alga has no lag phase – it enters directly into the exponential growth phase (Nyholm & Källqvist 1989), with a growth rate μ given by

(S1)

where t_2 and t_1 are the times at the end and beginning of the time period, respectively, and N_2 and N_1 are the cell counts or cell densities at times t_2 and t_1, respectively. An analysis of a biomass growth curve for *P. subcapitata* (Nyholm & Källqvist 1989) recorded under the same conditions as those required for the control of the respective WET bioassay, gives an average growth rate of $\mu_{0\text{-}3}$ = 1.77 d^{-1} for days 0-3, and a growth rate equal to $\mu_{3\text{-}4}$ = 0.62 d^{-1} for days 3-4. These growth rates are then employed to sequentially back calculate the initial cell density N_0, starting from the measurement on day 4, which is given in the data. Figure S3.1 shows box and whisker plots per mill for the final and the back calculated initial absorbances for all available *P. subcapitata* bioassays. Clearly, the initial cell densities are so close to zero so as assume a lower horizontal asymptote of zero and to safely apply the three-parameter log-logistic function.

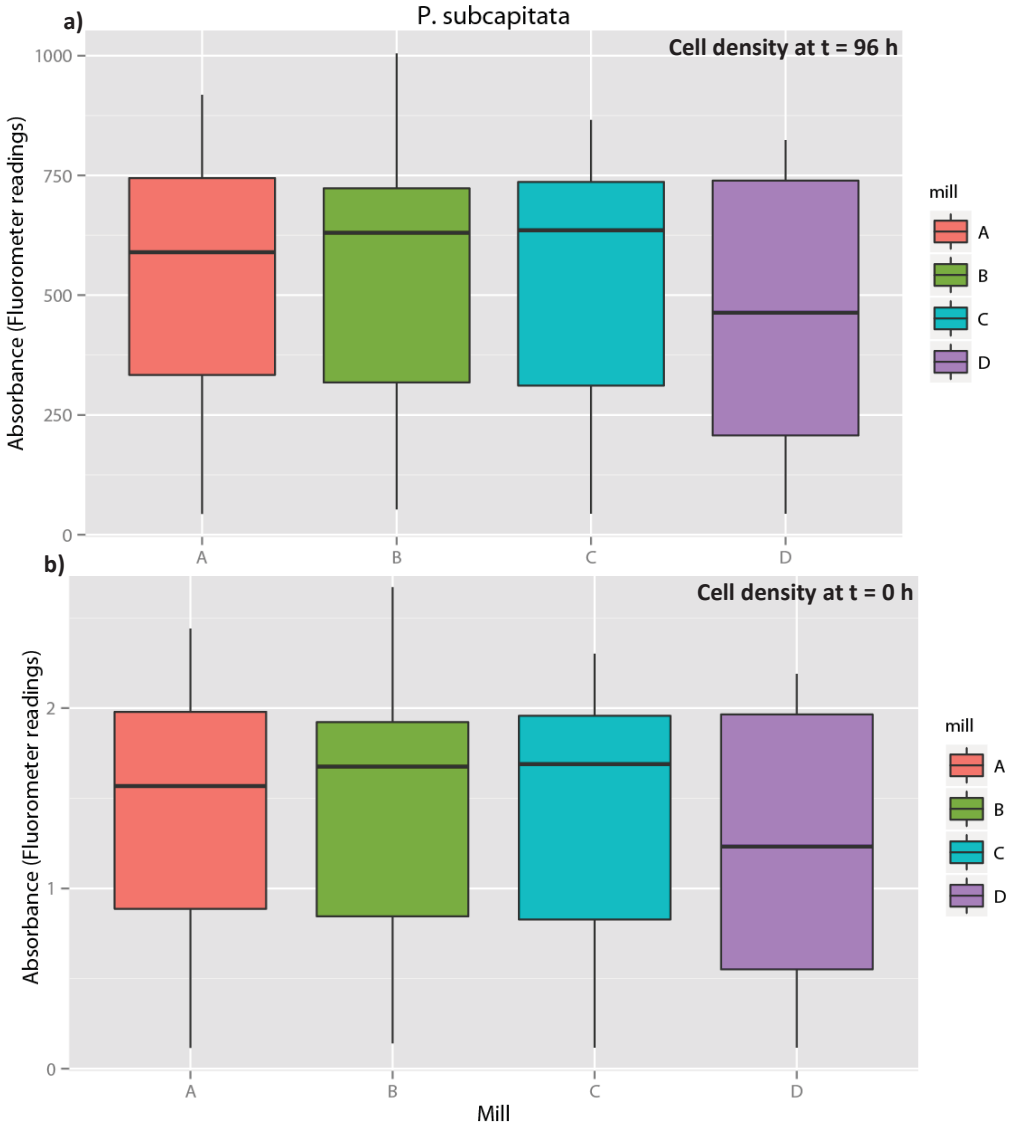

Figure S3.1 Box and whisker plots of absorbance measurements (representing cell density) aggregated per mill a) at the end of the bioassay (measured) and b) at the beginning of the bioassay (back-calculated).

5.2.2. tables

Table S3.1 Overview of all WET bioassay results (retained or excluded from further analysis) for *P. subcapitata*.

		Pseudokirchneriella subcapitata				
Sample	**Mill**	**(% effluent)**	**Standard error**	**Lower boundary of CI**	**Upper boundary of CI**	**Reason for exclusion (highlighted samples)**
15405	A	11.8	3.4	4.7	18.8	Unacceptable model fit (visual inspection)
15714	A	62.0	6.4	48.8	75.2	
16625	A	12.6	9.2	-6.6	31.8	
17446	A	45.4	3.8	37.5	53.4	
18321	A	113.7	24.4	63.0	164.3	
19459	A	202.0	NA	NA	NA	estimate > 200%
20620	A	8.6	75.2	-147.9	165.0	
21209	A	89.3	16.0	56.0	122.6	
22761	A	86.8	26.3	32.0	141.5	Non-convergence of optimisation function for model fit
23734	A	48.2	10.8	25.6	70.7	
24153	A	822.4	299.6	199.4	1445.5	
24643	A	106.3	16.6	71.8	140.8	
14824	B	61.9	11.4	38.2	85.6	
15398	B	67.5	12.5	41.5	93.5	
15728	B	369.9	395.7	-452.9	1192.7	
16713	B	104.4	26.6	49.1	159.7	
17794	B	101.4	20.2	59.4	143.5	
18540	B	821.1	1199.7	-1673.7	3316.0	
19675	B	90.7	806.8	-1587.2	1768.6	
20565	B	47863.7	949680.2	-1927104.3	2022831.7	
21604	B	364.1	708.5	-1109.3	1837.5	
22586	B	1144.1	3753.1	-6660.9	8949.2	
23635	B	257.1	261.9	-287.6	801.7	
24043	B	non-convergence of optimisation function: no parameters estimated				
24823	B	355.6	201.8	-64.1	775.3	
15756	C	175.5	63.9	42.6	308.3	
16951	C	231.8	180.3	-143.2	606.8	
17702	C	136.6	29.0	76.2	196.9	
18672	C	1319.0	13305.6	-26351.6	28989.5	
19677	C	non-convergence of optimisation function: no parameters estimated				
20841	C	10570.3	122874.8	-244961.8	266102.3	
21837	C	non-convergence of optimisation function: no parameters estimated				
22872	C	1968.5	66747.0	-136839.6	140776.5	
23669	C	6140.8	97862.4	-197375.2	209656.8	
24159	C	non-convergence of optimisation function: no parameters estimated				
24927	C	538.6	6178.1	-12309.5	13386.6	
14779	D	45.0	4.9	34.7	55.3	
15726	D	62.5	6.5	49.0	76.0	
16624	D	63.1	9.5	43.2	82.9	
17491	D	110.6	12.6	84.4	136.8	
18320	D	103.6	23.1	55.6	151.6	
19458	D	107.9	16.7	73.2	142.6	
20714	D	52.6	10.7	30.3	74.9	
21514	D	105.6	18.7	66.7	144.4	
22591	D	80.5	14.1	51.0	109.9	
23610	D	25.7	4.8	15.8	35.7	
23735	D	28.0	4.0	19.6	36.4	
24066	D	101.0	12.7	74.7	127.3	
24844	D	non-convergence of optimisation function: no parameters estimated				

Table S3.2 Overview of all WET bioassay results (retained or excluded from further analysis) for *C. dubia*.

		Ceriodaphnia dubia				
Sample	**Mill**	**(% effluent)**	**Standard error**	**Lower boundary of CI**	**Upper boundary of CI**	**Reason for exclusion (highlighted samples)**
9685	A	55.8	3.9	48.2	63.3	estimate > 200%
9877	A	59.3	2.4	54.6	63.9	
9949	A	33.9	2.8	28.3	39.5	
10452	A	77.1	3.1	71.1	83.1	
11141	A	85.6	5.0	75.9	95.4	Non-convergence of optimisation function for model fit
11475	A	93.3	4.1	85.3	101.2	
11707	A	129.8	18.7	93.3	166.4	
11995	A	non-convergence of optimisation function: no parameters estimated				
12361	A	non-convergence of optimisation function: no parameters estimated				Non-survival of test organisms in parallel survival bioassays
12802	A	non-convergence of optimisation function: no parameters estimated				
12922	A	non-convergence of optimisation function: no parameters estimated				
13106	A	58.0	6.1	46.0	70.1	
13191	A	5.9	0.8	4.4	7.5	
13198	A	71.6	6.8	58.3	84.9	
13252	A	non-convergence of optimisation function: no parameters estimated				
13360	A	non-convergence of optimisation function: no parameters estimated				
13610	A	58400.4	NA	NA	NA	
14388	A	184.6	57.3	72.2	296.9	
14389	A	non-convergence of optimisation function: no parameters estimated				
15405	A	124.0	13.8	97.1	151.0	
15714	A	200.0	86.8	29.8	370.1	
16625	A	146.9	44.1	60.4	233.4	
17446	A	770.6	NA	NA	NA	
18321	A	4730.4	NA	NA	NA	
19459	A	non-convergence of optimisation function: no parameters estimated				
20620	A	122.2	12.3	98.0	146.4	
21209	A	121.2	37.0	48.7	193.6	
22761	A	118.4	15.3	88.4	148.4	
23734	A	138.2	34.1	71.3	205.0	
24513	A	non-convergence of optimisation function: no parameters estimated				
24643	A	943.7	NA	NA	NA	
9525	B	92.0	3.5	85.2	98.9	
9625	B	non-convergence of optimisation function: no parameters estimated				
9760	B	2437.2	3586.1	-4591.5	9465.8	
9907	B	non-convergence of optimisation function: no parameters estimated				
9981	B	229.9	270.1	-299.5	759.3	
10242	B	non-convergence of optimisation function: no parameters estimated				
10271	B	non-convergence of optimisation function: no parameters estimated				
10442	B	non-convergence of optimisation function: no parameters estimated				
10555	B	non-convergence of optimisation function: no parameters estimated				
11050	B	non-convergence of optimisation function: no parameters estimated				
11140	B	non-convergence of optimisation function: no parameters estimated				
11239	B	non-convergence of optimisation function: no parameters estimated				
11873	B	non-convergence of optimisation function: no parameters estimated				
12360	B	non-convergence of optimisation function: no parameters estimated				
12533	B	non-convergence of optimisation function: no parameters estimated				
12741	B	non-convergence of optimisation function: no parameters estimated				
12874	B	non-convergence of optimisation function: no parameters estimated				
13118	B	non-convergence of optimisation function: no parameters estimated				
13441	B	non-convergence of optimisation function: no parameters estimated				
14258	B	62136.3	NA	NA	NA	
14391	B	non-convergence of optimisation function: no parameters estimated				

14824	B	non-convergence of optimisation function: no parameters estimated			
15398	B	non-convergence of optimisation function: no parameters estimated			
15728	B	300.5	203.3	-98.0	699.0
16713	B	232.0	196.8	-153.8	617.7
16953	B	non-convergence of optimisation function: no parameters estimated			
17431	B	225.6	132.8	-34.7	485.8
17794	B	non-convergence of optimisation function: no parameters estimated			
18540	B	non-convergence of optimisation function: no parameters estimated			
19675	B	15678.7	82351.8	-145727.9	177085.2
20565	B	non-convergence of optimisation function: no parameters estimated			
21604	B	non-convergence of optimisation function: no parameters estimated			
22586	B	non-convergence of optimisation function: no parameters estimated			
23635	B	non-convergence of optimisation function: no parameters estimated			
24043	B	non-convergence of optimisation function: no parameters estimated			
24823	B	non-convergence of optimisation function: no parameters estimated			
9614	C	2022.4	3796.6	-5418.9	9463.7
9928	C	447.8	396.9	-330.1	1225.6
10253	C	32.5	3.9	24.8	40.2
10506	C	non-convergence of optimisation function: no parameters estimated			
10574	C	195.1	63.7	70.3	319.9
11178	C	non-convergence of optimisation function: no parameters estimated			
11351	C	116.5	15.4	86.4	146.6
11572	C	160.2	35.2	91.1	229.3
12309	C	191.9	70.8	53.1	330.7
13064	C	non-convergence of optimisation function: no parameters estimated			
13307	C	non-convergence of optimisation function: no parameters estimated			
14259	C	100.3	18.2	64.7	135.9
14392	C	13.1	0.5	12.2	14.1
16951	C	152.9	67.3	20.9	284.8
17702	C	264.7	250.8	-226.9	756.4
19677	C	46697.1	387866.1	-713506.4	806900.6
20841	C	non-convergence of optimisation function: no parameters estimated			
21837	C	non-convergence of optimisation function: no parameters estimated			
22872	C	719.6	877.8	-1000.9	2440.0
24159	C	non-convergence of optimisation function: no parameters estimated			
24927	C	non-convergence of optimisation function: no parameters estimated			
10988	D	non-convergence of optimisation function: no parameters estimated			
12046	D	2782763.7	NA	NA	NA
12134	D	106.7	4.8	97.2	116.1
12306	D	841.2	2808.9	-4664.1	6346.6
12439	D	108.0	15.5	77.7	138.3
12669	D	124.0	14.4	95.8	152.3
12761	D	131.5	26.9	78.7	184.2
12921	D	117.7	19.4	79.8	155.7
13190	D	non-convergence of optimisation function: no parameters estimated			
13442	D	92.6	18.0	57.4	127.9
14256	D	251.6	181.3	-103.7	606.9
14390	D	64165.2	623098.4	-1157085.3	1285415.7
14779	D	non-convergence of optimisation function: no parameters estimated			
15726	D	178.1	96.5	-11.1	367.2
16624	D	335.7	190.6	-37.9	709.2
17491	D	237.6	204.7	-163.7	638.8
18320	D	non-convergence of optimisation function: no parameters estimated			
19458	D	228.0	84.7	62.1	393.9
21514	D	108.6	12.1	84.9	132.3
22591	D	188.9	55.1	81.0	296.8
23610	D	57.2	1.7	53.9	60.5
23735	D	92.6	3.5	85.8	99.4
24066	D	non-convergence of optimisation function: no parameters estimated			

24844	D	non-convergence of optimisation function: no parameters estimated

Table S3.3 Overview of all WET bioassay results (retained or excluded from further analysis) for *P. promelas*.

		Pimephales promelas				
Sample	**Mill**	**(% effluent)**	**Standard error**	**Lower boundary of CI**	**Upper boundary of CI**	**Reason for exclusion (highlighted samples)**
9685	A	88.0	39.2	6.6	169.4	Unacceptable model fit (visual inspection)
9877	A	304.1	337.4	-397.5	1005.8	
9949	A	non-convergence of optimisation function: no parameters estimated				
10452	A	101.2	5.4	89.9	112.5	
11141	A	99.7	1.6	96.3	103.2	estimate > 200%
11475	A	3.6	75.9	-154.3	161.4	
11707	A	115.4	37.0	38.6	192.3	
11995	A	138.5	54.4	25.5	251.6	
13106	A	0.0	0.1	-0.1	0.2	Non-convergence of optimisation function for model fit
13191	A	non-convergence of optimisation function: no parameters estimated				
13252	A	179.7	99.4	-27.0	386.4	
9760	B	non-convergence of optimisation function: no parameters estimated				Non-survival of test organisms in parallel survival bioassays
9907	B	non-convergence of optimisation function: no parameters estimated				
9981	B	non-convergence of optimisation function: no parameters estimated				
10242	B	non-convergence of optimisation function: no parameters estimated				
10271	B	non-convergence of optimisation function: no parameters estimated				
10442	B	non-convergence of optimisation function: no parameters estimated				
10555	B	non-convergence of optimisation function: no parameters estimated				
11050	B	non-convergence of optimisation function: no parameters estimated				
11140	B	non-convergence of optimisation function: no parameters estimated				
11239	B	non-convergence of optimisation function: no parameters estimated				
11873	B	non-convergence of optimisation function: no parameters estimated				
15398	B	non-convergence of optimisation function: no parameters estimated				
16953	B	non-convergence of optimisation function: no parameters estimated				
17431	B	non-convergence of optimisation function: no parameters estimated				
17794	B	non-convergence of optimisation function: no parameters estimated				
9614	C	non-convergence of optimisation function: no parameters estimated				
9928	C	non-convergence of optimisation function: no parameters estimated				
10253	C	non-convergence of optimisation function: no parameters estimated				
10506	C	non-convergence of optimisation function: no parameters estimated				
10574	C	non-convergence of optimisation function: no parameters estimated				
11178	C	non-convergence of optimisation function: no parameters estimated				
11351	C	non-convergence of optimisation function: no parameters estimated				
11572	C	non-convergence of optimisation function: no parameters estimated				
12309	C	non-convergence of optimisation function: no parameters estimated				
10988	D	non-convergence of optimisation function: no parameters estimated				
12406	D	non-convergence of optimisation function: no parameters estimated				
12134	D	non-convergence of optimisation function: no parameters estimated				
12306	D	non-convergence of optimisation function: no parameters estimated				
12439	D	non-convergence of optimisation function: no parameters estimated				
12669	D	non-convergence of optimisation function: no parameters estimated				
12761	D	non-convergence of optimisation function: no parameters estimated				

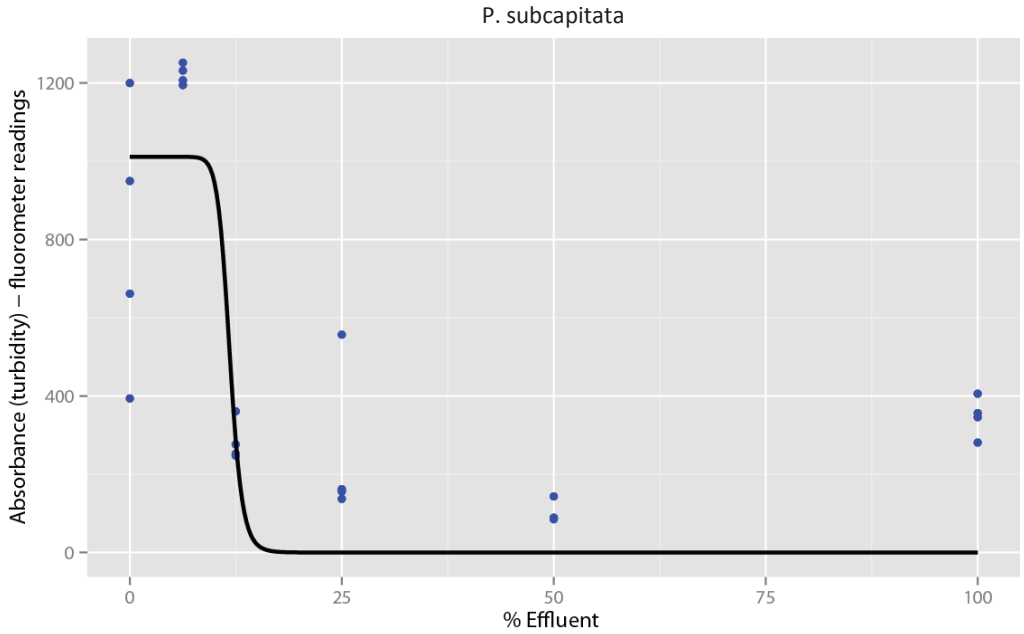

Figure S3.2 Example of a model fit deemed unacceptable by visual inspection.

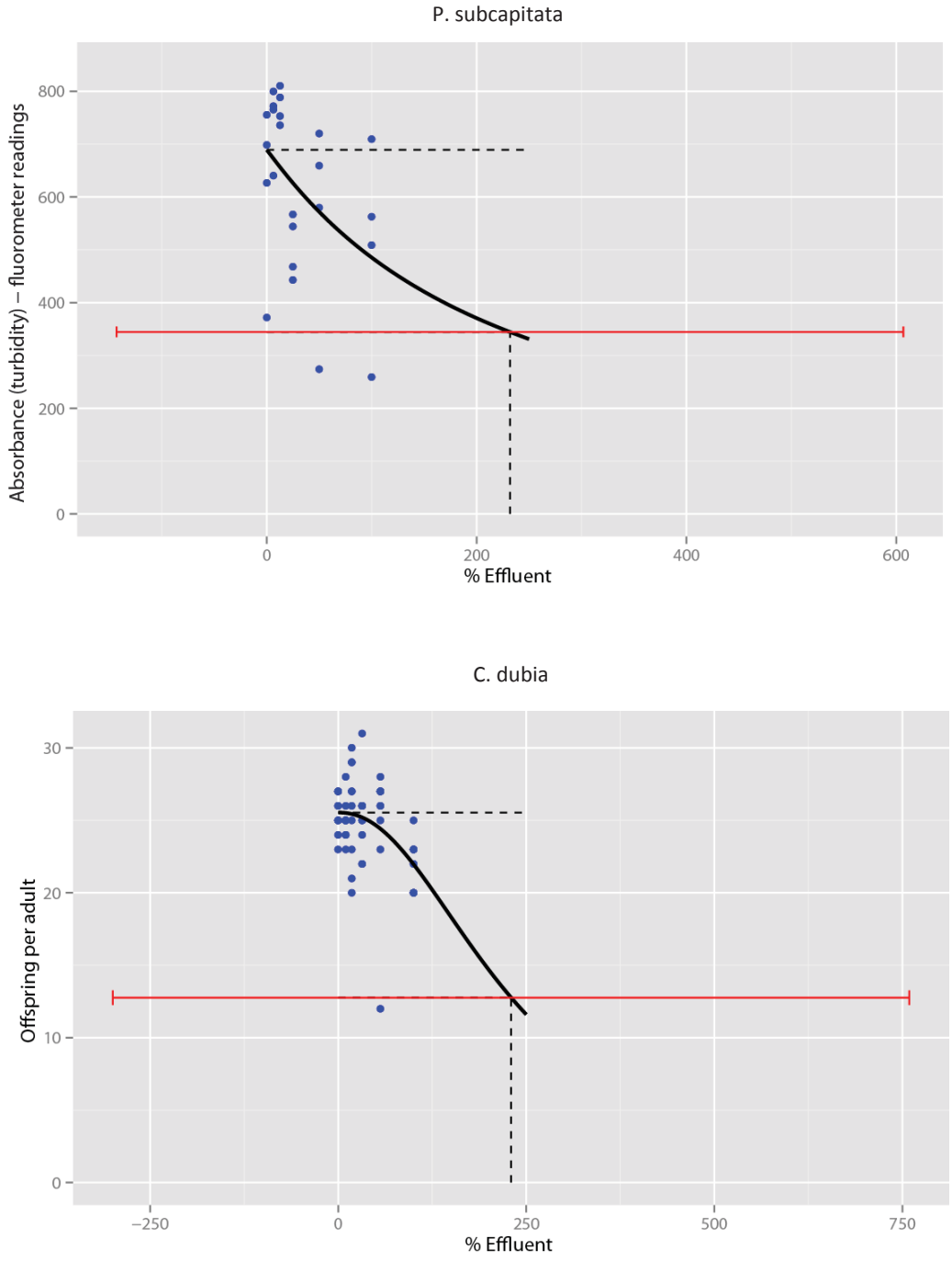

Figure S3.3 Examples of model fits deemed unacceptable due to extremely large uncertainty associated with the estimated which is beyond the cut-off point for extrapolation of 200%.

5.2.3. Error propagation

Experimentally estimated parameters are, more often than not, used in further calculations. In doing so, the error associated with the original parameter is forwarded to the values calculated further down the analysis chain. Given a relation the error in every is propagated to via the following relation:

(S2)

where is the standard deviation (of or), but can also be the standard error (i.e. an estimate of the standard deviation based on the population sample, divided by the square root of the number of observations in the sample).

5.2.3.1. Error propagation in effect factor calculation

The following equations shows how the original standard error estimated for the is propagated along the steps of the calculation

(S3)

(S4)

(S5)

(S6)

(e.g. for $n = 2$)

(S7)

5.2.3.2. Confidence intervals

For data that is assumed to be normally distributed, the 95% confidence interval in each case is constructed as follows:
Upper limit: estimate + 1.96 · standard error
Lower limit: estimate – 1.96 · standard error
(where 1.96 is the 0.975 quantile of the normal distribution)

5.2.4. tables

Table S3.4 Overview of estimated for *P. subcapitata*.

		Pseudokirchneriella subcapitata			
Sample	**Mill**		**Standard error**	**Lower boundary of CI**	**Upper boundary of CI**
15714	A	1.61	0.17	1.27	1.96
16625	A	7.93	5.80	-4.12	19.99
17446	A	2.20	0.19	1.82	2.59
18321	A	0.88	0.19	0.49	1.27
21209	A	1.12	0.20	0.70	1.54
22761	A	1.15	0.35	0.43	1.88
23734	A	2.08	0.47	1.10	3.05
24643	A	0.94	0.15	0.64	1.25
14824	B	1.62	0.30	1.00	2.24
15398	B	1.48	0.27	0.91	2.05
16713	B	0.96	0.24	0.45	1.47
17794	B	0.99	0.20	0.58	1.39
15756	C	0.57	0.21	0.14	1.00
17702	C	0.73	0.16	0.41	1.06
14779	D	2.22	0.24	1.71	2.73
15726	D	1.60	0.17	1.25	1.95
16624	D	1.59	0.24	1.09	2.09
17491	D	0.90	0.10	0.69	1.12
18320	D	0.96	0.22	0.52	1.41
19458	D	0.93	0.14	0.63	1.22
20714	D	1.90	0.39	1.10	2.71
21514	D	0.95	0.17	0.60	1.30
22591	D	1.24	0.22	0.79	1.70
23610	D	3.88	0.72	2.39	5.38
23735	D	3.57	0.51	2.50	4.64
24066	D	0.99	0.12	0.73	1.25

Table S3.5 Overview of estimated for *C. dubia*.

		Ceriodaphnia dubia			
Mill	**Sample**		**Standard error**	**Lower boundary of CI**	**Upper boundary of CI**
A	9685	1.79	0.12	1.55	2.04
A	9877	1.69	0.07	1.55	1.82
A	9949	2.95	0.25	2.46	3.44
A	10452	1.30	0.05	1.20	1.40
A	11141	1.17	0.07	1.04	1.30
A	11475	1.07	0.05	0.98	1.16
A	11707	0.77	0.11	0.55	0.99
A	13106	1.72	0.18	1.37	2.08
A	13198	1.40	0.13	1.14	1.66
A	14388	0.54	0.17	0.21	0.87
A	15405	0.81	0.09	0.63	0.98
A	15714	0.50	0.22	0.07	0.93
A	16625	0.68	0.20	0.28	1.08
A	20620	0.82	0.08	0.66	0.98
A	21209	0.83	0.25	0.33	1.32
A	22761	0.84	0.11	0.63	1.06
A	23734	0.72	0.18	0.37	1.07
B	9525	1.09	0.04	1.01	1.17
C	10253	3.08	0.37	2.35	3.81
C	10574	0.51	0.17	0.18	0.84
C	11351	0.86	0.11	0.64	1.08
C	11572	0.62	0.14	0.36	0.89
C	12309	0.52	0.19	0.14	0.90
C	14392	7.61	0.29	7.03	8.18
D	12134	0.94	0.04	0.85	1.02
D	12439	0.93	0.13	0.67	1.19
D	12669	0.81	0.09	0.62	0.99
D	12761	0.76	0.16	0.46	1.07
D	12921	0.85	0.14	0.58	1.12
D	13442	1.08	0.21	0.67	1.49
D	15726	0.56	0.30	-0.03	1.16
D	21514	0.92	0.10	0.72	1.12
D	22591	0.53	0.15	0.23	0.83
D	23735	1.08	0.04	1.00	1.16

Table S3.6 Overview of estimated for *P. promelas*.

			Pimephales promelas		
Sample	**Mill**		**Standard error**	**Lower boundary of CI**	**Upper boundary of CI**
10452	A	0.99	0.05	0.88	1.10
11141	A	1.00	0.02	0.97	1.04
11707	A	0.87	0.28	0.29	1.44
11995	A	0.72	0.28	0.13	1.31
13252	A	0.56	0.31	-0.08	1.20

5.2.5. Metal free ion activity tables and figure

Table S3.7 Free ion activities (as modelled in WHAM7) of metals in effluent samples for which *P. subcapitata* WET bioassays were also performed.

Samples for analysis alongside *Pseudokirchneriella subcapitata* WET tests

Mill	Sample	Metal	Free ion act. [M]	Mill	Sample	Metal	Free ion act. [M]
A	15714	Cr	5.71E-19	B	14824	Cr	1.05E-18
		Ni	1.10E-08			Ni	1.13E-07
		Cu	2.19E-13			Cu	1.81E-12
		Zn	9.21E-09			Zn	1.26E-08
		Cd	3.59E-10			Cd	4.79E-10
		Pb	2.52E-12			Pb	1.75E-12
	16625	Cr	6.43E-19		15398	Cr	3.74E-19
		Ni	6.88E-09			Ni	5.50E-08
		Cu	1.06E-13			Cu	3.86E-12
		Zn	5.90E-09			Zn	5.03E-08
		Cd	6.74E-11			Cd	8.48E-10
		Pb	1.04E-12			Pb	6.51E-12
	17446	Cr	2.00E-19		16713	Cr	3.03E-19
		Ni	5.05E-09			Ni	2.04E-08
		Cu	7.16E-14			Cu	4.75E-13
		Zn	4.65E-09			Zn	8.00E-09
		Cd	5.28E-11			Cd	3.37E-10
		Pb	1.57E-12			Pb	1.69E-12
	18321	Cr	3.51E-19		17794	Cr	3.29E-20
		Ni	2.00E-08			Ni	1.55E-08
		Cu	2.71E-13			Cu	9.76E-14
		Zn	7.91E-09			Zn	6.94E-09
		Cd	1.31E-10			Cd	7.95E-11
		Pb	2.77E-12			Pb	3.55E-12
	21209	Cr	2.16E-19				
		Ni	1.09E-08	C	15756	Cr	4.86E-19
		Cu	8.90E-14			Ni	1.94E-08
		Zn	6.95E-09			Cu	6.12E-13
		Cd	6.86E-11			Zn	2.83E-08
		Pb	2.49E-12			Cd	2.91E-10
	22761	Cr	3.26E-19			Pb	3.62E-11
		Ni	6.76E-09		17702	Cr	1.30E-18
		Cu	2.03E-13			Ni	2.05E-08
		Zn	6.11E-09			Cu	8.96E-13
		Cd	1.07E-10			Zn	3.20E-08
		Pb	2.07E-12			Cd	4.15E-10
	23734	Cr	2.50E-19			Pb	3.29E-11
		Ni	5.99E-09				
		Cu	1.98E-13				
		Zn	6.96E-09				
		Cd	1.15E-10				
		Pb	3.03E-12				
	24643	Cr	6.13E-19				
		Ni	8.66E-09				
		Cu	1.61E-13				

	Zn	5.75E-09
	Cd	8.18E-11
	Pb	2.76E-12

Samples for analysis with *Pseudokirchneriella subcapitata* WET tests (cont.)

Mill	Sample	Metal	Free ion act. [M]	Mill	Sample	Metal	Free ion act. [M]
D	14779	Cr	2.19E-19	D	20714	Cr	1.98E-19
		Ni	2.89E-09			Ni	1.21E-08
		Cu	1.98E-13			Cu	4.51E-13
		Zn	6.15E-09			Zn	9.22E-09
		Cd	9.81E-11			Cd	1.59E-10
		Pb	2.95E-12			Pb	1.47E-12
	15726	Cr	1.21E-19		21514	Cr	1.82E-19
		Ni	7.49E-09			Ni	1.87E-08
		Cu	2.79E-13			Cu	3.74E-13
		Zn	1.11E-08			Zn	1.97E-08
		Cd	3.17E-10			Cd	2.36E-10
		Pb	6.28E-12			Pb	3.15E-12
	16624	Cr	4.05E-20		22591	Cr	3.75E-19
		Ni	2.56E-09			Ni	1.27E-08
		Cu	4.21E-14			Cu	3.45E-13
		Zn	2.54E-09			Zn	1.47E-08
		Cd	5.65E-11			Cd	2.41E-10
		Pb	4.84E-13			Pb	1.93E-12
	17491	Cr	9.22E-20		23610	Cr	9.69E-20
		Ni	5.08E-09			Ni	6.62E-09
		Cu	1.38E-13			Cu	9.71E-14
		Zn	8.45E-09			Zn	5.05E-09
		Cd	1.08E-10			Cd	6.02E-11
		Pb	1.38E-12			Pb	1.41E-12
	18320	Cr	4.79E-20		23735	Cr	1.20E-18
		Ni	3.84E-09			Ni	3.75E-08
		Cu	5.27E-14			Cu	1.11E-12
		Zn	5.34E-09			Zn	4.24E-08
		Cd	6.09E-11			Cd	3.67E-10
		Pb	4.39E-13			Pb	1.18E-11
	19458	Cr	1.22E-19		24066	Cr	8.15E-20
		Ni	8.69E-09			Ni	6.88E-09
		Cu	1.72E-13			Cu	8.67E-14
		Zn	1.07E-08			Zn	6.56E-09
		Cd	1.56E-10			Cd	1.02E-10
		Pb	2.41E-12			Pb	7.06E-13

Table S3.8 Free ion activities (as modelled in WHAM7) of metals in effluent samples for which *C. dubia* WET bioassays were also performed.

Samples for analysis alongside *Ceriodaphnia dubia* WET tests

Mill	Sample	Metal	Free ion act. [M]	Mill	Sample	Metal	Free ion act. [M]
A	9877*	Cr	1.35E-18	A	14388	Cr	9.20E-19
		Ni	3.03E-09			Ni	7.41E-09
		Cu	6.15E-13			Cu	1.28E-13
		Zn	3.46E-08			Zn	9.81E-09
		Cd	2.02E-10			Cd	1.20E-10
		Pb	NA			Pb	1.37E-12
	9949	Cr	9.64E-19		15405	Cr	3.40E-19
		Ni	1.10E-08			Ni	1.08E-08
		Cu	6.50E-13			Cu	2.00E-13
		Zn	2.79E-08			Zn	1.18E-08
		Cd	1.28E-10			Cd	2.04E-10
		Pb	3.45E-12			Pb	1.18E-12
	10452	Cr	7.18E-20		15714	Cr	5.71E-19
		Ni	4.93E-09			Ni	1.10E-08
		Cu	6.57E-14			Cu	2.19E-13
		Zn	9.36E-09			Zn	9.21E-09
		Cd	3.47E-11			Cd	3.59E-10
		Pb	7.92E-13			Pb	2.52E-12
	11141	Cr	8.99E-19		16625	Cr	6.43E-19
		Ni	9.72E-09			Ni	6.88E-09
		Cu	2.07E-13			Cu	1.06E-13
		Zn	1.29E-08			Zn	5.90E-09
		Cd	7.18E-11			Cd	6.74E-11
		Pb	4.00E-12			Pb	1.04E-12
	11475	Cr	1.99E-20		20620	Cr	4.24E-19
		Ni	1.58E-09			Ni	1.75E-08
		Cu	1.80E-14			Cu	2.55E-13
		Zn	2.72E-09			Zn	6.40E-09
		Cd	1.81E-11			Cd	7.76E-11
		Pb	4.48E-13			Pb	5.37E-12
	11707	Cr	1.90E-19		21209	Cr	2.16E-19
		Ni	7.48E-09			Ni	1.09E-08
		Cu	1.43E-13			Cu	8.90E-14
		Zn	7.05E-09			Zn	6.95E-09
		Cd	1.92E-10			Cd	6.86E-11
		Pb	1.28E-12			Pb	2.49E-12
	13198*	Cr	4.99E-19		22761	Cr	3.26E-19
		Ni	8.53E-09			Ni	6.76E-09
		Cu	1.87E-13			Cu	2.03E-13
		Zn	8.93E-09			Zn	6.11E-09
		Cd	NA			Cd	1.07E-10
		Pb	6.36E-12			Pb	2.07E-12
					23734	Cr	2.50E-19
						Ni	5.99E-09
						Cu	1.98E-13
						Zn	6.96E-09
						Cd	1.15E-10
						Pb	3.03E-12

No results are presented for samples 9685 and 13106 (Mill A), and 9525 (Mill B) because no or too few metals were recorded for these samples.

* NA = non-available: the lack of measurement of a metal in a sample results in no free ion activity calculation.

Samples for analysis with *Ceriodaphnia dubia* WET tests (cont.)

Mill	Sample	Metal	Free ion act. [M]	Mill	Sample	Metal	Free ion act. [M]
C	10253	Cr	5.18E-18	D	12669	Cr	1.26E-19
		Ni	1.14E-08			Ni	2.79E-09
		Cu	3.76E-12			Cu	9.98E-14
		Zn	6.07E-08			Zn	1.14E-08
		Cd	5.65E-10			Cd	NA
		Pb	1.42E-11			Pb	3.65E-12
	10574	Cr	1.15E-17		12761	Cr	8.35E-20
		Ni	1.72E-08			Ni	3.78E-09
		Cu	3.51E-12			Cu	1.74E-13
		Zn	2.72E-08			Zn	1.28E-08
		Cd	6.19E-10			Cd	2.85E-10
		Pb	4.36E-12			Pb	2.00E-12
	11351	Cr	1.15E-19		12921	Cr	3.36E-19
		Ni	4.53E-09			Ni	5.03E-09
		Cu	1.19E-13			Cu	5.37E-13
		Zn	5.78E-09			Zn	6.12E-08
		Cd	4.01E-11			Cd	2.23E-10
		Pb	2.24E-12			Pb	5.05E-12
	11572	Cr	8.43E-19		13442	Cr	1.82E-19
		Ni	6.79E-09			Ni	5.27E-09
		Cu	1.85E-13			Cu	1.80E-13
		Zn	8.02E-09			Zn	7.21E-09
		Cd	2.62E-10			Cd	7.66E-11
		Pb	7.42E-11			Pb	2.49E-12
	12309	Cr	4.11E-19		15726	Cr	1.21E-19
		Ni	1.19E-09			Ni	7.49E-09
		Cu	3.67E-13			Cu	2.79E-13
		Zn	1.78E-08			Zn	1.11E-08
		Cd	1.10E-10			Cd	3.17E-10
		Pb	7.34E-12			Pb	6.28E-12
	14392	Cr	1.35E-18		21514	Cr	1.82E-19
		Ni	2.00E-08			Ni	1.87E-08
		Cu	5.93E-13			Cu	3.74E-13
		Zn	2.44E-08			Zn	1.97E-08
		Cd	4.23E-10			Cd	2.36E-10
		Pb	1.55E-11			Pb	3.15E-12
					22591	Cr	3.75E-19
						Ni	1.27E-08
						Cu	3.45E-13
						Zn	1.47E-08
						Cd	2.41E-10
						Pb	1.93E-12
					23735	Cr	1.20E-18
						Ni	3.75E-08
						Cu	1.11E-12
						Zn	4.24E-08
						Cd	3.67E-10
						Pb	1.18E-11

No results are presented for sample 12134 (Mill D) because no metals were recorded for this sample.

* NA = non-available: the lack of measurement of a metal in a sample results in no free ion activity calculation.

Table S3.9 Free ion activities (as modelled in WHAM7) of metals in effluent samples for which *P. promelas* WET bioassays were also performed.

Samples for analysis alongside *Pimephales promelas* WET tests

Mill	Sample	Metal	Free ion act. [M]
A	10452	Cr	7.18E-20
		Ni	4.93E-09
		Cu	6.57E-14
		Zn	9.36E-09
		Cd	3.47E-11
		Pb	7.92E-13
	11141	Cr	8.99E-19
		Ni	9.72E-09
		Cu	2.07E-13
		Zn	1.29E-08
		Cd	7.18E-11
		Pb	4.00E-12
	11707	Cr	1.90E-19
		Ni	7.48E-09
		Cu	1.43E-13
		Zn	7.05E-09
		Cd	1.92E-10
		Pb	1.28E-12
	11995	Cr	3.99E-19
		Ni	5.18E-09
		Cu	1.90E-13
		Zn	6.10E-09
		Cd	5.98E-11
		Pb	1.17E-12

No results are presented for sample 13252 (Mill A) because no metals were recorded for this sample.

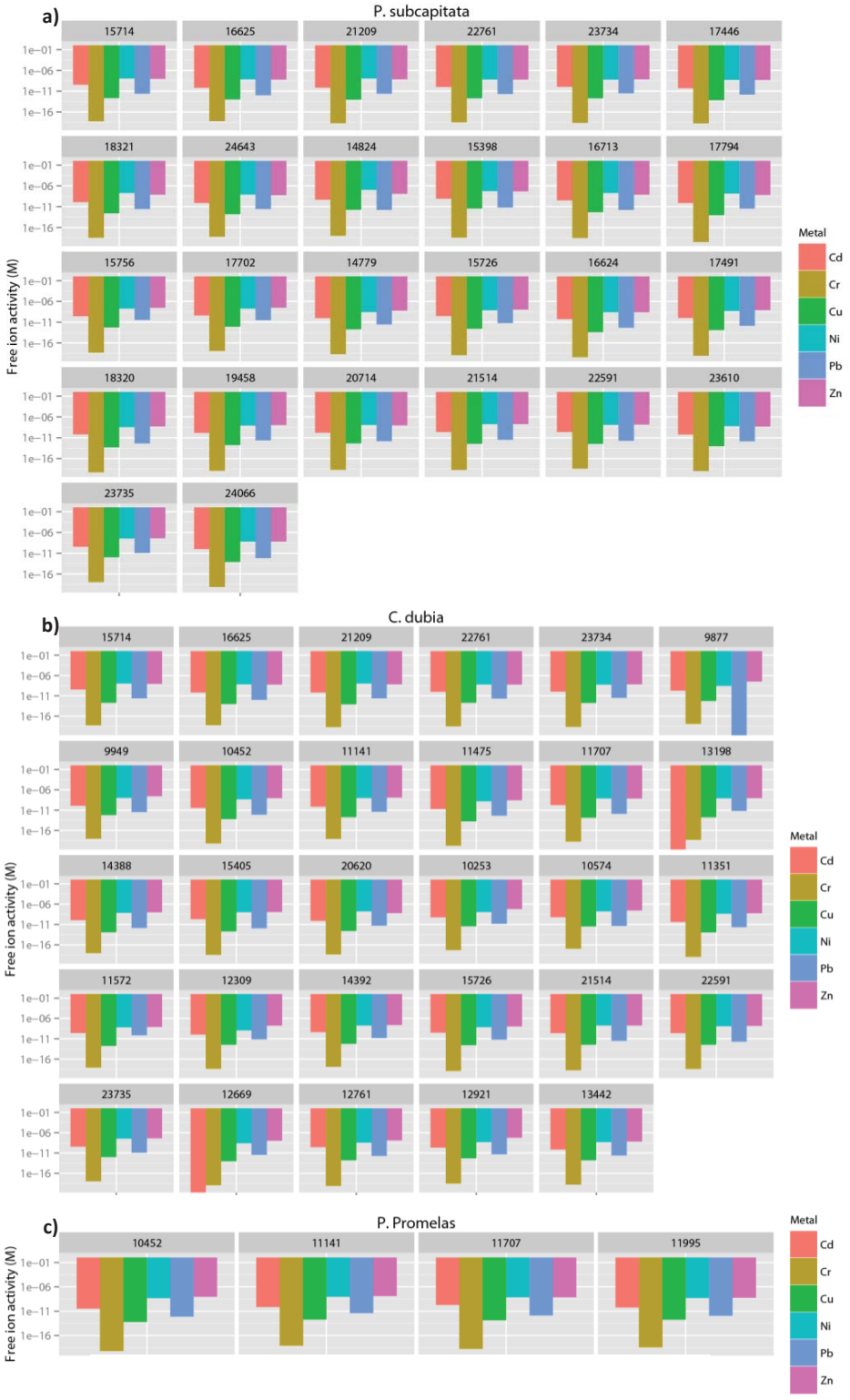

Figure S3.4 Free ion activity of metals in effluent samples per species and mill and sample, presented in logarithmic scale, as modelled in WHAM7.

5.2.6. Metal toxicity prediction models

Table S3.10 Models employed to predict metal toxicity to *P. subcapitata*.

***Pseudokirchneriella subcapitata*: 96 h growth**

Metal (ion)	Model type	End-point	Exposure type/time	Equation (where applicable)	Notes	Reference
Cd^{2+}	FIAM	Growth	Chronic/96 h	[M]		(Rodgher et al., 2012)
Cr^{3+}	FIAM	Growth	Chronic/72 h	[M]	Total metal EC_{50} in the reference converted to free ion EC_{50} via speciation modelling in WHAM7, using the same experimental conditions (pH, hardness etc)	(Vignati et al., 2010)
Cu^{2+}	Regression	Growth	Chronic/72 h	[M]	$R^2 = 0.95$, $p < 0.001$	(De Schamphelaere et al., 2003)
Ni^{2+}	BLM	Growth rate	Chronic/72 h	$2++$ $+$ [M]		(De Schamphelaere et al., 2006)
Pb	Total metal concentration	Growth	Chronic/96 h	[M]		(Chen et al., 1997)
Zn^{2+}	Regression	Growth	Chronic/72 h	[M]	Relation developed from experimental data in reference; $R^2 = 0.92$, $p < 0.001$	(Heijerick et al., 2002)

Table S3.11 Models employed to predict metal toxicity to *C. dubia*.

***Ceriodaphnia dubia*: 7 d reproduction**

Metal (ion)	Model type	Endpoint	Exposure time	Equation (where applicable)	Notes	Reference
Cd^{2+}	BLM	Survival	Acute	Acute modelled in HydroQual BLM version 2.2.3 and converted to chronic via ACR.	Geometric mean of freshwater ACRs for *D. magna* applied: 104.3	(HydroQual Inc. 2007; USEPA 2001)
Cr^{3+}	FIAM	Reproduction	Chronic/7 d	[M]	Total metal EC_{50} in the reference converted to free ion EC_{50} via speciation modelling in WHAM7, using the same experimental conditions (pH, hardness etc)	(Baral et al., 2006)
Cu^{2+}	BLM	Survival	Acute	Acute modelled in HydroQual BLM version 2.2.3 and converted to chronic via ACR.	Geometric mean of freshwater ACRs for *D. magna* applied: 2.55	(HydroQual Inc. 2007; USEPA 1984)
Ni^{2+}	BLM	Reproduction	Chronic/10 d	$2++$ $2+$ [M]		(De Schamphelaere et al., 2006)
Pb^{2+}	Regression	Reproduction	Chronic/7 d	[M]		(Esbaugh et al., 2012)
Zn	Total metal concentration	Reproduction	Chronic/7 d	[M]		(Cooper et al., 2009)

Table S3.12 Models employed to predict metal toxicity to *P. promelas*.

***Pimephales promelas*: 7 d growth**

Metal (ion)	Model type	Endpoint	Exposure time	Equation (where applicable)	Notes	Reference
Cd^{2+}	BLM	Survival	Acute	Acute modelled in HydroQual BLM version 2.2.3 and converted to chronic via ACR.	Geometric mean of freshwater ACRs for *P. promelas* applied: 13.1	(HydroQual Inc. 2007; USEPA 2001)
Cr^{3+}	FIAM	Survival	Acute/48 h	Acute converted to chronic via ACR	Total metal EC_{50} in the reference converted to free ion EC_{50} via speciation modelling in WHAM7, using the same experimental conditions (pH, hardness etc); freshwater ACR for *P. promelas* applied: 27	(Baral et al. 2006; USEPA 1980a)
Cu^{2+}	BLM	Survival	Acute	Acute modelled in HydroQual BLM version 2.2.3 and converted to chronic via ACR.	Freshwater ACR for *P. promelas* applied: 10.1	(HydroQual Inc. 2007; USEPA 1984)
Ni^{2+}	BLM	Survival	Acute/96 h	$2++$ $2+$ [M] Acute converted to chronic via ACR	Freshwater ACR for *P. promelas*: 49	(Deleebeecket al., 2007; USEPA, 1980b)
Pb^{2+}	Regression	Survival	Acute/96 h	[M]	Freshwater ACR for *O. mykiss* applied: 62	(Mager et al., 2011; USEPA, 1980c)
Zn^{2+}	BLM	Survival	Acute	Acute modelled in HydroQual BLM version 2.2.3 and converted to chronic via ACR.	Freshwater ACR for *P. promelas* applied: 5.64	(HydroQual Inc. 2007; USEPA 1980d)

5.2.7. Predicted metal EC_{50} tables

Table S3.13 Predicted metal EC_{50}s to *P. subcapitata.*

Predicted metal EC_{50}s for *Pseudokirchneriella subcapitata*

Mill	Sample	Metal	EC_{50} [M]	Mill	Sample	Metal	EC_{50} [M]
A	15714	Zn	2.12E-07	B	14824	Zn	1.44E-07
		Ni	1.57E-06			Ni	2.49E-06
		Cu	1.76E-09			Cu	7.00E-10
		Cd	6.00E-07			Cd	6.00E-07
		Cr	1.26E-08			Cr	1.26E-08
		Pb	1.28E-05			Pb	1.28E-05
	16625	Zn	2.06E-07		15398	Zn	6.51E-08
		Ni	1.53E-06			Ni	2.03E-06
		Cu	1.65E-09			Cu	1.07E-10
		Cd	6.00E-07			Cd	6.00E-07
		Cr	1.26E-08			Cr	1.26E-08
		Pb	1.28E-05			Pb	1.28E-05
	17446	Zn	1.63E-07		16713	Zn	1.92E-07
		Ni	1.53E-06			Ni	2.29E-06
		Cu	9.42E-10			Cu	1.40E-09
		Cd	6.00E-07			Cd	6.00E-07
		Cr	1.26E-08			Cr	1.26E-08
		Pb	1.28E-05			Pb	1.28E-05
	18321	Zn	1.48E-07		17794	Zn	5.67E-08
		Ni	1.57E-06			Ni	1.94E-06
		Cu	7.48E-10			Cu	7.70E-11
		Cd	6.00E-07			Cd	6.00E-07
		Cr	1.26E-08			Cr	1.26E-08
		Pb	1.28E-05			Pb	1.28E-05
	21209	Zn	1.72E-07				
		Ni	1.56E-06	C	15756	Zn	1.87E-07
		Cu	1.07E-09			Ni	1.77E-06
		Cd	6.00E-07			Cu	1.31E-09
		Cr	1.26E-08			Cd	6.00E-07
		Pb	1.28E-05			Cr	1.26E-08
	22761	Zn	1.97E-07			Pb	1.28E-05
		Ni	1.55E-06		17702	Zn	1.87E-07
		Cu	1.49E-09			Ni	1.79E-06
		Cd	6.00E-07			Cu	1.31E-09
		Cr	1.26E-08			Cd	6.00E-07
		Pb	1.28E-05			Cr	1.26E-08
	23734	Zn	1.54E-07			Pb	1.28E-05
		Ni	1.47E-06				
		Cu	8.26E-10				
		Cd	6.00E-07				
		Cr	1.26E-08				
		Pb	1.28E-05				
	24643	Zn	1.89E-07				
		Ni	1.54E-06				
		Cu	1.35E-09				
		Cd	6.00E-07				

	Cr	1.26E-08
	Pb	1.28E-05

Predicted metal EC_{50}s for *Pseudokirchneriella subcapitata* (cont.)

Mill	Sample	Metal	EC_{50} [M]	Mill	Sample	Metal	EC_{50} [M]
D	14779	Zn	1.74E-07	D	20714	Zn	1.72E-07
		Ni	1.48E-06			Ni	1.59E-06
		Cu	1.11E-09			Cu	1.07E-09
		Cd	6.00E-07			Cd	6.00E-07
		Cr	1.26E-08			Cr	1.26E-08
		Pb	1.28E-05			Pb	1.28E-05
	15726	Zn	1.07E-07		21514	Zn	1.30E-07
		Ni	1.55E-06			Ni	1.52E-06
		Cu	3.51E-10			Cu	5.56E-10
		Cd	6.00E-07			Cd	6.00E-07
		Cr	1.26E-08			Cr	1.26E-08
		Pb	1.28E-05			Pb	1.28E-05
	16624	Zn	1.28E-07		22591	Zn	1.84E-07
		Ni	1.52E-06			Ni	1.55E-06
		Cu	5.38E-10			Cu	1.27E-09
		Cd	6.00E-07			Cd	6.00E-07
		Cr	1.26E-08			Cr	1.26E-08
		Pb	1.28E-05			Pb	1.28E-05
	17491	Zn	1.03E-07		23610	Zn	1.67E-07
		Ni	1.57E-06			Ni	1.42E-06
		Cu	3.18E-10			Cu	1.01E-09
		Cd	6.00E-07			Cd	6.00E-07
		Cr	1.26E-08			Cr	1.26E-08
		Pb	1.28E-05			Pb	1.28E-05
	18320	Zn	1.48E-07		23735	Zn	1.72E-07
		Ni	1.54E-06			Ni	1.52E-06
		Cu	7.48E-10			Cu	1.07E-09
		Cd	6.00E-07			Cd	6.00E-07
		Cr	1.26E-08			Cr	1.26E-08
		Pb	1.28E-05			Pb	1.28E-05
	19458	Zn	1.30E-07		24066	Zn	1.58E-07
		Ni	1.47E-06			Ni	1.53E-06
		Cu	5.56E-10			Cu	8.82E-10
		Cd	6.00E-07			Cd	6.00E-07
		Cr	1.26E-08			Cr	1.26E-08
		Pb	1.28E-05			Pb	1.28E-05

Table S3.14 Predicted metal EC_{50}s to *C. dubia.*

Predicted metal EC_{50}s for *Ceriodaphnia dubia*

Mill	Sample	Metal	EC_{50} [M]	Mill	Sample	Metal	EC_{50} [M]
A	9877*	Zn	3.33E-07	A	14388	Zn	3.33E-07
		Ni	4.03E-08			Ni	5.11E-08
		Cu	2.03E-05			Cu	1.52E-05
		Cd	2.61E-07			Cd	1.61E-07
		Cr	2.70E-11			Cr	2.70E-11
		Pb	NA			Pb	2.92E-09
	9949	Zn	3.33E-07		15405	Zn	3.33E-07
		Ni	4.82E-08			Ni	3.79E-08
		Cu	2.15E-05			Cu	1.34E-05
		Cd	2.70E-07			Cd	1.53E-07
		Cr	2.70E-11			Cr	2.70E-11
		Pb	2.87E-09			Pb	1.92E-09
	10452	Zn	3.33E-07		15714	Zn	3.33E-07
		Ni	1.94E-08			Ni	5.63E-08
		Cu	2.56E-05			Cu	1.48E-05
		Cd	3.19E-07			Cd	1.68E-07
		Cr	2.70E-11			Cr	2.70E-11
		Pb	1.42E-09			Pb	2.68E-09
	11141	Zn	3.33E-07		16625	Zn	3.33E-07
		Ni	1.72E-08			Ni	5.06E-08
		Cu	2.80E-05			Cu	1.86E-05
		Cd	3.44E-07			Cd	2.01E-07
		Cr	2.70E-11			Cr	2.70E-11
		Pb	1.14E-09			Pb	2.59E-09
	11475	Zn	3.33E-07		20620	Zn	3.33E-07
		Ni	3.52E-08			Ni	4.65E-08
		Cu	1.73E-05			Cu	1.53E-05
		Cd	2.00E-07			Cd	1.66E-07
		Cr	2.70E-11			Cr	2.70E-11
		Pb	2.02E-09			Pb	2.47E-09
	11707	Zn	3.33E-07		21209	Zn	3.33E-07
		Ni	1.69E-08			Ni	4.35E-08
		Cu	2.67E-05			Cu	1.83E-05
		Cd	2.96E-07			Cd	2.09E-07
		Cr	2.70E-11			Cr	2.70E-11
		Pb	1.12E-09			Pb	2.08E-09
	13198*	Zn	3.33E-07		22761	Zn	3.33E-07
		Ni	3.44E-08			Ni	4.89E-08
		Cu	1.65E-05			Cu	8.49E-06
		Cd	NA			Cd	9.80E-08
		Cr	2.70E-11			Cr	2.70E-11
		Pb	1.85E-09			Pb	2.47E-09
					23734	Zn	3.33E-07
						Ni	3.06E-08
						Cu	1.37E-05
						Cd	1.47E-07
						Cr	2.70E-11
						Pb	1.82E-09

No results are presented for samples 9685 and 13106 (Mill A), and 9525 (Mill B) because no or too few metals were recorded for these samples.

* NA = non-available: there are no BLM-predicted EC_{50}s for the samples with no metal measurements.

Predicted metal EC_{50}s for *Ceriodaphnia dubia* (cont.)

Mill	Sample	Metal	EC_{50} [M]	Mill	Sample	Metal	EC_{50} [M]
C	10253	Zn	3.33E-07	D	12669*	Zn	3.33E-07
		Ni	1.20E-07			Ni	3.29E-08
		Cu	2.30E-06			Cu	2.15E-05
		Cd	4.31E-08			Cd	NA
		Cr	2.70E-11			Cr	2.70E-11
		Pb	4.83E-09			Pb	1.92E-09
	10574	Zn	3.33E-07		12761	Zn	3.33E-07
		Ni	2.31E-08			Ni	2.30E-08
		Cu	7.04E-06			Cu	2.27E-05
		Cd	8.99E-08			Cd	2.78E-07
		Cr	2.70E-11			Cr	2.70E-11
		Pb	1.73E-09			Pb	1.46E-09
	11351	Zn	3.33E-07		12921	Zn	3.33E-07
		Ni	2.74E-08			Ni	2.71E-08
		Cu	7.37E-06			Cu	3.49E-05
		Cd	8.28E-08			Cd	4.21E-07
		Cr	2.70E-11			Cr	2.70E-11
		Pb	1.92E-09			Pb	1.85E-09
	11572	Zn	3.33E-07		13442	Zn	3.33E-07
		Ni	5.06E-08			Ni	3.76E-08
		Cu	7.60E-06			Cu	2.23E-05
		Cd	9.06E-08			Cd	3.12E-07
		Cr	2.70E-11			Cr	2.70E-11
		Pb	2.68E-09			Pb	1.88E-09
	12309	Zn	3.33E-07		15726	Zn	3.33E-07
		Ni	4.82E-08			Ni	2.41E-08
		Cu	9.44E-06			Cu	2.37E-05
		Cd	1.32E-07			Cd	2.87E-07
		Cr	2.70E-11			Cr	2.70E-11
		Pb	1.95E-09			Pb	1.18E-09
	14392	Zn	3.33E-07		21514	Zn	3.33E-07
		Ni	1.12E-07			Ni	2.90E-08
		Cu	4.67E-06			Cu	2.35E-05
		Cd	8.26E-08			Cd	2.96E-07
		Cr	2.70E-11			Cr	2.70E-11
		Pb	3.28E-09			Pb	1.49E-09
					22591	Zn	3.33E-07
						Ni	4.75E-08
						Cu	1.33E-05
						Cd	1.87E-07
						Cr	2.70E-11
						Pb	2.27E-09
					23735	Zn	3.33E-07
						Ni	4.06E-08
						Cu	6.55E-06
						Cd	1.14E-07
						Cr	2.70E-11
						Pb	2.08E-09

No results are presented for sample 12134 (Mill D) because no metals were recorded for this sample.

* NA = non-available: there are no BLM-predicted EC_{50}s for the samples with no metal measurements.

Table S3.15 Predicted metal EC_{50}s to *P. promelas.*

Predicted metal EC_{50}s for *Pimephales promelas* WET tests			
Mill	**Sample**	**Metal**	**EC_{50} [M]**
A	10452	Zn	2.60E-05
		Ni	1.54E-07
		Cu	2.74E-05
		Cd	3.27E-07
		Cr	5.78E-12
		Pb	3.87E-10
	11141	Zn	2.67E-05
		Ni	1.62E-07
		Cu	2.71E-05
		Cd	3.84E-07
		Cr	5.78E-12
		Pb	3.39E-10
	11707	Zn	2.52E-05
		Ni	1.61E-07
		Cu	2.21E-05
		Cd	3.30E-07
		Cr	5.78E-12
		Pb	3.36E-10
	11995	Zn	2.48E-05
		Ni	1.81E-07
		Cu	2.10E-05
		Cd	2.22E-07
		Cr	5.78E-12
		Pb	5.54E-10

No results are presented for sample 13252 (Mill A) because no metals were recorded for this sample.

5.2.8. Metal *TU* tables and figure

Table S3.16 Estimated metal *TU* s for *P. subcapitata* samples.

Toxicity due to metals towards *Pseudokirchneriella subcapitata*

Mill	Sample	Metal	*TU* [-]	Mill	Sample	Metal	*TU* [-]
A	15714	Zn	4.35E-02	B	14824	Zn	8.80E-02
		Ni	6.99E-03			Ni	4.53E-02
		Cu	1.25E-04			Cu	2.58E-03
		Cd	5.98E-04			Cd	7.99E-04
		Cr	4.53E-11			Cr	8.29E-11
		Pb	1.97E-07			Pb	1.36E-07
	16625	Zn	2.87E-02		15398	Zn	7.71E-01
		Ni	4.49E-03			Ni	2.71E-02
		Cu	6.42E-05			Cu	3.61E-02
		Cd	1.12E-04			Cd	1.41E-03
		Cr	5.11E-11			Cr	2.97E-11
		Pb	8.09E-08			Pb	5.09E-07
	17446	Zn	2.86E-02		16713	Zn	4.17E-02
		Ni	3.31E-03			Ni	8.94E-03
		Cu	7.60E-05			Cu	3.39E-04
		Cd	8.80E-05			Cd	5.61E-04
		Cr	1.59E-11			Cr	2.40E-11
		Pb	1.23E-07			Pb	1.32E-07
	18321	Zn	5.36E-02		17794	Zn	1.22E-01
		Ni	1.28E-02			Ni	7.99E-03
		Cu	3.62E-04			Cu	1.27E-03
		Cd	2.18E-04			Cd	1.32E-04
		Cr	2.78E-11			Cr	2.61E-12
		Pb	2.16E-07			Pb	2.77E-07
	21209	Zn	4.04E-02				
		Ni	7.02E-03	C	15756	Zn	1.52E-01
		Cu	8.28E-05			Ni	1.10E-02
		Cd	1.14E-04			Cu	4.67E-04
		Cr	1.71E-11			Cd	4.84E-04
		Pb	1.94E-07			Cr	3.86E-11
	22761	Zn	3.09E-02			Pb	2.83E-06
		Ni	4.37E-03		17702	Zn	1.72E-01
		Cu	1.36E-04			Ni	1.14E-02
		Cd	1.79E-04			Cu	6.84E-04
		Cr	2.59E-11			Cd	6.91E-04
		Pb	1.62E-07			Cr	1.03E-10
	23734	Zn	4.52E-02			Pb	2.57E-06
		Ni	4.06E-03				
		Cu	2.40E-04				
		Cd	1.91E-04				
		Cr	1.98E-11				
		Pb	2.37E-07				
	24643	Zn	3.04E-02				
		Ni	5.63E-03				
		Cu	1.19E-04				
		Cd	1.36E-04				

		Cr	4.87E-11
		Pb	2.16E-07

Toxicity due to metals towards *Pseudokirchneriella subcapitata* (cont.)

Mill	Sample	Metal	*TU* [-]	Mill	Sample	Metal	*TU* [-]
D	14779	Zn	3.53E-02	D	20714	Zn	5.37E-02
		Ni	1.95E-03			Ni	7.62E-03
		Cu	1.78E-04			Cu	4.20E-04
		Cd	1.63E-04			Cd	2.64E-04
		Cr	1.74E-11			Cr	1.57E-11
		Pb	2.30E-07			Pb	1.15E-07
	15726	Zn	1.03E-01		21514	Zn	1.51E-01
		Ni	4.83E-03			Ni	1.23E-02
		Cu	7.96E-04			Cu	6.73E-04
		Cd	5.29E-04			Cd	3.93E-04
		Cr	9.64E-12			Cr	1.44E-11
		Pb	4.90E-07			Pb	2.46E-07
	16624	Zn	1.98E-02		22591	Zn	7.95E-02
		Ni	1.68E-03			Ni	8.19E-03
		Cu	7.82E-05			Cu	2.72E-04
		Cd	9.41E-05			Cd	4.02E-04
		Cr	3.22E-12			Cr	2.97E-11
		Pb	3.78E-08			Pb	1.51E-07
	17491	Zn	8.21E-02		23610	Zn	3.02E-02
		Ni	3.23E-03			Ni	4.67E-03
		Cu	4.34E-04			Cu	9.66E-05
		Cd	1.80E-04			Cd	1.00E-04
		Cr	7.32E-12			Cr	7.69E-12
		Pb	1.08E-07			Pb	1.10E-07
	18320	Zn	3.62E-02		23735	Zn	2.46E-01
		Ni	2.49E-03			Ni	2.47E-02
		Cu	7.04E-05			Cu	1.03E-03
		Cd	1.01E-04			Cd	6.12E-04
		Cr	3.80E-12			Cr	9.52E-11
		Pb	3.43E-08			Pb	9.23E-07
	19458	Zn	8.25E-02		24066	Zn	4.15E-02
		Ni	5.92E-03			Ni	4.51E-03
		Cu	3.10E-04			Cu	9.83E-05
		Cd	2.61E-04			Cd	1.70E-04
		Cr	9.72E-12			Cr	6.47E-12
		Pb	1.88E-07			Pb	5.52E-08

Table S3.17 Estimated metal *TU* s for *C. dubia* samples.

Toxicity due to metals towards *Ceriodaphnia dubia*

Mill	Sample	Metal	*TU* [-]	Mill	Sample	Metal	*TU* [-]
A	9877*	Zn	1.04E-01	A	14388	Zn	2.95E-02
		Ni	7.51E-02			Ni	1.45E-01
		Cu	3.03E-08			Cu	8.39E-09
		Cd	7.75E-04			Cd	7.47E-04
		Cr	4.98E-08			Cr	3.41E-08
		Pb	NA			Pb	4.69E-04
	9949	Zn	8.39E-02		15405	Zn	3.54E-02
		Ni	2.27E-01			Ni	2.85E-01
		Cu	3.02E-08			Cu	1.49E-08
		Cd	4.76E-04			Cd	1.34E-03
		Cr	3.57E-08			Cr	1.26E-08
		Pb	1.20E-03			Pb	6.14E-04
	10452	Zn	2.81E-02		15714	Zn	2.77E-02
		Ni	2.54E-01			Ni	1.95E-01
		Cu	2.57E-09			Cu	1.48E-08
		Cd	1.09E-04			Cd	2.13E-03
		Cr	2.66E-09			Cr	2.12E-08
		Pb	5.59E-04			Pb	9.39E-04
	11141	Zn	3.87E-02		16625	Zn	1.77E-02
		Ni	5.64E-01			Ni	1.36E-01
		Cu	7.39E-09			Cu	5.69E-09
		Cd	2.08E-04			Cd	3.35E-04
		Cr	3.33E-08			Cr	2.38E-08
		Pb	3.51E-03			Pb	3.99E-04
	11475	Zn	8.17E-03		20620	Zn	1.92E-02
		Ni	4.48E-02			Ni	3.77E-01
		Cu	1.04E-09			Cu	1.66E-08
		Cd	9.05E-05			Cd	4.67E-04
		Cr	7.38E-10			Cr	1.57E-08
		Pb	2.22E-04			Pb	2.18E-03
	11707	Zn	2.12E-02		21209	Zn	2.09E-02
		Ni	4.44E-01			Ni	2.51E-01
		Cu	5.34E-09			Cu	4.85E-09
		Cd	6.48E-04			Cd	3.29E-04
		Cr	7.04E-09			Cr	8.00E-09
		Pb	1.14E-03			Pb	1.19E-03
	13198*	Zn	2.68E-02		22761	Zn	1.83E-02
		Ni	2.48E-01			Ni	1.38E-01
		Cu	1.13E-08			Cu	2.39E-08
		Cd	NA			Cd	1.09E-03
		Cr	1.85E-08			Cr	1.21E-08
		Pb	3.43E-03			Pb	8.41E-04
					23734	Zn	2.09E-02
						Ni	1.96E-01
						Cu	1.45E-08
						Cd	7.81E-04
						Cr	9.26E-09
						Pb	1.66E-03

No results are presented for samples 9685 and 13106 (Mill A), and 9525 (Mill B) because no or too few metals were recorded for these samples.

* NA = non-available: the lack of measurement of a metal in a sample results in no toxicity calculation.

Toxicity due to metals towards *Ceriodaphnia dubia* (cont.)

Mill	Sample	Metal	*TU* [-]	Mill	Sample	Metal	*TU* [-]
C	10253	Zn	1.82E-01	D	12669	Zn	3.43E-02
		Ni	9.49E-02			Ni	8.46E-02
		Cu	1.63E-06			Cu	4.63E-09
		Cd	1.31E-02			Cd	0.00E+00
		Cr	1.92E-07			Cr	4.68E-09
		Pb	2.94E-03			Pb	1.90E-03
	10574	Zn	8.16E-02		12761	Zn	3.84E-02
		Ni	7.42E-01			Ni	1.65E-01
		Cu	4.99E-07			Cu	7.67E-09
		Cd	6.89E-03			Cd	1.03E-03
		Cr	4.26E-07			Cr	3.09E-09
		Pb	2.52E-03			Pb	1.37E-03
	11351	Zn	1.74E-02		12921	Zn	1.84E-01
		Ni	1.65E-01			Ni	1.85E-01
		Cu	1.61E-08			Cu	1.54E-08
		Cd	4.84E-04			Cd	5.29E-04
		Cr	4.26E-09			Cr	1.25E-08
		Pb	1.17E-03			Pb	2.73E-03
	11572	Zn	2.41E-02		13442	Zn	2.17E-02
		Ni	1.34E-01			Ni	1.40E-01
		Cu	2.44E-08			Cu	8.05E-09
		Cd	2.89E-03			Cd	2.46E-04
		Cr	3.12E-08			Cr	6.75E-09
		Pb	2.77E-02			Pb	1.32E-03
	12309	Zn	5.33E-02		15726	Zn	3.33E-02
		Ni	2.48E-02			Ni	3.11E-01
		Cu	3.89E-08			Cu	1.17E-08
		Cd	8.34E-04			Cd	1.11E-03
		Cr	1.52E-08			Cr	4.50E-09
		Pb	3.76E-03			Pb	5.33E-03
	14392	Zn	7.32E-02		21514	Zn	5.93E-02
		Ni	1.78E-01			Ni	6.44E-01
		Cu	1.27E-07			Cu	1.60E-08
		Cd	5.12E-03			Cd	7.97E-04
		Cr	4.98E-08			Cr	6.72E-09
		Pb	4.72E-03			Pb	2.11E-03
					22591	Zn	4.40E-02
						Ni	2.68E-01
						Cu	2.60E-08
						Cd	1.29E-03
						Cr	1.39E-08
						Pb	8.50E-04
					23735	Zn	1.27E-01
						Ni	9.23E-01
						Cu	1.69E-07
						Cd	3.21E-03
						Cr	4.44E-08
						Pb	5.67E-03

No results are presented for sample 12134 (Mill D) because no metals were recorded for this sample.

Table S3.18 Estimated metal *TU* s for *P. promelas* samples.

Toxicity due to metals towards *Pimephales promelas*

Mill	Sample	Metal	*TU* [-]
A	10452	Zn	3.59E-04
		Ni	3.20E-02
		Cu	2.40E-09
		Cd	1.06E-04
		Cr	1.24E-08
		Pb	2.04E-03
	11141	Zn	4.82E-04
		Ni	5.98E-02
		Cu	7.62E-09
		Cd	1.87E-04
		Cr	1.56E-07
		Pb	1.18E-02
	11707	Zn	2.80E-04
		Ni	4.65E-02
		Cu	6.46E-09
		Cd	5.82E-04
		Cr	3.29E-08
		Pb	3.80E-03
	11995	Zn	2.46E-04
		Ni	2.86E-02
		Cu	9.06E-09
		Cd	2.69E-04
		Cr	6.90E-08
		Pb	2.11E-03

No results are presented for sample 13252 (Mill A) because no metals were recorded for this sample.

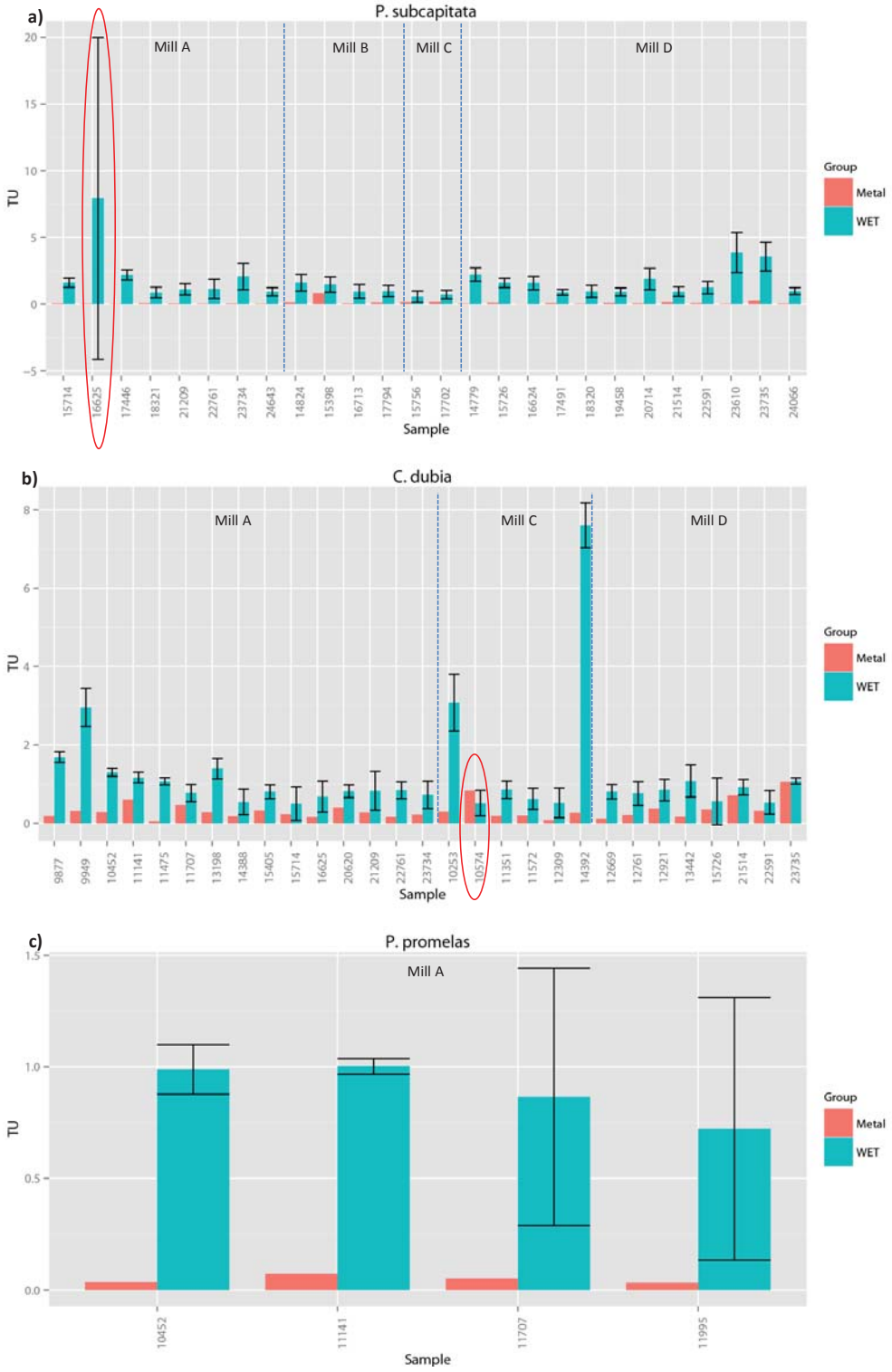

Figure S3.5 Estimated TU due to the whole effluent and due to the metals, per species, mill and sample. Indicated on the plots are the 95% confidence intervals for the TU_{WET} estimations, as well as two samples which were excluded from further analysis: a) sample 16625: prohibitively high uncertainty in TU_{WET} estimation b) sample 10574: TU due to metals > TU_{WET} (unrealistic scenario).

5.2.9. $EC50_{TOC}$ and final results tables

Table S3.19 Summary of all results for *P.subcapitata*.

Mill	Sample	TU_{WET}	ΣTU_{metal}	TU_{TOC}	C_{TOC}	$EC50_{TOC}$
A	15714	1.61	0.05	1.56	119	76.2
A	17446	2.20	0.03	2.17	118	54.4
A	18321	0.88	0.07	0.81	144	177.2
A	21209	1.12	0.05	1.07	127	118.5
A	22761	1.15	0.04	1.12	78.8	70.6
A	23734	2.08	0.05	2.03	98.4	48.6
A	24643	0.94	0.04	0.90	108	119.4
B	14824	1.62	0.14	1.48	50	33.8
B	15398	1.48	0.84	0.64	74	114.7
B	16713	0.96	0.05	0.91	30.4	33.5
B	17794	0.99	0.13	0.85	50	58.5
C	15756	0.57	0.16	0.41	72	177.1
C	17702	0.73	0.18	0.55	99	180.7
D	14779	2.22	0.04	2.18	155	71.0
D	15726	1.60	0.11	1.49	113	75.8
D	16624	1.59	0.02	1.56	144	92.1
D	17491	0.90	0.09	0.82	102	124.7
D	18320	0.96	0.04	0.93	131	141.5
D	19458	0.93	0.09	0.84	105	125.3
D	20714	1.90	0.06	1.84	127	69.1
D	21514	0.95	0.16	0.78	120	153.4
D	22591	1.24	0.09	1.15	85	73.6
D	23610	3.88	0.04	3.85	153	39.7
D	23735	3.57	0.27	3.30	40.6	12.3
D	24066	0.99	0.05	0.94	133	140.9

Table S3.20 Summary of all results for *C. dubia*.

Summary of results for *Ceriodaphnia dubia*

Mill	Sample	TU_{WET}	ΣTU_{metal}	TU_{TOC}	C_{TOC}	$EC50_{TOC}$
A	9877	1.69	0.18	1.51	127	84.2
A	9949	2.95	0.31	2.64	143	54.2
A	10452	1.30	0.28	1.01	122.8	121.2
A	11141	1.17	0.61	0.56	125	222.6
A	11475	1.07	0.05	1.02	111	109.0
A	11707	0.77	0.47	0.30	131	432.2
A	13198	1.40	0.28	1.12	115	102.8
A	14388	0.54	0.18	0.37	129	352.4
A	15405	0.81	0.32	0.48	95	196.6
A	15714	0.50	0.23	0.27	119	433.6
A	16625	0.68	0.15	0.53	145	275.6
A	20620	0.82	0.40	0.42	122	290.5
A	21209	0.83	0.27	0.55	127	230.3
A	22761	0.84	0.16	0.69	78.8	114.8
A	23734	0.72	0.22	0.50	98.4	194.9
C	10253	3.08	0.29	2.78	30.4	10.9
C	11351	0.86	0.18	0.67	55	81.6
C	11572	0.62	0.19	0.44	67	153.9
C	12309	0.52	0.08	0.44	65	148.3
C	14392	7.61	0.26	7.34	48	6.5
D	12669	0.81	0.12	0.69	187	272.8
D	12761	0.76	0.21	0.56	120	216.1
D	12921	0.85	0.37	0.48	128	268.2
D	13442	1.08	0.16	0.92	115	125.5
D	15726	0.56	0.35	0.21	113	535.9
D	21514	0.92	0.71	0.21	120	560.5
D	22591	0.53	0.31	0.22	85	394.9
D	23735*	1.08	1.06	0.02	40.6	1900.0

*The $EC50_{TOC}$ result for sample 23735 was excluded from the analysis as an outlier (see Figure 3.11)

Table S3.21 Summary of all results for *P. promelas*.

Summary of results for *Pimephales promelas*

Mill	Sample	TU_{WET}	ΣTU_{metal}	TU_{TOC}	C_{TOC}	$EC50_{TOC}$
A	10452	0.99	0.03	0.95	122.8	128.8
A	11141	1.00	0.07	0.93	125	134.4
A	11707	0.87	0.05	0.82	131	160.7
A	11995	0.72	0.03	0.69	156	225.9

5.3. Appendix for section 4.1 Spatial differentiation of ecotoxicity and human toxicity

5.3.1. Physical chemical properties

Table S4.1 presents the test set and chosen properties.

Table S4.1: Test set of chemicals and related properties used in MAPPE runs

Chemicals	Clusters	CAS	MW	K_{ow}	K_{aw}	K_h25C	Air decay rate	Air decay rate	Soil decay rate	Ssoil decay rate	Water decay rate
			[g/mol]	[-]	[-]	[Pa.m3.mol^{-1}]	[1/s]	[1/hour]	[1/s]	[1/hour]	[1/s]
								Omniitox database		Omniitox database	
Tetrachloroethylene	1a	127-18-4	166	7,59E+02	7,15E-01	1,77E+03	3,50E-07	1,26E-03	1,13E-07	4,08E-04	1,10E-07
Carbon tetrachloride	1a	56-23-5	154	4,37E+02	1,11E+00	2,76E+03	1,13E-08		3,19E-08	1,15E-04	1,13E-07
Butadiene	1a	106-99-0	54	9,77E+01	2,97E+00	7,36E+03	1,13E-08		3,50E-07	1,26E-03	1,13E-07
Methomyl	2a	16752-77-5	162	3,98E+00	7,43E-09	1,84E-05	3,32E-06		3,83E-07	1,38E-03	3,49E-08
Acephate	2a	30560-19-1	183	1,41E-01	2,02E-11	5,01E-08	5,59E-06	9,18E-02	3,64E-06	1,31E-02	1,50E-07
Formaldehyde	2b	50-00-0	30	2,24E+00	1,36E-05	3,37E-02	5,31E-05	1,60E-02	3,50E-06	1,26E-02	2,01E-06
PCBs	3a	1336-36-3	292	1,26E+07	1,68E-02	4,15E+01	4,07E-07		2,14E-07	7,70E-04	5,70E-07
Phthalate, di(n-octyl)	3a	117-84-0	391	1,26E+08	1,04E-04	2,57E-01	1,03E-05		5,72E-07	2,06E-03	5,73E-07
Benzene, hexabromo-	3a	87-82-1	551	1,17E+06	1,13E-03	2,81E+00	5,73E-09		1,34E-07	4,81E-04	1,34E-07
Cypermethrin	3a	52315-07-8	416	3,98E+06	7,75E-06	1,92E-02	1,07E-05		1,54E-07	5,56E-04	1,60E-06
Mirex	3a	2385-85-5	546	7,94E+06	3,27E-02	8,11E+01	1,13E-06		3,50E-09	1,26E-05	1,13E-06
Dicofol	3b	115-32-2	370	1,05E+05	9,77E-06	2,42E-02	1,72E-06		1,32E-07	4,75E-04	2,14E-07
Heptachlor epoxide	3b	1024-57-3	389	9,55E+04	8,48E-04	2,10E+00	2,59E-06		2,74E-08	9,87E-05	2,74E-08
p-Dichlorobenzene	4a	106-46-7	147	2,51E+03	9,73E-02	2,41E+02	3,50E-07		3,50E-08	1,26E-04	1,13E-07
Aldrin	4a	309-00-2	365	1,02E+03	1,78E-03	4,40E+00	3,86E-05	1,39E-01	1,13E-08	4,08E-05	1,10E-08
1,1,2,2-Tetrachloroethane	4a	79-34-5	168	2,45E+02	1,48E-02	3,67E+01	1,13E-08		3,50E-08	1,26E-04	1,13E-07
Anthracene	4b	120-12-7	178	3,47E+04	2,25E-03	5,56E+00	3,50E-06		3,50E-08	1,26E-04	3,50E-07
gamma-HCH	4b	58-89-9	291	5,01E+03	2,08E-04	5,14E-01	1,85E-07		1,13E-08	4,08E-05	1,13E-08
Methanol	5a	67-56-1	32	1,70E-01	1,84E-04	4,55E-01	4,91E-07	1,70E-03	3,50E-06	1,26E-02	3,50E-06

1,2-Dichloroethane	5a	107-06-2	99	3,02E+01	4,77E-02	1,18E+02	1,13E-07		3,50E-08	1,26E-04	1,13E-07
Ethyl acetate	5a	141-78-6	88	5,37E+00	5,41E-03	1,34E+01	9,92E-07		1,13E-06	4,08E-03	2,01E-06
N-Nitrosodiethylamine	5a	55-18-5	102	3,02E+00	1,47E-04	3,63E-01	3,21E-05	3,19E-02	1,13E-07	4,08E-04	3,21E-05
Dimethyl phthalate	6a	131-11-3	194	1,32E+02	4,24E-06	1,05E-02	1,13E-06		3,50E-07	1,26E-03	1,13E-06
Thioperoxydicarbonic diamide, tetramethyl-	6a	137-26-8	240	5,37E+01	1,23E-05	3,04E-02	1,13E-06	4,08E-03	3,50E-07	1,26E-03	1,13E-06
Propoxur	6b	114-26-1	209	3,16E+01	5,77E-08	1,43E-04	3,85E-05	1,63E-01	3,50E-07	1,26E-03	3,50E-07
Captan	6c	133-06-2	301	2,00E+02	2,62E-07	6,48E-04	1,13E-05		3,50E-07	1,26E-03	1,13E-05
Pronamide	6c	23950-58-5	256	2,69E+03	3,95E-07	9,77E-04	6,62E-06		9,97E-08	3,59E-04	1,97E-07
1H-Isoindole-1,3(2H)-dione, 2-(trichloromethyl)thio -	6c	133-07-3	297	7,08E+02	3,09E-06	7,66E-03	7,87E-06		1,40E-08	5,04E-05	1,40E-08
Benomyl	6c	17804-35-2	290	2,00E+02	1,99E-10	4,93E-07	3,86E-05	1,39E-01	1,13E-07	4,08E-04	1,13E-06
Hexachlorobutadiene	7a	87-68-3	261	6,03E+04	4,16E-01	1,03E+03	1,50E-08	4,03E-05	1,13E-07	4,07E-04	1,10E-07
Hexachlorocyclopentadiene	7a	77-47-4	273	1,10E+05	1,09E+00	2,70E+03	1,97E-07		4,58E-07	1,65E-03	2,23E-06
Trifluralin	7b	1582-09-8	336	2,19E+05	4,16E-03	1,03E+01	1,13E-06	7,77E-02	1,13E-07	4,08E-04	1,13E-07
Hexachlorobenzene	7b	118-74-1	285	3,16E+05	6,86E-02	1,70E+02	2,62E-08		3,50E-09	1,26E-05	3,50E-09
Heptachlor	7b	76-44-8	373	1,86E+05	1,19E-02	2,94E+01	3,50E-06		1,13E-07	4,08E-04	3,50E-07
Nitrobenzene		98-95-3	123	7.1E+01	9.7E-04	2.1E+00	3.9E-05		2.1E+00	9.7E-04	1.1E-07
Endosulfan		115-29-7	407	6.8E+03	2.6E-03		5.0E-06			2.6E-03	1.7E-06

Figure S4.1 presents the different substances in the chemical space.

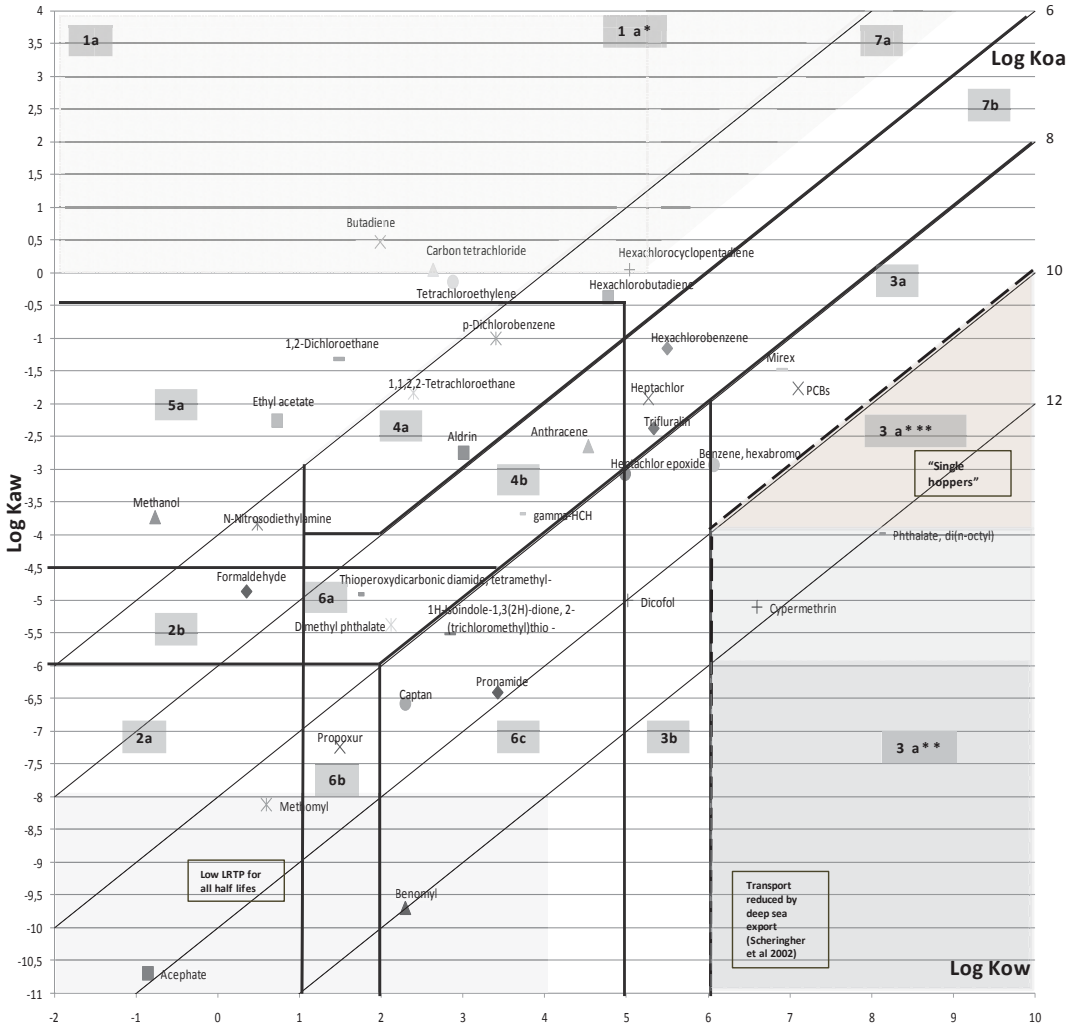

Figure S4.1: Sub-sections of the chemical space (1a, 2a …) with similar environmental behavior and location of the 36 representative chemicals in the test set (modified from Sala et al 2011)

5.3.2. Models description

MAPPE Global is a GIS based model that builds on the concept of the European version (Pistocchi 2008; Pistocchi et al 2010) and is a spatially-resolved steady state multimedia model. Currently, it computes only the removal rates of a substance with given physico-chemical properties. It is composed of an atmospheric boundary layer, soil, inland and seawater, for the whole world, with a resolution of 1°x1° (except for some parameters, which are defined at finer resolution). Advection at the global scale between cells is not yet modelled in term of transport but only in term of quantity subject to advection from each cell. Hence, the influence of distributing an emission over a region, which would reduce the maximum potential variability for some types of chemical, is not modelled at the global scale. The detailed model description, background parameters and input data are reported in Pistocchi et al 2011.

Nevertheless, we use MAPPE global to analyze spatial variability related to global pattern in removal rate and, as a further development, to build scenarios at global scale based on specific spatial patterns.

Generally, global scale multimedia models were used to illustrate the potential of certain persistent pollutants to migrate to, and accumulate in, polar regions (Mac Leod et al 2010).

In this study, we use a global model at high resolution to explore variability related to the interaction between chemical and environmental properties accounting for removal rates chemical–dependent. This means we focused on removal rates whose values are affected by chemical physical properties and not on those chemical- independent (e.g. assuming a persistent chemical emitted to air, the advection removal rate is chemical independent because it mainly reflects atmospheric mass transport). Actually, MAPPE Global computes chemical quantity subject to advection but yet the chemical transport in space. For this reason we used MAPPE to account for chemical specific variability in removal rates at global scale in order to support building global archetypes.

At equal emission rates (one unit of emission), the removal rates are expected to be different for different groups of chemicals and for different environmental conditions. Under this assumption, MAPPE Global model was run in order to assess the spatial variability in the removal rates for the test set of chemicals.

MAPPE Europe

In order to understand the spatial variability of chemicals distributions and fate, it is necessary to test models at higher resolutions. For this purpose, we ran the multimedia model MAPPE Europe. This is a GIS based model which provides a user-friendly way to simulate fluxes and concentrations of chemical pollutants emitted by industrial and agricultural activities, other chemical emission diffusive or point sources, or widespread used substances within households or urban environment. The target contaminants are organic compounds such as Persistent Organic Pollutants (e.g. polychlorinated biphenyls, dioxins), pesticides, pharmaceuticals, volatile organic compounds, or other industrial chemicals. Spatial extent is the European continent with resolution of 1x1 km. The analysis could be performed by grid cell (1*1 km), by watershed, by country and for overall Europe. There are some computational constraints in developing a multimedia model at high resolution. For the atmospheric part of Mappe Europe a source receptor matrix was used, but this implies a number of assumptions related to emission and receptor location. Using MAPPE Europe, we

calculated annual average environmental concentration in air, soil, surface water and European seas, as well fate factors and characterisation factors. The CF's are actually calculated using the effect factors provided by USEtox (potentially Affected Fraction of species [PAF].m^3.day.kg-1), in order to perform cross comparisons. The results serve also as a basis for determining condition that needs spatially resolved models at different resolutions.

5.3.3. Structure of the source receptor matrix of MAPPE Europe

In figure S.4.2, the structure of the SR matrix is presented with an example related to an emission from France.

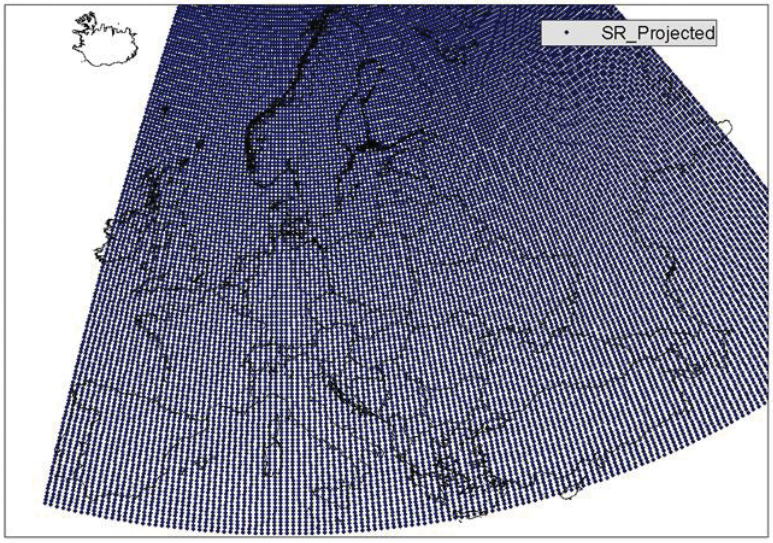

Figure S4.2: Map of the SR matrix composed by 19600 cells

Using the SR matrix it is possible to compute the concentration of a substance in the atmosphere, due to a specific location of the emission. In the example in fig S.4.3, for an emission in France, SR air concentration in the SR nodes are reported.

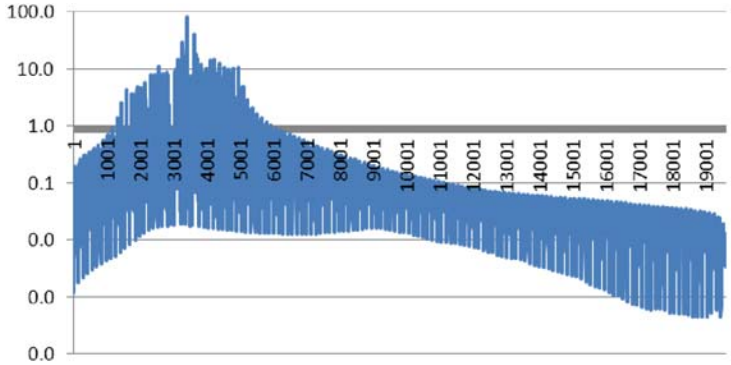

Figure S4.3: Fraction of chemical (in µg/Mt) in the 19600 nodes of the SR matrix after an emission of 1 Mt/year in France of a non-decaying chemical

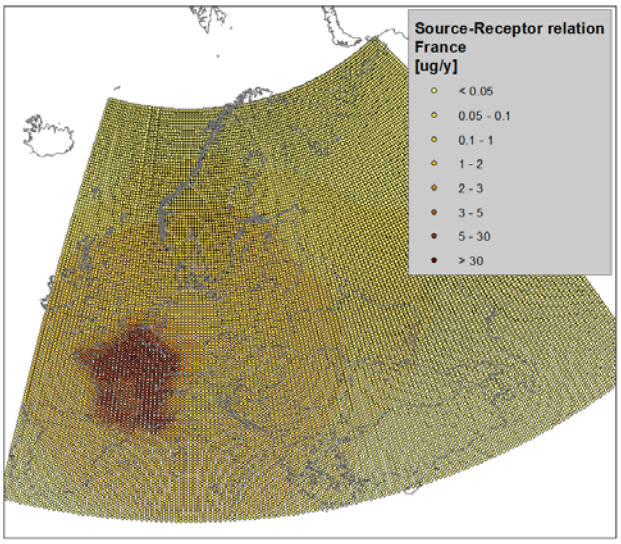

Figure S4.4: Map of the SR relations between after an emission in France

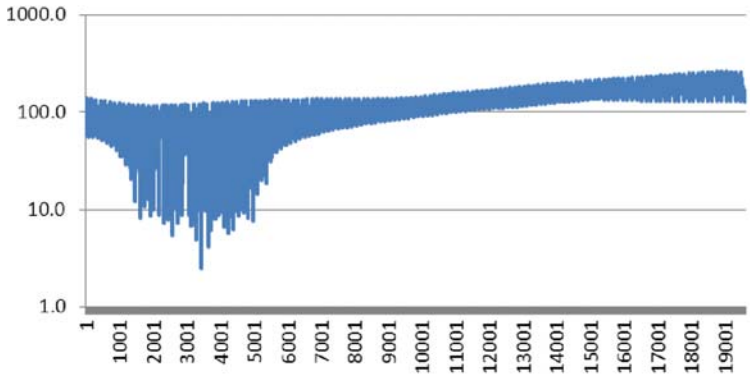

Figure S4.5: Travel time (in days) from France nodes to the other nodes of the SR matrix.

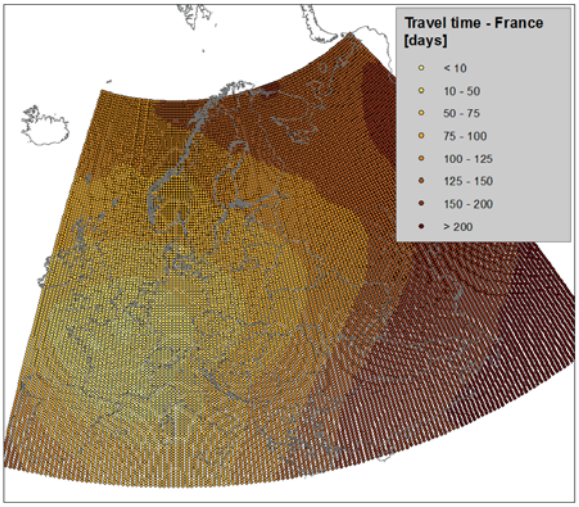

Figure S4.6: Map of the travel time (days) for each node of the SR matrix, after an emission in France

5.3.4. Landscape data for USEtox parametrization

Table S4.2shows the landscape parameters for the 17 subcontinental and the 8 zone continental resolution

Table S4.2: USEtox landscape parameters for the 17 subcontinental and the 8 zone continental resolution

ID #	Name	Continental scale													
		Area land	Area sea	Areafrac freshwater	Areafrac nat soil	Areafrac agr soil	Areafrac other soil	Temp	Wind speed	Rain rate	Depth freshwater	RiverFlow reg-cont	Fraction run off	Fraction infiltration	Soil erosion
		km^2	km^2	[-]	[-]	[-]	[-]	°C	$m.s^{-1}$	$mm.y^{-1}$	m	[-]	[-]	[-]	$mm.y^{-1}$
W1	West Asia	1.7E+07	7.4E+05	1.7E-02	0.88	1.0E-01	1.0E-20	1.2E+01	7.3E+00	2.2E+02	1.3E+01	0.0E+00	4.6E-01	2.7E-01	3.0E-02
W2	Indochina	3.3E+06	2.2E+06	3.6E-02	0.86	1.0E-01	1.0E-20	1.2E+01	4.9E+00	2.4E+03	1.3E+01	0.0E+00	2.7E-01	2.7E-01	3.0E-02
W3	N. Australia	6.6E+06	1.6E+06	9.9E-03	0.89	1.0E-01	1.0E-20	1.2E+01	4.4E+00	1.5E+03	3.0E+00	0.0E+00	2.0E-01	2.7E-01	3.0E-02
W4	S. Australia+	1.5E+06	6.4E+05	1.2E-02	0.89	1.0E-01	1.0E-20	1.2E+01	1.0E+01	5.1E+02	3.0E+00	0.0E+00	1.0E-01	2.7E-01	3.0E-02
W5	S. Africa	1.0E+07	6.2E+05	2.2E-02	0.88	1.0E-01	1.0E-20	1.2E+01	3.5E+00	1.0E+03	4.6E+01	0.0E+00	1.9E-01	2.7E-01	3.0E-02
W6	N. Africa	2.4E+07	9.7E+05	1.9E-02	0.88	1.0E-01	1.0E-20	1.2E+01	5.1E+00	5.1E+02	4.6E+01	0.0E+00	1.8E-01	2.7E-01	3.0E-02
W7	Argentina+	4.2E+06	1.1E+06	1.5E-02	0.89	1.0E-01	1.0E-20	1.2E+01	7.4E+00	7.0E+02	8.0E+00	0.0E+00	3.0E-01	2.7E-01	3.0E-02
W8	Brazil+	1.1E+07	5.8E+05	8.3E-03	0.89	1.0E-01	1.0E-20	1.2E+01	4.9E+00	1.8E+03	8.0E+00	0.0E+00	4.0E-01	2.7E-01	3.0E-02
W9	Central America	5.9E+06	1.3E+06	3.6E-02	0.86	1.0E-01	1.0E-20	1.2E+01	7.3E+00	2.0E+03	2.0E+01	0.0E+00	3.8E-01	2.7E-01	3.0E-02
W10	US+	1.4E+07	1.8E+06	3.4E-02	0.87	1.0E-01	1.0E-20	1.2E+01	7.0E+00	7.1E+02	2.0E+01	0.0E+00	3.7E-01	2.7E-01	3.0E-02
W12	N. Eur. + N. Canada	1.8E+07	5.6E+06	4.9E-02	0.85	1.0E-01	1.0E-20	1.2E+01	8.8E+00	4.9E+02	1.7E+01	0.0E+00	3.6E-01	2.7E-01	3.0E-02
W13	Europe+	8.6E+06	1.7E+06	1.6E-02	0.88	1.0E-01	1.0E-20	1.2E+01	6.8E+00	5.5E+02	1.5E+01	0.0E+00	1.7E-01	2.7E-01	3.0E-02
W14	East Indies	2.0E+06	1.4E+06	3.0E-02	0.87	1.0E-01	1.0E-20	1.2E+01	8.0E+00	1.5E+03	3.0E+00	0.0E+00	2.0E-01	2.7E-01	3.0E-02
IND	India	4.6E+06	4.6E+05	4.2E-02	0.86	1.0E-01	1.0E-20	1.2E+01	5.0E+00	1.2E+03	1.3E+01	0.0E+00	2.7E-01	2.7E-01	3.0E-02
CHI	China	6.4E+06	8.4E+05	4.6E-02	0.85	1.0E-01	1.0E-20	1.2E+01	6.1E+00	1.2E+03	1.3E+01	0.0E+00	2.7E-01	2.7E-01	3.0E-02
JAP	Japan	6.0E+05	4.2E+05	4.4E-02	0.86	1.0E-01	1.0E-20	1.2E+01	8.3E+00	2.4E+03	1.3E+01	0.0E+00	2.7E-01	2.7E-01	3.0E-02
North America	North America	1.4E+07	1.8E+06	3.4E-02	8.7E-01	1.0E-01	1.0E-20	1.2E+01	7.0E+00	7.1E+02	2.0E+01	0.0E+00	3.7E-01	2.7E-01	3.0E-02
Latin America	Latin America	2.1E+07	3.0E+06	1.8E-02	8.8E-01	1.0E-01	1.0E-20	1.2E+01	6.5E+00	1.6E+03	1.5E+01	0.0E+00	3.8E-01	2.7E-01	3.0E-02
Europe	Europe	8.6E+06	1.7E+06	1.6E-02	8.8E-01	1.0E-01	1.0E-20	1.2E+01	6.8E+00	5.5E+02	1.5E+01	0.0E+00	1.7E-01	2.7E-01	3.0E-02
Africa+Middle East	Africa+Middle East	3.4E+07	1.6E+06	2.0E-02	8.8E-01	1.0E-01	1.0E-20	1.2E+01	4.3E+00	6.6E+02	4.6E+01	0.0E+00	1.8E-01	2.7E-01	3.0E-02
Central Asia	Central Asia	1.7E+07	7.4E+05	1.7E-02	8.8E-01	1.0E-01	1.0E-20	1.2E+01	7.3E+00	2.2E+02	1.3E+01	0.0E+00	4.6E-01	2.7E-01	3.0E-02
Southeast Asia	Southeast Asia	1.7E+07	5.3E+06	4.1E-02	8.6E-01	1.0E-01	1.0E-20	1.2E+01	6.5E+00	1.5E+03	1.2E+01	0.0E+00	2.6E-01	2.7E-01	3.0E-02
Northern regions	Northern regions	1.8E+07	5.6E+06	4.9E-02	8.5E-01	1.0E-01	1.0E-20	1.2E+01	8.8E+00	4.9E+02	1.7E+01	0.0E+00	3.6E-01	2.7E-01	3.0E-02
Oceania	Oceania	8.1E+06	2.2E+06	1.0E-02	8.9E-01	1.0E-01	1.0E-20	1.2E+01	7.4E+00	1.3E+03	3.0E+00	0.0E+00	1.9E-01	2.7E-01	3.0E-02

ID #	Name	Global scale													
		Area land km^2	Area sea km^2	Areafrac freshwater [-]	Areafrac nat soil [-]	Areafrac agr soil [-]	Areafrac other soil [-]	Temp ^oC	Wind speed $m.s^{-1}$	Rain rate $mm.y^{-1}$	Depth freshwater m	RiverFlow cont-reg [-]	Fraction run off [-]	Fraction infiltration [-]	Soil erosion $mm.y^{-1}$
W1	West Asia	1.2E+08	3.6E+08	3.0E-02	8.7E-01	1.1E-01	1.1E-20	1.2E+01	3.0E+00	7.0E+02	2.5E+00	0.0E+00	2.5E-01	2.5E-01	3.0E-02
W2	Indochina	1.4E+08	3.6E+08	2.7E-02	8.7E-01	1.0E-01	1.0E-20	1.2E+01	3.0E+00	7.0E+02	2.5E+00	0.0E+00	2.5E-01	2.5E-01	3.0E-02
W3	N. Australia	1.3E+08	3.6E+08	2.8E-02	8.7E-01	1.0E-01	1.0E-20	1.2E+01	3.0E+00	7.0E+02	2.5E+00	0.0E+00	2.5E-01	2.5E-01	3.0E-02
W4	S. Australia+	1.4E+08	3.6E+08	2.7E-02	8.7E-01	1.0E-01	1.0E-20	1.2E+01	3.0E+00	7.0E+02	2.5E+00	0.0E+00	2.5E-01	2.5E-01	3.0E-02
W5	S. Africa	1.3E+08	3.6E+08	2.8E-02	8.7E-01	1.1E-01	1.1E-20	1.2E+01	3.0E+00	7.0E+02	2.5E+00	0.0E+00	2.5E-01	2.5E-01	3.0E-02
W6	N. Africa	1.1E+08	3.6E+08	3.2E-02	8.7E-01	1.2E-01	1.2E-20	1.2E+01	3.0E+00	7.0E+02	2.5E+00	0.0E+00	2.5E-01	2.5E-01	3.0E-02
W7	Argentina+	1.3E+08	3.6E+08	2.7E-02	8.7E-01	1.0E-01	1.0E-20	1.2E+01	3.0E+00	7.0E+02	2.5E+00	0.0E+00	2.5E-01	2.5E-01	3.0E-02
W8	Brazil+	1.3E+08	3.6E+08	2.8E-02	8.7E-01	1.1E-01	1.1E-20	1.2E+01	3.0E+00	7.0E+02	2.5E+00	0.0E+00	2.5E-01	2.5E-01	3.0E-02
W9	Central America	1.3E+08	3.6E+08	2.7E-02	8.7E-01	1.0E-01	1.0E-20	1.2E+01	3.0E+00	7.0E+02	2.5E+00	0.0E+00	2.5E-01	2.5E-01	3.0E-02
W10	US+	1.2E+08	3.6E+08	2.9E-02	8.7E-01	1.1E-01	1.1E-20	1.2E+01	3.0E+00	7.0E+02	2.5E+00	0.0E+00	2.5E-01	2.5E-01	3.0E-02
W12	N. Eur. + N. Canada	1.2E+08	3.6E+08	3.0E-02	8.8E-01	1.1E-01	1.2E-20	1.2E+01	3.0E+00	7.0E+02	2.5E+00	0.0E+00	2.5E-01	2.5E-01	3.0E-02
W13	Europe+	1.3E+08	3.6E+08	2.8E-02	8.7E-01	1.1E-01	1.1E-20	1.2E+01	3.0E+00	7.0E+02	2.5E+00	0.0E+00	2.5E-01	2.5E-01	3.0E-02
W14	East Indies	1.4E+08	3.6E+08	2.7E-02	8.7E-01	1.0E-01	1.0E-20	1.2E+01	3.0E+00	7.0E+02	2.5E+00	0.0E+00	2.5E-01	2.5E-01	3.0E-02
IND	India	1.3E+08	3.6E+08	2.7E-02	8.7E-01	1.0E-01	1.0E-20	1.2E+01	3.0E+00	7.0E+02	2.5E+00	0.0E+00	2.5E-01	2.5E-01	3.0E-02
CHI	China	1.3E+08	3.6E+08	2.8E-02	8.7E-01	1.0E-01	1.0E-20	1.2E+01	3.0E+00	7.0E+02	2.5E+00	0.0E+00	2.5E-01	2.5E-01	3.0E-02
JAP	Japan	1.4E+08	3.6E+08	2.6E-02	8.7E-01	1.0E-01	1.0E-20	1.2E+01	3.0E+00	7.0E+02	2.5E+00	0.0E+00	2.5E-01	2.5E-01	3.0E-02
North America	North America	1.2E+08	3.6E+08	2.9E-02	8.7E-01	1.1E-01	1.1E-20	1.2E+01	3.0E+00	7.0E+02	2.5E+00	0.0E+00	2.5E-01	2.5E-01	3.0E-02
Latin America	Latin America	1.2E+08	3.6E+08	3.1E-02	8.7E-01	1.2E-01	1.2E-20	1.2E+01	3.0E+00	7.0E+02	2.5E+00	0.0E+00	2.5E-01	2.5E-01	3.0E-02
Europe	Europe	1.3E+08	3.6E+08	2.8E-02	8.7E-01	1.1E-01	1.1E-20	1.2E+01	3.0E+00	7.0E+02	2.5E+00	0.0E+00	2.5E-01	2.5E-01	3.0E-02
Africa+Middle East	Africa+Middle East	1.0E+08	3.6E+08	3.5E-02	8.7E-01	1.3E-01	1.3E-20	1.2E+01	3.0E+00	7.0E+02	2.5E+00	0.0E+00	2.5E-01	2.5E-01	3.0E-02
Central Asia	Central Asia	1.2E+08	3.6E+08	3.0E-02	8.7E-01	1.1E-01	1.1E-20	1.2E+01	3.0E+00	7.0E+02	2.5E+00	0.0E+00	2.5E-01	2.5E-01	3.0E-02
Southeast Asia	Southeast Asia	1.2E+08	3.6E+08	3.0E-02	8.8E-01	1.1E-01	1.1E-20	1.2E+01	3.0E+00	7.0E+02	2.5E+00	0.0E+00	2.5E-01	2.5E-01	3.0E-02
Northern regions	Northern regions	1.2E+08	3.6E+08	3.0E-02	8.8E-01	1.1E-01	1.2E-20	1.2E+01	3.0E+00	7.0E+02	2.5E+00	0.0E+00	2.5E-01	2.5E-01	3.0E-02
Oceania	Oceania	1.3E+08	3.6E+08	2.8E-02	8.7E-01	1.0E-01	1.1E-20	1.2E+01	3.0E+00	7.0E+02	2.5E+00	0.0E+00	2.5E-01	2.5E-01	3.0E-02

ID #	Name	Urban scale			Human Population			Exposure	
		Area	Areafrac	Areafrac	Human pop	Human pop	Human pop	Human breathing rate	Water ingestion
		land	nat soil	other soil	world	continent	urban	world + cont + urban	world + cont
		km^2	[-]	[-]	[-]	[-]	[-]	m^3/(person*day)	l/(person*day)
W1	West Asia	240	0.67	0.33	6.58E+09	2.35E+08	1.47E+06	13	1.4
W2	Indochina	240	0.67	0.33	6.35E+09	4.65E+08	1.30E+06	13	1.4
W3	N. Australia	240	0.67	0.33	6.82E+09	3.20E+06	8.24E+05	13	1.4
W4	S. Australia+	240	0.67	0.33	6.80E+09	2.12E+07	1.03E+06	13	1.4
W5	S. Africa	240	0.67	0.33	6.50E+09	3.24E+08	1.25E+06	13	1.4
W6	N. Africa	240	0.67	0.33	6.03E+09	7.89E+08	2.30E+06	13	1.4
W7	Argentina+	240	0.67	0.33	6.75E+09	6.67E+07	2.89E+06	13	1.4
W8	Brazil+	240	0.67	0.33	6.58E+09	2.42E+08	2.62E+06	13	1.4
W9	Central America	240	0.67	0.33	6.51E+09	3.05E+08	2.76E+06	13	1.4
W10	US+	240	0.67	0.33	6.49E+09	3.28E+08	1.32E+06	13	1.4
W12	N. Eur. + N. Canada	240	0.67	0.33	6.80E+09	1.67E+07	6.56E+05	13	1.4
W13	Europe+	240	0.67	0.33	6.06E+09	7.59E+08	1.41E+06	13	1.4
W14	East Indies	240	0.67	0.33	6.61E+09	2.07E+08	1.30E+06	13	1.4
IND	India	240	0.67	0.33	5.25E+09	1.57E+09	1.76E+06	13	1.4
CHI	China	240	0.67	0.33	5.49E+09	1.33E+09	1.47E+06	13	1.4
JAP	Japan	240	0.67	0.33	6.67E+09	1.51E+08	4.56E+06	13	1.4
North America	North America	240	0.67	0.33	6.5E+09	3.3E+08	1.3E+06	13	1.4
Latin America	Latin America	240	0.67	0.33	6.2E+09	6.1E+08	8.3E+06	13	1.4
Europe	Europe	240	0.67	0.33	6.1E+09	7.6E+08	1.4E+06	13	1.4
Africa+Middle East	Africa+Middle East	240	0.67	0.33	5.7E+09	1.1E+09	3.6E+06	13	1.4
Central Asia	Central Asia	240	0.67	0.33	6.6E+09	2.4E+08	1.5E+06	13	1.4
Southeast Asia	Southeast Asia	240	0.67	0.33	3.1E+09	3.7E+09	1.0E+07	13	1.4
Northern regions	Northern regions	240	0.67	0.33	6.8E+09	1.7E+07	6.6E+05	13	1.4
Oceania	Oceania	240	0.67	0.33	6.8E+09	2.4E+07	1.9E+06	13	1.4

ID #	Name	Production-based intake rates											
		Exposed produce	Exposed produce	Unexposed produce	Unexposed produce	Meat	Meat	Dairy products	Dairy products	Fish freshwater	Fish freshwater	Fish coastal marine water	Fish coastal marine water
		world kg/(day*capita)	continent kg/(day*capita)	world kg/(day*capita)	continent kg/(day*capita)	world kg/(day*capita)	continent kg/(day*capita)	world kg/(day*capita)	continent kg/(day*capita)	world kg/(day*capita)	continent kg/(day*capita)	world kg/(day*capita)	continent kg/(day*capita)
W1	West Asia	1.36	1.39	1.13	0.65	0.10	0.08	0.24	0.26	0.01	0.011	0.04	0.05
W2	Indochina	1.35	1.55	1.11	1.21	0.10	0.05	0.25	0.01	0.01	0.008	0.03	0.06
W3	N. Australia	1.36	6.10	1.12	4.54	0.09	0.51	0.24	1.39	0.01	0.006	0.03	6.65
W4	S. Australia+	1.35	5.34	1.11	3.89	0.09	0.60	0.23	2.84	0.01	0.004	0.03	0.61
W5	S. Africa	1.41	0.38	1.12	1.08	0.10	0.03	0.25	0.06	0.01	0.006	0.04	0.03
W6	N. Africa	1.46	0.65	1.16	0.78	0.10	0.04	0.26	0.10	0.01	0.006	0.04	0.01
W7	Argentina+	1.34	3.74	1.11	1.64	0.09	0.23	0.23	0.57	0.01	0.002	0.03	0.31
W8	Brazil+	1.36	1.41	0.97	5.03	0.09	0.20	0.24	0.28	0.01	0.004	0.04	0.05
W9	Central America	1.40	0.62	1.07	2.10	0.10	0.09	0.24	0.20	0.01	0.003	0.04	0.04
W10	US+	1.22	4.28	1.12	0.96	0.08	0.35	0.21	0.69	0.01	0.003	0.04	0.04
W12	N. Eur. + N. Canada	1.36	1.61	1.12	0.60	0.09	0.15	0.24	0.75	0.01	0.008	0.03	1.43
W13	Europe+	1.24	2.34	1.09	1.35	0.08	0.19	0.17	0.80	0.01	0.003	0.04	0.02
W14	East Indies	1.38	0.77	1.13	0.58	0.10	0.02	0.24	0.01	0.01	0.013	0.03	0.13
IND	India	1.54	0.77	1.21	0.81	0.12	0.01	0.25	0.20	0.01	0.008	0.05	0.00
CHI	China	1.33	1.49	1.20	0.79	0.09	0.12	0.29	0.03	0.01	0.029	0.04	0.01
JAP	Japan	1.37	0.94	1.13	0.44	0.10	0.09	0.24	0.19	0.01	0.027	0.04	0.06
North America	North America	1.22	4.28	1.12	0.96	0.08	0.35	0.21	0.69	0.012	0.003	0.04	0.04
Latin America	Latin America	1.37	1.27	0.91	3.20	0.09	0.15	0.23	0.27	0.012	0.003	0.03	0.08
Europe	Europe	1.24	2.34	1.09	1.35	0.08	0.19	0.17	0.80	0.012	0.003	0.04	0.02
Africa+Middle East	Africa+Middle East	1.52	0.57	1.17	0.87	0.11	0.03	0.27	0.09	0.012	0.006	0.04	0.02
Central Asia	Central Asia	1.36	1.39	1.13	0.65	0.10	0.08	0.24	0.26	0.011	0.011	0.04	0.05
Southeast Asia	Southeast Asia	1.65	1.13	1.47	0.83	0.14	0.06	0.40	0.10	0.005	0.017	0.05	0.02
Northern regions	Northern regions	1.36	1.61	1.12	0.60	0.09	0.15	0.24	0.75	0.011	0.008	0.03	1.43
Oceania	Oceania	1.35	5.44	1.11	3.97	0.09	0.59	0.23	2.65	0.011	0.005	0.03	1.40

We provide an example of results obtained using the landscape parametrization in the USEtox tool with benzene (CAS 71-43-2) with substance data from the USEtox database in Table S4.3.

Table S4.3: CF results for benzene using the continental parametrization of USEtox presented in Table S4.2

Zone		Human health characterization factor [cases/$kg_{emitted}$]														
		Emission to urban air			Emission to cont. rural air			Emission to cont. freshwater			Emission to cont. sea water			Emission to cont. natural soil		
		cancer	non-canc.	total	cancer	non-canc.	total	cancer	non-canc.	total	cancer	non-canc.	total	cancer	non-canc.	total
W1	West Asia	2.1E-03	5.4E-04	2.7E-03	2.4E-04	6.0E-05	3.0E-04	2.1E-04	5.3E-05	2.6E-04	1.1E-04	2.7E-05	1.4E-04	2.1E-04	5.3E-05	2.6E-04
W2	Indochina	3.7E-04	9.4E-05	4.6E-04	1.5E-04	3.7E-05	1.8E-04	3.9E-04	9.8E-05	4.9E-04	3.9E-04	9.8E-05	4.9E-04	3.7E-04	9.4E-05	4.6E-04
W3	N. Australia	6.9E-04	1.7E-04	8.6E-04	9.2E-05	2.3E-05	1.1E-04	7.9E-05	2.0E-05	9.9E-05	2.7E-05	6.8E-06	3.3E-05	7.7E-05	2.0E-05	9.7E-05
W4	S. Australia+	1.1E-03	2.8E-04	1.4E-03	1.6E-04	4.0E-05	2.0E-04	1.5E-04	3.9E-05	1.9E-04	9.6E-05	2.4E-05	1.2E-04	1.4E-04	3.5E-05	1.7E-04
W5	S. Africa	1.7E-03	4.2E-04	2.1E-03	3.0E-04	7.5E-05	3.7E-04	1.2E-04	3.1E-05	1.5E-04	6.8E-05	1.7E-05	8.5E-05	2.5E-04	6.3E-05	3.1E-04
W6	N. Africa	5.2E-03	1.3E-03	6.6E-03	5.7E-04	1.4E-04	7.1E-04	3.0E-04	7.6E-05	3.8E-04	1.8E-04	4.6E-05	2.3E-04	4.9E-04	1.2E-04	6.2E-04
W7	Argentina+	7.8E-03	2.0E-03	9.8E-03	4.5E-04	1.1E-04	5.7E-04	4.1E-04	1.1E-04	5.2E-04	2.1E-04	5.3E-05	2.6E-04	3.9E-04	1.0E-04	4.9E-04
W8	Brazil+	6.5E-03	1.7E-03	8.2E-03	5.0E-04	1.3E-04	6.2E-04	4.0E-04	1.0E-04	5.0E-04	1.6E-04	3.9E-05	1.9E-04	4.1E-04	1.0E-04	5.2E-04
W9	Central America	7.3E-03	1.9E-03	9.2E-03	6.2E-04	1.6E-04	7.8E-04	5.1E-04	1.3E-04	6.4E-04	2.8E-04	7.2E-05	3.6E-04	5.2E-04	1.3E-04	6.5E-04
W10	US+	1.8E-03	4.5E-04	2.2E-03	2.4E-04	6.1E-05	3.0E-04	1.9E-04	4.9E-05	2.4E-04	1.0E-04	2.7E-05	1.3E-04	2.1E-04	5.3E-05	2.6E-04
W12	N. Eur. + N. Canada	4.6E-04	1.2E-04	5.7E-04	7.9E-05	2.0E-05	1.0E-04	7.0E-05	1.8E-05	8.8E-05	4.3E-05	1.1E-05	5.3E-05	7.0E-05	1.8E-05	8.7E-05
W13	Europe+	2.2E-03	5.7E-04	2.8E-03	4.7E-04	1.2E-04	5.9E-04	3.9E-04	1.0E-04	4.9E-04	2.0E-04	5.0E-05	2.5E-04	4.1E-04	1.0E-04	5.1E-04
W14	East Indies	1.8E-03	4.6E-04	2.3E-03	3.1E-04	7.7E-05	3.8E-04	2.9E-04	7.5E-05	3.7E-04	1.5E-04	3.8E-05	1.9E-04	2.6E-04	6.6E-05	3.2E-04
IND	India	4.5E-03	1.1E-03	5.6E-03	1.7E-03	4.4E-04	2.2E-03	1.4E-03	3.5E-04	1.7E-03	5.4E-04	1.4E-04	6.8E-04	1.5E-03	3.7E-04	1.8E-03
CHI	China	2.8E-03	7.1E-04	3.5E-03	9.2E-04	2.3E-04	1.2E-03	7.7E-04	1.9E-04	9.6E-04	3.5E-04	8.9E-05	4.4E-04	7.8E-04	2.0E-04	9.8E-04
JAP	Japan	2.0E-02	5.0E-03	2.5E-02	1.3E-03	3.3E-04	1.6E-03	1.2E-03	2.9E-04	1.4E-03	6.6E-04	1.7E-04	8.2E-04	1.1E-03	2.7E-04	1.3E-03

Table S4.3 (continued): CF results for benzene using the continental parametrization of USEtox presented in Table S4.2

Zone		Ecotox. Charact. factor [PAF.m^3.day.kg^{-1}]					
		Em.airU	Em.airC	Em.fr.waterC	Em.sea waterC	Em.nat.soilC	Em.agr.soilC
		freshwater	freshwater	freshwater	freshwater	freshwater	freshwater
W1	West Asia	1.1E-01	1.1E-01	9.8E+01	4.9E-02	1.1E+00	1.1E+00
W2	Indochina	1.2E-01	1.1E-01	1.7E+02	3.5E-02	1.4E+01	1.4E+01
W3	N. Australia	3.1E-02	3.1E-02	4.8E+01	8.8E-03	2.8E+00	2.8E+00
W4	S. Australia+	2.8E-02	2.8E-02	1.4E+01	1.7E-02	3.4E-01	3.4E-01
W5	S. Africa	2.9E-01	2.9E-01	4.8E+02	6.4E-02	2.0E+01	2.0E+01
W6	N. Africa	3.4E-01	3.3E-01	3.8E+02	1.1E-01	8.9E+00	8.9E+00
W7	Argentina+	4.9E-02	4.9E-02	6.4E+01	2.2E-02	2.0E+00	2.0E+00
W8	Brazil+	5.1E-02	5.0E-02	1.0E+02	1.5E-02	7.0E+00	7.0E+00
W9	Central America	2.0E-01	1.9E-01	1.4E+02	8.8E-02	1.1E+01	1.1E+01
W10	US+	2.7E-01	2.7E-01	1.6E+02	1.2E-01	5.0E+00	5.0E+00
W12	N. Eur. + N. Canada	3.0E-01	3.0E-01	9.6E+01	1.6E-01	2.3E+00	2.3E+00
W13	Europe+	9.4E-02	9.3E-02	1.3E+02	3.9E-02	3.2E+00	3.2E+00
W14	East Indies	3.5E-02	3.5E-02	2.2E+01	1.7E-02	1.3E+00	1.3E+00
IND	India	1.9E-01	1.8E-01	1.7E+02	5.7E-02	8.4E+00	8.4E+00
CHI	China	2.0E-01	2.0E-01	1.3E+02	7.6E-02	6.6E+00	6.6E+00
JAP	Japan	6.5E-02	6.4E-02	8.2E+01	3.2E-02	7.2E+00	7.2E+00

5.3.5. Details of the variability of removal rates from air

Aiming to identify the reasons for variability and to specify whether the variability follows similar spatial patterns for different chemicals, maps of distribution of values at global scale were calculated. Actually, maps could be used not only to visualize but also to analyze the spatial nature of pollutants. Analyzing the spatial pattern in the maps of the chemicals, the variability of the results in Fig. 5.1 could be explained as follows:

For chemicals in the group 1a, the dominant compartment is air. The variability could be driven by gas exchange in the atmosphere that basically depends on the variability of land cover. In fact, e.g. forest coverage is associated with higher gas exchange whereas desert of sealed soil have gas exchange close to zero. The following categories of ground surface are described in the model: agricultural or natural (bare) soil; impervious surface (urban, sealed soil); desert or permanently frozen soil; forest deciduous; forest evergreen (broadleaves or conifers); water (lakes and rivers; oceans and seas). See for example, for butadiene, the map removal rate from air without advection (Figure in Sala et al 2011). The pattern of variability suggests the dependence of the final result on the variability of the gas exchange and the differences in the global distribution of land cover influence the variability of the results. This is confirmed by comparing the pattern of distribution with the map of the removal rate due to gas exchange only (Figure in Sala et al 2011).

The environmental partitioning of 2a chemicals is mainly related to water. The high variability in the Kair values could be explained by the difference in precipitation among countries. Comparing the total removal rate of a highly hydrophilic chemical, such as acephate (Figure in Sala et al 2011), with the pattern of the map of the wet deposition removal rate (Figures in Sala et al 2011) and the pattern of the annual average precipitation map (Figure in Sala et al 2011) it is clear that the foremost removal rate process is the wet deposition. The same explanation may describe the spatial variability of methomyl, also in the 2a group but less hydrophilic (Figure in Sala et al 2011).

In the case of hydrophobic chemicals with a low affinity for air, such as PCBs in the 3a group, the pattern of variability may be explained by considering those chemicals emitted to air, with gas absorption (Figures in Sala et al 2011). However the additional patterns map (Figures in Sala et al 2011) shows that Kpart could account for the total variability, as the highest values in the total removal rate are in the same areas where particle dry deposition is uppermost.

Furthermore, to explain the different variability amongst chemicals within 3a (e.g. cypermethrin and hexabromobenzene), a combination of degradation rate and Kgas has to be taken into account. The variability of gas exchange drives (Fig S15 and S17 in Sala et al 2011) the overall variability of the Kair when the degradation rate is low (as in the case of hexacromobenzene – 4.9 10-4 1/d) and the persistence is high (over 1000 days of half life in air). In the opposite case, where the degradation rate is higher (as cypermethrin – 0.92 1/d or di(n-octyl)phthalate – 0.89 1/d) and the persistence is low (respectively 0.75 and 0.78 days of half life in air) the overall variability is very low (Figures in Sala et al 2011). Then, the degradation, as an elimination process from atmosphere, reduces the range of variability of

total air removal rates, which are originally associated with the wide spatial fluctuations of gas exchange or wet/dry deposition.

5.3.6. Detailed explanation of sensitivity analysis for removal rate from air

Environment specific inputs

As pointed out, the approach used for the model sensitivity analysis is described in Saltelli etl a. (2008) and in Ciuffo et al. (2012). The size of the Monte Carlo experiment is *N*=20.000. At the end of any experiment we paid attention to verify the stability of the Sobol indices. In all the applications they proved to be stable with no more than 5.000 iterations.

In addition we derived the 90% confidence interval of the indices as a further proof of their robustness. Confidence intervals have been numerically derived using the bootstrapping technique (Ciuffo et al. 2011).

In the following figures, the results of the sensitivity analysis for the four chemicals are reported.

Figure S4.7 reports the results for the acephate. The four charts give approximately the same figures and this means that neither the coverage combinations, nor the advection phenomenon exert any impact on the model outputs for this chemical. The air removal rate, in this case, is only affected by the value of the average precipitation in the cell and by the atmospheric boundary layer (both for their first order and combined effects). This is reasonable as the acephate is a highly hydrophilic chemical and also because, as it is well known in the literature, spatially resolute models usually overestimate the role of precipitation.

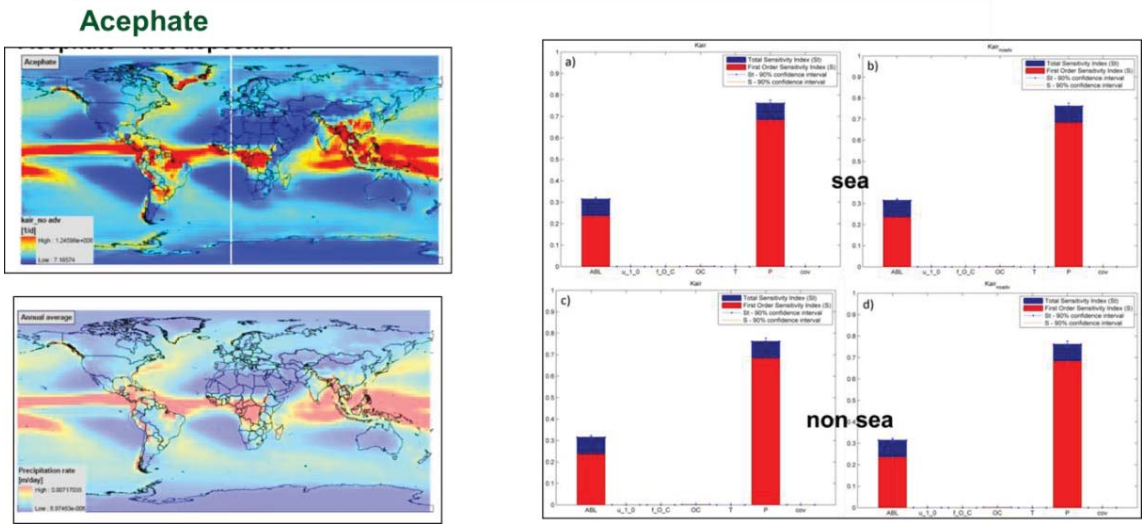

Figure S4.7. First order, total order sensitivity indices and their confidence interval for environment specific input factors of the MAPPE model with respect to acephate. Charts a) and c) refer to the total air removal rate, while b) and d) do not consider advection. Indices in charts a) and b) are calculated with sea and land coverage combinations, while c) and d) refer only to land coverage combinations. Two maps on the left show the similarities between air removal rate distribution for acephate and precipitation distribution

Confidence intervals are quite small around the calculated values as a good indication about the reliability of the results achieved. The two maps in Figure S4.7 show the similarities between air removal rate for acephate and precipitation distributions, confirming the results of the sensitivity analysis.

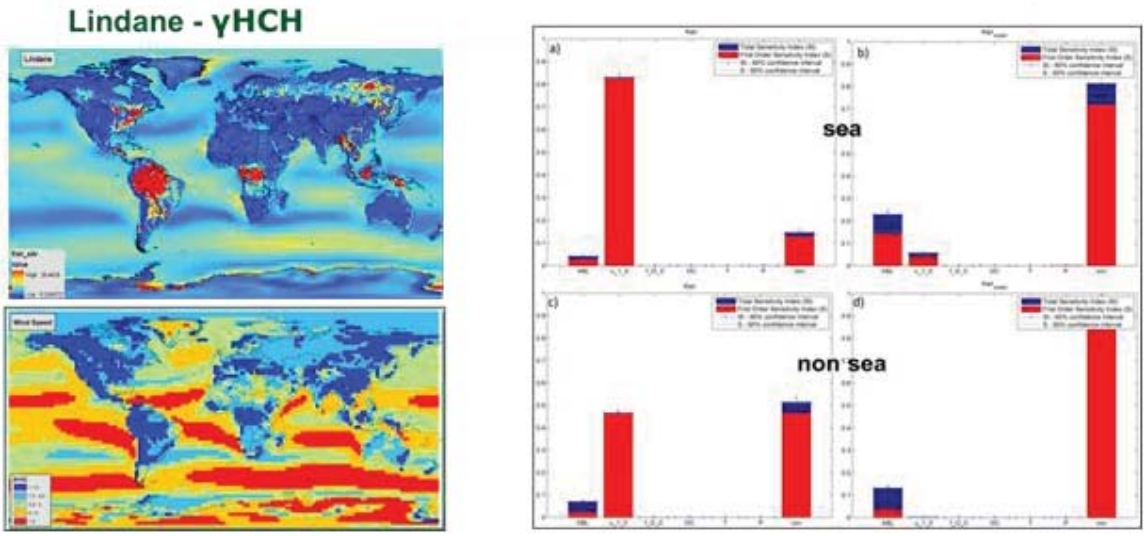

Figure S4.8. First order, total order sensitivity indices and their confidence interval for environment specific input factors of the MAPPE model with respect to γ-HCH. Charts a) and c) refer to the total air removal rate, Indices in charts a) and b) are calculated with sea and land coverage combinations, while c) and d) refer only to land coverage combinations. Two maps on the left show the similarities between air removal rate distribution for γ-HCH and wind speed distribution

Figure S4.8 reports on the results of the sensitivity analysis for the MAPPE model with respect to the γ-HCH (lindane). In this case both the coverage combinations and the advection have a significant impact on the results. On the contrary the precipitation has no influence on the outputs of the model. Comparing the chart in Figure S4.7 with those in Figure S4.8 it is possible to see that chemical specific factors have a significant effect on the model. For lindanelindane the coverage combinations and the wind speed have the most important effects. This quantitatively varies if we consider sea cells or not (see the difference between Figure S4.8a and Figure S4.8c). Also in this case the atmospheric boundary layer has an effect on the model outputs, even if lower than in the case of the acephate.

Differently from the other chemicals, with llindane, we performed also an additional analysis since the parameters of the relation between both K_{aw} and K_{deg} and the temperature T are available. Results are reported in Figure S4.9.

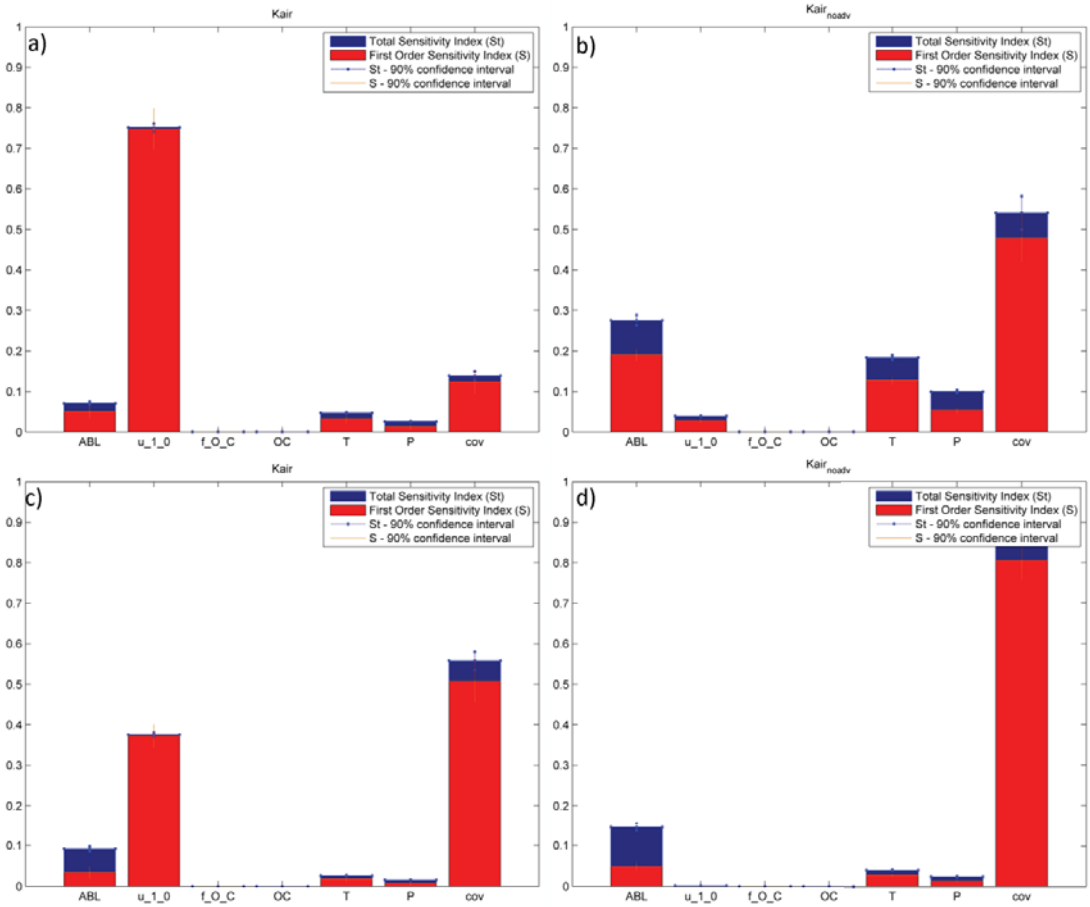

Figure S4.9. First order, total order sensitivity indices and their confidence interval for environment specific input factors of the MAPPE model with respect to γ-HCH with the influence of the temperature modelled. Charts a) and c) refer to the total air removal rate, while b) and d) do not consider advection. Indices in charts a) and b) are calculated with sea and land coverage combinations, while c) and d) refer only to land coverage combinations

Results are fairly different from the previous case. Apart from the organic carbon and its fluxes, all the inputs show an effect on the model outputs. This is particularly true considering sea cells without advection. Being a multimedia chemical, this behaviour for l lindanelindane was expected: the chemical does not show a clear preference toward a single medium. For this reason, without an explicit link with temperature we could conclude that the MAPPE model is not sufficiently accurate to reproduce the behaviour of chemicals like llindane.

In Figure S4.10 the results of the model sensitivity analysis for t di(n-octyl)phtalate are shown.

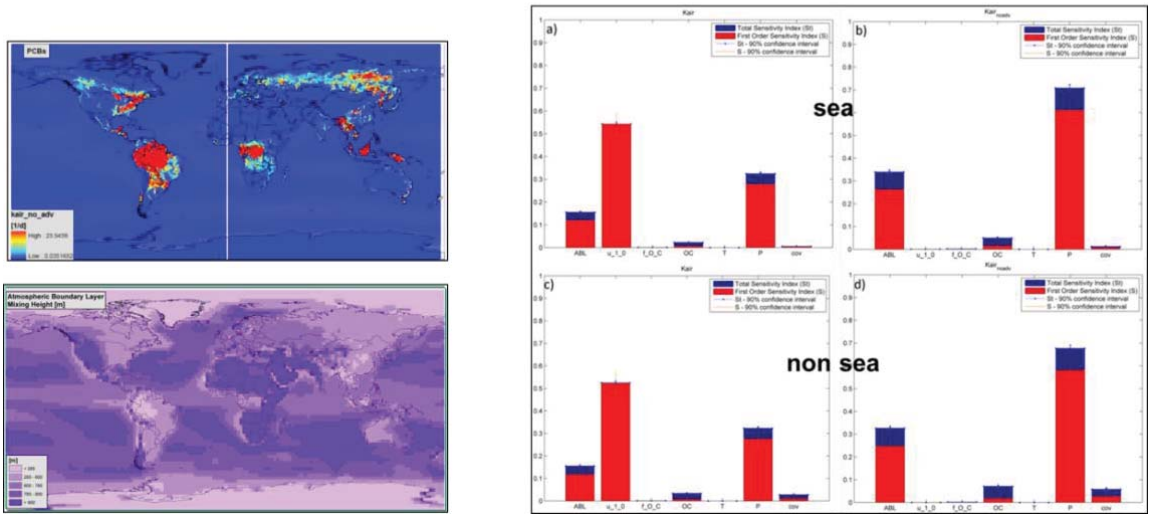

Figure S4.10. First order, total order sensitivity indices and their confidence interval for environment specific input factors of the MAPPE model with respect to di(n-octyl)phtalate. Charts a) and c) refer to the total air removal rate, while b) and d) do not consider advection. Indices in charts a) and b) are calculated with sea and land coverage combinations, while c) and d) refer only to land coverage combinations. Two maps on the left show the similarities between air removal rate distribution for di(n octyl) phtalate and atmospheric boundary layer distribution

Again the results are different from the other chemicals. For the di(n octyl) phtalate, almost all the input factors have an effect on the model outputs (apart from the organic carbon fluxes and the temperature that are not modelled for this chemical). The atmospheric boundary layer has still an important effect, even if most of the variance in the outputs is accounted for by wind speed and precipitation.

Before drawing any inference about the results of the sensitivity analysis for this chemical, it is worth noting that in absolute terms, the air removal rate for both lindane and di(n-octyl)phtalate are much lower than for acephate. This means that, on average, lindane and di(n-octyl)phtalate are expected to stay much longer in the air compartment than acephate. If this behaviour can be expected for Lindane, this is probably not the case for di(n-octyl)phtalate, which has and extreme lipophilic character (even though this feature might be explained by the fact that the chemical remains in air associated with particulates). For this reason the model behaviour should not be checked against the effects of the input factor, but, in this case, against the reliability of the output. In any case the fact that, different to the other chemicals, organic carbon has an effect on the model outputs can be seen as proof that the MAPPE model is able, within certain limits, to mimic the mechanisms that lead a chemical to follow their partitioning tendencies.

Finally, in Figure S5.6, the results of the model sensitivity analysis for butadiene are shown. Results are in principle similar to those of lindane even if, interestingly, the effect of advection is much lower. This is particularly evident for the analysis in which the cells of pure water are removed (Figure S4.11c-d). Considering that butadiene represents a more volatile character than llindane, this appears to be a contradictory behaviour of the MAPPE model.

Again, this further shows the power of sensitivity analysis in uncovering peculiar model behaviours.

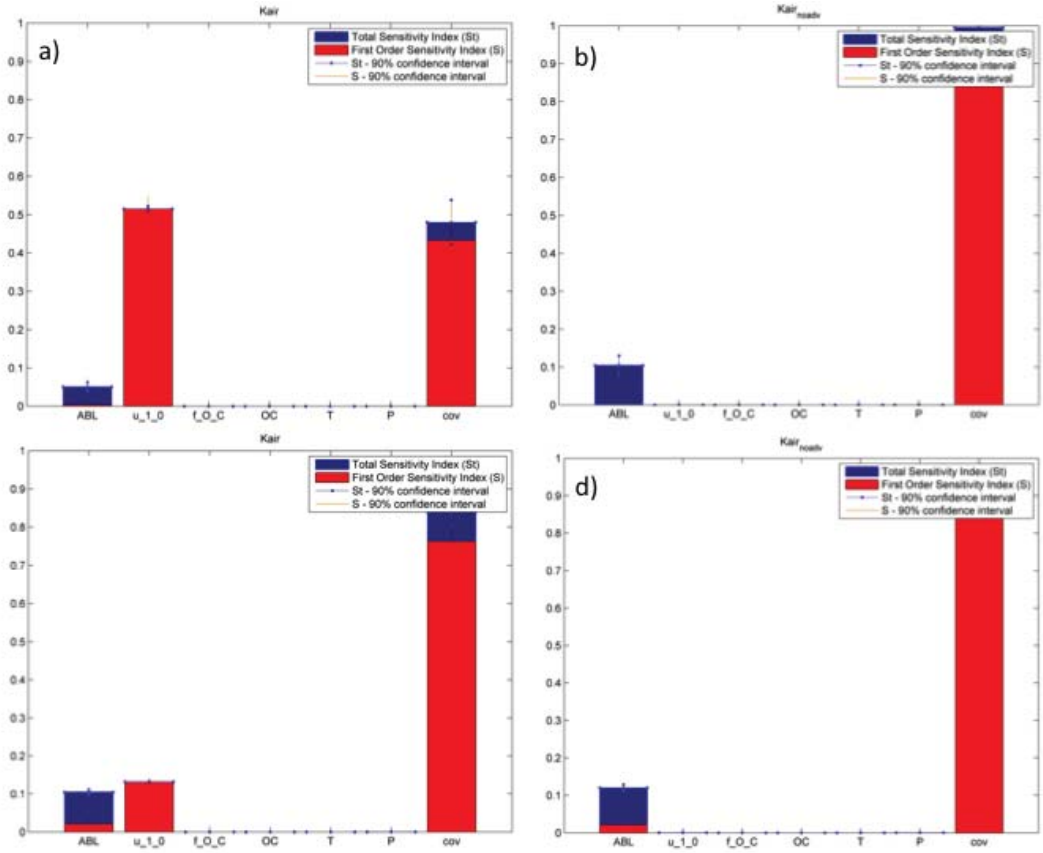

Figure S4.11. First order, total order sensitivity indices and their confidence interval for environment specific input factors of the MAPPE model with respect to butadiene. Charts a) and c) refer to the total air removal rate, while b) and d) do not consider advection. Indices in charts a) and b) are calculated with sea and land coverage combinations, while c) and d) refer only to land coverage combinations

Environment and chemical specific inputs

As already pointed out in previous sections, in order to quantify the effects on the outputs of choosing a specific chemical and to compare such effects with those of the other environment specific compounds, an additional sensitivity analysis has been carried out. Results are shown in Figure S4.12.

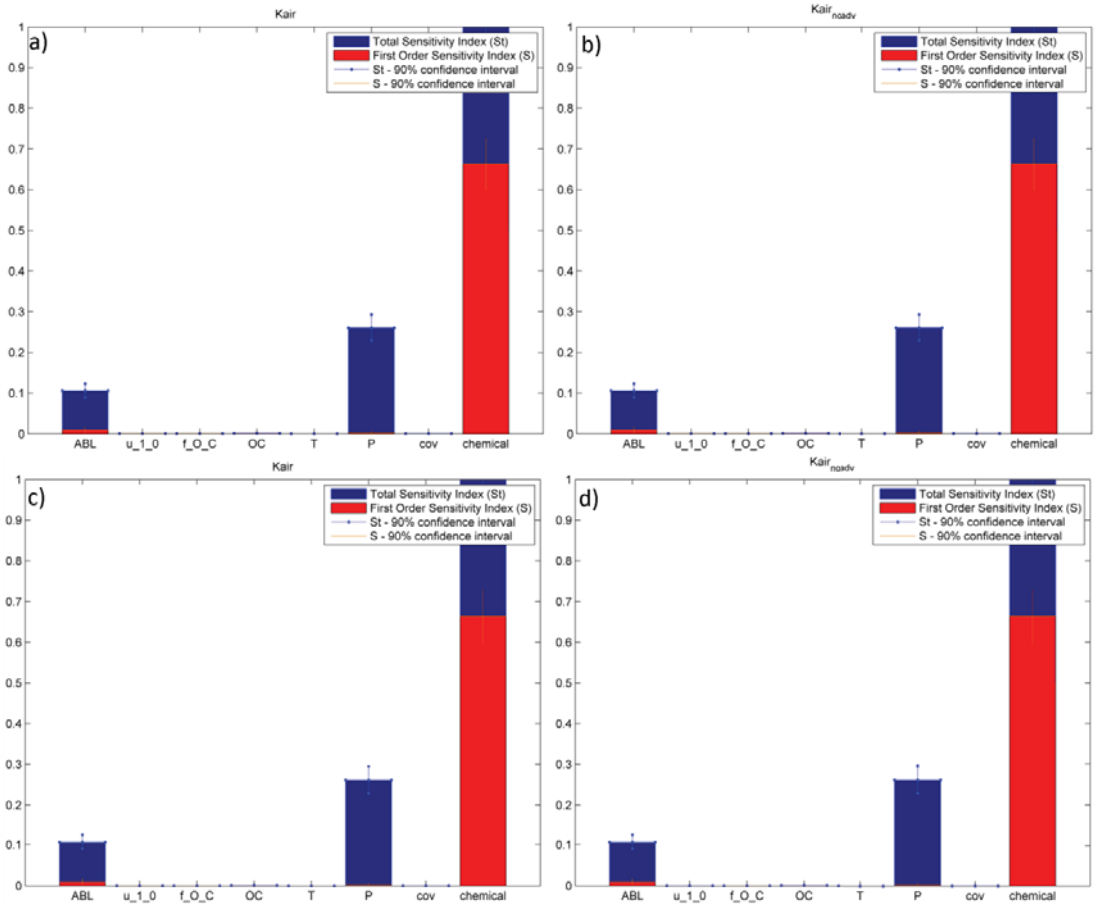

Figure S4.12. First order, total order sensitivity indices and their confidence interval for environment and chemical specific input factors of the MAPPE model. Charts a) and c) refer to the total air removal rate, while b) and d) do not consider advection. Indices in charts a) and b) are calculated with sea and land coverage combinations, while c) and d) refer only to land coverage combinations.

Results show that the choice of the chemical, alone, accounts for approximately 70% of the model output variance independently from all the other factors. Precipitation and the height of the atmospheric boundary layer have an effect only in combination between themselves and with the chemical. This is a clear indication that, once the properties of the chemical are known, precipitation and atmospheric boundary layer, alone, can provide a good indication of the time the chemical will remain in the air compartment.

It is interesting to note that, if we consider the scatter-plots reported in Figure S4.13 it is possible to identify two (or even more) categories of chemicals: a category of chemicals with also very high removal rate and another category (including the vast majority of the compounds) with much lower removal rates. Since most of the variance in the outputs lies within the first category, the scatter plots clearly explain why only ABL and P have showed up in the sensitivity analysis (confirming what wasstated for acephate, which in fact is one of these high air removal rate chemical).

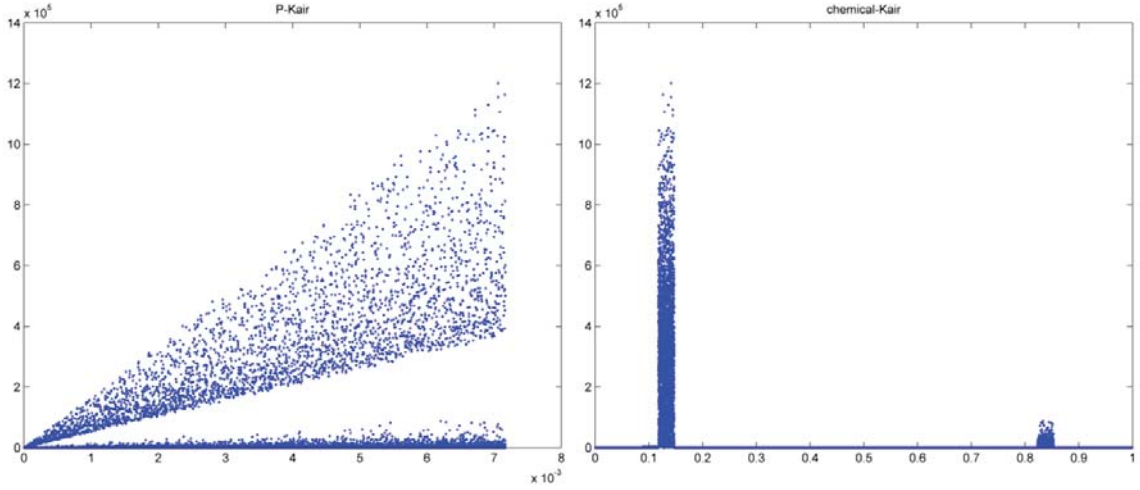

Figure S4.13. Scatter plots of the air removal rate (without advection) K_{air} (resulting from the MAPPE model) with respect to precipitation P and chemical input factors

In order to get further insights into the model, also for the other chemicals, we performed an additional sensitivity analysis without considering the chemicals pertaining to the first category of compounds (namely acephate, benomyl, methomyl and propoxur).

Results are shown in Figure S4.14.

In this case more input factors appear to exert an impact on the outputs, even if the situation does not change considerably with chemical, P and ABL account for most of the variance in the model outputs. The main difference with the previous case is that the environment specific factor also has an effect alone and not only in combination with the other factor. One can conclude that, according to what is predicted by the MAPPE model, the magnitude of the air removal rate is totally defined once the chemical, the height of the atmospheric boundary layer and the amount of precipitation are defined. Then, the calculation can be refined by knowing also the average wind speed and the coverage combination.

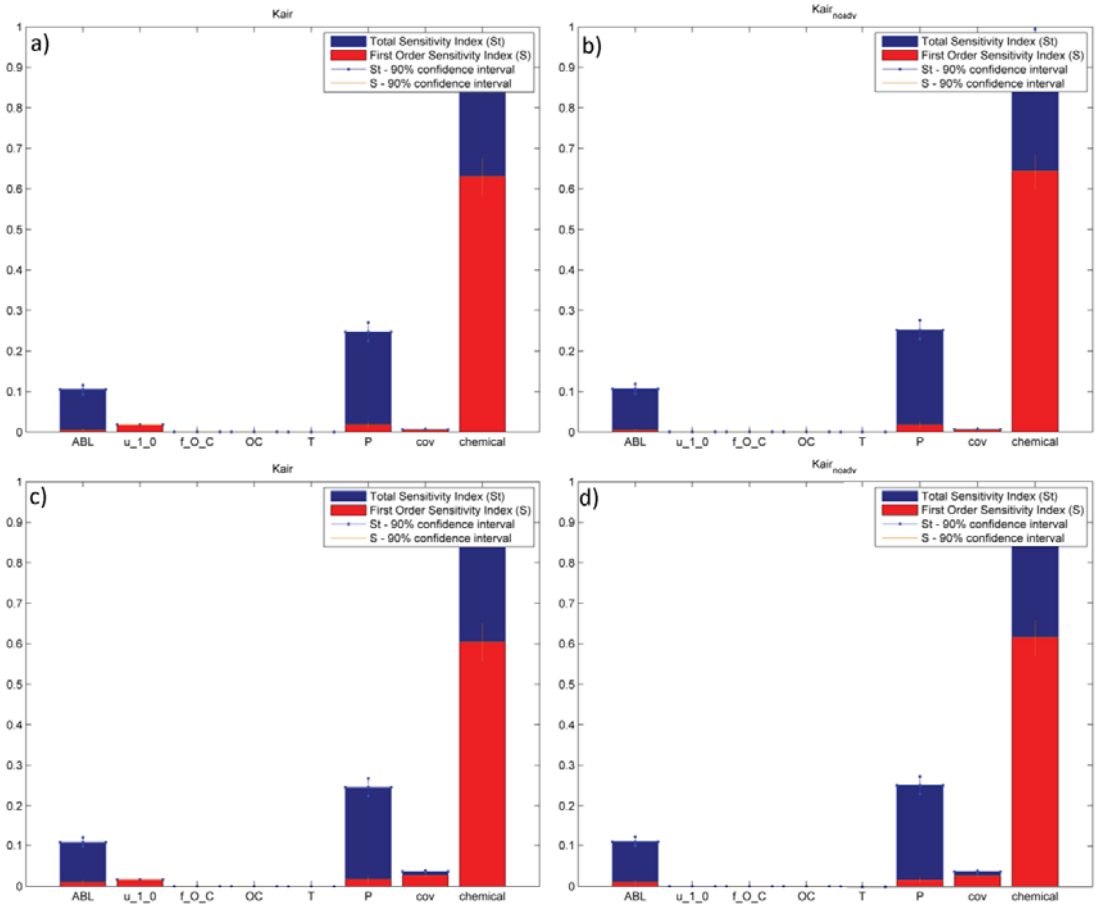

Figure S4.14. First order, total order sensitivity indices and their confidence interval for environment and chemical specific input factors of the MAPPE model (without considering acephate, benomyl, methomyl and propoxur among the chemicals). Charts a) and c) refer to the total air removal rate, while b) and d) do not consider advection. Indices in charts a) and b) are calculated with sea and land coverage combinations, while c) and d) refer only to land coverage combinations.

5.3.7. Detailed results sensitivity analysis for freshwater and soil

Environment specific inputs

In the following figures, the results of the sensitivity analysis for the five chemicals (acephate, γ-HCH, di(n-octyl)phthalate, mirex, butadiene) are reported.

In Figure S4.15, results of the sensitivity analysis of MAPPE for acephate are reported for the 4 selected model outputs. As expected, for acephate, having a strongly hydrophilic character, the soil removal rate is only influenced by the annual discharge *Q*. The erosion component of k_{soil} is influenced by the organic carbon and the sediment yield, but its impact on the total removal rate is clearly negligible. For the freshwater compartment, the outputs variance is driven by the annual discharge, the catchment retention time and their interaction.

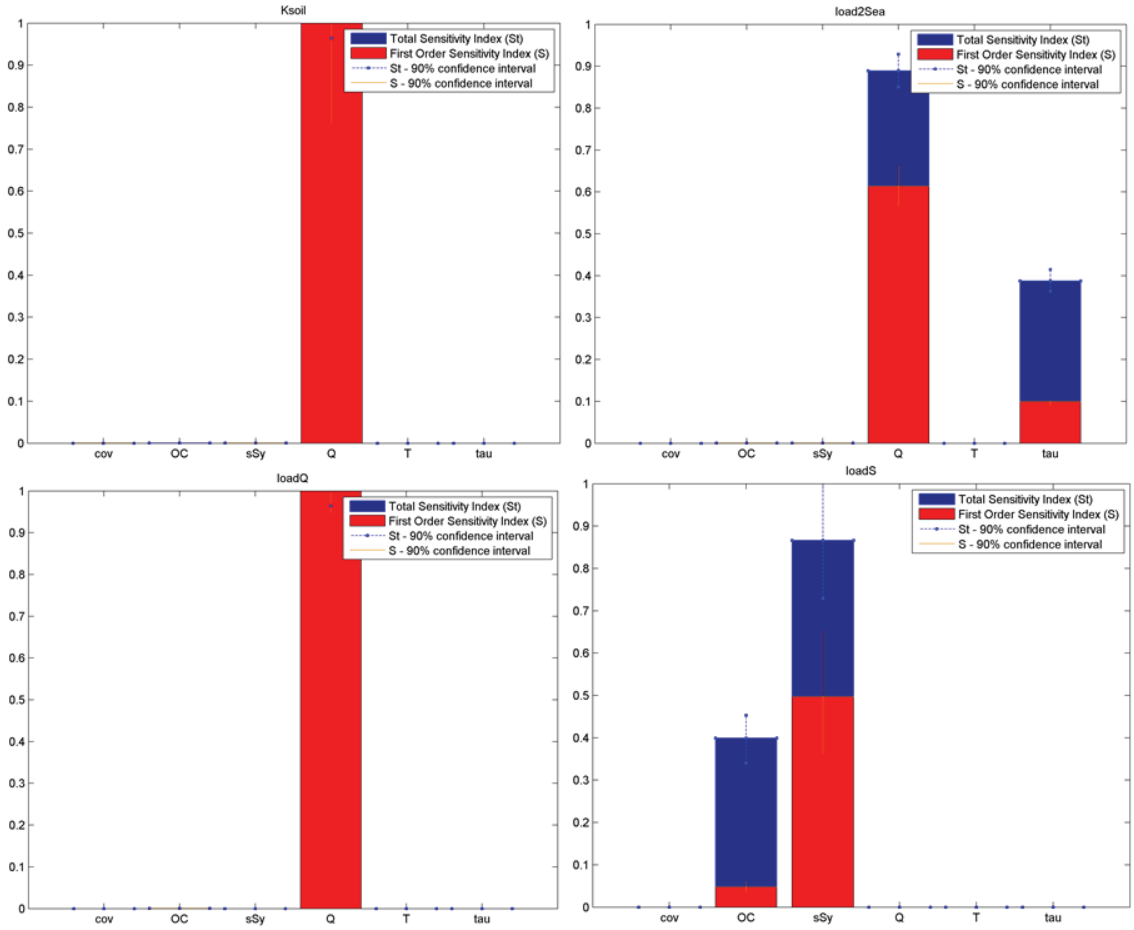

Figure S4.15. First order, total order sensitivity indices and their confidence interval of environment specific input factors of the MAPPE model for the acephate chemical. Four charts refer to four different model outputs

In Figure S4.16 results of the sensitivity analysis for lindane are reported. In contrast to the previous case, the annual discharge only marginally influences the total soil removal rate. The main driver here is the specific sediment yield, which accounts alone for about the 95% of the total variability of k_{soil}. Differently from the previous case, the same input is also responsible for almost the 100% of the *Load2Sea* variability, meaning that lindane is mainly affected by the amount of sediments rather than on the time they take to reach the sea. This is also clearly reflected from comparing the results for *LoadS* and *LoadQ*. In a way this confirms the peculiarity of Lindane that, emitted in air tends to remain in air and emitted at soil tends to remain to the soil as well.

In order to understand the meaning of having only one parameter accounting for almost all the output variability, in Figure S4.17, the scatter plots of K_{soil} versus Q for Acephate and sSy for lindane are reported.

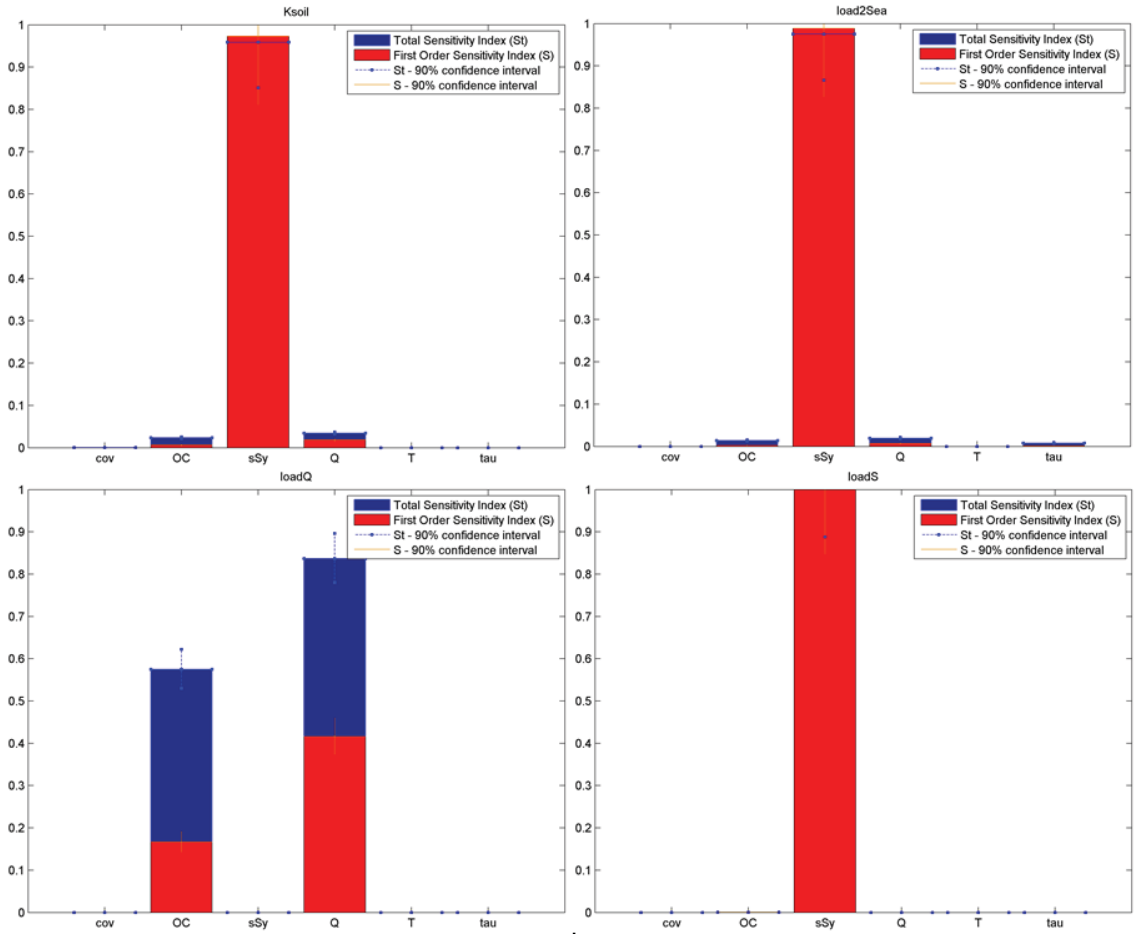

Figure S4.16. First order, total order sensitivity indices and their confidence interval of environment specific input factors of the MAPPE model for γ-HCH . Four charts refer to four different model outputs

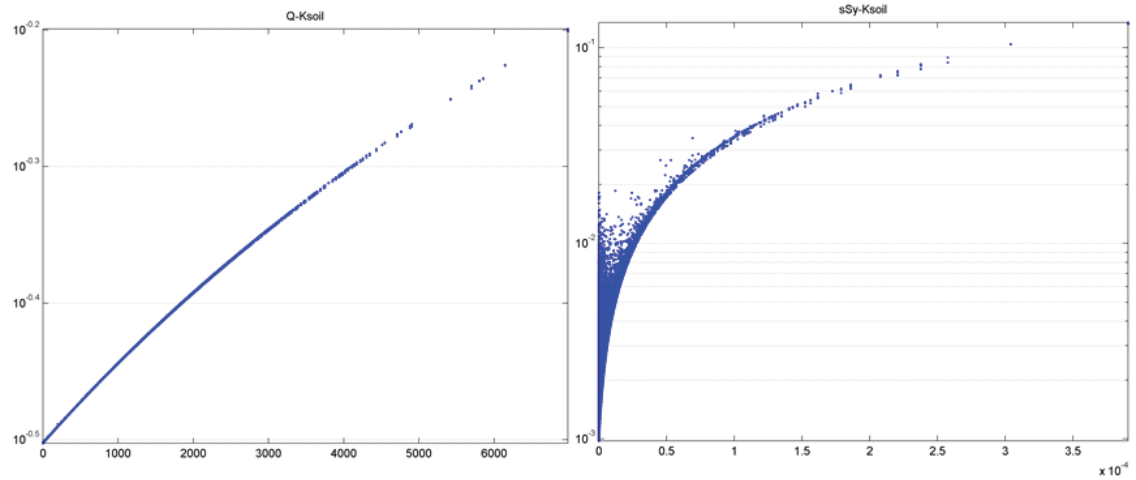

Figure S4.17. Figure S5.12. Scatter plots of Ksoil versus Q for acephate (left) and sSy for γ-HCH (right)

In both the cases, there is an approximate direct proportionality between k_{soil} and the input considered.

In Figure S4.18, results for di(n octyl) phthalate are reported. The situation in this case is even more extreme than in the case of lindane with the sediment yield accounting for 100% of the total variability of all the model outputs.

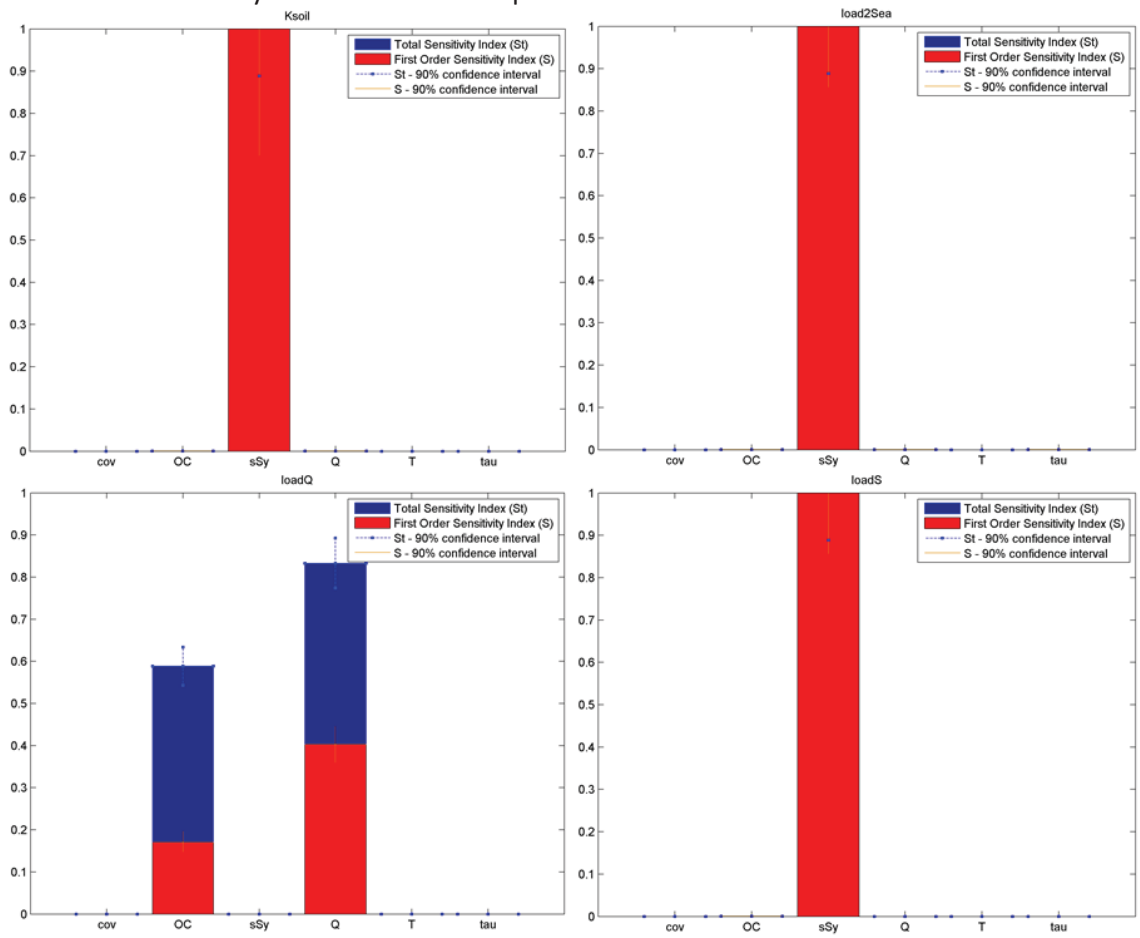

Figure S4.18. First order, total order sensitivity indices and their confidence interval of environment specific input factors of the MAPPE model for di(n-octyl)phthalate chemical. Four charts refer to four different model outputs

In order to confirm the results for di(n-octyl)phthalate, the same analysis has been carried out on another hydrophobic chemical, mirex. Results are reported in Figure S5.14 and show exactly the same behaviour to di(n-octyl)phthalate. Also for these two chemicals, in Figure S4.20 the scatter plots of Ksoil with respect to sSy are reported. As in the previous case, for both chemicals there is a direct relationship between input and output, but the overall variability of mirex is much higher than that of di(n-octyl)phthalate.

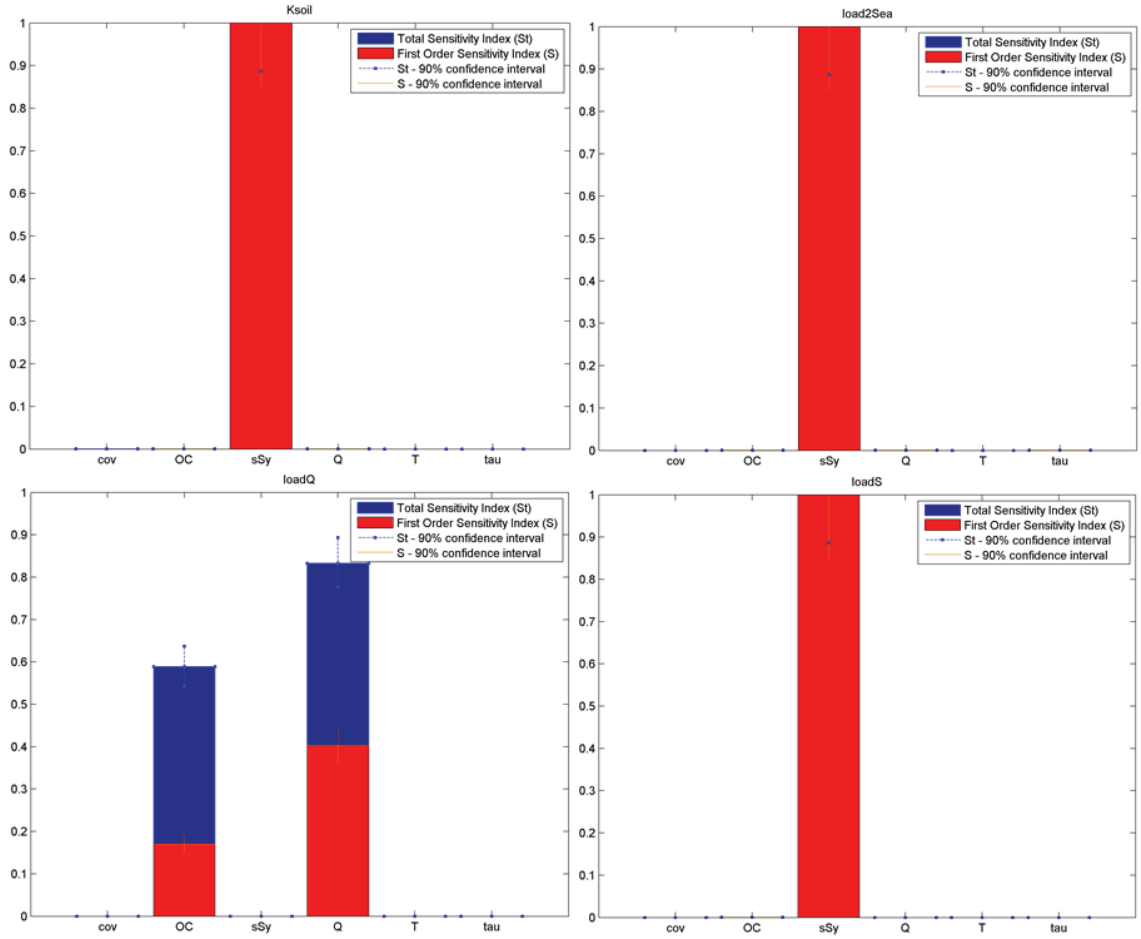

Figure S4.19. First order, total order sensitivity indices and their confidence interval of environment specific input factors of the MAPPE model for mirex. Four charts refer to four different model outputs

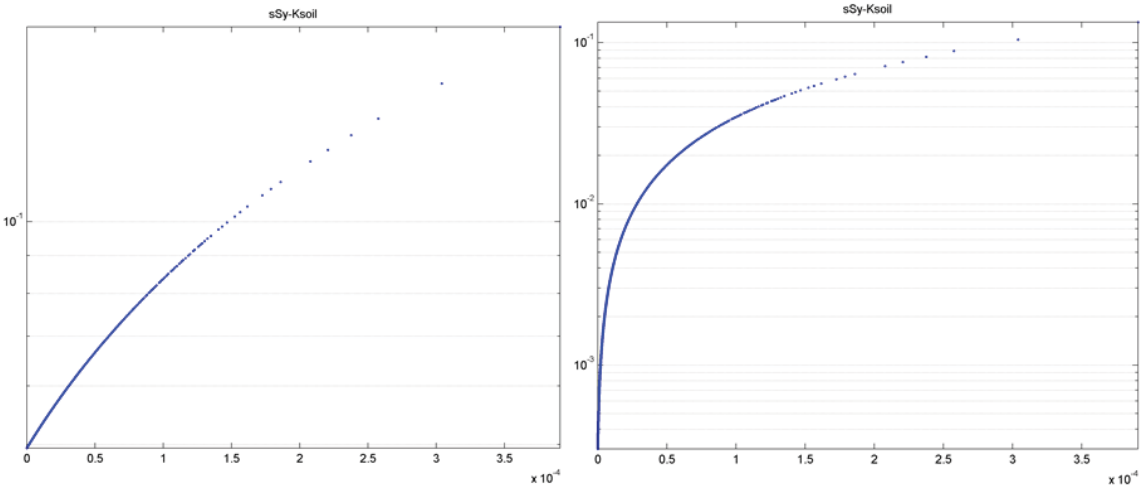

Figure S4.20. Scatter plots of Ksoil versus sSy for di(n octyl) phthalate (left) and mirex (right)

Finally, in Figure S4.21, results of the sensitivity analysis for butadiene are reported, a chemical with different characteristics that shows totally different results. In particular the most important inputs for k_{soil} are the concentration of organic carbon and the coverage type. This holds even if two of its components (loadQ and loadS) are not affected by the coverage and only marginally affected by organic carbon. The reason is, therefore, that the behaviour of butadiene is regulated by another phenomenon: volatilization (as expected due to high Koa). For load2Sea, the most important parameters are the discharge rate (that shows that runoff is more important than erosion for butadiene) and the catchment retention time.

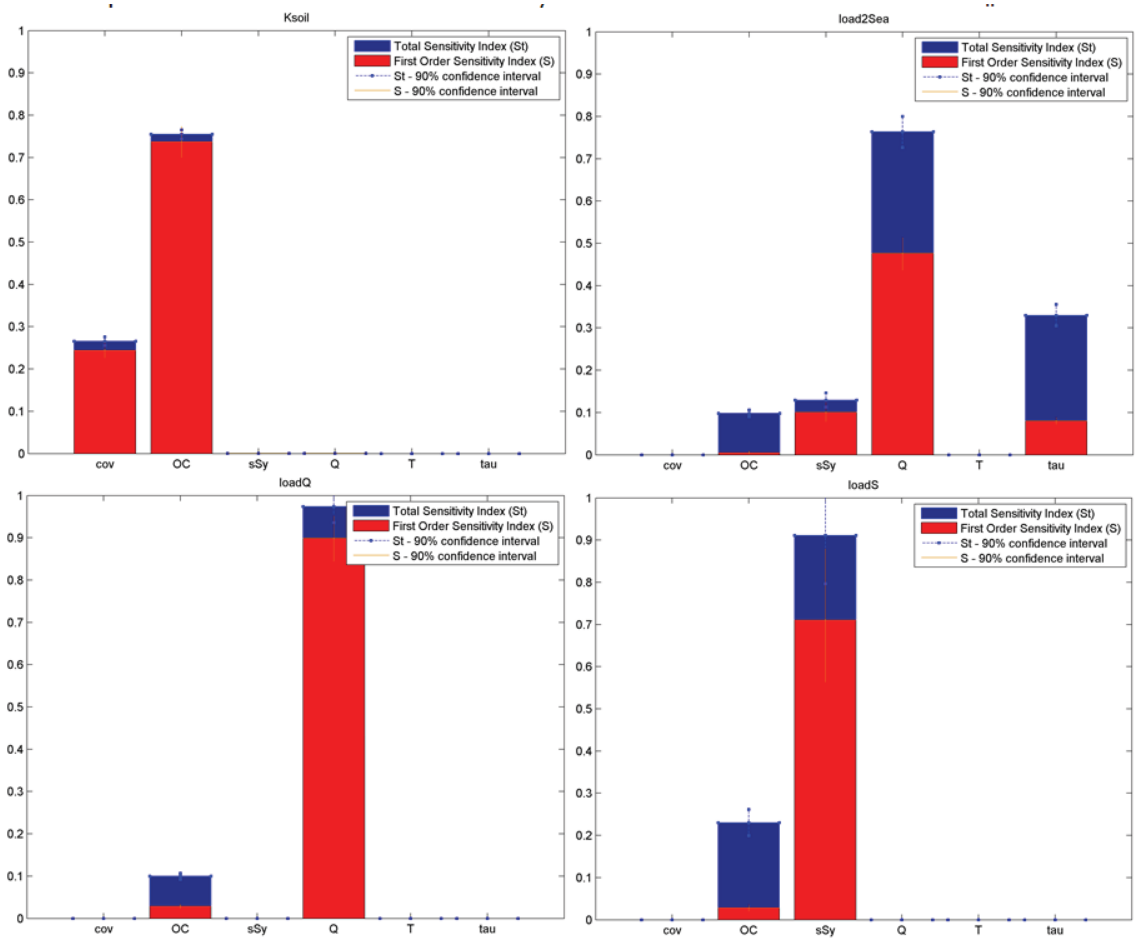

Figure S4.21. First order, total order sensitivity indices and their confidence interval of environment specific input factors of the MAPPE model for butadiene. Four charts refer to four different model outputs

Environment and chemical specific inputs

As for the case of the air compartment, in this section, results of the sensitivity analysis considering both environmental and chemical specific inputs are reported. Figure S4.22 shows the main results.

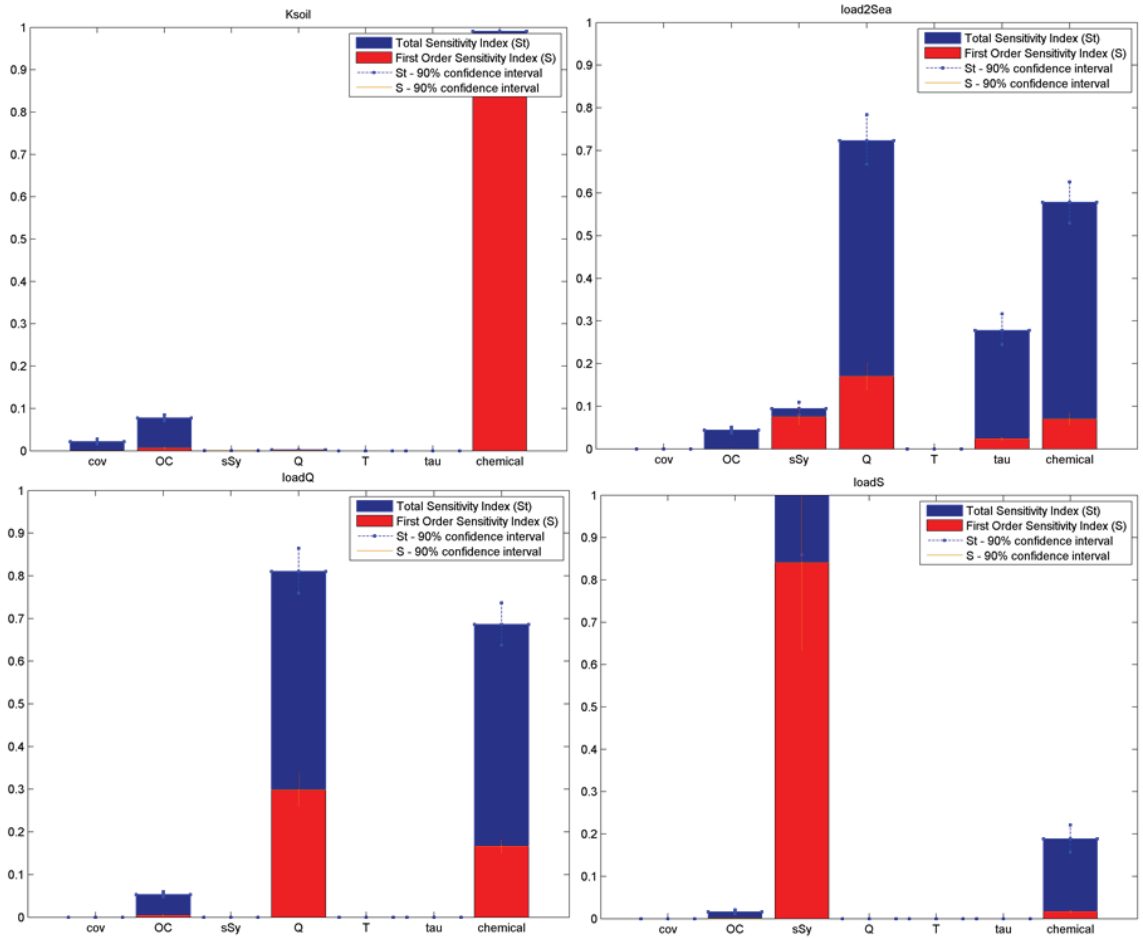

Figure S4.22. First order, total order sensitivity indices and their confidence interval of environment and chemical specific input factors of the MAPPE model. Four charts refer to four different model outputs

Results appear less straightforward than for the single chemical. In particular, the selection of the chemical accounts for almost the 90% of the k_{soil} variability. Another 10% of variability is due to the combination of organic carbon and coverage. Q and sSy do not apper to be influential and this was not expected, since they resulted the main factors for 4 out of the 5 chemicals analysed. The problem here is that in the sensitivity analysis, the absolute variability of k_{soil} is considered and not its variability in terms of orders of magnitude. Since the butadiene and the other volatile chemicals, in absolute terms, have the highest variability, the results here reflect their behaviour. However, for many hazardous chemical, whose k_{soil} is very low, it is also very important to know the precise magnitude of the removal rate. For example, the soil removal rate for mirex can vary from 10^{-4} to 10^{-1}. This range is almost negligible in absolute terms if compared with the range of variability of butadiene (0.5-2) but it is not in terms of magnitude. For this reason, in future work, we will repeat the sensitivity analyses on the logarithm of the relevant outputs.

For the load2Sea, the situation is considerably different with the chemical selection accounting, alone, for just the 10% of the total variability. The highest effect is caused by annual discharge and in terms of first order effects, by the sediment yield. Organic carbon

and catchment retention time also have a non-negligible effect on the output. This means that the definition of archetypes of the freshwater compartment needs to take into consideration several interacting parameters.

5.3.8. Detailed result of sensitivity – ocean compartment

Environment specific inputs

In the following figures, the results of the sensitivity analysis for the four chemicals are reported.

In Figure S4.23, results of the sensitivity analysis of MAPPE for acephate are reported for the 2 selected model outputs. As expected, for acephate, having a strongly hydrophilic character, without advection the ocean removal rate does not change at all, showing the meaningless results reported in the Figure. On the contrary, considering advection, the 100% of the removal rate variability is accounted for by the average current speed.

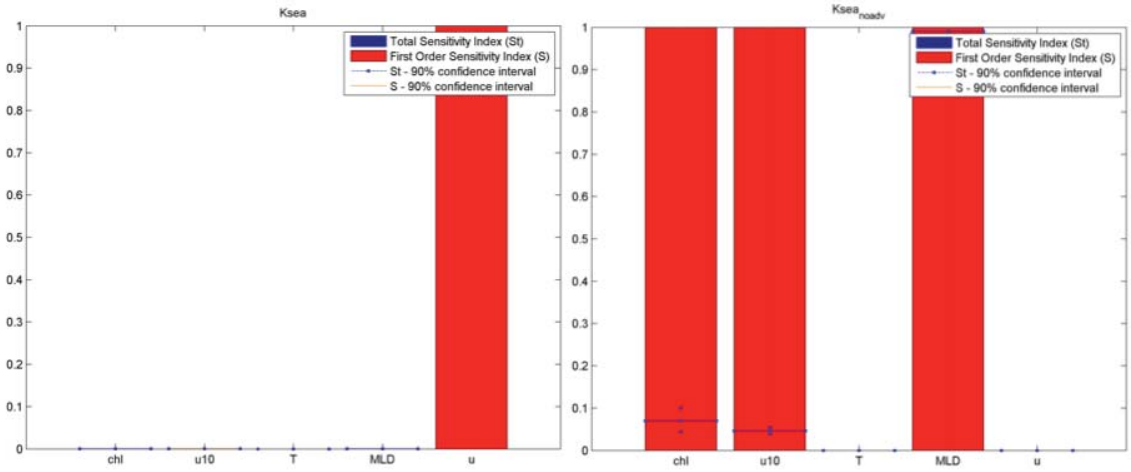

Figure S4.23. First order, total order sensitivity indices and their confidence interval of environment specific input factors of the MAPPE model for acephate. Two charts refer to two different model outputs

In Figure S5.19, results of the sensitivity analysis of MAPPE for lindane are reported for the 2 selected model outputs. Also in this case the advection represents the most important process for removal of the chemical. In this case, however, the wind speed and the depth of the ocean mixing layer also account for a share of output variability. As noted for the previous compartment, and also in this case, the multimedia character of lindane tends to result in highest concentrations in the compartment where it is emitted.

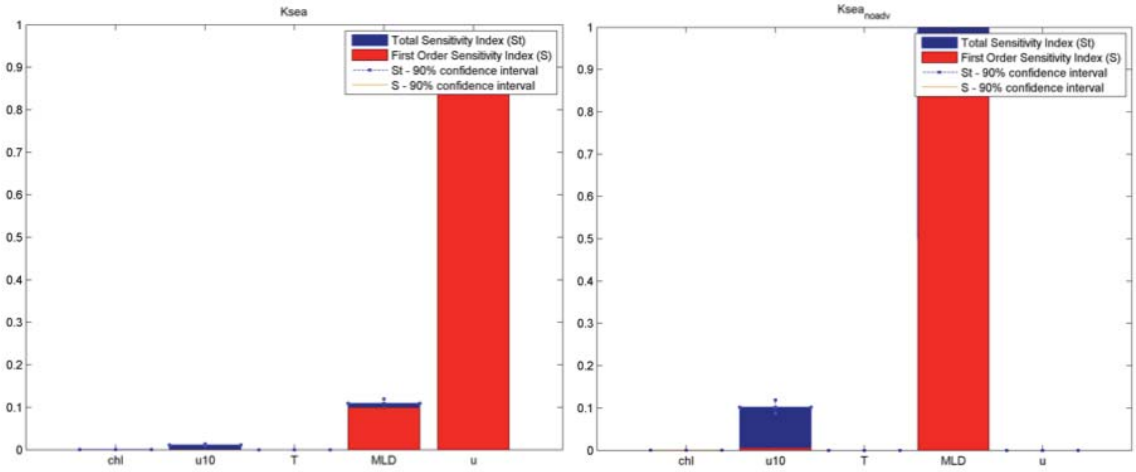

Figure S4.24. First order, total order sensitivity indices and their confidence interval of environment specific input factors of the MAPPE model for γ-HCH. Two charts refer to two different model outputs

In Figure S4.25, results of the sensitivity analysis of MAPPE the di(n-octyl)phthalate are reported for the 2 selected outputs. The different properties of the chemical results in other parameters being important. In particular, the main process regulating removal seems to be chemical sinking with organic carbon, which is affected by the depth of the ocean mixing layer and the chlorophyll concentration. Advection still accounts for a share ofoutput variability.

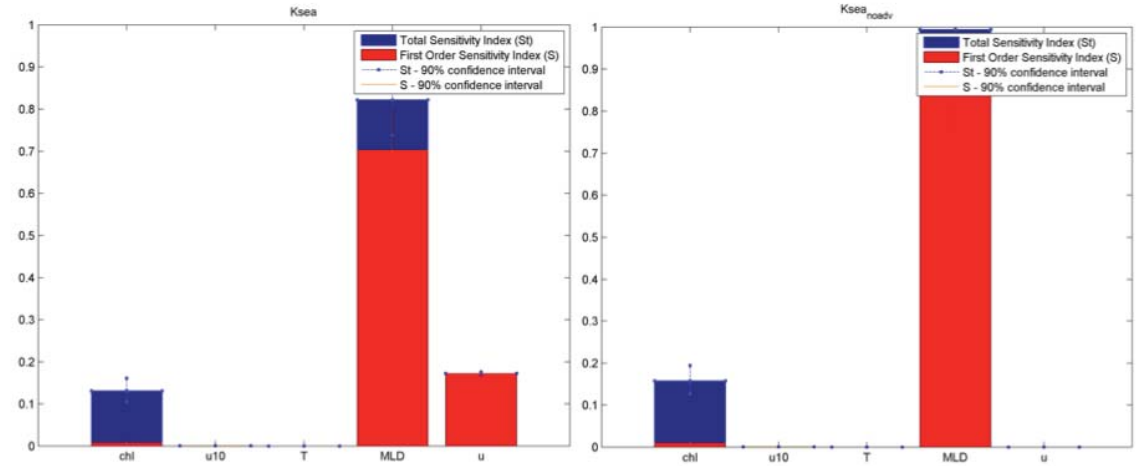

Figure S4.25. First order, total order sensitivity indices and their confidence interval of environment specific input factors of the MAPPE model for di(n-octyl)phthalate. Two charts refer to two different model outputs

Finally, in Figure S4.26, results of the sensitivity analysis of MAPPE for butadiene are reported. The different properties of the chemical results in other parameters being important. In particular, the main process regulating the removal seems to be chemical volatilization, which is affected by the depth of the ocean mixing layer and the wind speed.Advection only accounts for a small output variability.

With respect to the other compartments, the behaviour of MAPPE Global for the ocean compartment seems to better reflect the chemical characteristics. In the next section, the results of the analysis considering both environment and chemical specific inputs are shown.

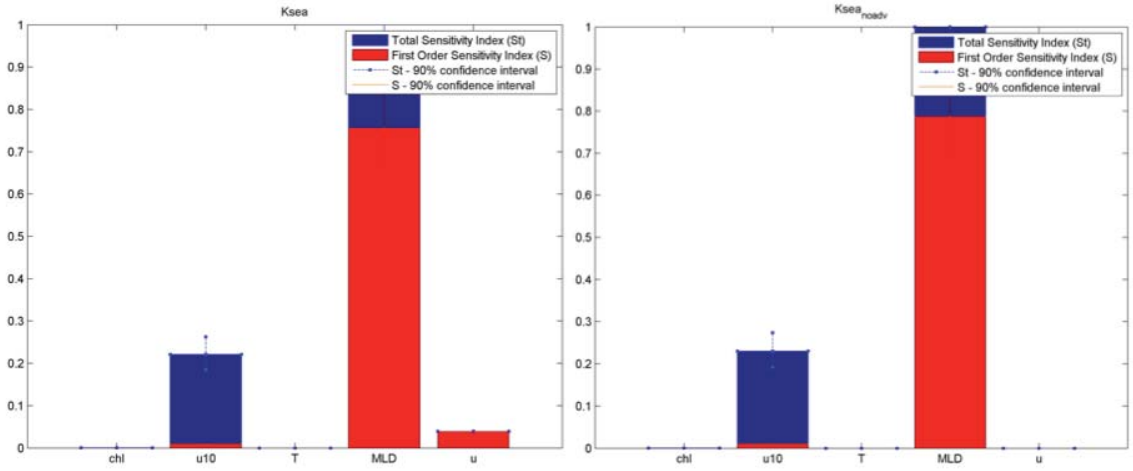

Figure S4.26. First order, total order sensitivity indices and their confidence interval of environment specific input factors of the MAPPE model for butadiene. Two charts refer to two different model outputs

Results – Environment and chemical specific inputs

In Figure S4.27 the results of this latter sensitivity analysis are reported. Both with and without advection the effect of the specific chemical on the outputs of MAPPE Global is significant. Amongst the other parameters, the ocean mixing layer depth in combination with the chemical and the wind speed plays an important role. Also in this case, therefore, the volatilization process, in absolute terms is responsible for the highest variability among the environmental parameters. An analysis on the logarithm of k_{sea}, may produce different outcomes.

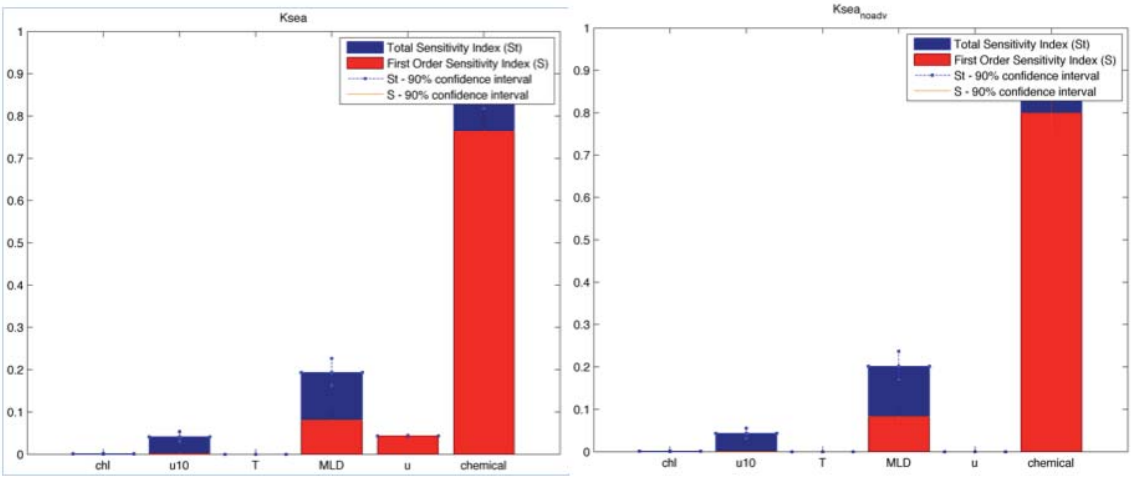

Figure 4.27. First order, total order sensitivity indices and their confidence interval of environment and chemical specific input factors of the MAPPE model. Two charts refer to two different model outputs

5.3.9. Comparison of the uncertainty in air removal rate using climatic vs. continental archetypes

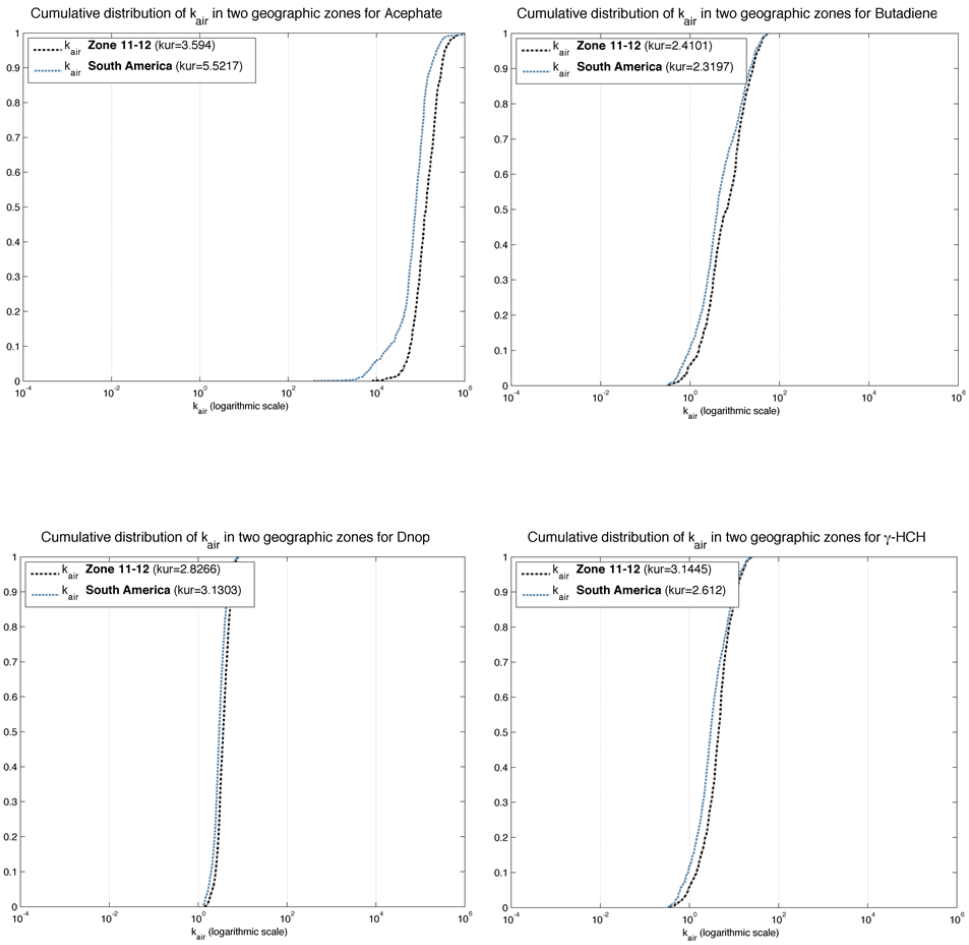

Figure S4.28. Cumulative distributions of k_{air} calculated in the cells of two different geographic zones: climatic zones 11 and 12 (according to Koppen Geiger Classification) and South America. The four pictures refer to four different chemicals. Values of k_{air} in abscissa are represented in logarithmic scale. In the legend the value of the distributions' kurtosis are also reported in parentheses.

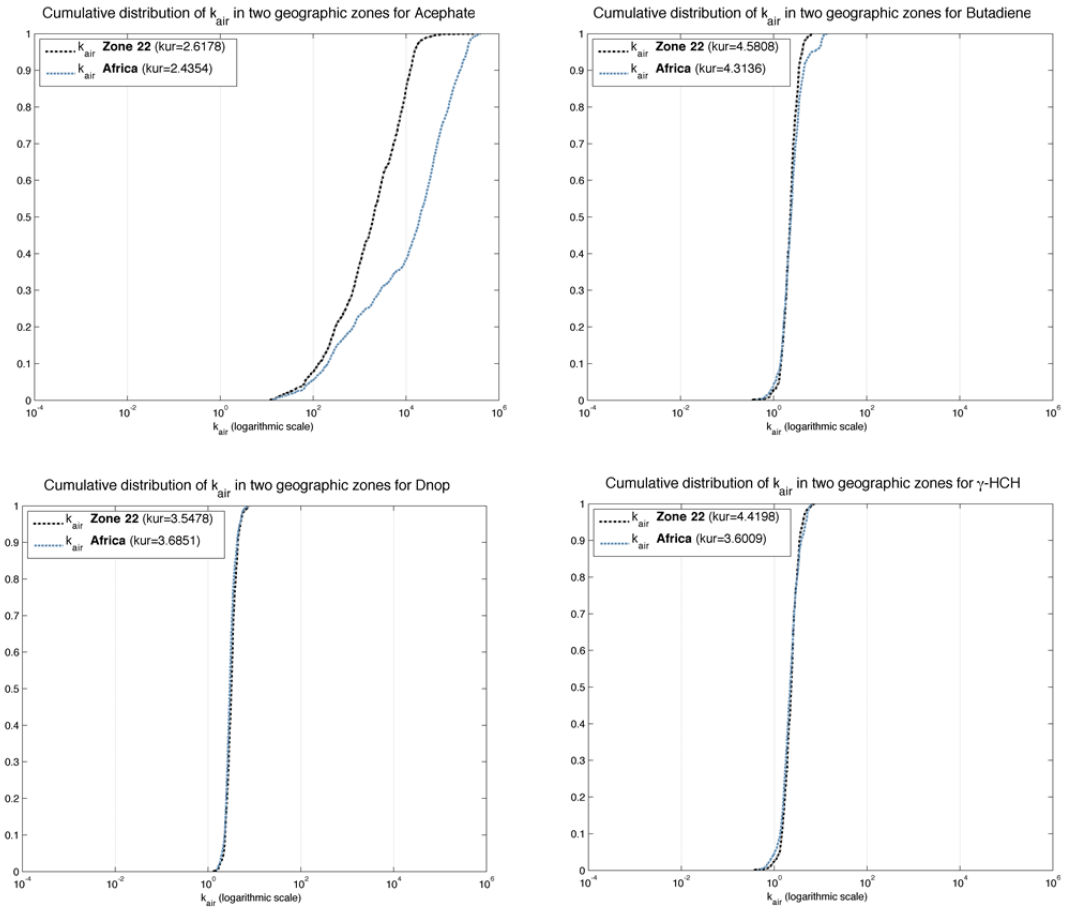

Figure S4.29.Cumulative distributions of k_{air} calculated in the cells of two different geographic zones: climatic zone 22 (according to Koppen Geiger Classification) and Africa. The four pictures refer to four different chemicals. Values of k_{air} in abscissa are represented in logarithmic scale. In the legend the value of the distributions' kurtosis are also reported in parentheses.

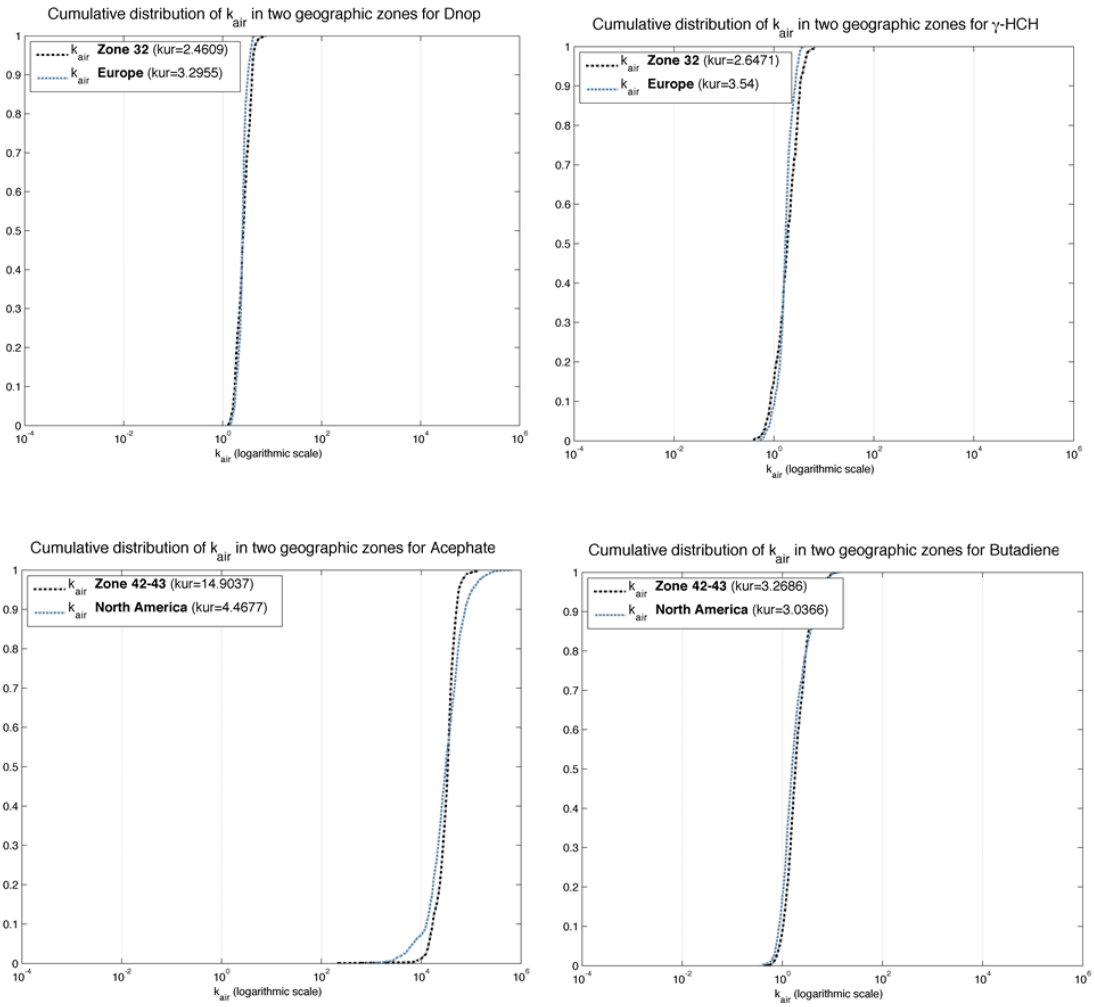

Figure S4.30. Cumulative distributions of k_{air} calculated in the cells of two different geographic zones: climatic zone 32 (according to Koppen Geiger Classification) and Europe. The four pictures refer to four different chemicals. Values of k_{air} in abscissa are represented in logarithmic scale. In the legend the value of the distributions' kurtosis are also reported in parentheses.

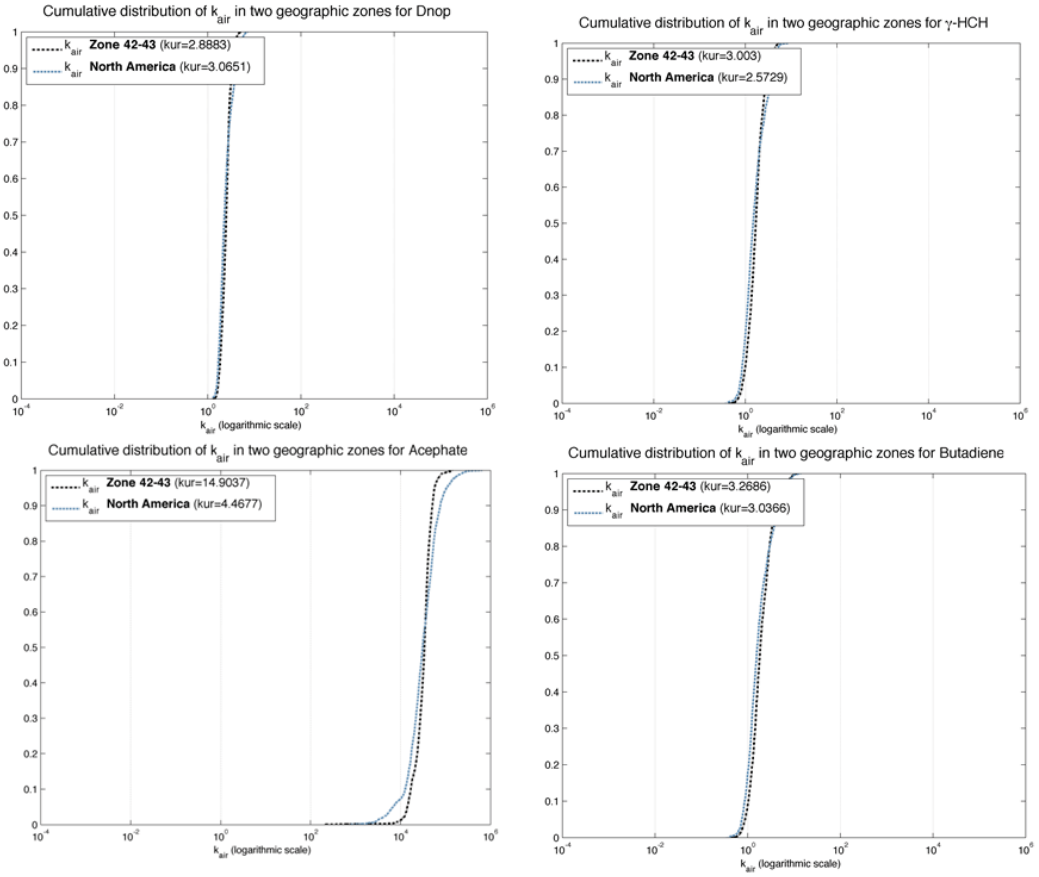

Figure S4.31. Cumulative distributions of k_{air} calculated in the cells of two different geographic zones: climatic zone 42-43 (according to Koppen Geiger Classification) and North America. The four pictures refer to four different chemicals. Values of k_{air} in abscissa are represented in logarithmic scale. In the legend the value of the distributions' kurtosis are also reported in parentheses.

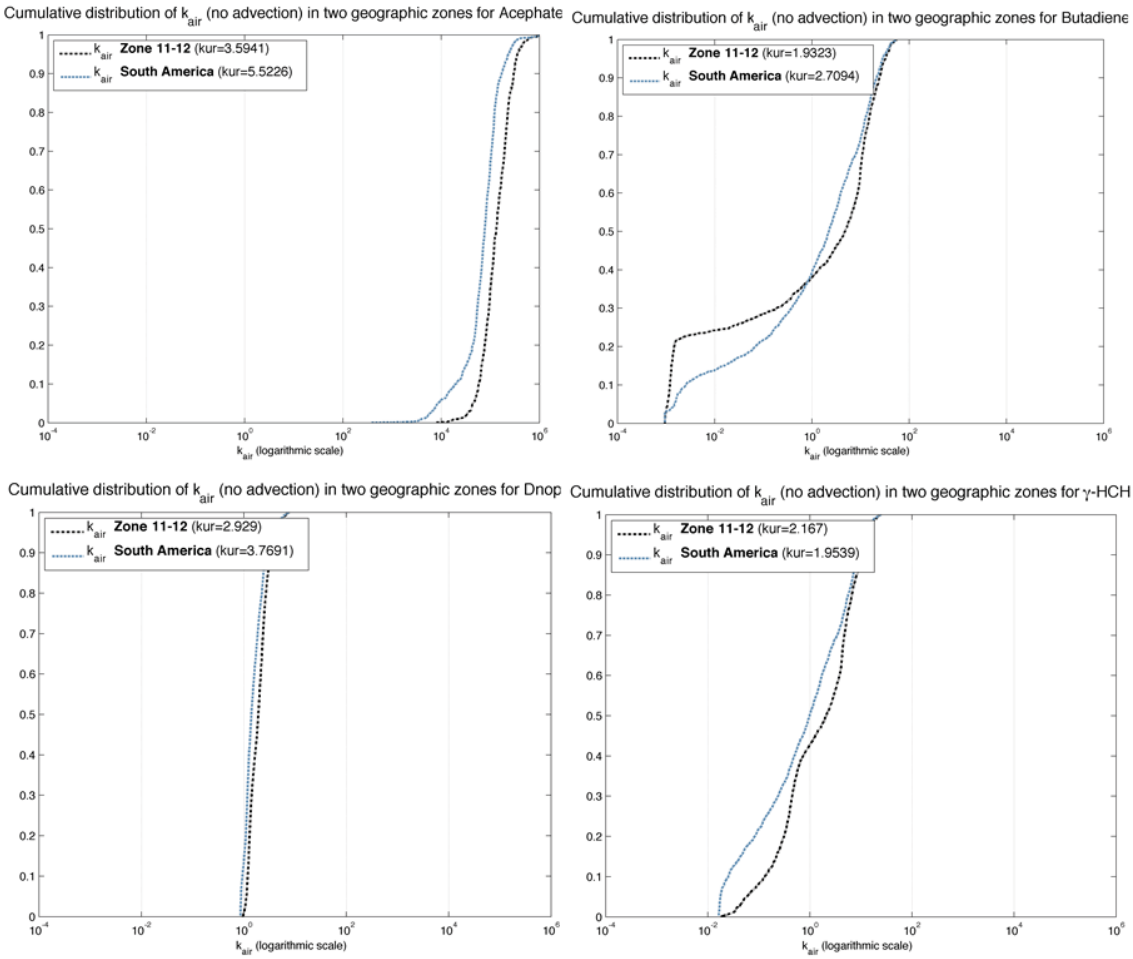

Figure S4.32. Cumulative distributions of k_{air} (without considering advection) calculated in the cells of two different geographic zones: climatic zone 11-12 (according to Koppen Geiger Classification) and South America. The four pictures refer to four different chemicals. Values of k_{air} in abscissa are represented in logarithmic scale. In the legend the value of the distributions' kurtosis are also reported in parentheses.

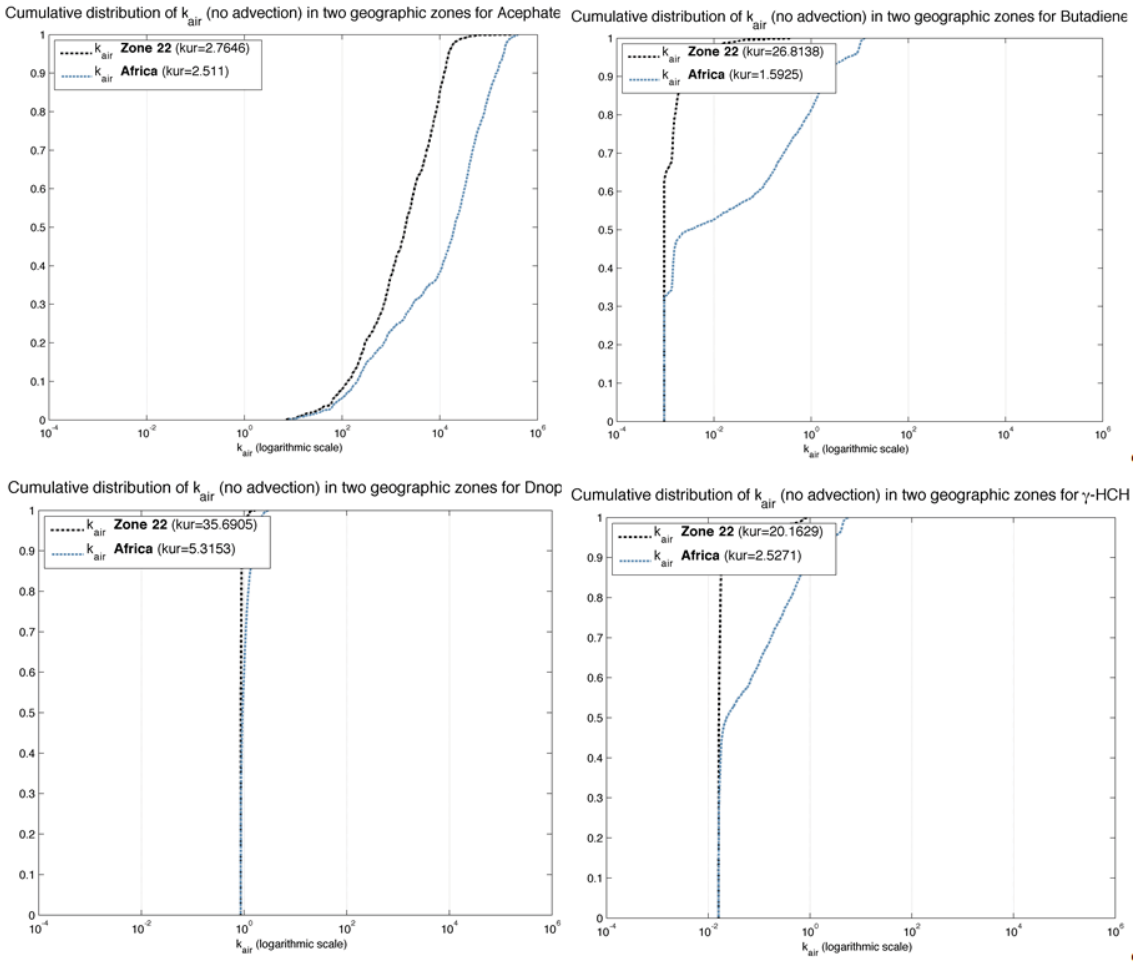

Figure S4.33. Cumulative distributions of k_{air} (without considering advection) calculated in the cells of two different geographic zones: climatic zone 22 (according to Koppen Geiger Classification) and Africa. The four pictures refer to four different chemicals. Values of k_{air} in abscissa are represented in logarithmic scale. In the legend the value of the distributions' kurtosis are also reported in parentheses.

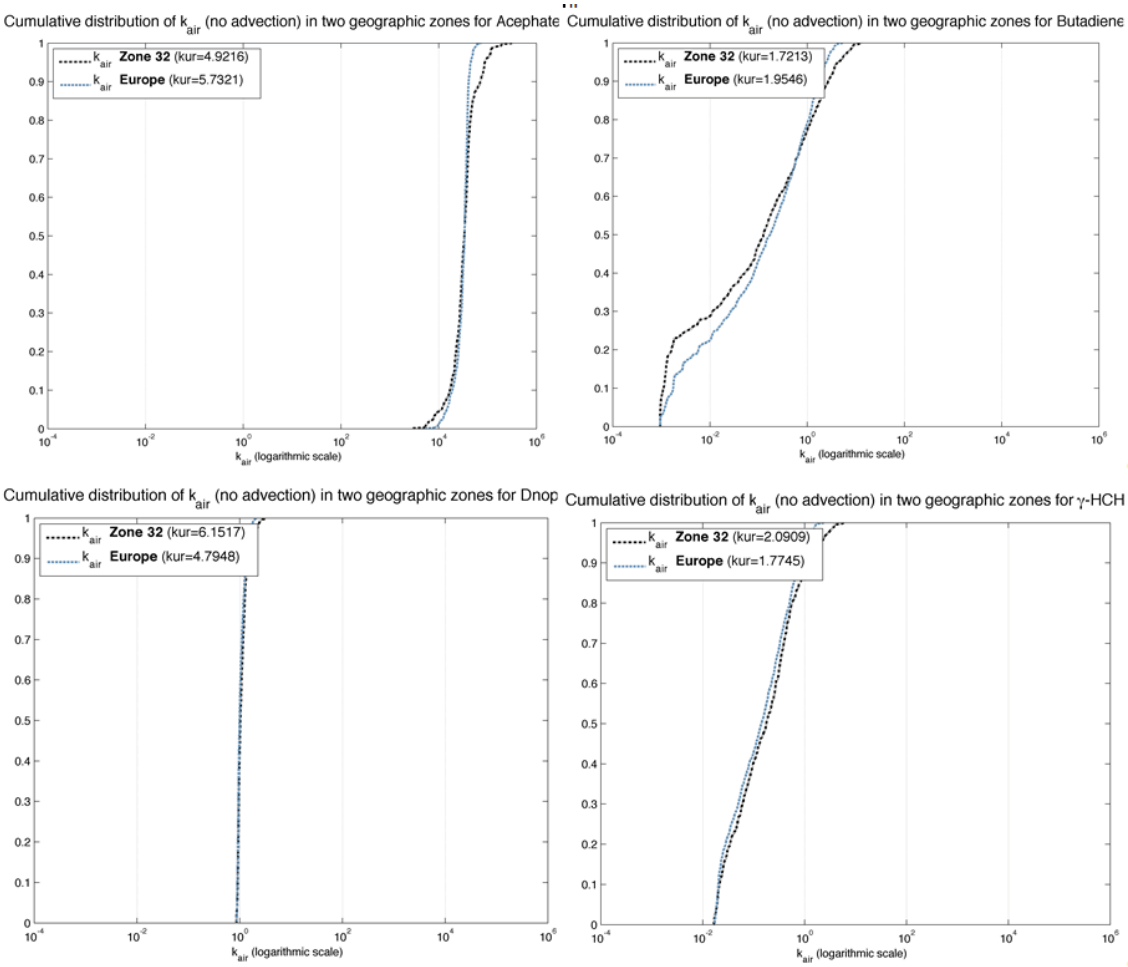

Figure S4.34. Cumulative distributions of k_{air} (without considering advection) calculated in the cells of two different geographic zones: climatic zone 32 (according to Koppen Geiger Classification) and Europe. The four pictures refer to four different chemicals. Values of k_{air} in abscissa are represented in logarithmic scale. In the legend the value of the distributions' kurtosis are also reported in parentheses.

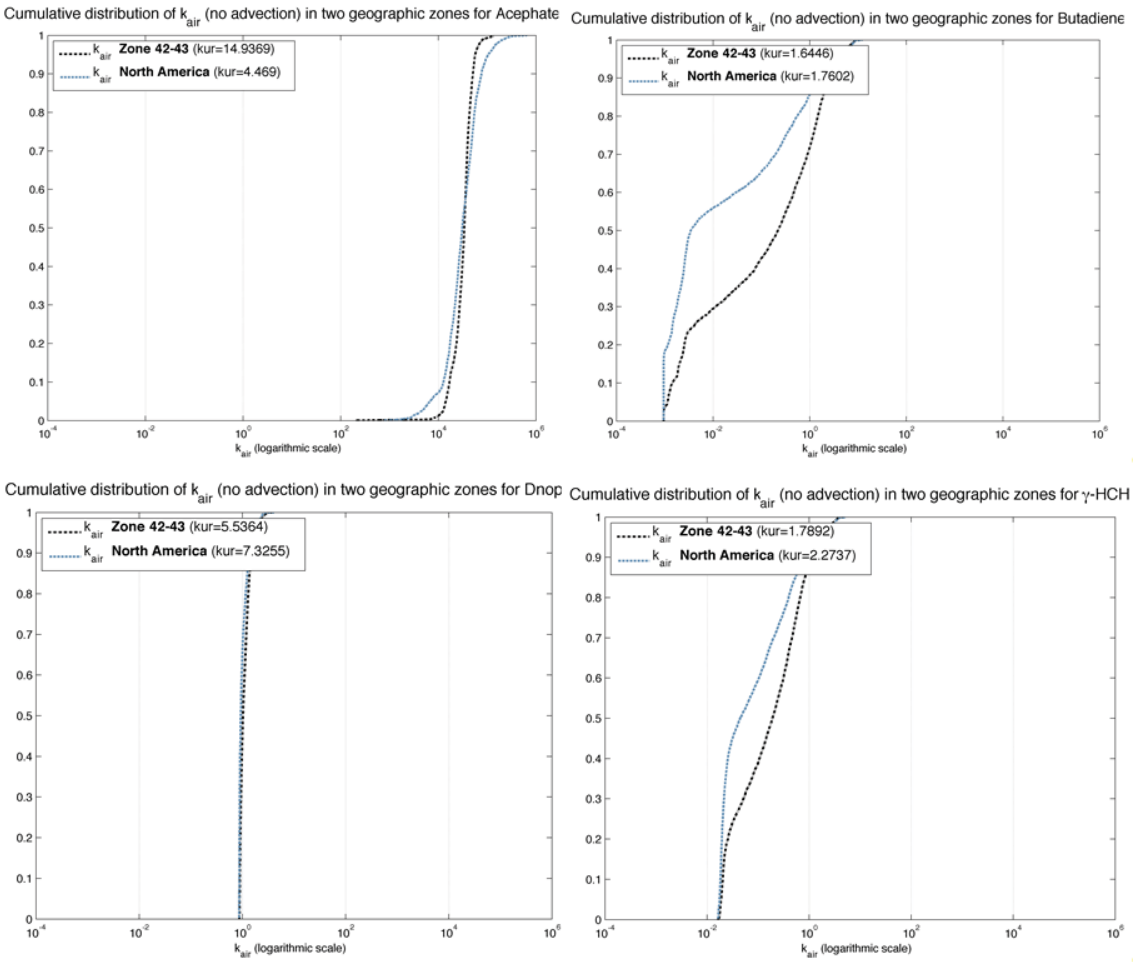

Figure S4.35. Cumulative distributions of k_{air} (without considering advection) calculated in the cells of two different geographic zones: climatic zones 42-43 (according to Koppen Geiger Classification) and North America. The four pictures refer to four different chemicals. Values of k_{air} in abscissa are represented in logarithmic scale. In the legend the value of the distributions' kurtosis are also reported in parentheses.

5.3.10. Spatial variability of freshwater CFs at different scale, detailed analysis

MAPPE Europe was used to calculate annual average environmental concentrations in air, soil, surface water and European seas as a basis for assessing drivers of variability that may result in differences in characterisation factors.

We calculate CF for freshwater. For other compartments (soil and sea), we calculate concentration and fate factors to be used to build CF for marine and terrestrial ecotoxicity.

MAPPE Europe was run for different compartments and at different resolutions considering two different emission scenarios:

- Agricultural emission related to a soil/water scenario: multiple uniform emission of 1 Kg/ha in Europe, assuming a 1% of drift. We considered all Europe, countries and watersheds. [endosulfan example]
- Industrial emission related to an air scenario: multiple point source emission from industrialized areas of a population weighted emission (Source receptor matrix for accounting for advection in air) [nitrobenzene and 1,1,1,2 tetrachloroethane example]

Agriculture scenario: Endosulfan emission in Europe

According to the higher variability associated with multimedia chemical, we decided to deepen the analysis of spatial variability running endosulfan. We built an emission scenario for soil, in which a uniform emission of 1kg/ha in soil in Europe, for agricultural use is assumed. This is a hybrid scenario (soil and water) because we assume 1% of the emission directly to water via drift, and site-specific runoff into water.

The model was run for all Europe and then for two specific cases: Germany and UK. The two countries where chosen as: they present different retention time to sea; Germany watersheds mainly end up in other countries while UK has direct loading to sea.

We calculated: concentration in soil and water, fate factors and freshwater characterisation factors.

All Europe

We ran the model under the assumption of emission of 1 Kg/ha in soil in all Europe. In Figure S4.36, the maps of concentration in soil and water are presented. For soil, the variability is within one order of magnitude whereas for water variability spans over three orders of magnitude (considering minimum and maximum possible values)

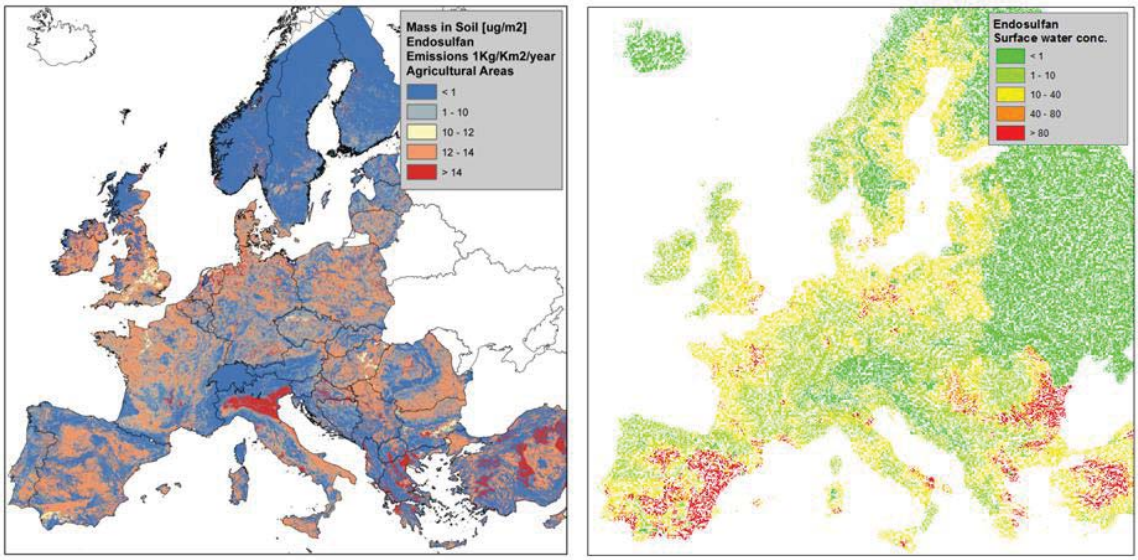

Figure S4.36. Map of concentration in soil (in µg/m^2) and water (in ng/l) after an emission of endosulfan to soil

The overall variability of fate factor in soil (Figure S4.37) is very low among countries.

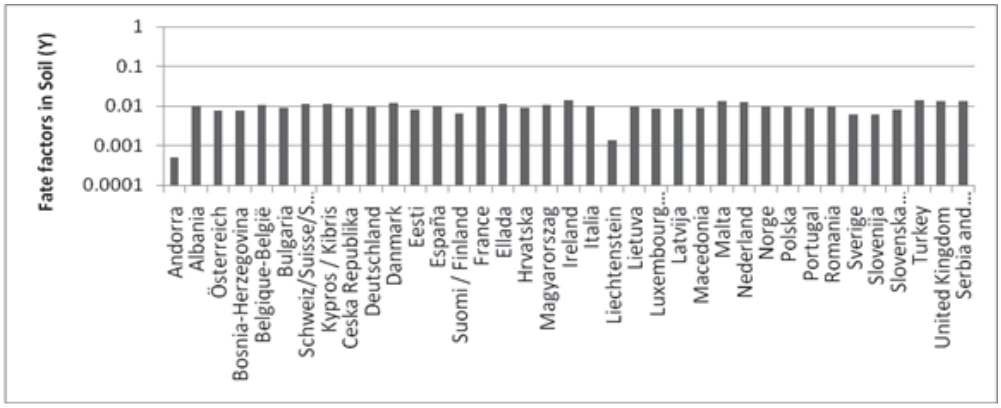

Figure S4.37. Fate factor in soil across Europe. Values expressed as FF (Y)

The fate factors and the characterisation factors for Europe were calculated with two different approaches: by country and by watershed. The CF's calculated by country are reported in Figure S4.38. The variability by country spans over 3 orders of magnitude if we consider small countries as Malta and Andorra. Otherwise, for other countries, the variability is of one order of magnitude. The average value for Europe (76.5) is close to the Usetox value (72.2). The latter calculated considering an emission to agricultural soil.

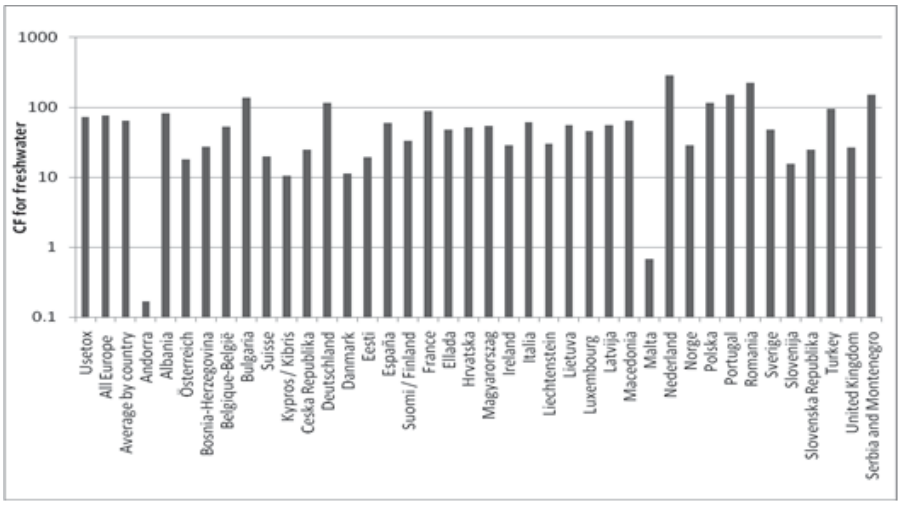

Figure S4.38. Characterisation factors (PAF.m3.day.kg-1) by country related to an emission of endosulfan to soil in all Europe

For calculating freshwater CF by watershed we consider all of the over 4000 watersheds in Europe.

MAPPE was run at watershed level, calculating concentrations, fate factors and CF for over 4000 watersheds and sub watersheds (Figure S4.34 a and b). The results for the major watersheds are presented in Figure S4.39 and frequency of CF values for all the watersheds is reported in Figure 4.41. More than 85% of freshwater CF's span from 1 to 100. This means that the uncertainty related to the use of the continental default factor provided by USEtox for endosulfan is low (1-2 order of magnitude). Cases of several orders of magnitude of differences accounted for less than 15% of the watershed and foremost, they refer to small watershed only. As presented in the figure 9, the major watersheds present CF within the same order of magnitude of USEtox.

Besides, the difference between the fate factor in soil and in water, is over one order of magnitude and this has to be further investigated.

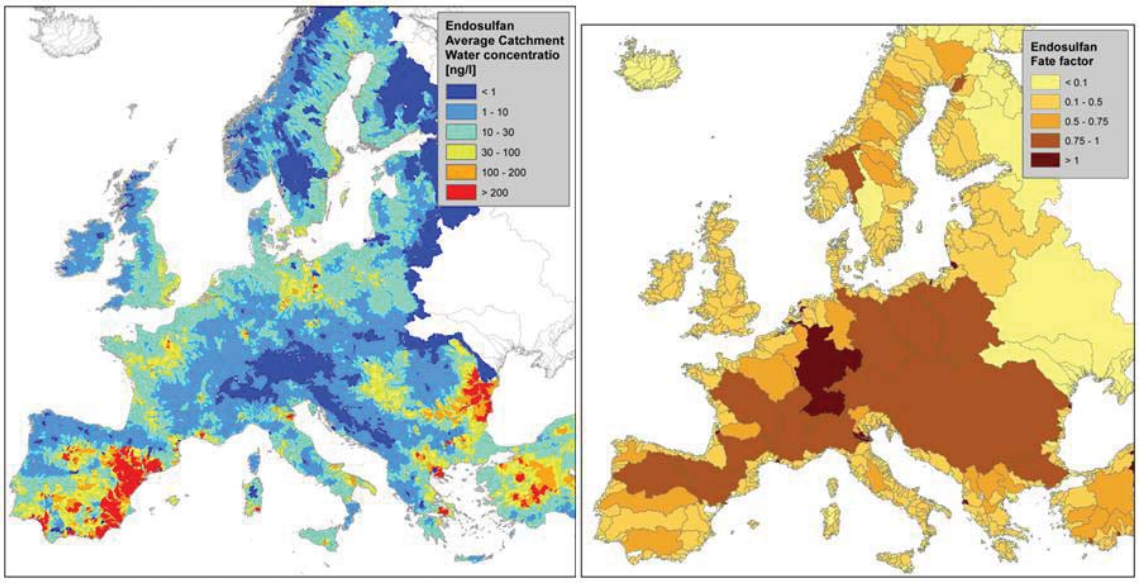

Figure S4.39. Maps of concentration (per watershed) and fate factor (in days) for river (for major watershed) in Europe related to uniform emission of endosulfan in soil.

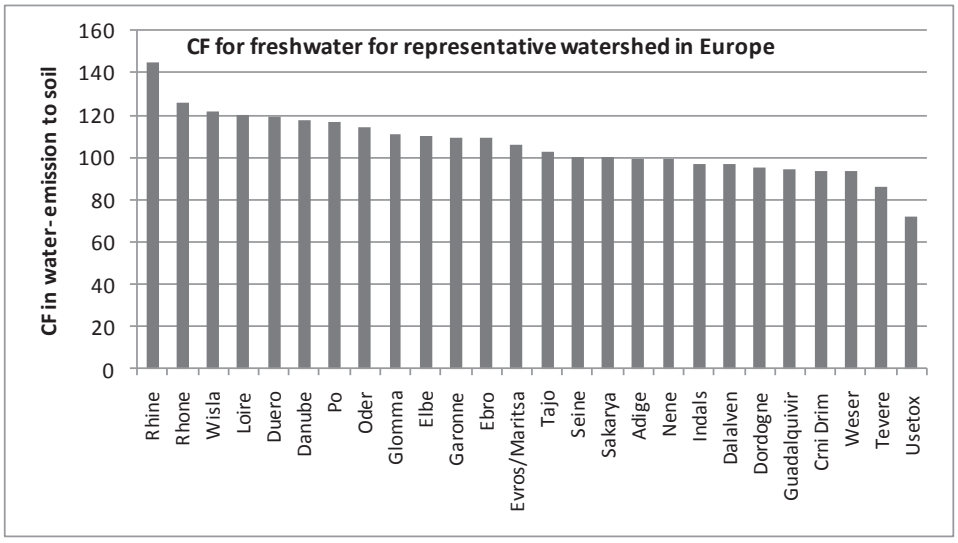

Figure S4.40. Carachterisation Factors (PAF.m3.day.kg-1) for freshwater due to a uniform emission of endosulfan to soil in representative European watershed (average of catchment area 10E5 Km^2)

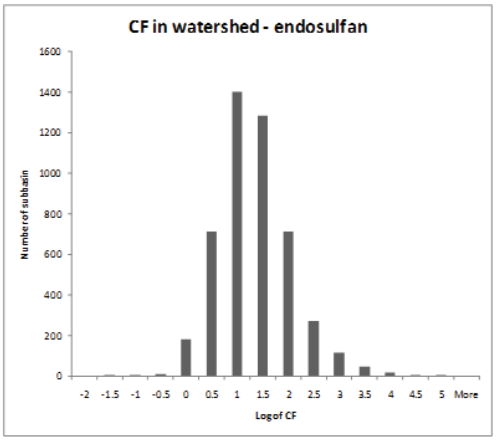

Characterisation factor at watershed level in Europe		
classes		%
0.01	0.1	0.15
0.1	1	4.05
1	10	44.39
10	100	41.89
100	1000	8.09
1000	10000	1.37
10000	100000	0.06

Figure S4.41. Frequency distribution of CF's in Europe and percentage of watershed within classes

Germany

We run the model under the assumption of a uniform multiple source emission of 1kg/ha in soil in Germany. In Figure S4.42, concentrations in water and soil related to this emission are presented.

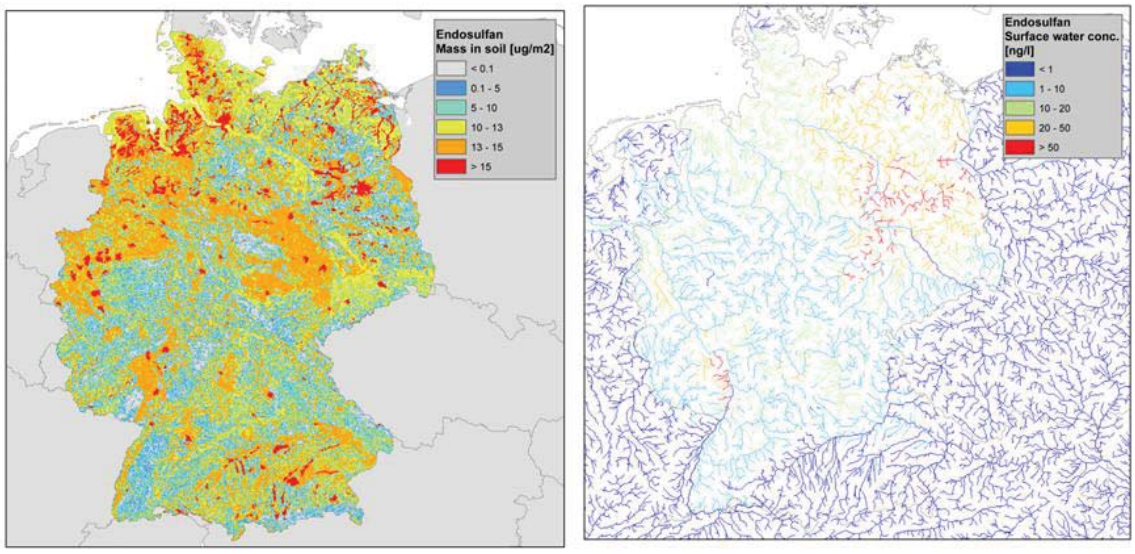

Figure S4.42. Concentration in surface water and soil related to a uniform emission of endosulfan in soil in Germany

For an emission to soil, the only country in which we find concentration in soil is Germany and the variability in concentration spans over an order of magnitude. The fate factor in soil for an emission to soil is equal to 9.8 E-3 y. The fate factor in water is 0.7 y.

The freshwater CF for an emission from Germany is calculated accounting also for the fate of the emitted chemical in other countries. The overall CF is 106.2 and it is mainly due to the quantity of endosulfan that remains in Germany. In the table associated to the Figure S4.43 the CF associated with each country are presented.

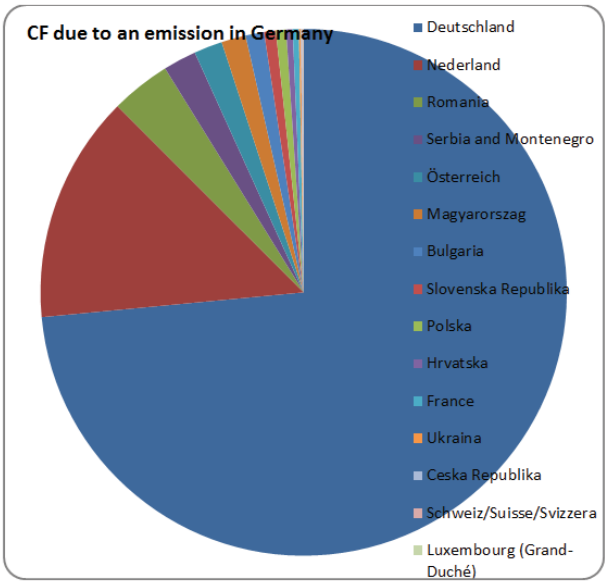

Country	CF
Deutschland	78.03048
Nederland	14.85975
Romania	3.906834
Serbia and Montenegro	2.159195
Österreich	1.854263
Magyarorszag	1.58891
Bulgaria	1.208144
Slovenska Republika	0.764978
Polska	0.658783
Hrvatska	0.430552
France	0.393838
Ukraina	0.132694
Ceska Republika	0.092913
Schweiz/Suisse/Svizzera	0.062627
Luxembourg (Grand-Duché)	0.020814
Belgique-België	0.001583
Danmark	0.00038

Figure S4.43. Contribution to the overall characterisation factor of an emission from Germany and associated CF table in EU country after an emission in soil in Germany. Countries not mentioned have CF (PAF.m3.day.kg-1) equal to zero

United Kingdom

As for Germany, we ran the model under the assumption of a uniform multiple source emission of 1kg/ha in soil in UK. In the figure concentration in water and the load to the sea related to the emission are presented.

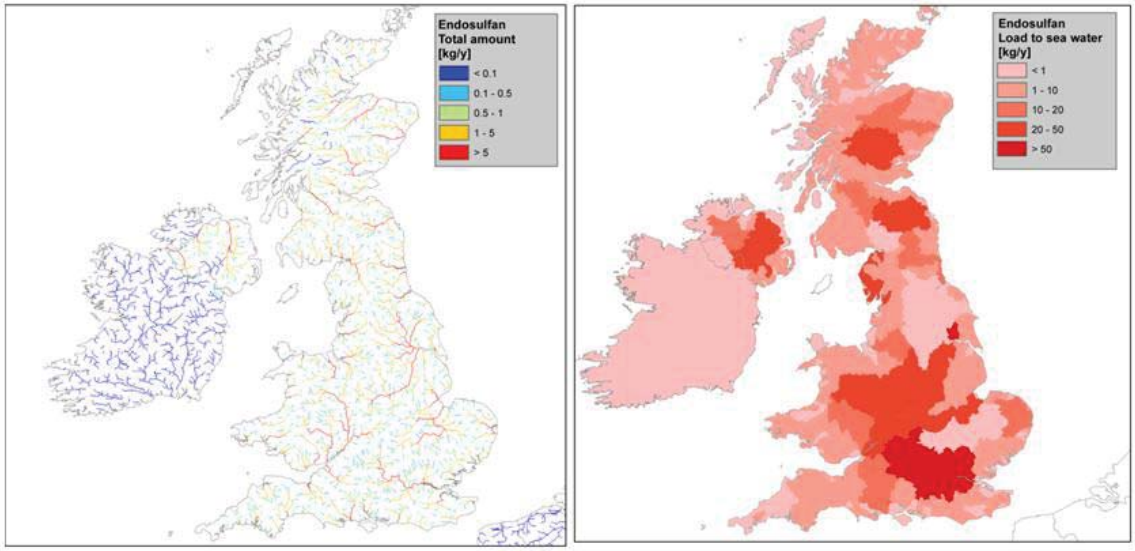

Figure S4.44. Mass of chemical (in Kg) in UK for each trait of the UK river network and the associated load to the sea

In UK, the fate factor in soil for an emission to soil is equal to 1.35 y. The CF's for freshwater in UK reflect the presence of relatively short river network, that quickly reaches the sea. The CF is lower than in Germany and it is equal to 26.27, of which only 0.12 is related to Ireland.

Since UK is completely surrounded by sea, it is relevant to account for concentrations in the sea and marine ecotoxicity related to coastal exposure has to be further explored.

Industrial scenario : 1,1,1,2 tetrachloroethane and nitrobenzene emission in Europe

In order to explore variability related to the source of emission, we ran MAPPE Europe for two chemicals: one is highly volatile (1,1,1,2 tetrachloroethane) and the second is a multimedia chemical (nitrobenzene). As the model setting changes accordingly to the emission assumptions, and further test on fate factors are needed, in this section we present result mainly related to concentration. A full set of fate factor and characterisation factors will be provided in the second phase, along with CF for human toxicity.

Example of 1,1,1,2 tetrachloroethane

The scenario for running the model was related to an industrial emission.

An emission of 1,1,1,2 tetrachloroethane was chosen to run the model considering a scenario of atmospheric emissions from industrialized (urban) areas in Europe. 1,1,1,2 tetrachloroethane has the highest solvent power of any chlorinated hydrocarbon and it was widely used as a solvent and as an intermediate in the industrial production of trichloroethylene, tetrachloroethylene, and 1,2-dichloroethylene.

The scenario assumes an overall amount of 100 tons emitted to air per year; this was scaling by country on the basis of population density. Thus, the emissions from the smaller European countries (like Estonia or Slovenia) are in a range 0.1-1 t/y, while the industrial states (as Germany, UK France and Italy) emitted more then 10t/y (besides, Spain and Poland are also close to this amount emitting 7-8 t/y); for the other cases the emissions vary between 1-4 t/y. Two maps of the results for 1,1,1,2 tetrachloroethane are reported in Figure S4.45.

In Figure S4.45a, the higher concentrations in atmosphere are related to the source of emissions (populated areas under the considered scenario) but also to climatic conditions (for instance, despite the higher emissions in Spain or Italy, the elevated air removal rate leads to relatively lower concentrations in southern Europe compared to those in the central part of Europe).

In Figure S4.45b, the spatial variability of 1,1,1,2-tetrachloroethane mass in soil after an emission to air is presented. In this case, the concentrations follow the pattern of the atmospheric deposition which explains why higher concentrations are predicted in the mountain areas, in which typically comparatively lower temperatures are expected.

In Figure S4.46, average concentrations by watershed are presented. They span over 3 orders of magnitude. Differences up to one order of magnitude, have been found for the 1,1,1,2-tetrachloroethane scenario described above, when comparing estimates of environmental concentrations (median or mean for Europe) produced by the highly resolved MAPPE model with non-spatial USEtox model.

Generally, USEtox tends to overestimate the forecasts of MAPPE model and predicts values close to the upper bound (95% quantile) of MAPPE results.

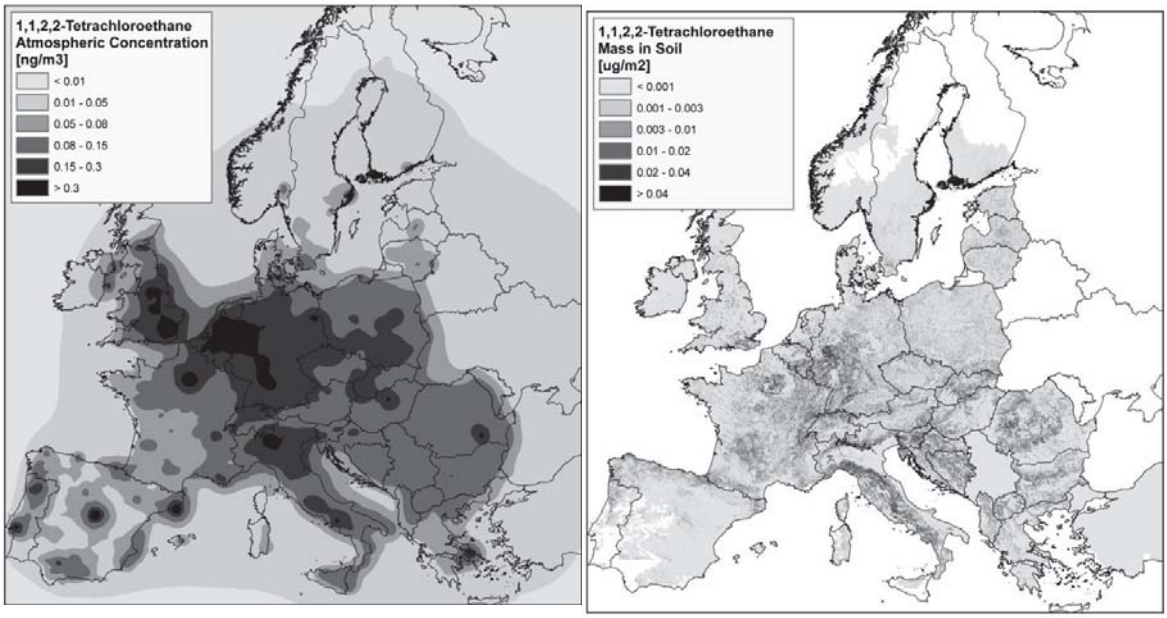

Figure S4.45. Concentration of 1,1,1,2 tetrachloroethane in air and in soil after an emission in air from highly industrialized areas

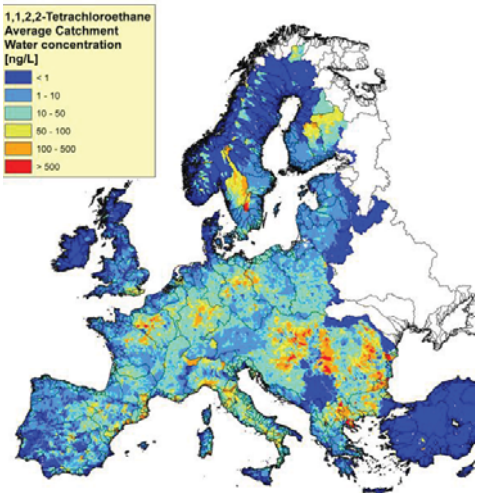

Figure S4.46.Average concentration of 1,1,1,2 tetrachloroethane in watershed after an emission to air

Example of Nitrobenzene

Map of surface water concentration after an emission in air of nitrobenzene under the same assumption of 1,1,1,2 tetrachloroethane are reported in Figure S4.47. The figure presents the concentration in water due to deposition from air and in Figure S4.48, variability of concentration in major watershed is presented. The variability in the concentration is high (up to 7 orders of magnitude). This variability is mainly related to the area of the catchment. In Figure S4.49 and S4.50, two coefficients of variability where assessed: firstly, the ratio of

standard deviation over media and then the latter ratio over the area of catchment. Figure S4.50 shows that, normalising the results by the area, the variability is not so high in the majority of watersheds.

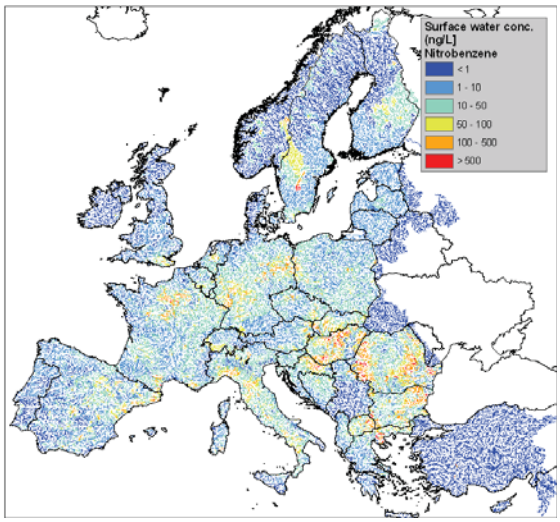

Figure S4.47. Concentration of nitrobenzene in water after an emission in air from highly industrialized area

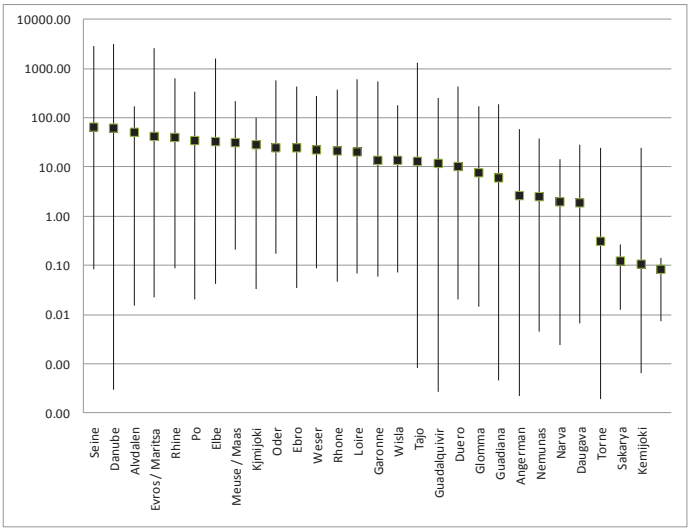

Figure S4.48. Spatial variability of Nitrobenzene concentration in the major watershed in Europe. Min max and average of the concentration in surface water (ng/L) are presented

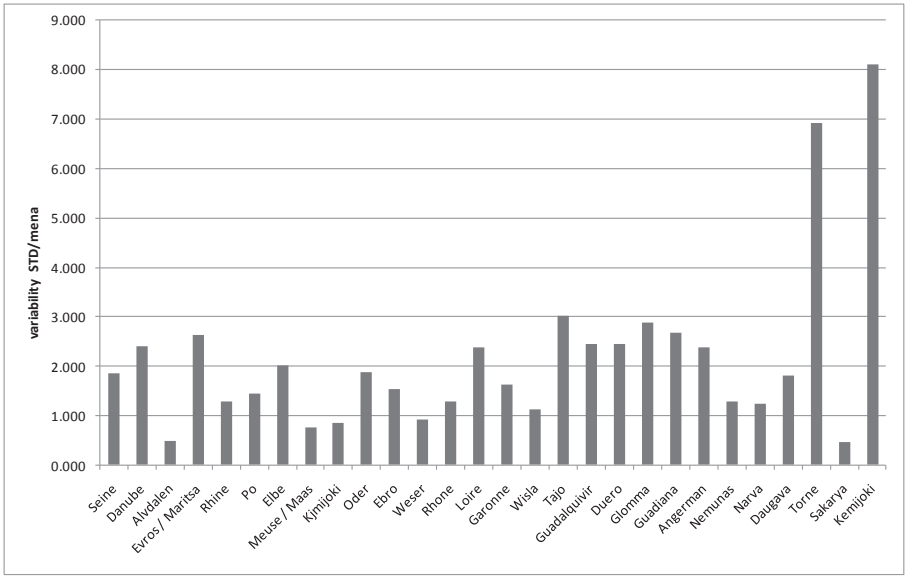

Figure S4.49. Variability in concentration by watershed, espressed as the ratio standard deviation over mean

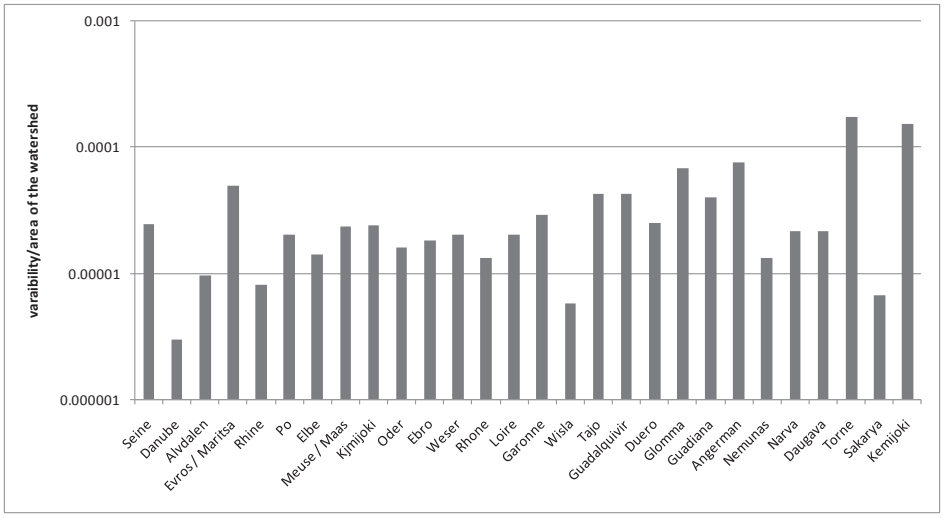

Figure S4.50. Variability compared with area of the watershed

In Figure S4.51 and S4.52, the variability of FF in soil is presented. These results have to be considered as preliminary result, as we are still testing the calculation of fate factors from point source emissions.

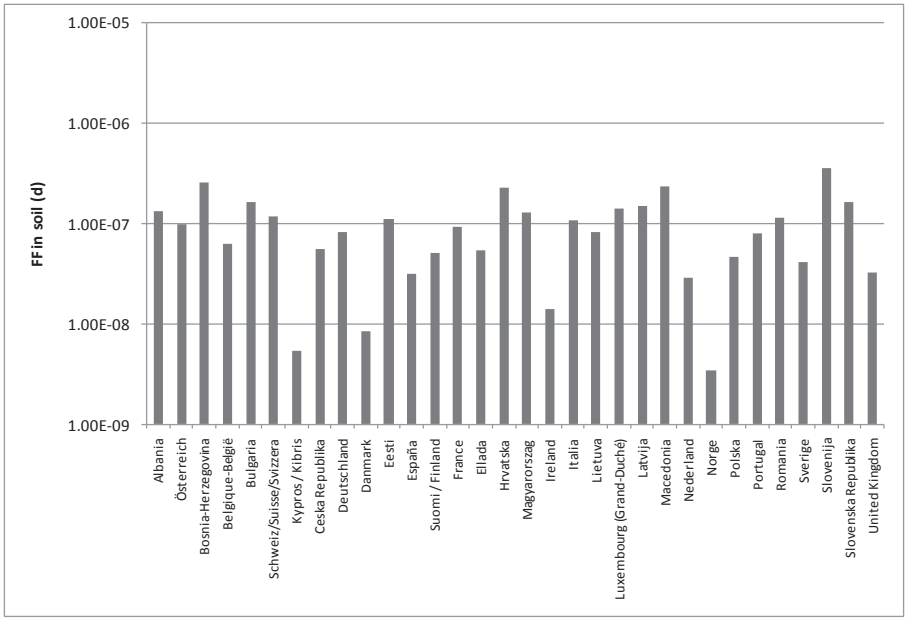

Figure S4.51. Variability of FF in soil (d) to to an emission of nitrobenzene in air

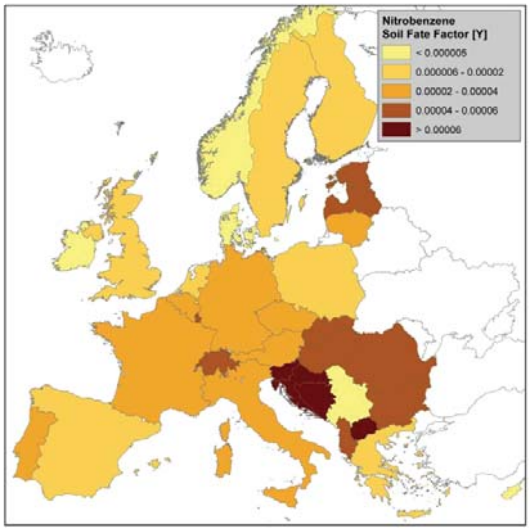

Figure S4.52. Fate factor in soil due to an emission in air of nitrobenzene

5.3.11. Selected set of pollutants

Table S4.4 shows the chemical data of the set of 36 pollutants of the OMNITOX set (Margni et al. 2002).

Table S4.4. USEtox landscape parameters for the 17 subcontinental and the 8 zone continental resolution

Name	CAS	Degradable with H and K_{ow} = 0; Non-degradable or specification of partitioning coefficients = 1	Molecular Mass (g/mole)	Henry's Constant (Pa m3 mol-1) or K_{aw}	Log K_{ow}	tropospheric degradation half life (hours)	water-column degradation half life (hours)	Soil surface layer degradation half life (hours)	Source	sediment degradation half life (hours)	vegetation degradation half life (hours)	Soil root zone degradation half life (hours)	Soil vadose layer degradation half life (hours)	Source
Tetrachloroethylene	127-18-4	0	166	1.77E+03	2.88	5.50E+02	1.75E+03	1.70E+03	OMNITOX	5.50E+03	1.70E+03	1.70E+03	1.70E+03	MACKAY
carbon tetrachloride (CCl4)	56-23-5	0	154	2.76E+03	2.64	1.70E+04	1.70E+03	6.04E+03	OMNITOX	1.70E+04	5.50E+03	5.50E+03	5.50E+03	MACKAY
1,3-butadiene	106-99-0	0	54	7.36E+03	1.99	1.70E+04		5.50E+02	OMNITOX	1.70E+03	5.50E+02	5.50E+02	5.50E+02	MACKAY
Methomyl	16752-77-5	0	162	1.84E-05	0.60	5.80E+01	5.52E+03	5.03E+02	OMNITOX	5.04E+02	5.04E+02	5.04E+02	5.04E+02	USES
Acephate	30560-19-1	0	183	5.01E-08	-0.85	3.44E+01	1.28E+03	5.29E+01	OMNITOX	5.28E+01	5.28E+01	5.28E+01	5.28E+01	USES
Formaldehyde	50-00-0	0	30	3.37E-02	0.35	3.63E+00	9.58E+01	5.50E+01	OMNITOX	3.84E+02	9.60E+01	9.60E+01	9.60E+01	HOWARD
PCBs	1336-36-3	0	292	4.15E+01	7.10	4.73E+02	3.38E+02	9.00E+02	OMNITOX	1.34E+03	3.36E+02	3.36E+02	3.36E+02	Estimate
Di(n-octyl) phthalate	117-84-0	0	391	2.57E-01	8.10	1.87E+01	3.36E+02	3.37E+02	OMNITOX	6.54E+03	3.36E+02	3.36E+02	3.36E+02	USES
Hexabromobenzene	87-82-1	0	551	2.81E+00	6.07	3.36E+04	1.44E+03	1.44E+03	OMNITOX	5.76E+03	1.44E+03	1.44E+03	1.44E+03	Estimate
Cypermethrin	52315-07-8	0	416	1.92E-02	6.60	1.80E+01	1.20E+02	1.25E+03	OMNITOX	1.25E+03	1.25E+03	1.25E+03	1.25E+03	USES
Mirex	2385-85-5	0	546	8.11E+01	6.90	1.70E+02	1.70E+02	5.50E+04	OMNITOX	5.50E+04	5.50E+04	5.50E+04	5.50E+04	MACKAY
Trifluralin	1582-09-8	0	336	1.03E+01	5.34	1.70E+02	1.70E+03	1.70E+03	OMNITOX	5.50E+03	1.70E+03	1.70E+03	1.70E+03	MACKAY
Dicofol	115-32-2	0	370	2.42E-02	5.02	1.12E+02	9.00E+02	1.46E+03	OMNITOX	3.84E+02	1.46E+03	1.46E+03	1.46E+03	CALTOX
1,4-dichlorobenzene	106-46-7	0	147	2.41E+02	3.40	5.50E+02	1.70E+03	5.50E+03	OMNITOX	1.70E+04	5.50E+03	5.50E+03	5.50E+03	MACKAY
Aldrin	309-00-2	0	365	4.40E+00	3.01	4.99E+00	1.75E+04	1.70E+04	OMNITOX	5.50E+04	1.70E+04	1.70E+04	1.70E+04	MACKAY
1,1,2,2-Tetrachloroethane	79-34-5	0	168	3.67E+01	2.39	1.70E+04	1.70E+03	5.50E+03	OMNITOX	1.70E+04	5.50E+03	5.50E+03	5.50E+03	MACKAY
Captan	133-06-2	0	301	6.48E-04	2.30	1.70E+01	1.70E+01	5.50E+02	OMNITOX	5.50E+02	5.50E+02	5.50E+02	5.50E+02	MACKAY
Pronamide	23950-58-5	0	256	9.77E-04	3.43	2.91E+01	9.77E+02	1.93E+03	OMNITOX	1.80E+02	1.93E+03	1.93E+03	1.93E+03	CALTOX
Anthracene	120-12-7	0	178	5.56E+00	4.54	5.50E+01	5.50E+02	5.50E+03	OMNITOX	1.70E+04	5.50E+03	5.50E+03	5.50E+03	MACKAY
gamma-HCH (lindane)	58-89-9	0	291	5.14E-01	3.70	1.04E+03	1.70E+04	1.70E+04	OMNITOX	5.50E+04	1.70E+04	1.70E+04	1.70E+04	MACKAY
dimethylphthalate (DMP)	131-11-3	0	194	1.05E-02	2.12	1.70E+02	1.70E+02	5.50E+02	OMNITOX	1.70E+03	5.50E+02	5.50E+02	5.50E+02	MACKAY
Methanol	67-56-1	0	32	4.55E-01	-0.77	3.92E+02	5.50E+01	5.50E+01	OMNITOX	7.20E+01	9.60E+01	9.60E+01	9.60E+01	HOWARD

Name	CAS	Degradable with H and K_{ow} = 0; Non-degradable or specification of partitioning coefficients = 1	Molecular Mass (g/mole)	Henry's Constant (Pa m3 mol-1) or K_{aw}	Log K_{ow}	tropospheric degradation half life (hours)	water-column degradation half life (hours)	Soil surface layer degradation half life (hours)	Source	sediment degradation half life (hours)	vegetation degradation half life (hours)	Soil root zone degradation half life (hours)	Soil vadose layer degradation half life (hours)	Source
1,2-Dichloroethane	107-06-2	0	99	1.18E+02	1.48	1.70E+03	1.70E+03	5.50E+03	OMNITOX	1.70E+04	5.50E+03	5.50E+03	5.50E+03	MACKAY
Ethyl acetate	141-78-6	0	88	1.34E+01	0.73	1.94E+02	9.58E+01	1.70E+02	OMNITOX	3.84E+02	9.60E+01	9.60E+01	9.60E+01	HOWARD
N-Nitrosodiethylamine	55-18-5	0	102	3.63E-01	0.48	6.00E+00	6.00E+00	1.70E+03	OMNITOX	2.40E+01	2.40E+03	2.40E+03	2.40E+03	HOWARD
Thiram	137-26-8	0	240	3.04E-02	1.73	1.70E+02	1.70E+02	5.50E+02	OMNITOX	1.70E+03	5.50E+02	5.50E+02	5.50E+02	MACKAY
Propoxur	114-26-1	0	209	1.43E-04	1.50	5.00E+00	5.50E+02	5.50E+02	OMNITOX	1.70E+03	5.50E+02	5.50E+02	5.50E+02	MACKAY
Folpet	133-07-3	0	297	7.66E-03	2.85	2.45E+01	1.38E+04	1.38E+04	OMNITOX	1.38E+04	1.38E+04	1.38E+04	1.38E+04	USES
Benomyl	17804-35-2	0	290	4.93E-07	2.30	4.99E+00	1.70E+02	1.70E+03	OMNITOX	5.50E+03	1.70E+03	1.70E+03	1.70E+03	MACKAY
Hexachlorobutadiene	87-68-3	0	261	1.03E+03	4.78	1.28E+04	1.75E+03	1.70E+03	OMNITOX	1.70E+03	1.70E+03	1.70E+03	1.70E+03	USES
Hexachlorocyclopentadiene	77-47-4	0	273	2.70E+03	5.04	9.77E+02	8.63E+01	4.20E+02	OMNITOX	1.68E+03	4.20E+02	4.20E+02	4.20E+02	HOWARD
Heptachlor epoxide	1024-57-3	0	389	2.10E+00	4.98	7.43E+01	7.03E+03	7.03E+03	OMNITOX	9.60E+01	7.02E+03	7.02E+03	7.02E+03	HOWARD
Hexachlorobenzene	118-74-1	0	285	1.70E+02	5.50	7.35E+03	5.50E+04	5.50E+04	OMNITOX	5.50E+04	5.50E+04	5.50E+04	5.50E+04	MACKAY
Heptachlor	76-44-8	0	373	2.94E+01	5.27	5.50E+01	5.50E+02	1.70E+03	OMNITOX	5.50E+03	1.70E+03	1.70E+03	1.70E+03	MACKAY

Name	PKa	BCF (kg-water/kg-fish)	Chemical Class (optional)	water - top - surface layer degradation half life (hours)	water - bottom - deep sea degradation half life (hours)	sediment (anaerobic) degradation half life (hours)	BCF (kg-water/kg-fish)	ED10 - oral - non cancer (mg / kg body weight - day, median estimate)	ED10 - inhalation - non cancer (mg / kg body weight - day, median estimate)	DALY/Incidence - oral- non cancer	DALY/Incidence - inhalation non cancer	ED10 - oral - cancer (mg / kg body weight - day, median estimate)	ED10 - inhalation - cancer (mg / kg body weight - day, median estimate)	Aquatic Ecotoxicological Effect Factor (PAF per kg/m3, median estimate)
Tetrachloroethylene		8.28E+01	Non dissociating compound	5.50E+02	5.50E+03	5.50E+03	8.28E+01	5.26E-01	2.08E+00	1.30E+00	1.30E+00	4.00E+00		6.13E+02
carbon tetrachloride (CCl4)		3.01E+01	Non dissociating compound	1.70E+03	1.70E+04	1.70E+04	3.01E+01	5.38E-02	4.09E+00	1.30E+00	1.30E+00	1.19E+00	1.19E+00	6.73E+01
1,3-butadiene		6.80E+00	Non dissociating compound	1.70E+02	1.70E+03	1.70E+03	6.80E+00	6.76E-01	6.76E-01	1.30E+00	1.30E+00		1.04E+01	2.01E+02
Methomyl		3.16E+00	Non dissociating compound	5.52E+03	5.04E+02	5.04E+02	3.16E+00	2.50E+00		1.30E+00	1.30E+00			7.01E+03
Acephate		3.16E+00	Non dissociating compound	1.26E+03	5.28E+01	5.28E+01	3.16E+00	2.04E-03		1.30E+00	1.30E+00	1.00E+01		7.26E+01

Name	PKa	BCF (kg-water/kg-fish)	Chemical Class (optional)	water - top - surface layer degradation half life (hours)	water - bottom - deep sea degradation half life (hours)	sediment (anaerobic) degradation half life (hours)	BCF (kg-water/kg-fish)	ED10 - oral - non cancer (mg / kg body weight - day, median estimate)	ED10 - inhalation - non cancer (mg / kg body weight - day, median estimate)	DALY/Incidence - oral- non cancer	DALY/Incidence inhalation - non cancer	ED10 - oral - cancer (mg / kg body weight - day, median estimate)	ED10 - inhalation - cancer (mg / kg body weight - day, median estimate)	Aquatic Ecotoxicological Effect Factor (PAF per kg/m3, median estimate)
Formaldehyde	1.33E+01	3.16E+00	Non dissociating compound	9.60E+01	3.84E+02	3.84E+02	3.16E+00	3.75E+00	2.52E-03	1.30E+00	1.30E+00		9.09E-02	7.42E+01
PCBs		5.80E+04	Mixture (of non dissociating compounds)	3.36E+02	1.34E+03	1.34E+03	5.80E+04			1.30E+00	1.30E+00			7.50E+05
Di(n-octyl) phthalate		6.35E+01	Non dissociating compound	3.36E+02	6.54E+03	6.54E+03	6.35E+01	3.09E+00		1.30E+00	1.30E+00			1.50E+01
Hexabromobenzene		9.42E+03	Non dissociating compound	1.44E+03	5.76E+03	5.76E+03	9.42E+03	1.61E-01		1.30E+00	1.30E+00			1.45E+06
Cypermethrin		2.07E+02	Non dissociating compound	1.20E+02	1.25E+03	1.25E+03	2.07E+02	1.00E+00		1.30E+00	1.30E+00			6.47E+06
Mirex		4.03E+04	Non dissociating compound	1.70E+02	5.50E+04	5.50E+04	4.03E+04	1.85E-02		1.30E+00	1.30E+00	7.14E-02		3.33E+03
Trifluralin		2.58E+03	Non dissociating compound	1.70E+03	5.50E+03	5.50E+03	2.58E+03	7.69E-01		1.30E+00	1.30E+00	2.94E+01		1.13E+04
Dicofol		1.46E+03	Hydrolyses app t1/2: 120 h [1]	8.99E+02	3.84E+02	3.84E+02	1.46E+03			1.30E+00	1.30E+00	1.32E+00		1.03E+04
1,4-dichlorobenzene		8.89E+01	Non dissociating compound	1.70E+03	1.70E+04	1.70E+04	8.89E+01	2.03E+00	7.69E+01	1.30E+00	1.30E+00	2.56E+01		7.63E+02
Aldrin		2.02E+04	Non dissociating compound	1.70E+04	5.50E+04	5.50E+04	2.02E+04	1.25E-03		1.30E+00	1.30E+00	1.18E-02	1.18E-02	8.27E+04
1,1,2,2-Tetrachloroethane		1.38E+01	Non dissociating compound	1.70E+03	1.70E+04	1.70E+04	1.38E+01	2.15E+00	2.32E+01	1.30E+00	1.30E+00	1.54E+00	9.09E-01	2.83E+02
Captan		2.86E+01	Non dissociating compound	1.70E+01	5.50E+02	5.50E+02	2.86E+01	3.33E+00		1.30E+00	1.30E+00			7.21E+03
Pronamide		8.73E+01	Non dissociating compound	9.79E+02	1.80E+02	1.80E+02	8.73E+01	7.69E+00		1.30E+00	1.30E+00	4.76E+00		3.66E+02
Anthracene		5.33E+02	Non dissociating compound	5.50E+02	1.70E+04	1.70E+04	5.33E+02	3.70E+01		1.30E+00	1.30E+00			3.92E+04
gamma-HCH (lindane)		3.08E+02	Non dissociating compound	1.70E+04	5.50E+04	5.50E+04	3.08E+02	2.63E-02	1.16E-01	1.30E+00	1.30E+00	1.23E+00		2.85E+04
dimethylphthalate (DMP)		3.40E+00	Non dissociating compound	1.70E+02	1.70E+03	1.70E+03	3.40E+00			1.30E+00	1.30E+00			4.14E+01

Name	PKa	BCF (kg-water/kg-fish)	Chemical Class (optional)	water - top - surface layer degradation half life (hours)	water - bottom - deep sea degradation half life (hours)	sediment (anaerobic) degradation half life (hours)	BCF (kg-water/kg-fish)	ED10 - oral- non cancer (mg / kg body weight - day, median estimate)	ED10 - inhalation - non cancer (mg / kg body weight - day, median estimate)	DALY/Incidence - oral- non cancer	DALY/Incidence - inhalation - non cancer	ED10 - oral - cancer (mg / kg body weight - day, median estimate)	ED10 - inhalation - cancer (mg / kg body weight - day, median estimate)	Aquatic Ecotoxicological Effect Factor (PAF per kg/m3, median estimate)
Methanol	1.53E+01	3.16E+00		5.50E+01	7.20E+01	7.20E+01	3.16E+00	3.79E+01		1.30E+00	1.30E+00			1.50E+00
1,2-Dichloroethane		2.75E+00	Non dissociating compound	1.70E+03	1.70E+04	1.70E+04	2.75E+00	8.70E-01	8.67E+01	1.30E+00	1.30E+00	3.23E-01	2.17E+00	2.57E+01
Ethyl acetate		3.16E+00	Non dissociating compound	9.60E+01	3.84E+02	3.84E+02	3.16E+00	7.14E+01		1.30E+00	1.30E+00			7.42E+00
N-Nitrosodiethylamine	3.89E+00	3.16E+00	Non dissociating compound	6.00E+00	2.40E+01	2.40E+01	3.16E+00			1.30E+00	1.30E+00	9.09E-04	1.33E-03	6.00E+00
Thiram	8.70E-01	4.29E+00		1.70E+02	1.70E+03	1.70E+03	4.29E+00	1.33E+00		1.30E+00	1.30E+00			4.00E+04
Propoxur	1.19E+01	2.95E+00		5.50E+02	1.70E+03	1.70E+03	2.95E+00	3.23E-02		1.30E+00	1.30E+00			3.21E+03
Folpet		3.12E+01	Non dissociating compound	1.38E+04	1.38E+04	1.38E+04	3.12E+01	1.00E+01		1.30E+00	1.30E+00	4.17E+01		8.07E+03
Benomyl		8.56E+00	Significant hydrolysis	1.70E+02	5.50E+03	5.50E+03	8.56E+00	1.33E+00		1.30E+00	1.30E+00			1.31E+03
Hexachlorobutadiene		9.56E+02	Non dissociating compound	1.70E+03	1.70E+03	1.70E+03	9.56E+02	1.40E-03	1.14E+00	1.30E+00	1.30E+00	2.94E+00	2.94E+00	5.82E+03
Hexachlorocyclopentadiene		1.52E+03	Hydrolyses app t1/2: 173 h [1]	8.65E+01	1.68E+03	1.68E+03	1.52E+03	5.56E-01	1.80E-03	1.30E+00	1.30E+00			4.38E+04
Heptachlor epoxide		1.36E+03	Non dissociating compound	7.02E+03	9.60E+01	9.60E+01	1.36E+03	2.33E-03		1.30E+00	1.30E+00	2.17E-02	2.17E-02	1.66E+05
Hexachlorobenzene		5.15E+03	Non dissociating compound	5.50E+04	5.50E+04	5.50E+04	5.15E+03	2.13E-02	1.50E-05	1.30E+00	1.30E+00	7.69E-02	7.69E-02	2.16E+04
Heptachlor		9.93E+03	Hydrolyses app t1/2: 23.1 h [1]	5.50E+02	5.50E+03	5.50E+03	9.93E+03	4.00E-02		1.30E+00	1.30E+00	4.76E-02	4.35E-02	1.02E+05

5.3.12. Intake fraction results for emission to water and to air

Figure S4.53 and Figure S4.54 present respectively exposed and unexposed produce ingestion intake fraction for an emission to water, and all pathways intake fractions for an emission to air.

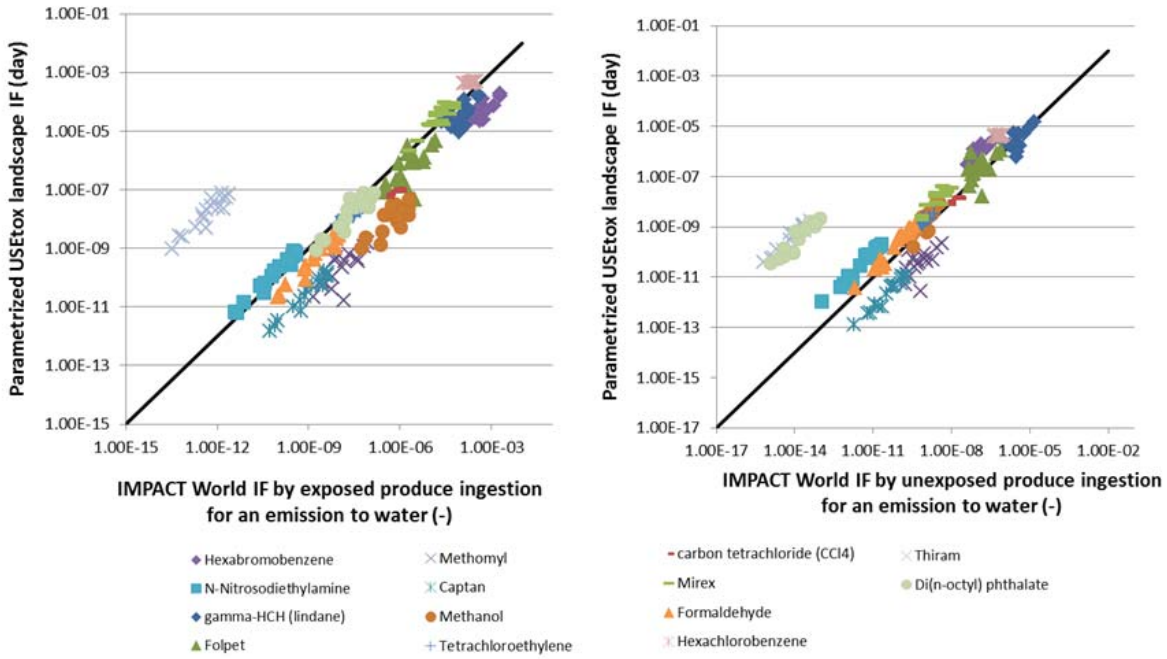

Figure S4.53: IF_w by exposed produce ingestion for an emission to water with default urban data for IMPACT World vs parametrized USEtox for selected chemicals by sub-continental zones (left); IF_w from unexposed produce ingestion for an emission to water for IMPACT World vs parametrized USEtox for selected chemicals for selected sub-continental zones (right)

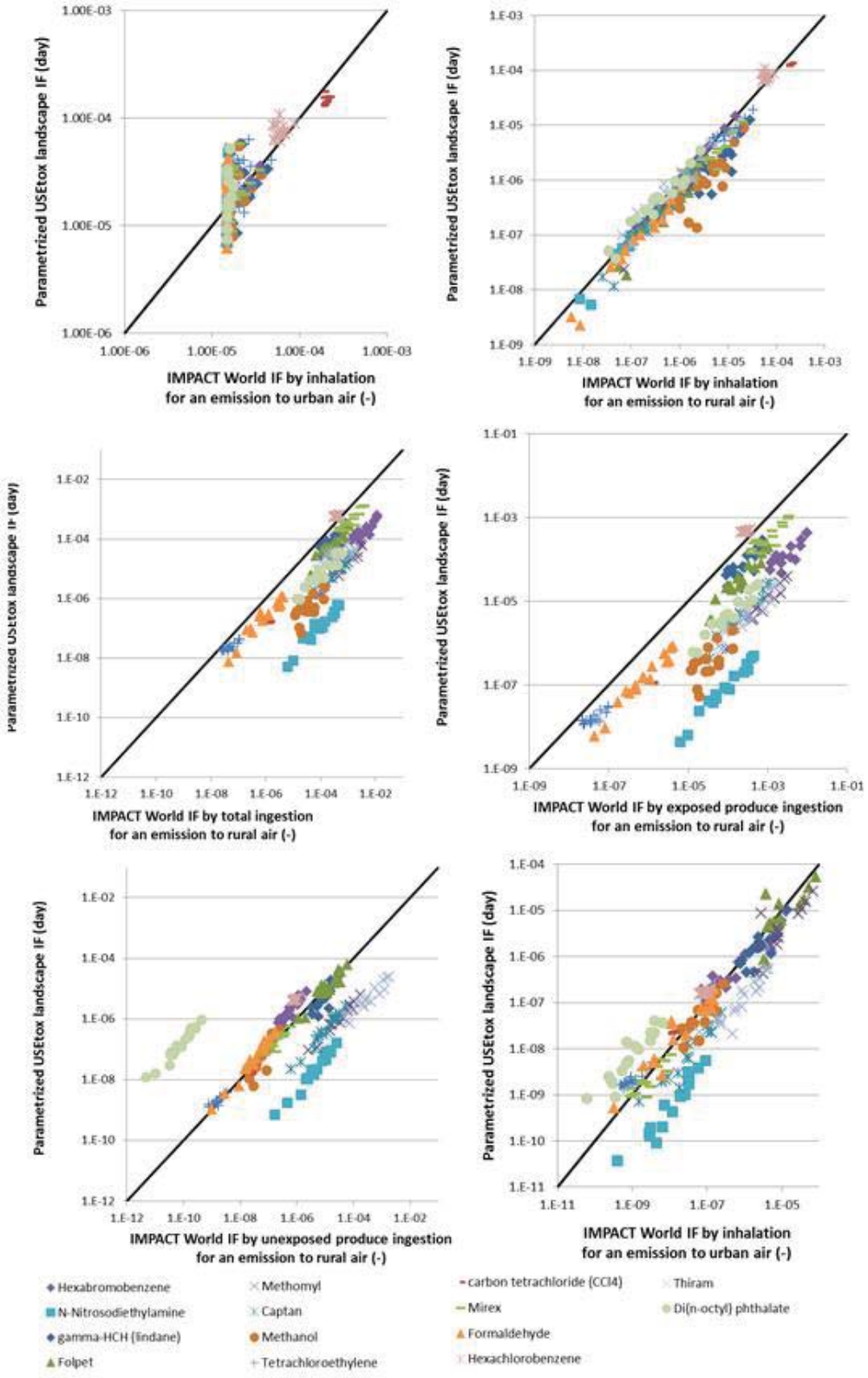
Parametrized USEtox landscape IF (day)
IMPACT World IF by inhalation for an emission to urban air (-)
IMPACT World IF by inhalation for an emission to rural air (-)
IMPACT World IF by total ingestion for an emission to rural air (-)
IMPACT World IF by exposed produce ingestion for an emission to rural air (-)
IMPACT World IF by unexposed produce ingestion for an emission to rural air (-)
IMPACT World IF by inhalation for an emission to urban air (-)
Hexabromobenzene
N-Nitrosodiethylamine
gamma-HCH (lindane)
Folpet
Methomyl
Captan
Methanol
Tetrachloroethylene
carbon tetrachloride (CCl4)
Mirex
Formaldehyde
Hexachlorobenzene
Thiram
Di(n-octyl) phthalate

Figure S4.54: IF_a by inhalation for an emission to urban air with default urban data for IMPACT World vs parametrized USEtox for selected chemicals by sub-continental zones (uppermost left), IF_a by inhalation for an emission to rural air for IMPACT World vs parametrized USEtox for selected chemicals by sub-continental zones (uppermost right), IF_a by total ingestion for an emission to rural air for IMPACT World vs parametrized USEtox for selected chemicals for all sub-continental zones (middle left), IF_a from exposed produce ingestion for an emission to water for IMPACT World vs parametrized USEtox for selected chemicals for all sub-continental zones (middle right), IF_a from unexposed produce ingestion for an emission to water for IMPACT World vs parametrized USEtox for selected chemicals for all sub-continental zones (bottom left), IF_a from direct water ingestion for an emission to water for IMPACT World vs parametrized USEtox for selected chemicals for all sub-continental zones (bottom right)

5.3.13. Classification of IMPACT Europe spatial model watersheds into archetypes

Table S4.5 shows the classification of IMPACT Europe spatial model watersheds into W1, W2 and W3 archetype categories.

Table S4.5. Classification of IMPACT Europe spatial model watersheds into W1, W2 and W3 archetype categories

Region No.	Volume (m3)	Advection rate (m3/h)	Is there a watershed after this one	Retention in watershed (d)	Retention after watershed (d)	Retention time until the sea (d)	Archetype watershed classification
W0	4.00E+13	4.15E+09		4.01E+02		4.01E+02	W0
W2	1.00E+08	1.24E+06		3.39E+00		3.39E+00	W2
W3	1.04E+07	2.49E+05		1.74E+00		1.74E+00	W1
W4	8.79E+09	8.15E+05	W4	4.50E+02	8.83E+02	1.33E+03	W3
W5	7.46E+10	6.78E+06	W5	4.58E+02	4.24E+02	8.83E+02	W3
W6	6.63E+07	9.28E+05		2.98E+00		2.98E+00	W2
W7	9.76E+07	1.47E+06	W7	2.77E+00	3.15E+00	5.92E+00	W2
W8	1.43E+08	1.88E+06		3.15E+00		3.15E+00	W2
W9	2.80E+07	5.28E+05		2.21E+00		2.21E+00	W2
W10	1.90E+08	2.04E+06		3.90E+00		3.90E+00	W2
W11	8.89E+07	8.80E+05		4.21E+00		4.21E+00	W2
W12	9.41E+07	5.88E+05		6.67E+00		6.67E+00	W2
W13	5.66E+06	9.99E+04		2.36E+00		2.36E+00	W2
W14	9.66E+07	1.23E+06	W14	3.28E+00	4.62E+00	7.90E+00	W2
W15	3.49E+08	3.15E+06		4.62E+00		4.62E+00	W2
W16	1.22E+08	1.04E+06		4.93E+00		4.93E+00	W2
W17	7.92E+07	1.43E+06		2.31E+00		2.31E+00	W2
W18	1.39E+11	1.60E+06	W18	3.62E+03	1.76E+03	5.38E+03	W3
W19	2.09E+11	4.94E+06		1.76E+03		1.76E+03	W3
W20	1.31E+11	3.71E+06	W20	1.48E+03	7.18E+00	1.48E+03	W3
W21	5.23E+07	5.74E+05	W21	3.80E+00	7.18E+00	1.10E+01	W2
W22	9.12E+08	7.72E+06	W22	4.93E+00	2.26E+00	7.18E+00	W2
W23	4.71E+08	8.69E+06		2.26E+00		2.26E+00	W2
W24	1.06E+11	9.15E+05	W24	4.83E+03	1.45E+02	4.97E+03	W3
W25	1.39E+10	4.04E+06	W25	1.43E+02	2.57E+00	1.45E+02	W3
W26	3.72E+08	6.05E+06		2.57E+00		2.57E+00	W2
W27	1.90E+07	4.81E+05		1.64E+00		1.64E+00	W1

W28	1.65E+07	4.59E+03		1.50E+02		1.50E+02	W3
W29	4.60E+07	8.49E+05	W29	2.26E+00	3.08E+00	5.34E+00	W2
W30	3.20E+07	5.53E+05	W30	2.41E+00	3.08E+00	5.49E+00	W2
W31	1.20E+08	1.63E+06		3.08E+00		3.08E+00	W2
W32	1.23E+07	2.08E+05	W32	2.46E+00	4.72E+00	7.18E+00	W2
W33	1.96E+08	1.73E+06		4.72E+00		4.72E+00	W2
W34	3.07E+06	2.08E+05		6.16E-01		6.16E-01	W1
W35	1.95E+08	1.72E+06		4.72E+00		4.72E+00	W2
W36	2.97E+06	1.34E+05		9.24E-01		9.24E-01	W1
W37	4.01E+07	4.40E+05	W37	3.80E+00	3.18E+00	6.98E+00	W2
W38	1.74E+08	2.28E+06		3.18E+00		3.18E+00	W2
W39	7.71E+06	3.91E+05		8.21E-01		8.21E-01	W1
W40	8.74E+07	3.18E+05		1.14E+01		1.14E+01	W2
W41	1.28E+08	4.53E+05		1.17E+01		1.17E+01	W2
W42	1.95E+10	2.30E+05		3.54E+03		3.54E+03	W3
W43	6.52E+07	2.79E+03		9.75E+02		9.75E+02	W3
W44	3.27E+07	1.18E+05		1.15E+01		1.15E+01	W2
W45	7.70E+07	1.51E+05		2.12E+01		2.12E+01	W2
W46	7.86E+07	2.09E+05		1.56E+01		1.56E+01	W2
W47	1.24E+07	2.93E+04		1.76E+01		1.76E+01	W2
W48	1.70E+06	1.15E+04		6.16E+00		6.16E+00	W2
W49	3.31E+07	1.19E+05		1.16E+01		1.16E+01	W2
W50	3.01E+07	9.79E+05		1.28E+00		1.28E+00	W1
W51	1.58E+07	7.11E+05		9.24E-01		9.24E-01	W1
W52	3.02E+07	1.06E+06		1.18E+00		1.18E+00	W1
W53	2.19E+07	1.37E+06		6.67E-01		6.67E-01	W1
W54	6.36E+06	7.38E+05		3.59E-01		3.59E-01	W1
W55	4.86E+07	1.23E+06		1.64E+00		1.64E+00	W1
W56	3.03E+07	1.60E+05		7.87E+00		7.87E+00	W2
W57	3.45E+06	1.75E+05		8.21E-01		8.21E-01	W1
W58	3.68E+07	1.11E+05		1.38E+01		1.38E+01	W2
W59	6.32E+06	3.21E+05		8.21E-01		8.21E-01	W1
W60	1.99E+07	9.87E+04		8.42E+00		8.42E+00	W2
W61	2.04E+06	2.96E+05		2.87E-01		2.87E-01	W1
W62	5.26E+06	2.67E+05		8.21E-01		8.21E-01	W1
W63	1.07E+06	1.08E+05		4.10E-01		4.10E-01	W1
W64	6.56E+06	2.22E+05		1.23E+00		1.23E+00	W1
W65	1.00E+07	1.30E+05		3.21E+00		3.21E+00	W2
W66	6.78E+07	2.10E+05		1.35E+01		1.35E+01	W2
W67	8.96E+08	4.67E+05		7.99E+01		7.99E+01	W3
W68	9.46E+06	1.51E+05		2.61E+00		2.61E+00	W2
W69	4.90E+06	2.21E+05		9.24E-01		9.24E-01	W1
W70	2.60E+06	1.51E+05		7.18E-01		7.18E-01	W1
W71	5.53E+06	3.46E+05		6.67E-01		6.67E-01	W1
W72	4.56E+07	3.50E+05		5.43E+00		5.43E+00	W2
W73	8.58E+06	3.87E+05		9.24E-01		9.24E-01	W1
W74	1.46E+08	4.50E+05		1.35E+01		1.35E+01	W2
W75	7.17E+07	3.39E+05		8.83E+00		8.83E+00	W2
W76	1.26E+08	1.66E+05		3.16E+01		3.16E+01	W2
W77	9.29E+07	3.18E+05		1.22E+01		1.22E+01	W2

W78	9.47E+07	2.58E+05		1.53E+01		1.53E+01	W2
W79	7.64E+09	9.19E+05	W79	3.46E+02	4.59E+02	8.05E+02	W3
W80	1.46E+08	2.20E+06	W80	2.77E+00	4.56E+02	4.59E+02	W3
W81	2.23E+10	2.42E+06	W81	3.83E+02	7.31E+01	4.56E+02	W3
W82	4.79E+09	2.73E+06		7.31E+01		7.31E+01	W3
W83	4.73E+07	1.60E+06		1.23E+00		1.23E+00	W1
W84	9.42E+06	3.19E+05		1.23E+00		1.23E+00	W1
W85	3.49E+09	1.57E+06		9.27E+01		9.27E+01	W3
W86	1.60E+07	7.23E+05		9.24E-01		9.24E-01	W1
W87	4.68E+07	8.64E+05		2.26E+00		2.26E+00	W2
W88	1.34E+07	4.96E+05		1.13E+00		1.13E+00	W1
W89	2.40E+07	1.39E+06		7.18E-01		7.18E-01	W1
W90	2.29E+07	1.55E+06		6.16E-01		6.16E-01	W1
W91	1.24E+07	8.40E+05		6.16E-01		6.16E-01	W1
W92	1.54E+08	6.08E+05		1.06E+01		1.06E+01	W2
W93	1.08E+08	6.75E+05		6.66E+00		6.66E+00	W2
W94	4.16E+07	5.83E+04		2.97E+01		2.97E+01	W2
W95	3.00E+07	1.52E+06		8.21E-01		8.21E-01	W1
W96	2.42E+07	5.79E+05		1.74E+00		1.74E+00	W1
W97	9.04E+06	7.34E+05		5.13E-01		5.13E-01	W1
W98	4.02E+09	7.11E+05		2.35E+02		2.35E+02	W3
W99	5.01E+07	1.85E+06		1.13E+00		1.13E+00	W1
W100	5.48E+09	4.96E+05		4.61E+02		4.61E+02	W3
W101	1.42E+07	9.59E+05		6.16E-01		6.16E-01	W1
W102	4.12E+11	5.55E+06		3.09E+03		3.09E+03	W3
W103	2.27E+07	1.03E+06		9.24E-01		9.24E-01	W1
W104	1.45E+10	3.20E+06		1.89E+02		1.89E+02	W3
W105	8.44E+09	1.04E+06		3.39E+02		3.39E+02	W3
W106	1.85E+07	1.25E+06		6.16E-01		6.16E-01	W1
W107	1.65E+07	4.47E+05		1.54E+00		1.54E+00	W1
W108	2.01E+07	4.29E+05		1.95E+00		1.95E+00	W1
W109	1.59E+07	4.04E+05		1.64E+00		1.64E+00	W1
W110	1.19E+07	2.69E+05		1.85E+00		1.85E+00	W1
W111	1.08E+08	3.01E+05		1.50E+01		1.50E+01	W2
W112	1.27E+07	1.03E+06		5.13E-01		5.13E-01	W1
W113	2.84E+08	6.94E+06		1.71E+00		1.71E+00	W1
W114	1.36E+08	2.20E+06		2.57E+00		2.57E+00	W2
W115	1.88E+11	6.18E+05		1.27E+04		1.27E+04	W3
W116	2.88E+11	1.79E+06		6.71E+03		6.71E+03	W3
W117	1.69E+11	8.55E+05		8.21E+03		8.21E+03	W3
W118	1.64E+07	2.13E+05		3.20E+00		3.20E+00	W2
W119	4.87E+09	7.42E+05		2.74E+02		2.74E+02	W3
W120	1.44E+08	2.25E+05		2.66E+01		2.66E+01	W2
W121	5.92E+10	7.79E+05		3.17E+03		3.17E+03	W3
W122	3.23E+07	5.34E+05		2.52E+00		2.52E+00	W2
W123	7.72E+06	5.63E+05		5.72E-01		5.72E-01	W1
W124	3.43E+08	2.24E+06		6.37E+00		6.37E+00	W2
W125	9.30E+06	2.52E+05		1.54E+00		1.54E+00	W1
W126	4.62E+09	8.42E+06	W126	2.28E+01	4.01E+02	4.24E+02	W3
W127	7.40E+09	2.50E+06	W127	1.23E+02	4.01E+02	5.24E+02	W3

W128	7.37E+09	5.03E+06	W128	6.11E+01	4.01E+02	4.62E+02	W3
W129	6.24E+07	5.03E+06		5.16E-01		5.16E-01	W1
W130	1.77E+06	3.40E+05		2.17E-01		2.17E-01	W1
W131	1.04E+07	1.56E+03		2.78E+02		2.78E+02	W3
W132	1.16E+08	4.43E+05		1.10E+01		1.10E+01	W2
W133	2.39E+07	2.36E+04		4.21E+01		4.21E+01	W2
W134	1.81E+07	4.31E+05		1.74E+00		1.74E+00	W1
W135	1.44E+07	3.39E+05		1.77E+00		1.77E+00	W1
W136	4.46E+07	1.47E+06		1.26E+00		1.26E+00	W1

5.4. Appendix for section 4.2 Human toxicity of pesticides

Experimental data for fitting leaf area index curves are derived from (*Lenz, 2007*) for wheat, from (*Chen et al., 2006*) for paddy rice, from (*Antón Vallejo, 2004*) for tomato, from (*Gong et al., 2006*) for apple, from (*Carranza et al., 2009*) for lettuce, and from (*Eremeev et al., 2008*) for potato.

Human ingestion intake fractions are calculated for recommended substance- and crop-specific application doses and times between application and harvest. Whereas intake fractions are independent of application doses, i.e. intake fractions are normalized to one unit mass applied, intake fractions are a function of the time between application and harvest. Wherever recommended application times were not available from authorized substance-crop combinations, typical crop-specific averages are calculated from existing information. Fungicides and insecticides can be applied in late life stage depending on pest infection; hence, the minimum pre-harvest interval serves as benchmark for calculating times to harvest. For herbicides, we face a different situation, as they are typically applied at pre-emergence or during early life stage of crops in order not to damage the cultivated species. However, there are two special cases. Firstly, conditions for apple as perennial plant are generally less strict, if herbicides are applied careful enough to not wetting the leaves. Secondly, herbicide application on potato is also allowed during later crop stages to help withering unwanted aerial plant parts. We, thus, differentiate typical times from application to harvest according to herbicides on the one hand (based on typical application to avoid damage of the cultivated species) and fungicides/insecticides on the other hand (based on minimum allowed pre-harvest intervals) as shown in Table S4.6. Average times for one nematicide and five acaricides are adopted from fungicides/insecticides.

Table S4.6: Typical average times between pesticide application and crop harvest for herbicides Δt_H [days] and aggregated over fungicides and insecticides $\Delta t_{F/I}$ [days]

crop	Δt_H	$\Delta t_{F/I}$
wheat	150 days	43 days
paddy rice	100 days	27 days
tomato	85 days	5 days
apple	150 days	14 days
lettuce	55 days	10 days
potato	60 days	14 days

Crop-specific human ingestion intake fractions are presented in Table S4.7 for 121 pesticides applied to the set of six selected crops.

Table S4.7: Target class TC (A: acaricides, F: fungicide, H: herbicide, I: insecticide, N: nematicides) and crop-specific human ingestion intake fractions iF [$kg_{intake} \cdot kg_{applied}^{-1}$] for the set of 121 pesticides. Bold values indicate substance-crop combinations registered for use in at least one of the countries listed in the Codex Alimentarius (*2010*)

pesticide	CAS-RN	TC	iF_{wheat}	iF_{rice}	iF_{tomato}	iF_{apple}	$iF_{lettuce}$	iF_{potato}

pesticide	CAS-RN	TC	iF_{wheat}	iF_{rice}	iF_{tomato}	iF_{apple}	$iF_{lettuce}$	iF_{potato}
1,3-Dichloropropene	542-75-6	N	1.8E-05	1.5E-04	1.2E-02	1.2E-03	2.9E-09	2.4E-07
2,4-D	94-75-7	H	1.0E-18	3.4E-13	3.4E-08	9.1E-19	1.1E-07	1.3E-09
Abamectin	71751-41-2	I	1.4E-08	3.3E-08	2.1E-05	1.6E-05	6.8E-03	9.8E-09
Acetamiprid	135410-20-7	I	2.8E-06	1.0E-05	2.7E-03	1.9E-04	1.6E-02	8.4E-08
Aclonifen	74070-46-5	H	5.6E-08	3.8E-07	2.6E-05	3.3E-06	3.0E-07	1.3E-09
α-Cypermethrin	67375-30-8	I	6.4E-07	1.2E-05	2.7E-03	1.6E-04	2.2E-02	3.2E-09
Azinphos-Methyl	86-50-0	I	1.5E-07	1.8E-06	5.0E-03	7.3E-04	2.6E-03	7.0E-09
Azoxystrobin	131860-33-8	F	2.1E-04	5.8E-04	1.1E-02	7.5E-03	3.4E-02	3.0E-08
Benalaxyl	71626-11-4	F	2.6E-06	2.4E-05	3.4E-03	2.7E-04	2.0E-02	4.2E-09
Benfluralin	1861-40-1	H	2.8E-13	3.0E-09	2.8E-06	2.7E-07	1.8E-07	2.8E-09
Benomyl	17804-35-2	F	1.9E-04	6.4E-04	9.6E-03	4.2E-03	5.6E-02	6.7E-09
β-Cyfluthrin	68359-37-5	I	3.8E-07	9.0E-06	2.7E-03	1.4E-04	2.0E-02	2.6E-09
Bifenthrin	82657-04-3	I	3.1E-07	8.3E-06	2.5E-03	1.0E-04	1.7E-02	7.5E-11
Buprofezin	69327-76-0	I	4.2E-07	8.9E-06	2.4E-03	1.2E-04	1.8E-02	3.7E-08
Butachlor	23184-66-9	H	1.9E-19	1.3E-15	5.1E-06	1.2E-09	5.3E-14	5.9E-09
Captan	133-06-2	F	2.6E-08	1.0E-06	4.6E-03	7.6E-04	2.4E-03	4.4E-08
Carbaryl	63-25-2	I	2.9E-07	5.7E-07	1.4E-03	2.2E-05	3.1E-03	4.0E-08
Carbendazim	10605-21-7	F	1.2E-06	1.2E-05	1.9E-03	1.0E-04	1.2E-02	4.0E-08
Carbofuran	1563-66-2	I	9.4E-09	4.5E-07	4.2E-04	1.2E-06	4.0E-03	2.2E-07
Carpropamid	104030-54-8	F	1.6E-04	4.0E-04	9.9E-03	5.2E-03	4.8E-02	1.1E-08
Chloropicrin	76-06-2	I	4.3E-05	1.6E-04	1.9E-02	1.4E-02	3.7E-03	1.1E-07
Chlorothalonil	1897-45-6	F	4.3E-07	2.8E-06	1.3E-03	4.9E-05	8.4E-03	1.6E-08
Chlorpyrifos	2921-88-2	I	3.5E-09	4.5E-07	8.4E-04	6.5E-06	7.9E-03	7.2E-09
Clofentezine	74115-24-5	A	7.8E-06	5.1E-05	4.4E-03	5.7E-04	2.3E-02	1.7E-08
Clomazone	81777-89-1	H	8.8E-06	1.1E-05	4.8E-04	6.1E-08	1.4E-07	8.6E-09
Cyhalothrin	68085-85-8	I	4.0E-05	1.7E-04	7.1E-03	2.2E-03	5.1E-02	5.4E-10
Cymoxanil	57966-95-7	F	2.7E-06	1.2E-05	2.8E-03	1.6E-04	1.5E-02	2.0E-07
Cypermethrin	52315-07-8	I	1.0E-06	1.7E-05	3.3E-03	2.4E-04	2.3E-02	2.0E-09
Cyproconazole	94361-06-5	F	6.6E-04	1.0E-03	1.3E-02	1.1E-02	5.1E-02	6.4E-08
Cyprodinil	121552-61-2	F	4.4E-06	3.8E-05	4.1E-03	5.0E-04	2.5E-02	1.9E-08
Cyromazine	66215-27-8	I	6.6E-07	4.3E-05	5.6E-03	1.0E-03	2.1E-02	1.6E-08
DDT	50-29-3	I	1.9E-04	4.3E-04	9.6E-03	5.6E-03	5.0E-02	9.9E-10
Deltamethrin	52918-63-5	I	5.8E-07	1.3E-05	2.0E-03	6.7E-05	1.4E-02	6.2E-12
Diazinon	333-41-5	I	2.2E-06	2.3E-05	3.3E-03	2.9E-04	2.1E-02	3.4E-08
Difenoconazole	119446-68-3	F	1.7E-05	9.9E-05	5.9E-03	1.3E-03	3.4E-02	1.6E-08
Dimethomorph	110488-70-5	F	3.7E-05	1.2E-04	5.5E-03	1.1E-03	2.7E-02	3.8E-08
Diquat	2764-72-9	H	1.1E-10	6.5E-08	6.4E-04	5.4E-08	8.4E-07	5.4E-09
Edifenphos	17109-49-8	F	4.1E-08	1.6E-06	1.4E-03	2.3E-05	1.1E-02	1.2E-08
Endosulfan	115-29-7	I	7.0E-08	2.4E-06	1.4E-03	3.2E-05	1.1E-02	6.4E-09
Epoxiconazole	133855-98-8	F	5.8E-04	9.3E-04	1.3E-02	1.0E-02	5.1E-02	2.2E-08
EPTC	759-94-4	H	5.2E-12	1.8E-10	1.5E-05	1.9E-11	3.0E-15	2.7E-09
Esfenvalerate	66230-04-4	I	7.1E-06	5.6E-05	5.0E-03	7.9E-04	3.5E-02	3.3E-08
Etofenprox	80844-07-1	I	3.9E-10	1.1E-07	5.6E-04	2.0E-06	5.6E-03	1.9E-09
Fenbutatin Oxide	13356-08-6	A	2.0E-07	1.8E-08	1.1E-06	5.9E-07	7.0E-03	1.3E-09
Fenhexamid	126833-17-8	F	2.1E-07	5.6E-06	2.1E-03	7.9E-05	1.4E-02	3.8E-08
Fenoxaprop-P	113158-40-0	H	1.8E-08	1.1E-07	7.3E-06	2.1E-10	1.3E-07	3.2E-10
Fenpropathrin	39515-41-8	I	4.2E-07	8.7E-06	2.5E-03	1.3E-04	2.0E-02	3.1E-08
Fenpropimorph	67564-91-4	F	9.8E-09	7.9E-07	1.0E-03	1.2E-05	9.6E-03	2.0E-08

pesticide	CAS-RN	TC	iF_{wheat}	iF_{rice}	iF_{tomato}	iF_{apple}	$iF_{lettuce}$	iF_{potato}
Fenpyroximate	134098-61-6	A	1.4E-07	4.4E-06	1.9E-03	6.0E-05	1.5E-02	2.0E-09
Ferbam	14484-64-1	F	2.7E-08	3.8E-07	1.7E-05	4.6E-05	3.7E-04	2.6E-08
Fipronil	120068-37-3	I	7.1E-10	1.2E-07	2.8E-03	1.7E-04	1.7E-03	1.5E-08
Fludioxonil	131341-86-1	F	1.8E-05	1.0E-04	6.0E-03	1.3E-03	3.3E-02	5.4E-10
Flufenacet	142459-58-3	H	1.6E-12	3.1E-09	8.6E-05	3.6E-12	2.1E-09	1.1E-08
Fosetyl	15845-66-6	F	2.8E-06	4.9E-06	5.6E-03	5.7E-04	1.3E-02	4.8E-10
Glyphosate	1071-83-6	H	3.7E-16	1.9E-08	5.0E-07	4.8E-08	2.9E-06	8.6E-12
Hexythiazox	78587-05-0	A	1.6E-07	4.1E-06	1.1E-03	1.1E-05	7.2E-03	1.0E-09
Imidacloprid	138261-41-3	I	1.2E-05	8.8E-05	6.8E-03	1.3E-03	4.2E-02	5.0E-08
Indoxacarb	173584-44-6	I	2.5E-07	5.9E-06	1.3E-03	2.1E-05	1.0E-02	9.2E-09
Iodosulfuron	185119-76-0	H	1.5E-11	1.0E-10	3.2E-09	1.3E-13	1.1E-08	4.4E-08
Iprodione	36734-19-7	F	4.9E-06	4.2E-05	4.0E-03	4.4E-04	2.1E-02	4.3E-08
Isoproturon	34123-59-6	H	4.0E-12	7.0E-10	3.5E-07	1.2E-17	5.7E-13	1.5E-09
λ-Cyhalothrin	91465-08-6	I	1.3E-07	4.4E-06	2.1E-03	6.9E-05	1.7E-02	2.0E-10
Malathion	121-75-5	I	7.6E-08	3.5E-06	6.0E-03	1.0E-03	4.6E-03	1.2E-08
Mancozeb	8018-01-7	F	3.7E-08	6.6E-07	2.8E-03	1.8E-04	2.5E-03	3.6E-09
Maneb	12427-38-2	F	4.8E-08	2.2E-06	1.0E-03	1.8E-04	8.0E-03	2.7E-09
MCPA	94-74-6	H	1.4E-18	2.9E-15	1.9E-07	3.9E-20	1.1E-12	4.0E-09
Mepanipyrim	110235-47-7	F	2.7E-05	1.2E-04	5.8E-03	1.4E-03	3.0E-02	2.0E-08
Metalaxyl-M	70630-17-0	F	1.7E-04	5.1E-04	7.8E-03	2.6E-03	4.1E-02	2.0E-08
Metam Sodium	137-42-8	H	1.4E-20	2.0E-18	2.4E-14	8.0E-21	1.5E-10	4.2E-10
Metconazole	125116-23-6	F	1.8E-04	4.3E-04	9.8E-03	5.5E-03	4.7E-02	3.0E-08
Methamidophos	10265-92-6	I	7.0E-09	2.8E-06	3.1E-03	2.1E-04	8.7E-03	2.8E-07
Methomyl	16752-77-5	I	2.5E-09	3.8E-07	3.0E-03	2.0E-04	2.6E-03	1.1E-07
Metribuzin	21087-64-9	H	1.2E-13	5.2E-11	3.5E-10	4.8E-21	5.6E-13	2.9E-09
Molinate	2212-67-1	H	1.1E-12	8.6E-11	1.2E-06	4.7E-15	1.2E-14	1.3E-09
Monocrotophos	6923-22-4	I	1.7E-07	6.6E-06	4.8E-03	4.8E-04	1.6E-02	3.4E-07
Myclobutanil	88671-89-0	F	6.8E-06	4.8E-05	4.2E-03	5.1E-04	2.2E-02	3.0E-08
Napropamide	15299-99-7	H	2.9E-05	3.2E-05	1.6E-03	4.8E-05	8.3E-05	5.6E-09
Norflurazon	27314-13-2	H	9.9E-04	3.4E-04	3.7E-03	2.0E-04	6.3E-04	6.0E-09
Oxadiargyl	39807-15-3	H	3.6E-13	3.2E-11	7.6E-06	6.5E-08	1.1E-12	9.5E-10
Paraquat	4685-14-7	H	1.9E-04	6.0E-06	1.5E-06	2.5E-06	1.7E-03	2.2E-12
Parathion-Methyl	298-00-0	I	1.1E-07	3.0E-06	5.0E-03	8.7E-04	4.3E-03	3.0E-08
Penconazole	66246-88-6	F	2.7E-07	5.3E-06	2.2E-03	7.8E-05	1.5E-02	1.1E-08
Pendimethalin	40487-42-1	H	6.4E-07	3.7E-06	4.0E-05	1.1E-05	2.9E-04	3.9E-09
Permethrin	52645-53-1	I	1.3E-07	4.3E-06	2.0E-03	6.7E-05	1.7E-02	1.2E-09
Phorate	298-02-2	I	6.9E-06	5.3E-05	4.7E-03	6.9E-04	2.1E-02	1.7E-08
Phosmet	732-11-6	I	1.3E-08	7.2E-08	2.8E-03	1.4E-04	2.3E-04	1.4E-09
Phoxim	14816-18-3	I	2.3E-09	1.6E-08	2.1E-03	6.0E-05	6.4E-04	6.6E-09
Picoxystrobin	117428-22-5	F	4.1E-08	2.0E-06	1.2E-03	1.7E-05	9.6E-03	1.9E-08
Pirimicarb	23103-98-2	I	1.2E-07	2.7E-06	4.3E-03	5.9E-04	4.2E-03	1.3E-08
Pirimiphos-Methyl	29232-93-7	I	6.2E-06	5.2E-05	4.7E-03	6.4E-04	2.3E-02	2.6E-08
Probenazole	27605-76-1	F	1.9E-09	8.4E-09	3.8E-03	1.7E-04	2.8E-04	2.6E-08
Propamocarb	24579-73-5	F	2.5E-05	9.3E-05	4.8E-03	6.4E-04	3.4E-02	5.9E-07
Propanil	709-98-8	H	9.4E-06	7.6E-06	1.8E-04	2.3E-07	1.4E-10	3.4E-09
Propargite	2312-35-8	A	9.9E-06	6.8E-05	5.0E-03	8.2E-04	3.7E-02	1.1E-08
Propiconazole	60207-90-1	F	8.2E-07	1.4E-05	3.0E-03	1.8E-04	1.8E-02	2.2E-08
Propoxycarbazone-Sodium	181274-15-7	H	2.2E-11	2.9E-10	7.8E-10	1.8E-13	4.9E-08	2.0E-08

pesticide	CAS-RN	TC	iF_{wheat}	iF_{rice}	iF_{tomato}	iF_{apple}	$iF_{lettuce}$	iF_{potato}
Propyzamide	23950-58-5	H	4.2E-06	6.0E-06	6.8E-04	8.8E-06	1.3E-06	4.5E-09
Prosulfocarb	52888-80-9	H	3.7E-17	4.1E-13	1.3E-06	1.1E-09	4.8E-08	2.7E-10
Prothioconazole	178928-70-6	F	1.7E-07	4.3E-06	1.9E-03	5.5E-05	1.4E-02	9.5E-09
Prothiofos	34643-46-4	I	1.4E-05	8.0E-05	5.1E-03	1.0E-03	3.7E-02	1.1E-08
Pymetrozine	123312-89-0	I	1.4E-07	3.7E-08	1.1E-03	1.3E-05	1.9E-04	5.0E-09
Pyraclostrobin	175013-18-0	F	1.8E-06	2.3E-05	3.3E-03	2.6E-04	2.1E-02	2.8E-09
Pyrimethanil	53112-28-0	F	3.6E-07	3.1E-06	1.5E-03	4.9E-05	1.1E-02	3.7E-08
Pyriproxyfen	95737-68-1	I	2.1E-08	1.4E-06	1.4E-03	2.2E-05	1.2E-02	6.7E-09
Pyroquilone	57369-32-1	F	5.2E-04	1.3E-03	9.5E-03	4.9E-03	5.3E-02	3.8E-07
Quinclorac	84087-01-4	H	2.1E-13	4.0E-11	3.2E-06	4.6E-16	2.3E-05	1.7E-08
Rimsulfuron	122931-48-0	H	7.1E-20	1.0E-16	6.0E-10	4.0E-20	1.2E-11	1.9E-09
Sethoxydim	74051-80-2	H	1.2E-14	6.2E-12	6.8E-10	6.1E-20	2.2E-14	1.3E-11
Simazine	122-34-9	H	5.9E-06	1.8E-05	2.5E-04	1.2E-10	1.9E-05	2.2E-08
S-Metolachlor	87392-12-9	H	8.8E-14	2.6E-11	3.4E-06	7.7E-14	2.5E-13	1.9E-09
Spinosad	168316-95-8	I	6.1E-09	7.2E-09	6.8E-05	2.8E-05	3.7E-03	5.9E-10
Spiromesifen	283594-90-1	I	8.9E-08	3.2E-06	1.7E-03	4.4E-05	1.4E-02	1.8E-09
Tebuconazole	107534-96-3	F	1.6E-05	9.5E-05	5.9E-03	1.3E-03	3.1E-02	3.5E-08
Thiacloprid	111988-49-9	I	6.4E-07	3.4E-06	1.1E-03	3.8E-05	7.7E-03	1.4E-08
Thiamethoxam	153719-23-4	I	1.4E-06	6.5E-05	2.8E-03	2.5E-03	3.8E-02	1.4E-07
Thiobencarb	28249-77-6	H	7.5E-20	3.1E-13	9.8E-06	1.8E-08	1.1E-13	2.9E-09
Thiophanate-Methyl	23564-05-8	F	9.3E-09	1.1E-08	1.3E-03	3.7E-05	4.4E-04	9.9E-09
Thiram	137-26-8	F	2.5E-08	1.1E-06	5.1E-04	3.0E-06	4.8E-03	8.1E-10
Triazophos	24017-47-8	I	1.1E-08	8.4E-07	4.1E-03	4.8E-04	3.3E-03	2.5E-08
Tricyclazole	41814-78-2	F	1.1E-05	1.3E-04	8.8E-03	3.9E-03	2.0E-02	8.2E-08
Trifloxystrobin	141517-21-7	F	1.5E-07	5.1E-06	6.2E-03	1.4E-03	7.9E-03	9.8E-09

The human effect assessment is based on dose-response information. Cancer dose-response slope factors are taken from USEtox (*Rosenbaum et al., 2008*). Non-cancer dose-response slope factors are calculated based on the chronic lifetime dose affecting 50% of a studied population extrapolated from no-observed effect levels NOEL with the assumption of a linear dose-response curve, which is in line with (*Huijbregts et al., 2005; Pennington et al., 2002*). Substance-specific NOEL along with information about tested receptor species and exposure duration of the studies are presented in Table S4.8, together with calculated dose-response slope factors. Extrapolation factors correcting for differences between studied receptor species and humans, cf_s, are derived from (*Huijbregts et al., 2010*) and are cf_s=4.1 for rat, cf_s=7.3 for mouse, cf_s=1.5 for dog, cf_s=2.4 for rabbit and cf_s=1.9 for monkey. Extrapolation factors correcting for differences between exposure duration of the study and chronic exposure, cf_{time}, are taken from (*Huijbregts et al., 2005*) and are cf_{time}=5 for subacute exposure and cf_{time}=2 for subchronic exposure.

Table S4.8: No-observed effect levels NOEL [$mg \cdot kg_{BW}^{-1} \cdot day^{-1}$], exposed animal receptor species, exposure duration, the reference, from which this information is derived, and dose-response slope factors β [incidence $risk \cdot kg_{intake}^{-1}$] for non-cancer effects of 121 pesticides. In addition, slope factors for cancer effects are added

pesticide	NOEL	receptor	exposure	reference	$\beta_{non\text{-}cancer}$	β_{cancer}
1,3-Dichloropropene	5	rat	subacute	(PPDB	2.0, 1.3E-01	4.1E-02

pesticide	NOEL	receptor	exposure	reference	$\beta_{non\text{-}cancer}$	β_{cancer}
				2011)		
2,4-D	1	rat	chronic	(US-EPA, 2011)	1.3E-01	0
Abamectin	0.12	rat	chronic	(US-EPA, 2011)	1.1E+00	n/a
Acetamiprid	15	rat	subacute	(PPDB 2.0, 2011)	4.2E-02	n/a
Aclonifen	50	rat	subacute	(PPDB 2.0, 2011)	1.3E-02	n/a
α-Cypermethrin	5	rat	subacute	(PPDB 2.0, 2011)	1.3E-01	n/a
Azinphos-Methyl	0.25	human	subacute	(OCSEH, 2010)	6.2E-01	0
Azoxystrobin	10	dog	subchronic	(OCSEH, 2010)	9.1E-03	n/a
Benalaxyl	5	rat	subchronic	(FAO, 2008)	5.1E-02	n/a
Benfluralin	25	dog	chronic	(US-EPA, 2011)	1.8E-03	n/a
Benomyl	5	rat	chronic	(US-EPA, 2011)	2.5E-02	n/a
β-Cyfluthrin	2.5	rat	chronic	(US-EPA, 2011)	5.1E-02	n/a
Bifenthrin	1.5	dog	chronic	(US-EPA, 2011)	3.0E-02	0
Buprofezin	3.6	rat	subacute	(PPDB 2.0, 2011)	1.8E-01	n/a
Butachlor	10	dog	subchronic	(Krieger and Krieger, 2001)	9.1E-03	n/a
Captan	12.5	rat	chronic	(US-EPA, 2011)	1.0E-02	9.7E-04
Carbaryl	9.6	rat	chronic	(US-EPA, 2011)	1.3E-02	8.1E-02
Carbendazim	10	rat	subacute	(PPDB 2.0, 2011)	6.4E-02	n/a
Carbofuran	0.5	dog	chronic	(US-EPA, 2011)	9.1E-02	0
Carpropamid	29.35	rat	subacute	(Motoyama and Yamaguchi, 2003)	2.2E-02	n/a
Chloropicrin	8	rat	subacute	(PPDB 2.0, 2011)	7.9E-02	0
Chlorothalonil	1.5	dog	chronic	(US-EPA, 2011)	3.0E-02	5.0E-04
Chlorpyrifos	1.5	dog	chronic	(US-EPA, 2011)	3.0E-02	0
Clofentezine	1.25	dog	chronic	(US-EPA,	3.7E-02	n/a

pesticide	NOEL	receptor	exposure	reference	$\beta_{non\text{-}cancer}$	β_{cancer}
				2011)		
Clomazone	4.3	rat	chronic	(PPDB 2.0, 2011)	3.0E-02	n/a
Cyhalothrin	0.5	rat	chronic	(US-EPA, 2011)	2.5E-01	n/a
Cymoxanil	47.6	rat	subacute	(PPDB 2.0, 2011)	1.3E-02	n/a
Cypermethrin	1	dog	chronic	(US-EPA, 2011)	4.6E-02	n/a
Cyproconazole	1.84	mouse	subacute	(PPDB 2.0, 2011)	6.1E-01	n/a
Cyprodinil	3	rat	chronic	(PPDB 2.0, 2011)	4.2E-02	n/a
Cyromazine	0.75	dog	subchronic	(US-EPA, 2011)	1.2E-01	n/a
DDT	0.05	rat	subchronic	(US-EPA, 2011)	5.1E+00	1.6E-01
Deltamethrin	2.5	rat	subacute	(PPDB 2.0, 2011)	2.5E-01	0
Diazinon	5	rat	subacute	(PPDB 2.0, 2011)	1.3E-01	0
Difenoconazole	20	rat	subacute	(PPDB 2.0, 2011)	3.2E-02	n/a
Dimethomorph	15	rat	subacute	(PPDB 2.0, 2011)	4.2E-02	n/a
Diquat	0.22	rat	chronic	(US-EPA, 2011)	5.8E-01	n/a
Edifenphos	10	rat	chronic	(Sasaki, 2003)	1.3E-02	n/a
Endosulfan	0.65	rat	chronic	(US-EPA, 2011)	2.0E-01	0
Epoxiconazole	7.5	rat	subacute	(PPDB 2.0, 2011)	8.5E-02	n/a
EPTC	2.5	rat	chronic	(US-EPA, 2011)	5.1E-02	n/a
Esfenvalerate	88.5	rat	subacute	(PPDB 2.0, 2011)	7.2E-03	n/a
Etofenprox	3.7	rat	chronic	(NYSDEC, 2006)	3.4E-02	n/a
Fenbutatin Oxide	5.2	rat	chronic	(US-EPA, 1994)	2.4E-02	n/a
Fenhexamid	17.4	dog	chronic	(OCSEH, 2010)	2.6E-03	n/a
Fenoxaprop-P	0.7	rat	subacute	(PPDB 2.0, 2011)	9.1E-01	n/a
Fenpropathrin	2.5	dog	chronic	(US-EPA, 2011)	1.8E-02	n/a
Fenpropimorph	0.3	rat	subacute	(PPDB 2.0,	2.1E+00	n/a

pesticide	NOEL	receptor	exposure	reference	$\theta_{non\text{-}cancer}$	θ_{cancer}
				2011)		
Fenpyroximate	1.3	rat	subacute	(PPDB 2.0, 2011)	4.9E-01	n/a
Ferbam	12.5	rat	chronic	(PPDB 2.0, 2011)	1.0E-02	0
Fipronil	0.35	rat	subacute	(PPDB 2.0, 2011)	1.8E+00	n/a
Fludioxonil	10	rat	subacute	(PPDB 2.0, 2011)	6.4E-02	n/a
Flufenacet	1.67	rat	subacute	(PPDB 2.0, 2011)	3.8E-01	n/a
Fosetyl	1424	rat	subacute	(PPDB 2.0, 2011)	4.5E-04	n/a
Glyphosate	10	rat	chronic	(US-EPA, 2011)	1.3E-02	n/a
Hexythiazox	2.5	dog	chronic	(US-EPA, 2011)	1.8E-02	n/a
Imidacloprid	13	rat	subacute	(PPDB 2.0, 2011)	4.9E-02	n/a
Indoxacarb	1.25	rat	chronic	(OCSEH, 2010)	1.0E-01	n/a
Iodosulfuron	7	dog	subacute	(PPDB 2.0, 2011)	3.3E-02	n/a
Iprodione	4.2	dog	chronic	(US-EPA, 2011)	1.1E-02	n/a
Isoproturon	20	rat	subchronic	(Makhteshim Agan UK Ltd, 2005)	1.3E-02	n/a
λ-Cyhalothrin	0.7	rat	subacute	(PPDB 2.0, 2011)	9.1E-01	n/a
Malathion	0.23	human	subchronic	(US-EPA, 2011)	2.7E-01	0
Mancozeb	0.6	dog	chronic	(OCSEH, 2010)	7.6E-02	n/a
Maneb	5	monkey	subchronic	(US-EPA, 2011)	2.4E-02	7.3E-03
MCPA	0.15	dog	chronic	(US-EPA, 2011)	3.0E-01	0
Mepanipyrim	2.45	rat	chronic	(PPDB 2.0, 2011)	5.2E-02	n/a
Metalaxyl-M	2.5	rat	subacute	(PPDB 2.0, 2011)	2.5E-01	n/a
Metam Sodium	5	rat	subacute	(CDPR, 2004)	1.3E-01	n/a
Metconazole	4	rabbit	subacute	(PPDB 2.0, 2011)	9.4E-02	n/a
Methamidophos	0.5	rat	chronic	(US-EPA, 2011)	2.5E-01	n/a
Methomyl	2.5	dog	chronic	(US-EPA,	1.8E-02	n/a

pesticide	NOEL	receptor	exposure	reference	$\beta_{non\text{-}cancer}$	β_{cancer}
				2011)		
Metribuzin	2.5	dog	chronic	(US-EPA, 2011)	1.8E-02	n/a
Molinate	0.2	rat	subacute	(US-EPA, 2011)	3.2E+00	n/a
Monocrotophos	0.0036	human	subacute	(OCSEH, 2010)	4.3E+01	n/a
Myclobutanil	2.49	rat	chronic	(US-EPA, 2011)	5.1E-02	n/a
Napropamide	30	rat	chronic	(US-EPA, 2011)	4.2E-03	n/a
Norflurazon	3.75	dog	subchronic	(US-EPA, 2011)	2.4E-02	n/a
Oxadiargyl	19.7	rat	subacute	(PPDB 2.0, 2011)	3.2E-02	n/a
Paraquat	0.45	dog	chronic	(US-EPA, 2011)	1.0E-01	n/a
Parathion-Methyl	0.025	rat	chronic	(US-EPA, 2011)	5.1E+00	0
Penconazole	3.8	rat	chronic	(PPDB 2.0, 2011)	3.3E-02	n/a
Pendimethalin	12.5	dog	chronic	(US-EPA, 2011)	3.7E-03	n/a
Permethrin	5	rat	chronic	(US-EPA, 2011)	2.5E-02	n/a
Phorate	0.05	dog	chronic	(US-EPA, 1988)	9.1E-01	n/a
Phosmet	2	rat	chronic	(US-EPA, 2011)	6.4E-02	n/a
Phoxim	0.375	dog	chronic	(EAEMP, 2000)	1.2E-01	n/a
Picoxystrobin	4.3	rat	subacute	(PPDB 2.0, 2011)	1.5E-01	n/a
Pirimicarb	37.5	rat	subacute	(PPDB 2.0, 2011)	1.7E-02	n/a
Pirimiphos-Methyl	0.25	human	subacute	(US-EPA, 2011)	6.2E-01	n/a
Probenazole	110	rat	chronic	(Tomlin, 2009)	1.2E-03	n/a
Propamocarb	41	rat	chronic	(PMEP, 1997)	3.1E-03	n/a
Propanil	5	rat	chronic	(US-EPA, 2011)	2.5E-02	n/a
Propargite	22.5	dog	chronic	(US-EPA, 2011)	2.0E-03	n/a
Propiconazole	1.25	dog	chronic	(US-EPA, 2011)	3.7E-02	n/a
Propoxycarbazone-Sodium	492	rat	chronic	(CDPR, 2005)	2.6E-04	n/a

pesticide	NOEL	receptor	exposure	reference	$\beta_{non\text{-}cancer}$	β_{cancer}
Propyzamide	7.5	dog	chronic	(US-EPA, 2011)	6.1E-03	1.5E-02
Prosulfocarb	1.9	rat	chronic	(OCSEH, 2010)	6.7E-02	n/a
Prothioconazole	25	dog	subacute	(PPDB 2.0, 2011)	9.1E-03	n/a
Prothiofos	5	rat	chronic	(Tomlin, 2009)	2.5E-02	n/a
Pymetrozine	3.7	rat	chronic	(PPDB 2.0, 2011)	3.4E-02	n/a
Pyraclostrobin	3	rat	chronic	(OCSEH, 2010)	4.2E-02	n/a
Pyrimethanil	139	rat	subacute	(PPDB 2.0, 2011)	4.6E-03	n/a
Pyriproxyfen	24	rat	subchronic	(PPDB 2.0, 2011)	1.1E-02	n/a
Pyroquilone	22.5	rat	chronic	(PPDB 2.0, 2011)	5.6E-03	n/a
Quinclorac	35	dog	chronic	(OCSEH, 2010)	1.3E-03	n/a
Rimsulfuron	3.4	rat	subacute	(PPDB 2.0, 2011)	1.9E-01	n/a
Sethoxydim	9.135	dog	chronic	(US-EPA, 2011)	5.0E-03	n/a
Simazine	0.52	rat	chronic	(US-EPA, 2011)	2.4E-01	0
S-Metolachlor	15	dog	subacute	(PPDB 2.0, 2011)	1.5E-02	n/a
Spinosad	9	rat	subacute	(PPDB 2.0, 2011)	7.1E-02	n/a
Spiromesifen	11.15	dog	chronic	(NYSDEC, 2006)	4.1E-03	n/a
Tebuconazole	10.8	rat	subacute	(PPDB 2.0, 2011)	5.9E-02	n/a
Thiacloprid	7.3	rat	subacute	(PPDB 2.0, 2011)	8.7E-02	n/a
Thiamethoxam	2	rat	chronic	(OCSEH, 2010)	6.4E-02	n/a
Thiobencarb	1	rat	chronic	(US-EPA, 2011)	1.3E-01	n/a
Thiophanate-Methyl	8	rat	chronic	(US-EPA, 2011)	1.6E-02	n/a
Thiram	5	rat	chronic	(US-EPA, 2011)	2.5E-02	0
Triazophos	1.5	rat	subacute	(PPDB 2.0, 2011)	4.2E-01	n/a
Tricyclazole	9.6	rat	chronic	(PPDB 2.0, 2011)	1.3E-02	n/a

pesticide	NOEL	receptor	exposure	reference	$\beta_{non\text{-}cancer}$	β_{cancer}
Trifloxystrobin	6.4	rat	subacute	(PPDB 2011)	2.0, 9.9E-02	n/a

Crops-specific human toxicity characterization factors are calculated based on crop- and substance-specific human ingestion intake fractions as well as on information for cancer and non-cancer effects as presented in Table S4.9 for cancer effects and in Table S4.10 for non-cancer effects. Crop-specific characterization factors are recommended for use to account for residues from direct pesticide application. To account, in addition, for continuous, diffuse emissions, generic characterization factors for emissions to rural air and agricultural soil as calculated by USEtox are recommended to be combined with loss fractions to air and soil during pesticide application.

Table S4.9: Crop-specific human cancer toxicity characterization factors CF [DALY·$kg_{applied}^{-1}$] as calculated by the presented modeling approach and non-cancer characterization factors for diffuse emissions to urban air and agricultural soil as calculated by USEtox for the set of 121 pesticides. Bold values indicate substance-crop combinations registered for use in at least one of the countries listed in the Codex Alimentarius (*2010*)

pesticide	CF_{wheat}	CF_{rice}	CF_{tomato}	CF_{apple}	$CF_{lettuce}$	CF_{potato}	$CF_{USEtox,air}$	$CF_{USEtox,soil}$
1,3-Dichloropropene	8.5E-06	7.1E-05	5.9E-03	5.5E-04	1.4E-09	1.1E-07	1.8E-08	4.1E-08
2,4-D	0.0E+00	0.0E+00	0.0E+00	0.0E+00	0.0E+00	0.0E+00	0.0E+00	0.0E+00
Abamectin	n/a	n/a	n/a	n/a	n/a	n/a	n/a	n/a
Acetamiprid	n/a	n/a	n/a	n/a	n/a	n/a	n/a	n/a
Aclonifen	n/a	n/a	n/a	n/a	n/a	n/a	n/a	n/a
α-Cypermethrin	n/a	n/a	n/a	n/a	n/a	n/a	n/a	n/a
Azinphos-Methyl	0.0E+00	0.0E+00	0.0E+00	0.0E+00	0.0E+00	0.0E+00	0.0E+00	0.0E+00
Azoxystrobin	n/a	n/a	n/a	n/a	n/a	n/a	n/a	n/a
Benalaxyl	n/a	n/a	n/a	n/a	n/a	n/a	n/a	n/a
Benfluralin	n/a	n/a	n/a	n/a	n/a	n/a	n/a	n/a
Benomyl	n/a	n/a	n/a	n/a	n/a	n/a	n/a	n/a
β-Cyfluthrin	n/a	n/a	n/a	n/a	n/a	n/a	n/a	n/a
Bifenthrin	0.0E+00	0.0E+00	0.0E+00	0.0E+00	0.0E+00	0.0E+00	0.0E+00	0.0E+00
Buprofezin	n/a	n/a	n/a	n/a	n/a	n/a	n/a	n/a
Butachlor	n/a	n/a	n/a	n/a	n/a	n/a	n/a	n/a
Captan	2.9E-10	1.2E-08	5.1E-05	8.5E-06	2.6E-05	4.9E-10	4.1E-09	1.4E-08
Carbaryl	2.7E-07	5.3E-07	1.3E-03	2.0E-05	2.9E-03	3.7E-08	5.3E-07	3.4E-07
Carbendazim	n/a	n/a	n/a	n/a	n/a	n/a	n/a	n/a
Carbofuran	0.0E+00	0.0E+00	0.0E+00	0.0E+00	0.0E+00	0.0E+00	0.0E+00	0.0E+00
Carpropamid	n/a	n/a	n/a	n/a	n/a	n/a	n/a	n/a
Chloropicrin	0.0E+00	0.0E+00	0.0E+00	0.0E+00	0.0E+00	0.0E+00	0.0E+00	0.0E+00
Chlorothalonil	2.5E-09	1.6E-08	7.7E-06	2.9E-07	4.9E-05	9.4E-11	1.7E-08	5.0E-09
Chlorpyrifos	0.0E+00	0.0E+00	0.0E+00	0.0E+00	0.0E+00	0.0E+00	0.0E+00	0.0E+00
Clofentezine	n/a	n/a	n/a	n/a	n/a	n/a	n/a	n/a
Clomazone	n/a	n/a	n/a	n/a	n/a	n/a	n/a	n/a
Cyhalothrin	n/a	n/a	n/a	n/a	n/a	n/a	n/a	n/a
Cymoxanil	n/a	n/a	n/a	n/a	n/a	n/a	n/a	n/a
Cypermethrin	n/a	n/a	n/a	n/a	n/a	n/a	n/a	n/a

pesticide	CF_{wheat}	CF_{rice}	CF_{tomato}	CF_{apple}	$CF_{lettuce}$	CF_{potato}	$CF_{USEtox,air}$	$CF_{USEtox,soil}$
Cyproconazole	n/a	n/a	n/a	n/a	n/a	n/a	n/a	n/a
Cyprodinil	n/a	n/a	n/a	n/a	n/a	n/a	n/a	n/a
Cyromazine	n/a	n/a	n/a	n/a	n/a	n/a	n/a	n/a
DDT	3.4E-04	7.8E-04	1.8E-02	1.0E-02	9.1E-02	1.8E-09	1.7E-05	5.4E-07
Deltamethrin	0.0E+00	0.0E+00	0.0E+00	0.0E+00	0.0E+00	0.0E+00	0.0E+00	0.0E+00
Diazinon	0.0E+00	0.0E+00	0.0E+00	0.0E+00	0.0E+00	0.0E+00	0.0E+00	0.0E+00
Difenoconazole	n/a	n/a	n/a	n/a	n/a	n/a	n/a	n/a
Dimethomorph	n/a	n/a	n/a	n/a	n/a	n/a	n/a	n/a
Diquat	n/a	n/a	n/a	n/a	n/a	n/a	n/a	n/a
Edifenphos	n/a	n/a	n/a	n/a	n/a	n/a	n/a	n/a
Endosulfan	0.0E+00	0.0E+00	0.0E+00	0.0E+00	0.0E+00	0.0E+00	0.0E+00	0.0E+00
Epoxiconazole	n/a	n/a	n/a	n/a	n/a	n/a	n/a	n/a
EPTC	n/a	n/a	n/a	n/a	n/a	n/a	n/a	n/a
Esfenvalerate	n/a	n/a	n/a	n/a	n/a	n/a	n/a	n/a
Etofenprox	n/a	n/a	n/a	n/a	n/a	n/a	n/a	n/a
Fenbutatin Oxide	n/a	n/a	n/a	n/a	n/a	n/a	n/a	n/a
Fenhexamid	n/a	n/a	n/a	n/a	n/a	n/a	n/a	n/a
Fenoxaprop-P	n/a	n/a	n/a	n/a	n/a	n/a	n/a	n/a
Fenpropathrin	n/a	n/a	n/a	n/a	n/a	n/a	n/a	n/a
Fenpropimorph	n/a	n/a	n/a	n/a	n/a	n/a	n/a	n/a
Fenpyroximate	n/a	n/a	n/a	n/a	n/a	n/a	n/a	n/a
Ferbam	0.0E+00	0.0E+00	0.0E+00	0.0E+00	0.0E+00	0.0E+00	0.0E+00	0.0E+00
Fipronil	n/a	n/a	n/a	n/a	n/a	n/a	n/a	n/a
Fludioxonil	n/a	n/a	n/a	n/a	n/a	n/a	n/a	n/a
Flufenacet	n/a	n/a	n/a	n/a	n/a	n/a	n/a	n/a
Fosetyl	n/a	n/a	n/a	n/a	n/a	n/a	n/a	n/a
Glyphosate	n/a	n/a	n/a	n/a	n/a	n/a	n/a	n/a
Hexythiazox	n/a	n/a	n/a	n/a	n/a	n/a	n/a	n/a
Imidacloprid	n/a	n/a	n/a	n/a	n/a	n/a	n/a	n/a
Indoxacarb	n/a	n/a	n/a	n/a	n/a	n/a	n/a	n/a
Iodosulfuron	n/a	n/a	n/a	n/a	n/a	n/a	n/a	n/a
Iprodione	n/a	n/a	n/a	n/a	n/a	n/a	n/a	n/a
Isoproturon	n/a	n/a	n/a	n/a	n/a	n/a	n/a	n/a
λ-Cyhalothrin	n/a	n/a	n/a	n/a	n/a	n/a	n/a	n/a
Malathion	0.0E+00	0.0E+00	0.0E+00	0.0E+00	0.0E+00	0.0E+00	0.0E+00	0.0E+00
Mancozeb	n/a	n/a	n/a	n/a	n/a	n/a	n/a	n/a
Maneb	4.0E-09	1.9E-07	8.5E-05	1.5E-05	6.7E-04	2.3E-10	9.2E-09	1.0E-08
MCPA	0.0E+00	0.0E+00	0.0E+00	0.0E+00	0.0E+00	0.0E+00	0.0E+00	0.0E+00
Mepanipyrim	n/a	n/a	n/a	n/a	n/a	n/a	n/a	n/a
Metalaxyl-M	n/a	n/a	n/a	n/a	n/a	n/a	n/a	n/a
Metam Sodium	n/a	n/a	n/a	n/a	n/a	n/a	n/a	n/a
Metconazole	n/a	n/a	n/a	n/a	n/a	n/a	n/a	n/a
Methamidophos	n/a	n/a	n/a	n/a	n/a	n/a	n/a	n/a
Methomyl	n/a	n/a	n/a	n/a	n/a	n/a	n/a	n/a
Metribuzin	n/a	n/a	n/a	n/a	n/a	n/a	n/a	n/a
Molinate	n/a	n/a	n/a	n/a	n/a	n/a	n/a	n/a
Monocrotophos	n/a	n/a	n/a	n/a	n/a	n/a	n/a	n/a
Myclobutanil	n/a	n/a	n/a	n/a	n/a	n/a	n/a	n/a

pesticide	CF_{wheat}	CF_{rice}	CF_{tomato}	CF_{apple}	$CF_{lettuce}$	CF_{potato}	$CF_{USEtox,air}$	$CF_{USEtox,soil}$
Napropamide	n/a	n/a	n/a	n/a	n/a	n/a	n/a	n/a
Norflurazon	n/a	n/a	n/a	n/a	n/a	n/a	n/a	n/a
Oxadiargyl	n/a	n/a	n/a	n/a	n/a	n/a	n/a	n/a
Paraquat	n/a	n/a	n/a	n/a	n/a	n/a	n/a	n/a
Parathion-Methyl	0.0E+00	0.0E+00	0.0E+00	0.0E+00	0.0E+00	0.0E+00	0.0E+00	0.0E+00
Penconazole	n/a	n/a	n/a	n/a	n/a	n/a	n/a	n/a
Pendimethalin	n/a	n/a	n/a	n/a	n/a	n/a	n/a	n/a
Permethrin	n/a	n/a	n/a	n/a	n/a	n/a	n/a	n/a
Phorate	n/a	n/a	n/a	n/a	n/a	n/a	n/a	n/a
Phosmet	n/a	n/a	n/a	n/a	n/a	n/a	n/a	n/a
Phoxim	n/a	n/a	n/a	n/a	n/a	n/a	n/a	n/a
Picoxystrobin	n/a	n/a	n/a	n/a	n/a	n/a	n/a	n/a
Pirimicarb	n/a	n/a	n/a	n/a	n/a	n/a	n/a	n/a
Pirimiphos-Methyl	n/a	n/a	n/a	n/a	n/a	n/a	n/a	n/a
Probenazole	n/a	n/a	n/a	n/a	n/a	n/a	n/a	n/a
Propamocarb	n/a	n/a	n/a	n/a	n/a	n/a	n/a	n/a
Propanil	n/a	n/a	n/a	n/a	n/a	n/a	n/a	n/a
Propargite	n/a	n/a	n/a	n/a	n/a	n/a	n/a	n/a
Propiconazole	n/a	n/a	n/a	n/a	n/a	n/a	n/a	n/a
Propoxycarbazone-Sodium	n/a	n/a	n/a	n/a	n/a	n/a	n/a	n/a
Propyzamide	7.1E-07	1.0E-06	1.1E-04	1.5E-06	2.1E-07	7.5E-10	2.6E-07	3.1E-07
Prosulfocarb	n/a	n/a	n/a	n/a	n/a	n/a	n/a	n/a
Prothioconazole	n/a	n/a	n/a	n/a	n/a	n/a	n/a	n/a
Prothiofos	n/a	n/a	n/a	n/a	n/a	n/a	n/a	n/a
Pymetrozine	n/a	n/a	n/a	n/a	n/a	n/a	n/a	n/a
Pyraclostrobin	n/a	n/a	n/a	n/a	n/a	n/a	n/a	n/a
Pyrimethanil	n/a	n/a	n/a	n/a	n/a	n/a	n/a	n/a
Pyriproxyfen	n/a	n/a	n/a	n/a	n/a	n/a	n/a	n/a
Pyroquilone	n/a	n/a	n/a	n/a	n/a	n/a	n/a	n/a
Quinclorac	n/a	n/a	n/a	n/a	n/a	n/a	n/a	n/a
Rimsulfuron	n/a	n/a	n/a	n/a	n/a	n/a	n/a	n/a
Sethoxydim	n/a	n/a	n/a	n/a	n/a	n/a	n/a	n/a
Simazine	0.0E+00	0.0E+00	0.0E+00	0.0E+00	0.0E+00	0.0E+00	0.0E+00	0.0E+00
S-Metolachlor	n/a	n/a	n/a	n/a	n/a	n/a	n/a	n/a
Spinosad	n/a	n/a	n/a	n/a	n/a	n/a	n/a	n/a
Spiromesifen	n/a	n/a	n/a	n/a	n/a	n/a	n/a	n/a
Tebuconazole	n/a	n/a	n/a	n/a	n/a	n/a	n/a	n/a
Thiacloprid	n/a	n/a	n/a	n/a	n/a	n/a	n/a	n/a
Thiamethoxam	n/a	n/a	n/a	n/a	n/a	n/a	n/a	n/a
Thiobencarb	n/a	n/a	n/a	n/a	n/a	n/a	n/a	n/a
Thiophanate-Methyl	n/a	n/a	n/a	n/a	n/a	n/a	n/a	n/a
Thiram	0.0E+00	0.0E+00	0.0E+00	0.0E+00	0.0E+00	0.0E+00	0.0E+00	0.0E+00
Triazophos	n/a	n/a	n/a	n/a	n/a	n/a	n/a	n/a
Tricyclazole	n/a	n/a	n/a	n/a	n/a	n/a	n/a	n/a
Trifloxystrobin	n/a	n/a	n/a	n/a	n/a	n/a	n/a	n/a

Table S4.10: Crop-specific human non-cancer toxicity characterization factors CF [DALY·$kg_{applied}^{-1}$] as calculated by the presented modeling approach and non-cancer characterization factors for diffuse emissions to urban air and agricultural soil as calculated by USEtox for the set of 121 pesticides. Bold values indicate substance-crop combinations registered for use in at least one of the countries listed in the Codex Alimentarius (*2010*)

pesticide	CF_{wheat}	CF_{rice}	CF_{tomato}	CF_{apple}	$CF_{lettuce}$	CF_{potato}	$CF_{USEtox,air}$	$CF_{USEtox,soil}$
1,3-Dichloropropene	3.3E-06	2.8E-05	2.3E-03	2.1E-04	5.4E-10	4.4E-08	4.5E-06	3.7E-06
2,4-D	1.2E-19	4.2E-14	4.2E-09	1.1E-19	1.4E-08	1.6E-10	7.6E-07	7.3E-07
Abamectin	4.0E-08	9.3E-08	6.0E-05	4.5E-05	2.0E-02	2.8E-08	n/a	n/a
Acetamiprid	3.1E-07	1.2E-06	3.1E-04	2.1E-05	1.8E-03	9.6E-09	n/a	n/a
Aclonifen	1.9E-09	1.3E-08	9.1E-07	1.1E-07	1.0E-08	4.5E-11	n/a	n/a
α-Cypermethrin	5.2E-08	9.7E-07	2.2E-04	1.3E-05	1.8E-03	2.7E-10	7.1E-07	6.7E-08
Azinphos-Methyl	1.1E-07	1.3E-06	3.6E-03	5.2E-04	1.9E-03	5.0E-09	4.5E-07	1.9E-06
Azoxystrobin	5.1E-06	1.4E-05	2.7E-04	1.8E-04	8.5E-04	7.5E-10	n/a	n/a
Benalaxyl	3.6E-07	3.3E-06	4.7E-04	3.7E-05	2.7E-03	5.7E-10	n/a	n/a
Benfluralin	1.4E-15	1.5E-11	1.4E-08	1.3E-09	9.1E-10	1.4E-11	8.0E-09	2.0E-08
Benomyl	1.8E-06	6.0E-06	9.1E-05	4.0E-05	5.3E-04	6.3E-11	2.2E-09	1.9E-09
β-Cyfluthrin	6.6E-08	1.5E-06	4.6E-04	2.3E-05	3.4E-03	4.5E-10	1.8E-06	1.3E-07
Bifenthrin	2.5E-08	6.8E-07	2.0E-04	8.3E-06	1.4E-03	6.1E-12	1.8E-06	1.2E-07
Buprofezin	1.6E-07	3.4E-06	9.0E-04	4.5E-05	6.8E-03	1.4E-08	4.4E-07	3.9E-07
Butachlor	4.8E-21	3.2E-17	1.3E-07	2.9E-11	1.3E-15	1.4E-10	n/a	n/a
Captan	7.1E-10	2.8E-08	1.3E-04	2.1E-05	6.5E-05	1.2E-09	4.3E-08	1.4E-07
Carbaryl	4.7E-08	9.3E-08	2.3E-04	3.6E-06	5.1E-04	6.4E-09	4.0E-07	2.5E-07
Carbendazim	6.0E-08	6.1E-07	9.1E-05	5.0E-06	6.1E-04	2.0E-09	2.3E-08	6.8E-08
Carbofuran	1.1E-08	5.1E-07	4.7E-04	1.3E-06	4.5E-03	2.5E-07	3.3E-06	5.0E-06
Carpropamid	9.3E-06	2.3E-05	5.8E-04	3.0E-04	2.8E-03	6.5E-10	n/a	n/a
Chloropicrin	9.1E-06	3.5E-05	4.1E-03	3.1E-03	7.8E-04	2.3E-08	n/a	n/a
Chlorothalonil	1.8E-08	1.1E-07	5.4E-05	2.0E-06	3.5E-04	6.7E-10	5.2E-07	1.5E-07
Chlorpyrifos	3.0E-09	3.7E-07	7.1E-04	5.5E-06	6.6E-03	6.1E-09	1.8E-06	1.1E-05
Clofentezine	7.7E-07	5.0E-06	4.3E-04	5.6E-05	2.2E-03	1.7E-09	n/a	n/a
Clomazone	7.1E-07	8.6E-07	3.9E-05	4.9E-09	1.1E-08	6.9E-10	n/a	n/a
Cyhalothrin	6.9E-06	2.9E-05	1.2E-03	3.8E-04	8.8E-03	9.3E-11	1.6E-06	1.9E-07
Cymoxanil	9.6E-08	4.3E-07	1.0E-04	5.6E-06	5.5E-04	7.3E-09	n/a	n/a
Cypermethrin	7.1E-08	1.1E-06	2.2E-04	1.6E-05	1.6E-03	1.4E-10	8.1E-07	8.6E-08
Cyproconazole	1.1E-03	1.7E-03	2.1E-02	1.9E-02	8.4E-02	1.1E-07	n/a	n/a
Cyprodinil	5.0E-07	4.3E-06	4.7E-04	5.7E-05	2.9E-03	2.1E-09	n/a	n/a
Cyromazine	1.2E-07	8.2E-06	1.1E-03	2.0E-04	3.9E-03	3.0E-09	1.6E-06	4.9E-07
DDT	6.4E-05	1.5E-04	3.3E-03	1.9E-03	1.7E-02	3.4E-10	1.4E-05	4.3E-07
Deltamethrin	7.2E-08	1.5E-06	2.5E-04	8.3E-06	1.8E-03	7.7E-13	6.6E-07	4.7E-08
Diazinon	7.2E-06	7.8E-05	1.1E-02	9.7E-04	7.0E-02	1.2E-07	3.0E-06	9.8E-06
Difenoconazole	1.5E-06	8.5E-06	5.0E-04	1.1E-04	2.9E-03	1.4E-09	n/a	n/a
Dimethomorph	4.2E-06	1.4E-05	6.3E-04	1.3E-04	3.1E-03	4.3E-09	n/a	n/a
Diquat	2.0E-10	1.2E-07	1.2E-03	9.7E-08	1.5E-06	9.7E-09	4.6E-06	5.4E-08
Edifenphos	5.6E-08	2.2E-06	1.9E-03	3.1E-05	1.5E-02	1.7E-08	2.2E-06	1.5E-06
Endosulfan	4.0E-08	1.4E-06	8.0E-04	1.8E-05	6.4E-03	3.7E-09	6.1E-07	4.5E-07
Epoxiconazole	1.3E-04	2.1E-04	2.9E-03	2.4E-03	1.2E-02	5.1E-09	n/a	n/a
EPTC	7.2E-13	2.4E-11	2.0E-06	2.7E-12	4.1E-16	3.7E-10	3.8E-08	2.6E-07
Esfenvalerate	1.4E-07	1.1E-06	9.6E-05	1.5E-05	6.8E-04	6.4E-10	n/a	n/a

pesticide	CF_{wheat}	CF_{rice}	CF_{tomato}	CF_{apple}	$CF_{lettuce}$	CF_{potato}	$CF_{USEtox,air}$	$CF_{USEtox,soil}$
Etofenprox	7.7E-11	2.2E-08	1.1E-04	3.9E-07	1.1E-03	3.8E-10	7.6E-07	1.3E-07
Fenbutatin Oxide	2.7E-08	2.5E-09	1.5E-07	8.1E-08	9.5E-04	1.8E-10	3.8E-06	9.4E-08
Fenhexamid	1.5E-09	4.0E-08	1.5E-05	5.6E-07	1.0E-04	2.7E-10	n/a	n/a
Fenoxaprop-P	4.3E-08	2.7E-07	1.8E-05	5.2E-10	3.3E-07	7.9E-10	n/a	n/a
Fenpropathrin	2.1E-08	4.3E-07	1.2E-04	6.5E-06	1.0E-03	1.5E-09	2.8E-07	5.4E-08
Fenpropimorph	5.6E-08	4.5E-06	6.0E-03	7.0E-05	5.5E-02	1.1E-07	n/a	n/a
Fenpyroximate	1.8E-07	5.8E-06	2.5E-03	7.9E-05	2.0E-02	2.7E-09	n/a	n/a
Ferbam	1.5E-08	2.1E-07	9.6E-06	2.5E-05	2.0E-04	1.4E-08	2.0E-07	1.1E-08
Fipronil	1.3E-09	2.1E-07	5.1E-03	3.0E-04	3.0E-03	2.6E-08	4.1E-06	4.7E-06
Fludioxonil	3.1E-06	1.7E-05	1.0E-03	2.3E-04	5.7E-03	9.3E-11	n/a	n/a
Flufenacet	1.6E-12	3.2E-09	8.9E-05	3.7E-12	2.2E-09	1.1E-08	n/a	n/a
Fosetyl	3.4E-09	5.9E-09	6.7E-06	6.9E-07	1.6E-05	5.8E-13	n/a	n/a
Glyphosate	4.1E-18	2.1E-10	5.6E-09	5.3E-10	3.2E-08	9.5E-14	7.3E-09	2.5E-08
Hexythiazox	6.6E-09	1.7E-07	4.3E-05	4.5E-07	3.0E-04	4.1E-11	1.3E-07	1.2E-07
Imidacloprid	7.3E-07	5.3E-06	4.1E-04	7.6E-05	2.5E-03	3.0E-09	3.2E-07	3.8E-08
Indoxacarb	6.7E-08	1.6E-06	3.4E-04	5.8E-06	2.8E-03	2.5E-09	n/a	n/a
Iodosulfuron	1.3E-12	9.0E-12	2.8E-10	1.1E-14	9.7E-10	3.9E-09	n/a	n/a
Iprodione	2.8E-07	2.4E-06	2.3E-04	2.5E-05	1.2E-03	2.4E-09	5.2E-07	1.2E-06
Isoproturon	1.4E-13	2.4E-11	1.2E-08	4.1E-19	1.9E-14	5.2E-11	n/a	n/a
λ-Cyhalothrin	3.1E-07	1.1E-05	5.0E-03	1.7E-04	4.2E-02	5.0E-10	n/a	n/a
Malathion	9.0E-10	4.1E-08	7.1E-05	1.2E-05	5.5E-05	1.4E-10	5.8E-09	6.0E-09
Mancozeb	2.7E-09	4.7E-08	2.0E-04	1.3E-05	1.8E-04	2.6E-10	3.3E-08	3.8E-08
Maneb	3.3E-09	1.5E-07	7.0E-05	1.2E-05	5.5E-04	1.9E-10	3.2E-08	3.6E-08
MCPA	1.1E-18	2.4E-15	1.5E-07	3.2E-20	8.8E-13	3.3E-09	2.0E-06	2.9E-06
Mepanipyrim	3.8E-06	1.7E-05	8.1E-04	1.9E-04	4.3E-03	2.9E-09	n/a	n/a
Metalaxyl-M	1.2E-04	3.5E-04	5.4E-03	1.8E-03	2.8E-02	1.4E-08	n/a	n/a
Metam Sodium	5.0E-21	6.9E-19	8.2E-15	2.7E-21	5.2E-11	1.4E-10	n/a	n/a
Metconazole	4.7E-05	1.1E-04	2.5E-03	1.4E-03	1.2E-02	7.7E-09	n/a	n/a
Methamidophos	1.5E-08	5.9E-06	6.5E-03	4.5E-04	1.8E-02	5.8E-07	2.6E-06	4.2E-06
Methomyl	2.1E-09	3.2E-07	2.5E-03	1.6E-04	2.2E-03	9.3E-08	2.3E-06	1.3E-06
Metribuzin	6.0E-15	2.5E-12	1.7E-11	2.4E-22	2.8E-14	1.4E-10	1.8E-07	2.0E-07
Molinate	2.0E-12	1.5E-10	2.1E-06	8.0E-15	2.0E-14	2.2E-09	1.2E-06	7.8E-06
Monocrotophos	2.4E-06	9.3E-05	6.6E-02	6.8E-03	2.2E-01	4.7E-06	1.3E-05	2.1E-05
Myclobutanil	3.1E-07	2.2E-06	1.9E-04	2.3E-05	1.0E-03	1.4E-09	2.3E-07	6.4E-08
Napropamide	3.4E-07	3.7E-07	1.8E-05	5.4E-07	9.5E-07	6.4E-11	5.4E-09	2.1E-08
Norflurazon	3.3E-05	1.1E-05	1.2E-04	6.5E-06	2.1E-05	2.0E-10	1.8E-07	1.6E-08
Oxadiargyl	3.1E-14	2.8E-12	6.6E-07	5.6E-09	9.9E-14	8.2E-11	n/a	n/a
Paraquat	4.2E-05	1.3E-06	3.3E-07	5.3E-07	3.6E-04	4.7E-13	5.4E-07	2.8E-09
Parathion-Methyl	1.5E-07	4.1E-06	6.9E-03	1.2E-03	5.9E-03	4.1E-08	1.5E-06	9.3E-07
Penconazole	1.1E-08	2.2E-07	9.0E-05	3.2E-06	6.0E-04	4.5E-10	5.8E-07	1.1E-07
Pendimethalin	6.3E-09	3.7E-08	3.9E-07	1.1E-07	2.9E-06	3.8E-11	3.3E-08	3.5E-08
Permethrin	3.2E-09	1.1E-07	4.9E-05	1.7E-06	4.1E-04	2.9E-11	1.7E-07	1.3E-08
Phorate	1.7E-05	1.3E-04	1.2E-02	1.7E-03	5.1E-02	4.1E-08	2.5E-07	2.1E-06
Phosmet	3.3E-09	1.9E-08	7.3E-04	3.6E-05	6.2E-05	3.8E-10	2.6E-07	2.5E-06
Phoxim	7.5E-10	5.1E-09	6.7E-04	2.0E-05	2.1E-04	2.2E-09	2.8E-07	4.9E-07
Picoxystrobin	1.6E-08	7.9E-07	4.8E-04	7.0E-06	3.8E-03	7.6E-09	n/a	n/a
Pirimicarb	7.4E-09	1.6E-07	2.6E-04	3.7E-05	2.6E-04	7.9E-10	6.3E-08	3.3E-07
Pirimiphos-Methyl	2.1E-06	1.8E-05	1.6E-03	2.2E-04	7.7E-03	8.7E-09	1.7E-07	1.1E-06

pesticide	CF_{wheat}	CF_{rice}	CF_{tomato}	CF_{apple}	$CF_{lettuce}$	CF_{potato}	$CF_{USEtox,air}$	$CF_{USEtox,soil}$
Probenazole	5.8E-12	2.6E-11	1.2E-05	5.4E-07	8.7E-07	8.2E-11	n/a	n/a
Propamocarb	8.6E-07	3.2E-06	1.6E-04	2.2E-05	1.2E-03	2.0E-08	3.1E-08	8.0E-08
Propanil	6.4E-07	5.2E-07	1.2E-05	1.6E-08	9.9E-12	2.3E-10	6.9E-07	4.7E-07
Propargite	1.1E-06	7.8E-06	5.7E-04	9.4E-05	4.2E-03	1.3E-09	2.4E-07	1.6E-07
Propiconazole	7.1E-08	1.2E-06	2.5E-04	1.5E-05	1.6E-03	1.9E-09	3.6E-07	1.4E-07
Propoxycarbazone-Sodium	1.5E-14	2.0E-13	5.4E-13	1.3E-16	3.4E-11	1.4E-11	n/a	n/a
Propyzamide	6.9E-08	9.9E-08	1.1E-05	1.4E-07	2.1E-08	7.4E-11	1.1E-07	1.3E-07
Prosulfocarb	6.6E-18	7.3E-14	2.4E-07	1.9E-10	8.7E-09	4.8E-11	n/a	n/a
Prothioconazole	4.1E-09	1.1E-07	4.7E-05	1.4E-06	3.4E-04	2.3E-10	n/a	n/a
Prothiofos	9.6E-07	5.5E-06	3.5E-04	7.1E-05	2.5E-03	7.4E-10	n/a	n/a
Pymetrozine	1.3E-08	3.5E-09	9.7E-05	1.2E-06	1.7E-05	4.6E-10	n/a	n/a
Pyraclostrobin	2.0E-07	2.6E-06	3.8E-04	3.0E-05	2.4E-03	3.2E-10	n/a	n/a
Pyrimethanil	4.4E-09	3.8E-08	1.9E-05	6.0E-07	1.4E-04	4.5E-10	n/a	n/a
Pyriproxyfen	2.6E-10	1.7E-08	1.7E-05	2.8E-07	1.4E-04	8.2E-11	2.6E-08	2.4E-09
Pyroquilone	7.9E-06	2.0E-05	1.4E-04	7.5E-05	8.1E-04	5.8E-09	n/a	n/a
Quinclorac	7.4E-16	1.4E-13	1.1E-08	1.6E-18	8.1E-08	6.1E-11	n/a	n/a
Rimsulfuron	3.6E-20	5.1E-17	3.0E-10	2.0E-20	6.0E-12	9.6E-10	n/a	n/a
Sethoxydim	1.7E-16	8.7E-14	9.5E-12	8.6E-22	3.1E-16	1.7E-13	9.5E-09	1.4E-08
Simazine	3.9E-06	1.2E-05	1.7E-04	7.7E-11	1.3E-05	1.5E-08	4.1E-06	2.9E-06
S-Metolachlor	3.6E-15	1.1E-12	1.4E-07	3.1E-15	1.0E-14	7.7E-11	n/a	n/a
Spinosad	1.2E-09	1.4E-09	1.3E-05	5.3E-06	7.1E-04	1.1E-10	n/a	n/a
Spiromesifen	9.8E-10	3.5E-08	1.9E-05	4.9E-07	1.5E-04	2.0E-11	n/a	n/a
Tebuconazole	6.8E-07	3.9E-06	2.4E-04	5.2E-05	1.3E-03	1.5E-09	2.9E-07	1.0E-07
Thiacloprid	1.5E-07	8.0E-07	2.5E-04	9.0E-06	1.8E-03	3.2E-09	n/a	n/a
Thiamethoxam	2.4E-07	1.1E-05	4.7E-04	4.4E-04	6.5E-03	2.3E-08	n/a	n/a
Thiobencarb	2.6E-20	1.1E-13	3.4E-06	6.2E-09	3.9E-14	9.9E-10	8.3E-07	2.3E-07
Thiophanate-Methyl	4.0E-10	4.7E-10	5.6E-05	1.6E-06	1.9E-05	4.2E-10	5.4E-08	1.7E-08
Thiram	3.7E-09	1.6E-07	7.5E-05	4.4E-07	7.1E-04	1.2E-10	1.2E-08	6.2E-08
Triazophos	7.7E-08	5.6E-06	2.7E-02	3.2E-03	2.2E-02	1.7E-07	5.7E-06	4.2E-06
Tricyclazole	4.0E-07	4.6E-06	3.1E-04	1.4E-04	7.1E-04	2.9E-09	n/a	n/a
Trifloxystrobin	4.0E-08	1.4E-06	1.7E-03	3.6E-04	2.1E-03	2.6E-09	n/a	n/a

Human toxicity impact scores are calculated for substance-crop combinations registered for use in at least one of the countries listed in the Codex Alimentarius (*2010*). Figure S4.55 lists substance-specific human toxicity impact scores grouped according to pesticide target class and ordered according to decreasing impact score per substance for all six selected crops.

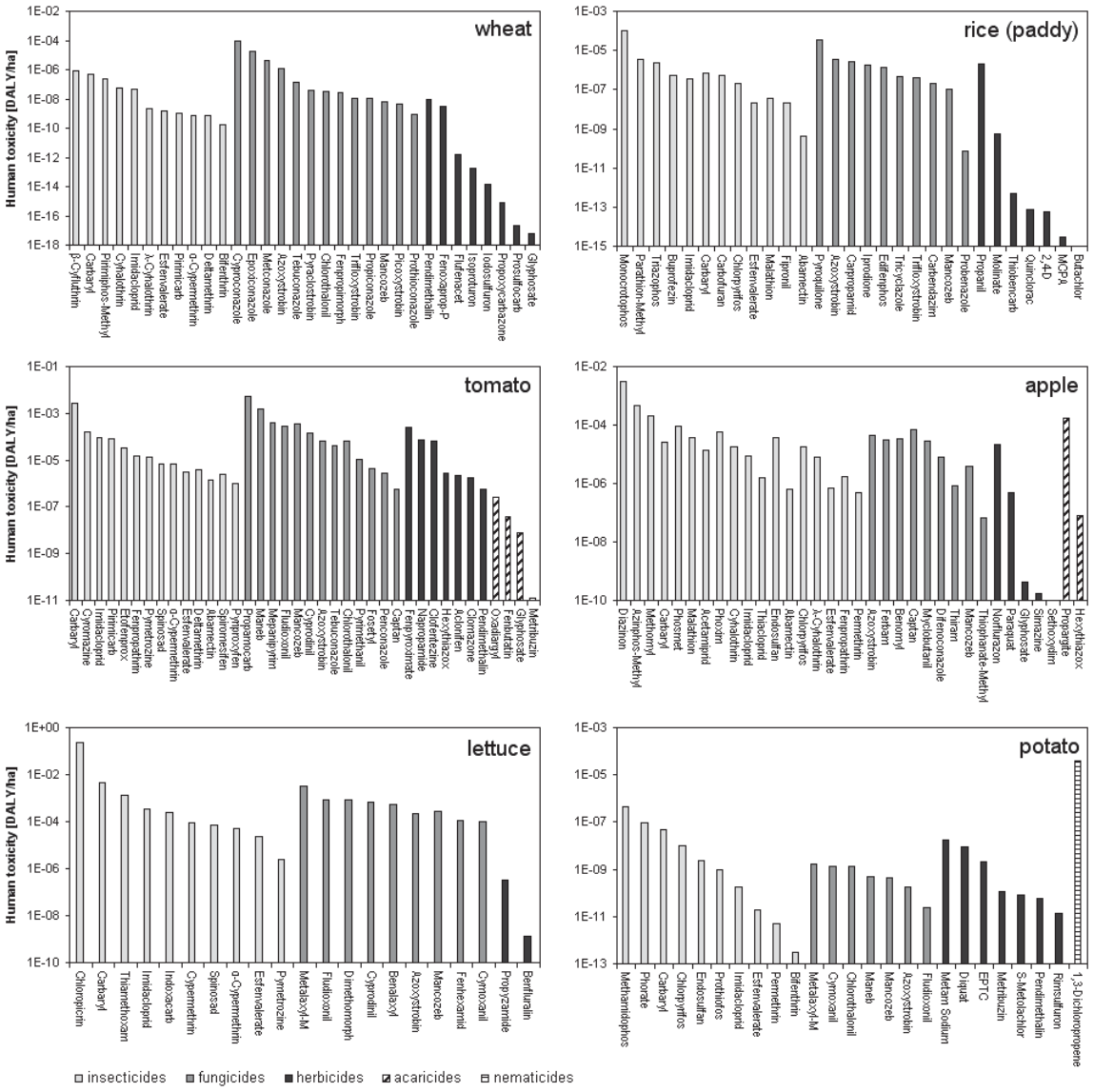

Figure S4.55: Crop-specific human toxicity impact scores aggregated over cancer and non-cancer effects for 181 officially authorized pesticide-crop combinations registered for use in at least one of the countries listed in the Codex Alimentarius (*2010*)

For a functional assessment of pesticides we developed an example of substitution of different pesticide target classes applied to wheat against a set of common pests. In Table S4.11, we present the background information for the three scenarios of substituting a mix of (a) insecticides, (b) fungicides and (c) herbicides based on the combination of applied dose and toxicity potential. Data on common wheat pests are derived from (*Jørgensen et al., 2010; Landwirtschaftskammer, 2009; Prescott et al., 1986*).

Table S4.11: Pesticide target class, scenario, selected pesticides (classified according to target class), target species, recommended application amount m_{app} [kg·ha^{-1}], substance-specific impact score $IS_{substance}$ [DALY·ha^{-1}], impact score aggregated over target class IS_{class} [DALY·ha^{-1}], and relative impact score ϑ_{IS} normalized to scenario #1 for three pesticide substitution scenarios on wheat

	scenario	pesticide	target pests*				m_{app}	$IS_{substance}$	IS_{class}	ϑ_{IS}
			A	B	C	D				
insecticides	#1	β-cyfluthrin	x	x	x		13.75	9.0E-07	1.4E-06	100%
		carbaryl		x	x	x	1.48	4.6E-07		
	#2	cyhalothrin	x	x	x	x	0.008	5.2E-08	5.3E-08	3.1%
		esfenvalerate		x	x	x	0.012	1.6E-09		
	#3	α-cypermethrin	x	x	x	x	0.015	7.9E-10	1.5E-09	0.1%
		deltamethrin	x	x	x	x	0.009	6.8E-10		
			E	F	G	H				
fungicides	#1	cyproconazole	x	x	x	x	0.08	8.8E-05	8.9E-05	100%
		azoxystrobin	x	x	x	x	0.238	1.2E-06		
	#2	epoxiconazole	x	x	x	x	0.125	1.7E-05	1.7E-05	18.8%
		pyraclostrobin	x	x	x	x	0.175	3.6E-08		
		fenpropimorph		x	x	x	0.45	2.5E-08		
	#3	tebuconazole		x		x	0.219	1.5E-07	1.8E-07	0.2%
		chlorothalonil	x	x	x		1.5	3.0E-08		
		mancozeb	x	x	x		2.35	6.3E-09		
			J	K	L	M				
herbicides	#1	pendimethalin	x	x			1.4	8.9E-09	1.2E-08	100%
		fenoxaprop-p	x		x		0.069	3.0E-09		
		prosulfocarb	x	x		x	3.5	2.3E-17		
	#2	iodosulfuron		x	x		0.01	1.3E-14	1.4E-14	<0.1%
		propoxycarbazone-sodium	x			x	0.05	7.7E-16		
	#3	glyphosate	x	x	x	x	1.37	5.7E-18	5.7E-18	<0.1%

* A: wheat bulb fly (*Delia coarctata*), B: cereal leaf beetle (*Oulema melanopa*), C: aphids (*Aphidoidea*), D: thrips (*Thysanoptera*), E: septoria leaf blotch (*Mycosphaerella graminicola*), F: wheat leaf rust (*Puccinia triticina*), G: wheat yellow rust (*Puccinia striiformis*), H: powdery mildew (*Blumeria graminis f. sp. Tritici*), J: slender meadow foxtail (*Alopecurus myosuroides*), K: annual meadow grass (*Poa annua*), L: common wild oat (*Avena fatua*), M: couch grass (*Elytrigia repens*).

5.4.1. References of Supporting Information

Antón Vallejo A. 2004. Utilización del Análisis del Ciclo de Vida en la Evaluación del impacto ambiental en el cultivo bajo invernadero mediterráneo. Ph.D. Dissertation, Univerisitat Politècnica de Catalunya, Barcelona.

California Department of Pesticide Regulation; Metam Sodium (Sodium N-Methyldithiocarbamate) Risk Characterization Document; 2004.

California Department of Pesticide Regulation; Summary of Toxicology Data Propoxycarbazone-Sodium; 2005.

Carranza C, Lanchero O, Miranda D, Chaves B. 2009. Análisis del crecimiento de lechuga (Lactuca sativa L.) 'Batavia' cultivada en un suelo salino de la Sabana de Bogotá. Agronomía Colombiana 27 : 41-48.

Chen J, Lin H, Liu A, Shao Y, Yang L. 2006. A semi-empirical backscattering model for estimation of leaf area index (LAI) of rice in southern China. International Journal of Remote Sensing 27:5417-5425.

Codex Alimentarius Commission; Codex pesticides residues in food online database. Joint FAO/WHO Food Standards Programme: 2010.

Eremeev V, Joudu J, Lääniste P, Mäeorg E, Makke A, Talgre L, Lauringson E, Raave H, Noormets M. 2008. Consequences of pre-planting treatments of potato seed tubers on leaf area index formation. Acta Agriculturae Scandinavica, Section B - Plant Soil Science 58:236-244.

European Agency for the Evaluation of Medicinal Products; Phoxim Summary Report, EMEA/MRL/756/00-FINAL; 2000.

Food and Agriculture Organization of the United Nations; Pesticide Residues in Food 2008. FAO Plant Production and Protection Paper 193; Rome, 2005.

Gong D, Kang S, Zhang L, Du T, Yao L. 2006. A two-dimensional model of root water uptake for single apple trees and its verification with sap flow and soil water content measurements. Agricultural Water Management 83 :119-129.

Huijbregts M, Hauschild M, Jolliet O, Margni M, McKone T, Rosenbaum RK, van de Meent D. 2010. USEtox™ User Manual Version 1.01.

Huijbregts MAJ, Rombouts LJA, Ragas AMJ, van de Meent D. 2005. Human-Toxicological Effect and Damage Factors of Carcinogenic and Noncarcinogenic Chemicals for Life Cycle Impact Assessment. Integrated Environmental Assessment and Management 1:181-244.

Jørgensen L N, Hovmøller MS, Hansen JG, Lassen P, Clark B, Bayles R, Rodemann B, Jahn M, Flath K, Goral T, Czembor J, du Cheyron P, Maumene C, de Pope C, Nielsen GC. 2010. EuroWheat.org - A Support to Integrated Disease Management in Wheat. Outlooks on Pest Management 21:173-176.

Krieger RI, Krieger WC. 2001. Handbook of Pesticide Toxicology (Second Edition). Academic Press: Orlando, FL.

Landwirtschaftskammer Nordrhein-Westfalen Schädlinge im Getreide; Münster, 2009.

Lenz VIS. 2007. A process-based crop growth model for assessing Global Change effects on biomass production and water demand - A component of the integrative Global Change decision support system DANUBIA. Ph.D. Disserstation, Universität Köln, Köln.

Makhteshim Agan UK Ltd; Safety data sheet Alpha Isoproturon 500; Berks, 2005.

Motoyama T, Yamaguchi I. 2003. Fungicides, Melanin Biosynthesis Inhibitors. In Encyclopedia of Agrochemicals, Plimmer JR Ed. John Wiley and Sons.

New York State Department of Environmental Conservation; Registration with Conditions of One New Pesticide Product, Pre-Strike Outdoor Fogger. EPA Reg. No. 11715-325-2724: 2006.

New York State Department of Environmental Conservation; Withdrawal of Application to Register the New Active Ingredient (NAI) Spiromesifen contained in Oberon 2SC Insecticide/Miticide (EPA Reg. No. 264-719) and Forbid 4F (EPA Reg. No. 432-1279) - (Chemical Code: 024875); 2006.

Office of Chemical Safety and Environmental Health; Acceptable Daily Intakes for Agricultural and Veterinary Chemicals, Current as of 30 September 2010; Commonwealth of Australia: Canberra, 2010.

Pennington DW, Crettaz P, Tauxe A, Rhomberg L, Brand K, Jolliet O. 2002. Assessing Human Health Response in Life Cycle Assessment Using ED10s and DALYs: Part 2 - Noncancer Effects. Risk Analysis 22:947-963.

Pesticide Management Education Program; Pesticide Information Profile: Propamocarb; Ithaca, NY, 1997.

Prescott JM, Burnett PA, Saari E E, Ranson J, Bowman J, de Milliano W, Singh RP, Bekele G. 1986 Wheat Diseases and Pests: a guide for field identification. International Maize and Wheat Improvement Center: Mexico 135.

Rosenbaum RK, Bachmann TM, Gold LS, Huijbregts MAJ, Jolliet O, Juraske R, Koehler A, Larsen HF, MacLeod M, Margni MD, McKone TE, Payet J, Schuhmacher M, van de Meent D, Hauschild MZ. 2008. USEtox - the UNEP-SETAC toxicity model: recommended characterisation factors for human toxicity and freshwater ecotoxicity in life cycle impact assessment. The International Journal of Life Cycle Assessment 13:532-546.

Sasaki M. 2003. Fungicides, Organophosphorus Compounds. In Encyclopedia of Agrochemicals, Plimmer. JR Ed. John Wiley and Sons.

The Pesticide Properties Database (PPDB 2.0) of the FOOTPRINT Project. University of Hertfordshire (last accessed April 10, 2011).

Tomlin CDS 2009. The Pesticide Manual, Fiveteenth Edition. BCPC Publications: Hampshire.

United States - Environmental Protection Agency; Integrated Risk Information System (IRIS). www.epa.gov/iris (last accessed April 22, 2011).

United States - Environmental Protection Agency; Phorate (Thimet) EPA Pesticide Fact Sheet 12/88; Washington, D.C., 1988.

United States - Environmental Protection Agency; Reregistration Eligibility Decision (RED) Fenbutatin-oxide; EPA 738-R-94-024; Washington, D.C., 1994.

5.5. Appendix for section 4.4 Higher (warm-blooded) predator ecotoxicity

5.5.1. Methodology

5.5.1.1. Correlations in residual standard errors

We did a pilot study to estimate the correlations in residual standard errors and the covariance in the ICE predictions, because ICE predictions were often made based on the same experimental LD50 value. As the experimental dataset underlying the ICE regressions of Raimondo et al. (2010) were not available due to confidentiality reasons, we considered a dataset with LD50 data from RTECS (Accelrys Inc. 2011) for 37 chemical substances in the species Mouse, Rabbit and Guinea Pig (see Table S1).

For species s1 and s2 we considered the ICE regression:

$$Log(LD50_x^{s2}) = a + b\,log(LD50_x^{s1}) + \varepsilon_x^{s1s2} \qquad \textit{S2.28}$$

where *s1* is called the surrogate species, *s2* is called the predicted species, and ε_x^{s1s2} is the so-called residual error. The variance of the ε_x^{s1s2} values was estimated by the mean squared error (MSE) of the corresponding linear regression. Once the parameters *a* and *b* have been estimated by values $\widehat{\alpha}$ (intercept) and $\widehat{\beta}$ (slope), we could define the residual error:

$$\varepsilon_x^{s1s2} = log(LD50_x^{s2}) - (\widehat{\alpha} + \widehat{\beta} log(LD50_x^{s1}) \qquad \textit{S2.29}$$

Table S4.12: Chemicals with LD50 data for mouse, rabbit and guinea pig used in our pilot study

CAS	Chemical name	LD50 mouse ($mg \cdot kgwwt^{-1}$)	LD50 rabbit ($mg \cdot kgwwt^{-1}$)	LD50 guinea pig ($mg \cdot kgwwt^{-1}$)
56073-10-0	Brodifacoum	5.00E+01	2.80E-01	4.00E-01
116-06-3	Aldicarb	5.41E-01	1.30E+00	1.00E+00
297-78-9	Telodrin	1.00E+01	4.00E+00	2.54E+00
1563-66-2	Carbofuran	5.37E+00	7.50E+00	9.20E+00
56-38-2	Parathion-ethyl	1.12E+01	1.00E+01	1.31E+01
900-95-8	Fentin acetate	8.70E+01	4.93E+01	1.80E+01
950-37-8	Methidathion	2.71E+01	7.10E+01	2.50E+01
10265-92-6	Methamydophos	1.62E+01	1.73E+01	3.00E+01
60-57-1	Dieldrin	6.00E+01	4.74E+01	3.09E+01
309-00-2	Aldrin	4.40E+01	6.32E+01	3.30E+01
22781-23-3	Bendiocarb	3.55E+01	3.74E+01	3.50E+01
2595-54-2	Mecarbam	1.06E+02	6.00E+01	6.50E+01
1113-02-6	Omethoate	3.12E+01	5.00E+01	7.07E+01
106-93-4	1,2-Dibromoethane	4.20E+02	5.50E+01	1.10E+02
29973-13-5	Ethiofencarb	1.35E+02	1.63E+02	1.13E+02
76-44-8	Heptachlor	6.80E+01	8.49E+01	1.16E+02
58-89-9	lindane	1.65E+02	1.08E+02	1.18E+02
301-12-2	Oxydemethon-methyl	3.00E+01	1.04E+02	1.20E+02

533-74-4	3,5-dimethyltetrahydro-2-H,1,3,5-thiadiazone-2-thione	2.78E+02	2.88E+02	1.60E+02
59669-26-0	Thiodicarb	2.26E+02	5.56E+02	1.60E+02
2176-62-7	Pentachloropyridine	1.31E+02	9.05E+01	1.70E+02
8001-35-2	Toxaphene	7.39E+01	5.72E+01	2.10E+02
101-27-9	Barban	1.35E+03	6.00E+02	2.40E+02
1912-24-9	Atrazine	1.75E+03	6.71E+02	2.50E+02
640-15-3	Thiometon	6.20E+01	9.50E+01	2.61E+02
63-25-2	Carbaryl	3.36E+02	7.10E+02	2.80E+02
333-41-5	Diazinon	1.11E+02	1.39E+02	3.05E+02
108-62-3	Metaldehyde	2.00E+02	6.02E+02	3.50E+02
17109-49-8	Edifenphos	3.61E+02	3.16E+02	3.74E+02
2597-03-7	Phenthoate	3.74E+02	2.10E+02	3.88E+02
2921-88-2	Chlorpyriphos	1.52E+02	1.41E+03	5.04E+02
1194-65-6	Dichlobenil	1.69E+03	2.32E+02	5.84E+02
1698-60-8	Chloridazon	2.74E+03	1.12E+03	1.01E+03
29232-93-7	Pirimiphos-methyl	1.18E+03	1.63E+03	1.41E+03
5598-13-0	Chlorpyrifos-methyl	1.88E+03	2.00E+03	2.25E+03
23564-05-8	Thiophanate-methyl	3.45E+03	2.26E+03	4.94E+03
71-55-6	1,1,1-trichloroethane	1.12E+04	5.66E+03	9.47E+03

Most noticeable was the high mutual correlation between the residual errors in the predicted values if a common surrogate species was used (correlation coefficient ≈0.9, see Table S2). Moreover the errors in the toxicities in the predictions from two different surrogate species were highly correlated. Table S2 shows the results. The reduction in residual standard error (RSE) in the bivariate linear regression with respect to linear regression from surrogate Guinea Pig is only (1 – 0.4752/0.4782) = 0.0063, that is a gain of less than 1%. We concluded that the residual standard errors in LD50 values predicted from a common surrogate are not independent. Since the combined dataset in this study was based on many LD50 values predicted from common surrogate species, we applied a conservative method to quantify the uncertainty of the HD50 value (correlation 1, see section 5.5.1.2).

Table S4.13: The correlation of the residual errors for toxicity predictions based on linear regressions

Surrogate species	Predicted species	Intercept	Slope	RSE	MSE	Correlation coeffcient
Mouse	Rabbit	0.2092	0.8679	0.5105	0.2606	0.8294
Mouse	Guinea Pig	0.1703	0.8812	0.5004	0.2504	
Rabbit	Mouse	0.4875	0.8001	0.4901	0.2402	0.8802
Guinea Pig	Mouse	0.4863	0.8047	0.4782	0.2287	
Rabbit + Guinea Pig	Mouse			0.4752	0.2258	

RSE = residual standard error, MSE = mean squared error

5.5.1.2. Conservative calculation of uncertainty

We used the ICE models to estimate 'predicted' LD50 values. The standard deviation of the predicted toxicity for chemical x in species j from surrogate species i ($s_{j,x}$) was calculated according to Mendenhall and Beaver (1994):

$$s_{j,x} = \sqrt{MSE_{ij} \cdot \left(1 + \frac{1}{n_{ij}} + \frac{(logLD50_{i,x} - \overline{logLD50}_i)^2}{S_{ss}}\right)} \qquad \textbf{S2.30}$$

In this equation, MSE_{ij} is the Mean Squared Error based on the Sum of Squares for Errors for the predicted toxicity value of species j from surrogate species i, given by Raimondo et al. (2010); n_{ij} is the total number of surrogate LD50 values used for derivation of the ICE model correlation between species i and j; $LD50_{i,x}$ is the experimental LD50 value for chemical x in surrogate species i as applied in our model predictions; $\overline{logLD50}_i$ is the average of all log-transformed experimental LD50 for surrogate species i (i.e. different chemicals) used for derivation of the ICE model correlation between species i and j; and S_{ss} is the sum of squared deviations in the surrogate toxicity value given by Raimondo et al. (2010). We approached the total number of warm-blooded wildlife species (N) with a number of experimentally tested species (n) and a number of modeled species (m). We assumed that the predicted species are a random sample of all species. Furthermore, we assumed that the computable covariances between predictions correspond to a random sample of pairs of species, e.g. predicted species j_1 and j_2. Therefore, the covariance between the predictions for all species j_1 up to j_N was denoted as s_{j1j2}, and the mean covariance $\frac{1}{N^2}\sum_{j1=1}^{N}\sum_{j2=1}^{N} s_{j1j2}$ was the average of the covariances and variances.

An upperbound to the mean covariance followed from the Cauchy-Schwartz inequality $s_{j1j2} = \sqrt{s_{j1}^2}\sqrt{s_{j2}^2}$ (Steele 2004, equality means correlation 1), and lead to the square of the mean standard deviation:

$$\frac{1}{N^2}\sum_{j1=1}^{N}\sum_{j2=1}^{N}s_{j1j2}=\frac{1}{N^2}\sum_{j1=1}^{N}\sum_{j2=1}^{N}\sqrt{s_{j1}^2}\sqrt{s_{j2}^2}=\frac{1}{N^2}\left(\sum_{j1=1}^{N}\sqrt{s_{j1}^2}\right)\left(\sum_{j2=1}^{N}\sqrt{s_{j2}^2}\right)=\left(\frac{1}{N}\sum_{j=1}^{N}s_j\right)^2 \qquad \textit{S2.31}$$

For the toxicity values predicted with the ICE-regressions from Raimondo et al. (2010), $\frac{1}{N}\sum_{j=1}^{N}s_j$ could be estimated by $\frac{1}{m}\sum_{j=1}^{m}s_j$. To be exact, s_j is $s_{j,x}$ i.e. the standard deviation of the predicted toxicity for chemical x in species j, calculated according to Mendenhall and Beaver (1994) (see below). If there were also *n* experimental values, then the square of the standard error of the mean ($SEM_{Co,x}$) was described by:

$$\frac{s_{Co,x}^2}{n+m}+\frac{m^2}{(n+m)^2}\left(\frac{1}{m}\sum_{j=1}^{m}s_{j,x}\right)^2 \qquad \textit{S2.32}$$

In this equation $s_{Co,x}^2$ is the variance of all LD50 values available for chemical x – both tested and predicted.

5.5.2. Results

Table S4.14: CF air indicates the characterization factor for the impact on warm-blooded predators due to an emission to air. CF freshwater indicates the characterization factor for the impact on warm-blooded predators due to an emission in fresh water. CF agr.soil indicates the characterization factor for the impact on warm-blooded predators due to an emission in agricultural soil.

CAS	CF air (yr/kg)	CF freshwater (yr/kg)	CF agr.soil (yr/kg)
2257-09-2	2.47E-17	9.05E-16	2.11E-17
2425-06-1	4.66E-15	1.19E-13	5.61E-15
2425-10-7	8.18E-17	1.82E-15	1.69E-16
2439-01-2	3.68E-17	1.43E-15	2.29E-17
2497-07-6	1.87E-16	1.57E-14	1.47E-15
2597-03-7	1.43E-17	1.19E-15	1.18E-17
3547-04-4	3.33E-15	3.23E-13	1.59E-15
3735-01-1	1.40E-17	1.75E-15	7.90E-17
4329-03-7	2.88E-15	1.07E-12	3.56E-16
5827-05-4	3.53E-17	4.76E-15	3.61E-16
7377-03-9	2.13E-19	4.15E-18	3.72E-19
100-00-5	2.00E-16	2.91E-15	2.64E-16
100-01-6	9.44E-18	1.80E-16	2.39E-17
10004-44-1	7.36E-20	4.71E-18	6.81E-19
100-17-4	1.48E-17	3.65E-16	2.79E-17
100-29-8	2.44E-17	1.11E-15	5.56E-17
10031-82-0	1.44E-17	7.57E-16	2.57E-17
100-40-3	1.52E-18	2.05E-16	8.12E-19
100-41-4	1.02E-17	1.35E-16	5.26E-18
100-42-5	1.12E-17	8.99E-16	6.52E-18
100-43-6	3.39E-17	2.58E-15	1.33E-16

100-44-7	1.71E-17	1.04E-16	8.82E-18
100-47-0	2.68E-17	2.29E-16	2.08E-17
100-51-6	9.31E-19	2.08E-17	1.84E-18
100-52-7	2.04E-17	3.72E-16	1.98E-17
100-54-9	5.85E-18	4.77E-17	6.64E-18
100-63-0	4.49E-17	1.50E-15	2.01E-16
100646-51-3	1.90E-17	8.11E-16	5.51E-18
100-66-3	3.07E-18	5.51E-17	1.77E-18
100-68-5	2.12E-17	6.02E-16	1.60E-17
100-75-4	3.57E-18	8.71E-17	8.56E-18
100-79-8	1.37E-19	2.32E-18	1.19E-19
100-97-0	1.06E-16	6.24E-18	2.14E-18
101-02-0	2.26E-16	7.21E-15	7.89E-17
101-05-3	4.03E-17	8.76E-16	4.88E-18
101-14-4	5.98E-17	9.54E-15	1.58E-16
101-21-3	2.83E-17	1.60E-15	1.06E-16
101-27-9	1.14E-17	2.38E-17	4.08E-20
101-42-8	5.95E-20	1.87E-18	2.68E-19
1014-69-3	1.35E-17	1.34E-15	9.55E-17
1014-70-6	1.38E-17	4.11E-16	2.52E-17
101-54-2	1.32E-17	1.16E-15	1.38E-16
101-61-1	7.14E-18	3.28E-15	2.47E-17
101-72-4	6.02E-18	2.20E-15	6.72E-17
101-77-9	5.32E-18	3.44E-16	1.59E-17
101-80-4	6.44E-18	5.10E-16	7.01E-17
101-81-5	2.31E-17	7.38E-16	1.32E-17
101-84-8	2.98E-17	7.61E-16	1.60E-17
101-90-6	3.09E-18	3.31E-16	4.24E-17
102-08-9	4.06E-17	4.34E-15	1.63E-16
102-09-0	4.53E-17	1.62E-15	5.30E-17
10222-01-2	2.17E-18	2.42E-17	3.41E-18
102-27-2	8.80E-18	2.26E-15	4.16E-17
1024-57-3	6.76E-14	3.52E-12	4.03E-14
10265-92-6	3.27E-17	2.01E-16	2.39E-17
103-05-9	1.42E-17	7.26E-16	2.94E-17
1031-07-8	5.44E-14	1.92E-12	8.52E-14
103112-35-2	9.85E-16	4.99E-14	4.51E-16
103-11-7	6.03E-19	1.53E-17	3.06E-19
10311-84-9	4.96E-15	5.00E-13	1.69E-15
103-23-1	5.44E-19	6.99E-19	4.06E-23
103-33-3	9.65E-17	2.84E-15	6.19E-17
103-65-1	3.82E-18	5.02E-17	1.93E-18
103-69-5	1.09E-17	1.60E-15	6.35E-17
103-72-0	3.50E-16	2.55E-15	1.78E-16
103-74-2	4.61E-20	4.08E-19	6.08E-20
103-76-4	2.89E-19	8.46E-19	1.30E-19
10380-28-6	1.96E-17	3.43E-16	3.01E-17
103-84-4	1.86E-18	2.82E-17	3.03E-18
103-85-5	1.17E-17	3.04E-16	3.61E-17
103-90-2	8.65E-19	8.19E-18	1.03E-18
104-40-5	7.62E-18	6.16E-16	6.41E-19
10443-70-6	2.52E-17	1.60E-15	1.13E-17
10453-86-8	3.29E-18	1.25E-15	4.34E-19
104-76-7	5.45E-18	1.39E-16	4.13E-18
104-85-8	3.65E-17	4.30E-16	2.85E-17
104-87-0	1.20E-17	3.93E-16	1.29E-17

104-88-1	4.51E-17	2.68E-15	1.18E-16
104-90-5	3.86E-17	7.97E-16	3.98E-17
104-93-8	1.33E-17	5.91E-16	1.04E-17
104-94-9	3.49E-18	2.03E-16	2.60E-17
105-11-3	7.46E-18	4.39E-16	5.69E-17
105-37-3	1.29E-19	4.36E-19	6.97E-20
105-38-4	2.96E-19	4.63E-18	1.79E-19
105-39-5	1.35E-17	4.32E-17	7.47E-18
105-46-4	1.73E-18	1.21E-17	9.40E-19
105512-06-9	1.34E-18	4.77E-17	4.53E-19
105-53-3	2.37E-20	1.77E-19	2.06E-20
105-54-4	1.32E-19	9.16E-19	7.12E-20
105-55-5	3.52E-19	1.83E-17	9.56E-19
105-60-2	9.48E-19	1.17E-17	1.38E-18
105-67-9	1.47E-18	1.55E-16	7.14E-18
105-75-9	3.62E-20	1.07E-18	3.87E-21
105-76-0	5.13E-19	1.51E-17	5.48E-20
10589-74-9	1.02E-18	1.66E-17	1.58E-18
10595-95-6	1.25E-17	1.10E-16	1.48E-17
105-99-7	2.61E-20	3.68E-19	1.20E-20
10605-21-7	2.36E-18	8.16E-17	7.13E-18
106-24-1	2.36E-18	5.65E-16	3.26E-18
106-40-1	2.96E-17	3.10E-15	1.37E-16
106-41-2	9.18E-17	2.53E-15	1.74E-16
106-42-3	1.26E-17	3.35E-16	6.55E-18
106-43-4	1.61E-17	1.08E-16	8.15E-18
106-44-5	4.28E-18	3.32E-17	1.09E-18
106-46-7	9.22E-16	5.14E-15	5.71E-16
106-47-8	5.86E-17	4.15E-15	3.63E-16
106-48-9	9.41E-17	3.48E-15	2.23E-16
106-49-0	4.27E-18	1.84E-15	2.27E-16
106-50-3	8.96E-19	2.23E-17	2.90E-18
106-51-4	3.69E-17	1.18E-16	2.59E-17
106-63-8	1.13E-19	1.72E-18	6.23E-20
1066-45-1	2.22E-16	7.82E-16	1.61E-16
106-69-4	1.02E-20	1.19E-20	1.57E-21
1067-14-7	9.63E-16	7.19E-14	6.19E-16
1067-33-0	4.66E-17	9.44E-16	8.79E-17
106-88-7	2.89E-17	9.65E-17	1.81E-17
106-89-8	5.77E-17	1.56E-16	3.36E-17
106-92-3	2.56E-18	6.74E-17	5.01E-18
106-93-4	2.16E-16	1.08E-15	1.27E-16
106-94-5	9.49E-18	5.25E-17	5.59E-18
106-95-6	1.28E-17	3.71E-16	1.00E-17
106-99-0	2.01E-20	5.60E-18	1.78E-20
107-02-8	8.26E-17	4.23E-16	6.39E-17
107-03-9	6.20E-19	3.44E-17	6.02E-19
107-05-1	4.25E-18	9.91E-17	2.54E-18
107-06-2	8.95E-17	3.06E-16	6.27E-17
107-07-3	4.45E-17	8.20E-17	2.48E-17
107-12-0	2.03E-16	3.73E-16	1.26E-16
107-13-1	1.65E-16	3.00E-16	9.02E-17
107-14-2	9.06E-17	2.21E-16	5.80E-17
1071-83-6	6.20E-19	8.36E-19	4.82E-21
107-18-6	1.59E-17	1.05E-16	1.21E-17
107-19-7	1.90E-17	2.46E-17	1.04E-17

107-20-0	1.05E-16	1.27E-16	5.73E-17
107-21-1	8.02E-19	3.44E-19	1.08E-19
107-22-2	2.93E-17	3.73E-18	7.81E-19
107-30-2	3.94E-17	4.83E-20	1.40E-17
107-41-5	1.40E-18	2.16E-17	3.13E-18
107-49-3	7.96E-18	1.18E-16	1.40E-17
107534-96-3	3.08E-16	1.01E-14	2.38E-16
107-66-4	3.95E-18	1.87E-16	1.14E-17
107-87-9	5.73E-18	3.63E-17	4.16E-18
1079-33-0	6.34E-18	2.41E-16	1.96E-17
107-98-2	1.46E-19	2.01E-19	8.03E-20
108-05-4	3.76E-19	4.15E-18	2.22E-19
108-10-1	2.42E-18	2.94E-17	1.48E-18
108-11-2	3.44E-18	5.89E-17	2.74E-18
108-20-3	2.17E-18	2.82E-17	1.52E-18
108-21-4	2.90E-19	1.23E-18	1.58E-19
108-24-7	7.27E-18	5.33E-20	1.73E-18
108-31-6	5.93E-18	2.16E-20	5.96E-24
1083-57-4	2.38E-19	2.45E-18	2.83E-19
108-42-9	4.72E-17	4.26E-15	2.69E-16
108-43-0	4.08E-17	2.11E-15	1.32E-16
108-45-2	5.09E-19	2.12E-17	3.10E-18
1085-98-9	4.00E-16	1.56E-14	3.69E-16
108-60-1	2.12E-17	2.90E-16	1.88E-17
108-62-3	6.52E-18	2.59E-16	2.56E-17
108-67-8	5.61E-18	5.04E-16	3.15E-18
108-68-9	3.91E-18	7.92E-16	4.65E-17
108-69-0	1.44E-18	6.73E-16	2.13E-17
108-70-3	5.90E-16	5.07E-15	3.11E-16
108-78-1	1.10E-18	5.52E-19	8.45E-20
108-83-8	4.36E-18	2.30E-16	4.89E-18
108-84-9	4.82E-19	5.32E-18	2.54E-19
108-85-0	3.13E-17	4.51E-16	1.70E-17
108-86-1	7.42E-18	3.88E-17	3.79E-18
108-87-2	3.48E-18	1.14E-16	2.30E-18
108-88-3	2.89E-17	3.37E-16	1.57E-17
108-89-4	2.44E-17	3.93E-16	3.39E-17
108-90-7	1.24E-17	7.36E-17	7.61E-18
108-93-0	3.69E-18	8.39E-17	5.43E-18
108-94-1	4.42E-18	3.31E-17	3.55E-18
108-95-2	7.71E-19	1.21E-17	7.90E-19
108-99-6	1.46E-17	2.18E-16	1.90E-17
109-01-3	2.98E-19	6.04E-18	8.31E-19
109-06-8	1.42E-17	1.81E-16	1.67E-17
109-07-9	2.38E-18	2.70E-17	3.02E-18
109-09-1	1.12E-16	1.22E-15	1.16E-16
109-21-7	1.32E-19	1.77E-18	6.96E-20
109-46-6	1.68E-18	2.06E-16	5.50E-18
109-57-9	3.80E-19	6.43E-18	7.00E-19
109-60-4	1.14E-19	4.84E-19	6.27E-20
109-65-9	1.94E-17	1.03E-16	9.77E-18
109-69-3	1.40E-17	9.31E-17	8.01E-18
109-70-6	5.46E-17	3.11E-16	2.99E-17
109-75-1	2.76E-17	1.73E-16	2.19E-17
109-79-5	5.76E-19	2.69E-17	3.23E-19
109-86-4	2.25E-18	2.46E-18	1.37E-18

109-87-5	8.12E-19	1.31E-18	4.85E-19
109-99-9	2.67E-18	1.80E-17	2.09E-18
110-02-1	1.10E-17	1.50E-16	7.13E-18
110-12-3	3.98E-18	7.78E-17	3.31E-18
110-19-0	1.24E-19	8.82E-19	6.69E-20
110-27-0	2.60E-19	2.41E-18	5.75E-20
110-40-7	3.42E-20	1.27E-18	6.14E-21
110-43-0	1.16E-17	1.66E-16	7.15E-18
110488-70-5	7.94E-17	1.71E-15	1.24E-16
110-49-6	2.39E-19	9.05E-19	1.54E-19
110-54-3	5.55E-20	1.71E-18	4.50E-20
110-62-3	2.83E-16	5.59E-15	2.10E-16
110-63-4	5.89E-19	4.73E-19	6.14E-20
110-65-6	4.83E-18	4.95E-18	6.30E-19
11067-81-5	1.54E-16	8.04E-15	2.59E-18
110-75-8	1.93E-18	6.38E-17	2.13E-18
110-80-5	8.54E-19	7.33E-18	8.65E-19
110-81-6	6.74E-19	2.21E-16	8.22E-19
110-82-7	6.13E-18	1.33E-16	3.53E-18
110-83-8	5.96E-19	6.34E-17	4.28E-19
110-86-1	5.05E-18	3.90E-17	3.99E-18
110-88-3	1.40E-19	2.43E-19	9.19E-20
110-93-0	1.25E-18	5.19E-16	2.22E-17
11096-82-5	2.69E-13	2.48E-12	9.34E-15
110-97-4	2.83E-19	7.93E-19	1.05E-19
11097-69-1	2.91E-14	1.58E-12	5.82E-15
110-98-5	1.00E-20	1.82E-20	2.47E-21
11104-28-2	5.81E-16	1.40E-14	2.97E-16
111-13-7	5.01E-18	7.40E-17	2.93E-18
111-15-9	3.76E-19	3.17E-18	3.60E-19
111-25-1	2.10E-17	2.05E-16	1.05E-17
111-27-3	3.97E-18	9.28E-17	3.81E-18
1113-02-6	6.15E-18	7.70E-18	1.05E-18
111-30-8	6.96E-18	2.33E-17	4.40E-18
111-36-4	7.04E-17	4.27E-16	3.61E-17
111-41-1	3.92E-18	6.57E-19	9.29E-20
11141-16-5	5.39E-16	1.30E-14	2.76E-16
111-44-4	1.10E-16	5.85E-16	8.50E-17
111-46-6	5.29E-20	1.49E-20	2.01E-21
1114-71-2	3.41E-18	1.27E-16	1.86E-18
111479-05-1	1.07E-17	4.67E-16	1.78E-18
111-48-8	4.89E-20	8.59E-20	1.12E-20
111-55-7	2.63E-20	1.52E-19	1.99E-20
1116-54-7	5.23E-20	2.15E-20	2.85E-21
111-69-3	2.50E-17	1.09E-16	1.65E-17
111-70-6	5.47E-18	1.48E-16	4.54E-18
111-76-2	3.34E-18	5.29E-17	4.61E-18
111-77-3	8.32E-20	4.04E-20	1.13E-20
1118-46-3	7.33E-19	5.74E-18	6.66E-19
111-87-5	3.89E-19	1.09E-17	2.79E-19
111-90-0	3.45E-20	1.13E-19	1.56E-20
111-91-1	1.10E-16	3.45E-15	2.65E-16
111991-09-4	1.27E-19	5.89E-19	9.17E-20
1120-71-4	1.13E-17	4.32E-17	7.97E-18
112-07-2	4.07E-19	1.32E-17	7.14E-19
112-12-9	1.11E-17	3.04E-16	5.47E-18

112-27-6	5.66E-20	9.32E-21	1.27E-21
1122-91-4	5.59E-17	3.49E-15	1.15E-16
112-30-1	7.03E-19	2.67E-17	2.56E-19
112-34-5	2.68E-19	6.58E-18	8.16E-19
112-36-7	1.42E-18	2.84E-17	3.68E-18
112-42-5	1.33E-17	5.61E-16	5.12E-18
112-53-8	3.17E-17	1.60E-15	5.41E-18
112-56-1	1.91E-17	8.71E-16	7.43E-17
1126-79-0	4.49E-18	1.70E-16	2.40E-18
112-70-9	6.77E-19	3.61E-17	1.03E-19
1129-41-5	5.57E-17	1.06E-15	1.10E-16
1134-23-2	6.63E-18	9.17E-16	1.01E-17
1135-99-5	1.29E-17	1.86E-16	2.36E-17
114-07-8	8.29E-18	1.47E-16	1.23E-17
114-26-1	1.45E-18	2.99E-17	3.77E-18
114369-43-6	1.53E-16	3.77E-15	1.76E-16
114-83-0	1.57E-17	4.77E-16	6.95E-17
115-18-4	2.01E-18	1.63E-16	8.02E-18
115-19-5	4.35E-18	4.11E-17	4.91E-18
115-20-8	6.52E-17	1.16E-15	1.02E-16
115-29-7	2.76E-15	1.84E-13	3.69E-16
115-31-1	2.14E-17	1.13E-15	1.65E-17
115-32-2	5.71E-15	3.69E-13	4.73E-16
115-77-5	5.78E-20	6.62E-21	8.80E-22
115-86-6	6.45E-18	2.24E-16	7.58E-19
115-90-2	6.04E-15	5.57E-13	3.71E-14
115-96-8	7.93E-18	5.33E-16	3.72E-17
116-02-9	1.39E-17	9.77E-16	2.75E-17
116-06-3	2.75E-15	1.23E-13	1.77E-14
116255-48-2	2.22E-15	5.06E-14	2.36E-15
1162-65-8	3.06E-17	5.29E-16	7.64E-17
116-29-0	8.83E-15	5.00E-13	3.93E-15
1163-19-5	3.94E-12	8.80E-15	5.27E-18
117-18-0	4.17E-17	4.12E-16	2.21E-17
117-80-6	5.78E-16	1.47E-14	7.47E-16
117-81-7	2.58E-18	7.11E-17	3.24E-20
117-84-0	1.64E-18	2.64E-18	5.80E-21
118-55-8	9.54E-19	5.76E-17	4.52E-19
118-61-6	2.01E-18	5.15E-17	1.44E-18
118-74-1	1.28E-14	4.47E-13	9.46E-15
118-75-2	1.05E-16	1.54E-15	1.78E-16
118-96-7	1.76E-18	5.82E-19	9.88E-20
119-12-0	6.39E-17	1.38E-15	3.01E-17
119168-77-3	4.81E-16	2.93E-14	1.48E-16
119-32-4	1.08E-18	3.00E-17	2.67E-18
119-33-5	3.20E-18	1.00E-16	4.66E-18
119-34-6	1.45E-18	2.05E-17	2.95E-18
119-38-0	1.92E-16	1.15E-14	1.47E-15
119446-68-3	3.08E-15	1.53E-13	1.33E-15
1194-65-6	2.07E-16	6.31E-15	3.91E-16
119-47-1	3.01E-17	1.04E-15	4.28E-19
119-61-9	3.81E-18	1.37E-16	4.55E-18
119-65-3	8.54E-17	3.56E-15	2.16E-16
119-84-6	3.30E-18	3.45E-17	3.70E-18
12002-53-8	8.13E-19	2.15E-17	4.91E-19
120068-37-3	2.37E-15	9.92E-14	2.72E-15

120-07-0	2.25E-19	1.33E-17	1.98E-18
120-12-7	1.05E-17	1.53E-17	3.52E-18
120-21-8	5.94E-19	1.55E-16	4.34E-18
120-32-1	1.71E-16	1.24E-14	1.01E-16
120-51-4	1.38E-18	3.79E-17	4.22E-19
120-62-7	4.43E-17	1.01E-14	2.38E-17
120-71-8	8.72E-19	3.93E-16	2.37E-17
12071-83-9	1.44E-19	6.04E-18	6.87E-19
120-72-9	1.69E-17	3.92E-15	2.65E-16
120-78-5	2.87E-19	1.51E-17	5.33E-20
120-80-9	7.00E-19	3.99E-17	1.53E-18
120-82-1	4.50E-15	3.78E-14	2.32E-15
120-83-2	1.50E-17	1.14E-17	7.00E-18
120-92-3	2.61E-18	2.28E-17	2.66E-18
120923-37-7	7.06E-20	5.04E-18	6.78E-19
121-14-2	6.19E-17	2.54E-16	4.01E-17
121-21-1	1.47E-17	1.10E-14	7.14E-18
12122-67-7	2.18E-18	4.62E-17	2.51E-18
121-29-9	4.19E-18	1.66E-15	1.10E-17
121-32-4	3.07E-18	8.44E-17	7.91E-18
121-33-5	1.69E-18	3.66E-17	3.94E-18
1214-39-7	3.38E-18	4.00E-17	5.28E-18
121-46-0	2.04E-19	4.03E-17	1.86E-19
121-54-0	1.16E-15	4.75E-14	6.89E-16
121552-61-2	6.72E-19	2.03E-16	2.23E-18
121-69-7	1.20E-18	4.20E-16	2.59E-17
121-73-3	2.68E-16	4.91E-15	2.78E-16
121-75-5	1.03E-15	1.50E-13	1.55E-15
121-79-9	1.17E-19	5.61E-18	4.84E-19
121-82-4	2.66E-17	6.07E-16	8.96E-17
121-87-9	5.17E-17	8.40E-16	9.81E-17
122-03-2	2.62E-17	8.27E-16	1.68E-17
122-10-1	1.76E-17	1.69E-17	2.19E-18
122-14-5	2.66E-16	2.02E-14	3.78E-16
122-34-9	2.18E-17	1.48E-15	1.78E-16
122-39-4	4.12E-17	8.30E-15	1.89E-16
122-42-9	5.08E-19	4.40E-17	1.14E-18
122-60-1	4.38E-18	2.67E-16	2.15E-17
122931-48-0	5.09E-20	7.45E-19	1.16E-19
122-99-6	2.29E-18	5.52E-17	5.73E-18
123-03-5	9.68E-16	2.70E-14	3.50E-15
123-05-7	3.61E-18	1.27E-16	2.08E-18
123-25-1	2.09E-20	2.46E-19	2.46E-20
123-30-8	1.04E-20	2.61E-19	3.87E-20
123312-89-0	5.74E-20	2.74E-19	4.01E-21
123-31-9	5.80E-19	6.18E-19	5.70E-20
123-33-1	8.06E-19	1.94E-18	2.95E-19
123-38-6	4.03E-18	2.54E-17	2.40E-18
123-42-2	1.12E-18	3.99E-18	7.81E-19
123-54-6	1.41E-17	1.07E-16	1.46E-17
123-72-8	1.94E-18	1.99E-17	1.28E-18
123-73-9	1.12E-17	1.10E-16	6.71E-18
123-86-4	2.01E-19	1.41E-18	1.11E-19
123-88-6	1.15E-18	1.17E-16	8.80E-18
123-91-1	1.39E-18	9.74E-18	1.40E-18
123-92-2	1.12E-19	9.52E-19	5.93E-20

123-96-6	2.72E-17	5.92E-16	1.62E-17
12407-86-2	3.87E-17	1.39E-15	8.93E-17
1241-94-7	5.10E-17	3.77E-15	3.80E-18
124-48-1	9.44E-17	4.22E-16	5.72E-17
124-63-0	6.83E-17	5.93E-16	5.80E-17
124-87-8	3.55E-15	6.84E-17	1.16E-17
126-22-7	4.65E-17	8.01E-16	1.02E-16
126-30-7	6.43E-19	3.30E-18	4.13E-19
126-33-0	1.38E-18	3.91E-18	6.00E-19
126535-15-7	3.94E-19	1.50E-17	2.40E-19
12672-29-6	3.73E-16	4.95E-14	1.34E-16
126-72-7	1.54E-18	1.80E-16	1.31E-18
126-73-8	1.93E-18	1.62E-16	7.09E-19
12674-11-2	2.94E-15	1.50E-13	1.04E-15
126-98-7	2.15E-16	1.18E-15	2.82E-16
126-99-8	6.26E-18	3.09E-16	5.35E-18
127-00-4	2.05E-17	2.02E-16	2.35E-17
127-07-1	1.90E-18	4.45E-19	6.70E-20
127-18-4	1.62E-17	7.27E-17	1.23E-17
127-47-9	2.38E-17	9.73E-16	8.83E-19
127-66-2	2.21E-17	5.50E-16	5.62E-17
12771-68-5	8.42E-17	1.71E-15	2.03E-16
12789-03-6	5.92E-14	1.33E-11	3.02E-14
127-91-3	3.33E-18	5.89E-16	1.77E-18
128-37-0	7.63E-17	4.41E-15	3.97E-17
129-00-0	3.20E-17	1.58E-16	5.49E-18
1300-21-6	6.22E-17	2.00E-16	3.60E-17
130-15-4	4.53E-16	6.71E-15	8.16E-16
13067-93-1	1.44E-15	2.98E-13	1.99E-15
13071-79-9	3.30E-16	3.26E-13	4.50E-15
131-11-3	7.17E-20	1.40E-18	4.22E-20
131-17-9	8.80E-19	8.44E-17	1.47E-18
13121-70-5	1.32E-15	7.63E-14	1.70E-17
13171-21-6	4.47E-17	8.08E-16	1.03E-16
131-79-3	2.28E-15	3.51E-13	5.31E-16
13194-48-4	2.18E-15	1.55E-13	1.62E-14
1319-77-3	1.70E-17	1.75E-15	1.09E-16
13256-06-9	6.44E-18	3.66E-16	3.91E-18
13256-11-6	5.15E-17	1.14E-15	1.46E-16
132-65-0	9.98E-16	5.18E-14	5.59E-16
13292-46-1	6.08E-18	2.67E-16	2.58E-18
1330-20-7	1.29E-17	3.17E-16	6.89E-18
133-06-2	4.24E-17	1.03E-15	9.90E-18
133-07-3	4.85E-16	4.63E-14	1.62E-15
1330-78-5	6.08E-17	2.95E-15	1.57E-17
13311-84-7	7.62E-17	2.30E-15	7.18E-17
13356-08-6	9.92E-08	1.90E-12	1.14E-15
13360-45-7	2.55E-17	6.68E-16	3.72E-17
1336-36-3	8.42E-15	1.01E-12	2.76E-15
134-20-3	3.26E-19	1.73E-17	8.68E-19
13457-18-6	1.05E-17	9.68E-16	2.19E-17
134-62-3	1.62E-17	9.48E-16	6.71E-17
135-01-3	9.50E-18	1.66E-16	4.89E-18
135-19-3	6.05E-17	7.68E-15	4.91E-16
135-23-9	7.48E-19	3.47E-17	5.50E-18
135-88-6	3.47E-18	1.69E-15	9.69E-18

13593-03-8	2.14E-16	2.65E-14	7.22E-17
136-25-4	4.84E-16	2.17E-15	2.70E-17
136-40-3	1.94E-18	5.82E-18	9.03E-19
13674-84-5	4.78E-18	2.39E-16	1.85E-17
13674-87-8	3.64E-17	1.27E-15	3.27E-17
13684-63-4	1.82E-18	5.75E-18	1.56E-20
137-09-7	6.32E-16	4.05E-18	6.30E-19
137-30-4	2.51E-17	9.48E-16	1.37E-16
13752-51-7	1.53E-19	2.24E-18	3.50E-19
13826-35-2	6.10E-18	2.34E-16	5.42E-18
138-86-3	4.52E-18	1.94E-15	2.50E-18
139-40-2	1.09E-17	5.07E-16	3.33E-17
139-65-1	1.95E-17	1.57E-15	1.58E-16
1397-94-0	6.26E-17	9.02E-16	2.72E-18
139-94-6	1.27E-18	1.72E-17	2.43E-18
140-11-4	9.88E-19	1.69E-17	9.26E-19
1401-55-4	3.29E-19	4.29E-19	6.22E-20
14026-03-0	3.06E-18	1.28E-16	1.28E-17
140-31-8	6.10E-19	1.96E-18	3.09E-19
140-57-8	1.02E-16	1.75E-14	6.38E-17
140-66-9	7.82E-18	1.19E-15	2.67E-18
140-67-0	1.68E-17	1.71E-15	1.63E-17
140-79-4	1.84E-18	7.75E-18	1.19E-18
140-88-5	1.37E-18	1.68E-17	7.82E-19
14088-71-2	1.79E-15	1.26E-13	1.41E-16
140-89-6	2.54E-16	1.77E-17	2.74E-18
141-03-7	2.54E-20	4.44E-19	1.25E-20
141-05-9	3.01E-19	7.66E-18	3.89E-19
141-28-6	2.46E-20	5.25E-19	2.53E-20
141-32-2	3.12E-18	4.95E-17	1.74E-18
141-66-2	3.17E-17	1.07E-16	1.47E-17
141-78-6	1.08E-18	2.20E-18	5.71E-19
141-90-2	7.81E-19	3.00E-17	2.76E-18
141-93-5	6.59E-18	2.16E-16	3.33E-18
141-97-9	3.25E-19	8.43E-19	2.05E-19
1420-06-0	3.48E-17	6.55E-15	6.51E-17
142-04-1	4.60E-17	1.56E-18	2.40E-19
14214-32-5	2.56E-17	8.62E-16	6.94E-17
14235-86-0	2.97E-15	2.07E-14	6.19E-18
142-96-1	1.31E-17	3.99E-16	6.74E-18
143-08-8	1.76E-18	5.23E-17	9.49E-19
143-22-6	2.02E-19	1.80E-18	2.41E-19
14324-55-1	2.80E-17	2.73E-15	1.21E-16
143390-89-0	8.71E-17	1.65E-15	1.23E-16
143-50-0	3.17E-14	1.92E-12	8.41E-15
144-21-8	2.97E-14	1.72E-18	2.69E-19
14437-17-3	4.05E-17	9.77E-16	2.61E-17
1445-75-6	1.38E-18	1.30E-16	6.30E-18
14484-64-1	2.23E-18	6.97E-18	1.17E-18
1456-28-6	1.41E-18	3.68E-17	5.20E-18
1461-22-9	2.16E-16	1.44E-14	1.09E-16
1461-25-2	6.25E-15	4.29E-15	3.01E-15
148-01-6	1.27E-18	9.35E-18	1.42E-18
14816-18-3	3.69E-17	5.95E-15	2.47E-17
14816-20-7	9.28E-16	2.58E-13	6.30E-16
148-24-3	5.85E-19	1.85E-16	1.28E-17

148-53-8	2.80E-18	7.06E-17	6.61E-18
148-79-8	1.57E-17	6.42E-16	5.30E-17
148-82-3	4.05E-16	3.10E-15	4.74E-16
150-19-6	2.30E-18	2.17E-16	2.02E-17
150-50-5	3.48E-16	1.71E-14	2.61E-17
150-68-5	1.08E-17	2.30E-16	2.62E-17
150-69-6	1.08E-18	3.62E-17	5.01E-18
150-76-5	3.84E-18	1.07E-16	9.37E-18
150-78-7	7.85E-18	2.82E-16	1.11E-17
151-67-7	1.85E-17	5.31E-17	1.19E-17
152-16-9	1.50E-16	9.74E-16	1.53E-16
15263-52-2	3.21E-18	6.64E-18	1.04E-18
15263-53-3	4.50E-18	9.30E-18	1.45E-18
15299-99-7	1.03E-18	4.09E-18	2.14E-19
15310-01-7	2.95E-18	1.40E-16	1.94E-18
15457-05-3	3.73E-16	1.26E-14	3.25E-16
15545-48-9	8.90E-18	4.06E-16	2.17E-17
1563-38-8	4.32E-18	4.56E-16	3.56E-17
1563-66-2	1.32E-15	7.58E-14	8.19E-15
156-60-5	1.35E-17	1.06E-16	1.20E-17
15662-33-6	2.22E-15	2.61E-14	3.93E-15
1570-64-5	1.46E-17	7.13E-16	3.60E-17
1582-09-8	2.09E-17	9.43E-15	3.45E-17
15972-60-8	8.19E-18	7.02E-16	1.70E-17
16071-86-6	1.23E-14	4.48E-20	7.65E-21
16090-02-1	3.39E-19	1.88E-17	3.73E-20
1610-18-0	1.00E-17	5.36E-16	2.66E-17
161050-58-4	2.05E-16	6.87E-15	1.62E-16
16118-49-3	2.24E-19	8.48E-18	8.13E-19
16338-97-9	1.48E-18	1.76E-16	1.32E-17
1634-04-4	6.43E-18	2.75E-17	5.35E-18
1634-78-2	1.25E-17	9.32E-17	1.10E-17
1639-66-3	1.44E-18	2.06E-17	7.55E-20
16423-68-0	3.48E-17	2.32E-16	5.14E-17
1646-87-3	4.50E-16	2.95E-15	4.58E-16
1646-88-4	2.63E-17	9.02E-17	1.41E-17
16568-02-8	7.66E-18	2.82E-17	5.71E-18
16752-77-5	4.93E-16	1.06E-14	1.39E-15
1689-99-2	5.01E-17	1.26E-15	2.21E-18
1698-60-8	6.12E-18	6.22E-16	2.31E-17
17109-49-8	3.14E-18	1.35E-16	1.90E-18
17372-87-1	1.54E-15	7.10E-16	1.79E-16
1746-01-6	5.25E-11	2.67E-09	2.78E-12
1746-81-2	9.40E-18	2.22E-16	2.52E-17
1757-18-2	3.91E-15	2.78E-12	1.63E-15
17606-31-4	6.95E-19	4.61E-16	1.46E-17
17754-90-4	1.57E-18	2.77E-16	1.59E-17
17804-35-2	1.35E-17	4.06E-16	3.15E-18
17924-92-4	1.13E-17	3.45E-16	7.66E-18
18181-70-9	1.14E-16	2.55E-14	2.35E-17
18181-80-1	6.31E-17	2.43E-15	4.73E-18
1825-21-4	2.56E-14	1.01E-12	1.27E-14
1835-49-0	1.33E-15	1.87E-14	2.04E-15
1836-75-5	6.55E-16	3.68E-14	2.20E-16
1836-77-7	2.93E-17	1.76E-15	5.20E-18
1861-32-1	5.78E-18	1.83E-16	1.07E-18

1861-40-1	7.99E-19	5.24E-17	3.93E-19
1871-57-4	4.60E-17	2.31E-15	2.84E-17
18854-01-8	6.76E-16	1.46E-13	1.28E-15
1897-45-6	1.25E-16	7.05E-16	6.41E-17
1910-42-5	2.30E-15	1.01E-16	1.59E-17
1912-24-9	4.33E-17	3.46E-15	3.85E-16
1912-26-1	5.15E-18	5.35E-16	1.65E-17
1918-13-4	7.47E-17	3.03E-15	1.55E-16
1918-16-7	4.08E-17	1.52E-15	1.03E-16
1918-18-9	5.50E-17	2.91E-15	7.20E-17
1928-43-4	1.49E-15	1.48E-13	1.19E-16
1928-45-6	2.90E-16	3.55E-14	1.11E-16
1929-73-3	1.42E-16	1.08E-14	6.00E-17
1929-77-7	5.02E-18	4.74E-16	5.33E-18
1929-82-4	5.25E-16	1.14E-14	4.25E-16
1929-88-0	5.73E-19	4.79E-17	5.02E-18
19335-11-6	3.70E-18	2.51E-16	3.66E-17
1934-21-0	2.70E-10	2.26E-19	3.84E-20
1937-37-7	2.88E-19	1.62E-17	7.72E-20
1948-33-0	5.97E-18	4.24E-16	2.12E-17
1955-45-9	1.64E-18	2.80E-18	9.49E-19
1966-58-1	9.06E-18	3.83E-16	1.69E-17
19666-30-9	1.18E-16	8.69E-15	3.16E-17
1967-16-4	4.18E-18	2.66E-16	8.22E-18
1982-47-4	5.05E-18	1.76E-16	3.21E-18
19937-59-8	1.67E-17	4.75E-16	6.08E-17
20056-92-2	3.45E-19	5.07E-17	1.37E-19
2008-41-5	2.56E-18	2.00E-16	1.88E-18
2028-63-9	2.47E-17	7.51E-17	1.66E-17
2032-59-9	3.27E-18	4.72E-16	4.77E-17
2032-65-7	4.15E-16	2.21E-14	1.35E-15
2034-22-2	1.09E-15	3.56E-14	4.66E-15
206-44-0	1.82E-17	1.06E-15	4.99E-18
2074-50-2	1.53E-15	7.63E-15	1.18E-15
20762-60-1	9.00E-17	5.15E-16	7.52E-17
20917-49-1	1.31E-17	7.39E-16	6.23E-17
2104-64-5	2.34E-15	3.55E-13	1.03E-15
2104-96-3	5.40E-17	1.55E-14	3.39E-17
21087-64-9	1.72E-20	4.33E-18	8.43E-20
21436-96-4	7.58E-19	2.99E-16	1.53E-17
21436-97-5	6.53E-19	3.29E-16	1.56E-17
2155-70-6	1.41E-16	1.71E-14	9.77E-17
21564-17-0	7.97E-18	8.91E-16	2.96E-17
21609-90-5	2.28E-15	1.71E-13	7.27E-17
21626-89-1	5.95E-18	8.21E-17	8.75E-18
2163-80-6	6.52E-15	6.24E-18	9.66E-19
2164-17-2	6.19E-17	1.21E-15	1.24E-16
21725-46-2	2.23E-17	4.51E-16	2.99E-17
21757-82-4	5.08E-18	2.84E-16	8.75E-19
2176-62-7	4.78E-16	3.98E-15	2.79E-16
21884-44-6	2.02E-17	3.11E-16	3.03E-17
21923-23-9	3.30E-15	1.63E-12	1.02E-15
2212-67-1	4.46E-18	2.68E-16	4.91E-18
2216-51-5	7.82E-19	3.24E-17	5.45E-19
22212-55-1	2.39E-17	1.09E-15	7.59E-18
2223-93-0	1.32E-16	1.69E-15	1.35E-17

2227-13-6	3.33E-15	3.30E-13	2.16E-16
2227-17-0	1.32E-13	1.03E-12	8.34E-16
2235-25-8	6.66E-18	2.00E-17	3.15E-18
2243-27-8	1.89E-17	2.21E-16	9.93E-18
2255-17-6	1.80E-15	2.77E-14	2.60E-15
2274-67-1	5.50E-16	2.67E-14	1.13E-15
2275-14-1	9.63E-16	8.41E-13	4.47E-16
2275-23-2	2.01E-18	1.73E-17	2.36E-18
22781-23-3	8.08E-17	2.15E-15	2.18E-16
22936-75-0	1.18E-17	9.31E-16	1.58E-17
22936-86-3	3.21E-17	1.15E-15	6.53E-17
23031-36-9	5.66E-18	3.53E-15	1.62E-17
2303-16-4	5.21E-17	8.31E-15	4.09E-17
2303-17-5	2.85E-17	6.06E-15	5.05E-17
2307-68-8	2.14E-17	1.75E-15	1.15E-17
2310-17-0	1.86E-16	1.31E-14	3.98E-17
23103-98-2	7.37E-18	8.57E-16	7.25E-17
2312-35-8	1.87E-16	2.32E-14	4.55E-17
23135-22-0	5.25E-17	2.39E-16	2.68E-17
23184-66-9	1.82E-17	2.34E-15	1.10E-17
23560-59-0	9.94E-17	4.37E-15	1.18E-16
23564-05-8	2.12E-20	6.21E-19	6.87E-20
2385-85-5	3.29E-14	1.91E-12	1.11E-14
23947-60-6	4.44E-19	4.58E-17	4.51E-18
23950-58-5	2.17E-17	1.95E-15	5.85E-17
24017-47-8	1.41E-14	1.03E-12	8.13E-14
2402-79-1	1.34E-16	2.36E-15	1.01E-16
24096-53-5	3.35E-16	4.60E-15	6.75E-16
2425-66-3	8.55E-17	6.89E-16	7.55E-17
24307-26-4	1.27E-16	5.04E-18	7.77E-19
24353-61-5	7.51E-16	1.53E-13	9.77E-15
2445-07-0	5.56E-17	3.47E-15	4.94E-16
24544-04-5	1.03E-18	4.01E-16	5.40E-18
24549-06-2	1.16E-18	4.43E-16	9.43E-18
24602-86-6	6.56E-18	1.57E-15	1.08E-18
2461-15-6	2.53E-19	9.03E-18	1.56E-19
2463-84-5	4.59E-17	4.77E-15	1.05E-16
2465-27-2	3.19E-17	4.39E-15	2.76E-16
24691-80-3	3.26E-18	1.17E-16	8.46E-18
2475-46-9	4.35E-18	1.10E-16	3.81E-18
2489-77-2	6.94E-19	1.48E-17	1.11E-18
24934-91-6	1.82E-17	2.06E-15	1.61E-17
25013-15-4	1.26E-18	9.43E-17	6.92E-19
25057-89-0	5.17E-17	3.07E-15	4.46E-16
25059-80-7	6.08E-19	1.18E-17	9.39E-19
25154-52-3	2.65E-19	4.55E-17	2.51E-19
25155-23-1	1.16E-17	8.13E-17	1.15E-20
25168-26-7	1.21E-16	3.35E-15	1.32E-17
2528-36-1	2.21E-18	1.47E-16	3.99E-19
25311-71-1	1.34E-16	4.63E-14	4.18E-16
25319-90-8	9.94E-17	7.85E-15	8.41E-17
25321-14-6	3.99E-17	8.39E-16	6.24E-17
25366-23-8	2.13E-17	2.90E-16	3.87E-17
2540-82-1	1.54E-17	4.15E-16	4.30E-17
2545-59-7	3.33E-16	3.39E-14	6.40E-17
25551-13-7	4.79E-19	4.30E-17	2.69E-19

25586-43-0	2.92E-16	1.13E-14	1.72E-16
25875-51-8	1.23E-16	7.97E-15	1.74E-16
2593-15-9	4.49E-17	1.66E-15	6.16E-17
2595-54-2	9.88E-17	7.25E-15	4.65E-16
26002-80-2	1.14E-18	3.52E-17	6.04E-21
26087-47-8	1.79E-18	2.12E-16	3.69E-18
260-94-6	4.98E-17	4.34E-15	1.10E-16
26140-60-3	5.99E-16	5.33E-14	2.73E-17
26225-79-6	1.15E-16	6.70E-15	4.59E-16
26259-45-0	1.28E-17	9.86E-16	1.96E-17
2631-37-0	2.46E-16	1.07E-14	3.90E-16
2631-40-5	4.92E-17	1.10E-15	8.05E-17
2634-33-5	2.83E-17	4.75E-16	6.98E-17
2636-26-2	2.41E-16	2.42E-14	6.06E-16
2642-71-9	2.55E-15	6.19E-13	2.64E-14
26444-49-5	2.61E-17	8.26E-16	5.69E-19
26471-62-5	1.73E-17	3.80E-16	1.01E-17
2655-19-8	3.08E-17	2.63E-15	5.35E-18
26761-40-0	2.23E-18	6.31E-17	4.36E-19
2686-99-9	7.40E-17	2.66E-15	1.71E-16
2691-41-0	1.03E-18	5.44E-17	8.15E-18
26952-21-6	7.36E-18	1.12E-16	3.95E-18
2698-41-1	1.89E-15	4.24E-14	2.64E-15
27304-13-8	3.27E-14	2.88E-12	1.61E-14
27314-13-2	5.61E-16	8.76E-15	9.84E-16
27355-22-2	9.68E-19	2.21E-17	1.07E-18
27541-88-4	4.71E-18	6.72E-17	6.62E-18
2782-70-9	2.42E-16	2.34E-14	5.41E-17
2782-91-4	6.88E-19	2.42E-17	2.97E-18
2797-51-5	2.33E-16	6.56E-15	6.86E-16
2813-95-8	5.24E-17	1.41E-15	3.24E-17
2814-20-2	3.16E-18	1.90E-16	1.31E-17
28249-77-6	6.13E-16	3.99E-14	1.12E-15
2835-39-4	5.16E-18	1.64E-16	2.89E-18
28434-00-6	2.75E-17	7.98E-15	2.28E-17
28434-01-7	1.43E-18	5.47E-16	4.78E-19
287-92-3	8.79E-20	1.44E-18	6.21E-20
288-32-4	9.41E-18	1.32E-16	1.93E-17
29069-24-7	4.08E-17	7.45E-16	3.02E-19
29091-05-2	5.44E-18	5.58E-16	7.23E-18
29104-30-1	1.10E-18	1.63E-16	2.84E-18
29171-20-8	2.70E-18	8.15E-16	2.41E-17
2921-88-2	2.01E-15	6.99E-13	2.32E-15
29232-93-7	1.64E-18	6.91E-16	5.28E-18
297-78-9	6.79E-13	5.17E-11	6.19E-13
297-97-2	1.17E-15	1.26E-13	7.30E-15
298-00-0	3.34E-15	4.19E-13	8.13E-15
298-02-2	2.38E-16	9.80E-14	9.10E-16
298-04-4	5.69E-16	2.46E-13	2.46E-15
298-06-6	8.36E-19	2.00E-16	6.54E-18
298-81-7	2.08E-18	1.39E-16	1.05E-17
29973-13-5	9.13E-18	2.47E-16	2.24E-17
299-84-3	1.31E-16	3.82E-14	1.02E-16
299-85-4	8.05E-17	9.09E-14	6.32E-16
299-86-5	7.93E-16	5.53E-14	1.96E-15
30043-49-3	3.91E-19	1.71E-18	2.65E-19

300-76-5	1.35E-17	2.75E-16	1.92E-17
301-11-1	1.12E-17	4.95E-16	2.74E-19
301-12-2	1.01E-18	1.13E-17	9.12E-19
302-17-0	1.36E-17	2.17E-16	2.25E-17
303-34-4	2.21E-17	2.45E-16	3.71E-17
30516-87-1	3.61E-19	1.78E-18	2.73E-19
30560-19-1	1.00E-18	9.17E-18	1.02E-18
3060-89-7	5.11E-18	1.57E-16	2.20E-17
306-37-6	2.79E-15	1.66E-17	2.55E-18
309-00-2	3.77E-16	6.43E-14	9.24E-16
311-45-5	6.35E-16	2.23E-14	1.78E-15
31218-83-4	1.31E-17	4.33E-15	6.45E-17
31431-39-7	1.06E-17	2.03E-16	1.24E-17
315-18-4	5.15E-17	3.54E-15	2.06E-16
315-22-0	2.60E-17	1.98E-17	3.33E-18
319-84-6	8.30E-14	3.44E-12	8.33E-14
319-85-7	6.40E-15	2.51E-13	4.61E-15
3244-90-4	1.35E-16	5.63E-14	1.33E-17
3252-43-5	2.41E-17	1.32E-16	2.15E-17
3254-66-8	1.75E-17	1.41E-15	5.13E-17
32598-13-3	1.04E-12	5.71E-11	2.62E-14
3268-49-3	9.86E-19	1.56E-17	1.19E-18
3276-41-3	1.55E-18	5.42E-17	6.34E-18
3279-46-7	3.32E-18	7.58E-17	7.81E-18
327-98-0	5.67E-15	2.50E-12	4.48E-15
32809-16-8	1.65E-17	8.94E-16	3.11E-17
3296-90-0	7.43E-18	1.11E-16	1.62E-17
330-54-1	1.50E-18	6.25E-17	5.03E-18
33089-61-1	2.49E-17	1.32E-14	1.54E-17
33125-97-2	1.72E-17	7.12E-16	3.27E-17
33213-65-9	9.66E-15	3.86E-13	1.34E-14
33245-39-5	1.61E-17	1.85E-15	1.45E-17
333-41-5	2.66E-15	4.64E-13	2.05E-14
3337-71-1	7.03E-19	1.32E-19	5.88E-21
3347-22-6	2.19E-16	4.00E-15	2.94E-16
33693-04-8	8.65E-17	2.67E-15	1.45E-16
3380-34-5	1.88E-16	1.68E-14	6.58E-17
33820-53-0	2.94E-18	2.09E-16	8.72E-19
3383-96-8	1.21E-14	1.06E-12	2.46E-16
34014-18-1	8.72E-18	1.28E-16	1.57E-17
34123-59-6	6.15E-18	8.37E-17	1.05E-17
34622-58-7	1.34E-17	1.22E-15	2.91E-17
34643-46-4	5.16E-16	3.08E-13	2.39E-16
34681-10-2	7.99E-17	1.86E-15	2.66E-16
34681-23-7	7.63E-18	2.29E-17	3.56E-18
34883-43-7	2.56E-16	1.22E-14	1.29E-16
35367-38-5	3.08E-18	1.17E-16	1.59E-18
35400-43-2	1.09E-15	2.10E-13	1.01E-16
35554-44-0	5.08E-17	6.08E-15	1.18E-16
35575-96-3	3.62E-18	4.65E-17	5.68E-18
3570-75-0	2.95E-18	3.03E-17	4.46E-18
36335-67-8	4.45E-18	4.35E-15	1.38E-17
36614-38-7	3.00E-17	5.45E-15	7.62E-17
36702-44-0	3.06E-18	1.28E-16	1.28E-17
36734-19-7	4.90E-19	8.52E-18	1.84E-19
3688-53-7	3.67E-19	7.07E-18	1.08E-18

3689-24-5	2.06E-17	4.39E-15	1.93E-17
371-40-4	9.39E-18	6.44E-16	3.76E-17
37248-47-8	1.73E-11	1.07E-19	1.44E-20
3766-81-2	1.64E-16	4.83E-15	2.27E-16
3811-49-2	6.02E-18	7.55E-16	1.62E-17
38260-54-7	1.78E-17	2.03E-15	5.39E-17
3878-19-1	2.73E-17	2.12E-15	1.46E-16
389-08-2	2.56E-18	5.45E-17	7.16E-18
39148-24-8	1.32E-16	2.35E-19	3.72E-20
39196-18-4	2.13E-14	6.84E-13	4.40E-14
39300-45-3	5.87E-17	3.26E-15	1.39E-18
3942-54-9	4.89E-17	1.10E-15	9.05E-17
39515-40-7	3.07E-17	4.32E-15	1.76E-18
39515-41-8	7.99E-17	5.43E-15	5.04E-18
39515-51-0	2.44E-17	1.27E-15	2.07E-17
396-01-0	6.14E-18	6.60E-17	9.88E-18
39765-80-5	6.95E-14	9.83E-12	1.80E-14
39801-14-4	9.18E-14	8.53E-12	4.74E-14
4005-51-0	7.98E-19	5.45E-18	8.24E-19
40321-76-4	2.66E-11	1.94E-09	8.91E-13
4044-65-9	5.32E-16	2.39E-14	1.20E-16
404-86-4	7.50E-17	3.14E-15	3.49E-17
40487-42-1	1.60E-17	1.47E-15	2.70E-17
40548-68-3	5.17E-18	8.89E-17	1.03E-17
40596-69-8	5.81E-19	1.69E-16	1.62E-19
41083-11-8	1.24E-14	8.71E-13	1.35E-15
41198-08-7	9.20E-16	1.11E-13	3.80E-16
41394-05-2	6.47E-18	1.16E-16	8.25E-18
41483-43-6	7.79E-19	6.89E-17	4.81E-18
4164-28-7	5.19E-18	1.57E-17	2.96E-18
4170-30-3	2.74E-17	4.27E-16	3.07E-17
41814-78-2	6.76E-17	1.48E-15	1.85E-16
42576-02-3	8.39E-18	2.93E-16	3.64E-18
42874-03-3	4.33E-16	3.18E-14	1.36E-16
4301-50-2	2.87E-15	1.76E-13	1.22E-15
43121-43-3	9.44E-16	1.57E-14	1.24E-15
43222-48-6	2.70E-16	1.21E-15	1.89E-16
4342-36-3	2.03E-16	2.14E-14	4.33E-17
443-48-1	8.41E-19	6.07E-18	9.22E-19
446-86-6	3.07E-18	1.61E-17	2.48E-18
452-86-8	5.92E-19	4.44E-17	5.77E-18
458-37-7	2.88E-19	7.31E-18	2.52E-19
462-06-6	1.55E-17	7.13E-17	8.75E-18
462-08-8	2.13E-18	2.74E-17	4.00E-18
464-45-9	5.00E-17	1.74E-15	8.01E-17
464-49-3	3.77E-17	1.07E-15	3.28E-17
4655-34-9	7.87E-18	1.72E-16	4.28E-18
465-73-6	2.62E-14	1.43E-11	8.86E-15
4658-28-0	1.22E-17	2.58E-16	1.27E-17
470-82-6	4.12E-17	1.11E-15	3.23E-17
470-90-6	5.50E-15	2.25E-13	1.21E-14
481-39-0	1.08E-16	2.43E-15	2.76E-16
481-42-5	4.59E-16	1.55E-14	1.23E-15
4824-78-6	1.44E-15	7.35E-13	2.70E-16
485-31-4	2.69E-17	1.92E-15	8.66E-18
4904-61-4	4.95E-17	1.06E-13	3.14E-17

495-54-5	1.63E-18	2.04E-16	1.98E-17
498-66-8	4.75E-20	4.11E-18	3.01E-20
50-00-0	1.13E-17	7.81E-17	8.38E-18
500-28-7	3.64E-17	3.19E-15	8.59E-17
50-06-6	1.41E-17	1.62E-16	2.19E-17
50-07-7	1.41E-17	4.94E-17	8.16E-18
50-18-0	3.37E-17	1.21E-15	1.82E-16
502-39-6	5.44E-17	2.38E-17	3.83E-18
50-24-8	2.18E-17	2.57E-16	3.71E-17
50-29-3	5.09E-14	2.98E-12	7.81E-15
50-33-9	2.54E-16	5.94E-15	2.43E-16
504-29-0	5.24E-18	9.06E-17	1.29E-17
50-44-2	5.53E-19	2.31E-17	3.49E-18
504-63-2	8.82E-20	4.32E-20	6.12E-21
50471-44-8	1.03E-17	3.27E-16	1.79E-17
50512-35-1	1.30E-19	6.33E-18	1.09E-19
505-29-3	1.64E-18	1.32E-16	1.01E-17
50-55-5	6.91E-18	1.77E-16	5.94E-18
50563-36-5	1.45E-17	5.53E-16	5.73E-17
50-65-7	4.31E-17	2.15E-15	1.18E-17
50-76-0	6.81E-19	3.95E-18	3.78E-19
509-14-8	1.11E-16	1.80E-17	6.14E-17
510-15-6	1.72E-16	1.04E-14	4.19E-17
51-03-6	7.74E-18	2.09E-15	6.29E-18
5103-71-9	9.75E-14	1.92E-11	4.91E-14
5103-74-2	5.00E-14	1.12E-11	2.55E-14
51207-31-9	1.04E-13	5.55E-12	2.34E-14
51218-45-2	5.69E-17	3.55E-15	3.42E-16
51218-49-6	1.06E-17	1.29E-15	1.25E-17
51235-04-2	2.42E-19	9.84E-18	1.19E-18
512-56-1	7.08E-19	7.38E-19	1.08E-19
51333-22-3	1.66E-16	2.21E-15	2.71E-16
513-37-1	6.42E-18	1.94E-16	4.07E-18
51338-27-3	1.86E-16	1.51E-14	5.67E-17
51-52-5	1.37E-19	4.56E-18	5.30E-19
51630-58-1	2.46E-17	1.15E-15	3.80E-19
51707-55-2	8.67E-19	1.08E-17	1.33E-18
51-79-6	1.84E-19	5.11E-19	7.71E-20
5221-49-8	1.43E-17	1.02E-14	2.30E-16
5221-53-4	6.69E-19	1.38E-16	3.62E-18
52-24-4	1.39E-17	5.03E-16	7.36E-17
52315-07-8	2.51E-14	4.95E-13	3.46E-14
5234-68-4	7.84E-19	3.41E-17	3.57E-18
525-82-6	4.77E-17	5.03E-15	1.12E-16
5259-88-1	1.01E-18	1.93E-17	2.89E-18
52-60-8	5.75E-16	2.68E-13	2.38E-16
52645-53-1	2.38E-16	1.55E-14	2.10E-17
52-68-6	2.45E-17	1.74E-16	1.10E-17
52756-25-9	3.41E-18	1.01E-16	4.95E-18
527-60-6	8.42E-20	7.29E-18	2.82E-19
52888-80-9	1.00E-18	9.33E-17	3.35E-19
52918-63-5	3.88E-15	1.41E-13	7.07E-17
5307-14-2	6.09E-19	1.09E-17	1.61E-18
53112-28-0	1.06E-18	1.58E-16	9.08E-18
532-27-4	2.62E-16	5.74E-15	4.82E-16
533-74-4	2.78E-19	2.57E-17	3.45E-18

53469-21-9	7.17E-15	8.62E-13	2.35E-15
536-33-4	1.47E-18	3.73E-17	4.86E-18
536-60-7	3.70E-17	1.25E-15	8.20E-17
536-90-3	7.27E-19	1.79E-16	1.46E-17
5377-20-8	4.09E-17	1.25E-15	9.58E-17
53-86-1	1.06E-14	5.08E-13	3.55E-15
5392-40-5	5.69E-18	1.22E-15	1.06E-17
53-96-3	9.31E-18	8.17E-16	2.72E-17
540-23-8	1.44E-18	3.90E-16	2.49E-17
540-59-0	9.33E-18	7.92E-17	8.01E-18
540-88-5	5.26E-18	1.46E-17	2.70E-18
54-11-5	8.21E-18	4.23E-16	5.85E-17
541-28-6	1.81E-17	1.99E-16	9.37E-18
541-73-1	9.20E-16	5.71E-15	6.75E-16
541-85-5	3.20E-18	7.00E-17	2.23E-18
542-18-7	9.26E-17	1.26E-15	4.79E-17
542-56-3	2.57E-17	2.05E-16	1.60E-17
542-59-6	4.23E-20	4.71E-20	7.53E-21
542-75-6	1.28E-17	4.85E-17	6.39E-18
54406-48-3	4.93E-18	1.62E-15	1.75E-18
544-25-2	1.57E-17	2.01E-15	1.21E-17
54-64-8	1.49E-15	1.53E-16	2.43E-17
54-85-3	6.35E-18	1.68E-17	2.57E-18
548-62-9	4.00E-16	3.80E-15	6.87E-16
55090-44-3	4.43E-18	2.65E-16	1.03E-18
55179-31-2	1.67E-16	7.29E-15	6.17E-17
55-18-5	5.69E-18	1.23E-16	1.08E-17
55-21-0	7.63E-19	6.17E-18	7.39E-19
55219-65-3	3.04E-16	6.05E-15	3.41E-16
552-41-0	5.87E-18	6.57E-16	6.86E-17
55268-74-1	5.59E-18	9.24E-17	8.27E-18
55285-14-8	2.31E-15	4.87E-13	3.79E-16
552-89-6	4.36E-17	2.29E-15	1.65E-16
55-37-8	1.09E-16	1.86E-14	4.87E-17
55-38-9	4.81E-16	7.80E-14	1.49E-15
554-00-7	4.59E-17	2.58E-15	1.11E-16
55406-53-6	3.51E-19	1.31E-17	4.88E-19
554-12-1	1.46E-18	2.93E-18	7.81E-19
554-84-7	1.42E-16	2.31E-15	2.47E-16
55512-33-9	1.38E-16	7.69E-15	4.65E-18
555-16-8	2.00E-17	4.83E-16	5.58E-17
555-37-3	2.66E-17	1.88E-15	1.77E-17
555-84-0	4.72E-19	6.06E-18	9.20E-19
555-89-5	6.46E-17	7.70E-15	2.44E-17
55-63-0	3.06E-18	7.52E-17	1.51E-18
556-52-5	6.85E-18	2.10E-18	2.91E-18
556-67-2	3.05E-19	3.67E-17	1.54E-19
556-82-1	1.82E-18	1.44E-16	6.50E-18
55-80-1	2.30E-17	1.62E-14	4.92E-17
55-91-4	1.23E-16	1.86E-14	1.09E-15
5598-13-0	6.34E-18	1.54E-15	9.40E-18
5598-52-7	1.18E-16	1.92E-15	2.28E-16
56-04-2	1.60E-18	6.72E-17	8.83E-18
56073-07-5	5.52E-15	8.17E-13	1.33E-16
56073-10-0	3.22E-12	2.88E-11	5.17E-15
56-23-5	5.69E-17	8.56E-17	4.96E-17

563-12-2	2.50E-16	1.77E-13	1.61E-16
563-41-7	1.70E-16	4.54E-18	8.60E-19
563-47-3	3.39E-18	1.89E-16	2.30E-18
56-35-9	5.74E-15	3.10E-13	1.90E-15
56-36-0	1.34E-16	8.24E-15	1.08E-16
563-80-4	4.51E-18	2.04E-17	3.02E-18
56-38-2	1.16E-15	2.57E-13	8.06E-16
56425-91-3	1.82E-15	8.56E-14	3.45E-15
56-53-1	2.66E-17	2.77E-15	4.81E-18
56-72-4	2.61E-14	1.77E-12	8.27E-14
56-75-7	1.74E-18	1.81E-17	2.66E-18
56-81-5	9.53E-20	1.10E-20	3.47E-21
569-64-2	4.26E-16	3.99E-15	6.07E-16
57018-04-9	3.61E-18	6.13E-16	4.71E-18
57057-83-7	1.25E-16	6.38E-15	1.31E-16
57-06-7	1.38E-17	5.64E-16	1.30E-17
57-13-6	3.16E-19	1.12E-20	1.38E-21
57-14-7	4.09E-17	5.28E-17	7.48E-18
57-15-8	3.99E-16	1.07E-14	8.14E-16
57369-32-1	2.10E-17	5.25E-16	6.78E-17
57-39-6	5.54E-17	1.06E-15	1.48E-16
57-43-2	8.44E-18	1.14E-16	1.24E-17
57-55-6	1.70E-20	1.14E-20	1.82E-21
576-24-9	3.06E-17	8.67E-16	3.88E-17
576-26-1	8.10E-18	2.20E-15	1.49E-16
57-63-6	8.77E-18	3.25E-16	8.01E-18
57646-30-7	4.49E-18	1.81E-16	1.37E-17
57653-85-7	2.00E-12	1.25E-11	3.64E-15
57-74-9	3.00E-14	4.03E-12	7.82E-15
57837-19-1	9.14E-18	2.33E-16	3.37E-17
578-54-1	1.32E-18	4.28E-16	2.03E-17
57-97-6	5.80E-17	2.36E-14	2.69E-17
58138-08-2	8.45E-16	1.41E-14	4.23E-16
58-14-0	8.77E-17	6.92E-15	5.78E-16
58-27-5	2.76E-16	6.95E-15	6.19E-16
583-78-8	5.04E-17	2.18E-15	6.93E-17
584-02-1	3.22E-18	4.55E-17	2.92E-18
584-79-2	4.72E-18	1.37E-15	3.92E-18
584-84-9	1.23E-17	2.70E-16	7.17E-18
586-98-1	2.40E-19	9.25E-19	1.17E-19
587-98-4	3.63E-17	3.13E-16	4.80E-17
58-89-9	1.24E-13	6.39E-12	2.33E-13
589-16-2	1.96E-18	6.53E-16	2.69E-17
589-18-4	1.38E-17	3.03E-16	3.22E-17
590-01-2	1.43E-19	1.11E-18	7.51E-20
590-21-6	1.79E-18	3.81E-17	1.33E-18
590-86-3	1.40E-18	2.26E-17	8.83E-19
591-27-5	1.97E-19	1.12E-17	1.62E-18
591-35-5	5.38E-18	3.24E-16	6.49E-18
5915-41-3	4.44E-17	1.52E-15	7.16E-17
591-78-6	3.76E-18	3.62E-17	2.43E-18
59-33-6	6.38E-17	7.53E-16	1.09E-16
593-60-2	2.01E-18	4.04E-17	1.55E-18
59-50-7	3.78E-18	3.57E-16	1.02E-17
59669-26-0	2.28E-16	7.83E-15	7.14E-16
597-25-1	4.77E-19	3.84E-18	5.95E-19

597-64-8	8.08E-17	1.11E-14	4.07E-17
598-16-3	2.81E-16	2.12E-15	1.46E-16
598-52-7	1.91E-18	5.96E-18	9.53E-19
598-55-0	5.51E-18	4.73E-18	1.25E-18
59-88-1	3.95E-18	6.51E-19	1.00E-19
59-89-2	7.67E-19	1.02E-17	1.50E-18
5989-27-5	4.28E-18	1.65E-15	2.41E-18
60-11-7	1.65E-16	2.61E-14	1.38E-16
60168-88-9	2.03E-15	4.83E-14	2.70E-15
602-01-7	3.22E-17	6.77E-16	5.04E-17
60207-31-0	1.53E-15	2.30E-14	2.55E-15
60207-90-1	2.80E-16	8.66E-15	3.65E-16
60-24-2	1.54E-18	8.48E-18	1.12E-18
60-29-7	8.62E-19	9.02E-18	7.45E-19
60-35-5	1.18E-19	3.26E-20	4.46E-21
604-75-1	5.37E-17	7.69E-16	7.74E-17
60-51-5	5.79E-17	4.30E-15	4.79E-16
60-54-8	5.28E-18	3.10E-18	5.24E-19
60-56-0	1.19E-19	1.25E-18	1.61E-19
60-57-1	5.41E-14	7.73E-12	7.39E-14
60599-38-4	9.63E-19	8.55E-18	1.29E-18
606-20-2	1.21E-17	3.40E-17	5.55E-18
60-80-0	5.34E-18	1.05E-16	1.58E-17
608-73-1	4.07E-14	1.86E-12	2.19E-14
608-93-5	1.58E-14	3.39E-13	9.65E-15
609-20-1	4.44E-18	2.14E-16	3.14E-17
610-39-9	1.19E-17	2.49E-16	1.77E-17
6109-97-3	7.66E-18	2.27E-15	7.61E-17
61213-25-0	2.34E-16	7.68E-15	3.00E-16
614-00-6	2.37E-17	7.20E-16	6.91E-17
615-53-2	4.40E-17	1.13E-15	8.67E-17
616-45-5	4.89E-19	3.84E-19	4.95E-20
61-73-4	6.35E-19	4.08E-17	6.16E-18
61-82-5	2.69E-18	5.12E-18	7.71E-19
618-85-9	8.83E-17	1.45E-15	1.32E-16
619-15-8	4.72E-17	9.96E-16	7.37E-17
61949-76-6	6.35E-16	2.03E-14	7.46E-18
61949-77-7	1.44E-16	4.60E-15	1.69E-18
619-72-7	4.31E-16	5.05E-15	6.86E-16
619-80-7	8.64E-18	9.87E-17	1.44E-17
621-64-7	4.89E-18	3.20E-16	2.02E-17
622-40-2	1.24E-19	5.25E-19	8.08E-20
623-00-7	6.14E-16	1.32E-14	7.83E-16
623-25-6	1.21E-16	3.15E-15	8.51E-17
62-38-4	4.73E-17	4.94E-16	7.49E-17
623-91-6	4.41E-19	1.12E-17	5.70E-19
62-44-2	1.86E-17	3.56E-16	3.37E-17
62-53-3	6.14E-18	3.83E-16	4.16E-17
625-53-6	7.44E-19	6.76E-18	8.32E-19
62-56-6	3.94E-18	2.77E-18	2.54E-19
626-17-5	5.99E-17	6.40E-16	9.20E-17
627-30-5	3.39E-18	4.19E-17	5.19E-18
62-73-7	1.19E-16	5.39E-16	3.73E-17
62-75-9	4.70E-17	2.46E-17	2.46E-17
628-63-7	1.57E-19	1.61E-18	8.52E-20
629-11-8	6.35E-19	7.68E-18	8.97E-19

629-40-3	4.64E-17	5.15E-16	7.23E-17
630-20-6	3.48E-16	1.39E-15	1.67E-16
6317-18-6	1.15E-17	3.75E-16	5.39E-17
632-22-4	6.30E-19	4.31E-18	6.27E-19
63-25-2	2.12E-18	1.20E-16	5.07E-18
63284-71-9	6.43E-15	1.39E-13	6.94E-15
634-66-2	1.61E-15	1.52E-14	8.19E-16
634-90-2	1.56E-15	1.47E-14	8.15E-16
634-93-5	6.48E-16	1.51E-14	4.96E-16
636-21-5	1.24E-18	3.25E-16	2.11E-17
637-07-0	2.44E-17	9.60E-16	1.95E-17
6392-46-7	2.94E-17	8.35E-15	9.10E-17
639-58-7	7.26E-16	9.72E-15	3.15E-16
64-00-6	3.47E-16	1.66E-14	6.67E-16
640-15-3	3.42E-17	3.55E-15	8.10E-17
64-17-5	1.26E-18	3.29E-19	6.00E-19
644-64-4	7.99E-18	3.48E-16	5.05E-17
645-56-7	2.21E-17	2.85E-15	7.98E-17
645-62-5	3.90E-18	2.00E-16	2.64E-18
646-06-0	1.16E-18	2.26E-18	7.51E-19
64628-44-0	1.74E-17	9.84E-16	2.95E-18
64-67-5	1.18E-17	4.27E-18	4.61E-18
64902-72-3	3.61E-18	4.59E-17	5.99E-18
65195-55-3	1.95E-13	1.04E-11	1.03E-13
65-30-5	2.07E-17	1.87E-16	3.54E-17
66063-05-6	2.98E-18	1.26E-16	6.39E-19
66215-27-8	2.27E-19	2.73E-18	6.74E-19
66230-04-4	1.09E-14	6.40E-13	5.80E-15
66246-88-6	1.16E-15	8.06E-14	3.66E-16
66-25-1	2.06E-18	5.88E-17	1.50E-18
66-27-3	2.29E-17	4.60E-17	1.03E-17
66332-96-5	2.92E-18	2.04E-16	3.73E-18
66-76-2	4.63E-17	5.49E-16	4.22E-17
66-81-9	1.65E-16	1.32E-15	2.00E-16
66841-25-6	2.39E-16	9.14E-16	1.80E-19
67129-08-2	1.27E-16	6.05E-15	5.17E-16
67-20-9	5.56E-18	1.37E-17	2.13E-18
67375-30-8	2.72E-15	2.05E-13	1.07E-16
67-45-8	3.28E-19	3.71E-18	5.69E-19
67-47-0	2.15E-19	1.64E-18	2.11E-19
67485-29-4	3.54E-15	2.03E-13	5.77E-17
67-56-1	2.28E-18	1.01E-18	1.18E-18
67-63-0	1.34E-18	2.77E-18	7.12E-19
67-64-1	3.83E-18	2.97E-18	2.01E-18
67-66-3	3.78E-16	1.33E-15	2.55E-16
67-72-1	1.59E-15	4.69E-15	8.01E-16
67747-09-5	9.74E-16	1.30E-13	1.58E-15
680-31-9	4.94E-18	1.76E-16	2.60E-17
68085-85-8	1.33E-15	3.60E-14	1.01E-17
68-12-2	3.97E-19	2.31E-19	8.15E-20
683-18-1	2.67E-17	8.74E-16	3.38E-17
68-35-9	6.39E-18	4.56E-17	7.02E-18
68359-37-5	6.67E-16	2.79E-14	1.64E-17
684-93-5	4.11E-18	2.27E-17	3.62E-18
68694-11-1	3.76E-16	1.17E-14	1.74E-15
68-89-3	7.50E-15	1.03E-18	1.62E-19

6923-22-4	2.23E-17	9.88E-17	1.34E-17
693-21-0	4.02E-18	5.84E-17	7.01E-18
69327-76-0	1.25E-18	2.51E-16	1.59E-18
693-54-9	9.49E-19	1.65E-17	4.83E-19
69409-94-5	1.31E-16	3.42E-15	1.04E-18
69581-33-5	1.23E-17	1.70E-16	2.47E-17
6959-48-4	3.77E-17	7.32E-16	6.55E-17
69806-50-4	2.22E-17	1.24E-15	5.83E-18
6988-21-2	1.89E-18	2.55E-17	3.57E-18
700-13-0	2.05E-19	1.77E-17	2.16E-18
7003-89-6	4.29E-16	2.64E-18	4.06E-19
70124-77-5	1.40E-16	4.20E-15	1.40E-18
70-25-7	6.81E-18	1.02E-17	1.57E-18
70-38-2	1.14E-19	1.32E-17	4.13E-20
706-14-9	1.76E-19	5.09E-18	1.76E-19
70-69-9	1.60E-17	1.44E-15	1.53E-16
709-98-8	2.09E-16	5.54E-15	2.48E-16
71-23-8	2.46E-18	7.01E-18	1.58E-18
71-36-3	1.50E-17	1.55E-16	1.29E-17
71-41-0	1.98E-17	3.63E-16	2.03E-17
71-43-2	2.73E-17	1.41E-16	2.06E-17
71-55-6	4.36E-18	8.79E-18	3.37E-18
71561-11-0	8.55E-17	6.27E-15	1.51E-16
71626-11-4	7.75E-20	4.84E-18	1.39E-19
71751-41-2	7.14E-13	3.94E-11	2.59E-13
7212-44-4	5.02E-18	4.92E-15	3.65E-18
72178-02-0	1.34E-15	2.25E-14	2.14E-15
72-20-8	6.01E-14	2.96E-11	4.59E-13
7227-91-0	1.80E-16	3.23E-15	1.46E-16
72-43-5	1.10E-16	1.42E-15	5.54E-18
72490-01-8	2.59E-19	6.84E-18	2.38E-20
72-54-8	1.87E-13	1.71E-11	6.31E-14
72-55-9	9.13E-15	9.50E-13	5.85E-15
72-56-0	1.53E-16	2.01E-14	1.41E-17
7287-19-6	1.01E-17	7.39E-16	2.30E-17
7292-16-2	8.12E-17	7.21E-15	7.44E-17
731-27-1	8.01E-16	6.23E-14	1.04E-15
732-11-6	3.18E-17	2.48E-15	9.48E-17
732-26-3	2.46E-15	4.05E-13	2.59E-16
73590-58-6	2.90E-18	4.10E-17	4.22E-18
738-70-5	5.99E-19	1.58E-17	2.36E-18
74051-80-2	2.24E-17	1.88E-15	1.08E-17
74115-24-5	2.05E-16	4.20E-15	2.31E-16
741-58-2	1.68E-17	3.01E-15	2.38E-17
74223-64-6	4.20E-19	5.82E-18	6.15E-19
74738-17-3	2.84E-16	1.42E-14	2.56E-16
74-83-9	2.65E-16	4.54E-16	1.53E-16
74-87-3	1.94E-18	4.76E-18	1.44E-18
74-96-4	1.38E-17	4.99E-17	9.03E-18
74-97-5	1.51E-17	4.19E-17	8.83E-18
75-01-4	7.67E-19	1.97E-17	1.01E-18
75-05-8	5.52E-17	6.63E-17	3.24E-17
75-07-0	6.43E-18	7.50E-18	3.34E-18
75-08-1	1.38E-18	3.51E-17	9.08E-19
75-09-2	4.22E-17	1.06E-16	2.36E-17
75-15-0	2.87E-18	1.70E-17	2.20E-18

75-18-3	3.36E-18	9.20E-18	1.85E-18
75-21-8	1.11E-16	1.17E-16	5.85E-17
75-25-2	7.39E-17	4.00E-16	4.38E-17
75-27-4	1.29E-16	5.06E-16	9.57E-17
75330-75-5	1.72E-18	4.05E-17	1.52E-19
75-34-3	4.13E-17	1.68E-16	2.94E-17
75-35-4	8.44E-18	2.14E-16	1.33E-17
75-36-5	1.71E-17	1.59E-17	9.84E-18
753-73-1	2.79E-17	2.57E-17	9.21E-18
75-47-8	7.57E-18	7.08E-17	4.54E-18
75-52-5	1.06E-17	6.84E-18	5.73E-18
75-56-9	2.81E-17	3.33E-17	1.55E-17
75-65-0	7.12E-18	4.20E-17	6.04E-18
756-79-6	1.49E-18	3.77E-18	8.11E-19
75-74-1	3.83E-18	9.27E-17	2.78E-18
758-17-8	1.02E-16	1.33E-17	3.85E-17
75-85-4	9.47E-18	1.22E-16	1.11E-17
75-86-5	2.29E-16	1.45E-15	2.16E-16
75-87-6	5.34E-17	6.35E-16	9.03E-17
75-89-8	4.63E-17	1.61E-16	3.37E-17
75-91-2	2.88E-17	2.40E-16	2.53E-17
759-73-9	8.76E-19	8.02E-18	1.11E-18
75-97-8	2.23E-17	9.54E-17	1.37E-17
759-94-4	6.22E-19	3.85E-17	7.52E-19
76-01-7	6.73E-16	2.18E-15	2.33E-16
760-23-6	2.42E-18	7.78E-17	1.43E-18
76-06-2	1.84E-16	7.12E-16	1.04E-16
76-13-1	3.31E-18	3.77E-18	2.95E-18
76-25-5	2.35E-16	3.23E-15	3.98E-16
76-29-9	3.00E-17	1.39E-15	3.65E-17
763-32-6	9.20E-19	4.85E-17	2.06E-18
76-38-0	1.78E-14	5.31E-14	9.99E-15
764-41-0	7.37E-17	3.58E-15	4.58E-17
76-44-8	3.38E-15	1.31E-12	1.74E-15
76578-14-8	1.05E-17	4.47E-16	3.04E-18
767-00-0	5.59E-17	9.21E-16	1.12E-16
76738-62-0	1.55E-15	3.61E-14	1.75E-15
7696-12-0	2.65E-17	7.21E-15	2.23E-17
7700-17-6	5.13E-19	3.25E-17	6.06E-19
7720-78-7	2.60E-18	6.71E-18	1.03E-18
77458-01-6	6.30E-16	2.50E-14	4.10E-16
7745-89-3	1.74E-16	4.65E-14	1.85E-15
77-47-4	3.79E-15	1.17E-16	1.81E-15
77-58-7	4.95E-12	3.92E-14	2.79E-14
77732-09-3	2.65E-17	2.73E-16	4.09E-17
77-73-6	1.58E-17	2.83E-15	1.07E-17
77-74-7	1.87E-17	5.35E-16	2.94E-17
77-75-8	6.71E-18	1.75E-16	1.33E-17
77-78-1	2.74E-17	1.40E-18	8.91E-18
7786-34-7	4.95E-18	3.28E-16	3.73E-18
77-99-6	4.34E-20	8.46E-21	1.12E-21
78-00-2	1.56E-17	2.24E-15	8.80E-18
780-11-0	4.58E-17	2.07E-15	6.97E-17
78-11-5	8.09E-18	1.08E-16	1.16E-17
78-30-8	2.73E-16	1.32E-14	7.06E-17
78-34-2	2.45E-16	1.81E-14	2.72E-16

78-40-0	2.00E-18	5.19E-17	6.01E-18
78-42-2	5.57E-18	4.52E-19	2.36E-23
78-48-8	3.97E-17	8.13E-15	2.58E-17
78-51-3	1.02E-18	6.98E-17	4.69E-19
78-59-1	4.66E-19	1.14E-16	5.56E-18
786-19-6	3.04E-15	9.27E-13	1.04E-15
78-62-6	3.30E-19	2.31E-18	2.51E-19
78-70-6	2.38E-18	9.89E-16	1.78E-17
78-83-1	4.55E-18	3.88E-17	3.59E-18
78-84-2	2.26E-18	1.96E-17	1.40E-18
78-87-5	2.30E-17	1.11E-16	2.40E-17
78-88-6	5.42E-17	8.36E-16	3.06E-17
78-92-2	2.16E-18	2.10E-17	1.76E-18
78-93-3	3.92E-18	6.14E-18	2.13E-18
78-94-4	5.30E-17	4.20E-16	4.55E-17
78-97-7	1.80E-17	8.63E-18	1.83E-18
78-99-9	6.18E-18	3.02E-17	3.34E-18
79-00-5	6.92E-17	3.13E-16	5.48E-17
79-01-6	1.12E-17	9.86E-17	9.62E-18
79-06-1	2.00E-18	1.37E-18	5.55E-20
791-28-6	8.93E-17	1.64E-15	9.96E-17
79-19-6	4.17E-17	1.43E-17	7.27E-18
79-20-9	3.06E-19	3.12E-19	1.66E-19
79-21-0	3.20E-17	1.18E-18	1.02E-17
79241-46-6	2.03E-17	1.13E-15	5.51E-18
79277-27-3	3.18E-19	3.62E-18	4.96E-19
793-24-8	1.20E-17	9.04E-15	3.94E-17
79-34-5	2.05E-16	1.38E-15	1.09E-16
79-44-7	4.44E-18	1.08E-17	2.88E-18
79-46-9	3.79E-17	1.34E-16	2.69E-17
79622-59-6	3.31E-17	7.17E-16	3.79E-17
80-00-2	1.52E-16	4.04E-15	1.45E-16
8001-35-2	2.29E-14	2.63E-13	3.10E-14
8003-19-8	1.42E-16	5.74E-16	7.89E-17
8003-34-7	6.54E-18	3.97E-15	1.43E-18
8004-87-3	3.12E-16	2.64E-15	4.06E-16
80-05-7	5.81E-17	4.33E-15	6.78E-17
80-06-8	4.59E-15	2.59E-13	1.73E-15
80-08-0	2.90E-17	4.90E-16	7.21E-17
80-12-6	7.57E-14	3.94E-15	7.21E-16
80-15-9	8.71E-17	2.06E-15	1.82E-16
8022-00-2	1.29E-17	3.43E-16	3.98E-17
8027-00-7	2.74E-15	2.02E-13	6.04E-16
80-33-1	6.43E-16	3.66E-14	3.74E-16
80-38-6	2.11E-16	8.40E-15	1.88E-16
80-46-6	1.94E-17	3.06E-15	3.42E-17
80-56-8	5.94E-18	1.27E-15	3.07E-18
80-62-6	3.20E-19	9.14E-18	2.78E-19
8065-36-9	1.17E-16	6.56E-15	1.03E-16
8065-48-3	1.76E-14	4.45E-12	2.67E-13
81405-85-8	6.23E-19	2.00E-17	4.27E-19
81406-37-3	3.63E-18	1.50E-16	5.17E-19
81-64-1	5.58E-20	2.46E-18	3.03E-20
816-57-9	1.12E-18	1.21E-17	1.47E-18
81-77-6	3.55E-18	8.46E-18	1.62E-21
81777-89-1	9.83E-17	3.09E-15	2.91E-16

818-08-6	5.63E-17	2.79E-15	2.81E-17
81-81-2	2.10E-16	8.93E-15	6.87E-16
81-82-3	3.34E-16	6.55E-15	3.82E-16
818-61-1	7.11E-19	2.24E-18	2.94E-19
81-88-9	3.49E-17	4.35E-16	5.88E-17
82097-50-5	1.16E-18	1.71E-17	1.80E-18
821-55-6	9.37E-18	1.50E-16	4.97E-18
82560-54-1	1.43E-16	1.82E-14	1.20E-16
82657-04-3	1.68E-15	1.30E-13	1.18E-16
82-68-8	1.53E-16	2.62E-15	7.03E-17
828-00-2	3.20E-19	5.29E-18	6.41E-19
83121-18-0	1.18E-17	6.01E-16	3.31E-18
83164-33-4	2.10E-16	1.17E-14	2.80E-17
83-34-1	3.09E-18	1.53E-15	6.24E-17
834-12-8	2.87E-17	1.23E-15	7.63E-17
83-59-0	6.15E-19	5.11E-17	3.11E-20
836-30-6	3.95E-19	1.04E-16	1.74E-18
83657-22-1	1.43E-16	5.58E-14	9.94E-16
83-66-9	1.57E-16	7.34E-15	8.98E-17
83-79-4	1.83E-16	8.60E-15	8.08E-17
841-06-5	6.53E-18	2.93E-16	2.18E-17
84-62-8	1.06E-19	2.42E-18	2.68E-20
84-65-1	1.07E-17	3.21E-16	9.31E-18
84-66-2	4.61E-19	1.58E-17	4.89E-19
84-69-5	8.71E-20	1.53E-18	4.28E-20
84-74-2	9.42E-18	4.13E-16	4.62E-18
84-75-3	2.78E-19	1.50E-17	5.67E-20
84852-15-3	5.38E-18	6.81E-16	3.85E-19
85-01-8	2.41E-16	3.07E-15	7.37E-17
85-41-6	6.02E-18	7.24E-17	1.01E-17
85-42-7	3.61E-17	1.32E-15	6.75E-17
85-43-8	4.79E-18	8.27E-16	3.94E-17
85-44-9	1.35E-17	4.66E-18	4.10E-20
85-68-7	2.60E-18	9.82E-17	6.62E-19
85-70-1	8.32E-20	1.54E-18	1.05E-20
86-30-6	4.61E-18	5.69E-16	8.49E-18
86-50-0	3.96E-16	4.59E-14	9.66E-16
86811-58-7	1.13E-17	6.80E-16	2.31E-18
86-86-2	7.59E-18	3.13E-16	3.87E-17
868-77-9	1.13E-19	1.28E-18	1.46E-19
868-85-9	5.35E-18	3.37E-18	2.74E-18
87130-20-9	7.15E-20	2.01E-17	5.40E-19
87-17-2	1.43E-18	5.02E-17	9.57E-19
87237-48-7	9.17E-17	4.22E-15	3.32E-17
872-50-4	2.56E-19	6.57E-19	9.82E-20
87-59-2	1.09E-18	5.73E-16	2.21E-17
87-61-6	1.32E-15	1.07E-14	6.79E-16
87-62-7	1.54E-18	6.03E-16	3.32E-17
87-64-9	2.89E-17	1.60E-15	6.45E-17
87674-68-8	8.52E-18	4.34E-16	4.29E-17
87-68-3	7.14E-14	4.74E-13	3.58E-14
88-04-0	4.51E-18	8.62E-16	2.19E-17
88107-10-2	6.97E-18	2.45E-16	3.69E-18
88-12-0	4.73E-19	6.13E-18	6.59E-19
88-18-6	2.20E-17	2.55E-15	3.99E-17
88-19-7	1.09E-17	1.21E-16	1.76E-17

88283-41-4	2.06E-16	7.71E-15	1.81E-16
886-50-0	1.64E-17	7.73E-16	1.70E-17
88671-89-0	9.26E-16	2.35E-14	1.26E-15
88-72-2	5.14E-17	4.07E-16	4.27E-17
88-73-3	2.30E-16	4.59E-15	2.89E-16
88-74-4	4.80E-17	1.12E-15	1.11E-16
89-61-2	3.73E-16	9.05E-15	3.91E-16
89-63-4	6.36E-17	1.36E-15	1.04E-16
89-72-5	1.85E-17	2.49E-15	4.26E-17
89-83-8	7.12E-18	1.57E-15	4.43E-17
89-98-5	2.96E-17	1.33E-15	4.25E-17
90-02-8	1.02E-17	4.49E-16	1.95E-17
9002-93-1	1.38E-16	1.92E-14	4.81E-17
90-04-0	2.46E-18	4.73E-16	3.60E-17
90-05-1	4.01E-18	1.42E-16	9.59E-18
9006-42-2	4.89E-19	1.61E-18	2.68E-19
900-95-8	2.82E-17	1.21E-15	4.50E-18
90-12-0	3.54E-17	3.68E-15	2.51E-17
90-13-1	2.56E-16	9.87E-15	1.50E-16
90-15-3	1.43E-17	4.29E-15	2.32E-16
90-43-7	1.40E-17	5.52E-16	1.10E-17
91-15-6	5.64E-16	6.82E-15	8.50E-16
91-17-8	4.63E-18	2.96E-16	2.62E-18
91-20-3	1.81E-16	5.43E-15	1.09E-16
91-22-5	1.55E-17	3.82E-16	3.02E-17
91-23-6	2.31E-17	4.42E-16	4.40E-17
91465-08-6	2.50E-15	5.14E-14	1.30E-17
91-53-2	2.44E-17	1.03E-14	1.18E-16
91-57-6	1.05E-16	1.13E-14	7.55E-17
91-58-7	2.66E-16	1.08E-14	1.57E-16
91-59-8	5.69E-18	3.68E-15	1.98E-16
91-63-4	1.22E-17	1.27E-15	5.09E-17
91-64-5	2.72E-17	5.08E-16	4.61E-17
91-66-7	1.07E-18	2.97E-16	2.12E-18
91-88-3	3.28E-18	3.93E-16	3.67E-17
919-86-8	1.17E-17	3.11E-16	3.61E-17
920-66-1	1.05E-17	9.60E-17	8.96E-18
924-16-3	3.80E-18	1.80E-16	4.62E-18
924-42-5	6.88E-18	8.67E-19	1.13E-19
92-52-4	6.55E-17	1.57E-18	3.13E-17
92-67-1	4.55E-17	3.70E-15	1.16E-16
92-87-5	3.35E-17	1.51E-15	1.21E-16
92-88-6	1.49E-17	7.14E-16	4.31E-17
928-96-1	5.17E-19	6.65E-17	2.40E-18
930-55-2	3.44E-18	2.70E-17	3.99E-18
93-08-3	2.30E-16	1.21E-14	5.91E-16
93-15-2	1.56E-17	3.80E-15	9.48E-17
932-83-2	5.69E-18	2.32E-16	2.21E-17
93-51-6	4.80E-18	4.77E-16	3.10E-17
93-78-7	5.89E-16	2.72E-14	2.78E-16
938-73-8	1.61E-18	2.60E-17	3.15E-18
93-89-0	4.31E-18	3.64E-17	2.41E-18
94-09-7	1.94E-18	7.00E-17	7.83E-18
94-11-1	2.56E-16	1.31E-14	1.70E-16
941-98-0	1.23E-16	6.02E-15	3.04E-16
94361-06-5	2.59E-15	6.43E-14	4.44E-15

944-22-9	4.24E-16	1.33E-13	1.20E-15
94-58-6	7.83E-18	7.55E-16	6.85E-18
94-59-7	9.74E-18	2.47E-15	3.16E-17
94-62-2	3.07E-17	3.93E-15	3.91E-17
947-02-4	8.27E-16	3.30E-14	4.39E-15
94-80-4	5.42E-16	3.31E-14	1.52E-16
94-96-2	1.53E-18	3.59E-17	3.25E-18
950-35-6	3.15E-16	4.09E-15	4.45E-16
950-37-8	1.28E-17	1.00E-15	6.86E-17
95-06-7	2.80E-18	9.42E-16	2.08E-17
95-16-9	2.37E-17	9.00E-16	5.62E-17
953-17-3	3.06E-16	2.84E-13	6.99E-16
95-33-0	1.76E-17	2.03E-15	5.26E-17
95465-99-9	3.89E-18	7.72E-16	5.22E-18
95-47-6	1.33E-17	3.47E-16	7.32E-18
95-48-7	1.36E-17	8.70E-16	2.73E-17
95-49-8	1.60E-17	1.07E-16	8.10E-18
95-50-1	1.17E-15	6.72E-15	8.17E-16
95-51-2	3.34E-17	3.26E-15	1.69E-16
95-53-4	1.25E-18	9.27E-17	8.77E-19
95-54-5	7.85E-19	3.90E-17	5.71E-18
95-56-7	6.50E-17	2.41E-15	9.62E-17
95-57-8	2.51E-16	1.29E-14	4.55E-16
95-63-6	4.03E-18	2.19E-16	2.09E-18
95-64-7	1.53E-18	6.78E-16	3.99E-17
95-65-8	7.20E-18	9.12E-16	6.22E-17
95-68-1	2.18E-18	8.58E-16	4.40E-17
956-90-1	4.24E-16	6.88E-15	5.39E-16
95-70-5	1.27E-18	6.88E-17	1.01E-17
95737-68-1	8.96E-18	1.58E-15	1.45E-18
95-74-9	5.18E-17	1.38E-14	5.49E-16
957-51-7	3.21E-17	7.37E-16	4.27E-17
95-76-1	6.57E-17	3.48E-15	2.72E-16
95-77-2	1.19E-17	4.24E-16	1.32E-17
95-79-4	6.87E-18	1.81E-15	6.92E-17
95-82-9	2.36E-18	2.24E-16	8.15E-18
95-87-4	4.96E-18	9.30E-16	4.86E-17
95-88-5	4.16E-18	3.51E-16	4.07E-17
95-92-1	3.09E-19	1.43E-18	2.37E-19
95-93-2	5.39E-18	2.02E-16	2.75E-18
95-94-3	8.79E-15	9.83E-14	4.50E-15
95-95-4	9.53E-17	4.73E-16	4.97E-17
959-98-8	1.11E-14	6.36E-13	1.79E-14
96-05-9	1.05E-17	4.48E-16	6.95E-18
96-09-3	2.09E-18	1.07E-17	1.18E-18
961-11-5	1.20E-17	3.75E-16	1.16E-17
96-12-8	1.23E-16	9.78E-16	6.97E-17
96-13-9	9.74E-18	1.38E-16	1.61E-17
96-17-3	4.63E-19	8.53E-18	3.61E-19
96-18-4	2.34E-16	1.31E-15	1.88E-16
96-22-0	5.65E-18	2.81E-17	3.82E-18
96-23-1	1.19E-16	1.63E-15	1.76E-16
96-24-2	1.03E-17	1.38E-17	2.27E-18
96-29-7	7.51E-18	8.71E-17	9.87E-18
96-33-3	2.36E-18	1.13E-17	1.28E-18
96-34-4	1.07E-17	2.27E-17	5.86E-18

96-45-7	6.46E-20	1.36E-18	1.33E-19
96-48-0	5.61E-19	5.00E-19	1.12E-19
96489-71-3	6.89E-16	1.42E-13	1.06E-16
97-00-7	1.17E-16	2.67E-15	2.13E-16
97-02-9	3.22E-17	4.61E-16	5.45E-17
97-11-0	4.80E-18	2.44E-15	1.14E-18
97-17-6	2.38E-16	9.44E-14	1.67E-16
97-23-4	5.79E-17	2.63E-15	2.43E-17
973-21-7	3.20E-16	1.51E-14	2.43E-16
97-53-0	1.13E-18	1.99E-16	1.02E-17
97-56-3	1.42E-16	1.83E-14	1.60E-16
97-63-2	9.74E-21	5.02E-19	2.10E-20
97-64-3	3.01E-19	4.23E-19	1.54E-19
97-74-5	1.14E-19	5.04E-18	6.26E-19
97-77-8	1.11E-17	9.36E-15	1.20E-16
97-86-9	6.58E-20	1.64E-18	3.74E-20
97-88-1	5.68E-20	1.44E-18	3.17E-20
97-99-4	6.18E-19	2.68E-18	3.86E-19
98-00-0	1.36E-18	3.22E-17	3.59E-18
98-01-1	1.12E-17	1.41E-16	1.31E-17
98-05-5	2.25E-15	1.55E-14	2.36E-15
98-06-6	4.82E-17	6.27E-16	2.42E-17
98-07-7	2.67E-16	2.75E-19	4.85E-17
98-08-8	6.08E-19	3.15E-18	3.21E-19
98-09-9	3.64E-17	3.87E-16	2.27E-17
98-13-5	2.31E-17	1.75E-16	1.17E-17
98-16-8	6.94E-17	3.98E-15	1.63E-16
98319-26-7	1.01E-16	2.17E-15	1.06E-16
98-51-1	9.89E-17	4.16E-15	4.95E-17
98-52-2	1.40E-17	1.09E-15	2.70E-17
98-54-4	6.16E-18	7.86E-16	1.96E-17
98-82-8	2.57E-17	3.02E-16	1.29E-17
98-85-1	4.71E-18	9.46E-17	7.52E-18
98-86-2	1.40E-17	2.79E-16	1.59E-17
98-87-3	3.14E-17	2.80E-16	1.71E-17
98-88-4	6.93E-18	9.34E-17	7.46E-18
98-92-0	2.13E-19	3.49E-19	4.53E-20
98-95-3	4.31E-17	7.63E-16	4.74E-17
99-08-1	6.67E-17	7.26E-16	7.50E-17
99-09-2	2.73E-17	4.67E-16	6.20E-17
99105-77-8	1.21E-17	1.70E-16	1.91E-17
99-30-9	7.93E-17	1.47E-15	1.08E-16
99-35-4	3.28E-17	3.76E-16	5.55E-17
99-51-4	3.29E-17	8.41E-16	3.58E-17
99-54-7	1.19E-16	3.06E-15	1.30E-16
99-56-9	2.37E-18	4.89E-17	7.08E-18
99-57-0	2.85E-18	4.34E-17	5.96E-18
99-59-2	9.89E-18	2.10E-16	2.29E-17
99607-70-2	1.64E-18	4.67E-17	4.18E-20
99-65-0	7.59E-16	8.59E-15	1.45E-15
99-71-8	2.57E-18	3.75E-16	8.65E-18
99-87-6	3.82E-17	1.25E-15	1.94E-17
99-89-8	8.94E-18	1.24E-15	3.34E-17
99-92-3	5.08E-19	2.58E-17	3.61E-18
99-93-4	6.38E-18	1.85E-16	2.38E-17
999-61-1	4.08E-19	3.56E-18	4.43E-19

99-97-8	4.91E-18	2.07E-15	3.21E-17
99-99-0	1.49E-17	3.43E-16	1.98E-17

5.5.3. References

Accelrys Inc. (2011) Registry of Toxic Effects of Chemical Substances (RTECS). Canadian Centre for Occupational Health and Safety (CCOHS). http://ccinfoweb.ccohs.ca/rtecs/search.html. Accessed June 6th - July 21st 2011

Adams WJ, Kimerle RA, Mosher RG (1985) Aquatic safety assessment of chemicals sorbed to sediments. In: Cardwell RD, Purdy R, Bahner RC (eds) Aquatic toxicology and hazard assessment:seventh symposium, vol STP 854. American Society for Testing and Materials, Philadelphia, PA, pp 429-453

Alexander M (2000) Aging, bioavailability, and overestimation of risk from environmental pollutants. Environ Sci Technol 34 (20):4259-4265. doi:10.1021/es001069+

Amacher M (1991) Methods for obtaining and analyzing kinetic data. In: Sparks DL, Suarez DL (eds) Rates of soil chemical processes vol Special Publication no. 27. Soil Science Society of America, Madison, WI, pp 19-59

Arnot JA, Mackay D, Bonnell M (2008) Estimating metabolic biotransformation rates in fish from laboratory data. Environ Toxicol Chem 27 (2):341-351

Arnot JA, Mackay D, Parkerton TF, Zaleski RT, Warren CS (2010) Multimedia modeling of human exposure to chemical substances: The roles of food web biomagnification and biotransformation. Environ Toxicol Chem 29 (1):45-55. doi:10.1002/etc.15

Asfaw A, Ellersieck MR, Mayer FL (2003) Interspecies correlation estimations (ICE) for acute toxicity to aquatic organisms and wildlife. II. User manual and software. EPA/600/R-03/106. United States Environmental Protection Agency. Washington, DC,

Batjes NH (2006) ISRIC-WISE derived soil properties on a 5 by 5 arc-minutes global grid (version 1.0). ISRIC –World Soil Information, Wageningen

Batjes NH (2008) ISRIC-WISE harmonized global soil profile dataset (version 3.1). ISRIC –World Soil Information, Wageningen

Batjes NH (2009) Harmonized soil profile data for applications at global and continental scales: updates to the WISE database. Soil Use and Management 25 (2):124-127. doi:10.1111/j.1475-2743.2009.00202.x

Belfroid A, Meiling J, Sijm D, Hermens J, Seinen W, Vangestel K (1994a) Uptake of hydrophobic halogenated aromatic-hydrocarbons from food by earthworms (eisenia-andrei). Archives of Environmental Contamination and Toxicology 27 (2):260-265

Belfroid A, Sikkenk M, Seinen W, Vangestel K, Hermens J (1994b) The toxicokinetic behavior of chlorobenzenes in earthworm (eisenia-andrei) experiments in soil. Environ Toxicol Chem 13 (1):93-99. doi:10.1897/1552-8618(1994)13[93:ttboci]2.0.co;2

Belfroid AC, Sijm DTHM, van Gestel CAM (1996) Bioavailability and toxicokinetics of hydrophobic aromatic compounds in benthic and terrestrial invertebrates. Environmental Review 4:276-299

Bhavsar SP, Gandhi N, Diamond ML (2008) Extension of coupled multispecies metal transport and speciation (TRANSPEC) model to soil. Chemosphere 70 (5):914-924

Buekers J, Degryse F, Maes A, Smolders E (2008) Modelling the effects of ageing on Cd, Zn, Ni and Cu solubility in soils using an assemblage model. Eur J Soil Sci 59 (6):1160-1170. doi:10.1111/j.1365-2389.2008.01053.x

Canadian Centre for Occupational Health and Safety (CCOHS) (2011) Registry of Toxic Effects of Chemical Substances (RTECS). Canadian Centre for Occupational Health and Safety (CCOHS). http://ccinfoweb.ccohs.ca/rtecs/search.html. Accessed June 6th - July 21st 2011

Christiansen KS, Borggaard OK, Holm PE, Vijver MG, Hauschild MZ, Peijnenburg WJGM (2012) Does the biotic ligand model approach improve the effect assessment of copper for plants in soil? submitted

Connell DW, Bowman M, Hawker DW (1988) Bioconcentration of chlorinated hydrocarbons from sediment by oligochaetes. Ecotoxicol Environ Saf 16 (3):293-302. doi:10.1016/0147-6513(88)90058-9

Cornelissen G, Gustafsson O, Bucheli TD, Jonker MTO, Koelmans AA, Van Noort PCM (2005) Extensive sorption of organic compounds to black carbon, coal, and kerogen in sediments and soils: Mechanisms and consequences for distribution, bioaccumulation, and biodegradation. Environ Sci Technol 39 (18):6881-6895. doi:10.1021/es050191b

Corwin DL, Lesch SM (2003) Application of soil electrical conductivity to precision agriculture: Theory, principles, and guidelines. Agron J 95 (3):455-471

Crout NMJ, Tye AM, Zhang H, McGrath SP, Young SD (2006) Kinetics of metal fixation in soils: Measurement and modeling by isotopic dilution. Environ Toxicol Chem 25 (3):659-663. doi:10.1897/05-069r.1

Davies CW (1962) Ion Association. Butterworth, London

de Caritat P, Reimann C, Chekushin V, Bogatyrev I, Niskavaara H, Braun J (1997) Mass Balance between Emission and Deposition of Airborne Contaminants. Environ Sci Technol 31 (10):2966-2972. doi:10.1021/es970193z

Degryse F, Smolders E, Parker DR (2009) Partitioning of metals (Cd, Co, Cu, Ni, Pb, Zn) in soils: concepts, methodologies, prediction and applications - a review. Eur J Soil Sci 60 (4):590-612. doi:10.1111/j.1365-2389.2009.01142.x

Degryse F, Voegelin A, Jacquat O, Kretzschmar R, Smolders E (2011) Characterization of zinc in contaminated soils: complementary insights from isotopic exchange, batch extractions and XAFS spectroscopy. Eur J Soil Sci 62 (2):318-330. doi:10.1111/j.1365-2389.2010.01332.x

Diamond ML, Gandhi N, Adams WJ, Atherton J, Bhavsar SP, Bulle C, Campbell PGC, Dubreuil A, Fairbrother A, Farley K, Green A, Guinee J, Hauschild MZ, Huijbregts MAJ, Humbert S, Jensen KS, Jolliet O, Margni M, McGeer JC, Peijnenburg W, Rosenbaum R, van de Meent D, Vijver MG (2010) The clearwater consensus: the estimation of metal hazard in fresh water. Int J Life Cycle Assess 15 (2):143-147. doi:10.1007/s11367-009-0140-2

Dijkstra JJ, Meeussen JCL, Comans RNJ (2004) Leaching of heavy metals from contaminated soils: An experimental and modeling study. Environ Sci Technol 38 (16):4390-4395. doi:10.1021/es049885v

Dijkstra JJ, Meeussen JCL, Comans RNJ (2009) Evaluation of a Generic Multisurface Sorption Model for Inorganic Soil Contaminants. Environ Sci Technol 43 (16):6196-6201. doi:10.1021/es900555g

DiToro DM, Zarba CS, Hansen DJ, Berry WJ, Swartz RC, Cowan CE, Pavlou SP, Allen HE, Thomas NA, Paquin PR (1991) Technical basis for establishing sediment quality criteria for nonionic organic-chemicals using equilibrium partitioning. Environ Toxicol Chem 10 (12):1541-1583. doi:10.1897/1552-8618(1991)10[1541:tbfesq]2.0.co;2

EC (2003) Technical Guidance Document in support of Commission Directive 93/67/EEC on Risk Assessment for new notified substances, Commission Regulation (EC) No 1488/94 on Risk Assessment for existing substances and Directive 98/8/EC of the European Parliament and of the Council concerning the placing of biocidal products on the market. Joint Research Centre, European Chemicals Bureau, Brussels, Belgium

Ewing SA, Christensen JN, Brown ST, Vancuren RA, Cliff SS, Depaolo DJ (2010) Pb Isotopes as an Indicator of the Asian Contribution to Particulate Air Pollution in Urban California. Environ Sci Technol 44 (23):8911-8916. doi:10.1021/es101450t

FAO/IIASA/ISRIC/ISS-CAS/JRC (2012) Harmonized World Soil Database (version 1.2)

Fedotov PS, Kordel W, Miro M, Peijnenburg W, Wennrich R, Huang PM (2012) Extraction and Fractionation Methods for Exposure Assessment of Trace Metals, Metalloids, and Hazardous Organic Compounds in Terrestrial Environments. Crit Rev Environ Sci Technol 42 (11):1117-1171. doi:10.1080/10643389.2011.556544

Finnveden G, Hauschild MZ, Ekvall T, Guinée J, Heijungs R, Hellweg S, Koehler A, Pennington D, Suh S (2009) Recent developments in life cycle assessment. Journal of Environmental Management 91 (1):1-21

Gaines JGL, Thomas HC (1953) Adsorption Studies on Clay Minerals. II. A Formulation of the Thermodynamics of Exchange Adsorption. The Journal of Chemical Physics 21 (4):714-718

Gandhi N, Diamond ML, Razavi R, Bhavsar SP, Hodge EM (2011a) A modeling assessment of contaminant fate in the Bay of Quinte, Lake Ontario: Part 1. Metals. Aquat Ecosyst Health Manag 14 (1):85-93. doi:10.1080/14634988.2011.550546

(2010) New Method for Calculating Comparative Toxicity Potential of Cationic Metals in Freshwater: Application to Copper, Nickel, and Zinc. Environ Sci Technol 44 (13):5195-5201. doi:10.1021/es903317a

Gandhi N, Huijbregts MAJ, Meent Dvd, Peijnenburg WJGM, Guinée J, Diamond ML (2011b) Implications of geographic variability on Comparative Toxicity Potentials of Cu, Ni and Zn in freshwaters of Canadian ecoregions. Chemosphere 82 (2):268-277

Garnier JM, Ciffroy P, Benyahya L (2006) Implications of short and long term (30 days) sorption on the desorption kinetic of trace metals (Cd, Zn, Co, Mn, Fe, Ag, Cs) associated with river suspended matter. Sci Total Environ 366 (1):350-360. doi:10.1016/j.scitotenv.2005.07.015

Golsteijn L, Hendriks HWM, van Zelm R, Ragas AMJ, Huijbregts MAJ (2012a) Do interspecies correlation estimations increase the reliability of toxicity estimates for wildlife? Ecotoxicol Environ Saf Volume 80:238–243

Golsteijn L, Van Zelm R, Veltman K, Musters G, Hendriks AJ, Huijbregts MAJ (2012b) Including ecotoxic impacts on warm-blooded predators in life cycle impact assessment. Integr Environ Assess Manag 8 (2):372–378. doi:10.1002/ieam.269

Griffin BA, Jurinak JJ (1973) Estimation of Activity Coefficients From the Electrical Conductivity of Natural Aquatic Systems and Soil Extracts. Soil Sci 116 (1):26-30

Groenenberg JE, Dijkstra JJ, Bonten LTC, de Vries W, Comans RNJ (2012) Evaluation of the performance and limitations of empirical partition-relations and process based

multisurface models to predict trace element solubility in soils. Environ Pollut 166 (0):98-107

Groenenberg JE, Römkens PFAM, Comans RNJ, Luster J, Pampura T, Shotbolt L, Tipping E, De Vries W (2010) Transfer functions for solid-solution partitioning of cadmium, copper, nickel, lead and zinc in soils: derivation of relationships for free metal ion activities and validation with independent data. Eur J Soil Sci 61 (1):58-73. doi:10.1111/j.1365-2389.2009.01201.x

Hauschild MZ, Huijbregts M, Jolliet O, MacLeod M, Margni M, van de Meent DV, Rosenbaum RK, McKone TE (2008) Building a model based on scientific consensus for life cycle impact assessment of chemicals: The search for harmony and parsimony. Environ Sci Technol 42 (19):7032-7037. doi:10.1021/es703145t

Henderson A, Hauschild M, van de Meent D, Huijbregts M, Larsen H, Margni M, McKone T, Payet J, Rosenbaum R, Jolliet O (2011) USEtox fate and ecotoxicity factors for comparative assessment of toxic emissions in life cycle analysis: sensitivity to key chemical properties. The International Journal of Life Cycle Assessment 16 (8):701-709. doi:10.1007/s11367-011-0294-6

Hendriks AJ, Traas TP, Huijbregts MAJ (2005) Critical body residues linked to octanol-water partitioning, organism composition, and LC50 QSARs: Meta-analysis and model. Environ Sci Technol 39 (9):3226-3236. doi:10.1021/es048442o

Hendriks AJ, Van der Linde A, Cornelissen G, Sijm D (2001) The power of size. 1. Rate constants and equilibrium ratios for accumulation of organic substances related to octanol-water partition ratio and species weight. Environ Toxicol Chem 20 (7):1399-1420

Houx NWH, Aben WJM (1993) Bioavailability of pollutants to soil organisms via the soil solution. Science of The Total Environment 134, Supplement 1 (0):387-395

Huijbregts MAJ (1999) Ecotoxicological effect factors for the terrestrial environment in the frame of LCA. Interfaculty Department of Environmental Science, University of Amsterdam,

Huijbregts MAJ, Guinee JB, Reijnders L (2001) Priority assessment of toxic substances in life cycle assessment. III: Export of potential impact over time and space. Chemosphere 44 (1):59-65. doi:10.1016/s0045-6535(00)00349-0

Humbert S, Marshall JD, Shaked S, Spadaro JV, Nishioka Y, Preiss P, McKone TE, Horvath A, Jolliet O (2011) Intake fraction for particulate matter: recommendations for life cycle impact assessment. Environmental Science and Technology 45 (11):4808-4816

Jager T (1998) Mechanistic approach for estimating bioconcentration of organic chemicals in earthworms (Oligochaeta). Environ Toxicol Chem 17 (10):2080-2090. doi:10.1897/1551-5028(1998)017<2080:mafebo>2.3.co;2

Jager T, Fleuren R, Hogendoorn EA, De Korte G (2003) Elucidating the routes of exposure for organic chemicals in the earthworm, Eisenia andrei (Oligochaeta). Environ Sci Technol 37 (15):3399-3404. doi:10.1021/es0340578

Janssen RPT, Peijnenburg WJGM, Posthuma L, Van Den Hoop MAGT (1997) Equilibrium partitioning of heavy metals in dutch field soils. I. Relationship between metal partition coefficients and soil characteristics. Environ Toxicol Chem 16 (12):2470-2478. doi:10.1002/etc.5620161206

Jensen J, Mesman M (2006) Foreword. In: Jensen J, Mesman M (eds) Ecological risk assessment of contaminated land, vol RIVM report number 711701047. National Institute for Public Health and the Environment, Bilthoven, the Netherlands, p 5

Kemp PF, Swartz RC (1988) Acute toxicity of interstitial and particle-bound cadmium to a marine infaunal amphipod. Marine Environmental Research 26 (2):135-153. doi:10.1016/0141-1136(88)90023-2

Kindler R, Siemens J, Kaiser K, Walmsley DC, Bernhofer C, Buchmann N, Cellier P, Eugster W, Gleixner G, Grunwald T, Heim A, Ibrom A, Jones SK, Jones M, Klumpp K, Kutsch W, Larsen KS, Lehuger S, Loubet B, McKenzie R, Moors E, Osborne B, Pilegaard K, Rebmann C, Saunders M, Schmidt MWI, Schrumpf M, Seyfferth J, Skiba U, Soussana JF, Sutton MA, Tefs C, Vowinckel B, Zeeman MJ, Kaupenjohann M (2011) Dissolved carbon leaching from soil is a crucial component of the net ecosystem carbon balance. Global Change Biology 17 (2):1167-1185. doi:10.1111/j.1365-2486.2010.02282.x

Kinraide TB (2009) Improved scales for metal ion softness and toxicity. Environ Toxicol Chem 28 (3):525-533

Kinraide TB, Yermiyahu U (2007) A scale of metal ion binding strengths correlating with ionic charge, Pauling electronegativity, toxicity, and other physiological effects. J Inorg Biochem 101 (9):1201-1213. doi:10.1016/j.jinorgbio.2007.06.003

Knezovich JP, Harrison FL (1988) The bioavailability of sediment-sorbed chlorobenzenes to larvae of the midge, chironomus-decorus. Ecotoxicol Environ Saf 15 (2):226-241. doi:10.1016/0147-6513(88)90076-0

Kooijman S (1987) A safety factor for LC50 values allowing for differences in sensitivity among species. Water Res 21 (3):269-276. doi:10.1016/0043-1354(87)90205-3

Lado LR, Hengl T, Reuter HI (2008) Heavy metals in European soils: A geostatistical analysis of the FOREGS Geochemical database. Geoderma 148 (2):189-199. doi:10.1016/j.geoderma.2008.09.020

Lair GJ, Gerzabek MH, Haberhauer G (2007) Retention of copper, cadmium and zinc in soil and its textural fractions influenced by long-term field management. Eur J Soil Sci 58 (5):1145-1154. doi:10.1111/j.1365-2389.2007.00905.x

Levard C, Hotze EM, Lowry GV, Brown GE (2012) Environmental Transformations of Silver Nanoparticles: Impact on Stability and Toxicity. Environ Sci Technol. doi:10.1021/es2037405

Lofts S, Spurgeon DJ, Svendsen C, Tipping E (2004) Deriving soil critical limits for Cu, Zn, Cd, and Ph: A method based on free ion concentrations. Environ Sci Technol 38 (13):3623-3631

Loibner A, Jensen J, Ter Laak T, Celis R, Hartnik T (2006) Sorption and aging of soil contamination. In: Jensen J, Mesman M (eds) Ecological risk assessment of contaminated land, vol RIVM report number 711701047. National Institute for Public Health and the Environment, Bilthoven, the Netherlands, pp 19-29

Ma YB, Lombi E, Oliver IW, Nolan AL, McLaughlin MJ (2006) Long-term aging of copper added to soils. Environ Sci Technol 40 (20):6310-6317. doi:10.1021/es060306r

MacLeod M, Bennett D, Perem M, Maddalena R, McKone T, Mackay D (2004) Dependence of intake fraction on release location in a multimedia framework: a case study of four contaminants in North America. Journal of Industrial Ecology 8 (3):89-102

Manneh R, Margni M, Deschênes L (2010) Spatial variability of intake fractions for canadian emission scenarios: a comparison between three resolution scales. Environmental Science and Technology 44 (11):4217-4224. doi:10.1021/es902983b

Margni M, Pennington D, Amman C, Jolliet O (2004) Evaluating multimedia/multipathway model intake fraction estimates using POP emission and monitoring data. Environmental Pollution 128 (1-2):263-277

Margni M, Pennington D, Birkved M, Larsen HF, Hauschild MZ (2002) Test set of organic chemicals for life cycle impact assessment characterisation method comparison. OMNITOX project report.

Matschonat G, Ingwersen J, Streck T (2003) Suitability of the ESS laboratory method to determine the equilibrium soil solution composition of agricultural soils, and suggestions for simplification of the experimental procedure. Journal of Plant Nutrition and Soil Science-Zeitschrift Fur Pflanzenernahrung Und Bodenkunde 166 (6):742-749. doi:10.1002/jpln.200321234

Mendenhall W, Beaver RJ (1994) Introduction to probability and statistics. Duxbury Press, Belmont, California, USA,

Mertens FM, Paetzold S, Welp G (2008) Spatial heterogeneity of soil properties and its mapping with apparent electrical conductivity. Journal of Plant Nutrition and Soil Science-Zeitschrift Fur Pflanzenernahrung Und Bodenkunde 171 (2):146-154. doi:10.1002/jpln.200625130

Meylan W, Howard PH, Boethling RS (1992) Molecular topology fragment contribution method for predicting soil sorption coefficients. Environ Sci Technol 26 (8):1560-1567. doi:10.1021/es00032a011

Nicholson FA, Smith SR, Alloway BJ, Carlton-Smith C, Chambers BJ (2003) An inventory of heavy metals inputs to agricultural soils in England and Wales. Sci Total Environ 311 (1-3):205-219. doi:10.1016/s0048-9697(03)00139-6

Nordberg M, Duffus JH, Templeton DM (2010) Explanatory dictionary of key terms in toxicology: Part II (IUPAC Recommendations 2010). Pure Appl Chem 82 (3):679-751. doi:10.1351/pac-rec-09-03-01

Nortcliff S (2002) Standardisation of soil quality attributes. Agriculture, Ecosystems & Environment 88 (2):161-168

Paquin PR, Gorsuch JW, Apte S, Batley GE, Bowles KC, Campbell PGC, Delos CG, Di Toro DM, Dwyer RL, Galvez F, Gensemer RW, Goss GG, Hogstrand C, Janssen CR, McGeer JC, Naddy RB, Playle RC, Santore RC, Schneider U, Stubblefield WA, Wood CM, Wu KB (2002) The biotic ligand model: a historical overview. Comparative Biochemistry and Physiology C-Toxicology & Pharmacology 133 (1-2):3-35

Parkhurst DL, Appelo CAJ (1999) User's guide to phreeqc- a computer
program for speciation, batch-reaction, one-dimensional transport, and inverse
geochemical calculations. U.S. Geological Survey, Denver, CO

Pavlou SP, Weston DP (1983) Initial evaluation of alternatives for development of sediment related criteria for toxic contaminants in marine waters (Puget Sound). Phase I: Development of conceptual framework. Bellevue, Washington

Peijnenburg W, Zablotskaja M, Vijver MG (2007) Monitoring metals in terrestrial environments within a bioavailability framework and a focus on soil extraction. Ecotoxicol Environ Saf 67 (2):163-179. doi:10.1016/j.ecoenv.2007.02.008

Pennington DW, Margni M, Ammann C, Jolliet O (2005) Multimedia fate and human intake modeling: spatial versus nonspatial insights for chemical emissions in Western Europe. Environmental Science and Technology 39 (4):1119-1128

Pennington DW, Payet J, Hauschild M (2004) Aquatic ecotoxicological indicators in life-cycle assessment. Environ Toxicol Chem 23 (7):1796-1807

Pettersen J, Hertwich EG (2008) Critical review: Life-cycle inventory procedures for long-term release of metals. Environ Sci Technol 42 (13):4639-4647. doi:10.1021/es702170v

Pistocchi A, Zulian G, Vizcaino P, Marinov D (2010) Multimedia assessment of pollutant pathways in the environment, European scale model (MAPPE-EUROPE). Office for Official Publications of the European Communities, Luxembourg, EUR 24256 EN.

Pizzol M, Bulle C, Thomsen M (2012) Indirect human exposure assessment of airborne lead deposited on soil via a simplified fate and speciation modelling approach. Sci Total Environ 421–422 (0):203-209

Pizzol M, Christensen P, Schmidt J, Thomsen M (2011) Eco-toxicological impact of "metals" on the aquatic and terrestrial ecosystem: A comparison between eight different methodologies for Life Cycle Impact Assessment (LCIA). Journal of Cleaner Production 19 (6-7):687-698

Popp M, Koellensperger G, Stingeder G, Hann S (2008) Novel approach for determination of trace metals bound to suspended solids in surface water samples by inductively coupled plasma sector field mass spectrometry (ICP-SFMS). J Anal At Spectrom 23 (1):111-118. doi:10.1039/b708482j

Prommer H, Tuxen N, Bjerg PL (2006) Fringe-Controlled Natural Attenuation of Phenoxy Acids in a Landfill Plume: Integration of Field-Scale Processes by Reactive Transport Modeling. Environ Sci Technol 40 (15):4732-4738. doi:10.1021/es0603002

Raimondo S, Vivian DN, Barron MG (2010) Web-based Interspecies Correlation Estimates (Web-ICE) for acute toxicity: user manual. Version 3.1. EPA/600/R-10/004. Office of Research and Development, U.S. Environmental Protection Agency. Gulf Breeze, FL.,

Rauch JN, Pacyna JM (2009) Earth's global Ag, Al, Cr, Cu, Fe, Ni, Pb, and Zn cycles. Global Biogeochem Cycles 23. doi:Gb2001

10.1029/2008gb003376

Reichenberg F, Mayer P (2006) Two complementary sides of bioavailability: Accessibility and chemical activity of organic contaminants in sediments and soils. Environ Toxicol Chem 25 (5):1239-1245. doi:10.1897/05-458r.1

Reuter HI, Lado LR, Hengl T, Montanarella L (2008) Continental-scale digital soil mapping using European soil profile data: soil pH. Hamburger Beiträge zur Physischen Geographie und Landschaftsökologie 19:91-102

RIVM; National Institute for Public Health and the Environment (2008) e-toxBase. http://www.e-toxbase.com/. 2008

RIVM; National Institute for Public Health and the Environment (2011) e-toxBase. http://www.e-toxbase.com/. Accessed December 2011

Robbins CW, Carter DL (1983) Selectivity coefficients for calcium-magnesium-sodium-potassium exchange in eight soils. Irrig Sci 4 (2):95-102. doi:10.1007/bf00273378

Rochat D, Margni M, Jolliet O (2004) Continent-specific intake fractions and characterization factors for toxic emissions: does it make a difference? International Journal of Life Cycle Assessment 11 (1):55-63

Rodrigues SM, Henriques B, da Silva EF, Pereira ME, Duarte AC, Groenenberg JE, Römkens PFAM (2010a) Evaluation of an approach for the characterization of reactive and available pools of 20 potentially toxic elements in soils: Part II – Solid-solution partition relationships and ion activity in soil solutions. Chemosphere 81 (11):1560-1570

Rodrigues SM, Henriques B, da Silva EF, Pereira ME, Duarte AC, Romkens P (2010b) Evaluation of an approach for the characterization of reactive and available pools of twenty potentially toxic elements in soils: Part I - The role of key soil properties in the variation of contaminants' reactivity. Chemosphere 81 (11):1549-1559. doi:10.1016/j.chemosphere.2010.07.026

Roelofs W, Huijbregts MAJ, Jager T, Ragas AMJ (2003) Prediction of ecological no-effect concentrations for initial risk assessment: Combining substance-specific data and database information. Environ Toxicol Chem 22 (6):1387-1393

Romkens PF, Guo H-Y, Chu C-L, Liu T-S, Chiang C-F, Koopmans GF (2009) Characterization of soil heavy metal pools in paddy fields in Taiwan: chemical extraction and solid-solution partitioning. J Soils Sediments 9 (3):216-228. doi:10.1007/s11368-009-0075-z

Römkens PFAM, Groenenberg JE, Bonten LTC, Vries Wd, Bril J (2004) Derivation of partition relationships to calculate Cd, Cu, Ni, Pb, Zn solubility and activity in soil solutions. Alterra, Wageningen

Rosenbaum R, Huijbregts M, Henderson A, Margni M, McKone T, van de Meent D, Hauschild M, Shaked S, Li D, Gold L, Jolliet O (2011) USEtox human exposure and toxicity factors for comparative assessment of toxic emissions in life cycle analysis: sensitivity to key chemical properties. The International Journal of Life Cycle Assessment 16 (8):710-727. doi:10.1007/s11367-011-0316-4

Rosenbaum RK, Bachmann TM, Gold LS, Huijbregts MAJ, Jolliet O, Juraske R, Koehler A, Larsen HF, MacLeod M, Margni M, McKone TE, Payet J, Schuhmacher M, van de Meent D, Hauschild MZ (2008a) USEtox-the UNEP-SETAC toxicity model: recommended characterisation factors for human toxicity and freshwater ecotoxicity in life cycle impact assessment. The International Journal of Life Cycle Assessment 13 (7):532-546. doi:10.1007/s11367-008-0038-4

Rosenbaum RK, Bachmann TM, Gold LS, Huijbregts MAJ, Jolliet O, Juraske R, Koehler A, Larsen HF, MacLeod M, Margni M, McKone TE, Payet J, Schuhmacher M, van de Meent D, Hauschild MZ (2008b) USEtox-the UNEP-SETAC toxicity model: recommended characterisation factors for human toxicity and freshwater ecotoxicity in life cycle impact assessment. Int J Life Cycle Assess 13 (7):532-546. doi:10.1007/s11367-008-0038-4

Rowell DL (1994) Soil science: Methods & applications. Longman Scientific & Technical, Longman Group UK Ltd, Harlow, Essex, UK

Ruby MV, Schoof R, Brattin W, Goldade M, Post G, Harnois M, Mosby DE, Casteel SW, Berti W, Carpenter M, Edwards D, Cragin D, Chappell W (1999) Advances in evaluating the oral bioavailability of inorganics in soil for use in human health risk assessment. Environ Sci Technol 33 (21):3697-3705. doi:10.1021/es990479z

Sauvé S, Hendershot W, Allen HE (2000) Solid-Solution Partitioning of Metals in Contaminated Soils: Dependence on pH, Total Metal Burden, and Organic Matter. Environ Sci Technol 34 (7):1125-1131. doi:10.1021/es9907764

Schuytema GS, Nebeker AV, Griffis WL, Miller CE (1989) Effects of freezing on toxicity of sediments contaminated with ddt and endrin. Environ Toxicol Chem 8 (10):883-891. doi:10.1897/1552-8618(1989)8[883:eofoto]2.0.co;2

Sedlbauer K, Braune A, Humbert S, Margni M, Schuller O, Fischer M (2007) Spatial differentiation in life cycle assessment: moving forward to more operational sustainability. Technikfolgenabschätzung - Theorie und Praxis (Technology assessment) 16 (3):24-31

Semple KT, Doick KJ, Jones KC, Burauel P, Craven A, Harms H (2004) Defining bioavailability and bioaccessibility of contaminated soil and sediment is complicated. Environ Sci Technol 38 (12):228A-231A

Shacklette HT, Boerngen JG (1984) Element concentration in soils and other surficial materials of the conterminous United States. USGS (United States Geological Survey) professional paper 1270,

Shaked S (2011) Multi-continental multimedia model of pollutant intake and application to impacts of global emissions and globally traded goods. PhD thesis. The University of Michigan, Ann Arbour

Shea D (1988) Developing national sediment quality criteria. Environ Sci Technol 22 (11):1256-1261. doi:10.1021/es00176a002

Siegfried BD (1993) Comparative toxicity of pyrethroid insectidicdes to terrestrial and aquatic insects. Environ Toxicol Chem 12 (9):1683-1689

Skeaff J, Delbeke K, Van Assche F, Conard B (2000) A critical surface area concept for acute hazard classification of relatively insoluble metal-containing powders in aquatic environments. Environ Toxicol Chem 19 (6):1681-1691. doi:10.1002/etc.5620190627

Smolders E, Degryse F, De Brouwere K, Van Den Brande K, Cornelis C, Seuntjens P (2000) Pore Water Based Kd Values of Heavy Metals in Soils from Flanders. Internal Report (in Dutch) to the Flemish Waste Agency, OVAM,

Sonmez S, Buyuktas D, Okturen F, Citak S (2008) Assessment of different soil to water ratios (1:1, 1:2.5, 1:5) in soil salinity studies. Geoderma 144 (1-2):361-369

Steele JM (2004) The Cauchy-Schwarz Master Class: An Introduction to the Art of Mathematical Inequalities. Cambridge University Press, New York,

Stiven GA, Khan MA (1966) Saturation percentage as a measure of soil texture in the lower Indus basin. Journal of Soil Science 17 (2):255-273. doi:10.1111/j.1365-2389.1966.tb01471.x

Sudduth KA, Kitchen NR, Wiebold WJ, Batchelor WD, Bollero GA, Bullock DG, Clay DE, Palm HL, Pierce FJ, Schuler RT, Thelen KD (2005) Relating apparent electrical conductivity to soil properties across the north-central USA. Comput Electron Agric 46 (1–3):263-283

Swartz RC, Ditsworth GR, Schults DW, Lamberson JO (1985) Sediment toxicity to a marine infaunal amphipod: Cadmium and its interaction with sewage sludge. Marine Environmental Research 18 (2):133-153

Swartz RC, Schults DW, Dewitt TH, Ditsworth GR, Lamberson JO (1990) Toxicity of fluoranthene in sediment to marine amphipods - a test of the equilibrium partitioning approach to sediment quality criteria. Environ Toxicol Chem 9 (8):1071-1080. doi:10.1897/1552-8618(1990)9[1071:tofist]2.0.co;2

Thakali S, Allen HE, Di Toro DM, Ponizovsky AA, Rooney CP, Zhao F-J, McGrath SP (2006a) A Terrestrial Biotic Ligand Model. 1. Development and Application to Cu and Ni Toxicities to Barley Root Elongation in Soils. Environ Sci Technol 40 (22):7085-7093. doi:10.1021/es061171s

Thakali S, Allen HE, Di Toro DM, Ponizovsky AA, Rooney CP, Zhao F-J, McGrath SP, Criel P, Van Eeckhout H, Janssen CR, Oorts K, Smolders E (2006b) Terrestrial Biotic Ligand Model. 2. Application to Ni and Cu Toxicities to Plants, Invertebrates, and Microbes in Soil. Environ Sci Technol 40 (22):7094-7100. doi:10.1021/es061173c

Tournassat C, Gailhanou H, Crouzet C, Braibant G, Gautier A, Gaucher EC (2009) Cation Exchange Selectivity Coefficient Values on Smectite and Mixed-Layer Illite/Smectite Minerals. Soil Sci Soc Am J 73 (3):928-942. doi:10.2136/sssaj2008.0285

Tournassat C, Gailhanou H, Crouzet C, Braibant G, Gautier A, Lassin A, Blanc P, Gaucher EC (2007) Two cation exchange models for direct and inverse modelling of solution major cation composition in equilibrium with illite surfaces. Geochim Cosmochim Acta 71 (5):1098-1114

Traas TP, van Leeuwen CJ (2007) Ecotoxicological effects. In: van Leeuwen CJ, Vermeire TG (eds) Risk assessment of chemicals: an introduction. Springer, pp 281-356

Tye AM, Young S, Crout NMJ, Zhang H, Preston S, Zhao FJ, McGrath SP (2004) Speciation and solubility of Cu, Ni and Pb in contaminated soils. Eur J Soil Sci 55 (3):579-590. doi:10.1111/j.1365-2389.2004.00627.x

Udo de Haes HA, Finnveden G, Goedkoop M, Hauschild MZ, Hertwich E, Hofstetter P, Jolliet O, Klöpffer W, Krewitt W, Lindeijer E, Mueller-Wenk R, Olsen I, Pennington D, Potting J, Steen B (2002) Life cycle impact assessment: striving towards best practice. Society of Environmental Toxicology and Chemistry (SETAC). Pensacola (US)

US EPA (2007) ECOTOX User Guide: ECOTOXicology Database System. Version 4.0. U.S. Environmental Protection Agency. http:/www.epa.gov/ecotox/. Accessed February 2012

Van Beelen P, Verbruggen EMJ, Peijnenburg W (2003) The evaluation of the equilibrium partitioning method using sensitivity distributions of species in water and soil. Chemosphere 52 (7):1153-1162. doi:10.1016/s0045-6535(03)00359-x

Van der Kooij LA, Van de Meent D, Van Leeuwen CJ, Bruggeman WA (1991) Deriving quality criteria for water and sediment from the results of aquatic toxicity tests and product standards: Application of the equilibrium partitioning method. Water Res 25 (6):697-705

Van Gestel CAM, Ma WC (1988) Toxicity and bioaccumulation of chlorophenols in earthworms, in relation to bioavailability in soil. Ecotoxicol Environ Saf 15 (3):289-297. doi:10.1016/0147-6513(88)90084-x

Van Zelm R, Huijbregts M, Posthuma L, Wintersen A, Van de Meent D (2009a) Pesticide ecotoxicological effect factors and their uncertainties for freshwater ecosystems. The International Journal of Life Cycle Assessment 14 (1):43-51. doi:10.1007/s11367-008-0037-5

Van Zelm R, Huijbregts MAJ, Van de Meent D (2009b) USES-LCA 2.0-a global nested multi-media fate, exposure, and effects model. The International Journal of Life Cycle Assessment 14 (3):282-284. doi:10.1007/s11367-009-0066-8

Veltman K, Huijbregts MAJ, Hendriks AJ (2010) Integration of Biotic Ligand Models (BLM) and Bioaccumulation Kinetics into a Mechanistic Framework for Metal Uptake in Aquatic Organisms. Environ Sci Technol 44 (13):5022-5028. doi:10.1021/es903697c

Veltman K, Huijbregts MAJ, Van Kolck M, Wang WX, Hendriks AJ (2008) Metal bioaccumulation in aquatic species: Quantification of uptake and elimination rate constants using physicochemical properties of metals and physiological characteristics of species. Environ Sci Technol 42 (3):852-858

Veltman K, McKone TE, Huijbregts MAJ, Hendriks AJ (2009) Bioaccumulation potential of air contaminants: Combining biological allometry, chemical equilibrium and mass-balances to predict accumulation of air pollutants in various mammals. Toxicol Appl Pharmacol 238 (1):47-55. doi:10.1016/j.taap.2009.04.012

Verbruggen EMJ, Posthumus R, van Wezel AP (2001) Ecotoxicological Serious Risk Concentrations for soil, sediment and (ground)water: updated proposals for first series of compounds. National Institute for Public Health and the Environment, Bilthoven, the Netherlands

Visconti F, de Paz JM, Rubio JL (2009) Principal component analysis of chemical properties of soil saturation extracts from an irrigated Mediterranean area: Implications for calcite equilibrium in soil solutions. Geoderma 151 (3–4):407-416

Voegelin A, Jacquat O, Pfister S, Barmettler K, Scheinost AC, Kretzschmar R (2011) Time-Dependent Changes of Zinc Speciation in Four Soils Contaminated with Zincite or Sphalerite. Environ Sci Technol 45 (1):255-261. doi:10.1021/es101189d

Vulava VM, Kretzschmar R, Rusch U, Grolimund D, Westall JC, Borkovec M (2000) Cation competition in a natural subsurface material: Modelling of sorption equilibria. Environ Sci Technol 34 (11):2149-2155

Wang P, De Schamphelaere KAC, Kopittke PM, Zhou DM, Peijnenburg W, Lock K (2012) Development of an electrostatic model predicting copper toxicity to plants. J Exp Bot 63 (2):659-668. doi:10.1093/jxb/err254

Wang P, Kinraide TB, Zhou D, Kopittke PM, Peijnenburg WJGM (2011) Plasma Membrane Surface Potential: Dual Effects upon Ion Uptake and Toxicity. Plant Physiol 155 (2):808-820. doi:10.1104/pp.110.165985

Wenger Y, Li D, Jolliet O (2012) Indoor intake fraction considering surface sorption of air organic compounds for life cycle assessment. The International Journal of Life Cycle Assessment 17 (7):919-931. doi:10.1007/s11367-012-0420-0

Yuan G, Lavkulich LM (1997) Sorption behavior of copper, zinc, and cadmium in response to simulated changes in soil properties. Commun Soil Sci Plant Anal 28 (6-8):571-587. doi:10.1080/00103629709369812

Ziegenfuss PS, Renaudette WJ, Adams WJ (1986) Methodology for assessing the acute toxicity of chemicals sorbed to sediments: testing the equilibrium partitioning theory. In: Poston TJ, Purdy R (eds) Aquatic toxicology and environmental fate, vol Vol 9 STP 921. American Society for Testing and Materials, Philadelphia, PA, pp 479-493